Cranfield University

Pericles Toukiloglou

Comparison of AVHRR, MODIS and VEGETATION for land cover mapping and drought monitoring at 1 km spatial resolution

School of Applied Sciences

PhD

Cranfield University

School of Applied Sciences

Natural Resources

Integrated Earth System Sciences Institute

PhD

2007

Pericles Toukiloglou

Comparison of AVHRR, MODIS and VEGETATION for land cover mapping and drought monitoring at 1 km spatial resolution

Supervisor: C.A.D. Sannier

May 2007

Dedicated to my parents, Pagratis and Olga Toukiloglou

Abstract

Low spatial resolution remote sensors are one of the best data sources for large area land cover mapping and drought monitoring. This study was concerned with identifying which of the three most operational such sensors (AVHRR, MODIS, and VEGETATION), were likely to help produce the best results within the mentioned applications.

A rigorous review of the sensors' characteristics led to the hypothesis that in land cover mapping and drought monitoring applications MODIS is most likely to achieve the best results followed by VEGETATION and lastly by AVHRR. This hypothesis was tested against experimental results generated within this study.

A methodology was developed allowing for unbiased relative comparison of the capacity of the sensors' Solar Reflective Bands (SRBs) to map land cover, and was applied to data collected over the UK and Greece, for which maps were produced using data collected by each sensor over the same dates and sites, and accuracy estimated using reference data. In the majority of cases the most accurate maps were produced by MODIS data; however, there were cases when maps produced by AVHRR and particularly VEGETATION data were more accurate.

Drought monitoring methodologies for low resolution data require historical Normalised Difference Vegetation Index (NDVI) records extending longer than MODIS and VEGETATION operational times. Towards solving this limitation, the relationships between the sensors' NDVI measurements over the same targets were investigated. It was found that NDVI data for one sensor could be predicted from NDVI data collected by another sensor with considerable accuracy. Consequently, MODIS and VEGETATION historical NDVI records could be extended based on past AVHRR data, and applications could be benefited by interchanging sensors for provision of NDVI data in the event of a sensor failure.

These extended datasets were used to assess drought conditions over Ethiopia with the aim of using the Vegetation Productivity Indicator (VPI) methodology. The sensors' NDVI data responsiveness to rainfall was assessed, finding MODIS NDVI data to best reflect rainfall conditions, and likely to produce more accurate VPI results.

Overall the experimental results generated in this study supported the initial hypothesis.

Acknowledgements

I would like to thank my parents Pagratis and Olga Toukiloglou for financing my education up until my MSc studies, which provided me with the background needed.

I would also like to thank my girlfriend Anne Dain-Owens for being very supportive and understanding during the difficult times of the PhD.

My thanks also go to my thesis committee members for their inputs and particularly my supervisor Christophe Sannier.

I would also like to thank Dr Sue White and Dr Hugh Eva for being my internal and external examiners respectively and helping me improve the final version of this document.

I would also like to thank my colleagues Elizabeth Farmer and Tim Brewer, for offering to take up part of my teaching assistant duties during the last stages of the present study, so that I could spend more time writing up.

My thanks also go to Prof. Richard Carter for helping me purchase the rainfall data from the National Meteorological Services Agency of Ethiopia, and Charles Marshall for providing some last minute statistical counselling.

And last but not least I would also like to thank all the good friends that I have made over the years of my stay in Silsoe (they are just too many to name individually), for enriching my life and exposing me to a wide range of cultures.

Table of Contents

List of Tables

List of Figures

List of Acronyms

5S: Simulation of Satellite Signal in the Solar Spectrum
6S: Second Simulation of Satellite Signal in the Solar Spectrum
ADDS: Africa Data Dissemination Service
ALI: Advanced Land imager
AMSU-A: Advanced Microwave Sounding Unit-A
AMSU-B: Advanced Microwave Sounding Unit-B
ARTEMIS: Africa Real Time Environmental Monitoring Information System
ATOVS: Advanced Television and Infrared Observational Satellite Operational Vertical Sounder
ATP: Automatic Picture Transmission
AU: Astronomical Unit
AVHRR: Advanced Very High Resolution Radiometer
BDF: Bidirectional Distribution Function
BGC: Biogeochemical
BIL: Band Interleaved by Line
BRDF: Bidirectional Reflectance Distribution Function
BT: Brightness Temperature
CCD: Charge Coupled Device
CEH: Centre for Ecology and Hydrology
CESBIO: Centre d'Etudes Spatiales de la Biosphère
CI: Confidence interval
CLASS: Comprehensive Large Array-data Stewardship System
CLIMPAG: Climate Impact on Agriculture
CNES: Centre National d'Etudes Spatiales
CORINE: Coordination of Information on the Environment
CTIV: VEGETATION'S image processing centre
CV-MVC: Constraint View angle Maximum Value Composite
DAAC: Distributed Active Archive Center
DCW: Digital Chart of the World
dd: Decimal degrees
DEM: Digital Elevation Maps
Df: Degrees of Freedom
DISC: Data and Information Services Center
DLR: Deutsches Zentrum fur Luftund Raumfahrt
DMSP: Defence Meteorological Satellite Program
DN: Digital Number
EC: European Commission
EEA: European Environment Agency
EM-DAT: Emergency Disaster Database
EOS: Earth Observing System
EOSDG: Earth Observing System Data Gateway
EROS: Earth Resources Observation System (EROS)
ERS-1: European Remote Sensing satellite one
ERS-2: European Remote Sensing satellite two

ESA: European Space Agency's
ESRI: Environmental Systems Research Institute
ETM+: Enhanced Thematic Mapper Plus
EVI: Enhanced Vegetation Index
FYROM: Former Yugoslav Republic of Macedonia
FAO: Food and Agriculture Organization
FAPAR: The Fraction of Absorbed Photosynthetically Active Radiation
FEWS NET: Famine Early Warning System Network
FOV: Field Of View
FTP: File Transfer Protocol
GAC: Global Area Coverage
GCPs: Global Control Points
GES: Goddard Earth Sciences
GIFOV: Ground-projected Instantaneous Field of View
GIMMS: Global Inventory Monitoring and Modelling Studies
GLC2000: Global Land Cover Map for the Year 2000
GMFS: Global Monitoring for Food Security
GSFC: Goddard Space Flight Centre
HEG: HDFEOS-to-GeoTiff
HIRS: High Resolution Infrared Radiation Sounder
HRPT: High Resolution Picture Transmission
HRVIR: High Resolution Visible IR
HyMap: Hyperspectral Mapper
IFOV: Field Of View
IGBP: International Geosphere–Biosphere Programme
IGBP-DIS: International Global Biosphere Programme-Data and Information System
ISODATA: Iterative Self-Organizing Data Analysis Technique
IT: Information Technology
JERS-1: Japanese Earth Resources Satellite one
JM Distance: Jeffries-Matusita Distance
JRC: European Commission's Joint Research Centre
LAC: Local Area Coverage
LAI: Leaf Area Index
LCCS: Land Cover Classification System
LCM2000: Land Cover Map 2000
LEA: Leaf Area Index
LISS: Linear Imaging Self-Scanning Sensor
LP: Land Processes
LUCAS: Land Use Cover Area frame statistical Survey
MARS: Monitoring Agriculture by Remote Sensing
MIR: Middle InfRared
MODIS: Moderate resolution Imaging Spectroradiometer
MSExcel: Microsoft Excel
MSU: Microwave Sounding Unit
MVC: Maximum Value Composite
NASA: National Aeronautics and Space Administration

NBARs: Nadir BRDF-adjusted Reflectances
NDVI: Normalised Difference Vegetation Index
NESDIS: National Environmental Satellite Data and Information Service
NIR: Near infrared
NOAA: National Oceanic and Atmospheric Administration
NSIDC: National Snow and Ice Data Center
OLS: Operational Linescan System
OSR: oil seed rape
PAL: Pathfinder AVHRR Land
PAR: Photosynthetically Active Radiation
POES: Polar Orbiting Environmental Satellites
PRTs: Platinum Resistance Thermometers
QIV: VEGETATION'S image quality centre
R^2: Correlation coefficient of determination
RMS: Root Mean Square
SE: Standard Error of the estimation
SL: Significance Level
SEI: Stockholm Environmental Institute
SiB2: A revised land surface parameterization for atmospheric GCMs
SMAC: Simplified Method for Atmospheric Corrections
SPOT: Satellite Pour l'Observation de la Terre
SRB: Solar Reflective Bands
SRIV: VEGETATION's primary receiving station in Kiruna, Sweden
SRVL: VEGETATION's L-band receiving station in Aussaguel, France
SSU: Stratospheric Sounding Unit
SWIR: Short-Wave InfraRed
SZA: Solar Zenith Angle
TCI: Temperature Condition Index
TEB: Thermal Emissive Bands
TIROS: Television InfraRed Operation Satellite
TM: Thematic Mapper
TOA: Top of the Atmosphere
TOMS: Total Ozone Mapping Spectrometer
TOVS: Television and Infrared Observational Satellite Operational Vertical Sounder
UK: United Kingdom
UMd: University of Maryland
UN: United Nations
UNEP: United Nations Environment Programme
VB6: Visual Basic 6
VCI: Vegetation Condition Index
VGT: VEGETATION
VIIRS: Visible and Infrared Imaging Radiometer
VIS: Visible
VITO: the Flemish Institute of Technological Research, Belgium
VPI: Vegetation Productivity Indicator
WMO: World Meteorological Organization

CHAPTER ONE

1 Introduction

1.1 Importance of vegetation monitoring

Vegetation plays a vital role in the Earth's biosphere. It is the primary source and producer of food in most terrestrial ecosystems. A plethora of organisms depend on it, either directly (vegetarian/omnivorous) or indirectly (carnivorous/omnivorous) for nutrition. It influences the climate on both a local and a global scale, by increasing the atmospheric content of moisture through the process of transpiration (Dickinson and Henderson-Sellers, 1988; Nobre et al. , 1991; O'Brien, 1996; Walker et al., 1995; Xue, 1996; Yukuan et al., 1994); by affecting the energy equilibrium through absorption and reflection of sunlight (Betts et al., 1996; Dickinson and Henderson-Sellers, 1988; Nobre et al. , 1991; Walker et al., 1995) and by absorbing and acting as a natural sink of the greenhouse gas CO_2 through the process of photosynthesis (Costa and Foley, 2000; DeFries et al., 2000; Houghton et al., 2000; Potter et al., 2001; Sellers et al., 1996; Zhan et al., 2000). Vegetation conserves biodiversity, by providing habitat to numerous species (Chapin et al., 2000; Houghton et al., 2000; Potter et al., 2001; Vitousek, 1994; Zhan et al., 2000). It affects the soil and prevents it from eroding (Douglas, 1999). It regulates the flow of biochemical cycles, such as those of carbon, water, oxygen and nitrogen (Houghton et al., 2000; Penner, 1994; Potter et al., 2001). What is more, vegetation has a socioeconomic impact on human societies by providing food, raw material, commercial commodities, fossil fuel, employment and recreation.

Despite the importance of vegetation in maintaining ecological balance and in supporting human life quality, there are factors that may threaten its functionality. In the past, the main threat was natural disaster events, including but not limited to climate change, droughts, diseases, fire and pest invasion. Anthropogenic activities, such as the clearing of vegetated areas for living space, agriculture, and raw resources, had only minor and localised effects on vegetation.

In modern human history natural disasters are no longer the sole main threat to the vegetation's functionality. Anthropogenic activities are now also a highly significant threat. This development can mainly be attributed to: i) the increase of the global human population, and ii) the achievement of technological advances. According to the United Nations (UN), in the last 55 years the human global population has almost tripled from 2.5 billion in 1950 to 6.5 billion in 2005; it is estimated to reach 9 billion by 2050 (UN, 2004). In general, more resources are needed to support a larger human population, and consequently the anthropogenic activities are intensified in order to meet the demand. Additionally, technological advances have allowed the acquisition of resources to become ever more effortless, which in turn has made the acquisition of resources more financially feasible. Hence, an increasing number of people can afford to acquire more resources than they previously could (particularly true for the citizens of the most prosperous countries); therefore, the total global demand for resources, and consequently anthropogenic activities, are driven even higher.

As a result, the rate that humans clear natural vegetation has exceeded the rate of vegetation regeneration (FAO, 2005). According to the Global Forest Resource assessment in 2005 (FAO, 2005) by the Food and Agriculture Organisation (FAO) of the United Nations (UN) it was estimated that for the period between 2000-2005, 13 million hectares were deforested every year, while in the same period only 6.7 million hectares per year were reforested, through either natural processes or plantations. This means that approximately an area around 7.3 million hectares of forest was lost every year. Meanwhile, vegetation species distributions have changed to meet commercial demands on a global scale.

The impact of human activities on vegetation has alarmed the scientific community. Environmental problems such as climate change and biodiversity impoverishment are directly linked to the effects of these activities. It is now clear that unless anthropogenic activities are regulated, the environmental problems will persist and potentially escalate.

Natural disasters have been and remain a threat to vegetation. In recent years, it is also believed that the frequency of meteorological disasters, such as droughts and floods, may have been intensified by climate change that has been induced by anthropogenic activities (e.g. release of greenhouse gases in the atmosphere). Moreover, natural

disasters are not only likely to disturb the functionality of natural vegetation and the environmental balance, but due to the increased density of human population around the globe today, there is an increased probability that they will affect (human) populated areas, and thus have a direct impact on human lives. In the past, millions of people have died due to such disasters. For example, according to the Emergency Disaster Database (EM-DAT), in the last century drought alone caused more than 11 million deaths and affected the lives of more than 2 billion people worldwide (EM-DAT, 2007).

It is evident that the beneficial role of vegetation in the Earth's biosphere could be jeopardised by anthropogenic activities and natural disasters. To safeguard against these threats, steps should be taken towards regulating human activities in order to conserve the natural vegetation and promote sustainable development. As far as natural disasters are concerned they can hardly be prevented; however, if disaster early-warning systems are in place and capable of identifying or predicting their occurrence at an early stage, emergency measures designed to minimise the harmful effects of the impending disaster (for instance the creation of fire protection zones or the stockpile of food and water in case of drought) could be implemented, potentially saving human lives and preserving vegetation that otherwise may have been lost.

Regardless of the nature of the threat to the functionality of vegetation in the Earth's biosphere, if sustainable development or disaster early-warning systems are to be achieved, scientists must to be able to monitor the Earth's vegetation resources (e.g. vegetation species composition and distribution, biomass, health status, Photosynthetic Active Radiation (PAR), vegetation moisture content, etc.) on a regular basis. The analysis of such data would help improve the understanding of the environmental processes in the Earth's biosphere. Such knowledge, combined with an ongoing and regular monitoring of the Earth's vegetation resources would allow the assessment of the nature, location, extent, and severity of anthropogenic threats to the vegetation's functionality, and assist policy makers in regulating human activities in the threatened areas in a manner that would allow sustainable development. The same data (from monitoring the Earth's vegetation resources) with improved environmental knowledge, would also allow scientists i) to estimate the possibility of a natural disaster occurrence based on the regular monitoring of certain biophysical properties, and to raise the alarm

when the occurrence possibility of the disaster has surpassed acceptable safe limits, or ii) to identify a disaster in progress.

1.2 The role of remote sensing

Data about the Earth's vegetation resources have not been regularly collected in the past. When such data were collected, conventional ground surveying methods were used based on sampling techniques (Eyles et al., 1993; Cochran, 1977; Gallego, 1995). In general, the accuracy and precision of such methods depend on various factors such as the surveyor's skill and perception, the type and quality of the equipment used, the data collection methodology, the choice of sampling sites, and the extrapolation method used. Ground surveys over large areas require a large number of surveyors, as a result such surveys are financially very costly and may contain a considerable amount of errors due to possible inconsistencies between surveyors' data collection methods. Regardless, the time needed to complete such surveys often proves to be overly long for the needs of certain applications (Hack and English, 1996; Running et al., 2002; Townshend et al., 1991). Moreover, the surveying of certain sites may be particularly challenging or financially expensive due to possible hazardous environmental conditions or lack of easy access. Finally, because ground survey methods are based on sampling techniques, it is possible that areas of significance for vegetation monitoring may be overlooked. For example, Tucker and Townshend (2000) found that sampling techniques are not adequate to estimate deforestation rates unless a very large number of samples are taken, which in turn would increase the total financial cost and the time needed to complete the survey even more.

These problems became apparent, for instance, during the early attempts to assess the global state of forests. Data from different countries were not only incomplete and outdated; but different vegetation definitions and data collection methods were employed leading to data inconsistencies (Anonymous, 1948, 1950, 1954; FAO, 1946, 1947, 1960, 1963; Kleinn et al., 2002; Kummer, 1992; Persson, 1974; Zon and Sparhawk, 1923). Additionally, each study took several years to complete; thus, a five year interval was established by FAO between successive global forest assessments (Mather, 2005). Such

time intervals between successive studies can be too long for the specific needs of the scientific community, particularly for the purpose of disaster early-warning.

Thanks to technological advances within the last decades, data regarding the Earth's vegetation resources collected remotely by sensors onboard aircrafts or spacecrafts, have become increasingly available and financially affordable. Surveys based on remotely sensed data may also require additional data collected by ground surveys; however, when they do, they require much less ground data than a solely ground based survey would require over the same areal extent. Due to the reduced, or no, need for ground data, errors and financial costs associated with large number of surveyors are reduced. Moreover, due to the remote nature of the data collection, constraints related to site accessibility or hazardous conditions, are minimised (data collection however can be restricted by cloud cover). Furthermore, the time needed to collect data over an area by air or space is considerably shorter than if that area was surveyed by ground; particularly when large areas are concerned.

The overall accuracy and precision of remote sensing surveys depends mainly on i) the sensor(s) used, ii) the accuracy and precision of the ancillary/ground data (if needed), and iii) the image processing methodology (or methodologies) used. The financial cost of a remote sensing survey depends primarily on the extent of the area studied, and the sensor and image processing requirements. Such a cost can be high, particularly if high spatial resolution data are required; something that led some authors in the early 1990s to question the cost-effectiveness of remote sensing (Allen, 1990; Meyer-Roux and Vossen, 1994). However, recently, technological advances in Information Technology (IT) and the wide spread use of remote sensing has led to considerable reductions in image processing and data purchasing costs (Cihlar, 2000; DeFries and Belward, 2000; Gallego, 1999). Overall, remote sensing is becoming more and more cost-effective (Gallego, 1998, 1999; Giovacchini and Brunetti, 1992; Taylor et al., 1997). Finally, due to the fact that data are collected faster by air or space than by ground (particularly over large areas), surveys based on remotely sensed data can be completed faster than ground based surveys; consequently, remote sensing based surveys can be repeated more frequently than their ground based counterparts, and therefore can monitor the Earth's vegetation resources more closely.

The ability of remote sensors to consistently collect data about the Earth's vegetation resources at frequent intervals (temporal resolution) on a global scale and at relatively low financial cost, led several authors to conclude that remote sensing based surveys are preferable to conventional ones (ground based) for monitoring vegetation over large areas (DeFries and Belward, 2000; DeFries and Townshend, 1994a; DeFries et al., 1995; Dymond et al., 2001; Hack and English, 1996; Liang, 2001; Lillesand, and Kiefer, 2000; Lioubimtseva, 2003; Mayaux and Lambin,1995; Nemani and Running, 1997; Price, 2003; Running et al., 2002; Sellers et al., 1992; Townshend, 1992; Woodcock and Strahler, 1987).

A group of satellite based sensors commonly referred to as "low resolution sensors" are of particular interest for monitoring vegetation over large areas. The term low resolution refers to the sensors' relatively poor ability to spatially distinguish features along the scan-line (spatial resolution). At nadir point, their Ground Instantaneous Field Of View (GIFOV), commonly used as a reference to a sensor's spatial resolution, is around 1 km, which is low compared to their high (0.5-50 m) or moderate (50-250 m) spatial resolution counterparts. The spatial resolution and the swath width of a sensor are inversely related to each other; as a result, low resolution sensors have swath widths much wider than their high resolution counterparts. Consequently, in a single pass low resolution sensors can collect data over much larger areas than higher spatial resolution sensors can. The low resolution sensors' swath widths combined with their typical orbit characteristics (sun-synchronous, near-polar orbits at about 700-850 km above the Earth's surface) allows low resolution sensors to collect data over the whole surface of the Earth in about a day; a feat that none of the high resolution sensors can claim. In addition to that, the financial cost of purchasing low resolution data is considerably lower than that of high resolution data or is free. Due to the above reasons, low resolution sensors are the main source of data for monitoring vegetation over large or homogeneously covered areas, where high level of spatial detail is not a primary concern, (DeFries and Townshend, 1994b; Loveland et al., 1991; Townshend et al., 1985, 1987, 1991; Tucker et al., 1985).

Satellite based sensors of higher spatial resolution such as the High Resolution Visible IR (HRVIR) onboard the Satellite Pour l' Observation de la Terre (SPOT) or the

Thematic Mapper onboard Landsat are impractical for large scale monitoring, due to i) their lower temporal resolution (typically more than 15 days, which operationally is further reduced due to cloud contamination), ii) their higher data purchasing cost, and iii) the higher financial cost and effort associated with processing large volumes of data (due to their lower area coverage per scene) (Braswell et al., 2003; Cihlar, 2000; DeFries and Belward, 2000; Townshend et al., 1991). One of the primary sources of remotely sensed low resolution data in the past has been the Advanced Very High Resolution Radiometer (AVHRR), first launched by the National Oceanic and Atmospheric Administration (NOAA) in October 1978 onboard the Television InfraRed Operation Satellite-N (TIROS-N). Since then 13 more AVHRR sensors have been flown into space. AVHRR was originally designed for meteorological and oceanographic studies, but the scientific community soon realised it could be used in numerous environmental, scientific and management contexts (Cracknell A.P., 2001). By the late 1990s it was the principal low resolution sensor used for vegetation monitoring over large areas (DeFries and Belward, 2000; Friedl et al. 2002; Lioubimtseva, 2003; Running et al. 1995; Strahler et al., 1999; Townshend and Justice, 2002; Townshend et al., 1991; Zhan et al., 2000). AVHRR's success led to the realisation of the low resolution sensors' contribution to the collection of scientific data, and triggered the development of further and increasingly more sophisticated sensors with similar properties (table 1.1).

Until the late 1990s AVHRR was practically the only operational low resolution sensor capable of vegetation monitoring; however, since the start of the new millennium it is no longer the obvious choice. Other low resolution sensors are also available and capable of carrying out the same tasks (table 1.1). These sensors have different technical characteristics, such as their spectral, radiometric, temporal and spatial resolution, or their calibration and atmospheric correction capabilities. Hence, data captured by these sensors over the same study areas and time, will differ. Consequently, it is reasonable to expect that remote sensing products based on different sensors will also differ, even if the same application methodologies are used. In some cases certain sensors may be better suited than others for specific applications and/or the environmental conditions of a study area. On the other hand, in some other cases (applications and/or environmental conditions) remote sensing products based on different sensors could be very similar. Either way, the

remote sensing and user community would benefit from knowing how the end-products of various applications based on different sensors compare with each other. Such knowledge would allow remote sensing data users to produce higher quality products by using data from a sensor that is more likely to result in a better product for a given application and study site. Additionally, such knowledge would allow data users to cross between different sensors that had been proven by research to produce similar products, in applications where for any reason the sensor from which the users were previously receiving data, became unavailable.

Table 1.1. List of sensors with bands, spatial resolution, swath width, and revisit time similar to AVHRR, their host satellites and launch dates.

Sensor	Satellite(s)	Launch date(s)
MODIS	TERRA	December 1999
	AQUA	May 2002
ATSR	ERS-1	June 1991
	ERS-2	April 1995
AATSR	ENVISAT	March 2002
MERIS	ENVISAT	March 2002
VEGETATION	SPOT 4	March 1998
VEGETATION/2	SPOT 5	May 2002
SeaWIFS	SeaStar	August 1997
MVISR	FY-1	May 2002
GLI	ADEOS II	December 2002
MR-2000	METEOR-2 N24	August 1993
MR-2000M	METEOR-3 N5	August 1991
	METEOR-3M N1	December 2001
MSU-M	Ocean-01 N7	October 1994
	OKEAN-O	September 1998
	SICH-1	August 1995
	SICH-1M	September 1999

1.3 Aims and Objectives

1.3.1 Aim

As discussed earlier an assessment of the relative performance of all available low resolution sensors in various vegetation monitoring applications would be beneficial to the remote sensing community and was considered a significant area of research. Due to the numerous low resolution sensors and vegetation monitoring applications available at the time, such a task could not realistically be accomplished by a single PhD study. Instead, it was deemed feasible to consider only the three most operational low resolution sensors at the time (Bartholomé and Belward, 2005); namely, the AVHRR (Goodrum et al., 2000; Kidwell, 1998), the Moderate resolution Imaging Spectroradiometer (MODIS) (Barnes et al., 1998; Running et al., 1994a), and the VEGETATION (Saint, 1995, 1997). The number of assessed vegetation monitoring applications also had to be limited. It was decided to limit the assessment to only two applications; these were land cover mapping and drought monitoring.

The interest of this study in vegetation land cover mapping was based on the need for regularly updated land cover datasets around the globe, in environmental studies, and in the formation of sustainable development policies. The significance of land cover mapping is underlined by several authors (Asrar and Dozier 1994; Bartholomé and Belward, 2005; Brown et al., 1999; DeFries and Belward, 2000; DeFries et al., 2000; Foody, 2002, 1996; Friedl et al., 2002; Giri et al., 2003, 2005; Haack and English, 1996; Henderson-Sellers et al., 1986; Liang, 2001; Loveland and Belward, 1997; Loveland et al., 1999; Muchoney et al., 2000; Nemani and Running, 1997; Reed, 1997; Running et al., 1995; Strahler et al., 1999; Townshend et al., 1991, 1994; Townshend, 1992; Tucker and Townshend, 2000; UN, 2002). Loveland et al., (2000) refer to (vegetation) land cover data as “among the most important and universally used terrestrial data set,” while Cihlar (2000) describes land cover mapping as “perhaps the most widely studied problem employing satellite data.” Therefore, it would not be an exaggeration to say that (vegetation) land cover mapping is probably the application for which remotely sensed data is most frequently used.

Similarly, the choice of drought monitoring was based on the potential beneficial role of such application not only to the quality of human life but also to human life itself. Droughts are a natural reoccurring phenomenon, associated with precipitation deficiency. Water shortage disturbs the ecology in a region, creates favourable conditions for wild fires, causes desertification and water-supply deficit, reduces or even destroys crop yields, and consequently causes socioeconomic problems or even famines (Changnon, 1999; Dalezios et al., 1991, 2000; Guo and Richard, 2004; Hayward, 2002; Kogan and Sullivan, 1993; Kogan, 2000; Palmer, 1965; Riebsame et al., 1990; Su et al., 2003; Tucker and Choudhury, 1987; Unganai and Kogan, 1998; Wheaton, 2000; Wilhite, 1993). Almost half of the world's agricultural areas are susceptible to drought (Kogan and Sullivan, 1993). In the last decade of the 20th century, droughts have claimed 50-150 million tons of grain (FAO, 2000). According to the World Meteorological Organization (WMO) of the United Nations (UN), since 1967, droughts have affected one in two people out of the 2.8 billion that have suffered from weather-related disasters. In the same period (since 1967), drought has been responsible for millions of deaths and has cost hundreds of billions of dollars in damage (Obasi, 1994). In developed countries the damage is mainly economic, but in developing countries droughts can cause human suffering and loss of life. It is important to be able to detect or predict a drought as soon as possible, so that the implementation of emergency measures and the organisation of aid will be given enough time to minimise the damage (Wilhite and Glatz, 1993; Wilhite, 1993; WMO, 1994). The conventional method of drought prediction/detection based on data from meteorological stations is not accurate or timely, because the network of such stations is usually sparse, especially in developing countries where the effects of drought produce dire situations (Seiler et al., 1998; Thenkabail et al., 2004; Unganai and Kogan, 1998). Alternatively, a remote sensing based drought monitoring/early warning system is likely to be more effective (Kogan, 1994; Su et al., 2003; Thenkabail et al., 2004; Tucker and Choudhury, 1987; Unganai and Kogan, 1998) being able to regularly collect information over large areas without the need for supplementing a ground based infrastructure. Moreover, satellite-based early warning systems can detect droughts 4-6 weeks earlier than previous methods and more importantly, far in advance of the harvest (Kogan, 2000).

An assessment of a sensor's performance for a given application could be based on the evaluation of the technical characteristics/specifications of all the available sensors in relation to the application's data requirements. All the technical characteristics /specifications of the sensors under consideration, which are likely to affect their performance in a given application, could be identified and gathered. This information could then be processed in a way that an objective and quantitative comparison of the sensors' theoretical performance could be carried out. Nevertheless, in this way the comparison of the sensors' performance would be hypothetical, and although such information would be insightful regarding the expected performance of the sensors, it could also be untrue in a real application due to overlooked information or possible violations of assumptions made in the theoretical comparison process. Vice versa, if only experimental data were available for the comparison, the reasons behind any possible differences between the performances of the sensors would be hard to discover. Thus, any cohesive comparative analysis of the sensors should rely on both theoretical and experimental data.

It was considered possible that the experimental results of the relative assessment of the three sensors in land cover mapping and drought monitoring could differ over different environmental conditions; hence, a very thorough assessment would have required experimental results over various study sites and dates. The amount of resources required for such an endeavour was too great; thus, instead it was decided to confine the experimental assessment of the three sensor's relative performances in land cover mapping and drought monitoring to as many sites and dates as possible over Europe and Africa, respectively. The choice of Europe was based on practical criteria and more particularly the availability of ancillary data; while Africa was chosen for the drought monitoring assessment, because of the continent's long history of susceptibility to this type of disaster.

Another consideration was that MODIS bands 1-7 can collect data with less than 1 km spatial resolution unlike any of the bands of VEGETATION and AVHRR (more details in section 2.3.1); however, it was considered that 1 km spatial resolution is adequate for land cover mapping and drought monitoring applications at national scales and for matters of compatibility it was decided to compare all three sensors at that spatial

resolution. Moreover, considering that the majority of land cover mapping and drought monitoring applications do not make use of Thermal Emissive Bands (TEBs) other than to detect clouds and ice, and the fact that MODIS is equipped with 16 TEBs (table 2.5) which dramatically increase the size of MODIS data sets and subsequently the resources needed to process them, it was decided that it would be considerably more practical not to use TEB data in the comparison other than the cloud/ice mask products derived from them.

To summarise, this study is concerned with the assessment of the relative performance of AVHRR, MODIS and VEGETATION for vegetation land cover mapping in Europe, and drought monitoring in Africa, using data from the sensors' SRBs at 1 km spatial resolution. The aim was to find out whether it is more advantageous to use one particular sensor over the other two in each of these applications.

1.3.2 Objectives

As mentioned earlier it was decided that the assessment of the sensors' relative performance in the chosen applications was to be derived both from a theoretical comparison of the sensors' likely performance based on their technical characteristics, and an experimental comparison of their results over Europe and Africa. It should be stressed that application results based on remotely sensed data do not solely depend on the sensor used to collect the data; others factors such as the methodology and ancillary data used, or the environmental conditions under which the data were collected, can all play a significant role. Therefore, in order to objectively compare the relative performance of a group of sensors in given applications, all factors contributing to the application result of each sensor (apart from the sensor's technical characteristics) must remain the same.

At the start of the present study, research was carried out to investigate whether adequate theoretical and experimental data already existed in the literature to support the comparative analysis of the three sensors in both applications of interest. Several authors have claimed that MODIS should outperform AVHRR in vegetation monitoring application (Cihlar, 2000; Friedl et al., 2002; Gitelson and Kaufman, 1998; Loveland and Belward, 1997; Loveland et al., 2000; Muchoney et al., 2000; Running et al., 1995;

Townshend et al., 1991; Zhan et al., 2000), mainly due to specially designed spectral bands for vegetation monitoring, improved calibration and atmospheric correction capability, and higher spatial, spectral and radiometric resolution. Similarly, other authors have advocated the superiority of VEGETATION over AVHRR (Bartholomé and Belward, 2005; Cihlar, 2000; Duchemin et al., 2002; Gond and Bartholomé, 2001; Lioubimtseva, 2003; Loveland and Belward, 1997; Saint, 1992) for analogous reasons. However, these claims were usually not accompanied with quantitative data, and only dealt with the comparison of either MODIS or VEGETATION to AVHRR, but not all three sensors simultaneously. In cases where quantitative information was provided, the sources only dealt with one sensor (Goodrum et al., 2000; Running et al., 1994a; Saint, 1995), or a single technical aspect of the sensors under consideration (e.g. Gitelson and Kaufman, 1998 evaluated the spectral difference between MODIS and AVHRR). All the information needed to carry out a quantitative comparative technical analysis of AVHRR, MODIS and VEGETATION could not be found in a single study.

Regarding land cover mapping application:

In the past, land cover datasets over large areas were created by compiling old maps and atlases (Matthews, 1983; Olson and Watts, 1982; Wilson and Henderson-Sellers, 1985), but such datasets had problems associated to conventional survey methods, such as inconsistent, missing and outdated data (Townshend et al., 1991). By the mid 1980s until the late 1990s, AVHRR became the dominant source of remotely sensed data for vegetation land cover mapping over large areas. AVHRR data were used in statistical clustering (Belward and Loveland, 1995; Belward, 1996; Chen et al., 1999, DeFries and Townshend, 1994b; Defries et al., 1995; Fleischmann and Walsh 1991; Goward et al., 1985; Justice et al., 1985; Koomanoff, 1989; Laporte et al., 1998; Liang, 2001; Loveland and Belward, 1997; Loveland et al., 1991, 1995, 2000; Townshend et al., 1987; Tucker et al., 1985), decision tree (DeFries et al., 1998; Friedl and Broadley, 1997; Hansen et al., 1996; Lloyd, 1990; Reed et al., 1994; Running et al., 1995) and artificial neural network (Gopal et al., 1999, 1994; Muchoney et al., 2000) land cover classification methodologies across the globe. Currently, the International Global Biosphere Programme-Data and Information System (IGBP-DIS) IGBP-DISCover (Loveland et al., 2000) and the

University of Maryland (Hansen et al., 2000) land cover datasets are two of the most established AVHRR-based datasets.

VEGETATION was launched in March 1998, and has been used to map vegetation land cover across the globe primarily under the Global Land Cover Map for the Year 2000 (GLC2000) project. The GLC2000 included 30 groups across the globe and used different classification techniques for different parts of the world. (Agrawal et al., 2003; Bartalev et al., 2003; Bartholomé and Belward, 2005; Bartholomé et al., 2002; De Badts, 2002; Eva et al., 2004, Fritz et al., 2003; Giri et al., 2005; Han et al., 2004; Latifovic et al., 2004; Ledwith 2003; Mayaux et al., 2002, 2004 ; Pekel et al., 2003; Tateishi et al., 2003 ; Wu et al., 2002). VEGETATION has also been used, outside the GLC2000 project, for example, Lioubimtseva (2003) used VEGETATION data in a maximum likelihood statistical clustering classifier to map large regions in Russia.

Finally MODIS, being the newest of the three sensors, launched in December 1999, had barely completed a year of operational time when the present study was initiated. MODIS was principally planned to be used with a univariate decision tree and an artificial neural network classifier to produce the MODIS global land cover/change product (MOD12) once every 6 months, provided that the sensor has completed collecting a year's data to meet the requirements of the intended classifier algorithm (Strahler et al., 1999). More information about the early results of this endeavour can be found in Friedl et al., 2002. It is evident that significant work has been done, and continues, in the area of land cover mapping with low resolution sensors.

The vast majority of studies present in the literature were focused on comparing and/or improving classification methodologies. No evidence could be found of a study that compared the ability of the three most operational low resolution sensors in land cover mapping, using the same methodology, imagery dates, ancillary data and study site.

Regarding drought monitoring application:

At the time of the study, no standard approach on drought monitoring had been established (Guo and Richard, 2004); however, almost all satellite-based methods make use of data collected in the red, near infrared (NIR) and occasionally thermal regions of the electromagnetic spectrum. The red and the NIR are the most important spectral

regions for vegetation monitoring (Townshend and Justice, 1988). These regions are important because chlorophyll pigments inside plants absorb radiation in the red region and strongly reflect it in the NIR due to the spongy mesophyll cells located in the interior or back of the vegetation leaves (Curran, 1985; Liang, 2004; Rees, 2001; Seller et al., 1996; Seller, 1985). When vegetation is under stress, the red reflectance increases, and the NIR decreases (Gray and McCrary, 1981; Guo and Richard, 2004; Seller et al., 1996; Seller, 1985; Tucker and Sellers, 1986; Unganai and Kogan, 1998).

Rouse et al. (1974) introduced a vegetation index based on these attributes of vegetation, the Normalised Difference Vegetation Index (NDVI) (see equation 1.1) (Goward et al., 1991; Kidwell, 1994, 1990; Kogan and Sullivan, 1993; Tarpley et al., 1984; Tucker, 1979).

$$NDVI = \frac{NIR - RED}{NIR + RED} \tag{1.1}$$

Theoretically, NDVI values can range from -1 to 1. Snow, water and clouds usually have negative NDVI values, because the red reflectance tends to be higher than the NIR for these surfaces. Bare soil and rocks reflect red and NIR radiation in a similar manner, thus they exhibit NDVI values close to zero (van Dijk, 1985). For vegetated surfaces, NDVI values usually range from 0.1 to 0.6, with the higher values being associated with greater green leaf and biomass (Tucker, 1979). Several studies that followed demonstrated that the NDVI is correlated to vegetation biomass, vigour (sometimes referred to as "greenness"), Leaf Area Index (LAI) and photosynthetic activity (Baret and Guyot, 1991; Choudhury, 1987; Curran, 1983; Daughtry et al., 1982; Gamon et al., 1995; Goward and Dye, 1987; Goward and Huemmrich, 1992; Goward et al., 1991; Jackson, 1983; Lenney et al., 1996; Muchoney et al., 2000; Peterson et al., 1987; Prince, 1991; Reed et al., 1994; Sellers, 1985; Teillet et al., 1997; Thenkabail et al., 2002, 2004b; Tucker et al., 1985; Tucker, 1979). Due to its traits (i.e. significant correlation with several vegetation parameters, calculation simplicity and strong reduction of variations caused by changing illumination conditions (Kimes et al., 1984)), NDVI became the most commonly used

vegetation index (Deering et al., 1975; Goward et al., 1991; Jensen, 1996; Oguro et al., 1999; Su et al., 2003).

Vegetation health/vigour depends on environmental resources such as soil, water availability and temperature (Clark, 1985; Kogan, 1995a). Since environmental induced stress to vegetation is reflected by NDVI values (Tucker and Choudhury, 1987), and assuming that all non-weather related environmental conditions remained constant for a certain location, any observed deviation from the historical "normal" values of the NDVI for that location should be weather related. Based on that logic, Kogan (1990) defined the Vegetation Condition Index (VCI) for drought monitoring as presented in equation 1.2.

$$VCI = \frac{NDVI - NDVI_{MIN}}{NDVI_{MAX} - NDVI_{MIN}} 100\% \quad (1.2)$$

$NDVI_{MIN}$ and $NDVI_{MAX}$ are the historical minimum and maximum NDVI values at the location and time (seasonal) that the NDVI measurement was taken. Assuming that NDVI values follow a normal distribution through time for a given location, VCI values less than 50% would suggest less than favourable conditions (possible drought) (Kogan 1995a; Kogan and Sullivan, 1993; Seiler et al., 1998; Singh et al., 2003; Thenkabail et al., 2004a; Unganai and Kogan, 1998). The use of VCI for drought monitoring assumes that any observed vegetation stress is related to water shortage, so as such, it is only applicable to rain-fed agriculture. It should also be noted that instead of using single day NDVI images, the Maximum Value Composite (MVC) method is used to compile NDVI images by retaining the highest NDVI value per pixel location out of a series of NDVI measurements over a predefined time period (usually a week, 10 days or a month). This is done because NDVI data contains noise due to cloud contamination, atmospheric attenuation (e.g. dust and haze) and viewing geometry related distortion (Cihlar et al., 1994; Cracknell, 1997; Eidenshink and Faundeen, 1994; Flieg et al., 1983; Goward et al. 1994; Goward et al., 1991; Gutman, 1991; Kogan and Sullivan, 1993; Kogan and Zhu, 2001; Kogan et al., 1994; Kogan , 1995a; NGDC, 1993; Rao et al., 1990; Unganai and Kogan, 1998). The MVC method is known to reduce such noise (Cihlar, 2000; Duchemin et al., 2002; Holben, 1986; Lioubimtseva, 2003; Muchoney et al., 2000; Strahler et al.,

1999). The VCI methodology has been applied around the world, mainly using NDVI data collected by AVHRR (Domenikiotis et al., 2004; Johnson et al., 1993; Kogan and Sullivan, 1993; Kogan, 1990b, 1995a, 1995b; Kogan, 1990b; Seiler et al., 1998).

Sometimes however, the weekly NDVI values tend to be depressed due to prolonged overcast periods (more than three weeks) giving the false impression of stressed vegetation and drought (Unganai and Kogan, 1998). In order to prevent such faulty conclusions, and also because vegetation can be under stress due to unfavourable temperature conditions, Kogan (1995a) proposed the use of another index, the Temperature Condition Index (TCI) as presented in equation 1.3.

$$TCI = \frac{BT_{MAX} - BT}{BT_{MAX} - BT_{MIN}} 100\% \quad (1.3)$$

Similar to VCI, BT_{MAX} and BT_{MIN} are the historical maximum and minimum brightness temperatures (BT) at the location and time (seasonal) that the BT measurement was taken. It was suggested that, when there is a choice of available thermal bands, the BT should be calculated from the band with the least response to the amount of water vapour in the atmosphere (Kogan, 1995a). TCI values less than 50% indicate temperatures higher than the historical normal and could imply drought or temperature conditions stressful for the vegetation (Dabrowska-Zielinska et al., 2002; Kogan 1995a, 1997; Seiler et al., 1998; Thenkabail et al., 2004a; Unganai and Kogan 1998). Generally, the TCI has been applied additionally to the VCI using mainly AVHRR data (Dabrowska-Zielinska et al., 2002; Kogan, 1995a; Seiler et al., 1998; Singh et al., 2003; Unganai and Kogan, 1998). The two indices can also be combined in the V/TCI, by applying different weights to each index (Kogan, 1995a) as presented in equation 1.4.

$$V/TCI = aVCI + bTCI \quad (1.4)$$

Sannier et al. (1998a) noted that the assumptions made by the VCI methodology - that the historical maximum and minimum NDVI values represent the maximum possible variation, and that the NDVI values follow a normal distribution - are unrealistic. Instead,

Sannier et al. (1998a) suggested another NDVI-based index, the Vegetation Productivity Indicator (VPI) which calculates the NDVI probability distribution (within each MVC compositing period) empirically based on a methodology typically used for assessing extreme hydrological events (Linsley et al., 1975). All available historical NDVI values for a given location and seasonal time period are ranked in ascending order. The probability (p) of an NDVI value being lower or equal to an NDVI value ranked at place m, out of n number of observations is as presented in equation 1.5.

$$p = \frac{m}{n+1} \quad \text{(Weibull, 1939)} \tag{1.5}$$

Sannier et al. (1998a) applied the VPI methodology to assess drought conditions and maize production in Southern Africa, using AVHRR MVC NDVI data.

For the purpose of this study the TCI and V/TCI methodologies were not considered because VEGETATION is not equipped with a thermal band and therefore can not be used for such analysis. Among the remaining two methodologies, it was decided to base the assessment of the sensors relative capacity to monitor drought conditions based on the VPI methodology. The decision was based on the observation made by Sannier et al. (1998a) that the VCI methodology was based on assumptions regarding the distribution of the historical NDVI values of a site which may not be true. The VPI methodology on the other hand was not based on any such assumption and as such it was deemed preferable.

The VPI methodology requires historical NDVI records sufficiently long to describe the historical NDVI value distribution over a specific site and date under a range of rainfall conditions, and such required time periods were considerably longer than that for which all three sensors were operational. Consequently, there were no VPI experimental results available for all three sensors that have been calculated over the same study area and using the same length of historical NDVI data. Not only that but at the time of the present study the historical NDVI records of MODIS and VEGETATION were not considered sufficiently long for the requirements of the VPI methodology.

Therefore, the relative capacity of the sensors at detecting drought conditions using the VPI methodology could not be assessed using experimental results. As an alternative it was suggested to investigate the relationship between NDVI data collected by the three sensors over the same targets and assess the possibility of simulating the NDVI data a sensor would have recorded based on the NDVI data recorded by another sensor over the same target. In the event that such simulation was possible, then MODIS and VEGETATION could extent their historical NDVI records in the past by simulating the NDVI data they would have recorded based on NDVI data collected by AVHRR in the past. If MODIS and VEGETATION were provided with sufficiently long and accurate simulated historical NDVI records for the requirements of the VPI methodology, then the VPI methodology could be applied on a certain study site using data from all three sensors; and consequently the sensors' data capacity at detecting drought conditions using the VPI methodology could be assessed using experimental data. Additional benefits of such possible simulation between sensors' NDVI data could also be that the three sensors could become interchangeable for the collection of NDVI data; therefore in the event that NDVI data became unavailable from one of the sensors, that data could still be substituted by the other sensors.

Therefore in order to meet the study's aim, the following objectives were set:

- To collect and analyse data regarding the characteristics (e.g. spatial, temporal, radiometric and spectral resolution) of MODIS, VEGETATION and AVHRR, in a way that hypotheses could be developed based on quantitative measures regarding their expected relative performance in vegetation land cover mapping and drought monitoring applications.
- To assess the three sensors' SRBs relative capacity in accurately mapping land cover over Europe at 1 km spatial resolution based on experimental results.
- To assess the relation between the NDVI values collected by the three sensors over the same targets, and assess the possibility of providing MODIS and VEGETATION with simulated NDVI data based on NDVI measurements taken by AVHRR.
- To assess the three sensors' relative capacity at monitoring drought conditions at 1 km spatial resolution using the VPI methodology based on experimental results over a study area in Africa; provided that MODIS and VEGETATION could be supplied with sufficiently long and accurately simulated historical NDVI records for the requirements of the VPI methodology.

The above objectives are dealt with in the following chapters:

Chapter 2 gives a description of the three sensors, and compares their spatial, temporal, radiometric and spectral resolutions, their calibration and atmospheric correction capabilities and data availability. Based on the findings of the comparison, hypotheses are developed regarding their expected performance in land-cover classification and drought monitoring applications.

In Chapter 3 a land cover mapping classification methodology which allows for an unbiased comparison of the three sensors' ability to produce accurate land cover maps is developed. That methodology is then applied on 1 km spatial resolution data collected by each sensor's SRBs over a series of dates and two study areas (one over the UK and

another over Greece) and the relative effectiveness of each sensor in accurately distinguishing between different land cover classes is assessed.

In Chapter 4, the relations between NDVI data collected by the three sensors over the same targets are assessed. A theoretical assessment is performed using estimated NDVI values of the three sensors over a series of targets, based on the targets' spectral profiles and the sensors' spectral resolutions. An experimental assessment is also performed based on composite NDVI data collected on the same dates by the three sensors over a sample of sites in Africa. Based on the results of the assessments, empirical regressions between the sensors' NDVI values are developed, and the possibility of simulating NDVI data between the three sensors is discussed.

Finally in Chapter 5, the three sensors' relative capacity at monitoring drought conditions using the VPI methodology based on experimental results over a series of sites in Ethiopia at 1 km spatial resolution is assessed; provided that MODIS and VEGETATION could be provided with sufficiently long and accurately simulated historical NDVI records for the requirements of the VPI methodology.

CHAPTER TWO

2 Theoretical assessment

2.1 Background

At the start of this chapter a brief description of AVHRR, MODIS and VGT is provided in order to familiarise the reader with the sensors' historical background, purpose and general description. The sensors' characteristics are then looked into in more detail in terms of spatial, temporal, radiometric and spectral resolution, calibration capabilities and data availability. The characteristics are reviewed in a manner that enables a quantitative comparison of the sensors, as well as enabling the formation of hypotheses regarding the sensors' expected relative performance in land cover mapping and drought monitoring applications.

2.2 Sensors

2.2.1 AVHRR

AVHRR is a low-resolution (spatial), cross-track, line-scanning multispectral radiometer (Barnes and Smallwood, 1982; Kidwell 1984; Schwalb, 1978), that operates on the Polar Orbiting Environmental Satellites (POES) of the National Oceanic and Atmospheric Administration (NOAA). It is equipped with four, five or six spectral bands, depending on the sensor version (table 2.1 displays the spectral band composition of each version) that are sensitive to the red, near-infrared and thermal parts of the electromagnetic spectrum.

The radiation detectors of the spectral bands are mounted behind a telescope aimed at a rotating mirror (360 rpm) that views the Earth (Schwalb, 1978). The collected data are recorded with a 10-bit radiometric resolution. The AVHRR views the Earth scene through a cross-track angle of 110.8° (± 55.4° from the satellite sub-point), from an

average altitude of about 850 km above the Earth's surface, collecting data in a single scan from an area of more than 2700 km in length (swath width). The sensor's GIFOV is 1.09 km at nadir point, but degrades considerably at high viewing angles (Kidwell, 1998).

Table 2.1: AVHRR versions /1 /2 and /3 and their respective spectral bands (Goodrum et al., 2000; Kidwell, 1998)

Spectral bands	AVHRR/1 onboard TIROS-N	AVHRR/1 onboard NOAA-6,8,10	AVHRR/2 onboard NOAA-7,9,11,12,14	AVHRR/2 onboard NOAA-13	AVHRR/3 onboard NOAA-15,16,17,18
1	0.550- 0.900 μm	0.580- 0.680 μm	0.580- 0.680 μm	0.580-0.680 μm	0.580 - 0.680 μm
2	0.725- 1.100 μm	0.725- 1.100 μm	0.725- 1.100 μm	0.725-1 μm	0.725-1.100 μm
3A	-	-	-	-	1.580-1.640 μm
3B	3.550- 3.930 μm	3.550- 3.930 μm	3.550- 3.930 μm	3.550-3.930 μm	3.550-3.930 μm
4	10.500-11.500 μm	10.500-11.500 μm	10.300-11.300 μm	10.300-11.300 μm	10.300-11.300 μm
5	-	-	11.500-12.500 μm	11.400-12.400 μm	11.500-12.500 μm

NOAA flew the first AVHRR version onboard the Television InfraRed Observation Satellite (TIROS-N) in 1978 (Tucker, 1996). The success of the satellite (TIROS-N) led to the launch of 13 more up to the date of this study. After the launch of the second satellite, they were renamed to NOAA. The launch dates and operational periods of each satellite are given in table 2.2 (Hillger and Toth, 2006; Kidwell, 1998; NOAA, 2006).

The TIROS-N/NOAA series satellites follow a near-polar (inclined by 98°) sun-synchronous orbit. Their orbital period is approximately102 minutes, which produces 14.1 orbits per day. However, because the Earth is not a perfect sphere and due to the gravitational influence of nearby planetary bodies, the orbit into which the satellite was initially placed drifts over time. Nevertheless the satellites view each location at almost the same Local Solar Time (LST) on every pass. Each of the satellites' equatorial LST at ascent or descent is given in table 2.3 (Goodrum et al., 2000; Kidwell, 1998).

AVHRR was originally designed for meteorological and oceanographic studies. However it was not long until scientists discovered its potential in further applications. AVHRR was soon used in an extensive list of applications, (Cracknell, 1997, 2001) such as land-cover classification (DeFries et al., 1995; Loveland et al., 2000), vegetation monitoring (Duchemin et al., 1999; Weiss et al., 2004), fire detection/monitoring (Kennedy et al., 1994; Matson et al., 1987), crop yield estimations (Dabrowska-Zielinska et al., 2002; Johnson et al., 1987), and more. It became one of the most valuable sources of data in numerous environmental, scientific and managements contexts (Cracknell,

2001). AVHRR became so popular among the scientific community that, in a survey carried out in 1999, it was found out that nine of the twelve most cited papers in the *International Journal of Remote Sensing* in the last 20 years, exclusively dealt with AVHRR (Cracknell, 1999).

Table 2.2: Launch and operation dates of the TIROS-N/NOAA satellite series

Satellite	AVHRR version	Launch Date	Date Range
TIROS-N	AVHRR/1	October 12, 1978	10/19/1978 – 1/30/1980
NOAA-6	AVHRR/1	June 27, 1979	6/27/1979 – 3/5/1983 and 7/3/1984 - 11/16/1986
NOAA-B	-	May 29, 1980	Failed to achieve orbit
NOAA-7	AVHRR/2	June 23, 1981	8/19/1981 – 6/7/1986
NOAA-8	AVHRR/1	March 28, 1983	6/20/1983-6/12/1984 and 7/1/1985 - 10/31/1985
NOAA-9	AVHRR/2	December 12, 1983	2/25/1985 -10/7/1988
NOAA-10	AVHRR/1	September 17, 1986	11/17/1986 - 9/16/1991
NOAA-11	AVHRR/2	September 24, 1988	11/8/1988 - 4/11/1995
NOAA-12	AVHRR/2	May 14, 1991	5/14/1991- present (standby)
NOAA-13	AVHRR/2	August 9, 1993	8/9/1993 - 8/21/1993
NOAA-14	AVHRR/2	December 30, 1994	4/11/1995 - present (standby)
NOAA-15	AVHRR/3	May 13, 1998	9/26/1998- present (secondary AM)
NOAA-16	AVHRR/3	September 21, 2000	2/27/2001- present (secondary PM)
NOAA-17	AVHRR/3	June 24, 2002	15/10/2002-present (primary AM)
NOAA-18	AVHRR/3	May 20, 2005	30/08/2005-present (primary PM)

The data from AVHRR are available in four formats (Huh, 1991):

- Automatic Picture Transmission (ATP). This is a direct broadcast at low resolution of the second and fourth (daytime) or the third and fourth (night) spectral bands, to ground stations over the world.
- High Resolution Picture Transmission (HRPT). These are the data that the sensor continuously transmits and can be received from ground stations that are within the sensor's range. Data from five spectral bands (bands 3A and 3B can not operate simultaneously, but the first is used during the day and the latter during the night) are transmitted at 10 bit accuracy and with a maximum spatial resolution of 1.1 km at nadir point.

- Global Area Coverage (GAC). These are on-board recordings of the whole global coverage for all transmitted bands at a resolution of 4 km. The data are sampled in the spacecraft from the 1.1 km resolution data by averaging the first four out of each five pixels along every third scan line. Every day, two global area coverages are completed.
- Local Area Coverage (LAC). These are on-board recordings at high resolution (1.1 km) of all transmitted bands for selected parts of the orbit. These data are archived in NOAA facilities.

Note: LAC and GAC data can be ordered from the National Environmental Satellite Data and Information Service (NESDIS) in hardcopy or softcopy format.

Table 2.3: Ascending and descending node times in LST.

Satellite	Ascending node	Descending node
TIROS-N	15:00	03:00
NOAA-6	19:30	07:30
NOAA-7	14:30	02:30
NOAA-8	19:30	07:30
NOAA-9	14:20	02:20
NOAA-10	19:30	07:30
NOAA-11	13:40	01:40
NOAA-12	19:30	07:30
NOAA-13	13:40	01:40
NOAA-14	13:30	01:30
NOAA-15	19:30	07:30
NOAA-16	14:00	02:00
NOAA-17	22:00	10:00
NOAA-18	14:00	02:00

2.2.2 MODIS

MODIS was built by Raytheon Santa Barbara Remote Sensing for NASA's Goddard Space Flight Center (Steitz et al., 1999) and was the most recent and technologically advanced low-resolution sensor in service at the time of the present study.

MODIS is a key element to NASA's "Mission to Planet Earth", as it was designed to improve our understanding of dynamics and processes that take place in the oceans, on the land and in the lower atmosphere (Maccherone and Cardwell, 2006a), on both global and local scales. Data from MODIS are used in a variety of applications, including but not limited to applications in agriculture and vegetation monitoring (Seelan et al., 2003; Zhang et al., 2003), in forestry (Leuning et al., 2005; Xiao et al., 2005), in disaster management (Ji et al., 2004; Tatem et al., 2004), in fire detection/monitoring (Giglio et al., 2003; Roy et al., 2002), in ice/snow detection (Hall et al., 1995; Klein and Barnett, 2003), in atmospheric quality and cloud detection (Hutchison et al., 2003; Ichokuet al., 2004), in land-cover classification/change (Friedl et al., 2002; Zhan et al., 2002), in volcanology (Tupper et al., 2004; Wright et al., 2002), and in oceanology and water quality (Carder et al., 2004; Hu et al., 2005).

The sensor was first launched onboard the NASA' Earth Observing System (EOS) series' satellite "Terra" (EOS AM-1) on the 18th of December 1999, followed by a second launch on the 4th of May 2002 onboard "Aqua" (EOS PM-1), also part of NASA's EOS series. Both satellites have a sun-synchronous, near polar orbit at an average altitude of 705 km (more details in table 2.4).

Table 2.4: Terra and Aqua orbit characteristics

	TERRA	AQUA
Orbit	Sun-synchronous, near-polar	Sun-synchronous, near-polar
Inclination	98.2°	98.2°
Period	98.5 min	98.5 min
Revisit Time	16 days	16 days
Altitude	705 km	705 km
Descending Node	22:30	01:30
Ascending Node	10:30	13:30

Table 2.5: MODIS spectral bands (Barnes et al., 1998; Maccherone and Cardwell, 2006b)

Primary Use	Band	Bandwidth
Land/Cloud/Aerosols Boundaries	1	0.620 – 0.670 µm
	2	0.841 – 0.876 µm
Land/Cloud/Aerosols Properties	3	0.459 – 0.479 µm
	4	0.545 – 0.565 µm
	5	1.230 – 1.250 µm
	6	1.628 – 1.652 µm
	7	2.105 – 2.155 µm
Ocean Colour/ Phytoplankton/ Biogeochemistry	8	0.405 – 0.420 µm
	9	0.438 – 0.448 µm
	10	0.483 – 0.493 µm
	11	0.526 – 0.536 µm
	12	0.546 – 0.556 µm
	13	0.662 – 0.672 µm
	14	0.673 – 0.683 µm
	15	0.743 – 0.753 µm
	16	0.862 – 0.877 µm
Atmospheric Water Vapour	17	0.890 – 0.920 µm
	18	0.931 – 0.941 µm
	19	0.915 – 0.965 µm
Surface/Cloud Temperature	20	3.660 - 3.840 µm
	21	3.929 - 3.989 µm
	22	3.929 - 3.989 µm
	23	4.020 - 4.080 µm
Atmospheric Temperature	24	4.433 - 4.498 µm
	25	4.482 - 4.549 µm
Cirrus Clouds Water Vapour	26	1.360 - 1.390 µm
	27	6.535 - 6.895 µm
	28	7.175 - 7.475 µm
Cloud Properties	29	8.400 - 8.700 µm
Ozone	30	9.580 - 9.880 µm
Surface/Cloud Temperature	31	10.780 - 11.280 µm
	32	11.770 - 12.270 µm
Cloud Top Altitude	33	13.185 - 13.485 µm
	34	13.485 - 13.785 µm
	35	13.785 - 14.085 µm
	36	14.085 - 14.385 µm

MODIS is equipped with 36 spectral bands spanning from visible to long-wave infrared, (20 solar reflective and 16 thermal emissive bands) (table 2.5). Bands 1-2, 3-7 and 8-36 have spatial resolutions of 250 m, 500 m and 1000 m at the nadir, respectively, and are all recorded with a 12-bit radiometric resolution. The sensor scans the Earth using a cross-tracking scanning system; a continuous rotating (20.3 rpm) double-sided mirror is used to collect incoming radiation from the Earth through a viewing angle of ±55°. At an altitude of 705 km and a ±55° viewing angle, the sensor can scan a cross track line of 2330 km, enabling it to survey large areas in a single pass and the entire globe in two days. The along-track Field Of View (FOV) of the sensor was designed to be 10 km. In order to achieve this along-track FOV, the sensor was equipped with a linear array of detectors for each spectral band. However, all the bands of the sensor do not share the same spatial resolution; therefore, a different number of detector elements were needed in each band's linear detector array if they were all to achieve an along-track FOV of 10 km. More specifically: bands 1 and 2 (250 m spatial resolution), 3 to 7 (500 m spatial resolution) and 3 to 37 (1000 m spatial resolution) were equipped with a 40-element, 20-element and 10-element linear detector array respectively (Barnes et al., 1998).

There are 44 available MODIS data products grouped under five disciplines, namely land, ocean, atmosphere, calibration and cryosphere. A list of product names along with a brief description is given in Appendix A (Maccherone and Cardwell, 2006c). The Goddard Earth Sciences (GES) Data and Information Services Center (DISC) Distributed Active Archive Center (DAAC), archives the atmospheric, oceanic and calibration products, while the land and cryospheric products are being archived by the Land Processes (LP) DAAC at the Earth Resources Observation System (EROS) Data Center and the National Snow and Ice Data Center (NSIDC DAAC), respectively. All products are available to be downloaded for free or ordered for a small handling fee, from NASA's Earth Observing System Data Gateway (EOSDG).

2.2.3 VEGETATION

The VEGETATION (VGT) sensor is a product of cooperation between the French Centre National d'Etudes Spatiales (CNES), the European Commission's Joint Research Centre (JRC), the Italian Agenzia Spaziale Italiana , the Belgian Federal Science Policy Office and the Swedish National Space Board.

As the name implies, VGT was primarily designed to monitor vegetation. It has found applications in land-cover mapping (Bartalev et al., 2003; Bartholomé et al., 2002), agriculture (Xiao et al., 2002a; Zhang et al., 2003), disaster management (Lupo et al., 2001; Ozer et al., 2000), plant health (Ceccato et al., 2001; Fraser and Latifovic, 2003), forestry (Mayaux et al., 2000; Stibig et al., 2003), fire detection/management (Eastwood et al., 1998; Phulpin et al., 2002), snow and ice detection (Xiao et al., 2001; Xiao et al., 2002b) and even in atmospheric studies (Schmullius et al., 2003; Xiangming et al., 2003) mostly through the use of its blue band.

So far, two versions of the sensor have been launched: VGT-1 onboard SPOT-4 on the 24th of March 1998, and VGT-2 onboard SPOT-5 on the 3rd of May 2002. Both satellites follow a sun-synchronous, near polar orbit at an average altitude of 822 km (more details in table 2.6).

Table 2.6: (SPOT-5 CNES, 2006b): SPOT 4 and 5 orbit characteristics.

	SPOT-4/SPOT-5
Orbit	Sun-synchronous, near-polar
Inclination	98.72°
Period	101.46 min
Cycle Duration	26 days
Altitude	822 km
Descending Node	10:30
Ascending Node	22:30

VGT-1 and VGT-2 are practically identical, with only slight differences between their spectral bands (SPOT-5 CNES, 2006b) as can be seen in table 2.7. VGT has 4 bands, the red (B2), near-infrared (NIR) (B3) and short-wave infrared (SWIR) bands were designed

for vegetation monitoring, while the blue (B0) was meant to help with atmospheric correction. Data collected by these bands are quantized with a 10-bit radiometric resolution.

VGT scans the Earth using a Charge Coupled Device (CCD). That means that a linear array of detectors (1728 detector elements) is used to scan an entire line simultaneously across its length by each of the four band cameras (SPOT-5 CNES, 2006a; Saint, 1995; SPOT-4 CNES, 2006). The cameras view the Earth through an angle of ±50.5° and from an average altitude of 822 km achieving a swath width of approximately 2250 km and a spatial resolution of 1.165 km at nadir. Due to the large extent of the swath width, VGT can cover almost the entire globe in a single day, with the exception of some areas around the equator.

Authorized users with the necessary equipment can receive data from VGT through the L band (510 kbps), data through this band are also received at the L band VGT receiving station (SRVL) in Aussaguel, France, in order to validate the band's image telemetry. However the VGT's primary receiving station (SRIV) is located in Kiruna, Sweden. Data are received there through the X band (3400 kbps) and forwarded to the VGT image processing centre (CTIV). The CTIV in turn, processes the data and consequently archives and distributes the resulting products. Additionally, an operations control centre located in Toulouse, France is responsible for monitoring and programming the VGT payload through the S band. Finally, the VGT image quality centre (QIV) is also located in Toulouse, France and is responsible for providing the CTIV with parameters for geometric and radiometric correction, it is also responsible for regularly calibrating the sensor (SPOT-5 CNES, 2006a; Saint, 1997).

Table 2.7: (SPOT-VEGETATION, 2006a): VGT-1 and VGT-2 bands

Spectral bands	Specified	VGT-1 (actual values)	VGT-2 (actual values)	Surface reflectance range
BLUE (B0)	0.430 - 0.470 µm	0.437 - 0.480 µm	0.438 - 0.475 µm	0.0 - 0.5
RED (B2)	0.610 - 0.680 µm	0.615 - 0.700 µm	0.615 - 0.690 µm	0.0 - 0.5
NIR (B3)	0.780 - 0.890 µm	0.772 - 0.892 µm	0.782 - 0.890 µm	0.0 - 0.7
SWIR	1.580 - 1.750 µm	1.600 - 1.692 µm	1.582 - 1.750 µm	0.0 - 0.6

The VGT products are grouped under two categories, the P (primary) products and the S (synthesis) products. The P products are radiometrically (in-band and absolute calibration) and geometrically corrected (resampled to the user's requested projection and at 1 km resolution) and contain values linearly scaled to equivalent Top Of the Atmosphere (TOA) reflectance values for all four bands, in addition to the viewing angle (zenith and azimuth), sun angles (zenith and azimuth), atmospheric correction data (aerosol optical depth at 550 nm and the vertically integrated gaseous contents for water vapour and ozone) and a status map (land, water, snow, ice and cloud). The P products are used to synthesise the S products. First the reflectance values of the P products are corrected for atmospheric interference and the NDVI for each pixel is calculated. Then the S product for a particular area of interest is synthesised by mosaicing all pixels with the highest NDVI value per pixel location, from each portion of the P products that falls within that area. If all the P products that were in the synthesis were captured in a single day the resulting product is coded as S1, alternatively if all P products from 10 successive days were used, the resulting product is coded as S10. Both S1 and S10 products have a 1 km spatial resolution. However the S10 products are also available at degraded resolution of 4 and 8 km and are coded as S10.4 and S10.8 respectively (SPOT-5 CNES, 2006a; Henry et al., 1996; SPOT-VEGETATION, 2006b).

2.3 Technical comparison

At this stage of the research, data were collected and processed in a way that the three sensors under consideration could be evaluated in an objective and quantitative manner, so that hypotheses could then be formed about their expected relative performance in vegetation land cover mapping and drought monitoring. Remote sensors are typically distinguished by their spatial, temporal, radiometric and spectral resolution, their data availability, and any integrated technology such as their on-board calibration capability; therefore, their expected relative performance was assessed based on these aspects.

2.3.1 Spatial resolution

The spatial resolution of a remote sensor refers to its ability to spatially distinguish features on the ground. It is critical in land cover mapping and drought monitoring applications. The minimum area unit which a sensor with low spatial resolution can distinguish is larger than it would be for a sensor with higher spatial resolution. The probability that the minimum area unit detectable by a sensor is composed purely by a single land cover class (pure pixel) is reduced as area increases; particularly when measurements are taken over heterogeneous areas.

In land cover classification application, the presence of non pure pixels (mixed pixels) is one of the prime causes of misclassification errors, especially when the classification accuracy is assessed with a pixel-to-pixel approach (Foody 1996b, 1999, 2002; Hseih et al., 2001; Huang et al., 2002; Karaska et al., 1995; Latty et al., 1985; Toll, 1985; Townshend et al., 2000). On the other hand, in drought monitoring applications, mixed pixels may be composed of vegetated and non-vegetated areas. In such cases the NDVI values calculated from such mixed pixels will be less responsive to vegetation stress status because only the vegetated portion of the mixed pixel will be affected by the drought stress. Therefore, land cover maps or drought monitoring applications based on data collected from sensors with low spatial resolution are more likely to contain misclassification errors or be less effective in detecting droughts, respectively, than if they were based on higher spatial resolution data.

A sensor's spatial resolution is commonly measured by the dimensions of the surface area of the earth covered by its pixel (known as the Ground-projected Instantaneous Field Of View (GIFOV)) at the point directly underneath the sensor (nadir). For instance the dimensions of the area scanned within one pixel by Landsat 5 TM visible bands at nadir is 30 m by 30 m; hence, the visible bands of Landsat 5 Thematic Mapper (TM) are commonly referred to as having 30 m spatial resolution.

Information regarding the GIFOV of AVHRR, VEGETATION and MODIS bands at the nadir viewing point of the sensors (vertical viewing angle 0°) is available in the literature as: 1.09 km (Goodrum et al., 2000) for AVHRR, 1.15 km for VEGETATION (Saint, 1992) and 1 km, 0.5 km and 0.25 km for MODIS 8-36, 3-7 and 1-2 bands

respectively (Running et al., 1994). However, the knowledge of the sensors' GIFOV at nadir point is not adequate to compare the sensors' spatial resolution.

The GIFOV of a sensor increases at higher viewing angles as it moves away from the nadir point. Its value is mainly a function of the altitude of its orbit, the curvature of the Earth, the viewing angle at which the sensor receives radiation, and the sensor's Instantaneous Field Of View (IFOV). The three compared sensors do not share the same altitude of orbit or IFOVs; hence it can not be expected that their GIFOVs would change in the same manner at different viewing angles.

Particularly for the case of VEGETATION, it is important to note that the sensor scans a whole line simultaneously using its CCD array, and as such the array as a whole does not scan the Earth at varying viewing angles. However, the angles at which each detector on VEGETATION's CCD array (1728 detectors for each band) receive radiation from the Earth scene increase for each detector placed further away from the central detector of the array. Hence, when referring to VEGETATION's viewing angles, the reference is to the viewing angle of the detectors and not the whole CCD array. Additionally, VEGETATION's optics system (telecentric lenses) combined with the use of a CCD array is designed to minimise distortion and retain a stable GIFOV across the scan line (Henry and Meygret, 2001b; Henry et al., 1996; Saint, 1992). VEGETATION's GIFOV still increases monotonically across the scan line, but not as much as it would if it were using a conventional optics system. At a 50° viewing angle VEGETATION's across-track GIFOV reaches a maximum value of about 1.7 km (Bartholomé and Belward, 2005).

It was decided to quantitatively compare the sensors' spatial resolution by calculating and comparing the values of the along-track and across-track GIFOV of each sensor at regular distance intervals on the ground away from their nadir points. The along-track and across-track GIFOVs of each sensor were to be calculated with the development of trigonometric equations. However, trigonometric equations could not account for the optics system of VEGETATION which greatly minimises the degradation of the sensor's GIFOV at viewing angles away from the nadir point. Hence the use of the equations was limited to MODIS and AVHRR.

If the IFOV (θ°) and the altitude (h) of a sensor's orbit are known, then the spatial resolution of the sensor (GIFOV) can be calculated, assuming that the Earth is a perfect sphere with a 6372.795 km radius (R). In figure 2.1, the across-track GIFOV of a sensor at a viewing angle of ϕ° will be equal to the length of the EF arc ($\overline{EF}$). The length of the $\overline{EC}$ will be equal to the difference between the arcs $\overline{EC}$ and $\overline{FC}$. But the length of $\overline{EC}$ and $\overline{FC}$ arcs can be calculated if the $E\hat{K}C$ and $F\hat{K}C$ angles are known (see equation 2.1).

$$\text{Across-track GIFOV} = \overline{EF} = \overline{EC} - \overline{FC} = \frac{(E\hat{K}C - F\hat{K}C)\pi R}{180} \tag{2.1}$$

The angles $E\hat{K}C$ and $F\hat{K}C$ can be calculated from the EKC and FKC triangles respectively (equations 2.2 – 2.5):

$$EC^2 = R^2 + R^2 - 2R^2 \cos E\hat{K}C \tag{2.2}$$

$$FC^2 = R^2 + R^2 - 2R^2 \cos F\hat{K}C \tag{2.3}$$

$$E\hat{K}C = a\cos(\frac{2R^2 - EC^2}{2R^2}) \tag{2.4}$$

$$F\hat{K}C = a\cos(\frac{2R^2 - FC^2}{2R^2}) \tag{2.5}$$

In turn, the length of EC and FC can be calculated from the AEC and AFC triangles respectively (equations 2.6, 2.7):

$$EC = \sqrt{AE^2 + h^2 - 2AEh\cos(\phi + \frac{\theta}{2})} \tag{2.6}$$

$$FC = \sqrt{AF^2 + h^2 - 2AFh\cos(\phi - \frac{\theta}{2})} \tag{2.7}$$

Finally in order to solve the above equations (2.6 & 2.7) the lengths of AE and AF should be calculated (equations 2.8 – 2.11).

For the triangle AEK:

$$EK^2=AE^2+AK^2-2(AK)(AE)\cos(\frac{\theta}{2}+\phi) \tag{2.8}$$

$$AE = AK\cos(\frac{\theta}{2}+\phi) \pm \sqrt{AK^2\cos^2(\frac{\theta}{2}+\phi) - AC^2 - 2(EK)(AC)} \tag{2.9}$$

$$AE = (h+R)\cos(\frac{\theta}{2}+\phi) \pm \sqrt{(h+R)^2\cos^2(\frac{\theta}{2}+\phi) - h^2 - 2hR} \tag{2.10}$$

And similarly for the AFK triangle

$$AF = (h+R)\cos(\phi-\frac{\theta}{2}) \pm \sqrt{(h+R)^2\cos^2(\phi-\frac{\theta}{2}) - h^2 - 2hR} \tag{2.11}$$

As for the along-track GIFOV, the Earth's curvature along the along-track is minute and can be assumed to be flat; additionally, there is no viewing angle on the along-track plane, thus figure 2.2 can be used for the along-track calculation. Because the triangle AUZ in figure 2.2 has equal sides AU=AZ then UAG and GAZ triangles are orthogonal, UG=GZ=UZ/2, and the angles $U\hat{A}G = G\hat{A}Z =$ θ°/2. Since the UGA triangle is an orthogonal then, as in equations 2.12 – 2.14:

$$UG=AG\sin(\frac{\theta}{2}) \tag{2.12}$$

$$\text{Along-track GIFOV} = 2\sin(\frac{\theta}{2})AG \tag{2.13}$$

$$\text{Along-track GIFOV(UZ)}=2AG\sin(\frac{\theta}{2}) \tag{2.14}$$

The AG length can be calculated from the AGK triangle in figure 2.1 (in equation 2.15):

$$AG = (h+R)\cos(\phi) \pm \sqrt{(h+R)^2\cos^2(\phi) - h^2 - 2hR} \tag{2.15}$$

Moreover, if the maximum viewing angle of a sensor was used $\phi°_{MAX}$ then the length of the $\overline{EC}$ arc would be equal to the sensor's swath width from one side of the nadir point; therefore, the total swath width of a sensor would be twice the EC arc length when the maximum viewing angle is used $\phi°_{MAX}$ (seen in equation 2.16).

$$\text{Swath width} = 2\,\overline{EC} = \frac{\pi R E\hat{K} C}{90} \quad (\text{for } \phi°_{MAX}) \tag{2.16}$$

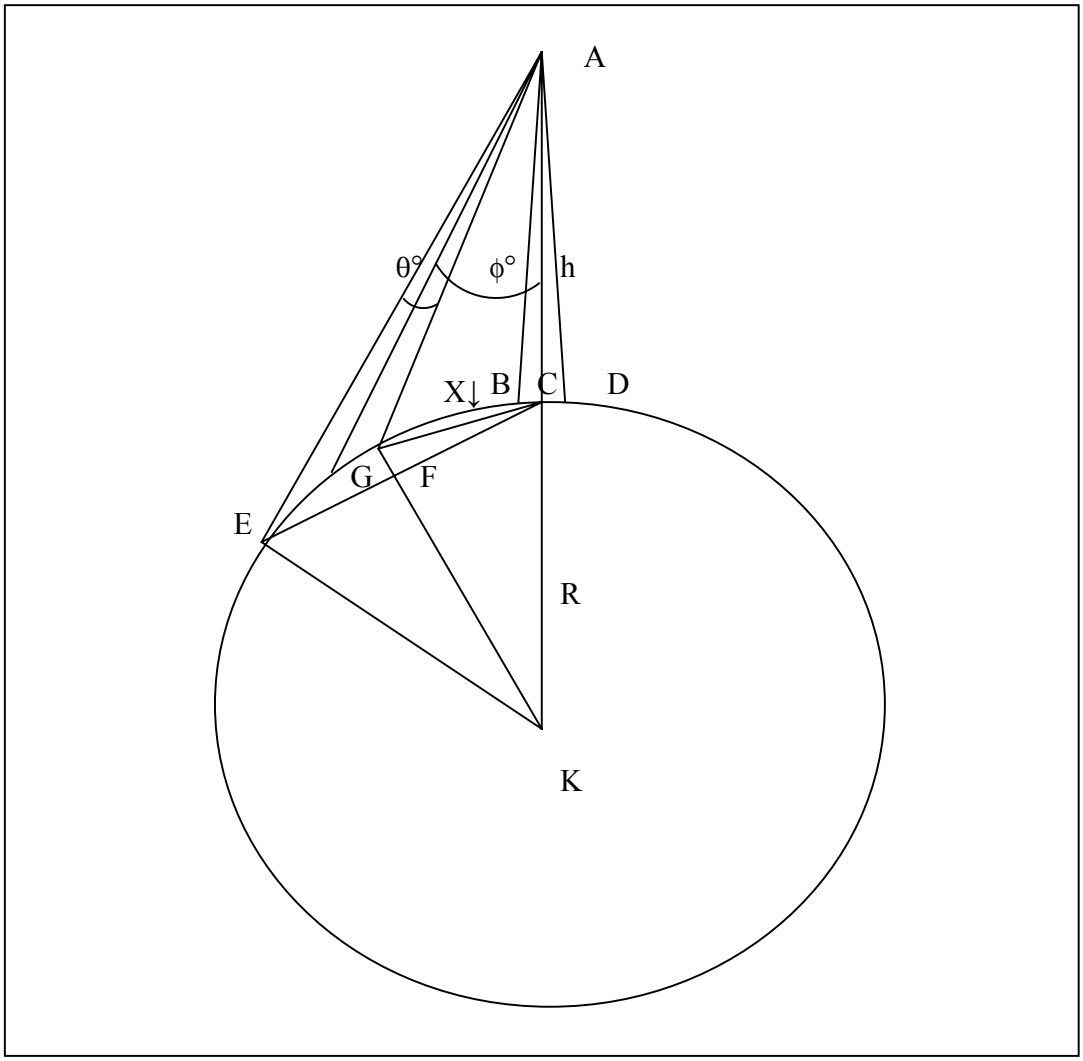

Figure 2.1: Assuming that the Earth is a perfect sphere with 6372.795 km radius (R), the across-track spatial resolution of the sensor when viewing the earth at an angle of f° and an IFOV of u°, will be equal to the length of the EF arc.

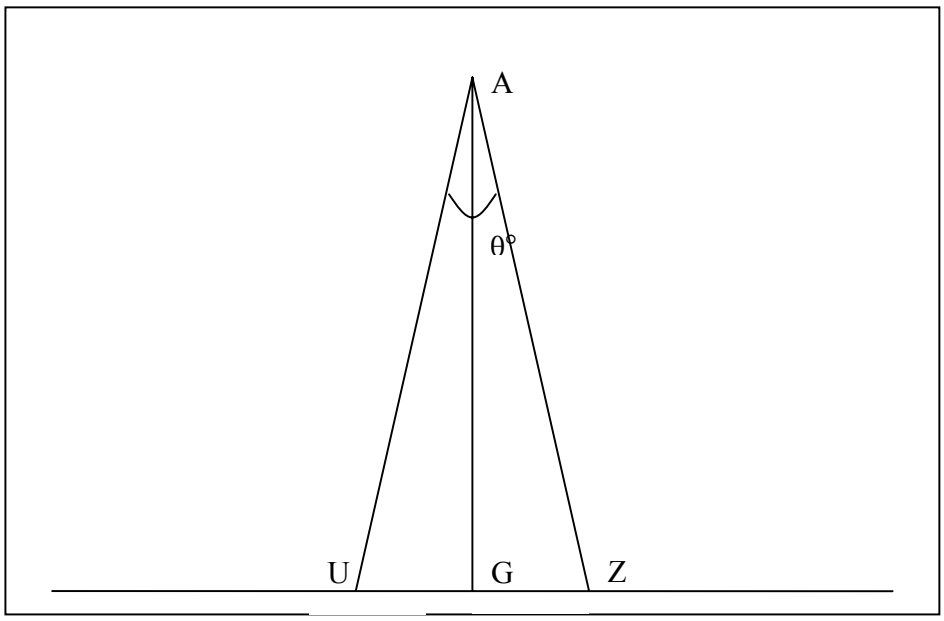

Figure 2.2: Assuming that the Earth's curvature is minuscule on the along-track the along-track GIFOV of a sensor on position A would be equal to the UZ length.

Therefore, the along and across track GIFOV of any sensor can be calculated at any viewing angle, given that the IFOV and orbit altitude of the sensor are known. In order to compare the sensors' GIFOVs at the same distance intervals away from their nadir points, the viewing angle at which each sensor must point in order to view the same distance from their nadir points, is required. It can be calculated from the same set of equations used to calculate the GIFOV, only this time, for an area where the centre is at point X on the ground (figure 2.1), the viewing angle is unknown, and the length of the $\overline{CX}$ arc is known.

The IFOV, orbit altitude, and maximum viewing angle of MODIS and AVHRR are known (table 2.8); and so, using the above equation, their along and across track GIFOVs at different distances away from their nadir points can be calculated. Table 2.9 displays the calculated along and across track GIFOVs of MODIS and AVHRR for increasing distance intervals of 100 km away from their nadir points.

Table 2.8: Altitude, IFOV, and maximum viewing angle of VGT, MODIS and AVHRR (Goodrum et al., 2000; Running et al., 1994; SPOT-VEGETATION, 2006)

	VGT	MODIS	AVHRR
Altitude (km)	822	705	833
IFOV (milliradians)	1.400	Bands(8-36): 1.418 Bands(3-7): 0.709 Bands(1-2) : 0.354	1.300
Maximum viewing angle (degrees)	±50.5	±55	±55.4
Swath width (km)	2250	2330	2930

Table 2.9: MODIS and AVHRR across and along track GIFOV at 100 km intervals from their nadir points (assuming that all sensors are equipped with conventional optic systems).

Distance from nadir (in km)	MODIS (in km)						AVHRR (in km)	
	Bands 8-36		Bands 3-7		Bands 1 and 2		Bands 1-5	
	Across	Along	Across	Along	Across	Along	Across	Along
0	1.00	1.00	0.50	0.50	0.25	0.25	1.08	1.08
100	1.02	1.01	0.51	0.51	0.26	0.25	1.10	1.09
200	1.09	1.04	0.55	0.52	0.27	0.26	1.16	1.12
300	1.21	1.10	0.61	0.55	0.30	0.27	1.25	1.16
400	1.38	1.16	0.69	0.58	0.35	0.29	1.39	1.22
500	1.61	1.25	0.80	0.62	0.40	0.31	1.57	1.28
600	1.89	1.34	0.94	0.67	0.47	0.34	1.79	1.36
700	2.23	1.45	1.11	0.72	0.56	0.36	2.05	1.45
800	2.64	1.56	1.32	0.78	0.66	0.39	2.37	1.55
900	3.12	1.67	1.56	0.84	0.78	0.42	2.75	1.65
1000	3.68	1.80	1.84	0.90	0.92	0.45	3.18	1.75
1100	4.34	1.92	2.17	0.96	1.08	0.48	3.69	1.87
1200	N/A	N/A	N/A	N/A	N/A	N/A	4.27	1.98
1300	N/A	N/A	N/A	N/A	N/A	N/A	4.94	2.10
1400	N/A	N/A	N/A	N/A	N/A	N/A	5.72	2.21

Based on the calculated GIFOVs of AVHRR and MODIS (table 2.9) and considering that the maximum value of VEGETATION's GIFOV does not exceed 1.7 km, it was concluded that:

- The best (lowest) GIFOV values were achieved by MODIS 1 and 2 bands. This is because they have the smallest IFOV values.
- The second best GIFOV values were also achieved by MODIS for bands 3 to 7 bands. This is also because they have the second smallest IFOV values.
- At short distances from the nadir point (up to 400 km) the GIFOV values of MODIS bands 8-36, AVHRR and the assumed values of VEGETATION were similar, due to minimal geometric distortion caused by high viewing angles and the curvature of the Earth.
- Beyond short distances however, the GIFOV of MODIS bands 8-36 and AVHRR, begin to deteriorate (increase) considerably. It can be seen in table 2.9 that at a distance of 600 km both of the sensors' GIFOVs have already exceeded the maximum GIFOV value of VEGETATION. Therefore over the majority of the sensors' swath widths, VEGETATION has the lowest GIFOV values.
- Beyond short distances it can also be seen that the GIFOV values of MODIS bands 8-36 deteriorate faster than the respective GIFOV values of AVHRR. This is the result of the combined effect of MODIS' higher IFOV values and lower orbit altitude (a sensor orbiting at a lower altitude than another would view targets away from the nadir point at higher angles).

The across and along track GIFOV values of MODIS and AVHRR can be seen more graphically in figures 2.3 and 2.4, respectively. The effect of the Earth's curvature is apparent in these graphs, both the along and across track GIFOV of each sensor increase in value with increasing distances from the nadir point; however, the increase rate of the across GIFOV values is considerably higher than the rate of the along GIFOV values, because the Earth curvature effect on the latter is minimal.

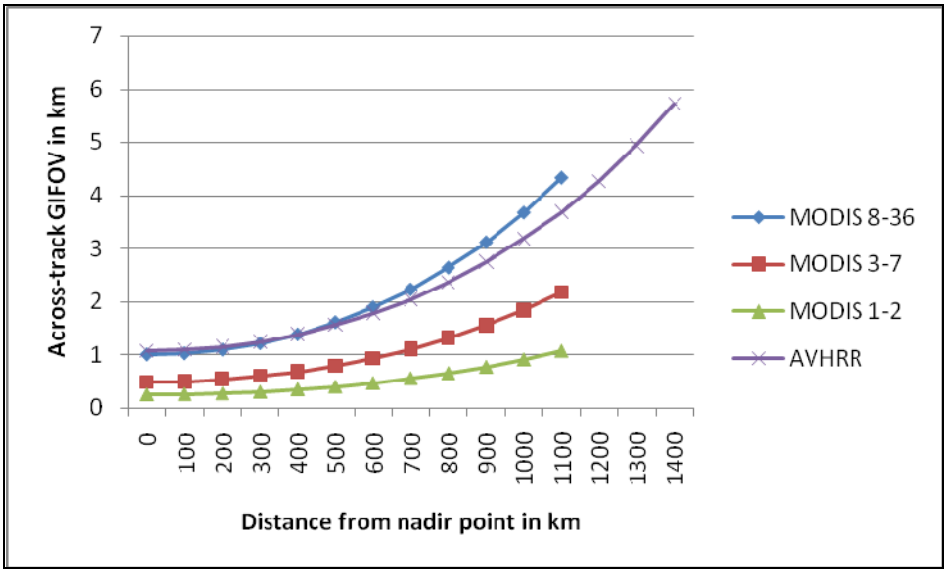

Figure 2.3: Graph of the calculated across-track GIFOV values of MODIS and AVHRR at increasing distances from the nadir point

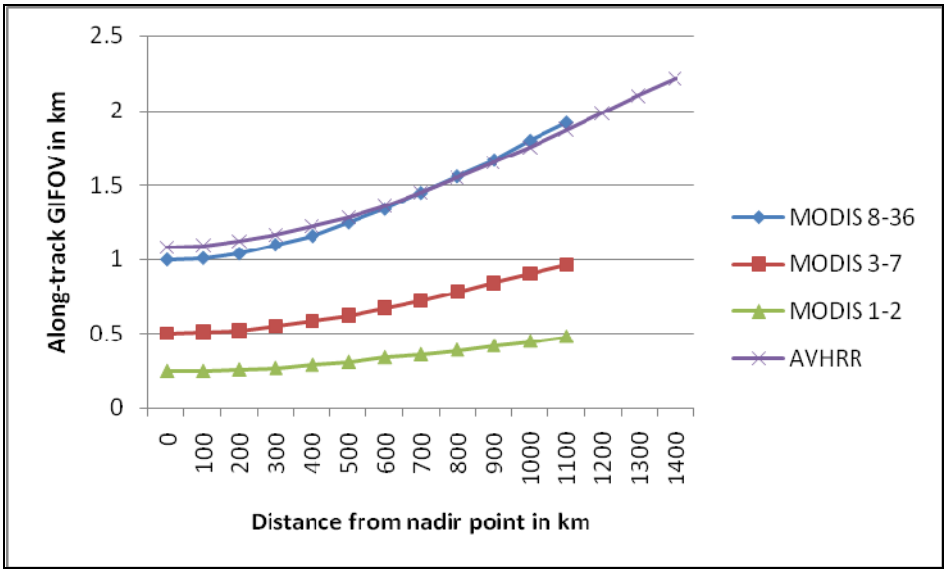

Figure 2.4: Graph of the calculated along-track GIFOV values of MODIS and AVHRR at increasing distances from the nadir point.

The GIFOV is not the only measure of a sensor's spatial resolution. The radiation recorded by a sensor is not the sum of a uniform contribution of radiation from the area covered by the GIFOV but is affected unequally from radiation coming from both within

and outside the GIFOV; due to atmospheric effects, optical system imperfections, image resampling, the motion of the target during acquisition, and signal processing effects. Areas in the centre of the GIFOV contribute more radiation than those further away, extending beyond the GIFOV to the neighbouring GIFOVs (Forster and Best, 1994; Markham, 1985; Schott, 1997; Schowengerdt, 1997; Townshend, 1981; Williams & Becklund, 1989). This effect is described by the Point Spread Function (PSF) which is the response of the sensor to a point source of radiation (figure 2.5). Thus the actual spatial resolution of a sensor is actually less than the sensor's GIFOV.

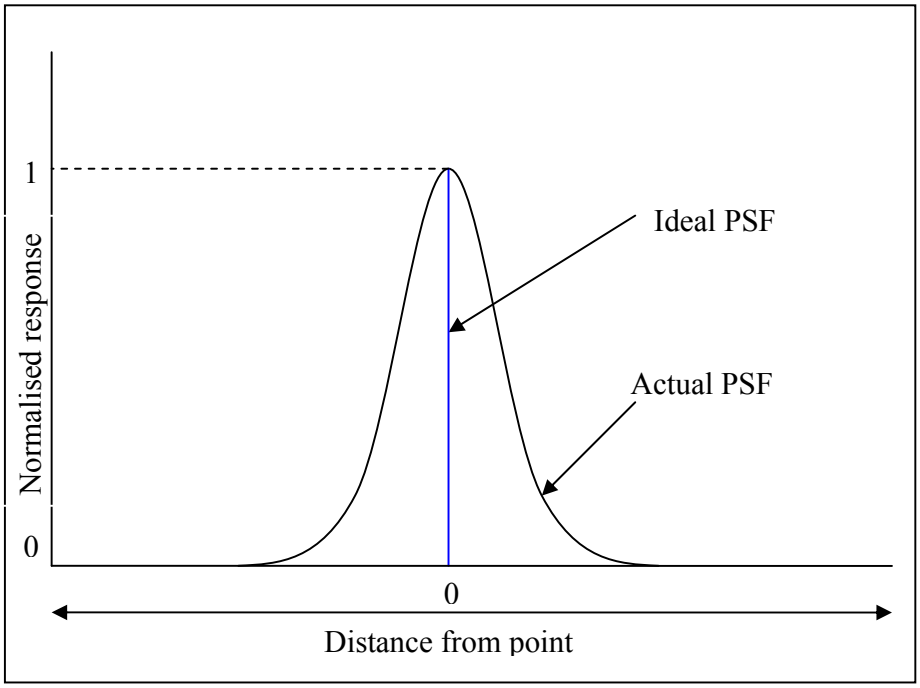

Figure 2.5: Comparison between the responses of a sensor with ideal PSF and a sensor with a less than ideal PSF to a point source of radiation.

In order to assist the perception of a measure of a sensor's spatial resolution in regard to the PSF effect, the concept of target is used which is composed of dark and light coloured lines as wide as a sensor's GIFOV, and placed next to each other in alternate order; thus, having one dark or light line within every width of two GIFOV (or in other words a spatial frequency equal to: $\frac{1}{2GIFOV}$). If the dark and light lines had brightness values of two and eight respectively then a sensor with an ideal PSF and constant GIFOV

values across its scan line, would record a consecutive series of values of alternating twos and eights when scanning the target. In reality, sensors do not have ideal PSFs and even if their GIFOV remained constant across their scan line they would more likely record something like a series of threes and sevens. The recorded image would be less contrasted and more blurred than the real target. Consequently the sensor's ability to spatially distinguish the dark and light lines is impaired. In extreme cases of very wide-shaped PSF or of targets with very high spatial frequencies (several lines per GIFOV), the ability to distinguish the lines is lost completely. Therefore, a measure of contrast preservation in relation to spatial frequency can also be used as a measure of spatial resolution. The contrast of an image can be measured by the contrast, or square wave, transfer function (CTF) (equation 2.17).

$$CTF = \frac{I_{MAX} - I_{MIN}}{I_{MAX} + I_{MIN}} \tag{2.17}$$

Where I_{MAX} and I_{MIN} are the sensor's highest and lowest recorded values, respectively. In the previous example, a sensor with an ideal PSF (or at a very low spatial frequency) would have a CTF value of $\frac{8-2}{8+2} = 0.6$ and another sensor with a less than ideal PSF could have a CTF value of $\frac{7-3}{7+3} = 0.4$ in the $\frac{1}{2GIFOV}$ spatial frequency. The value of a sensor's measured CTF when viewing a target of a certain spatial frequency normalised by the CTF value of a sensor with an ideal PSF (or at a very low spatial frequency), when viewing the same target, provides a measure of a sensor's ability to preserve contrast at the certain spatial frequency of the target. A sensor with a normalised CTF value of 1 for a certain spatial frequency would be able to retain all of the target's contrast at that spatial frequency. Normalised CTF values tend to be close to one for very low spatial frequencies (by default 1 for zero spatial frequency) and zero at very high spatial frequencies.

Commonly, instead of the CTF metric, the Modulation Transfer Function (MTF) is used. The MTF is defined the same way as the normalised CTF with the exception that

the input values (target values) are sinusoidally varying functions (Schott, 1997). The MTF value of a sensor changes in relation to the target's spatial frequency similarly to the CTF metric; hence it approaches values of one or zero, for very low and very high spatial frequencies respectively.

According to the sampling theorem, the Nyquist frequency is the highest spatial frequency an ideal sampling system (or sensor) can reproduce, and it is equal to that which is shown in equation 2.18:

$$\text{Nyquist frequency} = \frac{1}{2\Delta x} \tag{2.18}$$

Where Δx is the distance between sample centres, the Nyquist frequency for a remote sensor would then be equal to: $\frac{1}{2GIFOV}$

Table 2.10 (Barnes et al., 1998; Goodrum et al., 2000; SPOT-VEGETATION, 2006): MTF values at the Nyquist frequency for MODIS, VGT and AVHRR at the nadir

	Bands	Across-track MTF	Along-track MTF
AVHRR	All	≥0.3	≥0.3
VGT	B0	0.48	0.53
	B2	0.33	0.38
	B3	0.22	0.44
	B4	0.58	0.43
MODIS	1	0.37	0.42
	2	0.41	0.45
	3	0.38	0.54
	4	0.40	0.56
	5	0.26	0.50
	6	0.27	0.50
	7	0.34	0.46
	8	0.38	0.59
	9-19 and 26	≈0.40	≈0.60

The MTF values of AVHRR, MODIS and VEGETATION bands at their respective Nyquist frequencies were found in the literature (table 2.10). Considering that all sensors' bands do not share the same Nyquist frequencies (due to different GIFOV values), the following were derived from table 2.10:

- MODIS bands 1 and 2 have the highest MTF values compared with any of the other sensors' bands at the same spatial frequencies. This is because although the MTF values of the other sensors' bands at their respective Nyquist frequencies had comparable values, their GIFOV values were higher; therefore, their MTF values at their Nyquist frequencies were measured under lower spatial frequency. Hence, at higher spatial frequencies the MTF values of MODIS bands 1 and 2 would be comparably higher.
- Similarly, MODIS bands 3 to 7 have the second best MTF performance.
- The GIFOVs of the remaining sensor bands have similar values at the nadir point and therefore their MTF values at their Nyquist frequencies refer to similar spatial frequencies and can be compared. The MTF values of VEGETATION bands are higher or similar to the MTF values of the other sensor bands. However, the GIFOV of VEGETATION bands deteriorate considerably less across the scan line than the GIFOVs of the other sensors; consequently, based on the sensors' bands MTF values, the VEGETATION bands ability to distinguish between spatial features would be higher across the greater part of each of the sensors' bands scan lines, because the measurements would be under lower spatial frequencies.
- Finally, between the remaining bands of MODIS (8-19 and 26) and AVHRR, at distances close to the nadir point, MODIS should perform better than AVHRR due to higher MTF values. However, at greater distances away from the nadir point, AVHRR MTF performance may surpass that of MODIS (bands 8-19 and 26) due to AVHRR lower GIFOV values at such distances.

In summary, both GIFOV and MTF comparisons indicate the following order in terms of the quality of the sensors' spatial resolution in descending order:

1. MODIS bands 1 and 2
2. MODIS bands 3 to 7
3. VEGETATION
4. AVHRR or MODIS bands 8-19 and 26 (depending on the distance from the nadir point)

2.3.2 Temporal resolution

The time interval between two successive scans of the same area by a sensor determines the sensor's temporal resolution. Sensors with high temporal resolution collect data from a certain area more frequently than sensors with lower temporal resolution; this is important in both land cover classification and drought monitoring applications. Data collected for these applications can only be used if they are not cloud contaminated, and the probability of acquiring such data is increased at higher data collection rates. Additionally numerous land cover classification and drought monitoring methodologies rely on the interpretation of vegetation reflectance profiles over time and are therefore benefited by higher data collection rates (more detailed vegetation profiles over time).

Temporal resolution depends mainly on two factors: i) the orbit of the sensor's carrier space vehicle (satellite), and ii) the length of the sensor's swath width. The sensor's (satellite's) orbit determines the distance covered by an object on the Earth's surface along the equatorial plane in relation to the orbital plane, within the sensor's orbit period (the time needed by the sensor to complete an orbit). The swath width of a sensor combined with its orbit determines the length of its scan line along the equatorial plane. The combined knowledge of these two parameters can be used to calculate the number of orbits needed by a sensor to view a target for a second consecutive time within its swath width. The temporal resolution of the sensor for that target would then be equal to the number of orbits multiplied by the sensor's period.

The orbit of the satellite can be characterised by its major (a) and minor axis (b) (also known as apogee and perigee respectively), period ($P_{o)}$, and inclination to the equatorial plane of the Earth (i°) (figures 2.6 and 2.7).

If the Earth was a perfect sphere then a sensor's orbit period would be calculated by equation 2.18 (Smith et al., 1985):

$$P_o = 2\pi\sqrt{\frac{a^3}{GM}} \tag{2.18}$$

Where,
G= The gravitational constant
M= The Earth's mass
GM = $(3.98600434\pm0.00000002)10^{14}$ m^3 s^{-2}

However, the Earth is an oblate spheroid; as a result the orbit period is longer than it would be if the Earth was a perfect sphere and can be calculated using equation 2.19 (Rees, 2001).

$$P_n = 2\pi\sqrt{\frac{a^3}{GM}}\left(1+\frac{3J_2 a_e^{\,2}}{4a^2}\left(1-3\cos^2 i+\frac{1-5\cos^2 i}{(1-e^2)^2}\right)\right) \tag{2.19}$$

Where:
α_e= The Earth's equatorial radius ≈ 6378135 m
J_2= The dynamic form factor≈ 0.00108263
e = the orbit's eccentricity $e^2 = \frac{a^2-b^2}{a^2}$ (2.20)

Moreover, the Earth's oblate shape causes the orbital plane to rotate around the Earth's polar axis (vertically to the equatorial plane) by an angular velocity (procession angular velocity, Ω_p) (Rees, 2001) as presented in equation 2.21:

$$\Omega_p = -\frac{3J_2\sqrt{GM}\,a_e^{\,2}a^{-7/2}\cos i}{2(1-e^2)^2} \tag{2.21}$$

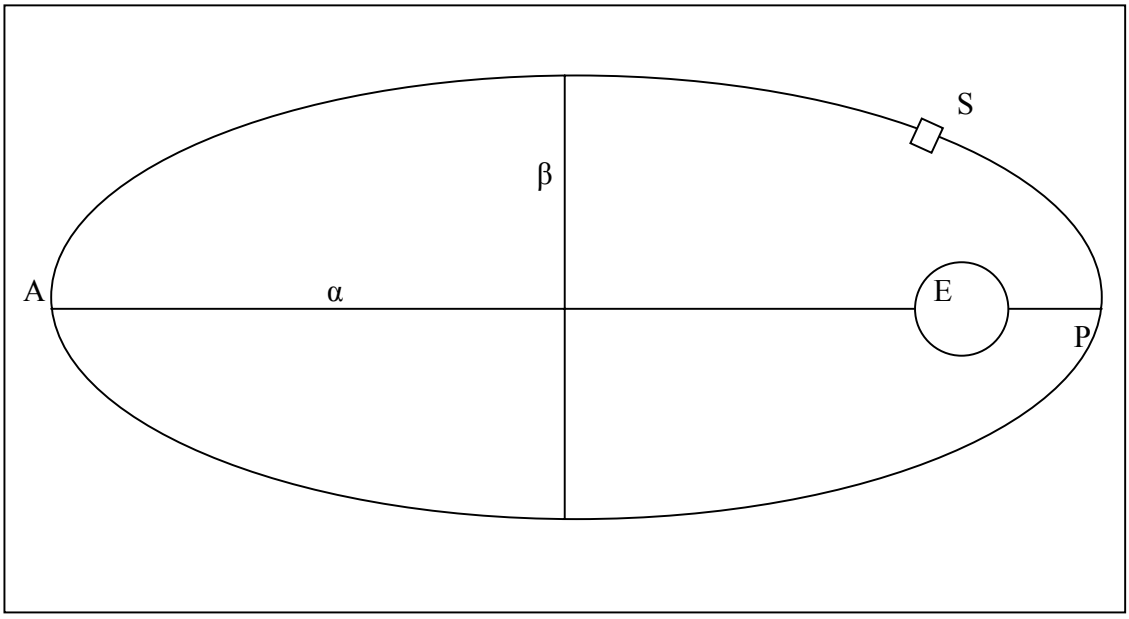

Figure 2.6: Points A and P are the furthest and closest point of the satellite's (S) orbit to the Earth's (E) centre, otherwise known as apogee and perigee respectively. Moreover α and β are the major and minor axis of the satellite's orbit.

If the inclination of a sensor's orbit is less than 90° (also known as a prograde orbit) then the cosine of its inclination becomes positive and the procession angular velocity becomes negative. Vice versa, if the inclination is higher than 90° (also known as a retrograde orbit), the procession angular velocity becomes positive. So at inclination values lower than 90° the orbital plane rotates opposite to the Earth's rotation, and in the same direction at inclination values higher than 90°.

Information regarding MODIS, AVHRR and VEGETATION (onboard their respective satellite vehicles) orbits can be found in the literature (table 2.11). Their orbits are near-circular; thus, it can be approximated that their eccentricity values are zero (e=0). Even though the sensors' orbit periods are already provided, they could still be calculated using equation 2.20 for validation reasons. The values of the sensors' orbit periods based on equation 2.20 are: 98.9 min for MODIS, 101.45 min for VEGETATION, and 101.68 min for AVHRR. The difference between estimated and provided period values is very small, and can be mainly attributed to simplifications regarding the sensor's orbit altitudes (they fluctuate), eccentricity (it is near circular, so it is slightly higher than zero), and the Earth's shape and mass (the constants for G, M and

Earth's radius). Nevertheless despite the small difference between the provided and calculated orbit period values, the period values provided by the literature were considered to be more accurate and were adopted for the remainder of the comparison.

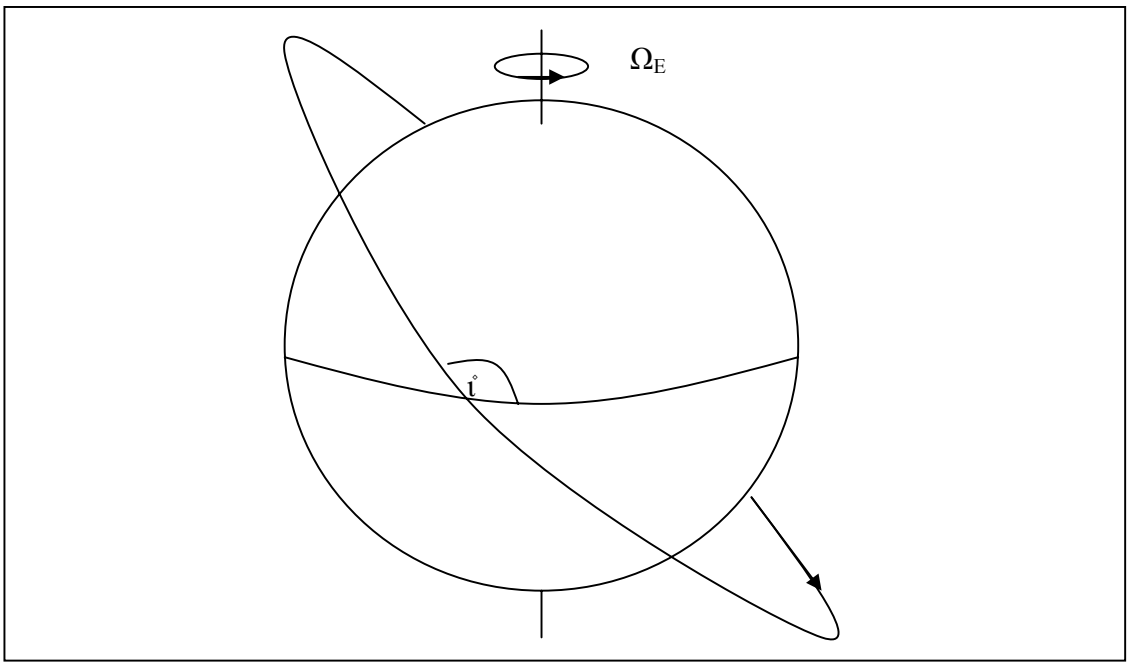

Figure 2.7: The angle between the equatorial and the orbital plane is the inclination angle of the orbit (i°)

The processing angular velocity of the sensors' orbital plane around the Earth's polar axis (Ω_p) could be calculated from equation 2.22; however the calculations can be made easier because it is known that the three sensors follow sun-synchronous orbits. Satellites on sun-synchronous orbits, have angular procession velocities (Ω_p) equal to the angular velocity of the Earth (Ω_s) orbiting around the Sun (Rees, 2001). The time needed for the Earth to complete a full orbit around the Sun (sidereal year), is slightly longer than a normal 365-day calendar year; Thus equation 2.22:

$$\Omega_p = \Omega_s = \frac{2\pi}{sidereal\_year} = \frac{2\pi}{(365.25)(24)(60)(60)} = 1.99102 \cdot 10^{-7}\, s^{-1} \qquad (2.22)$$

Table 2.11: Orbit characteristics of the sensor's carrier vehicles (Running et al., 1994; Goodrum et al., 2000; SPOT-VEGETATION, 2006)

	SPOT-4 & SPOT-5	TERRA & AQUA	NOAA-17& NOAA-18
Orbit	Sun-synchronous, near-polar	Sun-synchronous, near-polar	Sun-synchronous, near-polar
Inclination	98.72°	98.2°	98.8°
Period	101.46 min	98.5 min	101.35 min
Altitude	822 km	705 km	833 km
Descending Node	10:30	22:30 (TERRA)	10:00 (NOAA-17)
		01:30 (AQUA)	02:00 (NOAA-18)
Ascending Node	22:30	10:30 (TERRA)	22:00 (NOAA-17)
		13:30 (AQUA)	14:00 (NOAA-18)

The angular velocity of the Earth around its axis (Ω_E) is 2π per day. Similarly to the sidereal year, the Earth completes a full rotation around its axis within a sidereal day which is slightly shorter than a calendar 24-hour day. Hence equation 2.23:

$$\Omega_E = \frac{2\pi}{sidereal\_day} = \frac{2\pi}{(23)(60)(60)+(56)(60)+4} = \frac{2\pi}{86164} = 7.29212 \cdot 10^{-5}\, s^{-1} \quad (2.23)$$

Because the orbit inclinations of the three sensors are higher than 90° the processing angular velocities of their orbital plane vertical to the equatorial plane moves in the same direction as the Earth's rotation. Hence, the relative angular velocity (Ω_{RE}) on the equatorial plane of a target on the surface of the Earth in relation to the sensors' orbits is the difference between the two angular velocities, as presented in equation 2.24:

$$\Omega_{RE} = \Omega_E - \Omega_p = 7.27221 \cdot 10^{-5}\, s^{-1} \quad (2.24)$$

The velocity of a target on the surface of the Earth (V_s) located at latitude (λ) is shown in equation 2.25:

$$V_s=\Omega_E R\cos\lambda \quad (2.25)$$

R=Average radius of the Earth, 6372795 m

Consequently, the relative velocity of a target on the surface of the Earth (V_{RS}) located at latitude (λ) to the orbital plane of a sun-synchronous orbit is as shown in equation 2.26:

$$V_{RS} = \Omega_{RE} R\cos\lambda = 463.4432\cos\lambda \text{ m s}^{-1} \quad (2.26)$$

The distance (dx) covered by a target on the surface of the Earth across the equatorial plane in relation to the sensor's position after the sensor has completed a full orbit (sensor's period (P_n)), is presented in equation 2.27:

$$dx= P_n 463.4432\cos\lambda \text{ m} \quad (2.27)$$

After a number of periods (n), the relative distance on the equatorial plane between target and sensor (dx(n)), as long as it has not exceeded half of the Earth's circumference ($\pi R\cos\lambda$), would be as shown in equation 2.28:

$$dx(n)= nP_n 463.4432\cos\lambda \text{ m} \quad \text{for } dx(n) < \pi R\cos\lambda \quad (2.28)$$

Once dx(n) in equation 2.29 exceeds half of the Earth's circumference, the two objects (target and sensor) begin to move closer to each other on the equatorial plane, and their relative distance is:

$$dx(n)= \pi R\cos\lambda - nP_n 463.4432\cos\lambda \text{ m} \quad \text{for } \pi R\cos\lambda > dx(n) > 2\pi R\cos\lambda \quad (2.29)$$

And once the two objects cross each other again on the equatorial plane, their relative distance increases again. Therefore, a conditional function was developed to calculate the relative distance between sensor and target on the equatorial plane, after n number of orbits ($dx(n,\lambda)$) (equation 2.30):

$$dx(n,\lambda)=\begin{cases} nP_n 463.4432\cos\lambda - k\pi R\cos\lambda & k=even \\ 2\pi R\cos\lambda - (nP_n 463.4432\cos\lambda - (k-1)\pi R\cos\lambda) & k=odd \end{cases} \quad (2.30)$$

Where, k is the integer part of $\frac{\mathrm{nP_n}\,463.4432\cos\lambda}{\pi R\cos\lambda} = \frac{nP_n 463.4432}{\pi R}$

A sensor can scan an area equal to half of its swath width (W) from each side of its nadir point. However, because the three sensors' orbital planes are not vertical to the equatorial plane but inclined by i°, the length of their projected swath width across the equatorial plane (W_e) is:

$$W_e = W\cos(i-90) \quad (2.31)$$

Therefore, after an integer number of orbits n, if the relative distance ($dx(n,\lambda)$) between a target at latitude λ and a sensor (following a sun-synchronous orbit) on the equatorial plane is less than or equal to half of the sensor's swath width across the equatorial plane (We), then the target will be visible by the sensor. In other words, whenever the following function is satisfied, the target is visible by the sensor (equation 2.32):

$$dx(n,\lambda) \le \frac{W_e}{2} \quad \text{only for integer n numbers} \quad (2.32)$$

The temporal resolution of a sensor depends largely on the length of its swath width; however as seen in the previous section (2.3.1) the further away from the nadir point the greater the spatial resolution degradation. At the edges of the swath width the spatial resolution degradation may be too great for the data to be usable. Based on that, it was considered more appropriate that if the temporal resolutions of the sensors were to be compared then the comparison should not be done by just counting how many times each sensor views a given target within a given time, but also by setting a maximum spatial resolution threshold with which the target should be viewed with. With this in mind it

was decided to compare the temporal resolution of the sensors by counting the numbers of times each sensor views three targets at latitudes 0°, 30° and 70° within 10 days and with a maximum across-track GIFOV of 1.7 km. Three different latitudes were chosen to demonstrate the effect of latitude in temporal resolution and a 10 day period was considered a reasonable time period also frequently used for compositing NDVI data. The choice of an across-track GIFOV over an along-track GIFOV was based on the fact that the spatial resolution degradation over the same distance from the nadir is greater in the across than the along direction. As for the value of the across-track GIFOV threshold, 1.7 km was chosen partly because it was considered a fair spatial resolution for most low resolution application and partly because there were no accurate data available regarding the spatial resolution along the swath width of VEGETATION other than that the across-track GIFOV of the sensor did not exceed 1.7 km.

Within 10 days, MODIS will complete $\frac{(10)(24)(60)}{(98.5)} \approx 146$ orbits, VEGETATION $\frac{(10)(24)(60)}{(101.46)} \approx 142$ orbits and AVHRR $\frac{(10)(24)(60)}{(101.35)} \approx 142$ orbits. The equations developed in section 2.3.1 were used to calculate the swath width length of each sensor across which the maximum across-track GIFOV threshold was not exceeded; these lengths were: 1130 km, 2330 km, 1906 km, 1074 km and 2250 km for AVHRR, MODIS bands 1-2, MODIS bands 3-7, MODIS bands 8-36 and VEGETATION respectively.

For each sensor, target and number of orbits the number of times equation 2.32 was satisfied were counted. It is assumed that the initial position of each sensor is such that the sensor views the target at the nadir point; hence, all counts are increased by one to account for the first viewing. The results are displayed in table 2.12. It can be seen that the temporal resolution of the sensors is higher at higher latitudes; this is because the length of the Earth's circumference is shorter at higher latitudes. Consequently, the target with the lowest temporal resolution is the one located at the equator. If the comparison did not account for a maximum across-track GIFOV then the three sensors would likely have very similar results; as it is though, MODIS bands 1-2 had the highest temporal resolution, VEGETATION and MODIS bands 3-7 followed closely and MODIS bands 8-36 and AVHRR had the lowest. MODIS bands 1-7 and VEGETATION had

approximately half the revisit time of MODIS bands 8-36 and AVHRR over the three latitudes. However, even at 0° latitude the lowest average revisit period of the three sensors did not exceed two days, and within such a short time it is unlikely that the land cover or the vegetation condition of a study are likely change dramatically. Therefore, with such short revisit periods, the temporal resolution of the three sensors was considered unlikely to be a limiting factor in a land-cover or a drought monitoring application. It should be noted however that certain areas and particularly during certain seasons are frequently covered by clouds and in such cases the acquisition of cloud free data can be difficult. In such cases the use of MODIS bands 1-7 and VEGETATION would be advantageous due to their shorter revisit periods which in turn improves the chances of acquiring cloud free data.

Table 2.12: The number of times each target location is viewed by each sensor within 10 days and with a maximum across-track GIFOV of 1.7 km. The last three columns display the average revisit time of each sensor for the three chosen latitudes.

Sensors	**Number of orbits that viewed the target**			**Average revisit period in hours**		
Latitude	0º	30º	70º	0º	30º	70º
MODIS bands 1-2	9	11	25	26.67	21.82	9.60
MODIS bands 3-7	8	9	21	30.00	26.67	11.43
MODIS bands 8-36	5	5	12	48.00	48.00	20.00
VGT	8	10	23	26.67	24.00	10.43
AVHRR	5	6	12	48.00	40.00	20.00

2.3.3 Spectral resolution

2.3.3.1 Assessment based on the bandwidth and positioning of the sensors bands

Spectral resolution is a measure of a sensor's ability to resolve between narrow bandwidth intervals of the electromagnetic spectrum. It also refers to the range of the electromagnetic spectrum to which a sensor is sensitive.

Studies in the past have shown that the spectral resolution is a critical factor in vegetation studies; sometime more critical than the spatial resolution of the data (Gao, 1999; Thenkabail et al., 2002c). Accurate assessment of the vegetation's biophysical and biochemical properties is increased when data are available over a range of narrow wavebands (commonly referred to the contiguous range of wavelengths over which the response of a sensor's band is above half of its maximum) positioned at specific wavelengths (the optimum position may vary depending on the application), as opposed to data collected over a few and spectrally broad wavebands (Bork et al., 1999; Kumar et al., 2001). In studies carried out by Thenkabail et al., (1999, 2000, 2002a) the assessment of vegetation parameters such as the Leaf Area Index (LAI), wet biomass, dry biomass, plant height, plant nitrogen, and canopy cover was considerably more accurate when high spectral resolution data collected by Hyperion were used, as opposed to data collected by spectrally coarser Landsat-5 TM sensor. Similarly, in another study (Thenkabail et al., 2004b), high spectral resolution data (collected by Hyperion) were proven to be more successful in estimating vegetation biomass and classifying forested areas than spectrally broader data collected by IKONOS, Advanced Land Imager (ALI), and Enhanced Thematic Mapper Plus (ETM+). The improved performance of high spectral resolution data (Hyperion) in land-cover classification against coarser spectral resolution data (ETM) was further demonstrated by Thenkabail et al., (2002b, 2004c). Several authors support the advantages of data collected by specific and narrow wavebands for vegetation studies. Examples include measurements of photosynthetically active radiation (PAR) (Wiegard, 1991), biomass estimation (Friedl et al., 1994), LAI (Blackburn, 1999; Broge and Leblanc, 2000; Elvidge and Chen, 1995; Friedl et al., 1994), photosynthetic pigment concentration (Blackburn and Steele, 1999; Blackburn,1999; Broge and Leblanc, 2000),

percent green vegetation cover (Elvidge and Chen, 1995; McGwire et al., 2000), vegetation stress (Carter, 1994, 1998;), biochemical content of plants (Curran, 1994), change detection (Elvidge et al., 1993; Lyon et al., 1998), plant water content (Bauer et al., 1981; Penuelas et al., 1995), and land-cover classification accuracies (Janetos and Justice, 2000).

The majority of data regarding the biophysical and biochemical properties of vegetation are collected over certain wavebands; data collected beyond these wavebands are largely redundant (Blackburn, 1998; Broge and Leblanch. 2000; Carter, 1998; Schott J.R., 1997; Thenkabail et al., 2002b, 2002c, 2004b). For instance, Thenkabail et al., 2004b achieved better land-cover classification accuracies with the addition of more narrow wavebands within the 400 nm to 2500 nm range; however, beyond 22 critical wavebands, additional bands helped increase the classification accuracy only marginally and no further improvement in classification accuracy was achieved when more than 30 bands were used.

It is possible that data collected over spectrally broad wavebands are less effective in measuring biophysical and biochemical vegetation properties (and consequently less accurate at distinguishing between vegetation classes or assessing vegetation stress), than data collected over spectrally narrow wavebands; because, it is likely that the information content of their collected data is reduced due to averaging over a broader range of wavelengths. Averaging over broader wavebands could result in loss of information content either because data are averaged over spectral regions which are both critical and redundant for vegetation monitoring, or because even if the data were averaged only over critical spectral regions (for vegetation monitoring), an averaged value would contain less information than a series of values over critical spectral regions.

Additionally, the broader a waveband is the higher the possibility it will include spectral regions within its waveband over which the contribution of atmospheric effects (such as scattering and absorption) to the data collected by a sensor is considerable. In such cases, the collected data would not simply reflect vegetation properties but also the molecular and particle content of the atmosphere (mainly aerosols, water vapour, O_3, and CO_2). Atmospheric effects can be removed with various atmospheric correction processes; however these processes often require information that may not always be

available or accurately measured, and as a result the atmospheric correction is often only partially successful. Therefore, data collected over spectrally broader wavebands are more likely to be atmospherically contaminated and potentially result in inaccurate assessments of vegetation parameters.

Past research has identified the red and NIR as two of the most important spectral regions where information for vegetation studies are collected (Collins, 1978; Horler et al., 1983; Townshend and Justice, 1988). Radiation is absorbed by chlorophyll pigments inside the plants over the red region, and reflected by spongy mesophyll cells over the NIR region (Curran 1985; Liang, 2004; Rees 2001). More recent studies have also recognised the importance of data collected over the MIR region in measuring biophysical parameters of vegetation such as water, protein content, LAI, biomass, and height (Blackburn, 1998, 1999; Boyd and Duane, 2001; Braswell et al., 2003; Jakubauskas and Price 1997; Jensen, 2000; Kumar et al., 2001; Lambert et al., 1995; Saint, 1995; Thenkabail et al., 1995, 2002b, 2004b). Research has also pointed out the contribution of data collected over the blue spectral region in determining the carotenoid content of plants (Blackburn, 1999) as well as their ageing and browning conditions (Thenkanbail et al., 1999b, 2000). Some of the most critical wavebands for vegetation studies within the visible, NIR, and MIR regions (according to the literature) are displayed in table 2.13. Finally, although usually overlooked, data collected over the TEBs have been successfully used to improve vegetation assessment in applications such as drought monitoring (Dabrowska-Zielinska et al., 2002; Kogan 1995a, 1997; Seiler et al., 1998; Thenkabail et al., 2004a; Unganai and Kogan 1998) and land-cover classification (Lambin and Ehrlich, 1996a, 1996b; Liang, 2001; Nemani and Running, 1995; Nemani et al., 1993; Running et al., 1995).

Table 2.13: Wavelengths of importance for vegetation studies and their role

Waveband	Region	Importance
0.470 μm	Blue	Sensitive to carotenoid content (Blackburn, 1999)
0.495-0.499 μm	Blue	Sensitive to ageing and browning conditions (Thenkanbail et al., 1999b,2000)
0.555 μm	Green	Maximum reflectance peak in the visible region, sensitive to chlorophyll content (Blackburn, 1999; Thenkanbail et al., 2002b)
0.611 μm	Red	Sensitive to biomass and LAI (Thenkanbail et al., 2004b)
0.635 μm	Red	Sensitive to chlorophyll b (Blackburn, 1999)
0.670 μm	Red	Maximum absorption region for chlorophyll a (Gitelson and Merzlyak, 1996)
0.675 μm	Red	Maximum absorption area for most vegetation species due to chlorophyll a and b, sensitive to biomass and LAI (Blackburn, 1998)
0.680 μm	Red	Sensitive to chlorophyll a (Blackburn, 1999)
0.692 μm	Red	Sensitive to growth conditions, biomass and LAI (Thenkabail et al., 2004b)
0.722 μm	Red-edge	Sensitive to vegetation stress and structure, but resilient to soil background and atmospheric noise/radiation contribution (Baret et al., 1992; Dawson and Curran, 1998; Demetriades-Shah, 1990; Elvidge and Chen, 1995; Mauser and Bach, 1995)
0.783 μm	NIR	Sensitive to chlorophyll content (Curran et al., 1992)
0.845 μm	NIR	Sensitive to chlorophyll content (Schepers et al., 1996)
0.895 μm	NIR	Reflectance peak for most vegetation species, sensitive to biomass , chlorophyll and protein content (Thenkabail et al., 2000, 2002a)
0.943 μm	NIR	Absorption area due to vegetation water content (Thenkabail et al., 2004b)
0.970-0.980 μm	NIR	Sensitive to vegetation water content (Thenkabail et al., 2002a; Penuelas et al., 1993)
1.054 μm	NIR	Sensitive to vegetation water content (Thenkabail et al., 2004b)
1.094 μm	NIR	Sensitive to biomass and LAI (Thenkabail et al., 2004b)
1.104 μm	NIR	Sensitive to biomass and LAI (Thenkabail et al., 2004b)
1.145 μm	NIR	Sensitive to biomass and water content (Thenkabail et al., 2004b)
1.215 μm	NIR	Sensitive to vegetation water content (Thenkabail et al., 2004b)
1.285 μm	NIR	Sensitive to biomass and LAI (Thenkabail et al., 2004b)
1.467 μm	MIR	Sensitive to starch, lignin, cellulose and water content (Thenkabail et al., 2004b)
1.518 μm	MIR	More sensitive to changes in water content than NIR wavebands (Jensen, 2000)
1.659 μm	MIR	Sensitive to biomass, starch, lignin and assists the discrimination of leaf types (Gausman, 1973)
1.710 μm	MIR	Sensitive to starch and changes in water content (Jensen, 2000; Kumar et al., 2001)
2.022 μm	MIR	Sensitive to water content (Thenkabail et al., 2004b)
2.052 μm	MIR	Sensitive to water content and protein (Kumar et al., 2001; Olson, 1967)
2.050-2.140 μm	MIR	Lignin absorption area (Kumar et al., 2001)
2.264 μm	MIR	Sensitive to water content changes (Jensen, 2000)
2.315 μm	MIR	Sensitive to water content, lignin, starch and stress (Thenkabail et al., 2004b)

Tables 2.1, 2.5 and 2.7 display the spectral bands of AVHRR, MODIS and VEGETATION respectively. Just a quick glance at the tables reveals that MODIS is equipped with a lot more bands than the other two sensors. However, not all of them are intended for studies over land. The SRBs primarily designed for studies over land are bands 1 to 7; the remaining SRBs (8-19, and 26) were designed for oceanographic and atmospheric studies. Bands 8 to 16 were designed to be more responsive (higher calibration gain) to radiation than bands intended for land studies, because water bodies tend to reflect significantly less radiation over the visible and NIR spectral regions than vegetation or generally most land surfaces do. As a result, some of these SRBs may become saturated when measuring radiation over land surfaces. Two such SRBs likely to get saturated over land are the red bands 13 and 14, particularly when taking measurements at their high gain mode (these bands were designed in a way that they measure radiation at two different modes, a high gain mode and a low gain one). The NIR bands 15 to 19 may become saturated too, because vegetation strongly reflects NIR radiation as opposed to water bodies which largely absorb it. Over land surfaces the primary red and NIR bands of MODIS are its first and second bands, respectively.

MODIS red band (1^{st}) compared to that of VEGETATION or AVHRR, is narrower and more closely positioned to the red absorption regions (mostly sensitive in the 0.650-0.670 μm region, figure 2.9) where reflectance values over vegetation are correlated to chlorophyll content, LAI, and biomass (Blackburn, 1998, 1999; Curran et al., 1992; Gitelson and Merzlyak, 1996). As for MODIS NIR band (2^{nd}) it is also narrower and closer to the NIR reflectance peak region of most vegetation (mostly sensitive in the 0.850-0.880 μm region, figure 2.10) than the NIR bands of AVHRR or VEGETATION. Additionally, MODIS NIR band unlike that of AVHRR or VEGETATION does not encompass the wavelength regions where atmospheric absorption due to water and O_2 occurs (Clark et al., 1993; Heidinger et al., 2002b). MODIS is also equipped with narrower and more numerous (5, 6 and 7) bands in the MIR region than either AVHRR (3a) or VEGETATION (SWIR). In the blue region which is sensitive to vegetation senescing, browning and carotenoid content, MODIS also has narrower and more numerous bands (3, 8, 9, 10) than VEGETATION which has a single band (B0) or AVHRR which has none. MODIS is also equipped with green bands (4, 11 and 12)

which are sensitive to the chlorophyll content of vegetation (Blackburn, 1999; Thenkanbail et al., 2002b) as opposed to VEGETATION or AVHRR which have none. Finally in terms of TEBs which can improve the detection of cloud contaminated data in land-cover mapping and drought monitoring, MODIS again has narrower and more numerous bands than AVHRR which has 2 during day-time and 3 during night-time or VEGETATION which has none. It would therefore be expected that in terms of spectral resolution, data collected by MODIS over vegetated areas are more likely to help produce a more accurate assessment of the vegetation's biochemical and biophysical properties than data collected by AVHRR or VEGETATION.

As far as VEGETATION and AVHRR are concerned, VEGETATION's most sensitive region in the red spectral region is narrower and closer to the red absorption region of plants (the band is most sensitive in the 0.660-0.690 μm region, figure 2.9) than that of AVHRR (mostly sensitive in the 0.590-0.680 μm region, figure 2.9) which also encompasses part of the green spectral region. Moreover, VEGETATION's red band is also moderately sensitive to the red-edge spectral region where a rapid increase of reflectance values is observed over vegetated targets, the values of which are indicative of vegetation stress and structure (Baret et al., 1992; Dawson and Curran, 1998; Demetriades-Shah, 1990; Elvidge and Chen, 1995; Mauser and Bach, 1995). VEGETATION's NIR band is also narrower than the AVHRR respective band and unlike AVHRR it is not as sensitive to the spectral region between 940 nm and 1000 nm where atmospheric absorption due to water vapour occurs (Tanre et al., 1992) (figure 2.10). The SWIR band of VEGETATION although broader than that of AVHRR, is however, sensitive to important spectral regions for vegetation studies such as the 1.659 nm and 1.710 μm (Gausman, 1973; Jensen, 2000; Kumar et al., 2001) where the AVHRR SWIR band is not. And finally, both sensors are equipped with spectral bands that the other does not have; AVHRR is equipped with TEBs and VEGETATION with a band in the blue spectral region. Nevertheless the red, NIR and SWIR spectral regions are more important for vegetation studies than the blue or the thermal emissive regions. Thus, VEGETATION spectral resolution is likely to be better than that of AVHRR for vegetation studies due to the fact that its red, NIR and SWIR bands are better positioned and narrower (for the red and NIR bands) than those of AVHRR.

2.3.3.2 Assessment based on the simulated values of the sensors' red and NIR bands

In addition to the theoretical assessment of the sensors' ability to monitor vegetation based on the positioning and bandwidth of their spectral bands, it was decided to quantitatively assess the capacity of sensors' red and NIR bands in discriminating between targets of different land cover and NDVI values, based on the simulated values of the sensors' red and NIR band response when viewing a series of different land cover classes/targets. The simulation was limited particularly to the red and NIR bands because these were considered as two of the most important spectral regions for land-cover classification studies, and also because these two bands are necessary for the calculation of the NDVI, which in turn is necessary for the implementation of some of the most established drought monitoring methodologies, such as the VPI and VCI.

Ideally, the response of the red and NIR bands of the sensors should be simulated for a wide range of targets, and the simulation of the sensors' red and NIR bands over each target should be based on hyperspectral data across the bands' bandwidth collected over a representative sample of the target. However such hyperspectral data were not available, instead what was available was a single hyperspectral measurement over eight different land cover classes frequently found in UK land cover classifications, namely:

- Winter barley
- Sugar beet
- Forest
- Pasture
- Winter wheat
- Bare soil
- Winter oil seed rape (OSR)
- Urban

The hyperspectral reflectance R(λ) data (figure 2.8) were provided by a colleague (Dr. Graham Thomas) and were collected by the HyMap sensor for the needs of a different project. HyMap is equipped with 128 bands each of which has a bandwidth between 15-20 nm, and all together provide a contiguous cover of the spectral region

between 0.45-2.5 μm (HyVista, 2007). The sensor was mounted on an aircraft and flown over sites covered by the eight land cover classes/targets. The reflectance values collected were not atmospherically corrected; hence, the atmospheric contribution was also accounted for. Although the available hyperspectral data were not ideal for the purpose of simulating the response of the red and NIR bands of the sensor over a wide range of targets, it was decided to proceed with the simulation as its purpose was merely to provide an indicative measure against the theoretical assessment of the sensors' spectral resolution.

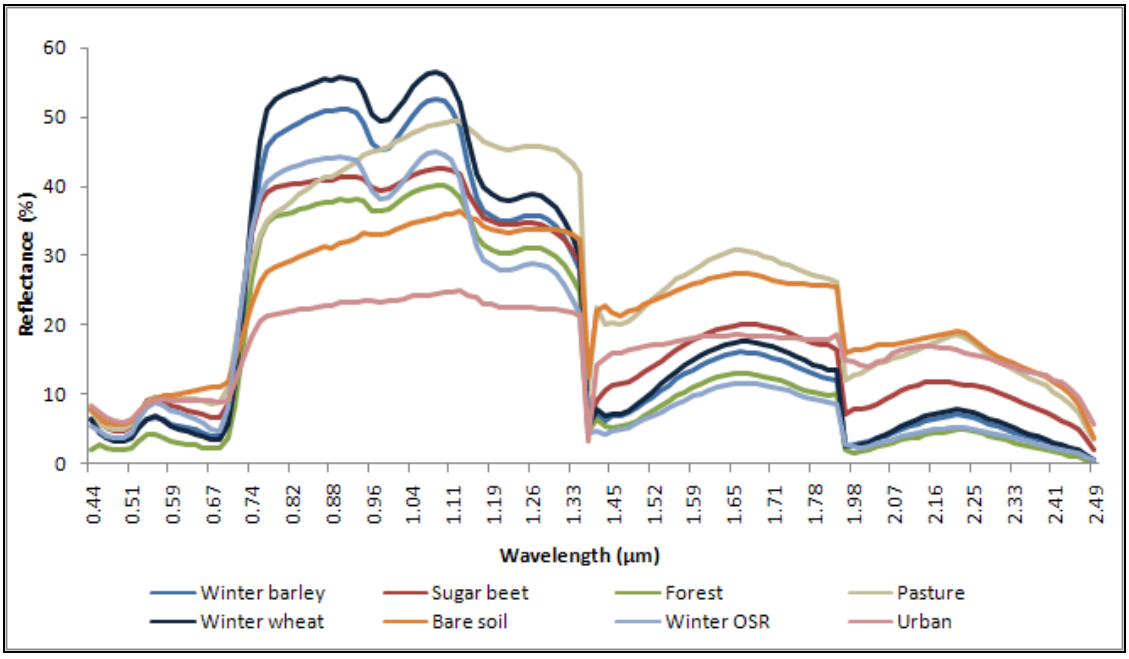

Figure 2.8: The spectral profiles of the eight selected land-cover types, collected by HyMap.

The following assumptions were made for the simulation, to simplify the process and permit the comparison of the sensors under the same conditions:

- All the targets are viewed by all sensors at the same time
- Same atmospheric path for all sensors (same atmospheric effects)
- Targets have Lambertian surfaces
- No radiometric resolution limitations
- Sensors are perfectly calibrated

The radiance (I) value recorded by a sensor when receiving radiation reflected by a target over the red or NIR region, under the above assumptions, would depend on i) the sensor's normalised spectral response $\Phi(\lambda)$ over the red or NIR region, and ii) the spectral radiance reaching the sensor from the target across the sensor's red or NIR bandwidth $I(\lambda)$.

The spectral response curves of the sensors over their red and NIR bands are provided by the sensors' manufacturers, and are displayed in figures 2.9 and 2.10. It can be seen that the sensors' response is not constant across their bandwidth; it is low across the edges, and high near the centre.

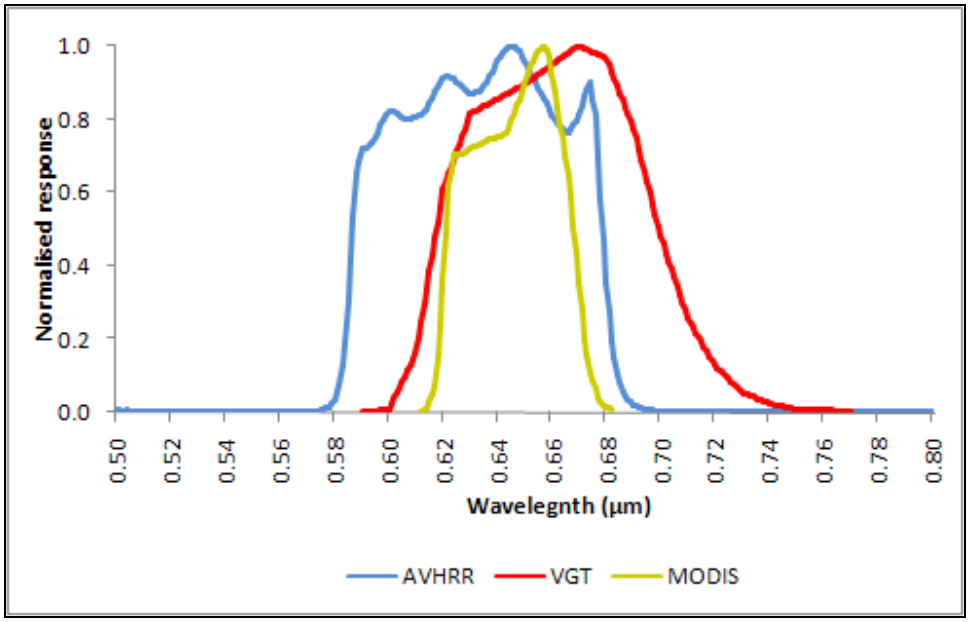

Figure 2.9 (NASA, 2003; Goodrum et al., 2000; SPOT-VEGETATION, 2006;): The spectral response curves of the red bands of AVHRR, VEGETATION, and MODIS (band 1)

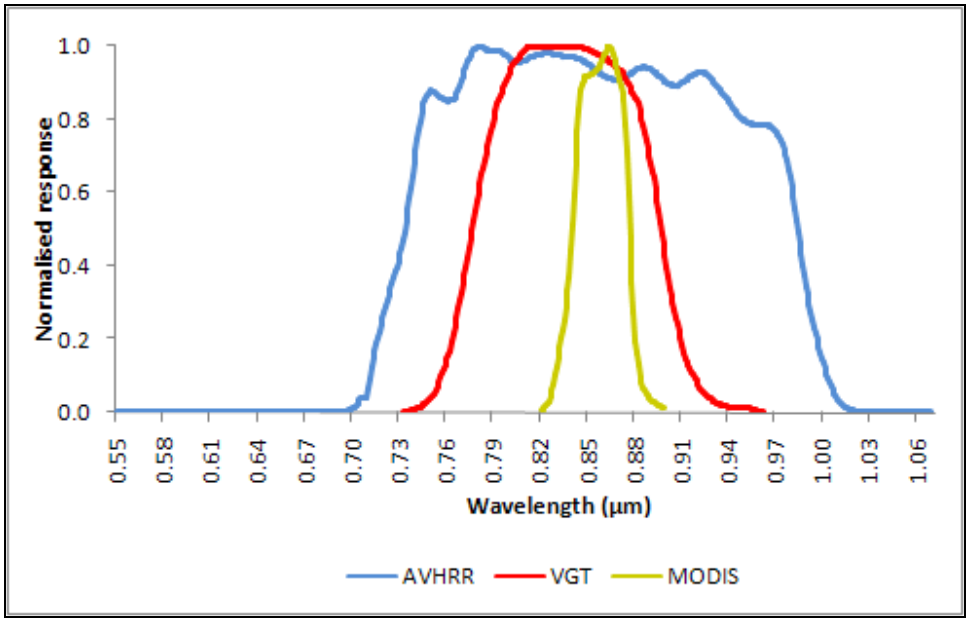

Figure 2.10 (NASA, 2003; Goodrum et al., 2000; SPOT-VEGETATION, 2006): The spectral response curves of the NIR bands of AVHRR, VEGETATION and MODIS (band 2)

The spectral radiance I(λ) reaching the sensor over its bandwidth depends, i) on the extraterrestrial solar irradiance (Iex(λ)) reaching the Earth across the sensor bandwidth, ii) the target's reflectance R(λ) values across the sensor bandwidth, iii) the atmospheric contribution over the sensor bandwidth, iv) the solar zenith angle (Z), and v) the Earth-Sun distance (D), as seen in equation 2.33.

$$I(\lambda) = \frac{\mathrm{R}(\lambda)\mathrm{Iex}(\lambda)\cos Z}{D^2 100\pi} \tag{2.33}$$

The extraterrestrial solar irradiance (Iex(λ)) reaching the Earth across the sensor bandwidth were found in the literature (Neckel and Labs, 1984). The solar zenith angle (Z) which is the angle between the Zenith of a target and the position of the sun, depends on the location of the target and the reception time. The Earth-Sun distance (D) depends on the orbit of the Earth around the Sun and can be calculated in Astronomical Units (AU) based on the number of days which have elapsed since the first day of the last January (Julian day (J)), as presented in equation 2.34:

$$D=1-0.01672\cos(0.9856(J-4)) \tag{2.34}$$

The spectral radiance (I) recorded by the sensor would be as seen in equation 2.35:

$$I = \frac{\int_{\lambda \min}^{\lambda man} d\lambda \varphi(\lambda) I(\lambda)}{\int_{\lambda \min}^{\lambda man} d\lambda \varphi(\lambda)} \tag{2.35}$$

Consequently, the reflectance value (Rt) of each target according to each sensor can be calculated as in equation 2.36:

$$Rt = \frac{\mathrm{ID}^2 100\pi}{Iex \cos Z} \tag{2.36}$$

Where Iex is the sensor's band spectral extraterrestrial solar irradiance shown in equation 2.37:

$$Iex = \frac{\int_{\lambda \min}^{\lambda man} d\lambda \varphi(\lambda) Iex(\lambda)}{\int_{\lambda \min}^{\lambda man} d\lambda \varphi(\lambda)} \tag{2.37}$$

The above equations were used to simulate the reflectance values of each target over the red and NIR bands of each sensor. The calculations were done using $d\lambda$ increments equal to the increments of the provided sensors' response data. When the required Iex(λ) or R(λ) values were not available for certain wavelengths, they were calculated by linearly interpolating between the two closest known values. The values of the Julian date and zenith solar angle were selected without much consideration, because provided that the same values were used for the calculation of all sensors' simulated data, all simulated data would be equally affected by them; their values were chosen to be 135 and 30º respectively.

The results of the simulation are displayed in figures 2.11 to 2.14. Figures 2.11 and 2.12 display the radiance values. Figures 2.13 and 2.14 display the reflectance values of each sensor for each target.

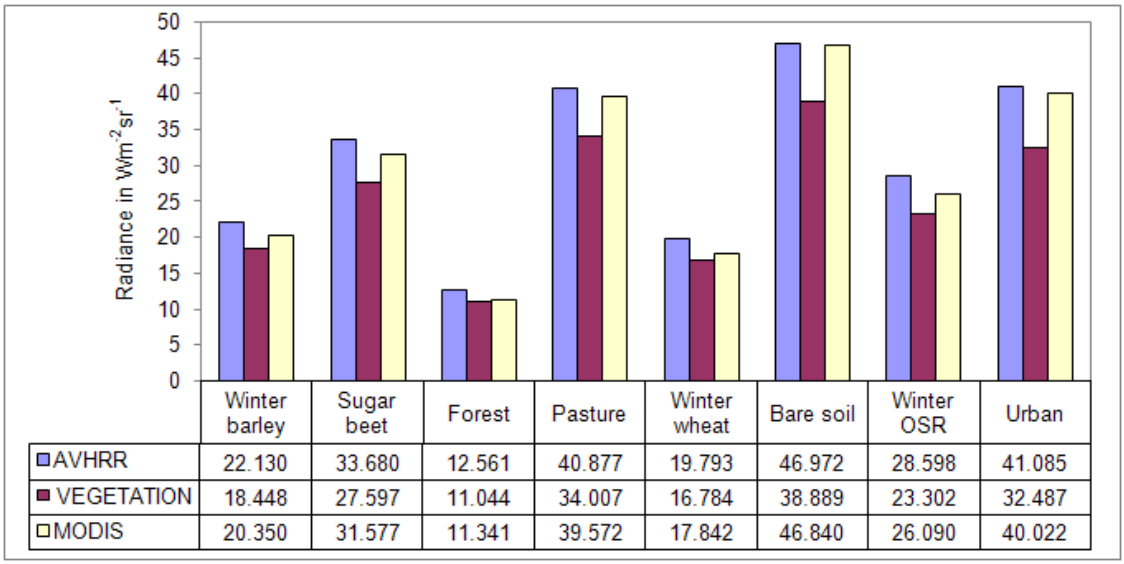

	Winter barley	Sugar beet	Forest	Pasture	Winter wheat	Bare soil	Winter OSR	Urban
AVHRR	22.130	33.680	12.561	40.877	19.793	46.972	28.598	41.085
VEGETATION	18.448	27.597	11.044	34.007	16.784	38.889	23.302	32.487
MODIS	20.350	31.577	11.341	39.572	17.842	46.840	26.090	40.022

Figure 2.11: The simulated radiance values which the AVHRR, VEGETATION and MODIS red bands would have recorded when viewing the eight land-cover targets.

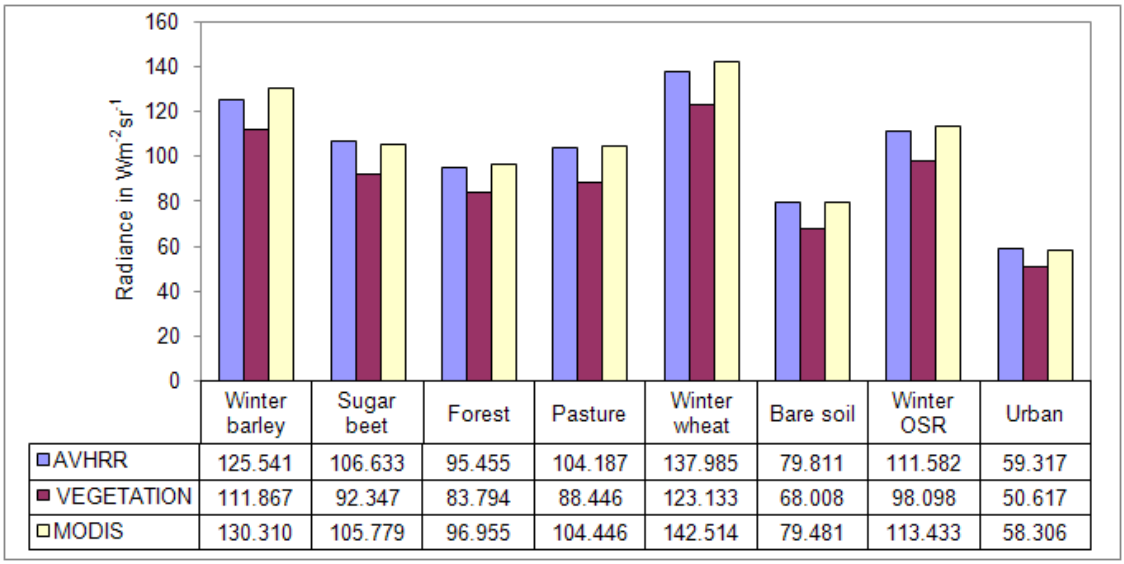

	Winter barley	Sugar beet	Forest	Pasture	Winter wheat	Bare soil	Winter OSR	Urban
AVHRR	125.541	106.633	95.455	104.187	137.985	79.811	111.582	59.317
VEGETATION	111.867	92.347	83.794	88.446	123.133	68.008	98.098	50.617
MODIS	130.310	105.779	96.955	104.446	142.514	79.481	113.433	58.306

Figure 2.12: The simulated radiance values which the AVHRR, VEGETATION and MODIS NIR bands would have recorded when viewing the eight land-cover targets.

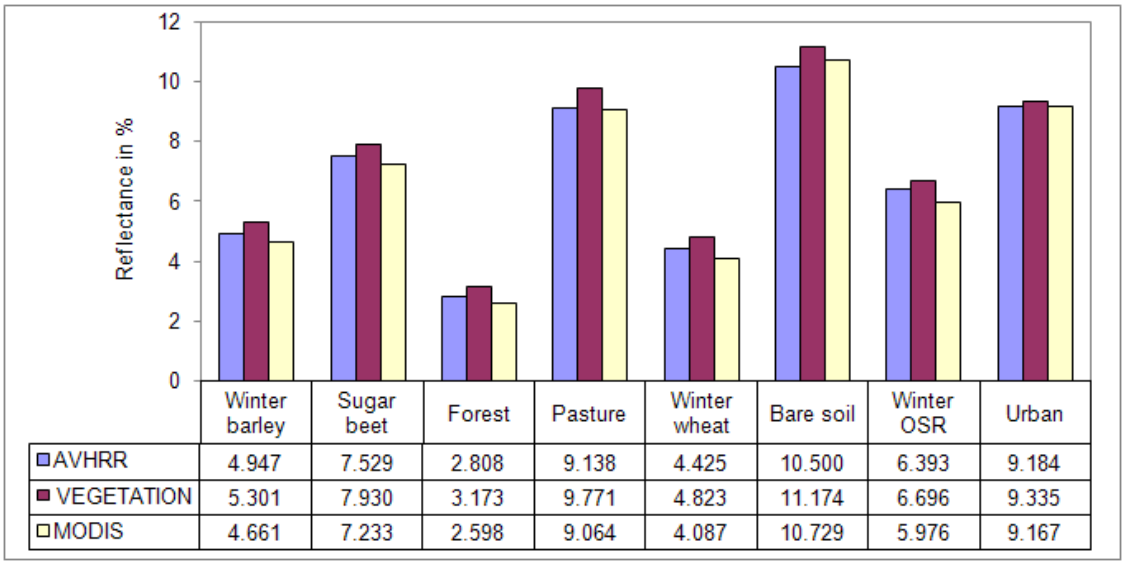

	Winter barley	Sugar beet	Forest	Pasture	Winter wheat	Bare soil	Winter OSR	Urban
AVHRR	4.947	7.529	2.808	9.138	4.425	10.500	6.393	9.184
VEGETATION	5.301	7.930	3.173	9.771	4.823	11.174	6.696	9.335
MODIS	4.661	7.233	2.598	9.064	4.087	10.729	5.976	9.167

Figure 2.13: The simulated reflectance values of AVHRR, VEGETATION and MODIS red bands for each of the eight different land-cover classes.

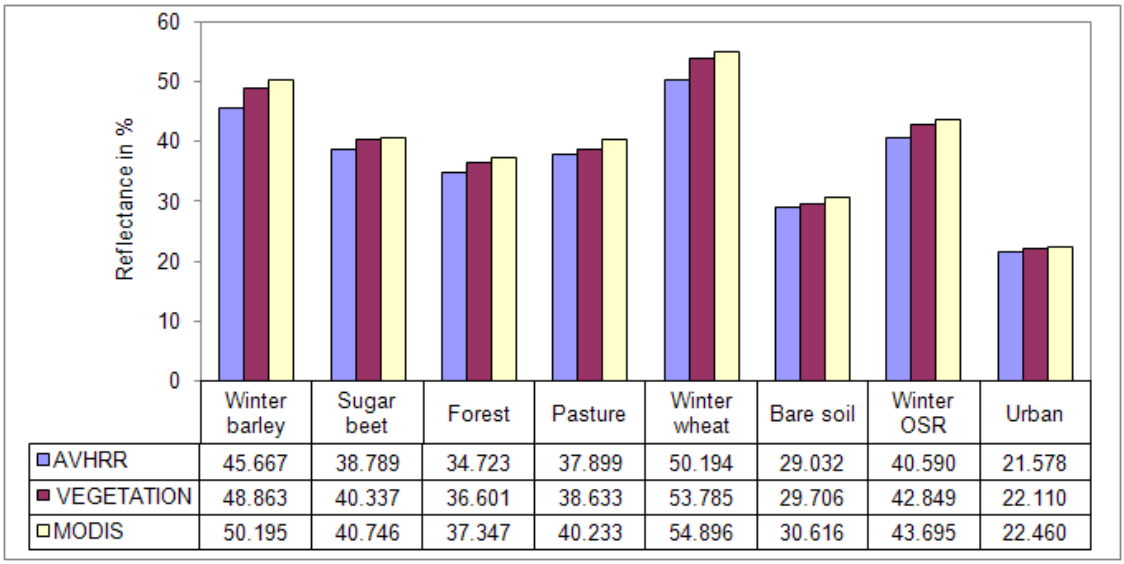

	Winter barley	Sugar beet	Forest	Pasture	Winter wheat	Bare soil	Winter OSR	Urban
AVHRR	45.667	38.789	34.723	37.899	50.194	29.032	40.590	21.578
VEGETATION	48.863	40.337	36.601	38.633	53.785	29.706	42.849	22.110
MODIS	50.195	40.746	37.347	40.233	54.896	30.616	43.695	22.460

Figure 2.14: The simulated reflectance values of AVHRR, VEGETATION and MODIS NIR bands for each of the eight different land-cover classes.

It can be seen from figure 2.13 that the lowest simulated reflectance values over the red band were recorded by MODIS. This was expected because MODIS red band is mostly sensitive to the spectral region where the maximum absorption of radiation over the red spectrum by plants is usually observed. On the other hand, the highest simulated reflectance values over the red band were recorded by VEGETATION; this is because although VEGETATION is more sensitive to the maximum absorption red region than AVHRR, it is also moderately sensitive to the red-edge region unlike AVHRR. Reflectance values over vegetation in the red-edge region are much higher than the ones recorded in the visible region, including the green region. Therefore, although VEGETATION is only moderately sensitive to the red-edge region, the high reflectance values recorded over that region contribute significantly to the overall reflectance value recorded by its red band.

Over the NIR bands, the highest simulated reflectance values were recorded by MODIS; this also came to no surprise, as MODIS NIR band is mostly sensitive to the spectral region where the maximum reflectance values are recorded over vegetation over the NIR region. Similarly, VEGETATION simulated reflectance values over its NIR band were higher than those of AVHRR because VEGETATION NIR band is narrower and more centred to the spectral region, where the maximum reflectance values over vegetation in the NIR region are recorded.

Since MODIS simulated reflectance values over the red and NIR region were the lowest and highest respectively, compared to those of AVHRR or VEGETATION when viewing the same vegetated target, it would then be expected that, for the same vegetated target it would also record the highest NDVI value. As for VEGETATION and AVHRR, their NDVI values may be closer together because AVHRR records lower and higher reflectance values over the red and NIR bands respectively than the respective values recorded by VEGETATION. The above assessments are verified by the calculation of the NDVI values, displayed in figure 2.15.

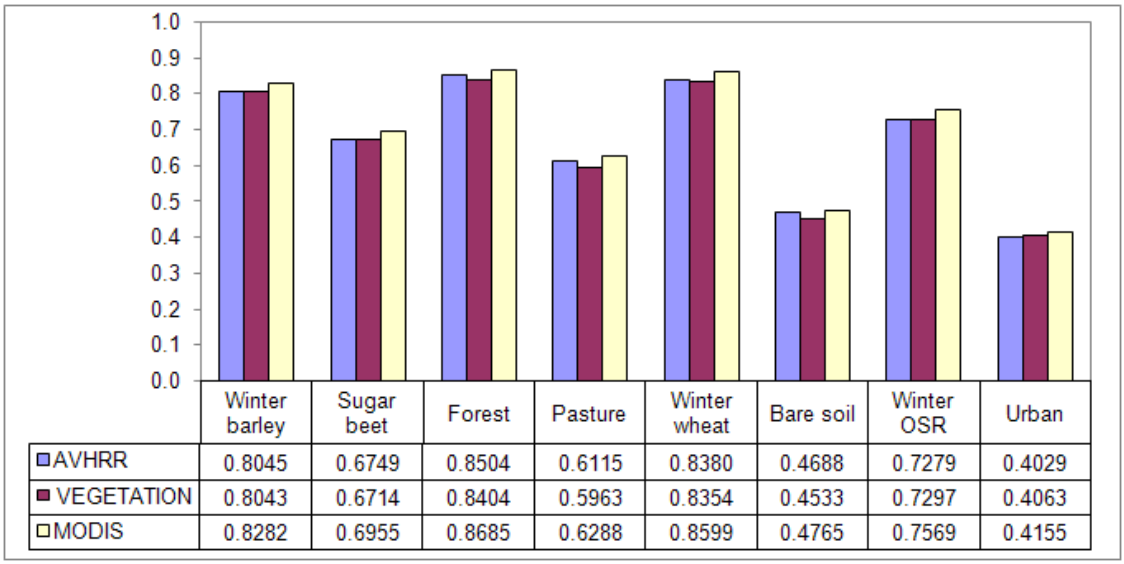

	Winter barley	Sugar beet	Forest	Pasture	Winter wheat	Bare soil	Winter OSR	Urban
AVHRR	0.8045	0.6749	0.8504	0.6115	0.8380	0.4688	0.7279	0.4029
VEGETATION	0.8043	0.6714	0.8404	0.5963	0.8354	0.4533	0.7297	0.4063
MODIS	0.8282	0.6955	0.8685	0.6288	0.8599	0.4765	0.7569	0.4155

Figure 2.15: The NDVI values of the eight different land-cover classes based on the simulated reflectance values of the AVHRR, VEGETATION and MODIS red and NIR bands.

However, the simulated reflectance values of the sensors' red and NIR bands do not clearly depict the sensors' relative ability to distinguish between different land cover classes. Normally a measure such as the Jeffries-Matusita (JM) or the Mahalanobis distance would be used to measure spectral separability; however, these measures require a sample of measurements over each target and the available hyperspectral data only allowed the simulation of one measurement over each target per sensor. Hence a different measure was needed, towards this goal a point was plotted for every target and sensor on a Cartesian system with x and y axis being the target's simulated reflectance values of the red and NIR bands respectively (figure 2.16). The closer together two points of the same sensor are plotted, the more similar the data collected by the sensor over its red and NIR bands for the two land cover classes are, and vice versa. Dissimilarity of data collected by a sensor for different targets is desirable, because without it different land-cover classes would not be able to be distinguished. The dissimilarity of data collected by a sensor over different targets can be assessed by measuring the Euclidean distance between their respective points on the Cartesian system. The Euclidean distance (d) between two points A and B in a two-dimensional space is (equation 2.38):

$$d(A,B) = \sqrt{(X_A - X_B)^2 + (Y_A - Y_B)^2} \quad (2.38)$$

The Euclidean distances between all the land-cover target pairs for each sensor based on their simulated reflectance values are displayed in table 2.14. MODIS simulated reflectance values achieved the highest Euclidean distance in 19 out of the total 28 land-cover target pairs; seven were achieved by VEGETATION; and the remaining two by AVHRR. Thus, data collected by MODIS red and NIR bands would overall be more successful in discriminating between the eight target classes in a land-cover classification, followed by VEGETATION and then AVHRR.

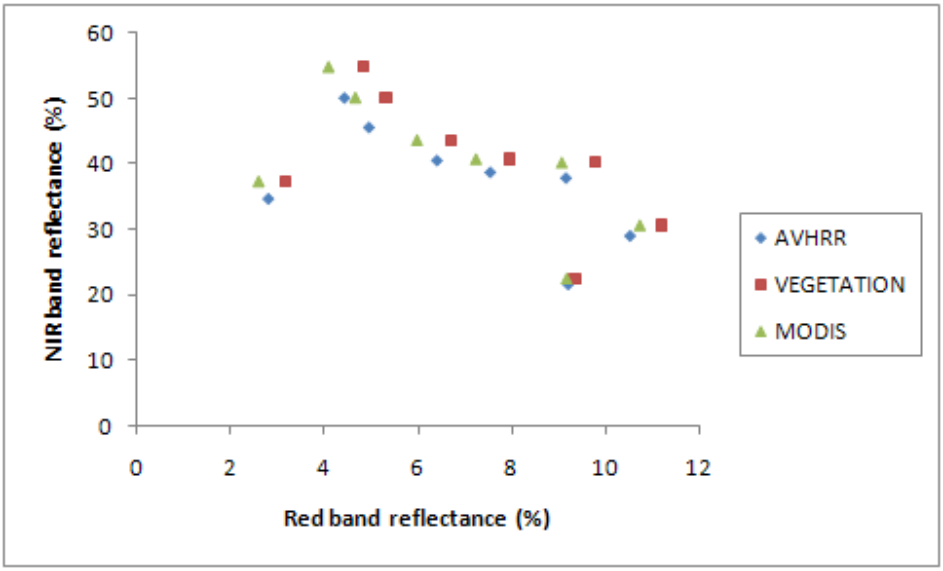

Figure 2.16: The eight different land-cover classes of each sensor plotted on a Cartesian system with x and y axes being the simulated reflectance values of the red and NIR bands respectively

Table 2.14: Euclidean distances between every land cover class pair and sensor. Higher Euclidean distances suggest greater ability to distinguish between the respective land-cover class pair.

Land cover class pairs	AVHRR	VEGETATION	MODIS
Winter barley/Sugar beet	7.347	8.922	9.793
Winter barley/ Forest	11.151	12.445	13.013
Winter barley/ Pasture	8.826	11.164	10.892
Winter barley/ Winter wheat	4.557	4.944	4.736
Winter barley/ Bare soil	17.537	20.038	20.498
Winter barley/ Winter OSR	5.279	6.174	6.632
Winter barley/ Urban	24.460	27.056	28.099
Sugar beet/ Forest	5.263	4.926	5.097
Sugar beet/ Pasture	6.788	7.724	8.477
Sugar beet/ Winter wheat	7.100	8.204	8.119
Sugar beet/ Bare soil	6.581	7.061	7.276
Sugar beet/ Winter OSR	13.357	14.663	15.139
Sugar beet/ Urban	11.274	12.524	10.198
Forest/ Pasture	7.082	6.904	7.081
Forest/ Winter wheat	15.555	17.262	17.612
Forest/ Bare soil	9.568	10.562	10.556
Forest/ Winter OSR	6.875	7.172	7.191
Forest/ Urban	14.610	15.747	16.273
Pasture/ Winter wheat	13.167	15.939	15.486
Pasture/ Bare soil	8.971	9.037	9.759
Pasture/ Winter OSR	3.843	5.219	4.639
Pasture/ Urban	16.322	16.529	17.773
Winter wheat/ Bare soil	22.016	24.902	25.172
Winter wheat/ Winter OSR	9.804	11.094	11.360
Winter wheat/ Urban	29.009	31.995	32.832
Bare soil/ Winter OSR	12.265	13.886	13.915
Bare soil/ Urban	7.570	7.816	8.305
Winter OSR/ Urban	19.216	20.907	21.473

Drought monitoring methodologies like the VCI and the VPI rely upon monitoring NDVI values of vegetated areas through time, and associate any abnormally low NDVI values (for the time of year and study area) to drought-related vegetation stress. The correct and early detection of drought conditions based on these methods is related to the responsiveness of the collected and analysed NDVI data to changes to the biophysical and biochemical properties of vegetation; the more responsive the NDVI the better. In order to quantitatively assess the responsiveness of each sensor's NDVI values to biophysical and biochemical vegetation changes, the response of the sensors' red and

NIR bands should be simulated and assessed in conjunction with meteorological data over a period ideally several decades long. Unfortunately, HyMap reflectance data upon which the sensors' response simulation relied were only available for a single date. Nevertheless, due to the fact that each land-cover target has different biophysical and biochemical properties, the relative NDVI responsiveness of each sensor to different biophysical and biochemical properties could be indicated by the difference in NDVI values between different land-cover targets for each sensor. The sensor that would have NDVI data demonstrating the highest NDVI value difference between different land-cover target pairs compared to the NDVI data of the other sensors, would likely be more responsive to different biophysical and biochemical vegetation properties.

Table 2.15: Absolute NDVI value difference between land-cover class pairs and sensors.

Land cover class pairs	AVHRR	VEGETATION	MODIS	Highest NDVI difference achieved by
Winter barley/Sugar beet	0.130	0.133	0.132	VEGETATION
Winter barley/Forest	0.046	0.036	0.040	AVHRR
Winter barley/Pasture	0.193	0.208	0.198	VEGETATION
Winter barley/Winter wheat	0.033	0.031	0.031	AVHRR
Winter barley/Bare soil	0.336	0.351	0.349	VEGETATION
Winter barley/Winter OSR	0.077	0.075	0.071	AVHRR
Winter barley/Urban	0.402	0.398	0.410	MODIS
Sugar beet/Forest	0.175	0.169	0.171	AVHRR
Sugar beet/Pasture	0.063	0.075	0.066	VEGETATION
Sugar beet/Winter wheat	0.163	0.164	0.163	VEGETATION
Sugar beet/Bare soil	0.206	0.218	0.217	VEGETATION
Sugar beet/Winter OSR	0.053	0.058	0.061	MODIS
Sugar beet/Urban	0.272	0.265	0.278	MODIS
Forest/Pasture	0.239	0.244	0.238	VEGETATION
Forest/Winter wheat	0.012	0.005	0.009	AVHRR
Forest/Bare soil	0.382	0.387	0.389	MODIS
Forest/Winter OSR	0.123	0.111	0.111	AVHRR
Forest/Urban	0.447	0.434	0.450	MODIS
Pasture/Winter Wheat	0.227	0.239	0.229	VEGETATION
Pasture/Bare soil	0.143	0.143	0.151	MODIS
Pasture/Winter OSR	0.116	0.133	0.127	VEGETATION
Pasture/Urban	0.209	0.190	0.212	MODIS
Winter wheat/Bare soil	0.369	0.382	0.380	VEGETATION
Winter wheat/Winter OSR	0.110	0.106	0.102	AVHRR
Winter wheat/Urban	0.435	0.429	0.441	MODIS
Bare soil/Winter OSR	0.259	0.276	0.278	MODIS
Bare soil/Urban	0.066	0.047	0.061	AVHRR
Winter OSR/Urban	0.325	0.323	0.339	MODIS

The NDVI absolute value difference for each land-cover target pair and sensor was calculated and is displayed in table 2.15. Both MODIS and VEGETATION recorded the highest NDVI value difference for 10 land-cover target pairs, and AVHRR in the remaining eight. As a side note, its is interesting to notice that in the majority of cases when the highest NDVI value difference between land-cover class pairs was recorded for MODIS data, the land-cover class pair involved were a vegetated and a non/sparsely vegetated class (Urban or Bare soil), suggesting that MODIS NDVI data may be particularly effective at discriminating between such land-cover classes. It is also worth noting, that the forest, winter barley and winter wheat classes all had similar NDVI values (figure 2.15) and subsequently low absolute value differences between them. It is possible that the hyperspectral measurements which were used for simulating the NDVI values over these classes were collected during a growing stage when the NDVI response of these classes was similar. Overall, despite the limitations of the simulated NDVI data the quantitative measurements agree with the theoretical assessment that the red and NIR bands of MODIS and VEGETATION are more responsive to differences in the biophysical and biochemical properties of vegetation than those of AVHRR.

2.3.4 Radiometric resolution

The radiometric resolution of a sensor refers to the dynamic range a sensor uses to quantize its response, in other words, the range of discrete Digital Numbers (DNs) it can record. High radiometric resolution sensors may be able to differentiate between radiation signals of similar radiance intensities, which otherwise might be indistinguishable to a sensor of lesser radiometric resolution. Consequently, the radiometric resolution of a sensor affects its ability to successfully distinguish between land cover classes of similar spectral profiles – important for land cover classification; or to detect fine spectral profile changes through time – important for drought monitoring applications.

Radiometric resolution is commonly measured in bits. A sensor with n bits of radiometric resolution can discriminate up to a range of values (dynamic range) equal to 2 raised to the power of n (equation 2.39):

$$\text{Dynamic range of a sensor with n-bit radiometric resolution} = 2^n \qquad (2.39)$$

Data collected by AVHRR are quantized at 10 bits (Goodrum et al., 2000), by VEGETATION at 10 bits (Henry et al., 1996; Saint, 1995), and by MODIS at 12 bits (Barnes et al., 1998). However, sensors with equal dynamic range such as AVHRR and VEGETATION do not necessarily have the same radiometric precision across their whole dynamic range. Sensor manufacturers often choose to distribute a sensor's dynamic range unevenly across the range of radiance values it's bands measure in order to achieve greater precision over ranges of radiance values of greater importance.

The most important spectral regions for vegetation monitoring, that also all three sensors under consideration have bands sensitive to, are the red, NIR and SWIR. Hence, for the purpose of this study, the comparison of the radiometric resolution of the three sensors was limited to these regions.

AVHRR's 10-bit quantization rate allows for up to 1024 possible levels of discrimination; however, these discrimination levels are not used equally across the range of the recorded reflectance values in the red, NIR and SWIR bands. For the red and NIR bands the first 501 levels of discrimination (0-500) are used for reflectance values up to

25% and the remaining 523 levels (501-1023) for reflectance values more than 25% (Goodrum et al., 2000). In the SWIR band the first 500 levels are used for reflectance values up to 12.5%, and the rest for higher reflectance values. Therefore, AVHRR's red and NIR bands quantization precision is $\frac{25}{501} = 0.0499\%$ for reflectance values up to 25% and $\frac{75}{523} = 0.1434\%$ in the 26%-100% reflectance range. Similarly, the SWIR band has a quantization precision of 0.025% and 0.1673% within the 0%-12.5% and 12.5%-100% reflectance range respectively.

VEGETATION quantizes data at a 10 bit rate too, but its red, NIR and SWIR bands are designed to saturate beyond 50%, 70%, and 60% reflectance values respectively (Saint, 1994; Henry et al., 1996). The available 1024 discrimination levels are equally distributed within the reflectance saturation range of each band; thus, the radiometric precision of the red, NIR and SWIR bands is 0.0488%, 0.0648%, and 0.0586% respectively.

MODIS digitises its measurements at a 12 bit rate (Barnes et al., 1998) and distributes them equally across the whole reflectance range of its red, NIR and SWIR bands; therefore it has a 0.0244% quantization precision for each band.

However, the radiometric resolution of a sensor is not solely governed by its quantization precision; it is also dependant on the residual electronic noise of the sensor. Parts of the sensor at temperatures higher than absolute zero cause residual electronic noise (Richards, 1993), that in turn create fluctuations in the sensor's response. This fluctuation, also referred to as dark current, is present even when the sensor receives a stable flux of radiation or no radiation at all. Therefore, due to the residual electronic noise, measurements taken by a sensor have a degree of radiometric uncertainty equal to the standard deviation of the sensor's response when viewing a source of stable radiation. Hence, any measurement quantized at a precision finer than the magnitude of the residual electronic noise would be futile. The radiometric resolution of a sensor cannot drop below the equivalent value of radiance ($Ne\Delta l$) or reflectance ($Ne\Delta\rho$) that would cause the sensor to generate a response equal to its dark current. The quantization precision of a sensor becomes a factor of its radiometric resolution when it is coarser than the magnitude of the sensor's residual electronic noise.

Table 2.16: Data quantization precision across the red, NIR and SWIR bands of MODIS, AVHRR and VEGETATION

Band	Reflectance values	MODIS	AVHRR	VEGETATION
RED	<25%	0.0244%	0.0499%	0.0488%
	25%-50%	0.0244%	0.1434%	0.0488%
	>50%	0.0244%	0.1434%	N/A
NIR	<25%	0.0244%	0.0499%	0.0648%
	25%-70%	0.0244%	0.1434%	0.0648%
	>70%	0.0244%	0.1434%	N/A
SWIR	<12.5%	0.0244%	0.025%	0.0586%
	12.5%-60%	0.0244%	0.1673%	0.0586%
	>60%	0.0244%	0.1673%	N/A

The residual noise is commonly expressed as a signal-to-noise-ratio (SNR) at a given reflectance or radiance value. The AVHRR SNR values for its red, NIR and SWIR bands are equal to or greater than 9, 9 and 20 respectively, for reflectance values of 0.5% (Goodrum et al., 2000); hence, the bands' respective $Ne\Delta\rho$ values are 0.0555% (or better), 0.0555% (or better) and 0.025% (or better). VEGETATION red band $Ne\Delta\rho$ value is 0.1% for reflectance values up to 10% and rises up to 0.3% for reflectance values in the 10%-50% range (VEGETATION red band saturates at 50% reflectance values) (Saint, 1994). As for the NIR and SWIR bands of VEGETATION, their $Ne\Delta\rho$ values are both 0.3% across their whole reflectance range (Saint, 1994).

According to Xiong et al., (2002) MODIS in-orbit assessment, MODIS red, NIR and SWIR (band 6) band SNR values are 196 at 21.8 $Wm^{-2}sr^{-1}\mu m^{-1}$, 519 at 24.7 $Wm^{-2}sr^{-1}\mu m^{-1}$, and 377 at 7.3 $Wm^{-2}sr^{-1}\mu m^{-1}$ radiance values. Consequently, the bands' respective $Ne\Delta l$ values are 0.111225 $Wm^{-2}sr^{-1}\mu m^{-1}$, 0.047592 $Wm^{-2}sr^{-1}\mu m^{-1}$ and 0.019363 $Wm^{-2}sr^{-1}\mu m^{-1}$. The residual electronic noise values of a sensor's band expressed in radiance ($Ne\Delta l$) cannot be directly compared to a sensor band's respective quantization precision values because the latter are expressed in reflectance values. Therefore, the $Ne\Delta l$ values were converted to $Ne\Delta\rho$ using the following equation:

$$Ne\Delta\rho = \frac{100\pi Ne\Delta l}{I_{EX}} \tag{2.40}$$

MODIS red NeΔρ value are 0.0218%,, NIR NeΔρ value are 0.0151%, and SWIR NeΔρ value are 0.0247%.

The radiometric resolution of each sensor's band is limited by the value of either the band's NeΔρ or quantization precision, whichever is coarser. Tables 2.16 and 2.17 display the NeΔρ and quantization precision values of the three sensors' red, NIR and SWIR bands; table 2.18 displays the radiometric resolution of each sensor and band based on the comparison of the data displayed in tables 2.16 and 2.17.

Table 2.17: NeΔρ values of MODIS, AVHRR and VEGETATION red, NIR and SWIR bands.

Band	Reflectance values	MODIS	AVHRR	VEGETATION
RED	<10%	0.0218%	0.0555%	0.1%
	10%-50%	0.0218%	0.0555%	0.3%
	>50%	0.0218%	0.0555%	N/A
NIR	<25%	0.0151%	0.0555%	0.3%
	25%-70%	0.0151%	0.0555%	0.3%
	>70%	0.0151%	0.0555%	N/A
SWIR	<12.5%	0.0247%	0.025%	0.3%
	12.5%-60%	0.0247%	0.025%	0.3%
	>60%	0.0247%	0.025%	N/A

Table 2.18: Radiometric resolution of MODIS, AVHRR and VEGETATION red, NIR and SWIR bands (expressed in % reflectance).

Band	Reflectance values	MODIS	AVHRR	VEGETATION
RED	<25%	0.0244%	0.0555%	0.1%
	25%-50%	0.0244%	0.1434%	0.3%
	>50%	0.0244%	0.1434%	N/A
NIR	<25%	0.0244%	0.0555%	0.3%
	25%-70%	0.0244%	0.1434%	0.3%
	>70%	0.0244%	0.1434%	N/A
SWIR	<12.5%	0.0247%	0.025%	0.3%
	12.5%-60%	0.0247%	0.1673%	0.3%
	>60%	0.0247%	0.1673%	N/A

From reviewing the results presented in table 2.18 it is apparent that MODIS has the highest radiometric resolution, followed by AVHRR and then VEGETATION.

2.3.5 Calibration

The raw data collected by a sensor are the sensor's response to the voltage of the electric current produced by the sensor's detectors when they are exposed to radiation. The data are recorded in the form of unitless integer Digital Numbers (DN), the values of which are a function of the radiance values of the detected radiation. The process of determining the function that relates the DN values to radiance values is called calibration. DN values transformed to radiance values through the process of calibration can then be converted to TOA reflectance values for the sensor's SRBs, or brightness temperatures (BT) for the sensor's TEBs.

The DN-radiance relation/function is carefully established for each band of a sensor before it is placed in orbit (pre-flight calibration) in controlled laboratory conditions by carrying out an extensive series of sensor response measurements against sources/targets of known radiance values. However, during launch and while in space, the sensors' response to radiation gradually changes, due to factors such as bombardment by energetic particles from space, deterioration of the electronics system, outgassing, and variations in the filter transmittance and spectral response (Liang, 2004; Gordon et al., 1983). Hence, after launch, the radiance-DN function determined during the pre-flight calibration is no longer reliable.

Methods exist for re-calibrating sensors after launch (post-launch/in-flight calibration). They rely on the regular monitoring of the sensor band's response against targets of either known or temporally stable (they could be unknown) spectral properties. When the sensor's response is monitored against a target of known spectral properties, then a function can be established to convert the DNs to absolute radiance values (absolute calibration). If however a target has spectral properties that are unknown but stable over time, it can be used as a reference to normalise variations of the sensor's response (multidate/relative calibration). Calibration reference targets can be located either outside (vicarious calibration) or inside the sensor (onboard calibration).

AVHRR does not have on-board calibration capability for its SRBs; thus, after launch these bands are calibrated with vicarious methods. One such method commonly used for the calibration of its SRB relies on the use of deserts as reference targets (Cosnefroy et

al., 1996; Heidinger et al., 2002b; Henry et al., 1993; Kaufman and Holben, 1993; Rao and Chen 1995, 1996). Deserts make good reference targets because they are near-Lambertian surfaces with very stable spectral properties over time (Cosnefroy et al., 1996); moreover, deserts occupy large areas thus even low resolution (spatial) sensors like AVHRR can measure radiance/reflectance from GIFOVs purely occupied by desert (pure pixels, not contaminated with land cover classes of unknown reflectance properties). Furthermore, due to the very high reflectance values of deserts, the contribution of the atmospheric effects to the measured radiance is so small that it can be ignored (Rao and Chen, 1995).

Rayleigh scattering (Briottet et al., 1997; Dilligeard et al., 1996; Kaufman and Holben, 1993; Meygret et al., 2000; Vermote et al., 1992) is another vicarious method that can be used for the calibration of AVHRR's red band. It is based on the fact that over clear oceans and under certain viewing (high viewing and solar zenith angles to increase the photon travel path, viewing to the west to avoid specular reflection), atmospheric (low haze, water vapour and no clouds) and wind conditions (low wind to avoid foam radiance), the majority (70-80%) of radiation reaching the sensor in the shortwave visible spectrum is caused by Rayleigh scattering (Fraser and Kaufman, 1986). The remaining percentage is mostly caused by aerosol, the optical thickness of which can be estimated by the NIR channel which is only slightly affected by Rayleigh scattering. Then by comparing the measured radiance caused by Rayleigh scattering to the radiance that theoretically would be caused by Rayleigh scattering (that can be modelled if meteorological and atmospheric conditions are known) the red band can be calibrated. A problem with this methodology is that it requires a calibrated NIR band.

AVHRR can also use the Sun glint method (Kaufman and Holben, 1993) for the vicarious calibration of its SWIR and NIR bands. The method is based on a similar idea to the Rayleigh scattering method, however this time a viewing geometry that the sunlight will reflect from the ocean to the sensor is required. In such case 87% of the recorded radiance is due to the specular reflectance (Kaufman and Holben, 1993). However the theoretical reflectance can not be estimated as in the Rayleigh scattering case because it will depend on wind speeds and wave structure (foam reflectance);

instead, it can be measured by another SRB as long as it has already been calibrated; because the reflectance over the sea is not wavelength dependant (Fresnel's laws).

It can be seen that the Rayleigh scattering and the Sun glint method require at least one SRB to be already calibrated. In order to tackle this problem, either one band is calibrated using another vicarious method, or, the NIR band is calibrated using the pre-flight calibration coefficients for the Rayleigh scattering method. Then the red band calibrated using the Rayleigh scattering method can be used to give a new estimate of the NIR using the Sun glint method. The new NIR estimate can be used again to calibrate the red band in the Rayleigh scattering method, and so on. The iteration continues until the process converges (Henry and Meygret 2001).

The cloud tops can also be used as reference targets for the vicarious calibration of SRBs (Henry and Meygret 2001; Vermote and Kaufman, 1995). The reflectance values of the clouds are variable and therefore unknown; but, their reflectance is flat over the SRBs and as such clouds can be used for calibrating SRBs if at least one band is calibrated (inter-band calibration). Particularly thick and high altitude clouds are preferred for this method; this way, the radiance measured by the sensor is mainly a function of only the cloud's reflectance and the atmospheric molecular and ozone content, out of which the contribution of the last two can be removed with atmospheric correction.

As for the thermal emissive bands (TEB), AVHRR uses two targets as references: a) cold deep space; and b) a blackbody on-board the sensor, the temperature of which is measured by four Platinum Resistance Thermometers (PRTs). The radiance of deep space is known by measurements during the pre-flight calibration, and the radiance emitted by the blackbody can be calculated using Planck's function and the mean temperature measured by the PRTs (Goodrum et al., 2000).

VEGETATION uses an onboard calibration lamp to provide a stable source of radiation as reference by illuminating the sensor's detectors once a month (Henry and Meygret, 2001). The stability of the lamp is cross-checked by regularly calibrating the sensor's SRBs using vicarious calibration methods. The vicarious methods officially used by SPOT are the Rayleigh scattering for bands B0 and B2, and the Sun glint for the B3 and SWIR bands (Henry and Meygret, 2001); other vicarious methods based on deserts

(Cosnefroy et al., 1996; Henry et al., 1993), or cloud tops (Vermote and Kaufman, 1995) are also occasionally used for validation purposes. The lamp's exact spectral properties are not known due to difficulties in assessing how these properties change in orbit, and also in the case of VGT-1 due to a "last-minute" modification before launch (Henry and Meygret, 2001). Hence, the lamp cannot be used for absolute calibration unless the calibration method is adjusted using data from the vicarious calibration methods (Henry and Meygret, 2001). Without the vicarious calibration adjustment the lamp can still be used for multidate calibration due to its very good in-orbit spectral stability (Henry and Meygret, 2001). It should be mentioned however that the performance of the lamp on-board VGT-2 was recently discovered not to evolve as anticipated and actions are now taken to re-calibrate VGT-2's historical data archive (VEGETATION, 2006).

MODIS SRBs are calibrated onboard using as reference targets deep space and a device called Solar Diffuser (SD) (Barnes et. al., 1998; Xiong et al., 2002, 2002c, 2005). The SD is a plate made out of space grade Spectralon that acts as a near-Lambertian surface. Once every week, (for the first two years of the sensor's operation and every second week thereafter) a deployable door on the along-track wall of MODIS, the Solar Diffuser Door (SDD), opens and allows sunlight to illuminate the SD. MODIS views both space and the SD in every 360° rotation of its double sided scanning mirror. If the SDD is closed then the last recorded SD reflectance values, when the SDD was last open, are used for the calibration. The space view radiance, similarly to AVHRR, is known based on measurements carried out during the pre-flight calibration. The SD's reflectance is calculated; its reflectance properties were known before launch but in orbit over time the SD's Lambertian properties deteriorate. It is for that reason the SD's performance is independently monitored by another device the Solar Diffuser Stability Monitor (SDSM). The SDSM monitors the SD performance and makes necessary adjustments to the calibration according to the changes it detects. MODIS also occasionally views the Moon as another reference target or for checking the SD stability. The Moon was selected as a reliable reference target because of its very high reflectance stability over time periods longer than the operation time of MODIS (Dinguirard and Slater, 1998; Liang, 2004)

.

MODIS' TEBs are also calibrated onboard using a deep space view and a blackbody on-board the sensor as reference targets. The temperature of the blackbody is measured by 10 detectors and consequently the radiance emitted by it can be calculated using Planck's function. During each full rotation of the double-sided scanning mirror of MODIS both targets are viewed (space and blackbody) and used for the calibration. More details about MODIS TEB calibration can be found in Xiong et al., 2005, 2002b and 2002.

The calibration of AVHRR SRBs is likely to be the least accurate out of the three sensors, because it relies solely on vicarious methods in contrast to VEGETATION or MODIS where onboard calibration methods are also used. Vicarious methods rely on assumptions or estimations regarding the atmospheric content or the spectral properties of the reference targets (e.g. stability, Lambertian surfaces), while on the other hand onboard calibration methods mainly rely on the spectral stability of their internal targets; hence, the margin of error in vicarious methods is larger. Moreover, the calibration of MODIS SRBs is more likely to be more accurate than the calibration of VEGETATION SRBs because not only are the spectral properties of the MODIS onboard calibration device known (absolute calibration possible), they are also regularly independently monitored by a second onboard calibration device (Barnes et al., 1998; Xiong et al., 2002); both are not true for VEGETATION. As an indication, estimations of the sensors' SRBs calibration accuracies are displayed in table 2.19.

Table 2.19: AVHRR's, VEGETATION's and MODIS' calibration uncertainties

Sensor	Bands	Absolute	Multidate
AVHRR	Red and NIR (Loeb, 1997; Rao and Chen, 1995, 1996, 1999)	5%	5%
	SWIR (Goodrum et al., 2000)	Not yet estimated	Not yet estimated
	TEBs (Goodrum et al., 2000)	0.3K	0.3K
VEGETATION	B0, B2 and B3 (Henry et al., 2004, Henry and Meygret 2001, 2001b)	5%	2%
	SWIR (Henry et al., 2004, Henry and Meygret 2001, 2001b)	10%	2%
	TEBs	N/A	N/A
MODIS	SRBs (-SWIR) (Heidinger et al., 2002; Xiong et al., 2005)	2%	2%
	SWIR (Heidinger et al., 2002; Xiong et al., 2005)	2%-3%	2%-3%
	TEBs (Xiong et al., 2004)	<1%	<1%

MODIS and AVHRR are the only sensors out of the three equipped with TEBs. The calibration of the two sensors' TEBs should be similarly accurate for both sensors, since practically the same onboard calibration method is employed for both of them.

In land-cover classification applications, calibration is critical if the class discrimination process relies on data collected over (an) image(s) different to the one being classified. This is because the DN values of data collected over the same land-cover classes at different times or location are likely to be significantly different, as they depend on variables such as the response of the used sensor and the illumination and viewing conditions of the land-cover class, which are image-specific. Therefore, if an image is classified based on classification criteria collected from another data source, both datasets must be calibrated or else significant misclassification errors may occur. It should also be noted that in such cases it is advisable to use training data collected during the same season as the image being classified so as to ensure that there is no mismatch between the spectral properties of the vegetation classes due to seasonal changes to the spectral properties of the vegetation. Moreover, absolute calibration of the data may not be necessary: If the data (training and classified) are calibrated in relation to (multidate

calibration) spectrally stable targets, then the effects of the varying sensor response and viewing and illumination conditions over time are normalised. Due to the fact that land-cover classification methods rely mainly on data collected over the SRBs rather than TEBs, data from the sensor with the most accurate SRB multidate calibration will result in the most accurate land-cover classification (all other parameters being equal). Hence, in terms of classification accuracy, data collected by VEGETATION are likely to perform almost as well as MODIS, but data collected by AVHRR are likely to result in more misclassification errors. Nevertheless, in all other land-cover classification cases, when images are classified using classification criteria extracted solely from the images being classified, then no data calibration is required; consequently, in such cases none of the sensors has an advantage over the other two as far as their calibration capabilities are concerned.

In drought monitoring methods, the spectral properties of vegetated areas are monitored and compared against previously collected historical data. Deviations of these spectral properties from the historical norm suggest changes in the biophysical and biochemical properties of the studied vegetation that could be triggered by drought-related stress. Due to the fact that these methods rely on the comparison of data collected over long periods of time, it is critical to ensure that any deviation from the historical data detected is due to changes of the spectral properties of the studied target, and not due to changes of response of the sensor(s) that collected the data, or the viewing and illumination conditions of the imaged scene (assuming no atmospheric contamination). Additionally, since the comparison is relative over time, the data need not be calibrated to absolute reflectance or temperature values; instead, a multidate calibration would suffice. As far as the calibration accuracy of the sensors' data is concerned, data collected by MODIS or VEGETATION should be equally efficient at detecting drought conditions; AVHRR however would be less effective due to its poorer multidate calibration capability.

2.3.6 Atmospheric correction

Radiation travelling through the atmosphere is altered through the processes of absorption and scattering caused by molecules and particles within the atmosphere. These atmospheric processes have a dual effect on remotely sensed data. The radiation reaching the top of the atmosphere from the Sun (Extraterrestrial irradiance), is altered as it travels through the atmosphere to the surface of the Earth; and the radiation reflected or emitted from the surface of the Earth is not equal to the radiation measured by sensors in orbit around Earth. Consequently, remotely sensed data are not solely dependant on the spectral properties of targets on the surface of the Earth, but also on the content of the atmosphere.

The atmospheric contribution to the measured radiation can be very significant and can cause considerable errors if TOA values are used to take quantitative measurements of surface parameters; moreover, it will never be constant since the atmospheric content is temporally and spatially variable; therefore, TOA data collected over different locations or time are not directly comparable. Atmospheric contamination is a major source of error in several vegetation monitoring applications (Cihlar et al., 1994; Cihlar, 2000; Eidenshink and Faundeen, 1994; Goward et al. 1994; Liang, 2001; Townshend and Justice, 2002; Vermote and Vermeulen, 1999); hence, it is common practice to remove it in cases when quantitative measurements are needed, or data collected over different dates and/or areas need to be used together (Berk et al., 1989; Campbell, 1996; Duggin, 1985; Fraser and Kaufman, 1985; Holben et al., 1991,1992; Kneizys et al., 1988; Liang, 2004; Ouaidrari and Vermote, 1999; Rees, 2001).

Atmospheric scattering is caused by three types of molecules and particles (Schott, 1997):

- Rayleigh scattering, caused by molecules or particles, the size of which is much smaller than the wavelength of the radiation travelling through them. The atmospheric content of these particles and molecules is spatially and temporally stable and their contribution to the remotely sensed data can be estimated based on the atmospheric pressure of the studied surface which in turn can be estimated by the surface's elevation (Russel et al., 1993; Vermote and Vermeulen, 1999). Rayleigh scattering mainly affects the visible region of the electromagnetic spectrum, with increased effect for radiation with smaller wavelengths (Liang, 2004).
- Mie scattering, caused by molecules or particles, the size of which is about the length of the wavelength of the radiation travelling through them. These particles and molecules are typically aerosol types such as pollen, dust, sea-salt, sulphate, nitrate, air pollutants, smoke, as well as other air contaminants (Liang, 2004; Schott, 1997). The concentration of these aerosols is variable over time and location; therefore, measurements for estimating the atmospheric contribution of the aerosols must be taken specifically for every image. This type of scattering affects mostly the visible region of the electromagnetic spectrum.
- Non-selective scattering, caused by particles much bigger than the wavelength of the radiation travelling through them. Clouds, rain, fog, and snow usually constitute these particles. Similarly to Mie scattering the concentration of these particles varies with time and location, but unlike Mie or Rayleigh non-selective scattering affects radiation almost equally across the electromagnetic spectrum (hence the name) (Bamber, 2006; Rees, 2003). Atmospheric haze is mainly due to non-selective scattering.

Atmospheric absorption is mainly caused by aerosols and gases. Since aerosol causes both absorption and scattering its effect on remotely sensed data is typically estimated for both processes combined (Liang, 2004). The gases which are mostly responsible for atmospheric absorption are water vapour (H_2O), ozone (O_3), oxygen (O_2), carbon dioxide

(CO_2), carbon monoxide (CO), nitrous oxide (N_2O), and methane (CH_4). Apart from ozone and water vapour, most gases absorb radiation over very narrow spectral wavebands and usually are not taken into account in atmospheric correction methods of most remotely sensed data unless they are collected by hyperspectral sensors (Liang, 2004). In the VIS, NIR, and MIR regions of the electromagnetic spectrum, water vapour mostly absorbs radiation with wavelengths over 700 nm and ozone radiation with wavelengths between 550 nm and 650 nm (Vermote et al., 1996). With the exception of water vapour, the concentration of the gases is rather globally stable over time or predictable and consequently their absorption effect can be easily accounted for (Liang, 2004; Tanre et al., 1992). It should be noted however, that the concentration of some of these gases may be abnormally higher over cities and industrial sites, or during certain events such as volcano eruptions or forest fires.

Several methods have been developed for atmospheric correction; however a detailed description of them is beyond the scope of the present study. In brief, some of them assume the existence of one or more objects in the imaged scene which have very low reflectance (dark objects) and attribute any recorded data in the SRBs to atmospheric contribution (Kaufman and Sendra, 1988; Liang et al., 1997), while others rely on objects in the image scene which are assumed to have spectrally stable properties over time (Hall et al., 1991; Kim and Elman, 1990), others require in situ measurements of the atmospheric content/profile or radiation reflected or emitted by the Earth's surface (Smith and Milton, 1999), others estimate the atmospheric effect by collecting data over the same target using different viewing angles and/or different wavebands (ERS-1, 1989; Mackay et al., 1998), others estimate the atmospheric effect based on typical model atmospheres based on the date and location the data were collected from (Cracknell and Hayes, 1993), and finally others utilise radiative transfer equation models and require information about the atmospheric content/profile in order to estimate its effect on the remotely sensed data (Jensen, 2005). Examples of such methods are the LOWTRAN (Kneizys et al., 1988, 1983), the MODTRAN (Berk et al., 1989), the Simplified Method for Atmospheric Corrections (SMAC) (Rahman and Dedieu, 1994), the Second Simulation of Satellite Signal in the Solar Spectrum (6S) (Vermote et al., 1997) and the Simulation of the Sensor Signal in the Solar Spectrum (5S) (Tarne et al., 1990).

Any of the above methods can be used for the atmospheric correction of data collected either by AVHRR, VEGETATION or MODIS with different degrees of success; however, the methods typically adopted by each sensor are presented next.

The SRB data of AVHRR are atmospherically corrected using the 5S radiative transfer equation model (DeFelice et al., 2003; Tanre et al., 1992). In order to run the model, knowledge of the imaged scene elevation or pressure (for the Rayleigh scattering correction), and ozone, aerosol and water vapour atmospheric content is required (Tanre et al., 1992). This knowledge can be obtained as follows: The elevation can be obtained from maps where the elevation of a location is noted, or provided by Digital Elevation Maps (DEM); the aerosol atmospheric content is estimated from AVHRR's SRBs using the dark-object method (Fell et al., 2001; Tanre et al., 1992), and the ozone and water vapour atmospheric content are estimated from measurements by other sensors such as the Television and Infrared Observational Satellite Operational Vertical Sounder (TOVS) or the Total Ozone Mapping Spectrometer (TOMS) (DeFelice et al., 2003; Meyer et al., 2003; Smith et al., 1985; Tanre et al., 1992). Just to note, TOVS is composed of the High Resolution Infrared Radiation Sounder (HIRS), the Microwave Sounding Unit (MSU) and the Stratospheric Sounding Unit (SSU), and flies onboard the same NOAA satellites as AVHRR; Since NOAA-15, TOVS was renamed to Advanced TOVS (ATVOS) and the MSU and SSU sensors were replaced by the more advanced Advanced Microwave Sounding Unit-A (AMSU-A) and Advanced Microwave Sounding Unit-B (AMSU-B) respectively.

The TEB data of AVHRR are atmospherically corrected using either the split-window (Becker and Li, 1990; Erbertseder et al., 1999; Prata et al., 1995; Wan and Dozier, 1996) or the single image (Erbertseder et al., 1999; Lim et al., 2004; Prata et al., 1995; Schroedter et al., 2003) methodology.

VEGETATION data are also atmospherically corrected using a radiative transfer equation model, the SMAC which is based on 5S and 6S (Berthelot and Dedieu, 2000; Leroy et al., 1998; Maisongrande et al., 2004; Passot, 2000). Consequently, this method also requires data about the altitude of the imaged scene and water vapour, ozone and aerosol atmospheric contents (Berthelot and Dedieu, 2000; Leroy et al., 1998; Maisongrande et al., 2004; Passot, 2000). Ozone and aerosol atmospheric contents are

provided by the Centre d'Etudes Spatiales de la Biosphère (CESBIO) using climatology and a fixed model respectively (the aerosol content is estimated based on latitude and waveband); the water vapour is estimated from meteorological models based on data downloaded from Meteo-France (Berthelot and Dedieu, 2000; Maisongrande et al., 2004; Passot, 2000). All atmospheric content data are estimated on an 8 km by 8 km grid, the same as the DEM used for the extraction of the elevation data.

MODIS SRB data are atmospherically corrected using the 6S model (Vermote and Vermeulen, 1999). The water vapour, ozone and aerosol atmospheric content which are required for the 6S model are estimated using MODIS wavebands (Kaufman and Tanre, 1998; Menzel et al., 2002; Vermote and Vermeulen, 1999). The Rayleigh correction is also based on the elevation of the imaged scene and is extracted from a 8 km by 8 km grid DEM (Vermote and Vermeulen, 1999).

Finally, data collected by MODIS TEBs are atmospherically corrected using mainly either the split-window or the day/night (Wan and Li, 1997; Wan, 1999, 2006) method; also although an unofficial method for MODIS, the single band method has also been used successfully (Lim et al., 2004).

Within the present study, emphasis was not given to the comparison of the expected performance of the atmospheric correction processes of the sensors' TEB data due to their relatively minor importance in land-cover classification and drought monitoring applications; instead, hypotheses were made regarding the expected accuracy of the three sensors' SRB data atmospheric correction processes.

Out of the three sensors, MODIS SRB data are likely to be more accurately atmospherically corrected. This is because, although all three sensors utilise rather similar radiative transfer equation models, the atmospheric parameters used as input in these models are more likely to be more accurate for MODIS. For instance, MODIS' aerosol content estimation should be more accurate than AVHRR's because more SRBs are used for its estimation (Kaufman and Tanre, 1998; Vermote and Vermeulen, 1999); and it should also be more accurate than VEGETATION's because the atmospheric aerosol content is variable over time and location and therefore it is unlikely that it would be as accurately estimated using VEGETATION's static model which depends only on location, as for MODIS' real-time measurements. Moreover, the water vapour and ozone

estimates of MODIS are available at a much better spatial resolution (about 1 km at nadir point) than the ones provided from TOVS or TOMS data for AVHRR (HIR's, AMSU-A's, AMSU-B's and TOVS' IFOVs are about 20 km, 50 km, 16 km, and 50 km respectively (Goodrum et al., 2000; Kempler, 2006)). Also, data collected by TOMS are collected over a different platform and possibly not at the same time as AVHRR's data collection; consequently, the atmospheric content estimated by TOVS may be different from the atmospheric content at the exact time when data were collected by AVHRR. Similarly, the water vapour atmospheric content estimates for VEGETATION are based on data provided by Meteo-France, which are not synchronised to the time that data from VEGETATION were collected, which also leads to possible errors due to changes of the atmospheric content over time. Additionally, VEGETATION's ozone content estimates are based on climatology and not on real-time data, thus they can not accommodate possible deviations from the expected atmospheric conditions. And finally, MODIS wavebands are narrower than AVHRR's or VEGETATION's and spectral regions of radiation absorption are avoided. For instance, water vapour - one of the most variable atmospheric parameters - does not affect the NIR band of MODIS (Vermote and Vermeulen, 1999; Fensholt, 2004; Fenshold and Sandholt, 2005), something which is not true for the respective band of AVHRR (Tanre et al., 1992; Huete et al., 1999).

In land cover classification applications, atmospheric correction is necessary when the training data are not extracted from the data being classified because TOA (not atmospherically corrected) reflectance or temperature values recorded at a different time or location by the same sensor and over targets of the same spectral properties/profiles/signatures are likely to be significantly different due to possible different atmospheric conditions at the time of their reception (Fraser and Kaufman, 1985; Fraser et. al., 1977; Liang, 2004; Ress, 2001; Vermote and Vermeulen, 1999). However, if the training data are extracted from the data being classified, then atmospheric correction would have only a small impact on the classification accuracy (Kawata et al., 1990; Song et al., 2001) and would not be required (Cracknell and Haeys, 1993; Foody et al., 1996; Jensen et al., 1993; Singh, 1989; Song et al., 2001). An exception applies in cases of considerably different atmospheric conditions across an image; in such cases, areas covered by the same land-cover classes may appear to have

different spectral properties (based on uncorrected measurements) due to different atmospheric conditions above them. In terms of atmospheric correction, MODIS would have an advantage over AVHRR and VEGETATION in land-cover applications only if the training data are not extracted from the data being classified.

In drought monitoring methodologies such as the VPI, VCI or TCI, atmospheric correction is required. These methods rely on the detection of abnormal measurements in relation to historical data records; hence, unless the atmospheric contribution is removed from both historical and assessed data, neither can the historical normal spectral properties of the studied area be established, nor can the analyst safely attribute any deviations (or no deviations) of the apparent spectral properties of the studied vegetation to actual changes (or no changes) of the vegetation condition, without eliminating the possibility of these deviations (or no deviations) being caused by atmospheric conditions. Therefore, MODIS atmospherically corrected data should contain fewer errors when used for the assessment of drought conditions than the respective data from AVHRR or VEGETATION, due to its more accurate atmospheric correction which reduces assessment errors caused by atmospheric contamination.

2.3.7 Data availability and cost

Data collected by AVHRR, VEGETATION and MODIS are made available at near real-time (1-2 days from reception) by each sensor's data distribution website. If internet access is unavailable or slow (due to the large volume of remotely sensed data), then data users can either request data by post, or, in the case of MODIS and AVHRR, set-up a receiving station and download the data directly from the sensor in real time.

In land-cover mapping applications data availability is not an issue for any of the three sensors because land-cover change is a process which normally takes place within time periods much longer than the slowest data retrieval option (by post) from any of the three sensors.

In drought monitoring applications however, the early detection of droughts could potentially save lives; consequently, the data on which the assessment is based should be accessible as close to real-time as possible. If a sufficiently fast internet connection is available then this data availability requirement can be met for any of the three sensors. On the other hand, if there is no sufficient internet infrastructure available, then recently collected data by VEGETATION could take several days to be received by post (depending on location), while data collected by AVHRR or MODIS could be downloaded in real-time using a receiving station. In terms of data availability, drought monitoring methods based on AVHRR or MODIS data would potentially be able to detect drought conditions earlier than methods that rely on VEGETATION data only if there is not sufficient internet infrastructure for VEGETATION data download.

Data collected by AVHRR and MODIS can be downloaded for free (either through the internet or a receiving station), or for a small handling fee if they are requested by post. The cost of VEGETATION data is subject to various conditions. Synthesis products are free (S-products) when downloaded through the internet, or at a small handling fee when sent by post; the daily products however, (P-products), are only available for a cost, unless the data are requested for scientific and non-profitable purposes, and the request is approved by the Flemish Institute of Technological Research, Belgium (VITO).

Thus, in land-cover mapping applications based on synthesis products, such as a series of MVC NDVI images, there is no data acquiring cost for data collected by any of

the three sensors. If however, single-date data are required for a commercial or non VITO-approved application, the data purchasing cost for VEGETATION data will be higher than for data collected by AVHRR or MODIS, which are both freely available.

Since most drought monitoring methods are based on synthesis products that are available for free for any of the three sensors, there is no financial advantage in using data from a specific sensor over the other two.

It should also be noted that in terms of future availability, NASA is planning to replace both AVHRR and MODIS by 2009 with the Visible and Infrared Imaging Radiometer Suite (VIIRS) (Gao, 2000; Johnson, 2006; Townshend and Justice, 2002). Nevertheless, AVHRR will continue to operate until 2020, under the European Space Agency's (ESA) space programme onboard a series of three satellites (METOP-A to METOP-C), the first of which (METOP-A) was launched on the 15th of May 2007 (ESA, 2007). As far as VEGETATION is concerned, there is talk of the possibility of a third sensor being launched in 2008 (Veroustraete et al., 2005).

2.3.8 Summary

Based on an overall assessment of the reviewed technical characteristics of the three sensors and their likely effect on land cover mapping and drought monitoring, MODIS was regarded to be better equipped in the majority of aspects, followed by VEGETATION and then AVHRR. However, the relative advantages of each sensor may be more significant than others over certain applications and study areas, and the same sensor may not always provide the most accurate results. For instance although MODIS was considered to have more relative advantages than VEGETATION for land cover mapping, under certain circumstances the few advantages of VEGETATION over MODIS could be significant. For example in the event that data collected by MODIS' bands 8-36 were used in a land-cover classification over a rather heterogeneous study area. In such a case, the lower spatial resolution of MODIS' 8-19 bands (particularly at high viewing angles) in relation to that of VEGETATION's bands may result in a higher proportion of mixed pixels (more than one land-cover class within a pixel) within the MODIS' image than in VEGETATION's. The number of mixed pixels would increase proportionally to the heterogeneity of the study area; consequently if the heterogeneity of a study area was considerably high, the misclassification errors caused by mixed pixels could be significant enough to overcome the relative advantages of MODIS over VEGETATION.

Hence, under certain circumstances the data collected by the sensor with the most overall relative advantages may not always produce the most accurate products; however, in the majority of cases it was hypothesised that in land cover mapping and drought monitoring applications MODIS is most likely to achieve the best results followed by VEGETATION and lastly by AVHRR. This hypothesis is subsequently tested with experimental data in the following chapters. In Chapter 3, the sensors' performance in land cover mapping is assessed by comparing the classification accuracies of the maps produced by each sensor over the same series of sites and dates. According to the hypothesis it is expected that over most sites and dates the maps produced by MODIS would be more accurate those produced by VEGETATION, and consequently those produced by VEGETATION are expected to be more accurate than those produced by

AVHRR. In Chapter 5 the VPI measurements of each sensor over a series of sites and dates are compared with rainfall data, according to the hypothesis it is expected that over most sites and dates the VPI measurements which are more closely related to the rainfall data would be those of MODIS, followed by VEGETATION and then AVHRR.

CHAPTER THREE

3 Land cover mapping

3.1 Background

In Chapter 2 the relative advantages and disadvantages of each of the three sensors (AVHRR, VEGETATION and MODIS) for land-cover mapping were assessed based on the sensors' technical characteristics. Based on the results of the assessment it was hypothesised that among the three sensors, the one that was more likely to help produce a more accurate land cover map was MODIS, followed by VEGETATION and then AVHRR. In this chapter the hypothesis developed in the previous chapter is tested with experimental data.

A methodology suitable for the relative comparison of the sensors' data effectiveness in land-cover mapping was developed and applied on data collected by each sensor over the study sites of the United Kingdom (UK) and Greece. The reasoning behind the development of the classification methodology, choice of imagery dates, ancillary data, study sites, classification schemes, and accuracy assessment is presented. The results of the assessment are then discussed and compared to the hypothesis made earlier.

3.2 Introduction

The purpose of this part of the study was to compare the relative effectiveness of data collected by the SRBs of AVHRR, MODIS and VEGETATION in producing accurate land cover maps at 1 km spatial resolution, based on experimental results. Towards this goal the following steps had to be taken:

- To select study areas where the experiment/assessment would take place.
- To develop a classification methodology which would help assess the relative effectiveness of each of the three sensors' data in land cover mapping, in an objective manner.
- To identify the acquisition/reception dates of the sensor data that would be used in the experiment/assessment.
- To identify and acquire suitable reference data for the study areas.
- To produce land cover maps using the methodology developed, for all data collected by the three sensors over the identified study areas acquired on the selected dates.
- To assess the accuracy of each land cover map.
- To draw conclusions regarding the sensors' relative effectiveness in land cover mapping.

The above steps are further discussed in more detail in the following sections.

3.3 Study areas

The relation between the relative effectiveness of each sensor's data in land cover mapping is likely to differ over areas of different land cover composition. Therefore, in order to conclusively reach a decision regarding the relative effectiveness of the three sensors' data, the assessment would have to take place over all regions on Earth with different land cover compositions. Due to the Earth's landscape complexity, such an attempt would require an amount of resources that would far exceed those available for

this study. Therefore, it was decided to limit the assessment to two study sites. Due to ancillary data availability issues, it was seen as more practical to select two study sites within Europe. In order to help assess the sensors relative effectiveness in land cover mapping over as wide a range of land cover compositions as possible, it was decided to select two study sites with some of the most contrasting environmental conditions within Europe. As such the United Kingdom (UK) and Greece were selected. The UK is located in the most North-Western part of Europe, it is surrounded by the Atlantic and its landscape is mostly dominated by plains, Greece on the other hand is located in the most South-Eastern part of Europe, it is surrounded in the most part by the Mediterranean sea and its landscape is mostly dominated by mountains; as such the two study sites have distinctly different environmental conditions and consequently land cover compositions.

3.3.1 United Kingdom

The UK consists of a group of islands located in the North-Western part of Europe (Longitudes -8˚ 12' - 1˚ 48', Latitudes 40˚ 57' - 60˚ 54'). It is surrounded by the English Channel, the Celtic Sea, the Irish Sea and the North Sea (figure 3.1).

The UK is composed of England, Wales, Scotland and Northern Ireland, and covers an area of about 244, 880 km^2. England's terrain is dominated by level or rolling plains, with a few low mountains in the North-West, the highest being less than 1 km high. Scotland's terrain is characterised by numerous lochs and firths, highlands in the North and West (reaching heights of 1.3 km) and lowlands in the East and South. Finally the terrain of Wales and Northern Ireland is mostly mountainous with their highest peaks reaching almost 1.1 km. and 850 m respectively (CIA, 2006; Wikipedia, 2006a).

The UK's climate is temperate, wet and cloudy especially in the Northern and Western parts. Temperatures are cool, but due to the effect of the Gulf Stream and the Atlantic, only very rarely extreme temperatures are recorded; thus, on average the temperature ranges from about -5˚ C to 32˚ C throughout the year.

Figure 3.1: The map of UK (source: CIA the World Factbook)

3.3.2 Greece

Greece is located in the South-Eastern part of Europe, (Longitude 19˚ 24' - 28˚ 18', Latitude 34˚ 42'- 41˚ 48') at the tip of the Balkan Peninsula and at the junction of Africa, Europe and Asia. In the North it is bordered by Albania, the Former Yugoslav Republic of Macedonia (F.Y.R.O.M.) and Bulgaria, to the East it is bordered by Turkey, and the rest of Greece is surrounded by the Ionian and Aegean Sea (figure 3.2).

Greece is divided into 13 regions (Diamerismata), Thrace, Macedonia, Thessaly, Epirus, Central Greece, Attica, Peloponnesus, Ionian Islands, Evia and Sporades, Cyclades, Northern East Aegean Islands, Dodecanese and Crete, covering an area of about 131,990 km^2. The terrain is dominated by mountains (the highest peak is Olympus reaching more than 2.9 km) extending up to the coastline and covering more than two thirds of the country, and thousands of islands (about 3000) in the Ionian and Aegean Sea. The few lowland plains are mostly located in Thessaly and Macedonia.

The Greek climate is very diverse due to the intermingling of mountainous and coastal environment; the climate is Mediterranean along the Greek coastline, Alpine in

the Western mainland and Temperate in the central and Eastern mainland. However, due to the very long coastline of Greece (one of the longest in the world, more than 15,000 km) in relation to its area, most regions are in close vicinity to the coast and hence the Greek climate is generally characterised as Mediterranean. Temperatures vary considerably depending on location mainly due to rapid elevation changes and the effect of the sea; overall mountainous regions are cooler than lowland or coastal regions. Winters tend to be short, wet and cool, summers are long, hot and dry, and autumn and spring are the shortest seasons with very changeable weather being transitional seasons between summer and winter.

Figure 3.2: The map of Greece (source: CIA the World Factbook)

3.4 Methodology

3.4.1 Background

The relative effectiveness of data collected by the SRBs of AVHRR, MODIS and VEGETATION in land cover mapping was intended to be assessed by comparing the classification accuracy of the land cover maps produced using data from each sensor. Hence in order for the assessment to be objective, any factor other than the sensor's characteristics which could effect the classification accuracy of each of the compared land cover maps in a different way, had to be minimised (if a factor affected the classification accuracy of each map in the same way/magnitude, then that factor would not affect the assessment result, since the assessment was intended to be only relative). Mainly five such factors were identified:

- The classification algorithm used to produce the land cover maps. Some classification algorithms are more successful than others and land cover maps produced by different classification algorithms do not have the same accuracies. Additionally, different classification results may be achieved using the same classification algorithm and data, if the training process differs.
- The land cover composition of the study areas. Study areas covered with land cover classes of similar spectral properties would be more difficult to classify accurately than a study area covered with land cover classes, the spectral properties of which are quite distinct. Also the heterogeneity of a land cover composition in combination with the spatial resolution of a sensor will determine the percentage of mixed class pixels in the received data. Mixed class pixels are a major source of misclassification errors; hence, study areas with more heterogeneous land cover composition are more difficult to classify. Finally the number of existing land cover classes within a study area also affects the classification accuracies of land cover maps produced for that area; the probability of incorrectly classifying a land cover class increases with the number of possible land cover classes.

- The quality of the reference data used. Errors in the reference data can reduce the effectiveness of the classification methodology to accurately identify the class of the land cover, as well as hinder the accuracy assessment of the produced land cover maps either by registering misclassified pixels as correct and thus overestimating the classification accuracy or vice versa.
- The land cover classification schemes of the compared land cover maps. Certain land cover classes may be more difficult to distinguish than others, and the probability of misclassification errors is increased with the number of possible land cover classes.
- The acquisition date of the data used to produce the compared land cover maps. That is because the land cover composition may be different on different dates and consequently the difficulty of the classification may differ. Also, the atmospheric conditions are likely to be different on different dates; hence, the atmospheric contribution to the received data may differ, as is subsequently the sensor's ability to distinguish land cover classes.

Therefore for the purpose of this study the land cover map accuracies could only be comparable to each other if:

- The land cover maps were produced using the same classification algorithm
- The land cover maps cover the same area
- The land cover maps were produced and assessed using the same reference data
- The land cover maps have the same classification scheme
- The land cover maps were produced using data collected by each sensor on the same date

Moreover, in order to improve the validity of the results, land cover maps produced using data from each sensor had to be produced and compared for as many dates as possible over the two study areas.

3.4.2 Selection of classification algorithm

Land-cover classification methodologies based on data collected by low resolution sensors tend to rely on multitemporal data to take advantage of the high temporal resolution of these sensors (Cihlar et al., 2000). This is not to say that only multitemporal low resolution sensor data are used for land cover mapping; for instance Pokrant, (1991), and Beaubien and Simard (1993) produced land cover maps of Canada using single date AVHRR images. However, in most cases multitemporal and particularly MVC NDVI data are preferred for such applications. MVC NDVI data are preferred over daily data in multitemporal datasets because the MVC process minimises errors associated with atmospheric and cloud contamination, varying GIFOV sizes due to different viewing angles, and varying illumination and viewing angles of non-Lambertian surfaces (Cihlar, 2000; Duchemin et al., 2002; Holben, 1986; Lioubimtseva, 2003; Muchoney et al., 2000; Strahler et al., 1999). Examples of land cover maps produced using methodologies which relied on multitemporal MVC NDVI data include among others DeFries and Townshend (1994b), Loveland et al. (2000), Hansen et al. (2000), Belward and Loveland, (1995), Belward (1996), Tucker et al. (1985), Justice et al. (1985), Goward et al., (1985), Townshend et al., (1987), Koomanoff (1989), Malingreau (1986), Loveland and Belward, (1997), Muchoney et al. (2000), Laporte et al. (1998), and Chen et al. (1999). Research has shown that the classification accuracy of such methods may be further improved if the land cover identification process also relied on thermal data (Lambin and Ehrlich,1996a, 1996b; Liang, 2001; Nemani and Running, 1995; Nemani et al., 1993; Running et al., 1995), NDVI metrics (DeFries et al., 1998; Hansen et al., 2000; Lloyd, 1990; Reed et al., 1994), latitude data (DeFries and Townshend, 1994b; Friedl and Brodley, 1997; Gopal et al., 1999), reflectance data (Defries et al., 1995; Hansen et al., 2000) and ancillary environmental data (Loveland et al., 1991, 1995).

So far, land cover maps have been produced based on a variety of algorithms/methods. The majority of these algorithms/methodologies are based either on statistical clustering (Belward and Loveland, 1995; Belward, 1996; Chen et al., 1999, DeFries and Townshend, 1994b; Defries et al., 1995; Fleischmann and Walsh 1991; Goward et al., 1985; Justice et al., 1985; Koomanoff, 1989; Laporte et al., 1998; Liang,

2001; Lioubimtseva, 2003; Loveland and Belward, 1997; Loveland et al., 1991, 1995;Loveland et al., 2000; Loveland et al., 2000; Townshend et al., 1987; Tucker et al., 1985), decision trees (DeFries et al., 1998; Friedl and Brodley, 1997; Hansen et al., 1996; Lloyd, 1990; Reed et al., 1994; Running et al., 1995), artificial neural networks (Gopal et al., 1999, 1994; Muchoney et al., 2000) or a combination of artificial neural networks and decision trees (Friedl et al., 2002; Strahler et al., 1999).

According to studies, artificial neural network classifiers tend to produce more accurate land cover maps than conventional statistical classifiers (Foody, 1996b; Gopal et al., 1999; Muchoney et al., 2000; Pal and Mather, 2003; Strahler et al., 1999). Their advantages lay in the fact that i) they make no assumption about the distribution of the data and can detect and exploit nonlinear data patterns, ii) they can accommodate ancillary data with ease, iii) their architecture can easily be modified to optimise performance, iv) they need less reference data than statistical classifiers, and v) each class can handle multiple subcategories (Foody et al., 1995; Gopal et al., 1999; Pal and Mather, 2003; Strahler et al., 1999). However, their design is highly complex, requiring substantial expertise, and the training process is quite lengthy (Foody and Arora, 1997; Friedl and Brodley, 1997; Kavzoglu, 2001; Pal and Mather, 2003;Wilkinson, 1997).

Decision trees have also been shown to produce better results than statistical classifiers (Friedl and Brodley, 1997; Gopal et al., 1999; Muchoney et al., 2000; Pal and Mather, 2003). Decision tree classifiers are i) capable of handling nonlinear relations between land cover classes and spectral data, ii) make no assumptions about the data distribution, iii) can handle data at different spatial resolution, iv) are quick to execute and v) train (Friedl and Brodley, 1997; Pal and Mather, 2003). In a study, Friedl and Broadley (1997) found that hybrid decision trees perform better than univariate or multivariate trees, and Brodley and Utgoff (1992) showed in another study that multivariate trees performed better than univariate.

If the aim of this study was to achieve good classification accuracy results based on low resolution data, it would seem that according to results of previous studies the best course of action would have been to apply a methodology based on multitemporal data, and either an artificial neural network or a decision tree algorithm. This however was not the aim of this study; this study aimed to assess the relative effectiveness of data

collected by the SRBs of AVHRR, MODIS and VEGETATION in land cover mapping in an objective manner. Thus, focus was not given to developing a method which would produce highly accurate land cover maps, but a method which would produce and compare land cover maps in a way that the process can be replicated for each of the sensors' data. Differences in the sensors' data characteristics are stressed, and any other factors which could potentially differentiate the classification outcome of each sensor, were minimised.

The use of multitemporal data in a land cover classification requires more resources than if single date data were used (increased image processing) instead. Hence, multitemporal data should be preferred over single date data only when there is an advantage to it. The temporal resolution of all three sensors at the latitudes of the two study sites is approximately one day which exceeds the requirements of multitemporal classification methodologies; hence, the use of multitemporal data would not give a relative advantage or disadvantage to any of the sensors. Additionally, classification methods based on multitemporal data mainly rely on MVC NDVI values which are calculated from data received only by the red and NIR bands of the sensors. Consequently if the present study made use of such a classification methodology, then the effect of the sensors' remaining SRBs would greatly be overlooked. For the above reasons it was decided that it would be better for this study if the classification method used was based on single date multi-spectral data than multitemporal.

The classification algorithms that would more likely produce the most accurate land cover maps are based on decision trees and/or artificial neural networks. These algorithms however require significant input from the analyst, which in turn would diminish the reproducibility and objectivity of the method. On the other hand, an unsupervised statistical clustering classification algorithm (Richards, 1992) offers the highest consistency, reproducibility and objectivity of the known classification algorithms (Cihlar, 2000; Viovy, 2000). The result of an unsupervised classification algorithm however, can still be heavily influenced by the choice of classes and the allowable dispersion around a class mean, which are controlled by the analyst. This problem can be resolved by requesting a very large number of classes, which could later be merged into the intended land cover classes based on objective criteria (Cihlar and

Beaubien, 1998; Cihlar et al., 1998; Cihlar, 2000; Driese et al., 1997; Homer et al., 1997; Kelly and White, 1993; Vogelmann et al., 1998). This approach would also potentially improve the accuracy of the produced land cover maps by reducing mismatches which may occur between spectral and thematic classes (Cihlar, 2000). It was therefore decided that an unsupervised statistical clustering classification algorithm set to identify a large number of classes (the exact number would have to be determined in a later stage) would be better suited for the purpose of this study.

Overall therefore it was decided to compare the relative accuracy of land cover maps produced by single date data collected by each sensor, using an unsupervised statistical clustering classification algorithm set to identify a large number of classes.

3.4.3 Selection of data acquisition dates

Data received over the same area at different times will not be the same even if they were received by the same sensor whose response has not changed (perfectly calibrated). These differences are caused by different illumination conditions, viewing angles, atmospheric conditions and even by probable changes in the viewed scene's land cover composition.

However, the effect of these parameters would practically be the same on each land cover map produced using data collected by AVHRR, MODIS and VEGETATION if the data were collected on the same day. This is because the overpass times of these sensors (table 2.11) are temporally close enough to each other, so as to assume that there is not sufficient time for these parameters (and consequently their effect on land cover mapping) to change significantly.

Therefore, for the purpose of this study, land cover maps produced using data from different sensors over a study area were compared to each other only if the data used were captured from all sensors on the same date. At the time of the study the time period when data were available for all three sensors extended from the beginning of 2000 to the end of 2003. Thus, the data dates for this study had to be chosen from within that time period.

Apart from the time period limitation, there were two other criteria which had to be considered during the date selection process. Radiation reflected or emitted from land surfaces towards a sensor can be significantly altered or even be blocked out by clouds present in the radiation's path. Measurements collected by sensors over cloud covered (completely or partially) surfaces are not representative of the surfaces' actual spectral profiles, and will result in classification errors if used for land cover mapping. To avoid such errors it is usual practice to detect and mask out any cloud contaminated data before data are used for land cover mapping. Even if these processes were perfectly effective (which is not always the case), considerable parts of the study areas could be masked, reducing the total area and land cover type diversity the results of the study would be based on, and consequently reducing the validity of these results. Hence it was decided to select dates when the majority of the study areas were least covered by clouds.

Finally it was desirable that the findings of this study are representative for different phenological stages of vegetation. So, it was intended to carry out the assessment using data from a range of dates across the seasonal cycle.

The date selection process was aided with the use of NASA's Earth Observation System (EOS) Data Gateway website. The website offers the option to search and download/order data collected by NASA's sensors such as AVHRR and MODIS based on criteria set by the user, such as location, data reception date and/or time, sensor and data product etc. Once a group of data products are selected based on the requested criteria, the user is provided with an option to download and preview any of the selected data products before choosing to order them.

The search engine of the website was set to select all 1 km spatial resolution, daily reflectance data products received by MODIS/TERRA over the UK and Greece, during daytime, within the 26/02/2000-31/12/2003 period. The search engine returned more than 1400 images per study area. The image previews of each of the selected images were then downloaded and visually inspected in order to identify the dates when cloud cover over the majority of the study areas was relatively low.

Table 3.1: Identified dates with low cloud cover over the majority of the UK study area within the 26/02/2000-31/12/2003 period

01/09/2002	23/01/2003	18/03/2003	17/04/2003
02/09/2002	09/02/2003	19/03/2003	18/04/2003
11/09/2002	14/02/2003	22/03/2003	04/05/2003
13/09/2002	15/02/2003	23/03/2003	30/05/2004
24/09/2002	18/02/2003	27/03/2003	12/06/2003
18/10/2002	21/02/2003	30/03/2003	13/06/2003
19/10/2002	22/02/2003	31/03/2003	14/06/2003
24/10/2002	14/03/2003	04/04/2003	15/06/2003
26/10/2002	15/03/2003	07/04/2003	16/06/2003
04/01/2003	16/03/2003	08/04/2003	13/07/2003
05/01/2003	17/03/2003	16/04/2003	04/08/2003

Table 3.2: Identified dates with low cloud cover over the majority of the Greek study area within the 26/02/2000-31/12/2003 period

13/04/2000	04/07/2000	20/08/2000	16/03/2001	11/10/2001
14/04/2000	07/07/2000	21/08/2000	24/03/2001	21/10/2001
24/04/2000	10/07/2000	22/08/2000	25/04/2001	23/10/2001
20/05/2000	11/07/2000	24/08/2000	02/05/2001	09/09/2001
05/06/2000	12/07/2000	28/08/2000	04/05/2001	20/09/2001
14/06/2000	26/07/2000	18/09/2000	10/06/2001	24/09/2001
21/06/2000	27/07/2000	20/09/2000	11/06/2001	30/09/2001
25/06/2000	03/08/2000	25/10/2000	12/06/2001	10/10/2001
26/06/2000	04/08/2000	15/11/2000	03/10/2001	23/10/2001
03/07/2000	19/08/2000	11/12/2000	10/10/2001	06/11/2001

The dates which were identified for the UK and Greek study areas are displayed in tables 3.1 and 3.2 respectively. This initial selection was further refined by rejecting dates when:

- the received images did not capture the whole of the study areas
- the study areas were imaged at the edges of the scenes where the spatial resolution of the sensors is most degraded
- cloud cover was relatively high compared to other dates

After applying the above criteria it was realised that only a small proportion of dates met the selection criteria, and consequently it was not possible to satisfy the study's intention to carry out the assessment using data from a range of dates across the seasonal cycle.

Nevertheless, when having to choose between dates of similar attributes (in terms of the selection process), the dates with the longest temporal spread between them were selected. The dates which were finally selected for the UK and Greek study areas are displayed in tables 3.3 and 3.4 respectively.

Table 3.3: Selected dates for the UK study area

17/03/2003
19/03/2003
22/03/2003
23/03/2003
16/04/2003
18/04/2003
13/07/2003

Table 3.4: Selected dates for the Greek study area

13/04/2000
05/06/2000
14/06/2000
04/07/2000
07/07/2000
03/08/2000
20/08/2000
25/10/2000
24/03/2001
04/05/2001
03/10/2001
23/10/2001

3.4.4 Reference data selection

Reference data were needed to identify the land-cover of the classes produced by the unsupervised classification algorithm and also to help assess the accuracy of the maps produced. Ideally, such data are provided by surveys carried out at a time period very close to the reception date of remotely sensed data used for the classification; so as to minimise potential errors due land cover changes which may have occurred between the survey and the data reception dates. A considerable amount (about 1% of the study's area) of randomly selected and evenly spaced sample sites should be surveyed so as to insure that the reference data provides an unbiased and fairly accurate representation of the study area's land cover class composition. To meet the above criteria, a ground survey had to be designed and carried out during the 2001-2003 period, which would survey a total area of about 3,700 km^2 in sample sites across the study areas. The resources required for such an endeavour were not available for this study, so alternative sources of reference data had to be found.

At the time of this stage of the study, the alternative sources of reference data were the following:

- Previously created maps and atlases. Such sources have been used in the past by Olson and Watts (1982), Matthews (1983) and Wilson and Henderson-Sellers (1985) to produce global land cover maps. However, the majority of such data were collected several decades before this study and do not reflect any recent land cover changes. Moreover, such data were collected by various surveyors and under different projects, consequently the data are likely to contain inconsistencies caused by different land cover definitions, survey methodologies and surveyors perceptions. Finally such data may not be available for parts of the study sites (Townshend et al., 1991).
- The Global Land Cover Map for the Year 2000 (GLC2000) (Bartholomé and Belward, 2005; Fritz et al., 2003; Giri et al., 2005; Mayaux et al., 2002). The GLC2000 is a global land cover map at a 1km spatial resolution created under the coordination of the Joint Research Centre (JRC) of the European Commission (EC) (Bartholomé and Belward, 2005). The project was first conceived in 1999

and was completed by the end of 2003 (Bartholomé, 2004). The land cover identification was based on classification of VEGETATION data received in the period between 1st of November 1999 to 31st of December 2000 (Giri et al., 2005), trained with reference data extracted from the visual interpretation of higher spatial resolution imagery collected by Landsat TM and SPOT HRV in 2000 (Bartholomé and Belward, 2005). There was no specific classification method used for the whole project; instead, the globe was divided among more than 30 different teams, and each team was given the freedom to choose their own classification method (Fritz et al., 2003; Mayaux et al., 2002). Nevertheless, all teams had to use the same classification scheme based on the Land Cover Classification System (LCCS) (Di Gregorio and Jansen, 2000) developed by the Food and Agriculture Organization (FAO) and the United Nations Environment Programme (UNEP). The GLC2000 land cover classification scheme is provided in Appendix B.

- The International Geosphere-Bioshpere Programme Data and Information Systems (IGBP-DIS) global land cover dataset (IGBP DISCover) (Loveland et al., 1999, 2000). This dataset was produced by the U.S. Geological Survey (USGS), the University of Nebraska-Lincoln and the JRC (Hansen and Reed, 2000; Loveland et al., 2000; Loveland and Belward, 1997). The dataset was produced on a continent-by-continent basis, by applying an unsupervised classification on an AVHRR NDVI monthly MVC dataset spanning from April 1992 to March 1993, and relying on ancillary data such as maps and atlases for reference data (Loveland et al., 2000). The dataset has a 1 km spatial resolution and uses the 17 IGBP land cover classes (Belward, 1996; Hansen and Reed, 2000; Loveland et al., 2000). The IGBP DISCover dataset was first released on July 1997. The IGBP DISCover land cover classification scheme is provided in Appendix B.
- The 1km spatial resolution global dataset produced by the University of Maryland (UMd) (Hansen et al., 2000). Land cover classes were identified by applying a decision tree algorithm on data collected by AVHRR in the time period between April 1992 and March 1993 (Hansen et al., 2000). The class membership was decided based on AVHRR data metrics such as the minimum annual red

reflectance, the peak annual NDVI and the minimum channel three brightness temperature (Hansen et al., 2000) (a complete list of the metrics is provided in Appendix B). Reference data were extracted from higher spatial resolution data collected mainly by the Landsat Multispectral Scanner System (MSS), and a few by the Landsat TM and the Linear Imaging Self-Scanning Sensor (LISS). The land cover classification scheme of this dataset is provided in Appendix B.

- Two global land cover datasets produced by UMd at a spatial resolution of one degree (DeFries and Townshend, 1994b; DeFries et al., 1995). Both datasets were based on a supervised maximum likelihood classification algorithm applied on AVHRR data collected in 1987, and used areas of agreement between the global datasets produced by Olson and Watts (1982), Matthews (1983) and Wilson and Henderson-Sellers (1985) as reference data (DeFries and Townshend, 1994b; DeFries et al., 1995). The first dataset (DeFries and Townshend, 1994b) used monthly MVC NDVI AVHRR data spatially averaged to one degree and classified land cover into 12 classes (the classification scheme is provided in Appendix B). The second dataset (DeFries et al., 1995) used metrics derived from 10-day composites of NDVI, reflectance and temperature values (a complete list of the metrics used is provided in Appendix B) and classified the land cover into 13 classes (the classification scheme is provided in Appendix B)
- The global land cover dataset at 8 km spatial resolution produced by UMd (DeFries et al., 1998). DeFries et al. (1998) applied a decision tree algorithm on data collected by AVHRR in 1984, to classify land cover into 13 classes based on a simplified IGBP classification (the classification scheme is provided in Appendix B). The classifier was based on metrics derived from the reflectance, temperature and NDVI values of the AVHRR data, and trained with reference data extracted from higher spatial resolution imagery received by Landsat MSS, Landsat TM and LISS.
- The global land cover dataset at one degree spatial resolution produced by Gopal et al. (1999). Gopal et al. (1999) used the same dataset, classification scheme and reference data as DeFries and Townshend (1994b); however, instead of a supervised maximum likelihood classification algorithm, a neural network

classifier was used, and an overall classification accuracy higher than the one achieved by DeFries and Townshend (1994b) was achieved (Gopal et al., 1999).

- The MODIS land cover dataset (MOD12) at 1 km spatial resolution produced by UMd (Friedl et al., 2002; Strahler et al., 1999). This dataset was intended to be reproduced every half year once a full year and a half of MODIS data were received (Strahler et al., 1999). However at the time of the study the only dataset available was the one produced by Friedl et al., (2002) by applying mainly a decision tree classifier (a neural network classifier was intended to be used too) on the following data collected during the July 2000 – December 2000 period: i) MODIS Nadir Bidirectional Reflectance Distribution Function (BRDF)-adjusted Reflectance values (NBARs) for the first seven bands (1-7) for every 16 days, ii) MODIS 16 day MVC Enhanced Vegetation Index (EVI) and iii) USGS land/sea mask. The classification was trained using reference data extracted from ancillary data and higher spatial resolution imagery collected by Landsat TM (Friedl et al., 2002). The land cover was classified into the IGBP (Loveland et al., 2000) classification scheme, the classes of which can be relabelled to provide compatibility with other classification schemes (Friedl et al., 2002; Strahler et al., 1999) such as the BioGeoChemical biome scheme (BGC) (Running et al., 1995), and the Leaf Area Index/Fraction of Photosynthetically Active Radiation biome scheme (LAI/FPAR) (Myneni et al., 1997) and the SiB2 (Sellers et al., 1996) (The classification schemes are provided in Appendix B).
- The Pan-European Land Cover Monitoring (PELCOM). PELCOM (Champeaux et al., 2000; Mucher et al., 2001, 2000) was produced by classifying data collected by AVHRR in 1997 (both supervised and unsupervised classification algorithms were used). The classification was mainly based on monthly MVC NDVI AVHRR data from the Deutsches Zentrum fur Luftund Raumfahrt (DLR) archive, and to a lesser degree on daily AVHRR images mosaiced together acquired from the archive of the Monitoring Agriculture by Remote Sensing (MARS) project. Reference data were extracted from the Coordination of Information on the Environment (CORINE) dataset (CLC1990) and other ancillary data sources such

as the Digital Chart of the World (DCW). PELCOM used a land cover classification scheme of 16 classes (provided in Appendix B).

- The Stockholm Environmental Institute (SEI) land cover map of Europe (SEI, 2006). The dataset was released in 1999 by SEI; it was produced by combining a variety of different ancillary data sources such as the "Forest Map of Europe" at 1 km spatial resolution produced by ESA in the early 1990s (ESA, 1992), the "Land Use Map of Europe" produced by FAO (FAO-Cartographia, 1980) in the 1970s, the AGRISTAT database from FAO (FAO-Agristat, 1990) and land use maps of the former USSR. The land cover classification scheme includes 90 classes. The dataset is available freely to collaborators on projects that SEI participates in and at a nominal cost for anyone else. The dataset was revised again in 2002 (Cinderby, 2002; Emberson and Cinerby, 2002).
- The Land Use Cover Area frame statistical Survey (LUCAS) by Eurostat and the Directorate General responsible for Agriculture (Delincé, 2000, 2001; Lucas, 2003). Data were collected in two phases. In the first phase, data were collected by surveying points selected by a two stage area frame systematic sampling design during springtime; in the first stage Primary Sampling Units (PSU) were selected by taking the cross-sections of a 18 by 18 km grid covering the study area, and in the second stage Secondary Sampling Units (SSUs) were selected by taking 10 points regularly distributed (in a rectangular area of 1500 × 600 m) around the centre of each PSU. In the second phase data were collected by interviewing farmers in autumn about yield and agricultural techniques, (Lucas, 2003). The dataset is available for free for research purposes. At the time of the present study two surveys had already been carried out, one in 2001 and the other in 2003. Land cover is classified under 57 classes displayed in Appendix B.
- The Land Cover Map 2000 (LCM2000) was created at the Centre for Ecology and Hydrology (CEH) Monks Wood under the Defra-funded project: CS2000 Module 9, Data Integration for Localised Results and Support for Indicators of Countryside Character and Quality. The LCM2000 extent is limited only within the UK and classifies UK land cover under 26 classes (The LCM2000's classification scheme is provided in Appendix B). The methodology made use of

Landsat TM images composed from scenes received in the winter and summer of 1998 (or the closest available year). The images were segmented into parcels of spectrally uniform pixels using an automated procedure. The class membership of each parcel was then determined by a maximum likelihood classification algorithm, trained with reference data which were collected by field visits using a minimum mapping area of half a hectare. Post-classification, classes which appeared to be out of context or were classified with a low confidence level were reviewed again (Fuller et al., 2002). The dataset is available in both vector and raster format. The raster format is available in two spatial resolutions 25 m and 1 km. The latter, is further available either as the dominant class within each 1 km^2 or in Countryside Information System (CIS) format. The dataset is freely available only in the 1 km dominant class raster format.

- The CORINE Land Cover map 1990 (CLC1990) was produced by the European Environment Agency (EEA) within the 1986-1996 period (EEA, 2006a, 2006b). It should be stressed that a more recent dataset the CLC2000 was released by the EEA at the end of 2004, but was not yet available at the time when this part of the study was carried out. Two versions of the CLC1990 dataset were available, the CLC1990 06/1999 and the CLC1990 12/2000. The most recent version at the time of the study (CLC1990 12/2000) extended over most of the EU15 countries apart from Sweden and Finland, 12 central and eastern European countries and parts of Morocco and Tunisia (a complete list of countries is provided in Appendix B). A hierarchical classification scheme comprised of three levels was used, containing 5, 15 and 44 classes in each level respectively (the scheme is provided in Appendix B). Land cover classes were identified by means of visual interpretation of false colour printouts of satellite imagery captured by Landsat MSS and TM, and SPOT HRV and XS, at a scale of 1:100000 (The imagery used for the UK and Greece were captured during the 1989-1990 and 1987-1991 time period, respectively (EEA, 2006c)). The minimum mapping unit area was set to 25 hectares. The interpretation process was further aided by the use of ancillary data such as existing maps, statistics and aerial photographs and in some cases by reference data collected by field visits. The dataset is available in vector and raster

format. The raster format is available in 100 m and 250 m spatial resolutions; both datasets were created by rasterizing the vector and assigning to each pixel the class of the vector polygon which overlays the centre of the pixel. The CLC1990 is freely available from EEA for non commercial purposes.

This study required reference data which had to be as recent, accurate, and unbiased as possible. Based on these criteria several of the above potential reference datasets were rejected.

Any dataset which was produced based on data collected from any of the three sensors assessed in this study (AVHRR, MODIS and VEGETATION), would introduce bias and should not be used for the purposes of this study. These datasets were: i) the GLC2000, ii) the IGBP DISCover, the UMd datasets created by iii) Hansen et al. (2000), iv) DeFries and Townshend (1994b), v) DeFries et al. (1995), vi) DeFries et al., (1998) and vii) Gopal et al. (1999), viii) the MOD12 and the ix) PELCOM.

The datasets produced by Olson and Watts (1982), Matthews (1983), Wilson and Henderson-Sellers (1985) and SEI were also rejected. The decision was based on the grounds that these datasets were created based on maps and ancillary data which were collected several decades before the current study and from various different sources, introducing possible errors due to recent land cover changes, and inconsistencies between different data collection methods and land cover class identification criteria.

The LUCAS dataset can provide reference data over a series of sample locations across the study areas. Such data were not considered sufficient for the requirements of this part of the present study. This is because land cover information collected over points could help provide land cover information with confidence over areas as large as the sensors' GIFOV only if the areas of interest are particularly homogeneous or a significantly high number of points were used. However there was no reason to assume that the study areas were highly homogeneous, and the number and distributions of the point samples of LUCAS were not considered sufficient to provide reference information over the entire extent of the two study sites with confidence. Thus LUCAS was also rejected.

Out of the remaining two reference datasets, (LCM2000 and CLC1990) the LCM2000 was more recently produced and at a higher spatial resolution than CLC1990. However, it was decided to use the CLC1990 dataset instead, due to the following factors:

- The CLC1990 covers both study areas (UK and Greece) unlike the LCM2000 which only covers the UK
- The CLC1990 is freely available at a higher spatial resolution (100 m and 250 m) than the LCM2000 which is available for free only in the 1 km dominant class raster format.
- The CLC1990 is likely to be more thematically accurate than the LCM2000. This assumption was based on the fact that land cover class assignment over the whole CLC1990 extent was based on visual interpretation of high resolution imagery, in comparison to the LCM2000 where land cover class assignment was based on a maximum likelihood classification algorithm, trained by reference data collected by field visits. The visual interpretation of high resolution imagery is assumed to be a more accurate land cover classification method than a maximum likelihood algorithm, this can be backed up by the literature where it can be seen that the visual interpretation of high resolution imagery is accepted as a valid method of attaining reference data (Belward and Loveland, 1995; Belward, 1996; DeFries et al., 1998; Friedl et al., 2002; Hansen et al., 2000; Liang, 2001; Malingreau et al., 1989; Muchoney et al., 2000; Strahler et al., 1999) which by default is considered to be 100% accurate. However, land cover maps produced based on maximum likelihood algorithms are not considered to be 100% accurate.

Therefore, the CLC1990 was considered to be the best choice from the available reference datasets at the time.

3.4.5 Reference data manipulation

3.4.5.1 Reclassification of CLC1990

At the time of the study the CLC1990 dataset was available on the EEA website in Environmental Systems Research Institute (ESRI) Band Interleaved by Line (BIL) format at either 100 m or 250 m spatial resolution. Considering that the average GIFOV of AVHRR, MODIS and VEGETATION is at best about 1 km at nadir point (apart from MODIS bands 1-2 (250 m) and 3-7 (500 m)), and that the CLC1990 was produced with a minimum mapping area of 25 ha and a positional accuracy of 150 m (EEA, 2006a), it was considered that the use of the 100 m spatial resolution CLC1990 version would not have been very realistic for the purposes of the study, and the 250 m version was preferred instead.

The CLC1990 dataset although it was never officially validated at the time of the study (an accuracy assessment was carried out later on in 2006 for the more recent version of the CORINE land cover map (the CLC2000) by comparing its agreement with the LUCAS dataset (EEA, 2006d), but no comparison was carried out for the CLC1990) was considered likely to contain errors due to possible land cover changes that may have occurred since the dataset's production (the data which were used to produce it were received more than a decade before the current study) and also because in general reference data are known to contain errors (Bauer et al., 1994; Bowers and Rowan, 1996; Foody, 2002; Merchant et al., 1994).

Errors in the reference data can cause errors in the production of land cover maps by mis-labelling the land-cover of the classes produced by the unsupervised classification algorithm and/or errors in accuracy assessment of the produced maps. Since no information about the accuracy of the reference data was available, it was not possible to estimate the effect of these errors on the assessed accuracy of the produced land cover maps, nor was there any evidence to suggest that maps produced using different sensors' data will be equally affected. Classification errors identified in land cover maps caused by errors in the used reference data can not be distinguished from errors caused by limitations of the sensor data (or any other factor for that matter). Therefore, in order to assess the relative effectiveness of the sensors in land cover mapping by means of

comparing the classification accuracies of the land cover maps produced using data from each sensor, classification errors caused by reference data errors had to be minimised.

The following actions were taken towards minimising potential errors in the CLC1990 reference data.

- Land cover classes which may have changed since the production of the CLC1990 dataset (e.g. burnt areas may have been reforested, trees in agroforestry areas may have been felled etc) were ignored in the analysis. By doing so probable errors due to land cover change in the reference data were minimised.
- Land cover classes which shared essentially the same land cover surface but were differentiated by land use (e.g. grassland and pastures) were merged together. This way the number of possible land cover classes a surface can be classified under was reduced and consequently the probability of assigning an incorrect land cover class over a surface was also reduced.
- Agricultural classes which are one of the highest contributors in misclassification errors over large areas (Hansen et al., 2000; Loveland et al., 1999) were all merged under a single thematic class (Agriculture). The probability of misclassification errors was reduced by reducing the total number of land cover classes, and possible errors in the reference data caused by possible changes in the agricultural use of land since the date the reference data were collected were minimised.
- The sea and ocean classes were removed because the study was only interested in land cover.

Due to the distinct differences between the spectral properties of land and water surfaces, the successful identification of water bodies was not considered to be particularly challenging for any of the three sensors. Water bodies covered a considerable percentage of both study areas (60% and 64% in the UK and Greek study area respectively). Consequently land cover maps produced over both study areas based on data from any of the three sensors, would have considerably higher estimated overall classification accuracies if the water body classes were included in the classification

scheme than if they were not. In such a case (water body classes included) differences between the land cover accuracies of each sensor's land cover maps which may have been more evident if the water body classes were not included, could have been overshadowed. On those grounds it was decided to remove the most spatially dominant water body classes (the sea and the ocean) from the land cover classification scheme.

It should also be noted that the classes which were aggregated into the Agriculture class were not necessarily spectrally similar. Nonetheless, this would not cause misclassification problems because the sensor data would be classified using an unsupervised classification algorithm with many classes; therefore, each spectrally dissimilar sub-class would be assigned to one or more unsupervised classes, and all unsupervised classes of each sub-class would then be assigned to the Agriculture class.

The reclassification of the CLC1990 was carried out in ERDAS IMAGINE. The CLC1990 was first imported to ERDAS IMAGINE so as to be converted to a format best handled by the software. The imported raster pixel values representing the original land cover classes of CLC1990 were then altered according to table 3.5 using the Recode function of ERDAS. Figures 3.3 and 3.4 display the original and reclassified versions of the CLC1990 dataset, respectively.

Table 3.5: The reclassification of the original CLC1990 land cover scheme in order to improve its classification accuracy.

Original Code	Original CORINE class	New code	New Land-cover class
1	Continuous urban fabric	1	Urban/Built-up
2	Discontinuous urban fabric	1	Urban/Built-up
3	Industrial or commercial units	1	Urban/Built-up
4	Road and rail networks and associated land	1	Urban/Built-up
5	Port areas	1	Urban/Built-up
6	Airports	1	Urban/Built-up
7	Mineral extraction sites	1	Urban/Built-up
8	Dump sites	0	Unknown/Removed
9	Construction sites	1	Urban/Built-up
10	Green urban areas	1	Urban/Built-up
11	Sport and leisure facilities	0	Unknown/Removed
12	Non-irrigated arable land	2	Agriculture
13	Permanently irrigated land	2	Agriculture
14	Rice fields	2	Agriculture
15	Vineyards	2	Agriculture
16	Fruit trees and berry plantations	2	Agriculture
17	Olive groves	2	Agriculture
18	Pastures	3	Grassland
19	Annual crops associated with permanent crops	2	Agriculture
20	Complex cultivation patterns	2	Agriculture
21	Land principally occupied by agriculture	2	Agriculture
22	Agro-forestry areas	0	Unknown/Removed
23	Broad-leaved forest	4	Broad-leaved
24	Coniferous forest	5	Coniferous
25	Mixed forest	6	Mixed forest
26	Natural grasslands	3	Grassland
27	Moors and heathland	7	Moors and heathland
28	Sclerophyllous vegetation	8	Sclerophyllous vegetation
29	Transitional woodland-shrub	9	Transitional woodland-shrub
30	Beaches, dunes, sands	10	Bare soil/sparsely vegetated
31	Bare rocks	10	Bare soil/sparsely vegetated
32	Sparsely vegetated areas	10	Bare soil/sparsely vegetated
33	Burnt areas	0	Unknown/Removed
34	Glaciers and perpetual snow	11	Glaciers and perpetual snow
35	Inland marshes	12	Inland marshes
36	Peat bogs	13	Peat bogs
37	Salt marshes	14	Salt marshes
38	Salines	15	Salines
39	Intertidal flats	16	Intertidal flats
40	Water courses	17	Water bodies
41	Water bodies	17	Water bodies
42	Coastal lagoons	17	Water bodies
43	Estuaries	18	Estuaries
44	Sea and ocean	0	Unknown/Removed
49	NODATA	0	Unknown/Removed
50	Sea and ocean	0	Unknown/Removed

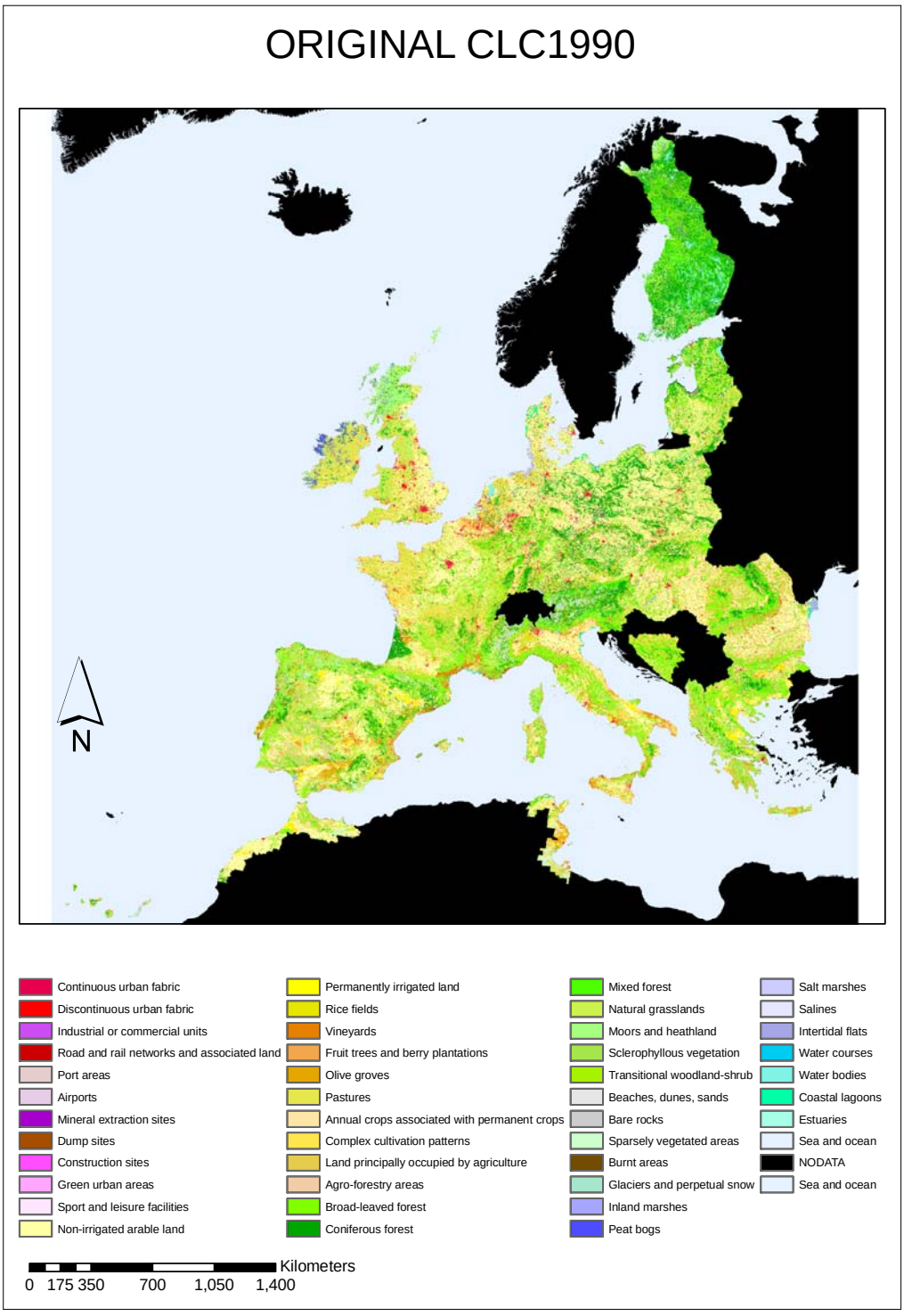

Figure 3.3: The original CLC1990 dataset (version 12/2000) at 250 m resolution

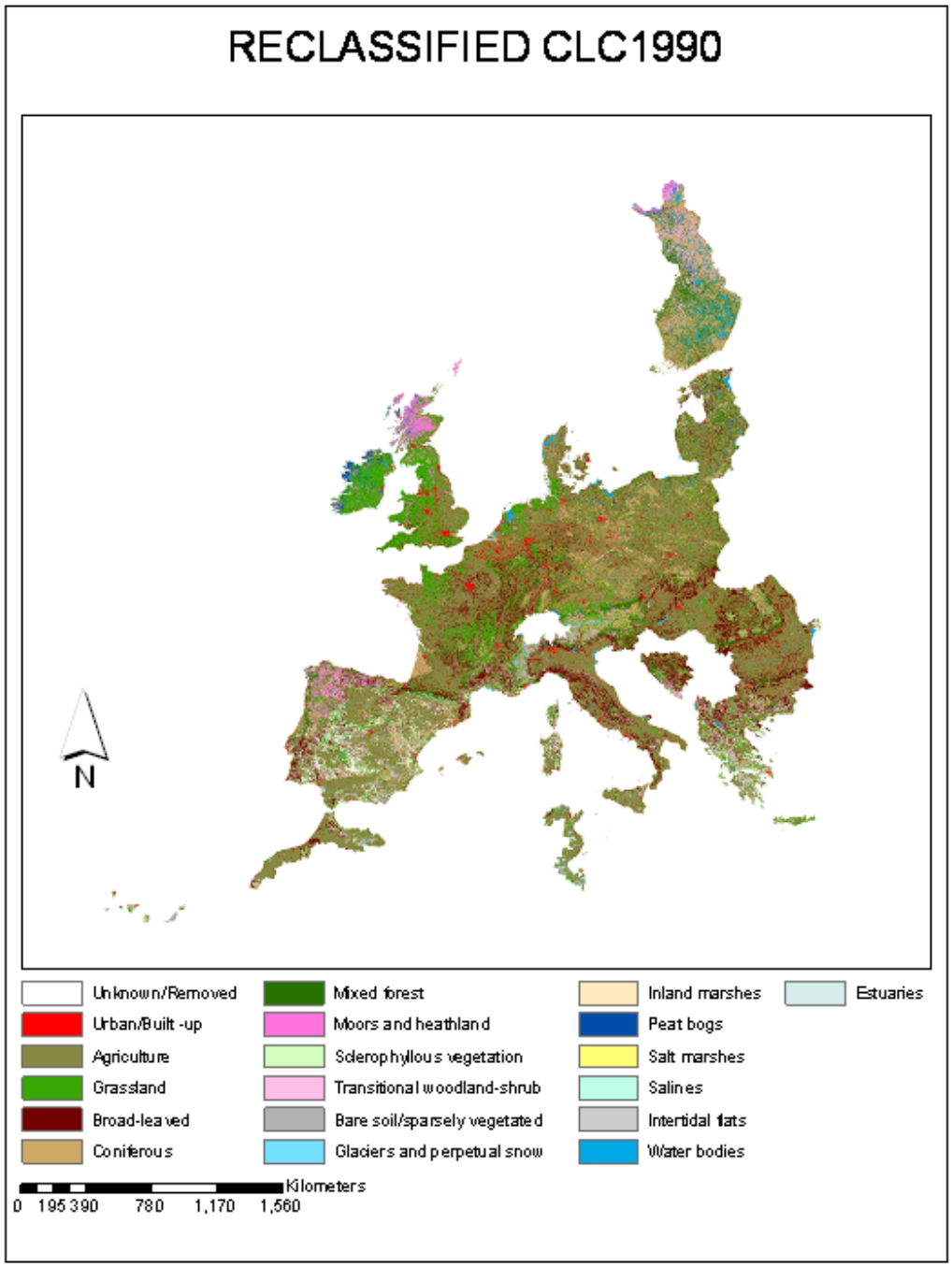

Figure 3.4: The reclassified CLC1990 dataset (version 12/2000) at 250 m resolution

Two rectangular areas covering the extent of each study area were then extracted from the reclassified CLC1990 image using the subset function of ERDAS. The dimensions of these areas are given in table 3.6.

Table 3.6: Dimensions of the UK and Greek study areas (Projection: Lambert Azimuthal Equal-area, Spheroid: GRS 1980, Datum GRS 1980)

	UK Study Area	Greek Study Area
Upper Left X	-1217438.193	844436.807
Lower Right X	-423938.193	1604686.807
Upper Left Y	1282017.649	-529518.065
Lower Right Y	290017.649	-1329768.065

The two study areas did not contain all of the 18 reclassified CLC1990 land cover classes; hence any non-existent land cover class was removed from the classification land cover scheme of each study area. The new classification schemes for the UK and Greek study areas are displayed in table 3.7.

Table 3.7: Existing reference classes in the UK and Greek study areas

	UK	Greece
0	Unknown/Removed	Unknown/Removed
1	Urban/Built-up	Urban/Built-up
2	Agriculture	Agriculture
3	Grassland	Grassland
4	Broad-leaved	Broad-leaved
5	Coniferous	Coniferous
6	Mixed forest	Mixed forest
7	Moors and heathland	Moors and heathland
8	Transitional woodland-shrub	Sclerophyllous vegetation
9	Bare soil/sparsely vegetated	Transitional woodland-shrub
10	Inland marshes	Bare soil/sparsely vegetated
11	Peat bogs	Inland marshes
12	Salt marshes	Peat bogs
13	Intertidal flats	Salt marshes
14	Water bodies	Salines
15	Estuaries	Intertidal flats
16	N/A	Water bodies
17	N/A	Estuaries

Before the reclassified CLC1990 reference data could be used for either helping to assign land-cover classes to the classes produced by the unsupervised classification algorithm or assessing the classification accuracy of the produced land cover maps, there was one more issue which had to be resolved. The reference data had a spatial resolution of 250 m while the average GIFOV of the three sensors at nadir point is about 1 km (Apart from MODIS 1-7 bands). As a result, a single pixel of sensor data is composed of 16 pixels of reference data and as such could potentially be composed of up to 16 different reference land cover classes. Subsequently, the problem rises of how to assign a single land cover class to an area covered by potentially more than one reference land cover classes, which in turn would help assign land cover classes to the produced unsupervised classes and assess the classification accuracy of the produced land cover maps.

In order to resolve the problem, the spatial resolution of CLC1990 data had to be degraded to 1 km. Two different approaches were suggested, regarding the spatial degradation rule that had to be adopted i) to retain the dominant class within the 16 pixels (dominant class rule) or ii) to create new classes based on the class composition within each square kilometre pixel.

The established approach in such cases would be the first option; to keep the dominant class (Cihlar et al., 1996; Cihlar, 2000; Foody, 2002; Hansen et al., 2000). Studies have shown that classifications based on low resolution data (spatial), overestimate the area of dominant classes, as opposed to the non-dominant that are under-estimated (Hay et al., 1997; Lioubimtseva, 2003; Mayaux and Lambin, 1995; Moody and Woodcock, 1995; Moody, 1998; Nelson and Holben, 1986; Strahler et al., 1999; Townshend and Justice, 1988). In other words, in low resolution (spatial) pixels, classification methods tend to identify the dominant class within the pixel.

The second approach was based on the argument that the radiation emanating from an area is the sum of all radiation sources, so that different composition of radiation sources (classes) within an area could result in different radiation values, and consequently distinct spectral signatures.

The research of the best spatial degradation strategy for classification purposes was beyond the original aim of this study; but, it was considered an interesting issue and it

was decided to pursue both approaches in the first study site (UK) and retain the best performing approach in the second (Greece).

3.4.5.2 Spatial degradation of the reclassified CLC1990 using the dominant class rule

The dominant class rule was the simpler of the two spatial degradation rules to implement. The process was assisted with the use of two Visual Basic 6 (VB6) programs written by the author for this study.

Before these programs could process the reference data, the data had to be exported in binary format so that they could be handled more easily by these programs. The data were exported in generic binary format, as unsigned 8-bit integers.

The reference data in binary format was then scanned by the first program (named Data_extractor) using a 4 by 4 pixel frame and the number of pixels belonging to each land cover class of the reference data classification scheme found within the 4x4 pixel area of the matrix were counted. The information regarding the number of pixels belonging to each land cover class within each 4x4 pixel frame were then stored in the form of separate bands in a new binary file as 8-bit integers using a Band Interleaved by Pixel (BIP) format. The newly created binary file therefore had 1 km spatial resolution and band number equal to the number of land cover classes in the reference data. The value of each pixel's band specified the number of the reference pixels of the land cover class represented by the particular band, which were present within the 1x1 km pixel.

The binary file created by the Data_extractor was then read by the second VB6 program (referred to from now on as Majority_extractor). The Majority_extractor read all bands of each pixel of the latter binary file and stored in a new binary file the number of the band which had the highest value within each pixel. The values were stored as unsigned 8-bit integers.

The values of each pixel of the final binary file identified the reference land cover class which was most dominant within the square kilometre area covered by that pixel. The process was repeated for both study areas. The spatially degraded reference datasets

along with their new classification schemes are displayed in figures 3.5 and 3.6 and table 3.8 respectively.

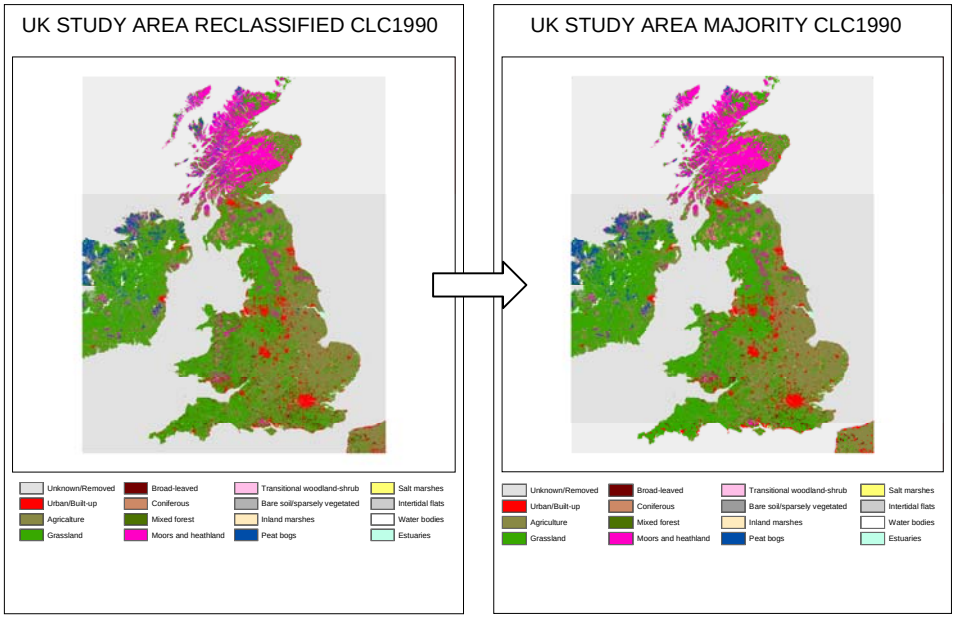

Figure 3.5: The spatial degradation of the reclassified CLC1990 dataset over the UK study area using the majority rule

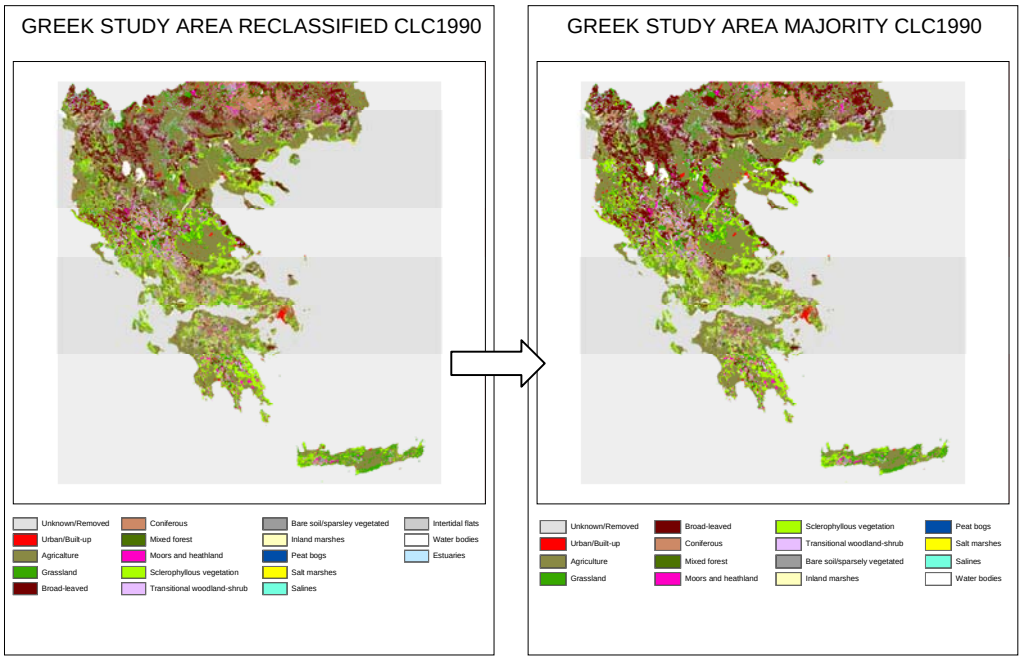

Figure 3.6: The spatial degradation of the reclassified CLC1990 dataset over the Greek study area using the majority rule

Table 3.8: Majority land cover classification scheme for the UK and Greek study areas

	UK	Greece
0	Unknown/Removed	Unknown/Removed
1	Urban/Built-up	Urban/Built-up
2	Agriculture	Agriculture
3	Grassland	Grassland
4	Broad-leaved	Broad-leaved
5	Coniferous	Coniferous
6	Mixed forest	Mixed forest
7	Moors and heathland	Moors and heathland
8	Transitional woodland-shrub	Sclerophyllous vegetation
9	Bare soil/sparsely vegetated	Transitional woodland-shrub
10	Inland marshes	Bare soil/sparsely vegetated
11	Peat bogs	Inland marshes
12	Salt marshes	Peat bogs
13	Intertidal flats	Salt marshes
14	Water bodies	Salines
15	Estuaries	Water bodies

By comparing tables 3.7 and 3.8 it can be seen that two land cover classes of the Greek study area classification scheme were lost after the spatial degradation (Intertidal flats and Estuaries). Such a possibility was anticipated, since some minor classes may not occur as the majority over an area of a square kilometre anywhere within the extent of a study area. The maps of the newly created reference data are displayed in figures 3.5 and 3.6.

3.4.5.3 Spatial degradation of the reclassified CLC1990 using the mixed class rule

The spatial degradation of the reclassified CLC1990 dataset using the class composition rule was also assisted with the use of VB6 software developed by the author for the purpose of this study.

The reclassified CLC1990 dataset of each study area was exported to a binary file and processed using the Data_extractor just as was done for the majority class spatial degradation rule; however, the binary file produced by the Data_extractor was further processed by different software, the Combination_extractor. The Combination_extractor read the binary file produced by the Data_extractor and determined the percentage of

coverage of each land cover class within each square kilometre pixel using a 10% coverage interval. A unique integer number (combination class number) was assigned to each new land cover class combination which was discovered. The software recorded the combination class number of each pixel to a new binary file (an unsigned 16-bit integer was used so that up to 65536 possible class compositions could be recorded) and also created a separate text file which described the class composition of each combination class number.

The software provided a description of each class composition using a code. The code was made up of a string of numbers, each number representing the cover percentage occupied by a certain land cover class within the square kilometre area of the class composition. Land cover classes which occupied 0%-10%, 10%-20%, 20%-30%, 30%-40%, 40%-50%, 50%-60%, 60%-70%, 70%-80%, 80%-90% and 90%-100% of the total area of the pixel were given the numbers 0, 1, 2, 3, 4, 5, 6, 7, 8 and 9 respectively. The order the numbers were written in the code followed the order of the reclassified CLC1990 classification scheme, thus the first number of the string referred to the first land cover class of the classification scheme, the second number to the second land cover class and so on. Some examples of different codes and the respective land cover compositions which they describe are given in table 3.9.

Table 3.9: Examples of combination codes and their respective class composition descriptions (letters are indicative only)

	Class composition	Code	Description
1	Class A	90000000000	90%-100% Class A
2	Class B	06003000000	60%-70% Class B, 30%-40% Class E
3	Class C	00200000060	20%-30% Class C, 60%-70% Class J
4	Class D	00001008000	10%-20% Class E, 80%-90% Class H
5	Class E	12230000000	10%-20% Class A, 20%-30% Class B, 20%-30% Class C, 30%-40% Class D
6	Class F	00040000200	40%-50% Class D, 20%-30% Class I
7	Class G	00100000700	10%-20% Class C, 70%-80% Class I
8	Class H	00030006000	30%-40% Class D, 60%-70% Class H
9	Class I	50000000003	50%-60% Class A, 30%-40% Class K
10	Class J	00002005000	20%-30% Class E, 50%-60% Class H
11	Class K	0000090000	90-100% Class F

When Combination_extractor was run for both study areas 9183 and 12698 existing class compositions were found in the UK and Greek study areas respectively (table 3.10). The total number of compositions discovered in either of the two study areas was too large for classification purposes. In order to reduce the number of class combinations two steps were taken: i) the coverage percentage interval was increased from 10% to 25% (land cover class coverages of 0%-25%, 25%-50%, 50%-75% and 75%-100%, were now represented in the code as 0, 1, 2, and 3 respectively) and ii) in composition where at least 75% of a pixel was covered by a single land cover class any other land cover class present within that pixel was ignored. The Combination_extractor was modified accordingly and was run again for both study areas (table 3.11).

Table 3.10: Existing class combinations discovered in the UK and Greek study areas by using a 10% coverage interval

UK study area		Greek study area	
1	9000000000000000	1	900000000000000000
2	0005000100000100	2	600000110000000000
3	0006000300000000	3	000000350010000000
4	0009000000000000	4	000000070020000000
.	.	.	.
.	.	.	.
9180	1050100000000000	12695	010700000010000000
9181	0420300000000000	12696	104100002000000000
9182	0010300003001000	12697	301000001030000000
9183	0500130000000000	12698	100300001300000000

Table 3.11: Existing class combinations discovered in the UK and Greek study areas by using a 25% coverage interval and by ignoring minor classes in pixels which are covered at least 75% by a single land cover class

UK study area		Greek study area	
1	3000000000000000	1	300000000000000000
2	0002000000000000	2	200000000000000000
3	0002000100000000	3	000000120000000000
4	0003000000000000	4	000000030000000000
.	.	.	.
.	.	.	.
953	2000010001000000	995	100000002100000000
954	0000100000100000	996	000000201010000000
955	0120000000100000	997	100000021000000000
956	0101000000100000	998	000010201000000000

In table 3.11 it can be seen that after the modifications the number of existing class compositions were significantly reduced for both study areas (956 and 998 for the UK and Greek study areas respectively); nevertheless, the total number of class compositions were too numerous for any practical land cover classification scheme.

It was possible that some of the identified class compositions occupied only a very small portion of a study area. To test this possibility a program was written in VB6 which counted the number of pixels occupied by each class combination (Histogram_extractor). When the Histogram-extractor was run for both study areas it was discovered that hundreds of class combinations indeed existed only over a few pixels (figures 3.7 and 3.8). If such class compositions were removed from the classification the total number of classes could drop to a more manageable number without significantly affecting the final land cover map. Therefore it was decided to remove any class combination present in a study area which covered less than 0.25% of the total area. The Combination_extractor was further modified to conform to the new rule and was run again for both study areas.

The class combinations produced by the modified Combination_extractor for the UK and Greek study site are displayed in tables 3.12 and 3.13 respectively. It can be seen that the total number of class combinations in each study area were reduced significantly (38 and 66 class combinations for the UK and Greek study areas respectively); but not enough for a practical land cover classification scheme. As a last attempt to reduce the total number of classes it was suggested to merge class compositions together. Class compositions consisting of the same land cover classes were merged together regardless of each land cover's coverage ratio, and class combinations containing the "Unknown" land cover class were removed. The new land cover classification schemes for the UK and Greek study areas after the merging was performed are displayed in table 3.14.

The final reference datasets of each study area which were produced either by the majority or the class composition spatial degradation rule were imported back to ERDAS. Once imported, the datasets had to be georeferenced again because all georeferencing information was lost during the Export-Import processes. Additionally, the UK and Greek study area datasets were re-projected to the Ordnance System Great Britain (OSGB) and Transverse Mercator (Spheroid: GRS 1980, Datum: EGSA87) projection systems respectively; because, these are the projection systems most frequently used in

the production of maps within these respective regions. The maps of the newly created reference data are displayed in figures 3.9 and 3.10.

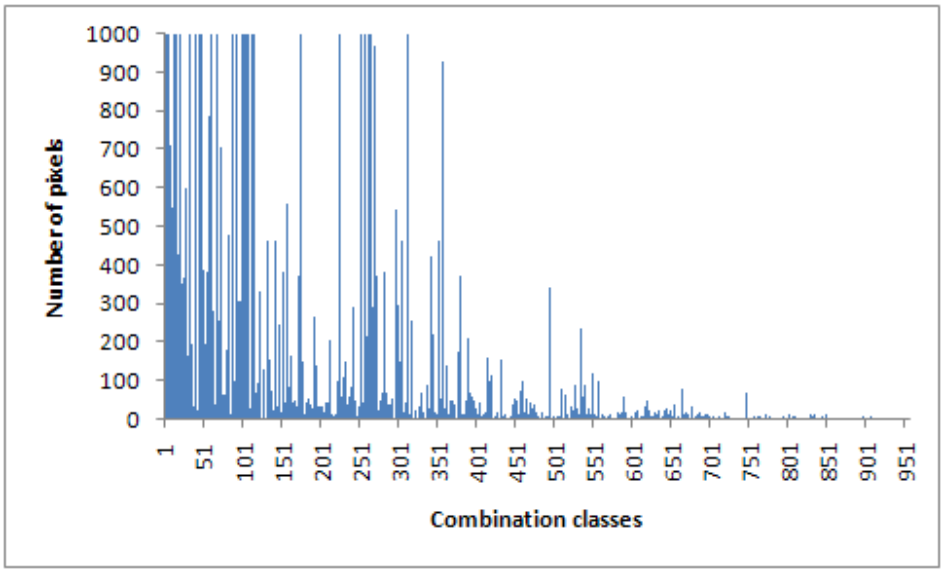

Figure 3.7: Several class combinations occupied more than 1000 pixels however a Y axis maximum of 1000 was used in this graph so that class combinations occupying small number of pixels could easily be seen. From this graph it becomes obvious that the majority of class combinations within the UK study area are only occupying a small portion of the total area.

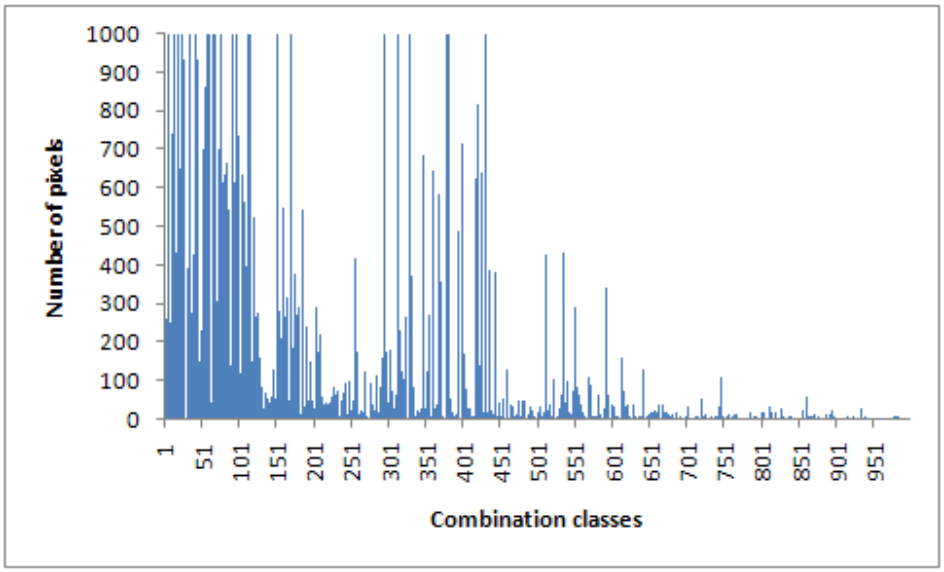

Figure 3.8: Several class combinations occupied more than 1000 pixels however a Y axis maximum of 1000 was used in this graph so that class combinations occupying small number of pixels could easily be seen. From this graph it becomes obvious that the majority of class combinations within the Greek study area are only occupying a small portion of the total area.

Table 3.12: Existing class combinations discovered in the UK study area by using a 25% coverage interval, by ignoring minor classes in pixels which are covered at least 75% by a single land cover class and by ignoring class combinations which cover less than 0.25% of the total study area

Class ID	Class combination code	Description
1	3000000000000000	≥75% Unknown
2	0002000000000000	50%-75% Grassland
3	0002000100000000	50%-75% Grassland 25%-50% & Moors and heathland
4	0003000000000000	≥75% Grassland
5	1002000000000000	25%-50% Unknown & 50%-75% Grassland
6	2001000000000000	50%-75% Unknown & 25%-50% Grassland
7	0001000200000000	25%-50% Grassland & 50-75% Moors and heathland
8	0000000300000000	≥75% Moors and heathland
9	0002000200000000	50% Grassland 50% & Moors and heathland
10	0201000000000000	50%-75% Urban/Built-up & 25%-50% Grassland
11	0012000000000000	25%-50% Agriculture & 50%-75%Grassland
12	0000000200010000	50%-75% Moors and heathland & 25%-50% Peat bogs
13	0000000000030000	≥75% Peat bogs
14	0001000000020000	25%-50% Grassland & 50%-75% Peat bogs
15	0000000200000000	50%-75% Moors and heathland
16	0002000000010000	50%-75% Grassland & 25%-50% Peat bogs
17	0000000000000030	≥75% Water bodies
18	0021000000000000	50%-75% Agriculture & 25%-50% Grassland
19	0102000000000000	25%-50% Urban/Built-up & 50%-75%Grassland
20	0300000000000000	≥75% Urban/Built-up
21	0000030000000000	≥75% Coniferous
22	0001020000000000	25%-50% Grassland & 50%-75% Coniferous
23	0002100000000000	50%-75% Grassland & 25%-50% Broad-leaved
24	0011000000000000	25%-50% Agriculture & 25%-50% Grassland
25	0002010000000000	50%-75% Grassland & 25%-50% Coniferous
26	0000020100000000	50%-75% Coniferous & 25%-50% Moors and heathland
27	0000010200000000	25%-50% Coniferous & 50%-75% Moors and heathland
28	0111000000000000	25%-50% Urban/Built-up & 25%-50% Agriculture & 25%-50%Grassland
29	0210000000000000	50%-75% Urban/Built-up & 25%-50% Agriculture
30	0000000000000003	≥75% Estuaries
31	0030000000000000	≥75% Agriculture
32	0120000000000000	25%-50% Urban/Built-up & 50%-75%Agriculture
33	0020000000000000	50%-75% Agriculture
34	0022000000000000	50% Agriculture & 50% Grassland
35	0020100000000000	50%-75% Agriculture & 2%5-50% Broad-leaved
36	0011100000000000	25%-50% Agriculture & 25%-50% Grassland 25-50% & Broad-leaved
37	0001200000000000	25%-50% Grassland & 50%-75% Broad-leaved
38	0000300000000000	≥75% Broad-leaved

Table 3.13: Existing class combinations discovered in the Greek study area using a 25% coverage interval, by ignoring minor classes in pixels which are covered at least 75% by a single land cover class and by ignoring class combinations which cover less than 0.25% of the total study area

Class	Class combination	Description
1	300000000000000000	>75% Unknown
2	000000030000000000	≥75% Moors and heathland-shrub
3	000030000000000000	≥75% Broad-leaved
4	000010200000000000	25%-50% Broad-leaved & 50%-75% Mixed forest
5	000120000000000000	25%-50% Grassland & 50%-75% Broad-leaved
6	003000000000000000	≥75% Agriculture
7	002010000000000000	50%-75% Agriculture & 25-50% Broad-leaved
8	012000000000000000	25%-50% Urban/Built-up & 50%-75% Agriculture
9	001100000000000000	25%-50% Agriculture & 25%-50% Grassland
10	000300000000000000	≥75% Grassland
11	001200000000000000	25%-50% Agriculture & 50%-75% Grassland
12	000003000000000000	75% Mixed forest
13	000200000000000000	50%-75% Grassland
14	002000000000000000	50%-75% Agriculture
15	002100000000000000	50%-75% Agriculture & 25%-50%Grassland
16	000003000000000000	≥75% Coniferous
17	000002000100000000	50%-75% Coniferous & 25%-50% Transitional woodland-shrub
18	001002000000000000	25%-50% Agriculture & 50%-75% Coniferous
19	000001000200000000	25%-50% Coniferous & 50%-75% Transitional woodland-shrub
20	000002100000000000	50%-75% Coniferous & 25%-50% Mixed forest
21	000020100000000000	50%-75% Broad-leaved & 25%-50% Mixed forest
22	000020000000000000	50%-75% Broad-leaved & 25%-50% Mixed forest
23	001000200000000000	25%-50% Agriculture & 50%-75% Mixed forest
24	030000000000000000	≥75% Urban/Built-up
25	000000000200000000	50%-75% Transitional woodland-shrub
26	001020000000000000	25%-50% Agriculture & 50%-75% Broad-leaved
27	002000000100000000	50%-75% Agriculture & 25%-50% Transitional woodland-shrub
28	002001000000000000	50%-75% Agriculture & 25%-50% Mixed forest
29	000020000100000000	50%-75% Broad-leaved & 25%-50% Transitional woodland-shrub
30	001000000100000000	25%-50% Agriculture & 25%-50% Transitional woodland-shrub
31	102000000000000000	25%-50% Unknown & 50%-75% Agriculture
32	201000000000000000	50%-75% Unknown and 25%-50% Agriculture
33	000001200000000000	25%-50% Coniferous & 50%-75% Mixed forest
34	001000000200000000	25%-50% Agriculture & 50%-75% Transitional woodland-shrub
35	000000200100000000	50%-75% Mixed forest & 25%-50% Transitional woodland-shrub
36	000002000000000000	50%-75% Coniferous
37	000210000000000000	50%-75% Grassland & 25%-50% Broad-leaved
38	000200000100000000	50%-75% Grassland & 25%-50% Transitional woodland-shrub
39	002001000000000000	50%-75% Agriculture & 25%-50% Coniferous
40	000010000100000000	25%-50% Broad-leaved & 25%-50% Transitional woodland-shrub
41	001010000000000000	25%-50% Agriculture & 25%-50% Broad-leaved
42	000100000100000000	25%-50% Grassland & 25%-50% Transitional woodland-shrub
43	000000000030000000	≥75% Bare soil/Sparsely vegetated
44	000010000200000000	25%-50% Broad-leaved & 50%-75% Transitional woodland-shrub
45	000000000300000000	≥75% Transitional woodland-shrub
46	000002000000000000	50%-75% Mixed forest
47	000100000200000000	25%-50% Grassland & 50%-75% Transitional woodland-shrub
48	000110000100000000	25%-50% Grassland & 25%-50% Broad-leaved & 25%-50% Transitional woodland-shrub
49	000000000000000030	≥75% Water bodies
50	000000100200000000	25%-50% Mixed forest & 50%-75% Transitional woodland-shrub
51	002000001000000000	50%-75% Agriculture & 25%-50% Sclerophyllous vegetation
52	000000003000000000	≥75% Sclerophyllous vegetation
53	001000002000000000	25%-50% Agriculture & 50%-75% Sclerophyllous vegetation
54	001000001000000000	25%-50% Agriculture & 25%-50% Sclerophyllous vegetation
55	000010002000000000	25%-50% Broad-leaved & 50%-75% Sclerophyllous vegetation
56	200000001000000000	50%-75% Unknown & 25%-50% Sclerophyllous vegetation
57	000200001000000000	50%-75% Grassland & 25%-50% Sclerophyllous vegetation
58	000020001000000000	50%-75% Broad-leaved & 25%-50% Sclerophyllous vegetation
59	000100002000000000	25%-50% Grassland & 50%-75% Sclerophyllous vegetation
60	000100001000000000	25%-50% Grassland & 25%-50% Sclerophyllous vegetation
61	000000001200000000	25%-50% Sclerophyllous vegetation & 50%-75% Transitional woodland-shrub
62	001100001000000000	25%-50% Agriculture & 25-50% Grassland & 25%-50% Sclerophyllous vegetation
63	002000002000000000	50% Agriculture & 50% Sclerophyllous vegetation
64	000000002100000000	50%-75% Sclerophyllous vegetation & 25-50% Transitional woodland-shrub
65	100000002000000000	25%-50% Unknown & 50%-75% Sclerophyllous vegetation
66	000000002000000000	50%-75% Sclerophyllous vegetation

Table 3.14: Final land cover classification schemes of the UK and Greek study areas using the class composition spatial degradation rule.

Code	UK study area	Greek study area
1	Urban/Built-up	Urban/Built-up
2	Grassland	Grassland
3	Agriculture	Agriculture
4	Broad-leaved	Broad-leaved
5	Coniferous	Coniferous
6	Moors and heathland	Moors and heathland
7	Peat bogs	Water bodies
8	Water bodies	Mixed forest
9	Estuaries	Sclerophyllous vegetation
10	Grassland & Moors and heathland	Bare soil/Sparsely vegetated
11	Urban/Built-up & Grassland	Transitional woodland-shrub
12	Agriculture & Grassland	Grassland & Broad-leaved
13	Moors and heathland & Peat bogs	Agriculture & Broad-leaved
14	Grassland & Peat bogs	Agriculture & Grassland
15	Grassland & Coniferous	Coniferous & Transitional woodland-shrub
16	Grassland & Broad-leaved	Agriculture & Coniferous
17	Coniferous & Moors and heathland	Agriculture & Mixed forest
18	Urban/Built-up & Agriculture	Sclerophyllous vegetation & Transitional woodland-shrub
19	Agriculture & Broad-leaved	Urban/Built-up & Agriculture
20	Urban/Built-up, Agriculture & Grassland	Agriculture & Transitional woodland-shrub
21	Agriculture, Grassland & Broad-leaved	Broad-leaved & Transitional woodland-shrub
22	N/A	Grassland & Transitional woodland-shrub
23	N/A	Agriculture & Sclerophyllous vegetation
24	N/A	Grassland & Sclerophyllous vegetation
25	N/A	Mixed forest & Transitional woodland-shrub
26	N/A	Broad-leaved Sclerophyllous vegetation
27	N/A	Grassland, Broad-leaved & Transitional woodland-shrub
28	N/A	Agriculture, Grassland & Sclerophyllous vegetation

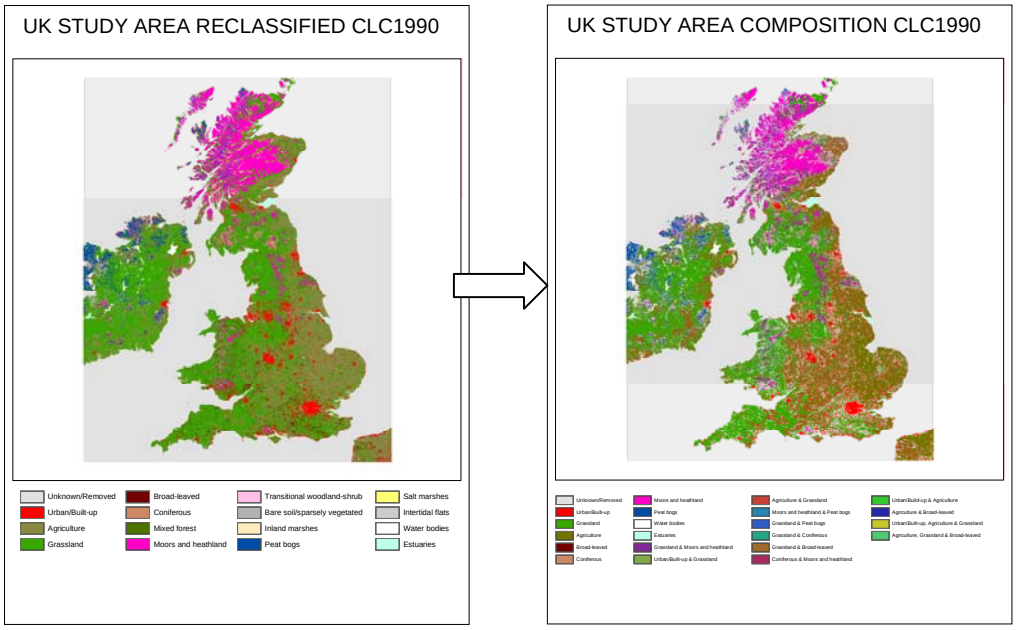

Figure 3.9: The spatial degradation of the reclassified CLC1990 dataset over the UK study area using the class composition rule

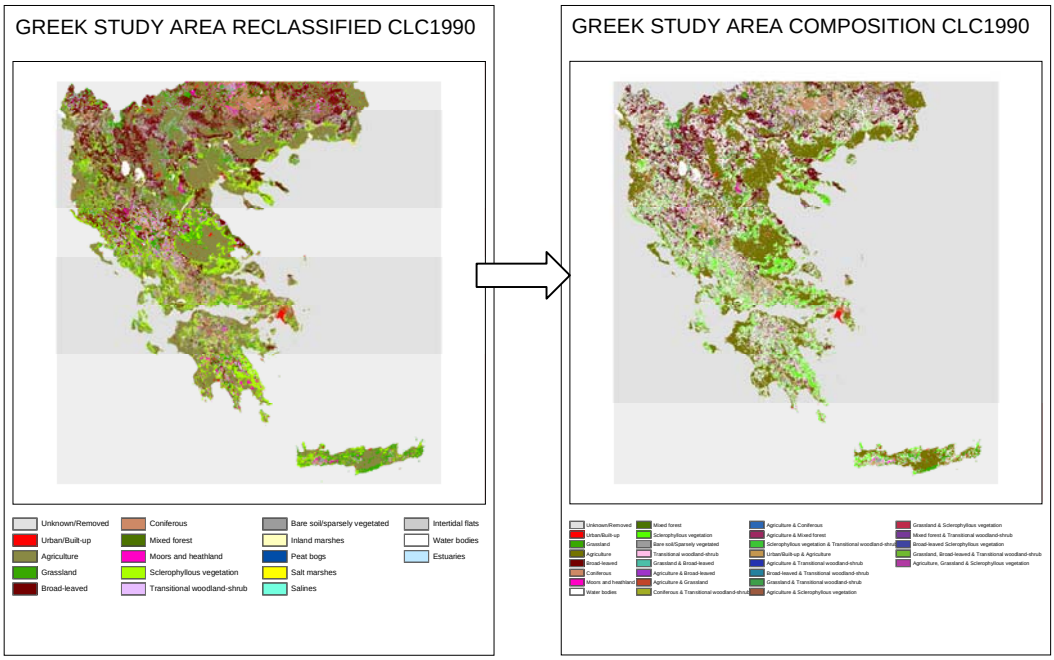

Figure 3.10: The spatial degradation of the reclassified CLC1990 dataset over the Greek study area using the class composition rule

3.4.6 Image processing

3.4.6.1 Sensor data acquisition and import

AVHRR

Data were acquired online from NOAA's Comprehensive Large Array-data Stewardship System (CLASS) website: http://www.class.noaa.gov (20 February 2003). The search engine of the website was used to select and consequently download 1 km Level 1B AVHRR data (either LAC or HRPT), captured during daytime on each of the pre-selected dates over each study area. In cases when more than one image were found for a single date (either because the study area was captured again on a different pass of the same sensor or it was captured by another AVHRR sensor onboard a different NOAA satellite) the image where the study area was most closely situated to the image centre was selected (to minimise spatial resolution degradation at the image edges).

The data files contained calibration and Global Control Points (GCPs) information besides the raw DN values of the three (1, 2 and 3A) AVHRR reflective bands. This information could be read and used by ERDAS to radiometrically and geometrically correct the data during the import process. Due to the intention to classify each image without the use of data extracted from a different image, the images did not need to be radiometrically corrected (calibrated) and that option was not chosen during the import process. On the other hand the images needed to be geometrically corrected and georeferenced in order to accurately cross-reference features between the sensor and reference data, therefore the option to geometrically correct the images was chosen.

MODIS

Data were acquired online from NASA's EOSDG website at: http://redhook.gsfc.nasa.gov/~imswww/pub/imswelcome/plain.html (10 March 2003). The search engine of the website was used to select and consequently download MODIS/TERRA 1km reflective solar bands scaled integers, (In EOS Hierarchical Data Format (HDF)), captured during daytime on each of the pre-selected dates over each study area (Since the 25th of September 2006, the above MODIS data were no longer available through the EOSDG website but were made available through the:

http://ladsweb.nascom.nasa.gov/data/ (12 January 2007) website instead). Similarly to AVHRR if more than one images were found for a single date the image where the study area was most closely situated to the image centre was selected. Data collected by the thermal bands have been used effectively to improve classification accuracies (Lambin and Ehrlich,1996a, 1996b; Liang, 2001; Nemani and Running, 1995; Nemani et al., 1993; Running et al., 1995); nevertheless the download and use of MODIS thermal data was deemed an unnecessary use of storage space and processing resources, as it was expected (based on the theoretical comparison performed in Chapter 2) that even with only the reflectance data used, MODIS data would produce more accurate land cover maps than those produced using data collected by either AVHRR or VEGETATION. Furthermore, although reflectance data were available to be downloaded at spatial resolutions of 250 m and 500m for the bands 1-2 and 3-7 respectively, it was decided to download all MODIS data at 1 km resolution (data collected by bands 1-7 were spatially degraded to 1 km by means of averaging). The decision was based on the fact that the reference data were produced at a 1 km spatial resolution in order to match the spatial resolution (at nadir point) of AVHRR, VEGETATION and all MODIS bands other than the first seven; therefore if MODIS data at 250 m or 500 m spatial resolution were used, they would require a different reference dataset and bias would have been introduced to the comparison. It should also be mentioned that for each date the data of the first seven spectral bands were stored in separate EOS-HDF files to the data of the remaining MODIS spectral bands, hence both had to be downloaded for each date.

Additionally cloud mask products (MOD35_L2) were available for each of the selected MODIS images. These cloud mask products were also downloaded, because at a later stage of the image processing, cloud contaminated pixels had to be identified and masked before applying the classification algorithm (to minimise classification errors due to cloud contamination).

The MODIS data (both daily reflectance and cloud mask products) could have been imported to ERDAS using the MODIS EOS-HDF format; however this option was not preferred. Instead the Data Pool HDFEOS-to-GeoTiff (HEG) tool was used to export the data to GeoTiff format which could also be handled by ERDAS. The HEG tool was developed to handle particularly MODIS data and is freely available though the Land

Processes (LP) Distributed Active Archive Center (DAAC) Data Pool File Transfer Protocol (FTP) site. It was preferred to use the HEG tool because the import process was considerably faster than that of ERDAS and the GeoTiff files occupied less storage space than the respective IMG files. When the HEG tool exported the GeoTiffs from the EOS-HDF files it also geometrically corrected the images. The pixel values of the GeoTiffs could be converted to reflectance values using the scale coefficients provided within each EOS-HDF file; however such a conversion was not needed for the purpose of this study and pixel values were left scaled to save storage space (the scaled integers required 16 bits of data storage space per pixel value as opposed to 32 bits which they would have occupied if converted to reflectance values (float)). As mentioned earlier the first seven spectral bands of MODIS were stored in separate HDF files to the remaining spectral bands; therefore, for each date two multi-band GeoTiffs were exported. The two multi-band GeoTiffs of each date were then layerstacked together to form single multi-band images, containing all spectral bands.

VEGETATION

VEGETATION daily P-products data captured over the UK and Greek study areas during daytime at the pre-selected dates, were provided freely by the CTIV processing centre at VITO. The data were made available for this study through FTP (vusftp.vgt.vito.be) after an application describing the intended use of the requested VEGETATION data was submitted and approved.

For every requested date (for both study areas), the following data were provided:

- Spectral band B0 in HDF format
- Spectral band B2 in HDF format
- Spectral band B3 in HDF format
- Spectral band MIR in HDF format
- Solar azimuth angle in HDF format
- Status map in HDF format
- Solar zenith angle in HDF format
- Viewing azimuth angle in HDF format
- Viewing zenith angle in HDF format

- Water vapour grid in HDF format
- Ozone grid in HDF format
- Aerosol grid in HDF format
- A quick look of the image
- A text file providing information regarding the data (such as acquisition date, georeferencing details, segment number, image number of lines and columns etc)

The data stored in the spectral band HDF files contained the reflectance values of each band, scaled to integers (to save storage space) by multiplying the reflectance values by 0.0005. Each spectral band was imported to ERDAS using the HDF raster format. For each date four IMG files were created (one for each band of VEGETATION), these were then stacked together using the layerstack function of ERDAS to form a single 4-band image for each date.

The status map provided information for every pixel regarding the radiometric quality of every spectral band, the probability of cloud presence in the pixel area and whether the pixel was covered by land, water or ice. Similarly to MODIS, this information was considered valuable for the cloud mask image processing step which was going to follow; thus the status map of each date was also imported to ERDAS using the HDF raster format.

The metadata file within each dataset contained georeferencing information of each image. All images had to be georeferenced in order to associate the images with the reference data; therefore the text file of each date was stored for later use. The remainder of the data were not needed (their use was primarily for atmospheric correction, which like the radiometric correction of the data, was not needed for the same reasons) and were discarded.

3.4.6.2 Cloud and snow/ice masking

Land cover classification algorithms such as the maximum likelihood (which was intended to be used in this study), rely on the recorded spectral properties of different land covers to properly identify them. Clouds, snow and ice commonly display higher reflectance values in the visible spectral bands (hence their white colour) and lower brightness temperatures than most land surfaces. The presence of either of them within an area where data are collected from a remote sensor would alter the apparent recorded spectral properties of the land cover class which normally covers that area (or the land cover class indicated by the reference data). Consequently if data collected from such an area (covered with either clouds, snow or ice) were used in a maximum likelihood classifier either for training the classifier or to identify the land cover class the area is covered with, misclassification errors would be caused. In order to minimise such classification errors, it is necessary to detect and remove/mask cloud and snow/ice contaminated pixels from sensor data before using them for land cover classification purposes. It could be argued that snow and ice are land cover classes themselves and should not have been removed; however, snow and ice are not land cover classes included in the classification scheme of CLC1990 and as such the reference data would not be able to be used to identify them. Moreover, because the extent of snow and ice cover is dependant on environmental conditions which change over time (e.g. temperature) even if they were included in the CLC1990 classification scheme, the accuracy of the reference data would vary from date to date.

AVHRR

Clouds, snow and ice are usually detected by using a range of criteria, such as the values of indices based on the recorded reflectance and/or brightness temperature values, or the values of the recorded reflectance and brightness temperatures themselves. The values of these criteria are determined after sampling the spectral profiles of a number of cloud, snow or ice contaminated pixels equally spread across the extent of each image. The process of determining the values of the criteria must be repeated for each image if

the images are not radiometrically corrected as was the case for the AVHRR data in this study. Additionally the process is not always very successful and cloud/snow/ice free pixels can be marked as contaminated and vice versa. Therefore, this method of cloud/snow/ice detection was considered to be best suited to dealing with a large number of radiometrically corrected images, which was not the case in the present study (19 non-radiometrically corrected AVHRR images).

Instead it was believed that a more accurate cloud/snow/ice detection could be achieved by means of visual interpretation; after all the samples needed to determine the cloud/snow/ice detection criteria are commonly taken from cloud/snow/ice contaminated pixels which have been visually identified. All AVHRR images were displayed and visually interpreted for clouds/snow/ice on ARCGIS ARCMAP. Then a shapefile was created for each image by digitising polygons around cloud/snow/ice contaminated and clear areas; a Field ID value of zero was given to polygons enclosing cloud/snow/ice contaminated pixels and a value of one to the remaining polygons. Each shapefile was then converted to raster format with a pixel size of 1 km and pixel values based on the Field ID attribute. Each raster was then multiplied by its respective AVHRR image; thus, all cloud/snow/ice contaminated pixel values in the newly created cloud masked AVHRR images were converted to zero, while the rest of the pixel values remained unchanged.

MODIS

As mentioned earlier MODIS cloud mask products (MOD35_L2) for each of the MODIS images were downloaded and converted to GeoTiffs along with the reflectance MODIS data. Each pixel of the imported (cloud mask) GeoTiffs had a signed 8-bit integer value which was the value of a binary number converted to integer in the decimal system. The value of each binary number depended on the cloud contamination probability, illumination conditions (whether it is day or night), location (whether it is located in the Sun glint path or in a coastal area), and cover (whether it is covered by water, land, ice, snow, or desert) of its corresponding pixel (table 3.15).

Table 3.15 (King, 2006): Description of MODIS cloud mask (MOD35_L2) binary pixel values

Bits	Field Description	Bit Interpretation Key
0	Cloud Mask Flag	0 = Not Determined 1 = Determined
1-2	Unobstructed FOV Quality Flag	0 = Confident Cloudy 01 = Probably Cloudy 10 = Probably Clear 11 = Confident Clear
3	Day/Night Flag	0 = Night 1 = Day
4	Sun glint Flag	0 = Yes 1 = No
5	Snow/Ice Background Flag	0 = Yes 1 = No
6-7	Land/Water Background Flag	00=Water 01=Coastal 10=Desert 11=Land

Each binary number was formed by placing the bit interpretation keys next to each other (table 3.15) starting from the 7^{th} bit field and ending with the 0^{th} bit field (7, 6, 5, 4, 3, 2, 1, 0). The interest was in masking any pixels which did not meet the following criteria:

- Determined cloud mask flag
- Confident clear (cloud)
- Day flag
- Negative snow/ice background flag

There were eight possible binary values which met the above criteria:

- 11111111
- 10111111
- 01111111
- 00111111
- 11101111
- 10101111
- 01110111
- 00101111

The most and least significant bits were the 7th and 0th respectively (King, 2006). When the cloud mask products were converted to GeoTiffs using the HEG tool, the binary numbers were converted to signed 8-bit integers in the decimal system. The converted new values of the above eight binary numbers were calculated using the following equation:

$$Number_{10} = \begin{cases} -((|1-6^{th}\,bit|)\times 2^6 + (|1-5^{th}\,bit|)\times 2^5 + (|1-4^{th}\,bit|)\times 2^4 + (|1-3^{rd}\,bit|)\times 2^3 + (|1-2^{nd}\,bit|)\times 2^2 + (|1-1^{st}\,bit|)\times 2^1 + (|1-0^{th}\,bit|)\times 2^0 + 1) & 7^{th}\,bit = 1 \\ (|1-7^{th}\,bit|)\times 2^7 + (|1-6^{th}\,bit|)\times 2^6 + (|1-5^{th}\,bit|)\times 2^5 + (|1-4^{th}\,bit|)\times 2^4 + (|1-3^{rd}\,bit|)\times 2^3 + (|1-2^{nd}\,bit|)\times 2^2 + (|1-1^{st}\,bit|)\times 2^1 + (|1-0^{th}\,bit|)\times 2^0 & 7^{th}\,bit = 0 \end{cases}$$

The calculated values of each of the eight binary numbers in signed 8-bit integer format using a decimal system were the following:

- -1
- -65
- 127
- 63
- -17
- -81
- 111
- 47

Consequently, reflectance image pixels whose corresponding cloud mask pixel value was not equal to any of the above eight integers had to be masked. To do so each cloud mask raster was recoded to a new raster, by assigning the value one to pixels with the cloud mask value equal to any of the above eight numbers, or the value zero to any pixel with any other cloud mask value. Then each of the new rasters was multiplied with its corresponding reflectance image, creating a new reflectance raster. Thus, a new reflectance image was created for each date, where any pixels which were either potentially cloud contaminated, recorded during night time, covered by snow/ice or the cloud mask flag was not determined for them, were masked.

VEGETATION

VEGETATION status maps were imported to ERDAS along with the reflectance data for each date/image. Status maps provided information for each pixel of their corresponding image, regarding the presence of clouds within their extent, whether they are located on water or land, covered by snow/ice or not, and whether the radiometric quality of their spectral bands is bad or good. Similarly to MODIS, this information was stored using an 8-bit binary number, starting with the 7^{th} bit field and ending with the 0^{th} (7, 6, 5, 4, 3, 2, 1, 0), also the most and least significant bits were the 7^{th} and 0^{th} respectively (table 3.16).

Table 3.16 (SPOT-VEGETATION, 2006b): Description of VEGETATION status map binary pixel values

Bits	Field Description	Bit Interpretation Key
0 -1	Cloud Mask Flag	00= Clear 10= Shadow 01= Uncertain 11= Cloud
2	Snow/Ice Background Flag	0 = No 1= Yes
3	Land/Water Background Flag	0=Water 1=Land
4	MIR Radiometric Quality Flag	0=Bad 1=Good
5	B3 Radiometric Quality Flag	0=Bad 1=Good
6	B2 Radiometric Quality Flag	0=Bad 1=Good
7	B0 Radiometric Quality Flag	0=Bad 1=Good

According to table 3.16, pixels which were not cloud contaminated, covered with snow/ice and had good radiometric quality for all four spectral bands, had a corresponding status map binary pixel value of either 11110000 or 11111000. When the status maps were imported to ERDAS the binary values were converted to unsigned 8-bit integers in the decimal system; therefore, the above two binary numbers were converted to 240 and 248.

Consequently any reflectance image pixel with corresponding status map pixel value other than 240 or 248 needed to be masked (pixels which were either covered by snow/ice or clouds, or had bad radiometric quality). A new raster image was created from each imported status map raster by recoding pixel values equal to 240 or 248 to one, and any other pixel value to zero. Then each recoded status map raster was multiplied with its corresponding reflectance raster image.

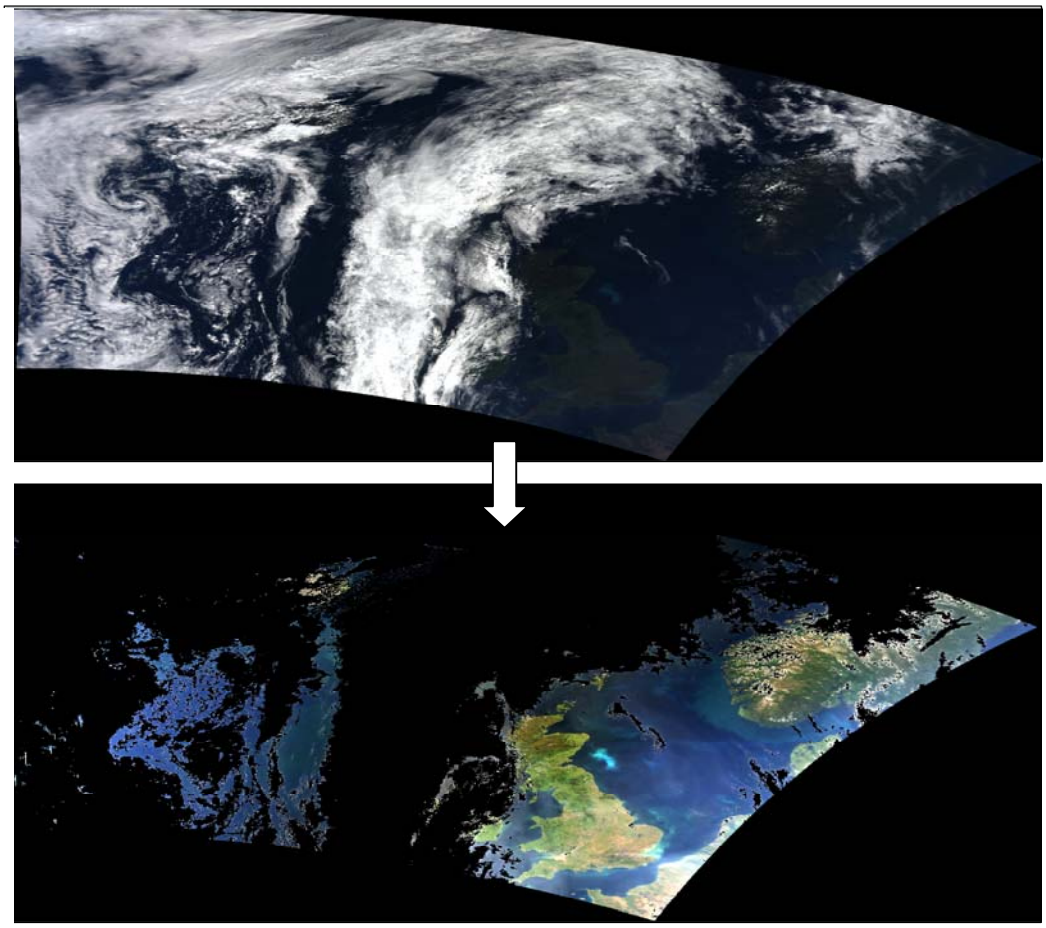

Figure 3.11: Example of a MODIS image (13/07/2003) being masked from pixels containing clouds, snow and ice (Red: Band 1, Green: Band 4, Blue: Band 3)

3.4.6.3 Sensor data georeferencing, sub-setting and rectification

AVHRR

The AVHRR imagery were already geometrically corrected and georeferenced to Longitude and Latitude (Datum:WGS72, Spheroid: WGS72) during the import process. Nevertheless, the data had to be projected so that their projection system matched the projection system of the reference data (OSGB and Transverse Mercator (Spheroid: GRS 1980, Datum: EGSA87) for the UK and Greek study areas, respectively).

The re-projection function of ERDAS was used to project all AVHRR images using a rigorous transformation (ensuring better accuracy than a polynomial approximation), a Nearest Neighbourhood (NN) resampling method (so that the pixel values of the images were not altered due to interpolation) and a pixel size of 1 km.

Once projected a few of the AVHRR images were overlaid over the reference data of either the UK or Greek study area, to test whether the images were accurately georeferenced. It was discovered that there was a slight shift between the AVHRR and the reference data of the order of a couple pixels/km. It was believed that the problem was probably caused by the uncertain quality of GCPs used in the georeferencing of the images during the import process.

To solve this problem, a second order polynomial was used to transform the coordinates of every AVHRR image so that they would overlay correctly over the reference data (rectification). Before doing so however, it was noticed that the extent of each image was not limited within the extent of their respective study areas. Image data beyond the extent limits of the two study areas was not needed for the purpose of this study. On the contrary such data would consume computer resources unnecessarily, such as storage space and processing speed. Moreover, the process of transforming the coordinates of an image using a polynomial is more accurate when dealing with a smaller area than a larger one. Thus each image was sub-setted before being rectified so as to include only data within the extent of the respective study areas.

The coefficients of each polynomial (one for the X and one for the Y coordinates of each image), were calculated using the coordinates of clearly identifiable features (GCPs) in both sensor and reference data, which were then inserted into the polynomial to form

equations. These coordinates were inserted into each polynomial to form 2nd order equations which were consequently solved to calculate the coefficients. A second order polynomial required a minimum of 6 equations/GCPs to be solved (and calculate the coefficients); however, an average of about 40 GCPs were collected per image to form an equal number of polynomial equations (per X and Y coordinates). This was done so that possible errors in the selection of GCPs were averaged out. Moreover, it was ensured that the selected GCPs were equally spaced and spread across the extent of each study area, so as to ensure that the transformation equation was representative for the whole extent of the study area. The polynomials were then used to transform sensor data coordinates to match those of the reference data using a NN resampling method (so that the original values of the pixels will not be altered by interpolation) and 1 km pixel size. A Root Mean Square (RMS) error of less than half a pixel was achieved for every image, which was considered satisfactory.

MODIS

The MODIS data were geometrically corrected and georeferenced to Longitude and Latitude (Datum:WGS84, Spheroid: WGS84) by the HEG tool. However, similarly to AVHRR, the data had to be projected to the same projection system as the reference data. As with AVHRR, the re-projection function of ERDAS was used (Rigorous transformation, NN resampling method and 1 km pixel size).

When the re-projected sensor data was overlaid with the reference data to test whether they matched, it was discovered that that the match was satisfactory for the UK study area but not for the Greek one. Moreover, several images extended beyond the extent of their respective study areas. This problem was dealt with in the same way as for the AVHRR data. Each image was sub-setted within the extent of their respective study areas, and then second order polynomials were used to transform the coordinates of each image to match the coordinates of the reference data. Similarly to the process followed for AVHRR, an average of 40 GCPs were used to calculate the polynomial coefficients of each image, and the new rectified images were resampled using a NN method and a

pixel size of 1 km. Again an RMS error of less than half a pixel was achieved for every image and was considered satisfactory.

VEGETATION

The imported VEGETATION data were geometrically corrected but were missing georeference information. The images could be manually georeferenced by providing information regarding the image map model and projection system through ERDAS Layer Info. The information required for every image was:

- Upper left corner X and Y coordinates
- Pixel size both in X and Y direction
- Projection information

This information was provided for every image within the text file which accompanied it. Therefore using this information, all images were manually georeferenced through ERDAS Layer Info.

The projection system used by the imported VEGETATION images was not the same as the reference data; therefore, similarly to what was done to the AVHRR and MODIS data, each image was re-projected to the same projection system as the reference data (rigorous transformation, NN resampling method, 1 km pixel size).

The re-projected images were then overlaid with the reference data to test whether the images matched together well. A visual inspection of a sample of re-projected images revealed that the images did overlay correctly over the reference data for both study areas. Moreover, the extent of each image was practically within the extent of their respective study area, so there was no need to rectify or put into sub-sets any of the images unlike AVHRR and MODIS.

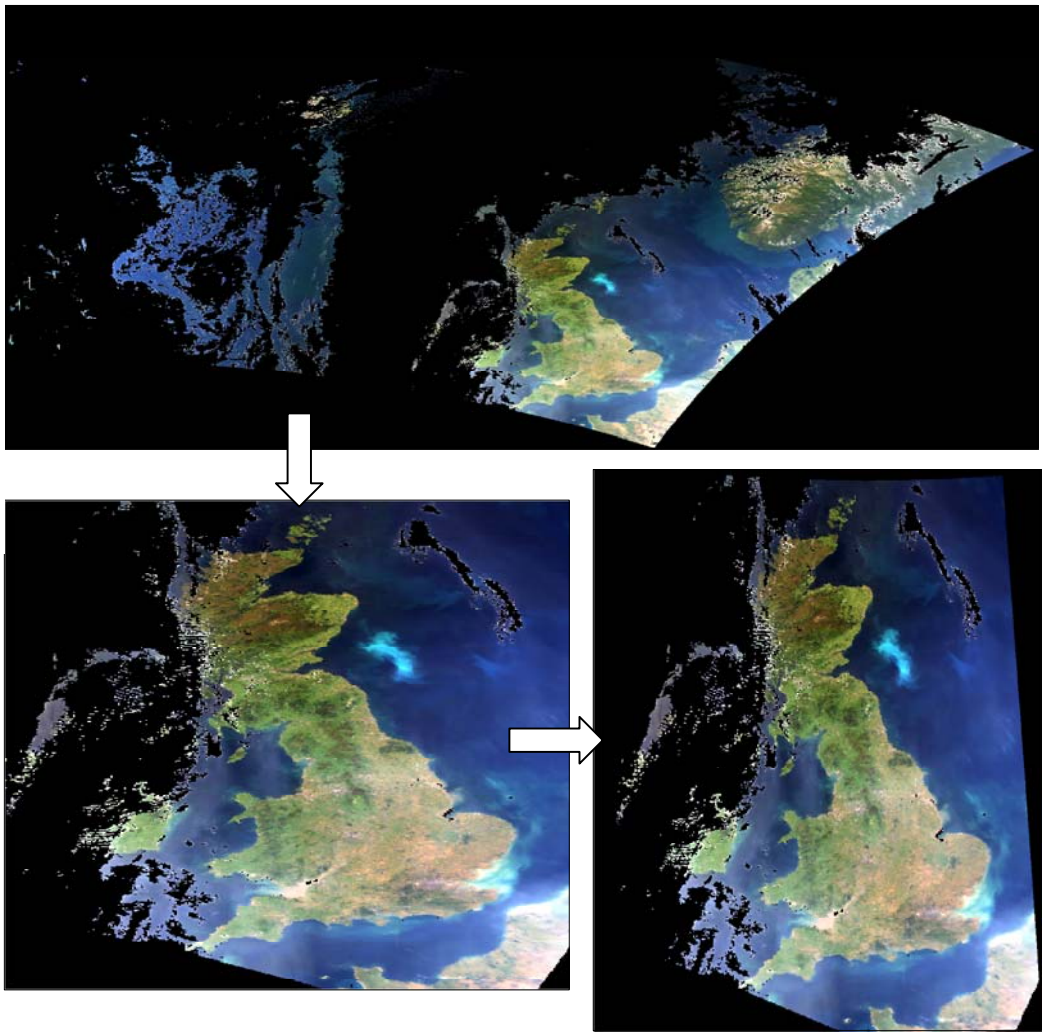

Figure 3.12: Example of a MODIS image (13/07/2003) being sub-setted to the extent of the UK study area and subsequently being projected to the OSGB projection system (Red: Band 1, Green: Band 4, Blue: Band 3).

3.4.6.4 Sea/Ocean mask

In the reference data manipulation section (3.4.5) it was pointed out that sea/ocean classes were not to be included in the land cover classification schemes. Thus sensor data pixels covered with sea/ocean were not needed. On the contrary if these pixels were not removed/masked before the unsupervised maximum likelihood classification processing step, due to the very high percentage of such pixels in both study areas (60% and 64% in the UK and Greek study area respectively) a considerable number of unsupervised classes would likely have been assigned to them. In doing so less unsupervised classes would have been discriminated within the land area of each study area which was not desirable; because, the study was only interested in land cover classes, and also because the use of a large number of unsupervised classes helped minimise any bias introduced to the comparison due to the choices of the analyst.

It was decided therefore to mask from the sensor data all pixel locations identified by the reference data as covered by either sea or ocean. The original CLC1990 dataset was recoded so that any pixel covered by sea or ocean (values 44 and 50, table 3.5) was given a new value of zero and pixels covered with any other land cover class was given a new value of one, forming a raster sea/ocean mask. The newly created sea/ocean mask was then spatially degraded to a pixel size of 1km using a majority rule to match the spatial resolution of the sensor data. The extent of each study area was then put into a sub-set from the sea/ocean mask using the coordinates displayed in table 3.6, and the sub-set of each study area was consequently reprojected to the same projection system as their respective reference data (using a rigorous transformation, a NN resampling method and a 1 km pixel size). Finally, pixels covered by sea/ocean were masked out from each sensor image by multiplying each image to the respective sea/ocean mask sub-set of their study area.

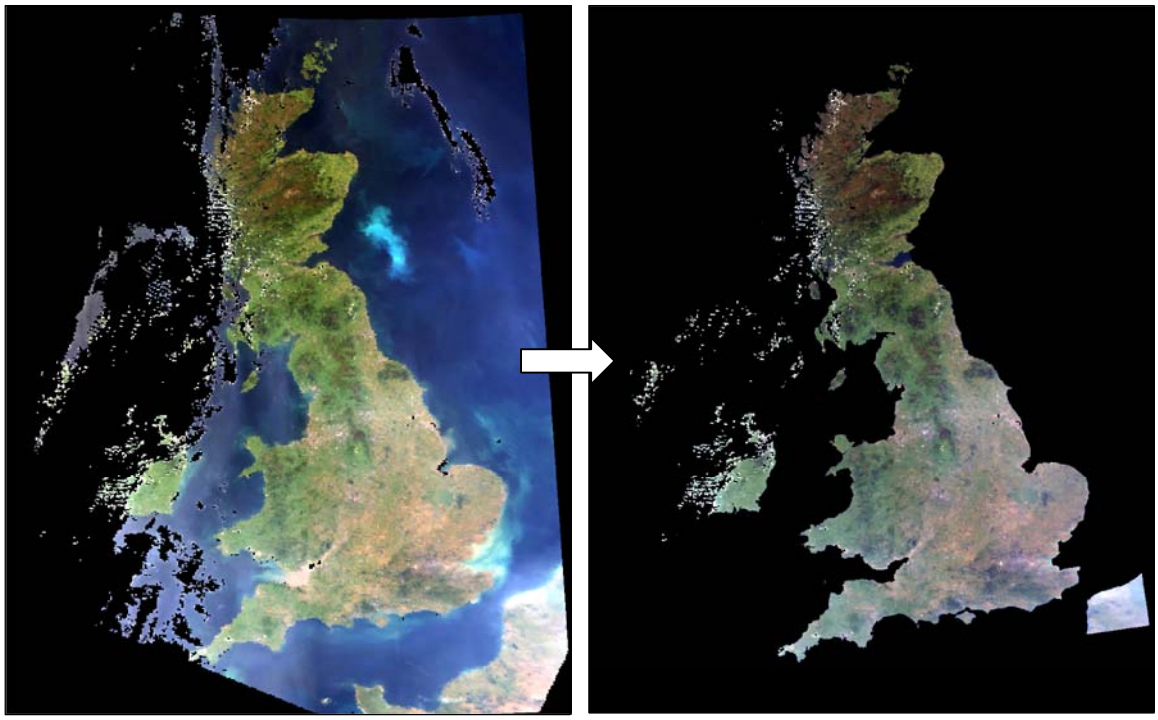

Figure 3.13: Example of a MODIS image (13/07/2003) being masked from pixels covered with sea/ocean (Red: Band 1, Green: Band 4, Blue: Band 3).

3.4.6.5 Sensor data extent matching per date

The study intended to compare the classification accuracy of each land cover map produced using data collected over the same study area and on the same date by each of the three sensors. Nevertheless, data collected by each sensor over the same study area and approximately at the same time (the overpass time if each sensor was relatively close to each other, table 2.11) did not necessarily capture the same extent; areas captured by one sensor may have been missed by another. Moreover, during the cloud/ice/snow contaminated and bad radiometric quality pixel masking processing step the same pixel locations (areas) may not have been masked for all the sensor images of the same study area and date. That could have been caused due to i) small changes in the cloud coverage of each image, ii) different success achieved in detecting and masking cloud/snow/ice covered pixels between images of different sensors, and/or iii) different radiometric quality of each sensor pixel over the same location (VEGETATION for example had a

few sensor elements on its CCD array which have malfunctioned over the years of operation).

These differences in area covered by the sub-setted and cloud/snow/ice/sea/ocean masked images of each sensor over the same date and study area meant that if these images were used as they were for producing land cover maps, the resulting land cover maps would have not been produced over the exact same areas.

To solve this problem, it was decided to mask any pixel location from all sensor images of the same date and study area, where data were not available for all three sensors. The first spectral band of each sensor image was recoded to form a new raster. Pixels with no data (value equal to zero) retained their pixel value, while the remaining pixel values were recoded to the value of one, creating a no-data raster mask for each image. Then all no-data masks of the same date and study area were multiplied together, forming a new no-data raster mask for all sensor images of the same date and study area. Finally each sensor image was multiplied by the combined no-data raster mask of the same date and study area. Thus the newly masked sensor images had data for the exact same pixel locations over the same study area and date.

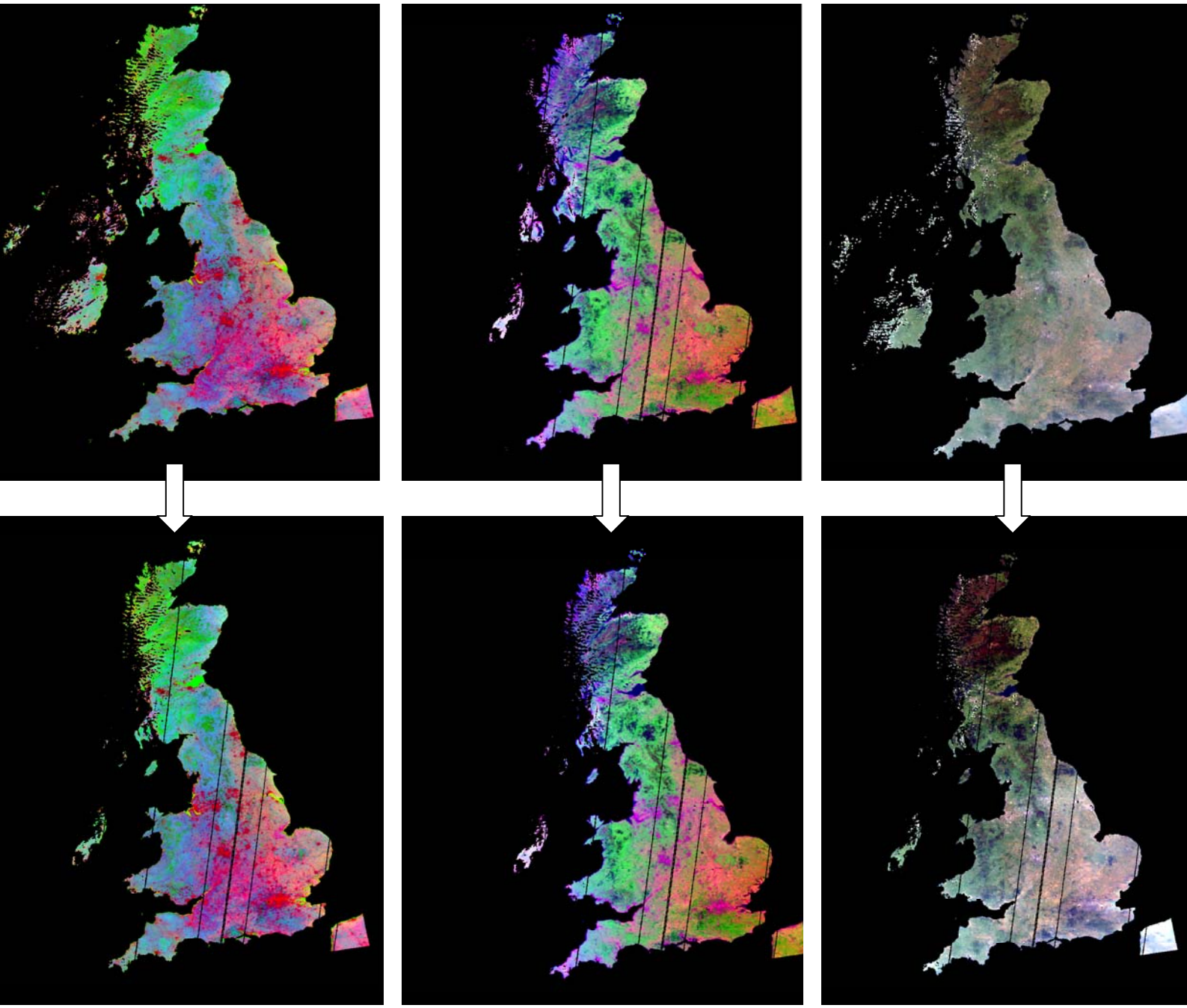

Figure 3.14: Example of an AVHRR, VEGETATION and MODIS image (from left to right) all captured on the same day (13/07/2003) being masked from pixels where data are not available to all three sensors. The black lines running along the images were caused by sensor elements on the VEGETATION's CCD array which have malfunctioned and were consequently masked out due to bad radiometric quality.

3.4.6.6 MODIS spectral band removal

When the pixel values of MODIS data were sampled it was revealed that practically over the whole extent of both study areas the pixel values of bands 15, 16 and 13 and 14 at their high gain setting (13H and 14H), shared the same value (65533). The cause of this was believed to be the fact that these bands were originally designed for measurements over the sea/ocean. Radiation over the wavelengths of the latter bands are reflected less over the sea/ocean than over land surfaces; consequently, due to the fact that these bands were primarily intended for use over the sea/ocean they were designed to be more sensitive to radiation (higher gain) than if they were designed for use over land surfaces. As a result data recorded by these bands over most land surfaces become saturated, recording the maximum reflectance value.

The data recorded over these bands therefore were of no use for land cover classification purposes, since they provide no discrimination between different land cover classes. Moreover, their presence may hinder the classification algorithm because different land cover classes would appear to have more similar spectral properties than they really do. Hence, bands 13H, 14H, 15 and 16 were removed from the MODIS images before applying the unsupervised maximum likelihood classification algorithm.

3.4.6.7 MODIS datasets

Each MODIS image contained information for each pixel over 18 spectral bands (after bands 13H, 14H, 15 and 16 had been removed). The spatial resolution of MODIS spectral bands 1-2 and 3-7 was 250 m and 500 m (GIFOV at nadir point) respectively, while the remaining bands of MODIS had a spatial resolution of 1 km (GIFOV). However as explained earlier for reasons of compatibility with the AVHRR, VEGETATION and reference data, the spatial resolution of the first seven bands of MODIS (1-7) was degraded to 1 km by averaging the value of all MODIS pixels covering an area of a square kilometre.

Nevertheless, even after the spatial degradation of the first seven bands to the same pixel size as the other MODIS bands, the actual spatial resolution of the first seven bands was still better than that of the other bands. This is due to the PSF effect as seen in section 2.3.1. The radiation recorded by a remote sensor over the area of a pixel has not originated solely from the apparent pixel area, but a proportion was originated from neighbouring areas. The total area where radiation was actually recorded from by a sensor due to PSF (represented as a circle in figure 3.15) over a pixel covering an area A (represented by a box in figure 3.15) would be larger than the total area where radiation was actually recorded from by a sensor of the same PSF ratio over a cluster of smaller sized pixels whose total area sum is also equal to A. This is because the extra area where radiation is recorded from due to the PSF effect would be overlapping for neighbouring pixels; thus, due to the overlap a smaller total area is covered, this can be seen clearly in figure 3.15. Therefore even though all spectral bands of the MODIS imagery had the same pixel size, the spatial resolution of the first two bands was better than bands 3-7, whose spatial resolution was in turn better than the remaining MODIS bands.

The availability of MODIS data at several different wavebands and spatial resolutions provided the opportunity to test whether MODIS data from only a few spectral bands with higher spatial resolution would help produce more accurate land cover maps than if data from more spectral bands with lower spatial resolution were used. To carry out this test, the layerstack function of ERDAS was used to produce three new datasets from each MODIS image. The first dataset (from now on referred to as MODIS1) was composed of the first two MODIS bands, the second dataset (from now on referred to a MODIS2) was composed of the first seven MODIS bands and the third (from now on referred to as MODIS3) dataset composed of all MODIS' reflective bands which were not removed (1-12, 13L, 14L, 17-19, and 26). Each of the new datasets of MODIS was then treated independently for the remainder of the study, as if they were from different sensors.

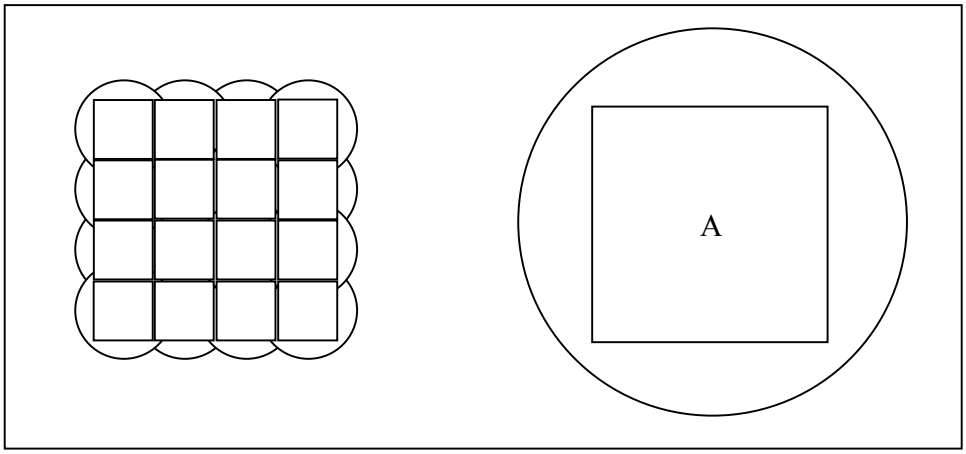

Figure 3.15: Boxes represent the apparent area of the pixels on the ground, the sum of the area of the smaller pixels on the left is equal to the area (A) of the larger pixel on the right. Due to the PSF effect the radiation recorded over each pixel actually originated over a greater area around the pixel, represented by a circle around each pixel. It can be seen that over a cluster of neighbouring pixels, and a larger pixel of the equal total area and PSF effect, radiation would be recorded over a smaller area by the former (the area covered by the sum of circles on the left) than the latter (the large circle on the right).

3.4.6.7 Multidate datasets

The spectral properties of vegetation land cover classes change over time as the biochemical and biophysical properties of vegetation change over time, either due to seasonal adaptation or different growth stages. It is possible that over a certain time period the spectral properties of different vegetation land cover classes may be similar, but dissimilar over another time period. It is unlikely that the spectral properties of all land cover classes within a study are most distinct on the same date; data collected by a sensor over the same study area at different dates may be better suited at discriminating between different land cover classes.

In land cover classification applications it is desirable to use data which can provide the maximum discrimination between all the involved land cover classes. Hence, if remotely sensed data of a study area are available for multiple dates, the discrimination of land cover classes is likely to be more successful if it is based on land cover class spectral properties extracted from a multidate dataset composition, than if they were extracted from a single date dataset.

In the present study, datasets were available for seven dates over the UK study area and 12 dates over the Greek one. It was therefore possible to produce a multidate dataset composition for each sensor (AVHRR, VEGETATION, MODIS1, MODIS2 and MODIS3) and study area, and test whether land cover maps based on multidate composition datasets are more accurate than the ones based on their single date counterparts.

Three dates were chosen for each study area for the creation of the multidate composition datasets. Greater differences in vegetation biochemical and biophysical properties are more likely to be recorded between data collected at dates as far apart from each other as possible; hence, the dates for the multidate compositions were chosen accordingly. For the UK study area these dates were:

- 23/03/2003
- 18/04/2003
- 13/07/2003

And for the Greek study area:

- 04/07/2000
- 04/05/2001
- 03/10/2001

Single date images could be layerstacked together to produce multidate image composites; however before the layerstack was performed an extra step had to be taken. Images captured at different dates do not share the same extent nor are they covered by cloud, snow and ice over the same locations. Consequently, it was highly likely that over certain pixels data may not be available for all three dates. Such pixels would cause problems in the unsupervised maximum likelihood classification at a later stage and had to be masked.

The first band of each single date image selected was recoded into a new raster in a way that pixels with values equal to zero retained their original values, and all other

pixels were given the value of one. Then, the three newly created rasters of the three dates needed for each multidate composition were multiplied together, producing a new raster which was effectively the desired raster mask. The raster mask of each multidate composition was then multiplied with each of its composing date datasets, masking out any pixel where data were not available for all three dates. Once masked the three date datasets needed for the multidate composition of each sensor and study area were layerstacked together.

3.4.6.8 Unsupervised Maximum likelihood classification algorithm

It was already decided (section 3.4.2) that the use of an unsupervised maximum likelihood classification algorithm set to identify a large number of classes, would ensure the reproducibility of the classification method for each sensor and minimise any possible bias introduced by the analyst to the comparison of the sensors' potential to produce accurate land cover maps. However, the exact number of classes the algorithm should be set to identify, was not yet determined.

The number of classes was estimated through trial and error. A sample of images from each sensor and study area was classified into 500 classes, which was thought to be a sufficiently large number. The classifications were carried out using the Iterative Self-Organizing Data Analysis Technique (ISODATA) (Jensen, 1996; Richards, 1992) function of ERDAS. The classifier was set to achieve a convergence threshold of 95% or stop after 100 iterations. The band histograms of some of the most dominant classes were then inspected. According to the requirements of the maximum likelihood classification algorithm, band values of pixels belonging to the same class must follow a normal distribution. The inspection of the band histograms however indicated that the pixel value distribution of some classes was multi-modal, suggesting that the inspected class could potentially be split into more classes.

The process of trial and error was repeated for 1000, 1500 and 2000 classes. The frequency of normal distributions identified in the inspection process varied depending on the number of classes used and the sensor, date and study area of the classified

imagery. Overall, it was decided that when the unsupervised classification algorithm was set to identify 2000 classes with 95% convergence threshold and a maximum of 100 iterations, the majority of the most dominant classes had approximately normal distributions; hence, it was decided to use the above settings. If a higher number of classes were used the ratio of classes with multi-modal distributions would probably be reduced further; however, at the same time the number of minor classes whose pixels are too few for the classes to be representative would also increase, and the computational requirements of the methodology would also become too demanding. Hence it was not attempted to classify the images into more than 2000 classes.

With the classification algorithm parameters determined, the classification algorithm was applied to all of the processed sensor images (AVHRR, MODIS1, MODIS2, MODIS3 and VEGETATION)

3.4.6.9 Production of land cover maps

The unsupervised classification algorithm produced images with approximately 2000 classes each (the classification algorithm did not always succeed in identifying 2000 separate classes). However, although each image was broken down to approximately 2000 spectrally similar classes, the land cover class of each unsupervised class was not yet determined. This was done by cross-referencing the produced images to the reference data of its respective study area.

The ERDAS Grouping tool was used to identify the composition of reference land cover classes within the area of each unsupervised class. In many cases it was discovered that the area of each unsupervised class was composed by more than one land cover class in the reference data. This was believed to be caused either because i) the sensor data were not successful in spectrally distinguishing the involved land cover classes, or ii) due to significant spectral variability within the same land cover class or even iii) due to possible land cover changes between the date the images were captured and the date the reference data was produced. To solve this problem, it was decided that each

unsupervised class was to be assigned to the most dominant reference land cover class within its extent.

For each classified image and reference land cover class, a text file was created listing which unsupervised classes were assigned to that reference land cover class. Then these text files along with their respective classified image were fed to a VB program (Reclassifier) developed by the author. When the Reclassifier was executed, it replaced the pixel values of the classified image to the values of the reference land cover classes they were assigned to, creating a new raster in the process. These newly created rasters were the final land cover maps.

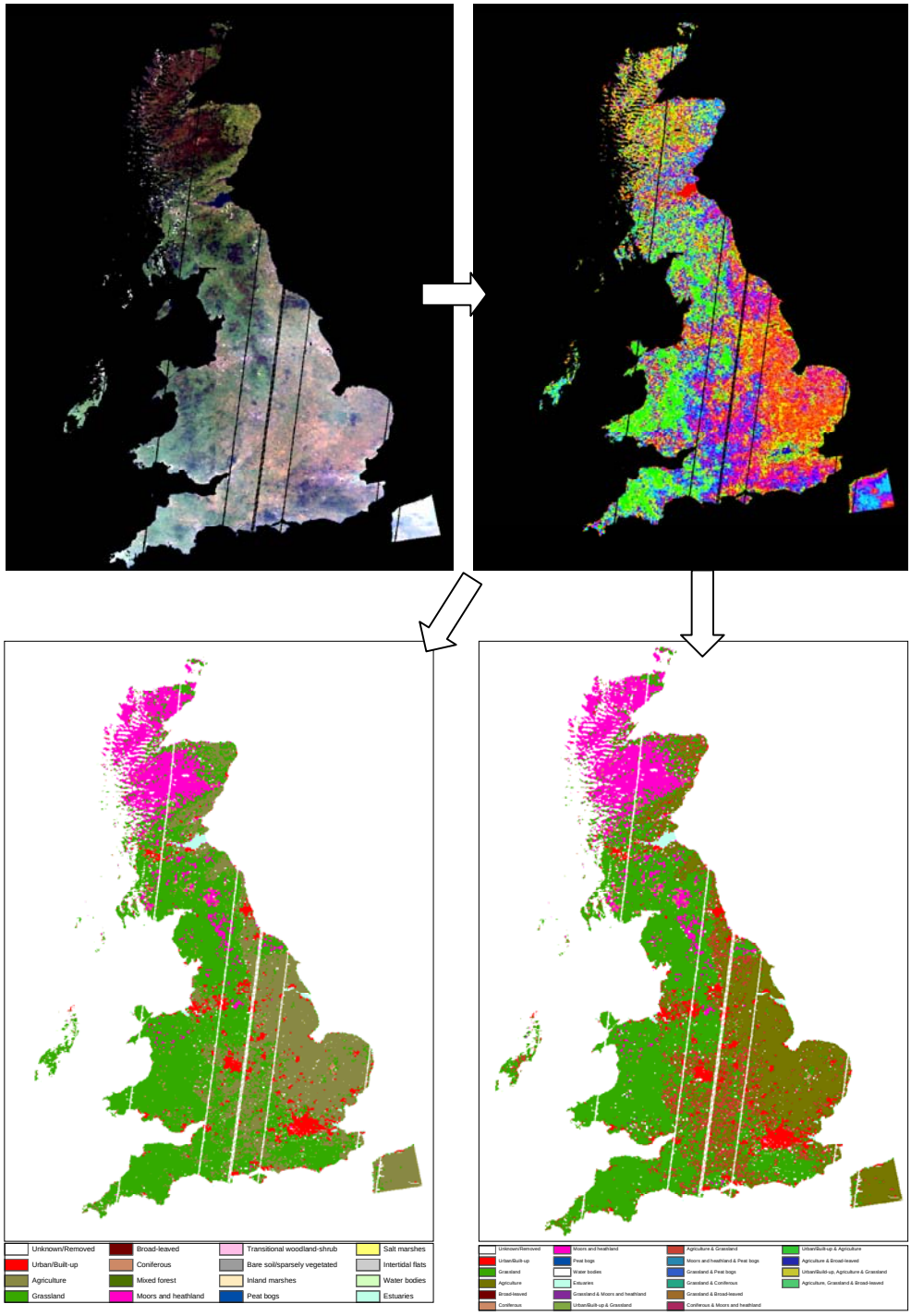

Figure 3.16: Example of a MODIS2 image (13/07/2003) being classified into 2000 unsupervised classes (top right) which were consequently assigned to land cover classes either according to the dominant class classification scheme (bottom left) or the combination class classification scheme (bottom right)

3.5 Results

3.5.1 Background

The most broadly accepted form of land cover map accuracy assessment among the remote sensing scientific community is through the use of confusion/error matrices (Foody, 2002). Confusion/error matrices demonstrate the level of agreement between two land cover maps. The classification accuracy of a classified image/map can be assessed by constructing a confusion matrix between it and a map which is known to be accurate (e.g. the reference data). If high levels of agreement are demonstrated by the produced confusion matrix the classification accuracy of the assessed classified image is also high, and vice versa.

Confusion matrices are two-dimensional with equal number of rows and columns. Each row and column represents a different land cover class, and each land cover class is assigned to the same row and column number. For the construction of a confusion matrix a sample of locations/pixels is taken from areas where both classified and reference data are available. The land cover class of each pixel is extracted from both classified and reference datasets, and the sum of pixels sharing the same class combinations are counted and displayed on the confusion/error matrix. The place where each total count is displayed on the confusion matrix depends on the count's classified and reference land cover class combination; counts of pixels with classified and reference land cover classes i and j respectively are displayed in i^{th} row and j^{th} column of the matrix. Ideally the numbers in the diagonal of the matrix (top left corner to bottom right corner) are the highest, suggesting that the majority of pixels were classified under the same land cover class as indicated by the reference data. Values outside the diagonal suggest that pixels were misclassified under a land cover class other than the one indicated by the reference data. The total classification accuracy of a map is calculated by dividing the sum of counts within the diagonal of the matrix to the sum of counts within the whole matrix, or in other words, the sum of all correctly classified locations/pixels divided by the sum of all of the assessed locations/pixels (equation 3.2). Besides the total classification accuracy, the accuracy with which each class was classified can be calculated by dividing the number of pixels out of those assessed which have successfully been classified in the

respective class to the sum of the assessed pixels actually classified in that class (user accuracy) or to the sum of the assessed pixels actually belonging to that class (producer accuracy). The total classification accuracy as well as the user and producer accuracy of each class was to be calculated; however it was decided that for the purpose of this study the comparison of the land cover maps should be on the basis of the total classification accuracy and not the accuracies of individual classes. This was because a particular class may be important and dominant under certain environmental conditions but may not even exist in different environmental conditions, and this study was interested in comparing the ability of the sensors to accurately classify land cover in general and not just certain classes.

In addition to the total classification accuracy of a map, other measures which could be derived from a confusion/error matrix and were useful for the purpose of the present study were the Kappa statistic (K) and the Kappa variance var(K). The Kappa is an indicator of whether the agreement between two datasets (or in case of the present study whether the classification accuracy of an assessed map) can be attributed to luck or not; Kappa values less than or equal to zero indicate chance agreement and values of one indicate perfect agreement (Agresti, 1990; Cohen, 1960; Viera and Garret, 2005). For a confusion/error matrix of n by n dimensions and if X(i,j) represents a matrix count in row i and column j then the Kappa is equal to:

$$K = \frac{\theta_1 - \theta_2}{1 - \theta_2} \tag{3.1}$$

$$\text{Observed agreement, } \theta_1 = \frac{\sum_{i=1}^{i=n} X(i,i)}{\sum_{i,j=1}^{i,j=n} X(i,j)} \tag{3.2}$$

$$\text{Chance agreement, } \theta_2 = \frac{\sum_{i=1}^{i=n}\left(\sum_{j=1}^{j=n} X(i,j)\sum_{j=1}^{j=n} X(j,i)\right)}{\left(\sum_{i,j=1}^{i,j=n} X(i,j)\right)^2} \tag{3.3}$$

And the Kappa variance of a confusion matrix can help determine whether the level of agreement of one classified image to the reference data is significantly different to the respective level of agreement of a different classified image. Two confusion/error matrices with Kappa values K1 and K2, and Kappa variance (equation 3.5, Congalton and Green, 1999) values var(K1) and var(K2), will indicate that the involved classified images have significantly different classification accuracies at a 95% confidence level, if the value of Delta Kappa (equation 3.4) is more than 1.96.

$$\text{Delta Kappa}=\frac{|K1-K2|}{\sqrt{\text{var}(K1)+\text{var}(K2)}} \tag{3.4}$$

$$\text{var}(K)=\frac{1}{\sum_{i,j=n}^{i,j=1} X(i,j)}\left[\frac{\theta_1(1-\theta_1)}{(1-\theta_2)^2}+\frac{2(1-\theta_1\theta_2-\theta_3)}{(1-\theta_2)^3}+\frac{(1-\theta_1)^2(\theta_4-4\theta_2^{\,2})}{(1-\theta_2)^4}\right] \tag{3.5}$$

$$\theta_3=\frac{\sum_{i=1}^{i=n} X(i,i)\left(\sum_{j=1}^{j=n} X(i,j)+\sum_{j=1}^{j=n} X(j,i)\right)}{\left(\sum_{i,j=1}^{i,j=n} X(i,j)\right)^2} \tag{3.6}$$

$$\theta_4=\frac{\sum_{i,j=1}^{i,j=n} X(i,j)\left(\sum_{k=1}^{k=n} X(j,k)+\sum_{j=1}^{j=n} X(k,i)\right)^2}{\left(\sum_{i,j=1}^{i,j=n} X(i,j)\right)^3} \tag{3.7}$$

Hence, in order to determine which of the three sensors data collected over a particular study area and time helped produce the most accurate land cover map within a certain confidence level, the above metrics (classification accuracy, Kappa and Kappa variance) need to be calculated for each of the classified images (land cover maps) produced using data collected by each sensor over that particular area and time.

The values of the classification accuracy, Kappa and Kappa variance metrics are dependant on of the sample of pixels used in the construction of the confusion matrix. It is therefore imperative in order not to bias the assessment, that the samples used are representative for each image. As such, care should be taken not to over-sample or under-sample certain classes or portions of the classified images.

It is common practice in classification methodologies to divide the reference data into two sets; one set is used for training or labelling purposes in supervised or unsupervised classification algorithms respectively, and the other set used for accessing the accuracy of the produced maps. This is done so bias is not introduced in the assessment by assessing the classification accuracy with the same data used in the classification process. This however could not be applied in this study because the entire reference data had to be used in the classification process because the unsupervised algorithm produced hundreds of classes which occupied very small areas, and due to their size these classes could not be successfully labelled if only a portion of the reference data was used. Nonetheless, the assessment of the land cover maps of all three sensors is likely to be equally effected by the use of the same data for both labelling and assessment purposes, and considering that this study is interested in comparing the relative classification accuracy of the sensors' map and not in measuring the absolute accuracy of the produced maps, this could be allowed.

It could be argued that a selection of samples from each classified image is not necessary because reference data were available for each pixel of the classified images. However the use of neighbouring pixels may result in the underestimation of the Kappa variance values due to spatial autocorrelation, which in turn could lead to misleading results of classification significant difference tests between classified images. Therefore, it was considered necessary to calculate the overall classification accuracy and particularly the Kappa and Kappa variance of each classified image based on sampled pixel values. A systematic sample, provides an equal coverage across the extent of an image/area, and a random sample of 11% is very likely (most land cover classification studies use lower sampling rates for accuracy assessment (Achard et al., 2001; Hodges, 2002; Mayaux et al., 2006; Scepan, 1999)) to be representative of the majority of land cover classes over an area/image. Hence, it was believed that the use of an 11%

systematic random sample would provide an unbiased representation of each classified image; and it was decided to use such a sample to calculate the overall accuracy, Kappa and Kappa variance of each classified image.

A VB program (named "CMatrix_extractor") was developed by the author; the program's function was to compare a classified image against a reference image of the same area, and consequently construct a confusion matrix, and calculate the values of the total classification accuracy (or agreement), Kappa and Kappa variance using an 11% systematic random sample. The program was used to compare every produced land cover map/classified image against its respective reference data. The produced confusion matrices are provided in the appendix while the calculated classification accuracies, Kappa and Kappa variance values are provided below for each study area separately.

3.5.2 UK study area

Dominant class land cover scheme

The total classification accuracy, Kappa and Kappa variance values of each classified image using a 11% sample, and the classification land cover scheme produced using the dominant class spatial degradation rule are displayed in tables 3.17, 3.18 and 3.19 respectively; while the delta Kappa values for each pair of classified images of the same date are displayed in table 3.20.

Table 3.17: Total classification accuracy values of the produced land cover maps over the UK study area, using the dominant land cover class classification scheme (11% sample)

	AVHRR	VEGETATION	MODIS1	MODIS2	MODIS3
Multidate	69.79%	73.36%	71.74%	75.53%	75.30%
17/03/2003	65.69%	63.32%	60.17%	69.48%	69.60%
19/03/2003	64.23%	62.40%	56.52%	68.67%	69.33%
22/03/2003	63.27%	62.93%	60.49%	68.93%	68.64%
23/03/2003	59.23%	62.11%	58.04%	72.16%	70.69%
16/04/2003	63.22%	64.71%	57.82%	68.61%	68.06%
18/04/2003	57.80%	62.24%	57.68%	68.25%	68.24%
13/07/2003	61.88%	67.66%	64.74%	69.43%	69.23%

Table 3.18: Kappa values of the produced land cover maps over the UK study area, using the dominant land cover class classification scheme (11% sample)

	AVHRR	VEGETATION	MODIS1	MODIS2	MODIS3
Multidate	0.5180	0.5748	0.5494	0.6127	0.6068
17/03/2003	0.4439	0.3815	0.3338	0.5124	0.5175
19/03/2003	0.4761	0.4336	0.3449	0.5381	0.5475
22/03/2003	0.4164	0.3948	0.3655	0.5027	0.5020
23/03/2003	0.3701	0.3913	0.3434	0.5701	0.5449
16/04/2003	0.4372	0.4499	0.3424	0.5157	0.5113
18/04/2003	0.3370	0.4039	0.3363	0.5158	0.5172
13/07/2003	0.4246	0.5100	0.4723	0.5430	0.5420

Table 3.19: Kappa variance values of the produced land cover maps over the UK study area, using the dominant land cover class classification scheme (11% sample)

	AVHRR	VEGETATION	MODIS1	MODIS2	MODIS3
Multidate	2.88E-05	2.67E-05	2.76E-05	2.54E-05	2.68E-05
17/03/2003	1.68E-05	1.74E-05	1.60E-05	1.64E-05	1.61E-05
19/03/2003	1.94E-05	2.02E-05	1.98E-05	1.84E-05	1.85E-05
22/03/2003	2.51E-05	2.56E-05	2.52E-05	2.38E-05	2.34E-05
23/03/2003	2.27E-05	2.21E-05	2.21E-05	1.90E-05	1.99E-05
16/04/2003	1.69E-05	1.77E-05	1.76E-05	1.67E-05	1.66E-05
18/04/2003	1.48E-05	1.47E-05	1.41E-05	1.35E-05	1.35E-05
13/07/2003	1.91E-05	1.79E-05	1.85E-05	1.72E-05	1.71E-05

Table 3.20: Delta Kappa values for each pair of classified images over the UK study area and of the same date using the dominant land cover class classification scheme (11% sample). Classifications which were not found to be significantly different are displayed in bold text.

	Multidate	17/03/2003	19/03/2003	22/03/2003	23/03/2003	16/04/2003	18/04/2003	13/07/2003
AVHRR vs VGT	7.62	10.67	6.76	3.03	3.16	2.15	12.31	14.04
AVHRR vs MODIS1	4.17	19.24	20.95	7.17	4.00	16.12	**0.14**	7.79
AVHRR vs MODIS2	12.86	11.90	10.08	12.35	30.97	13.55	33.58	19.66
AVHRR vs MODIS3	11.91	12.85	11.61	12.30	26.78	12.79	33.86	19.51
VGT vs MODIS1	3.46	8.27	14.02	4.11	7.21	18.08	12.61	6.25
VGT vs MODIS3	5.24	22.52	16.81	15.35	27.89	11.24	21.04	5.56
VGT vs MODIS3	4.37	23.52	18.33	15.31	23.70	10.49	21.32	5.40
MODIS1 vs MODIS2	8.70	31.39	31.23	19.60	35.36	29.58	34.16	11.83
MODIS1 vs MODIS3	7.79	32.46	32.75	19.57	31.09	28.85	34.45	11.67
MODIS2 vs MODIS3	**0.82**	**0.89**	**1.55**	**0.11**	4.04	**0.77**	**0.27**	**0.16**

Combination class land cover scheme

The total classification accuracy, Kappa and Kappa variance values of each classified image using a 11% sample, and the classification land cover scheme produced using the combination class spatial degradation rule are displayed in tables 3.21, 3.22 and 3.23 respectively; while the delta Kappa values for each pair of classified images of the same date are displayed in table 3.24.

Table 3.21: Total classification accuracy values of the produced land cover maps over the UK study area, using the combination land cover class classification scheme (11% sample)

	AVHRR	VEGETATION	MODIS1	MODIS2	MODIS3
Multidate	54.79%	57.85%	56.74%	60.11%	59.97%
17/03/2003	55.03%	52.78%	50.54%	58.56%	58.65%
19/03/2003	52.88%	50.50%	46.12%	55.90%	56.97%
22/03/2003	51.03%	50.65%	48.49%	55.64%	55.90%
23/03/2003	47.09%	49.65%	46.82%	59.22%	57.56%
16/04/2003	52.01%	52.81%	46.98%	56.98%	56.21%
18/04/2003	47.71%	51.98%	48.25%	57.52%	57.18%
13/07/2003	49.79%	54.78%	52.00%	56.80%	56.80%

Table 3.22: Kappa values of the produced land cover maps over the UK study area, using the combination land cover class classification scheme (11% sample)

	AVHRR	VEGETATION	MODIS1	MODIS2	MODIS3
Multidate	0.3942	0.4361	0.4205	0.4705	0.4668
17/03/2003	0.3656	0.3123	0.2851	0.4219	0.4244
19/03/2003	0.3878	0.3494	0.2907	0.4309	0.4427
22/03/2003	0.3318	0.3170	0.2890	0.3999	0.4005
23/03/2003	0.2932	0.3143	0.2824	0.4594	0.4356
16/04/2003	0.3606	0.3640	0.2790	0.4245	0.4151
18/04/2003	0.2792	0.3327	0.2897	0.4284	0.4225
13/07/2003	0.3382	0.4067	0.3715	0.4371	0.4393

Table 3.23: Kappa variance values of the produced land cover maps over the UK study area, using the combination land cover class classification scheme (11% sample)

	AVHRR	VEGETATION	MODIS1	MODIS2	MODIS3
Multidate	0.000021	0.000021	0.000020	0.000021	0.000021
17/03/2003	0.000013	0.000013	0.000012	0.000014	0.000014
19/03/2003	0.000016	0.000016	0.000015	0.000016	0.000016
22/03/2003	0.000018	0.000018	0.000018	0.000019	0.000019
23/03/2003	0.000016	0.000016	0.000016	0.000017	0.000017
16/04/2003	0.000013	0.000014	0.000013	0.000014	0.000014
18/04/2003	0.000011	0.000011	0.000011	0.000012	0.000012
13/07/2003	0.000015	0.000015	0.000015	0.000015	0.000015

Table 3.24: Delta Kappa values for each pair of classified images over the UK study area and of the same date using the combination land cover class classification scheme (11% sample). Classifications which were not found to be significantly different are displayed in bold text.

	Multidate	17/03/2003	19/03/2003	22/03/2003	23/03/2003	16/04/2003	18/04/2003	13/07/2003
AVHRR vs VGT	6.52	10.37	6.83	2.47	3.74	0.66	11.31	12.65
AVHRR vs MODIS1	4.11	16.00	17.52	7.15	**1.93**	16.01	2.28	6.18
AVHRR vs MODIS2	11.89	10.77	7.63	11.21	29.16	12.31	31.32	18.25
AVHRR vs MODIS3	11.20	11.27	9.70	11.33	24.92	10.51	30.04	18.62
VGT vs MODIS1	2.43	5.41	10.61	4.67	5.68	16.54	9.17	6.51
VGT vs MODIS3	5.34	21.04	14.44	13.66	25.42	11.56	19.87	5.58
VGT vs MODIS3	4.72	21.56	16.52	13.78	21.20	9.77	18.62	5.97
VGT vs MODIS2	7.80	26.83	25.18	18.32	31.14	28.17	29.38	12.11
MODIS1 vs MODIS3	7.15	27.37	27.28	18.44	26.89	26.36	28.10	12.49
MODIS2 vs MODIS3	**0.58**	**0.48**	2.07	**0.11**	4.12	**1.79**	**1.22**	**0.40**

3.5.3 Greek study area

In the UK study area the classification land cover scheme based on the dominant rule spatial degradation rule produced more accurate land cover maps than the classification scheme based on the combination class spatial degradation rule. Hence, in the Greek study area only the classification scheme based on the dominant class spatial degradation rule was used.

The total classification accuracy, Kappa and Kappa variance values of each classified image using a 11% sample, and the classification land cover scheme produced using the

dominant class spatial degradation rule are displayed in tables 3.25, 3.26 and 3.27 respectively; while the delta Kappa values for each pair of classified images of the same date are displayed in table 3.28.

Table 3.25: Total classification accuracy values of the produced land cover maps over the Greek study area, using the majority land cover class classification scheme (11% sample).

	AVHRR	VEGETATION	MODIS1	MODIS2	MODIS3
Multidate	49.54%	53.73%	45.59%	47.29%	44.71%
13/04/2000	43.83%	49.59%	46.85%	50.26%	46.45%
05/06/2000	45.11%	49.80%	45.10%	47.26%	44.54%
14/06/2000	45.73%	51.23%	46.34%	48.63%	44.46%
04/07/2000	43.98%	51.92%	47.29%	49.18%	47.57%
07/07/2000	46.66%	51.67%	46.37%	48.81%	45.73%
03/08/2000	48.90%	47.73%	48.28%	50.69%	49.22%
20/08/2000	43.86%	51.16%	46.97%	48.78%	47.08%
25/10/2000	43.97%	42.79%	43.75%	48.31%	47.33%
24/03/2001	43.99%	50.46%	45.14%	49.93%	46.94%
04/05/2001	47.02%	49.22%	45.15%	48.22%	45.24%
03/10/2001	46.79%	48.66%	45.30%	47.88%	46.19%
23/10/2001	39.45%	44.95%	42.10%	45.53%	41.54%

Table 3.26: Kappa values of the produced land cover maps over the Greek study area, using the dominant land cover class classification scheme (11% sample).

	AVHRR	VEGETATION	MODIS1	MODIS2	MODIS3
Multidate	0.3369	0.4063	0.2729	0.3070	0.2696
13/04/2000	0.2008	0.3162	0.2665	0.3288	0.2654
05/06/2000	0.2508	0.3252	0.2444	0.2885	0.2318
14/06/2000	0.2670	0.3526	0.2652	0.3084	0.2379
04/07/2000	0.2227	0.3706	0.2949	0.3283	0.3104
07/07/2000	0.2811	0.3672	0.2703	0.3167	0.2587
03/08/2000	0.2992	0.2969	0.2846	0.3326	0.3052
20/08/2000	0.2412	0.3595	0.2918	0.3256	0.2992
25/10/2000	0.2215	0.2232	0.2140	0.2951	0.2758
24/03/2001	0.2361	0.3527	0.2703	0.3474	0.3012
04/05/2001	0.2818	0.3237	0.2515	0.3150	0.2595
03/10/2001	0.2877	0.3155	0.2582	0.3043	0.2821
23/10/2001	0.1590	0.2575	0.2155	0.2665	0.2243

Table 3.27: Kappa variance values of the produced land cover maps over the Greek study area, using the dominant land cover class classification scheme (11% sample).

	AVHRR	VEGETATION	MODIS1	MODIS2	MODIS3
Multidate	0.000026	0.000026	0.000024	0.000026	0.000025
13/04/2000	0.000022	0.000024	0.000024	0.000025	0.000025
05/06/2000	0.000019	0.000022	0.000020	0.000021	0.000019
14/06/2000	0.000023	0.000026	0.000024	0.000025	0.000023
04/07/2000	0.000016	0.000019	0.000018	0.000019	0.000019
07/07/2000	0.000017	0.000018	0.000017	0.000018	0.000017
03/08/2000	0.000019	0.000023	0.000019	0.000021	0.000020
20/08/2000	0.000016	0.000018	0.000017	0.000018	0.000017
25/10/2000	0.000016	0.000024	0.000017	0.000019	0.000019
24/03/2001	0.000017	0.000019	0.000018	0.000019	0.000019
04/05/2001	0.000018	0.000020	0.000018	0.000019	0.000019
03/10/2001	0.000017	0.000018	0.000016	0.000018	0.000017
23/10/2001	0.000020	0.000026	0.000022	0.000026	0.000024

Table 3.28: Delta Kappa values for each pair of classified images over the Greek study area and of the same date using the dominant land cover class classification scheme (11% sample). Classifications which were not found to be significantly different are displayed in bold text.

	AVHRR vs VGT	AVHRR vs MODIS1	AVHRR vs MODIS2	AVHRR vs MODIS3	VGT vs MODIS1	VGT vs MODIS2	VGT vs MODIS3	MODIS1 vs MODIS2	MODIS1 vs MODIS3	MODIS2 vs MODIS3
Multidate	9.58	9.07	4.16	9.41	18.81	13.76	19.03	4.85	**0.47**	5.25
13/04/2000	17.00	9.68	18.67	9.45	7.11	**1.79**	7.23	8.83	**0.16**	8.94
05/06/2000	11.67	**1.03**	5.90	3.08	12.58	5.61	14.66	6.86	2.03	8.90
14/06/2000	12.26	**0.26**	5.93	4.28	12.49	6.21	16.48	6.17	4.01	10.13
04/07/2000	25.05	12.40	17.91	14.84	12.58	6.93	9.87	5.57	2.57	2.95
07/07/2000	14.61	**1.88**	6.06	3.89	16.35	8.42	18.30	7.86	2.00	9.83
03/08/2000	**0.36**	2.35	5.31	**0.96**	**1.89**	5.44	**1.28**	7.60	3.29	4.31
20/08/2000	20.33	8.80	14.57	10.07	11.43	5.69	10.18	5.73	**1.25**	4.48
25/10/2000	**0.26**	**1.31**	12.55	9.25	**1.43**	11.00	8.05	13.47	10.26	3.13
24/03/2001	19.44	5.79	18.60	10.92	13.53	**0.86**	8.40	12.68	5.10	7.55
04/05/2001	6.82	5.01	5.44	3.64	11.77	**1.40**	10.33	10.41	**1.31**	8.97
03/10/2001	4.75	5.15	2.84	**0.96**	9.87	**1.89**	5.69	7.96	4.17	3.79
23/10/2001	14.65	8.72	15.95	9.90	6.08	**1.25**	4.74	7.36	**1.29**	6.01

3.6 Discussion

3.6.1 UK study area

Dominant class land cover scheme

A review of table 3.17 revealed that for each of the selected dates (including the multidate composition) the land cover maps produced using the MODIS2 dataset were more accurate than the respective maps of the other datasets, with the exception of two dates (17/03/2003 and 19/03/2003) where the highest accuracy was achieved by the MODIS3 datasets. Nevertheless, according to table 3.20 the classifications carried out using the MODIS2 and MODIS3 datasets were not significantly different at a 95% confidence level (Delta Kappa<1.96) for all but one date (23/03/2003); however, classifications carried out using either MODIS2 or MODIS3 datasets were significantly different to classification carried out using any of the other datasets. Therefore, the most accurate land cover maps using the dominant class land cover classification scheme over the UK study area were produced by the MODIS2 and MODIS3 datasets (equally efficient).

The only date when MODIS2 produced a significantly more accurate map than MODIS3 was on the 23/03/2003. The Delta Kappa value calculated for the two classifications on that date was just 4.004 (table 3.20) indicating that the difference between the classifications was significant but yet not great. The difference between the two datasets is that MODIS3 had additional spectral bands to MODIS2, which were also recorded at a lower spatial resolution. Since the land cover map produced using the MODIS2 dataset had the highest accuracy on that day, then it is indicative that the lower accuracy of the land cover produced by MODIS3 was caused by the additional spectral bands. The higher spectral resolution (in terms of additional spectral bands) of the MODIS3 is an advantage over the MODIS2 dataset, and could not have been the reason for the lower performance of the dataset; therefore lower performance of the MODIS3 dataset must have been caused from the lower spatial resolution of the additional spectral bands. Lower spatial resolution can increase the number of mixed class pixels and occurrence of misclassification errors. However, the difference in spatial resolution

between the two datasets caused a significant difference only on a single day (23/03/2003) out of the whole (including the previous day 22/03/2003). Therefore it was hypothesised that on the specific date the spatial resolution of the sensor may have been worse than the other dates due to prevailing atmospheric conditions, such as haze which in turn would have caused the PSF of the sensors of MODIS to deteriorate.

Land cover maps produced by the MODIS1 datasets were in most cases the least accurate. MODIS1 had the same radiometric resolution as MODIS2 and MODIS3 which had produced the most accurate maps; therefore the improved radiometric resolution of MODIS over AVHRR and VEGETATION was not the reason that MODIS2 and MODIS3 produced more accurate land cover maps. In addition MODIS1 had better spatial resolution than the AVHRR or VEGETATION datasets, yet it produced less accurate maps than them. Hence, the better performance of the MODIS2 and MODIS3 over the other datasets was attributed mainly to their improved spectral resolution (more spectral bands).

Between the MODIS1, AVHRR and VEGETATION datasets the VEGETATION datasets have produced significantly more accurate land cover maps in most of the cases (five out of eight); followed by the AVHRR datasets which produced the most accurate land cover map in the remaining cases (three out of eight); and finally by the MODIS1 dataset which produced the least accurate maps apart from 18/04/2003 when the accuracy of the produced map was not significantly different to that of the respective AVHRR dataset, and on 13/07/2003 and multidate datasets when the maps produced by the MODIS1 datasets were significantly more accurate (with a 95% confidence) than those produced by the respective AVHRR datasets.

The datasets of VEGETATION had lower spatial and radiometric resolution than MODIS1 as well as wider spectral bands; hence, the better performance of the VEGETATION datasets over MODIS1 was attributed to the additional spectral bands they contained. In comparison to the AVHRR datasets, the VEGETATION datasets must have helped produce more accurate maps in most cases due to their narrower spectral bands and improved spatial resolution. In the three cases (17/03/2003, 19/03/2003 and 22/03/2003) when maps produced by the AVHRR datasets were more accurate than the ones produced by the respective VEGETATION datasets two hypotheses were made: i)

the UK study area was closer to the centre of the AVHRR swath on those three specific days than that of VEGETATION (full data swaths of VEGETATION were not provided to test this hypothesis); thus, the AVHRR datasets may have had equal or better spatial resolution than VEGETATION over the majority of the UK study area on those dates, hence causing less misclassification errors due to mixed class pixels, and ii) the cloud masking process may have been more successful on the AVHRR datasets than those of VEGETATION on those three dates, thus the classification accuracy of the maps produced by the VEGETATION datasets may have had more misclassification errors caused by cloud contaminated pixels.

It is noteworthy that on one of the two dates (13/07/2003) the MODIS1 dataset produced a more accurate map than the respective dataset of AVHRR, all datasets except AVHRR (MODIS1, MODIS2, MODIS3 and VEGETATION) had produced the most accurate map out of all days (except for the multi-date datasets). It is likely that the reason why all datasets apart from AVHRR produced the most accurate map on the same day could be because that day (13/07/2003) was in the middle of the summer when vegetation growth is at its peak and biophysical and biochemical differences between different vegetation land covers are more evident. A probable reason why the AVHRR dataset did not produce the most accurate land cover map of all the AVHRR datasets (except for the multi-date datasets) on that day (like the datasets of the other two sensors), is that unlike MODIS and VEGETATION the spectral bands of AVHRR were not designed particularly well for vegetation monitoring (section 2.3.3). This is also likely to be the reason why on that day the MODIS1 dataset produced a more accurate land cover map than the respective AVHRR dataset.

The only other case when a MODIS1 dataset produced a more accurate land cover map than its respective AVHRR dataset was when the land cover maps were produced using the multi-date datasets. It was believed that this was due to the fact that on the multi-date composites the 13/07/2003 date was included which gave the MODIS1 dataset a relative advantage.

It is also worth mentioning that among the land cover maps produced by each sensor (AVHRR, MODIS1, MODIS2, MODIS3 and VEGETATION) in all cases the one produced using the multidate composite was the most accurate. This result supports the

original expectations expressed in section 3.4.6.7 that land cover class spectral profiles extracted from multi-temporal composites are more likely to help distinguish between different land cover classes than those extracted from single-date images.

Combination class land cover scheme

A comparison between tables 3.17 and 3.21 shows a significant difference between the land cover maps produced using the two different land cover classification schemes. In all cases, the land cover map produced using the combination class land cover scheme was less accurate (by about 15%) than the respective map produced using the dominant class land cover scheme. This result was in agreement with results of previous studies which showed that when coarse spatial resolution imagery is used, classification algorithms tend to identify the dominant classes within land cover class mixtures (Hay et al., 1997; Lioubimtseva, 2003; Mayaux and Lambin, 1995; Moody and Woodcock, 1995; Moody, 1998; Nelson and Holben, 1986; Strahler et al., 1999; Townshend and Justice, 1988) and minor classes are almost entirely lost (Lioubimtseva, 2003). Moreover, a shortcoming of mixed class classification approaches pointed out by Price (2003) is that "Different fractions of different surface types can yield the same value of observed radiance or apparent reflectance", in such cases the distinction of classes based on their spectral profiles would be difficult, leading to misclassification errors, and lower classification accuracies. Hence, in the majority of cases, map producers prefer to use classification schemes based on the most dominant class (Cihlar et al., 1996; Cihlar, 2000; Foody, 2002; Hansen et al., 2000). In addition to the above arguments it should also be pointed out that the combination class land cover scheme had four classes more than the dominant class one; hence the possibility of classifying a pixel under the wrong land cover class was increased.

A further comparison between tables 3.17 and 3.21 and tables 3.20 and 3.24 revealed that despite the noticeable reduction in the produced maps classification accuracies, the relative differences between the classification accuracies of the maps produced by different datasets were practically the same as those produced using the dominant class classification scheme.

Thus, as in the dominant class land cover classification scheme, for all dates (including the multi-date composites) the most accurate maps were produced using the MODIS2 and MODIS3 datasets. Moreover maps produced using either the MODIS2 or MODIS3 dataset of the same date had classification accuracies which were not significantly different at a confidence level of 95%, apart from the maps produced using the 23/03/2003 and 19/03/2003 datasets. The same reasoning discussed in the dominant class classification section could be used to explain why the MODIS3 dataset helped produce a land cover map on the 23/03/2003 with significantly lower accuracy than that produced with the respective dataset of MODIS2. The classification accuracies of the two datasets 19/03/2003 were barely significantly different (Delta Kappa = 2.07).

Likewise among the land cover maps produced using the MODIS1, AVHRR and VEGETATION datasets, the maps produced using the VEGETATION datasets were significantly more accurate in most of the cases (five out of eight) and the maps produced using the AVHRR datasets were most accurate in the remaining three cases. Notably the dates when the maps produced using the AVHRR datasets were significantly more accurate than those produced using the VEGETATION datasets were the same as those in the dominant class classification scheme (17/03/2003, 19/03/2003 and 22/03/2003).

Moreover, similarly to the results in the dominant class classification scheme the maps produced using the MODIS1 dataset were significantly more accurate than those produced using the AVHRR datasets on the 13/07/2003 and the multi-date composite. The only difference is that the map produced using the MODIS1 dataset on the 18/04/2003 was significantly different to the one produced using the respective AVHRR dataset unlike the results of the dominant class classification scheme; nevertheless the value of the Delta Kappa was barely higher than the threshold (2.28>1.96). Due to the fact that the 16/04/2003 and 18/04/2003 datasets were temporally close to each other, it was expected that the classification accuracies of the maps for these dates would be similar for the same sensor; because, the recorded spectral properties of the land cover classes should not have changed significantly. This expectation proved true for the maps produced using the MODIS1 datasets with only about 1.47% difference between the classification accuracies of the produced maps; however the difference in the classification accuracies of the maps produced using the AVHRR datasets for the same

dates was about 4.31% which was relatively high compared to the map's total accuracy (47.55%). Due to this it was assumed that the cloud (ice and snow were not expected on that day) masking process or the rectification process was not as successful in the AVHRR dataset on that date (18/04/2003) than in other cases such as on the 16/04/2003. Therefore the better performance of the MODIS1 dataset on that day was attributed to the above possible explanation.

Since the relative differences between the classification accuracies of the maps produced by each dataset were practically the same to those observed for the dominant class classification scheme, the same reasoning provided there was also applicable here.

3.6.2 Greek study area

Over the UK study area two land cover classification schemes created from the same dataset (CLC1990) using a different spatial degradation rule (dominant or combination class) were tested. The land cover classification scheme based on the dominant class spatial degradation rule proved to consistently produce more accurate land cover maps than the one based on the combination class spatial degradation rule. As such it was decided to use only the classification scheme based on the dominant class spatial degradation rule over the Greek study area.

Something that became immediately obvious was that the overall classification accuracies of the land cover maps produced over the Greek study area using the dominant class land cover scheme were considerably lower than the classification accuracies of the respective land cover maps produced over the UK study area (tables 3.17 and 3.25). This result was believed to have been caused by the two study areas different land cover class composition.

The two classification schemes created over the UK and Greek study areas using the dominant class spatial degradation rule were quite similar; both classification schemes had the same numbers of classes (15), out of which 13 were common in both schemes (including the most dominant ones). However, the percentage of area covered by each of the study areas' common land cover classes were considerably different (table 3.29). The percentage of area covered by each class over a study area can have a significant impact

on classification accuracy of maps produced over that study area. High percentage of areas covered by land cover classes which are relatively easy to distinguish would help produce land cover maps of relatively high classification accuracy, and vice versa. The differences between the ratios of area covered by each land cover class in the two study sites were believed to be part of the reason that significantly different land cover accuracies were achieved. It is indicative that for the UK study area the highest user accuracies (derived from the confusion matrices displayed in the Appendix C) were usually associated with the Urban/Built-up, Agriculture and Grassland classes, which all together covered 77% of the UK study area, as opposed to 47% of the Greek study area.

Table 3.29: Proportions of areas occupied by each of the dominant land cover CLC1990 classes of the UK and Greek study areas.

UK	Coverage	Greece	Coverage
Urban/Built-up	5.00%	Urban/Built-up	1.00%
Agriculture	23.64%	Agriculture	35.92%
Grassland	48.28%	Grassland	10.44%
Broad-leaved	1.36%	Broad-leaved	14.74%
Coniferous	3.71%	Coniferous	5.85%
Mixed forest	0.06%	Mixed forest	4.95%
Moors and heathland	11.67%	Moors and heathland	2.13%
Transitional woodland-shrub	0.43%	Sclerophyllous vegetation	12.82%
Bare soil/sparsely vegetated	0.41%	Transitional woodland-shrub	8.54%
Inland marshes	0.05%	Bare soil/sparsely vegetated	2.20%
Peat bogs	3.13%	Inland marshes	0.06%
Salt marshes	0.10%	Peat bogs	0.01%
Intertidal flats	0.47%	Salt marshes	0.15%
Water bodies	0.89%	Salines	0.02%
Estuaries	0.80%	Water bodies	1.16%

Another reason behind this difference in classification accuracy between the land cover maps of the two study areas was believed to be the different land cover class heterogeneity of the two study areas. The Greek study area was a lot more mountainous than the UK, and this combined with the fact the coast line of the former was significantly longer than the latter in relation to their extent, resulted in a more heterogeneous land cover class environment either due to the more rapidly changing environmental conditions or the different land uses through the area. The ratios of land cover classes occupying each study area, displayed in table 3.29 show that the Greek

study area is less dominated by a few land cover classes than the UK study area. The higher heterogeneity of the Greek study area is further supported by the findings in table 3.10; over the Greek study area 12698 different existing class combinations were found, as opposed to 9183 found in the UK study area. Considering that the extent of the Greek study area was smaller than that of the UK (the CLC1990 datasets used to count the existing class combinations in the Greek and the UK study areas covered 196833 km^2 and 320259 km^2 respectively), if the two study areas covered the same area then the Greek study area would proportionally have 2.25 times more different class combinations in relation to the UK study area.

The higher land cover class heterogeneity of the Greek study area in relation to the UK, caused the effect of the two main factors that cause errors in classifications: i) mixed class pixels and ii) within class variability and (Hseih et al., 2001; Latty et al., 1985; Toll, 1985) to be amplified more over the Greek study area. The higher the land cover class heterogeneity of an area the higher the percentage of areas within it where two or more different land cover classes border. Consequently, higher percentage of land cover class border areas results in a higher percentage of pixels covered by a mixture of classes, which in turn are one of the main causes of misclassification errors. Also because in the present study the reference data was produced by assigning to each pixel the land cover class which was most dominant within its extent the spectral variability within each land cover class was likely to be more variable over more heterogeneous environments. This is because the more heterogeneous an area is the higher the chance that a group of pixels would be composed of different land cover class combinations but share the same dominant class within their extent; hence although all pixels in that group are assigned under the same land cover class, the spectral properties of each pixel may vary considerably, causing more errors in classifications based on pixels' spectral properties.

Due to the higher land cover class heterogeneity of the Greek study area and the negative impact this had on the classification accuracy of the produced land cover maps, the spatial resolution of the remotely sensed data became more important over the Greek study area than in the UK one. This is because the percentage of mixed class pixels recorded over an area depends a lot more on the spatial resolution of the sensor recording

the data if the area has high land cover class heterogeneity than low; over heterogeneous areas low spatial resolution causes that percentage to rise and vice versa.

Consequently land cover maps produced using datasets with relatively low spatial resolution were not expected to be among the most accurate maps; the AVHRR and MODIS3 were such datasets. As expected it can be seen in table 3.25 that maps produced using either the AVHRR or MODIS3 datasets were in fact among the least accurate. The amplified effect of the spatial resolution over the Greek study area was particularly demonstrated by the land cover maps produced using the MODIS3 datasets. Over the UK study area the maps produced by the MODIS3 datasets were among the most accurate ones along with those produced by the MODIS2 datasets. However, over the Greek study area the maps produced by the MODIS3 datasets were among the least accurate, while those produced by the MODIS2 datasets were still among the most accurate.

However this is not to say that over the Greek study area it was expected that the highest spatial resolution datasets would produce the most accurate maps. Despite the increased importance of the spatial resolution over the Greek study area, the spectral resolution of the datasets was still expected to be an important factor. Hence, although the MODIS1 datasets had the highest spatial resolution of the other datasets they were not expected to produce the most accurate maps; this is because the MODIS1 datasets contained the least spectral bands among the datasets, and therefore had least spectral information to base the distinction between the different land cover classes. In table 3.25 it can be seen that as expected the land cover maps produced using the MODIS1 datasets were not among the most accurate ones, similarly to the UK study area.

The datasets which were expected to produce the most accurate land cover maps had to have a relatively high spectral and spatial resolution; these were the datasets of VEGETATION and MODIS2. In table 3.25 it can be seen that this was the case. Nevertheless something unexpected was noticed; the MODIS2 datasets had both higher spectral and spatial resolution than those of VEGETATION, yet the VEGETATION datasets produce the most accurate land cover maps more times than those of MODIS2. In more detail, out of the 13 cases, the most accurate land cover map was produced six times (04/07/2000, 05/06/2000, 07/07/2000, 14/06/2000, 20/08/2000 and the multi-date composite) using the VEGETATION dataset, two times (03/08/200 and 25/10/2000)

using the MODIS2 dataset, and fives times (03/10/2001, 04/05/2001, 13/04/2000, 23/10/2001 and 24/03/2001) by either of the two datasets (VEGETATION or MODIS2) since the classification accuracies of the produced maps were not significantly different at a 95% confidence level.

The reason behind this was believed to be associated with yet another unexpected result. The multi-date composite of each sensor was expected to produce more accurate land cover maps than any of their respective single date datasets due to the additional multi-temporal spectral information that helped distinguish between land cover classes. That expectation was confirmed for all sensors in the UK study area (table 3.17) and for the AVHRR and VEGETATION datasets on the Greek study area but not for any of the MODIS datasets (MODIS1, MODIS2 and MODIS3).

The cause of both of these unexpected results was believed to be related to the rectification accuracy of the MODIS datasets. Images which are not very well rectified to each other do not overlay very accurately; hence, the spectral signatures extracted from pixels of multi-date composites constructed from a series of inaccurately rectified single-date images, may not be extracted over the same locations and land cover classes, but may be extracted over a series of neighbouring locations which may be covered by different land cover classes. The extraction of such spectral signatures would cause misclassification errors because the same land cover classes may have apparently different multi-temporal spectral signatures due to differences in the land cover class of their neighbouring pixels. That was believed to be the reason for the reduced accuracy of the land cover maps produced using the multi-date composites of MODIS.

The probable inaccurate rectification of the MODIS imagery was also believed to be the reason why the land cover maps produced using the VEGETATION datasets were more accurate than those produced by the MODIS2 datasets in more cases. Probable inaccurate rectification of the MODIS images with the reference data caused a portion of spectral profiles to be attributed to incorrect land cover classes, an effect which would have been amplified by the heterogeneity of the Greek study area. Several studies have shown that inaccurate rectification between classified and reference data can cause significant misclassification errors (Canters, 1997; Czaplewski, 1992; Foody, 2002;

Muller et al., 1998; Riemann et al., 2000; Stehman, 1997; Todd et al., 1980) particularly over heterogeneous study areas (Foody, 2002; Loveland et al., 1999; Scepan, 1999).

Nevertheless, even though the MODIS datasets were likely to have been inaccurately rectified, the land cover maps produced using the MODIS2 datasets were still relatively quite accurate in comparison to the maps produced using the other datasets (table 3.25). It was therefore assumed that had the MODIS2 datasets been more accurately rectified the land cover maps produced using the MODIS2 datasets would have at least produced maps as accurate as the VEGETATION datasets

The only case when a map produced by the VEGETATION dataset was not the most or second most accurate was on the 25/10/2000 which may have been caused by cloud contaminated pixels which were probably not successfully identified and masked. On the other hand the only case when a map produced by MODIS2 was not among the two most accurate ones was in the case of the multi-date composites; however this can also be attributed to the probable errors in the MODIS2 dataset rectification.

The comparison of the classification accuracies of the maps produced by the MODIS1 and MODIS3 datasets over the Greek study area was difficult to predict. MODIS3 datasets had higher spectral resolution than the MODIS1 datasets, but on the other hand the MODIS3 datasets also had lower spatial resolution than the latter. Over the UK study area, the higher spectral resolution of the MODIS3 datasets gave them a clear advantage; however, over the Greek study area the importance of the spatial resolution of the datasets was significantly increased, hence a prediction of the comparison was not obvious. The results displayed in tables 3.25 and 3.28 did not provide a conclusive answer. Out of the 13 cases produced by each dataset, five classification accuracies were not significantly different, three were higher for the maps produced by MODIS1, and five were higher for the maps produced by MODIS3. It is likely that the result of the comparison may have been clearer if it was not believed that the MODIS datasets may had different accuracies of rectification between different dates causing inconsistencies in the comparison. Nevertheless, it would appear that MODIS3 datasets had a slight advantage over those of MODIS1, the three cases (05/06/2000, 07/07/2000 and 14/06/2000) when maps produced by MODIS1 were more accurate than those produced by MODIS3 may have been caused by conditions which may have

amplified the effect of the spatial resolution on the classification accuracy of the produced maps. Such conditions could have been the degradation of the spatial resolution on both datasets due to haze in the atmosphere (stronger PSF effect) or high viewing angles. Such spatial resolution deterioration would cause more classification errors over a heterogeneous area to maps produced by the MODIS3 than the MODIS1 datasets due to the lower spatial resolution of the former.

As far as the comparison between the classification accuracies of the maps produced using the MODIS3 and AVHRR datasets is concerned, it was expected that maps produced by MODIS3 would be more accurate than those produced by AVHRR. This is because MODIS3 datasets had a higher spectral resolution than that of the AVHRR datasets and the spatial resolution of two datasets was about the same apart from high viewing angles when the spatial resolution of the MODIS3 datasets degraded faster than the AVHRR datasets (section 2.3.1). The results displayed in tables 3.25 and 3.28 confirmed the above expectation; in the majority of cases the MODIS3 dataset produced more accurate maps. Out of the five cases when maps produced by the AVHRR dataset were more accurate than the respective maps produced by MODIS3, one was when the maps were produced using the multi-date composites and were likely to have been caused due to possible rectification inaccuracies in the MODIS3 datasets. Then three out of the four remaining cases were the same dates as when maps produced by MODIS1 were also more accurate than those produced by MODIS3 reinforcing the suspicion that on those dates data were likely to have been recorded under certain conditions (such as haze or high viewing angles) which caused the spatial resolution of the MODIS datasets to degrade. The fifth case (04/05/2001) was likely to have been caused by rectification errors in the MODIS dataset.

Finally MODIS1 datasets were expected to produce more accurate maps than the ones produced using the AVHRR datasets. This is because it was not believed that the single extra SWIR band of the AVHRR dataset would have been enough to overcome the MODIS1 advantage due to higher spatial resolution, particularly in an area as heterogeneous as the Greek study area. The results in tables 3.25 and 3.28 were not surprising, in the majority of cases maps produced using the MODIS1 datasets were more accurate than the respective ones produced by AVHRR. In more detail, the classification

accuracies of the two datasets were not significantly different in four cases, the accuracy of the maps produced by MODIS1 was higher in five cases, and in the remaining four cases the accuracy of the maps produced by AVHRR was higher. The four cases when the maps produced by AVHRR datasets were more accurate than the ones produced by MODIS1 were likely to have been caused by inaccuracies in the rectification of the MODIS datasets. As expected one of those cases was the multi-temporal composite. The remaining three cases (03/08/2000, 03/10/2001 and 04/05/2001) were on the same dates as the cases when maps produced by AVHRR datasets were either more accurate or not significantly different from those produced by MODIS3, reinforcing the probability that the rectification of the MODIS' datasets may have been inaccurate.

3.7 Conclusions

The experimental results in this part of the study confirmed the hypothesis formed in Chapter 2 based on the theoretical comparison of the three sensors' characteristics. In the majority of cases the land cover maps produced using 1 km spatial resolution data collected by MODIS SRBs were overall more accurate than the respective maps produced by VEGETATION which in turn were in most cases more accurate than the respective maps produced by AVHRR.

Moreover, it was shown that it is more likely to achieve higher classification accuracies if only the first seven bands of MODIS are used. The remaining spectral bands of MODIS were not designed for land surface applications and as a result do not provide significant information for the distinction of different land cover classes as can be seen by the results produced by the MODIS2 and MODIS3 datasets in the UK study area. On the contrary due to their lower spatial resolution, these spectral bands could increase the ratio of mixed class pixels in a scene and cause a reduction in the classification accuracy of the produced maps; this is particularly true over heterogeneous areas as demonstrated by the classification accuracy results over the Greek study area.

On a further note, the image registration of the MODIS data was found to be relatively inaccurate compared to the other two sensors. Such image registration inaccuracies decrease the potential classification accuracy of a land cover map produced

using data collected by MODIS. Unless the image registration of MODIS data is rectified, the misclassification errors it could cause may be significant enough to overcome relative advantages over the other sensors, particularly over heterogeneous study areas. In such cases the land cover classification accuracies achieved using data collected by MODIS may be similar to those achieved using data collected by VEGETATION or AVHRR over the same sites and dates, as seen by the experimental results of the three sensors over the Greek study area.

The results of the present study have also confirmed the results of previous studies (Hay et al., 1997; Lioubimtseva, 2003; Mayaux and Lambin, 1995; Moody and Woodcock, 1995; Moody, 1998; Nelson and Holben, 1986; Strahler et al., 1999; Townshend and Justice, 1988) that low spatial resolution data tend to identify the most dominant class within pixel-size areas.

As a last note, the results have also shown that when data are accurately rectified, land cover maps produced using multidate data are likely to be more accurate than maps produced using single date data.

3.8 Future work

The reference data used in this part of the study were not collected at a time near the collection of the sensor data used for the land cover mapping. In fact, the reference data used were collected up to 10 years before the sensor data used in this study were collected. This temporal mismatch between the reference and sensor data was due to lack of available reference data which were collected near the time when all three sensors were operational. This temporal mismatch could have introduced possible errors in the classification and accuracy assessment processes, due to possible land cover changes which may have occurred between the collection of the reference and the sensor data. This could have been particularly true for the agriculture class as significant areas of land may have been brought in or out of agriculture. Relatively shortly after the completion of this part of the study, the release of a more recent reference dataset was announced by EEA, the CLC2000 08/2005. It would be interesting to repeat the current methodology using the more recent reference CLC2000 dataset, thus minimising possible assessment

errors which may have occurred in this study, caused by the temporal mismatch of the reference and sensor data.

During the last stages of this study it was discovered that the registration accuracy of some MODIS images over the Greek study area may have not been very accurate. The registration inaccuracy of MODIS data was believed to be the primary cause for the unexpected relatively low classification accuracies achieved using the MODIS data; however there was not sufficient time to try to improve the registration accuracy of the MODIS data and repeat the assessment. In the future if the data collected by MODIS over the Greek study area were to be rectified so as to improve their registration accuracy and repeat the assessment, the results of the new assessment would help verify whether the data collected by MODIS did not help produce land cover maps at the expected accuracy levels due to image registration inaccuracies or not.

The present study was carried out over limited dates and study areas. In the future it would be interesting to test the validity of this study's results by applying the same methodology over more dates and different study areas preferably covered with different land cover class compositions.

Finally, the efficiency of the three sensors to accurately map land cover was based on data collected by their SRBs at 1 km spatial resolution; however it can be argued that the full capacity of MODIS and AVHRR was not used. The first seven SRBs of MODIS are capable of collecting data at higher spatial resolution than 1 km, and it is possible that at higher spatial resolution land cover could be mapped more accurately due to the potential reduction of mixed class pixels. Also although land cover classifications are primarily based on SRB data, studies have shown that they could potentially be improved with the use of TEB data (Lambin and Ehrlich,1996a, 1996b; Liang, 2001; Nemani and Running, 1995; Nemani et al., 1993; Running et al., 1995). In this study the TEB data of MODIS and AVHRR were not used in the assessment as their inclusion would have required a lot more storage space and processing time (double in the case of MODIS) and their importance was considered secondary to SRB data; however, it would be interesting to see in a future study whether their inclusion would have significantly altered the results.

CHAPTER FOUR

4 NDVI data simulation

4.1 Background

One of the aims of the present study was the assessment of the relative capacity of data collected by AVHRR, MODIS and VEGETATION in monitoring drought conditions using the VPI methodology. For the correct implementation of the VPI methodology the use of long historical NDVI records is necessary. The available historical NDVI data collected over a site must be sufficiently long to be able to support adequately accurate assessments regarding the probabilities associated with the occurrence of various NDVI values. However out of the three sensors only AVHRR was considered to have sufficiently long historical NDVI records. In this part of the study the relation between the NDVI values collected by the three sensors over the same targets and dates was investigated. In the event that the NDVI values of the different sensors were found to be highly correlated, then it could be possible to simulate through regression analysis the NDVI response of a sensor, based on NDVI data recorded by another sensor over the same target and date. If such NDVI data simulation was possible and sufficiently accurate then MODIS and VEGETATION could be provided with sufficient historical NDVI records to meet the requirements of the VPI methodology, by simulating the NDVI data the two sensors were likely to have recorded in the past based on NDVI data collected by AVHRR. Additionally, other applications which require NDVI could be benefited from such simulation possibility; either by extending the historical NDVI records of MODIS and VEGETATION, or by providing an alternative source of NDVI data in the event that the sensor that normally provided a certain application with NDVI data was no longer operational.

4.2 Introduction

Based on the theoretical comparison of the technical characteristics of AVHRR, MODIS and VEGETATION it was hypothesised that NDVI data collected by MODIS or VEGETATION used in a methodology such as the VPI were likely to help detect drought conditions more accurately than NDVI data collected by AVHRR.

At the time this part of the study was initiated (2003), MODIS and VEGETATION had respectively collected NDVI data for a period of about three and five years each. Such short historical NDVI records were not sufficiently long to safely establish the historical distribution of NDVI values over certain areas and time, as is required by drought monitoring methodologies such as the VPI or the VCI (Guo and Richard, 2004; Sannier et al., 1998; Thenkabail et al., 2004a). Thus, despite the relative advantages of MODIS and VEGETATION over AVHRR, data collected by the former could not be used to efficiently detect drought conditions using either the VPI or the VCI methodology. On the other hand the historical NDVI record of AVHRR extended for more than two decades and had already been used in such drought monitoring methodologies in the past (Johnson et al., 1993; Kogan 1995b; Kogan and Sullivan, 1993; Unganai and Kogan, 1998).

Data collected by AVHRR in the past could not be used directly to provide MODIS and VEGETATION with the NDVI data for the time period they were not yet operational; because, NDVI values calculated from the measurements taken by the three sensors over the same area and time will differ. This was demonstrated in Chapter 2 (section 2.3.3); the simulated red and NIR band reflectance measurements of each of the three sensors were not the same over the same land cover targets, even though the simulation did not account for any other factors that could cause differences between the sensors' measurements other than the different spectral relative response of the sensors' red and NIR bands. Thus, if NDVI data collected by AVHRR were to be used to provide MODIS or VEGETATION with historical data for a methodology such as the VPI or the VCI, then NDVI values based on measurements taken by MODIS or VEGETATION over a particular area would differ from the historical NDVI values provided by AVHRR even if the spectral properties of that particular area have not changed over time. In such

a case, the results produced by a VCI or VPI methodology regarding the state of stress of the vegetation occupying that area would have been misleading.

However, although NDVI values collected by the three sensors over the same targets differ, it was of interest to test whether these values were correlated with each other. In such a case, if the correlation between the sensors' NDVI measurements over the same targets and dates was significantly high, then regression analysis could be used to simulate the NDVI measurements a sensor would collect based on NDVI measurements collected by another sensor over the same target and date. Consequently, if NDVI data for MODIS and VEGETATION could be simulated based on NDVI data collected by AVHRR, then MODIS and VEGETATION could be provided with simulated historical NDVI records as long as the historical records of AVHRR. Moreover, if the NDVI data simulation of MODIS and VEGETATION was sufficiently accurate for the requirements of the VPI methodology, then the VPI methodology could be applied not only using NDVI data collected by AVHRR but also using NDVI data collected by MODIS and/or VEGETATION.

In addition, a successful simulation of one sensor's NDVI data based on the NDVI data collected by another would not only potentially benefit drought monitoring applications alone, but also other applications where NDVI data collected by any of the three sensors are needed. This could be for applications that require long historical records similarly to the VPI, or monitoring applications where the continuous reception of NDVI data is crucial and the existence of a second or even third back up sensor would allow uninterrupted monitoring even if NDVI data became unavailable from two of the three sensors.

This idea was encouraged by the results of the spectral simulation performed earlier (2.3.3). When the sensors' simulated NDVI values over the same series of targets (figure 2.15) were plotted against each other (figures 4.1, 4.2 and 4.3) highly linear correlations could be seen. That was confirmed when regression analysis was performed; the equations, correlation coefficients of determination (R^2), Standard Error (SE) of the estimations, SE of the regression coefficients, and the Significance Levels (SL) of each regression are displayed in table 4.1. It can be seen that all regressions were significant

(SL<0.001) and more than 99% (R^2>0.99) of variability between the sensor's NDVI values could be explained.

Table 4.1: Statistics of the regression analysis between the simulated NDVI values of AVHRR, MODIS and VEGETATION.

	Equation	R^2	Scale SE	Constant SE	SE	SL
MODIS/AVHRR	MODIS=1.0285AVHRR-0.0003	0.99931	0.011037	0.00762	0.004904	<0.001
VGT/AVHRR	VGT=1.0052AVHRR-0.0087	0.99809	0.017923	0.012375	0.007964	<0.001
MODIS/VGT	MODIS=1.022VGT+0.0094	0.99894	0.013576	0.009308	0.00607	<0.001

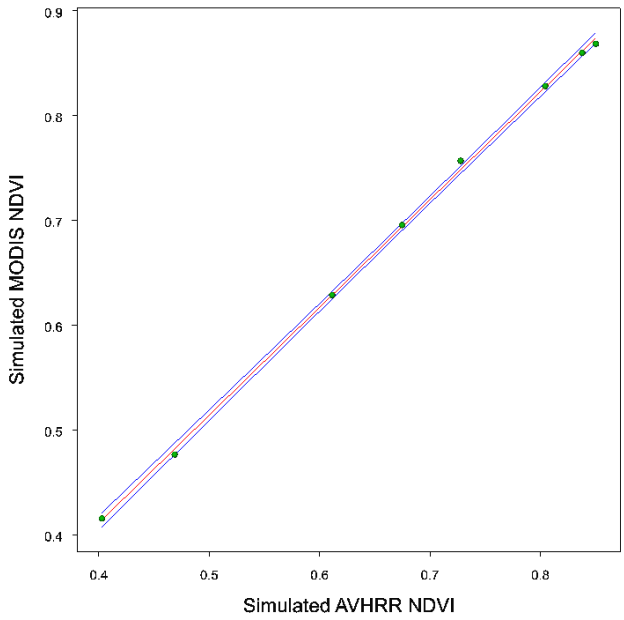

Figure 4.1: Scatter plot of MODIS and AVHRR simulated NDVI values which themselves are displayed in figure 2.15 (The trendline and 95% CI are displayed in red and blue respectively).

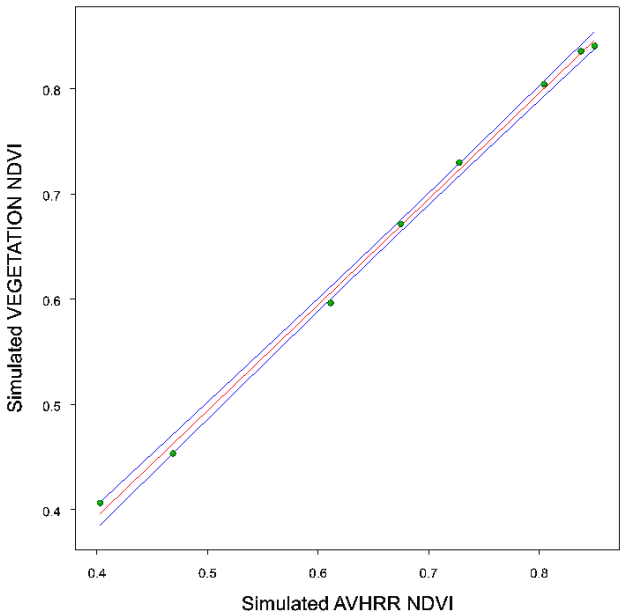

Figure 4.2: Scatter plot of VEGETATION and AVHRR simulated NDVI values which themselves are displayed in figure 2.15 (The trendline and 95% CI are displayed in red and blue respectively).

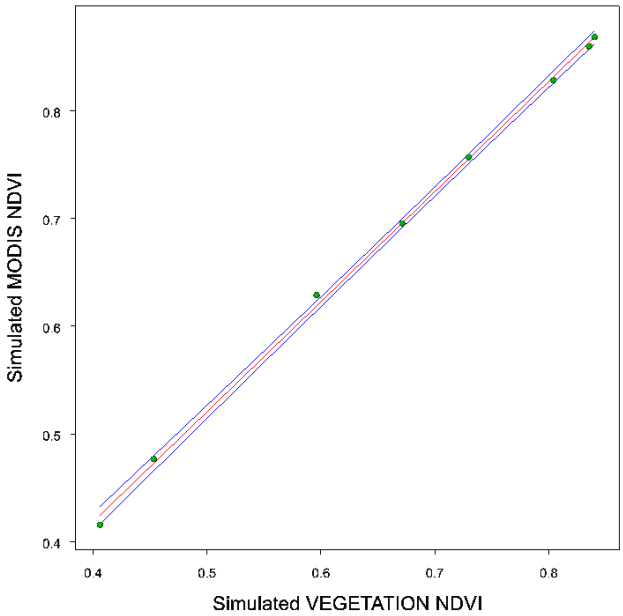

Figure 4.3: Scatter plot of MODIS and VEGETATION simulated NDVI values which themselves are displayed in figure 2.15 (The trendline and 95% CI are displayed in red and blue respectively).

It was considered of particular interest to investigate whether the relationships between the simulated NDVI data of the three sensors were significantly different to the respective relationships between the sensors' real NDVI data. This was considered possible, because the sensors' NDVI values were simulated under certain assumptions which are not always true in real conditions.

For instance, in the simulation it was assumed that all sensors viewed the earth's surface from the same position (that of HyMap) and at the same time. This is not true in reality because the three sensors follow different orbits (table 2.11); hence, the three sensors view a certain area at different times and from different viewing angles. Because the majority of land cover surfaces do not have near-Lambertian properties (Kimes et al., 1985; Leeuwen et al., 1994; Vierling et al.,1997), differences in the sensor-target-sun geometry could cause significant variation between the measurements of the three sensors (Burgess and Pairman 1997; Cihlar et al., 1994b; Goward et al. 1991; Gutman, 1991; Holben 1986; Li et al. 1996; Privette et al., 1995). Differences in the sensor-target-sun geometry would also cause significant variation between the atmospheric contribution to the sensors' measurements; because, at greater viewing and solar zenith angles radiation travels further through (and consequently interacts more with) the atmosphere, and vice versa.

The HyMap data used in the simulation have not been previously atmospherically corrected; however, the NDVI measurements required for applications such as the VPI are preferably atmospherically corrected, so that atmospherically induced variations in multi-temporal data are minimised. The data collected by the three sensors however are not equally affected by atmospheric effects due to differences in the sensors' spectral bandwidths (Fenshold and Sandholt, 2005; Fensholt, 2004; Huete et al., 1999; Luo and Trishchenko, 2005; Tanre et al., 1992; Vermote et al., 1996), and atmospheric correction processes. Consequently, variations between the sensors' measurements over the same area and approximately the same time could be caused due to unequal atmospheric contribution to the sensors' measurements.

Moreover, the HyMap data used in the simulation were not affected or obscured by cloud cover, however measurements taken by the three sensors could be. Cloud contamination can significantly reduce the NDVI value a sensor would normally record

over a non cloud cover target. As such, cloud contaminated data are removed and not used in applications interested in the assessment of the biophysical and biochemical properties of land surfaces, such as the VPI methodology. However, the three sensors are not equally equipped in the identification and consequent removal of cloud contaminated data. Hence, the sensors' different efficiency at detecting cloud contaminated data could introduce differences between the sensors' NDVI measurements, which were not accounted for in the simulation.

Further, as already discussed in sections 2.3.5 and 2.3.4, the calibration accuracies of the sensors were different, and so were their radiometric resolutions; however in the simulation it was assumed that all sensors' bands were perfectly calibrated and the effect of the radiometric resolution was not accounted for. The violation of these assumptions in real conditions may cause differences between the real and simulated relationships of the sensors' NDVI values.

Additionally, when the NDVI values of the three sensors were simulated over a series of eight targets, the spatial resolution of each sensor was not accounted for. It was assumed that for each target each sensor recorded radiation over an area covered entirely by a single land cover class. In reality however, and particularly over heterogeneous areas this assumption would not be true. The radiation emanating from a heterogeneous area would depend on the proportion of different land cover classes it is composed of, which in turn would be dependant on the extent of the area considered and the degree of heterogeneity. Since sensors of different spatial resolution would measure radiation over areas of different size for the formation of each pixel in their data, then it is likely that over heterogeneous areas the radiation emanating from the extent of each of the sensors' pixel equivalent area on the surface of the earth would be different. Thus, differences in the spatial resolution of the sensors could also be a factor which could cause a different relationship between the NDVI values of the three sensors than the relationship predicted by the simulation.

Finally the regression between the simulated NDVI values of the three sensors was only based on the simulation of the sensors' response over eight different land cover classes on a single date. The relationship between the NDVI values of the sensors may vary over different dates and land cover classes.

The correlation between the sensors' NDVI values and consequently the probability of succeeding in simulating NDVI data was expected to be higher if MVC NDVI values were used instead of single-date NDVI data. The MVC technique is known to minimise the effect of varying Solar Zenith Angles (SZAs) (variations of SZA within the same sensor can be caused by orbital drift (Cracknell, 1997; Kaufmann et al., 2000)), viewing angles and atmospheric contamination (Cihlar et al. 1994b; Cihlar, 2000; Cracknell 1997; Duchemin et al., 2002; Eidenshink and Faundeen, 1994; Flieg et al. 1983; Goward et al. 1994; Holben , 1986; Kogan and Zhu 2001; Lioubimtseva, 2003; Muchoney et al., 2000; Strahler et al., 1999) from multi-temporal NDVI data collected by a sensor. Due to these properties of the MVC technique for NDVI data collected by the same sensor, it was believed that the MVC technique would also minimise differences between NDVI values of different sensors caused by the same effects. Consequently, a regression between MVC NDVI data collected from different sensors was considered more likely to be successful, than a regression between single date NDVI data collected from different sensors.

The simulation was intended to be based on MVC NDVI data recorded by each of the three sensors over predefined study sites within the time period that the operational time of the sensors overlapped. The MVC NDVI data recorded by each sensor over the same site locations and composite periods were to be plotted against each other, and through regression analysis it was anticipated to derive equations which would allow the prediction of the MVC NDVI value of one sensor over a specific area and composite period based on the respective MVC NDVI value recorded by another sensor.

The simulation was not expected to be perfect, as that would imply that there are no differences between the three sensors' NDVI measurements, which is not true as explained briefly in the present chapter and more extensively in Chapter 2 of this study. However, it was believed to be a possible option for providing MODIS and VEGETATION with fairly accurate historical MVC NDVI records spanning long enough to be used in methodologies such as the VPI or the VCI.

At the time this part of the study was undertaken the three sensors were operational at the same time for only a few years; that may have been the reason that no other similar study regarding the regression between NDVI measurements from the three different

sensors could be found published in the literature at the time. Nevertheless, two such studies have been found at a later stage. Gallo et al. (2004) compared MVC (16-day composites) NDVI data collected by MODIS and AVHRR over the conterminous USA during 2001, and found that MODIS and AVHRR MVC NDVI values over the same sites and composite periods were linearly related, with the relation explaining more than 90% of variability in the MVC NDVI data of the sensors. Similarly, Thenkabail et al. (2004a) compared MVC (monthly composites) NDVI data collected by MODIS and AVHRR over Afghanistan, Pakistan and western India during the 2000-2001 period, and found a linear relation between the MVC NDVI values of the two sensors over the same sites and composite periods, over certain months the regression model that was developed could explain up to 95% of the variability in the data of the two sensors.

In the event that the investigation of the relationships between the sensors' composite NDVI values carried out in this part of the study, provided evidence to suggest that regression equations could potentially be used to simulate composite NDVI data for MODIS and VEGETATION based on NDVI data collected by AVHRR, then the validity of these regression equations were to be tested in the next stage of the study. More particularly in the next stage of the study, the validity of the regression equations developed in this part of the study were to be tested for providing MODIS and VEGETATION with simulated composite NDVI data for the requirements of the VPI methodology, over a study area in Africa which had not been identified yet at this stage of the study.

4.3 Study sites

Due to the fact that the decision had already been made to select a study area over Africa for the next stage of the study, it was considered more appropriate to investigate the relationships between the sensors' composite NDVI values using composite NDVI data collected by each of the three sensors over Africa. It was decided to extract MVC NDVI data over locations equally spread across the continent so that the MVC NDVI values used in the regression provided a good representation of the range of NDVI values occurring across the continent. Additionally, it was decided to investigate the relationship

between the sensors' composite NDVI values under conditions that would improve the chance of a high correlation between them. This was done so that the results of the current investigation could be used as a measure of the best likely scenario. As such it was decided to use composite NDVI data collected over homogeneously covered sites, so that differences between the sensors' composite NDVI values caused by differences between the sensors' spatial resolutions and image registration accuracies would be minimised.

In a study carried out by Sannier et al. (1998b) the compatibility of the FAO Africa Real Time Environmental Monitoring Information System (ARTEMIS) and the NASA Pathfinder AVHRR Land (PAL) MVC NDVI records was explored. MVC NDVI data were extracted from both datasets over seven sites; their names and coordinates in decimal degrees (dd) are displayed in table 4.2. These sites were selected because their land cover is highly homogeneous and as a group provide a representative range of NDVI values occurring in Africa. These properties of the sites also satisfied the requirements of the present study and were therefore adopted as sample sites. The site locations are plotted in figure 4.4.

Table 4.2: Names and coordinates (in dd) of the seven selected sites where MVC NDVI data were to be collected from each sensor

Site name	Longitude	Latitude
Nile Delta	30.967° E	30.917° N
Al Haruj al Aswad	17.317° E	27.383° N
Rub al Khali	53.017° E	19.183° N
Niger Delta	4.533° W	14.417° N
Congo Basin	23.267° E	0.767° N
Okavango Delta	22.483° E	19.167° S
Etosha Pan	16.233° E	18.883° S

Figure 4.4: The location of the seven selected sites where MVC NDVI data were to be collected from each sensor

4.4 Datasets

4.4.1 AVHRR

At the time of the present study there were two main sources of historical MVC NDVI data collected by AVHRR over Africa, the PAL dataset (Kempler, 2006b; James and Kalluri, 1994) and the dataset produced by the NASA Goddard Space Flight Centre (GSFC) (Los et al., 1994; Tucker et al., 1994, 2005). The temporal coverage of the Pathfinder dataset spans from July 1981 to September 1994 (Kempler, 2006b) and did not include the time period when the operational time of AVHRR overlapped with either MODIS or VEGETATION; therefore the dataset was not considered for the purpose of the present study. On the other hand the NASA/GSFC (also used by FAO-ARTEMIS) extended over the time period when the operational time of the three sensors overlapped, and therefore was selected. Moreover the latter dataset had recently been re-processed (Tucker et al., 2005) to account for SZA variations and stratospheric volcanic aerosols released by the eruption of El Chichon and Mt Pinatubo.

The NASA/GSFC AVHRR MVC NDVI dataset originated from the Global Inventory Monitoring and Modelling Studies (GIMMS) group. The GIMMS group has produced AVHRR MVC NDVI composites for all continents except for Antarctica, dating from July 1981 to present. The data used were collected by several AVHRR sensors onboard different satellites over time (table 4.3).

Table 4.3: Time periods when AVHRR data from each NOAA satellite were used in the production of the GIMMS AVHRR MVC NDVI dataset

Satellite	Period
NOAA 7	Jul 81 - Feb 85
NOAA 9	Feb 85 - Nov 88
NOAA 11	Nov 88 - Sep 94
NOAA 9(descend)	Sep 94 - Jan 95
NOAA 14	Jan 95 - Oct 00
NOAA 16	Nov 00 - Dec 03
NOAA 17	Jan 04 - present

The level-1b AVHRR data of the red and NIR bands were geolocated using a procedure by Saleous et al. (2000) and resampled to 8 km pixels; the data used were limited to those collected at viewing angles of less than or equal to 40° (Tucker et al., 2005). This limitation was imposed to minimise the effects of reflectance anisotropy over vegetated areas at high viewing angles. There is strong reflectance anisotropy in the red spectral region over most vegetated areas, while almost no anisotropy is observed in the NIR region (Huete et al., 1999; Fensholt and Sandholt, 2005). As a result, at high sensor-target-sun angles reflectance values over the red spectral region are reduced in relation to the NIR region and NDVI values are overestimated (Cihlar et al., 1994b; DeFries et al., 1998; Gowards et al., 1991; Huete et al., 1992; Lind and Fensholt, 1999; Strahler et al., 1999; Zhu and Yang, 1996).

Data collected by AVHRR sensors onboard NOAA-7 to NOAA-14 were processed differently to the data collected by AVHRR onboard NOAA-16 and NOAA-17. The red and NIR band data collected by the AVHRR sensors onboard the satellites NOAA-7 to NOAA-14 were calibrated using the technique described by Vermote and Kaufman (1995). Cloud contaminated pixels were detected and masked using the fifth band. Next if the data were collected between April 1982 and December 1984 or June 1991 and December 1993, then the data were corrected for stratospheric volcanic aerosol released by the El Chichon and Mt Pinatubo eruptions as proposed by Vermote et al., (1997b). MVC NDVI values were then calculated (a 10-day composite interval was used for Africa and 15-day for the rest of the world), and consequently adjusted for sensor degradation according to Los (1998). Finally the MVC NDVI values were corrected for SZA effects using the empirical mode decomposition described by Pinzon et al., (2005).

The red and NIR band data collected by AVHRR sensors onboard NOAA-16 and NOAA-17 were calibrated using the sensors' respective pre-flight calibration coefficients (Tucker et al., 2005). Cloud contaminated pixels were detected and masked using the fifth band. NDVI values were then calculated from the calibrated data, which were further used in the MVC technique. Next the produced MVC NDVI fields were corrected for SZA effects (Pinzon et al., 2005). The resulting MVC NDVI values were then inter-calibrated with VEGETATION which in turn was previously inter-calibrated with AVHRR on NOAA-14 (Tucker et al., 2005). As a final step the AVHRR NDVI dataset

was processed to match the dynamic range of MODIS and VEGETATION (Tucker et al., 2005).

Table 4.4: Information regarding the projection and extent of the GIMMS AVHRR MVC NDVI dataset over Africa

Projection	Albers Conical Equal Area
Datum	Clarke 1866
Spheroid	Clarke 1866
Pixel size	8 km x 8 km
Upper left latitude	4604032.51
Upper left longitude	-4603990.26
Lower right latitude	-4603967.50
Lower right longitude	4604009.74

The MVC NDVI data were scaled to 8-bit integers. In order to retrieve the original values the values of the 8-bit integers must be divided by 250 (equation 4.1). After the conversion the NDVI values greater than one such as 1.0200, 1.0160, and 1.0120, indicate water-covered, masked and missing pixels respectively. Information regarding the projection and extent of the dataset over the African continent is provided in table 4.4. More details regarding the production of the dataset can be found in Tucker et al. (2005).

$$\text{AVHRR NDVI value} = \frac{NDVI_{scaled}}{250} \tag{4.1}$$

4.4.2 MODIS

MVC NDVI data were available from both MODIS sensors onboard TERRA and AQUA. However AQUA was launched in May 2002 and at the time of the present study there was little temporal overlap between the operational time of MODIS onboard AQUA and the operational times of AVHRR and VEGETATION. Thus only MVC NDVI data collected by MODIS onboard TERRA (launched in late 1999) were used; the data were available in four different datasets:

i) at 250 m spatial resolution and a composite time interval of 16 days (MOD13Q1)
ii) at 500 m spatial resolution and a composite time interval of 16 days (MOD13A1)
iii) at 1 km spatial resolution and a composite time interval of 16 days (MOD13A2)
iv) at 1 km spatial resolution and a monthly composite time interval (MOD13A3).

Out of the four datasets the third (MOD13A2) was chosen because it was the closest match to the respective AVHRR dataset in terms of spatial resolution and composite time interval.

The calculation of the NDVI values of the MOD13A2 (Huete et al., 1999) product were based on aggregated surface reflectance values of the sensor's red and NIR bands (product MOD09). In the production of the MOD09 (Vermote and Vermeulen, 1999) the raw data of the first seven MODIS bands were geolocated (Wolfe et al., 1999) calibrated (Xiong et al., 2002, 2002c), atmospherically corrected for water vapour, aerosol Rayleigh scattering and ozone (Vermote et al., 1997a) cloud masked (Ackerman et al., 1996) and normalised for BRDF effects using a Walthall empirical BRDF model (Strahler et al., 1999b; Walthall et al., 1985).

The Walthall BRDF model required, over each pixel location, a minimum of five observations of good data integrity and no cloud or shadow coverage, during the 16-day composite period (Huete et al., 1999; Walthall et al., 1985). When fitted the Walthall BRDF model produced for each pixel location a BRDF normalised reflectance value for each spectral band. The BRDF normalised surface reflectance values of the red and NIR bands were then used to calculate the NDVI values for the MOD13A2 product.

The use of the MVC technique was not preferred, particularly due to the fact that the NDVI data were calculated from atmospherically corrected data (Huete et al., 1999).

NDVI values collected over near-Lambertian land cover surfaces at high viewing and/or solar zenith angles have lower NDVI values than NDVI values collected at lower viewing and/or solar zenith angles; this is because atmospheric contamination reduces NDVI values (Huete et al., 1999) and the magnitude of this reduction is increased when the atmospheric path length is increased due to higher viewing and/or solar zenith angles. However, the majority of land cover surfaces do not have near-Lambertian properties, but exhibit strong anisotropy related to vegetation canopy, shadows and soil background (Kimes et al., 1985; Leeuwen et al., 1994; Vierling et al.,1997). Bidirectional effects due to surface anisotropy are unequal over different spectral bands (Gutman, 1991; Roujean et al., 1992), and therefore are not removed by rationing the red and NIR in the NDVI calculation (Walter-Shea et al., 1997). Particularly over vegetation, NDVI measurements tend to be higher when collected at higher viewing angles mainly due to greater vegetation depth (greater absorption of radiation in the red spectral region). The atmospheric contamination and bidirectional effects counteract each other (Huete et al., 1999) and could result in either overestimation or underestimation of the NDVI. However if the NDVI values were calculated from atmospherically corrected data, the atmospheric effect would be removed and the bidirectional effects would become more prominent (Cihlar et al., 1994a, 1994b). Consequently the NDVI data selected by the MVC methodology are more likely to be affected by bidirectional affects if the NDVI data were calculated using atmospherically corrected data. The MVC methodology was considered better suited for use with non atmospherically corrected data (Cihlar et al., 1994a).

In those cases where less than five suitable observations were available for each pixel location, the Walthall model could not be used. Instead, the NDVI values of the two observations recorded with the lowest viewing and solar zenith angles were calculated, and the highest NDVI value of the two observations was selected for the MOD13A2 product. This is referred to as Constraint View angle Maximum Value Composite (CV-MVC). Moreover, if only one suitable observation was available then that observation was used for the calculation of the NDVI of MOD13A2. Finally, if there were no suitable observations at all, then the NDVI values were calculated for all observations and the observation with the highest NDVI value was selected.

The MOD13A2 dataset included other data besides the NDVI, such as:

- the Enhanced Vegetation Index (EVI) which is beyond the scope of this study
- quality assurance for both EVI and NDVI
- reflectance values of the first, second, third and seventh bands of MODIS
- average view, solar zenith and relative azimuth angles for each pixel

The NDVI, EVI and reflectance data were stored as scaled 16-bit integers and should be divided by 10000 in order to recover their original values (equation 4.2). The MOD13A2 products were not produced for whole continents (like the respective datasets of AVHRR and VEGETATION) but were available for areas of approximately the size of 10° by 10°. The data are available in a Sinusoidal projection (Datum: WGS 1984, Spheroid: WGS1984). More information regarding the MOD13A2 and MOD09 products can be found in Huete et al. (1999) and Vermote and Vermeulen (1999), respectively.

$$\text{MODIS NDVI value} = \frac{NDVI_{scaled}}{10000} \tag{4.2}$$

4.4.3 VEGETATION

MVC NDVI data collected by VEGETATION were available in the form of two products, the S-10 and the recently developed D-10. The difference between the two products is that the latter accounts for variations in the sensor-target-sun geometry unlike the former. BRDF effects were normalised in the D-10 product by applying the Bidirectional Distribution Function (BDF) methodology (Duchemin et al., 2000, 2002) that made use of the BRDF model developed by Roujean et al. (1992). However, the D-10 products were not available for dates earlier than July 2001 as opposed to the S-10 products which were available from as early as April 1998. At the time of the present study the temporal overlap between the D-10 products and the operational times of AVHRR and MODIS was a little more than a year and was not considered long enough for a regression analysis between the NDVI datasets of the three sensors; hence, it was decided to use the S-10 products instead.

The S-10 products were created using data collected by the sensor's spectral bands over a 10-day interval. For each 10-day interval, all data recorded over each pixel location were calibrated to TOA reflectance values (Henry and Meygret, 2001) and investigated for cloud contamination using criteria based on the TOA reflectance values of the B0 and SWIR bands (SPOT-VEGETATION, 2006a). NDVI values were then calculated from the TOA reflectance values of each observation, and for each pixel location the observation with the highest NDVI value were selected using the MVC technique (only cloud-free observations with good data integrity are used in the MVC technique). Consequently, for each pixel location the TOA reflectance values of the observation selected by the MVC technique were atmospherically corrected using the SMAC methodology (Rahman and Dedieu, 1994). Reflectance values were corrected for Rayleigh scattering based on surface altitude information, ozone and aerosol atmospheric contents based on data provided by CESBIO using climatology and a fixed model, and the water vapour based on data provided by Meteo-France using meteorological models. (Berthelot and Dedieu, 2000; Maisongrande et al., 2004; Passot, 2000). The NDVI value used by the S-10 product for each pixel location was calculated from the atmospherically corrected reflectance value of the observation selected by the MVC technique.

The NDVI values were stored as scaled 8-bit integers, the true NDVI values could be recovered by dividing the values of the scaled integers by 250 and subtracting 0.1 (equation 4.3).

$$\text{VEGETATION NDVI value} = \frac{NDVI_{scaled}}{250} - 0.1 \tag{4.3}$$

S-10 products were available for continental composites including Africa. The projection system used and the extent of the S-10 African composites are given in table 4.5. Moreover, information regarding the radiometric quality and cloud cover of each pixel in the S-10 composite was provided in the form of a status map.

Table 4.5: Information regarding the projection and extent of the VEGETATION S-10 continental composite of Africa

Projection	Plate Carrée
Datum	WGS1984
Spheroid	WGS1984
Pixel size	≈ 0.00893° by 0.00893°
Upper left latitude	38° N
Upper left longitude	26° E
Lower right latitude	35° S
Lower right longitude	60° W

4.5 Methodology

4.5.1 Acquisition of sensor NDVI data

At the start of this study, it was decided to carry out a simple linear regression analysis between the MVC NDVI values calculated from the measurements taken by each of the three sensors within the same composite time intervals and study sites, using data collected by each sensor until the end of 2002. Through the duration of the study more data became available from each sensor that could have been used to further reinforce the validity of the study's results. Nevertheless, this was not considered necessary as the initial results of the analysis were encouraging and data storage resources were limited.

The earliest data were available from the composite NDVI datasets of AVHRR, MODIS and VEGETATION for July 1981, February 2000 and April 1998, respectively. Thus, the time periods when the sensors' composite NDVI datasets overlapped up to the end of 2002 were: April 1998 – December 2002 for VEGETATION/AVHRR, and February 2000 - December 2002 for both MODIS/AVHRR, and MODIS/VEGETATION.

The recently re-processed (by the GIMMS group of NASA) MVC NDVI datasets of AVHRR over Africa were available to be downloaded from the Famine Early Warning System Network (FEWS NET) Africa Data Dissemination Service (ADDS) website

http://earlywarning.cr.usgs.gov/adds/datatheme.php (20 May 2005)) in BIL and Windisp formats. The data were available for each 10-day composite interval in a single image for the whole of Africa. Because all seven study sites were located within the extent of the image, data did not have to be downloaded separately for each study site. In total 171 files were downloaded for the time period between 01/04/1998 and 31/12/2002.

The MODIS MOD13A2 data were available to be downloaded from the EOS Data Gateway website (http://edcimswww.cr.usgs.gov/pub/imswelcome/ (10 March 2004)) in EOS-HDF format. The search engine of the website was used to select all MOD13A2 data available for each of the seven study sites between the time period 16/02/2000 and 31/12/20002. In total 462 files were selected and consequently downloaded.

Lastly, VEGETATION S-10 products were available to be downloaded in HDF format from the VITO website for the distribution of free VEGETATION products (http://free.vgt.vito.be/home.php (18 April 2003)). Similarly to AVHRR, a synthesis for the whole African continent covering in its extent all seven study sites was available for each 10-day composite interval. In total 171 files were downloaded for the time period between 01/04/1998 and 31/12/2002.

4.5.2 Image processing

4.5.2.1 Data import

All image processing was performed using ERDAS IMAGINE, therefore beforehand all data had to be converted into file formats compatible with that software.

Each of the AVHRR images were imported to ERDAS IMAGINE as generic binary using the settings displayed in table 4.6.

Each of the MODIS files contained several other fields besides the NDVI (such as the EVI, viewing and zenith solar angles etc). From these fields only the NDVI and its quality assurance were needed for this study. The HEG tool was used to create a geotiff file for every NDVI and NDVI quality assurance field of each MODIS files. These geotiff files could then be processed using ERDAS IMAGINE.

Table 4.6: Import information for the AVHRR MVC NDVI data

Data type	8-bit integer
Number of rows	1152
Number of columns	1152
Number of bands	1
File header size	512

Each of the VEGETATION files was compressed and contained the NDVI and status map data in two separate HDF files. Both NDVI and status map data from each VEGETATION file were imported to ERDAS IMAGINE using the HDF (Raster) option.

4.5.2.2 Data georeference

All data from all three sensors were already georeferenced; however, during the import process, although the geometry of the images remained intact, the data from AVHRR and VEGETATION did not retain their georeference information. This was corrected by updating the "Layer Info" of each image regarding the extent and map model of each image according to tables 4.4 and 4.5.

4.5.2.3 NDVI data restoration and quality assurance

Before proceeding any further, all images were visually inspected for signs of significant geometric and radiometric distortion. No obvious distortion was found in any of the MODIS and VEGETATION images. However, out of the AVHRR images, 11 were identified as distorted, the dates of which are given in table 4.7, an example of such a distorted image is displayed in figure 4.5. The identified images were removed from the study.

Apart from cases of obvious data distortion, such as the example shown in figure 4.5, other sources of error, such as cloud cover, could render some of the NDVI data unsuitable for the purpose of this study and had to be removed/masked.

Table 4.7: MVC NDVI images from AVHRR with significant geometric or radiometric distortion

Year	Month	10-day composite
1998	June	1st
1998	June	2nd
1999	May	3rd
2000	May	3rd
2000	December	3rd
2001	August	2nd
2002	February	2nd
2002	February	3rd
2002	June	1st
2002	June	2nd
2002	July	2nd

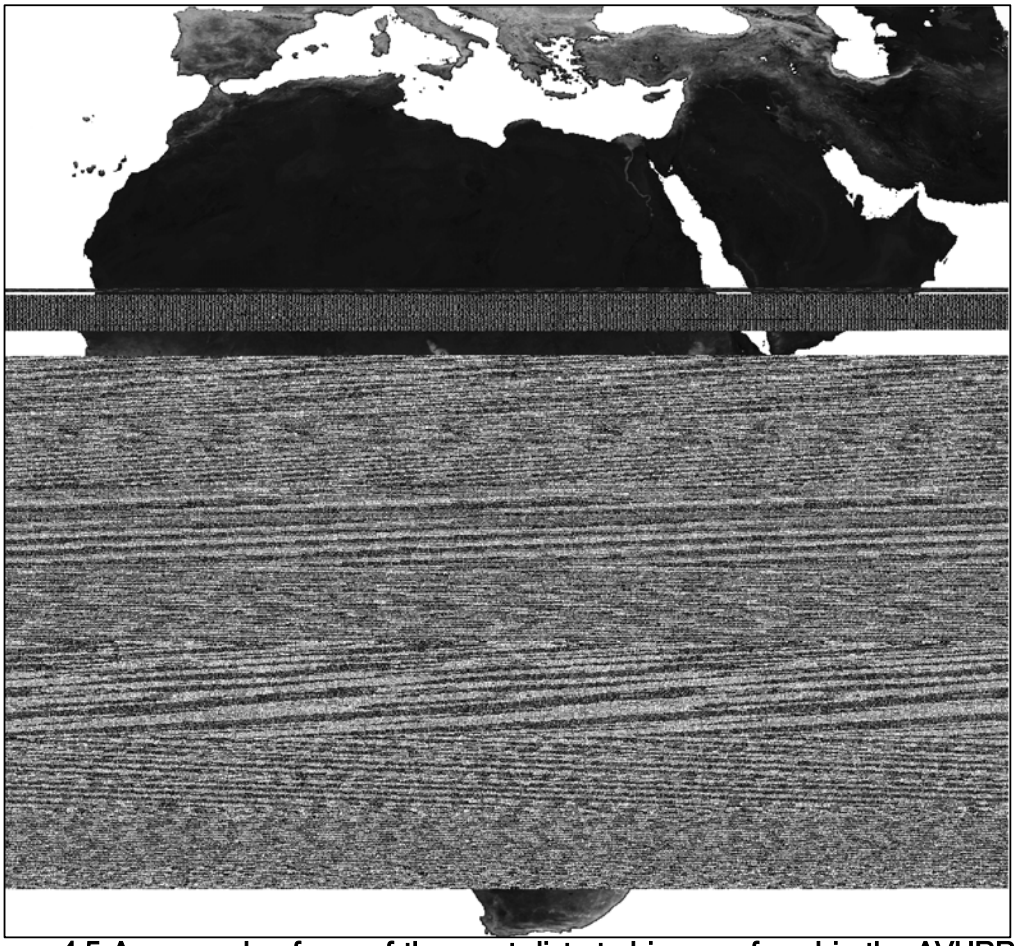

Figure 4.5 An example of one of the most distorted images found in the AVHRR MVC NDVI dataset (3rd composite May 1999).

Pixel locations in the AVHRR MVC NDVI dataset with no cloud free observations during the 10-day composite period or missing data were given a scaled NDVI value of 255 or 254, respectively. No further information regarding the quality of the NDVI data were included in the dataset; thus, the quality assurance of the AVHRR dataset could only be based on those two criteria. It was decided to remove/mask any pixels with scaled NDVI values of 254 or 255 from the dataset. Such pixels could not be removed/masked by replacing their values with zero, because zero is a valid NDVI value. A model was written in ERDAS IMAGINE, that when executed did the following for each AVHRR image:

- restored the original NDVI value of every pixel using equation 4.1
- and then replaced any pixel with NDVI values of $\frac{254}{250} = 0.016$ or $\frac{253}{250} = 1.012$ with the value of two

The value two is outside the valid range of NDVI and identified a pixel for which the NDVI value should be ignored.

From each MOD13A2 file, a NDVI image and a NDVI quality assurance image was created. Every pixel in the NDVI quality assurance image provided information for the quality of the data stored in the respective pixel location of the NDVI image. The data quality for each NDVI pixel was described with a 16-bit binary number, with the first bit being the least significant bit. The way which was used to depict the data quality of the NDVI data using a 16-bit binary is displayed in table 4.8. The pixel values of the NDVI quality assurance image were the 16-bit binary numbers converted into the decimal system.

It can be seen in table 4.8 that the quality assurance image provided a variety of information regarding the NDVI quality. For the purpose of this study it was decided to retain NDVI data that according to the quality assurance information:

- were of ideal quality
- their usefulness was rated to be within the first three highest levels
- were not contaminated with clouds
- were not collected over areas covered with snow/ice or shadow

All possible binary numbers (384 different numbers) that depicted such criteria according to table 4.8 were formed, and consequently converted into the decimal system. Next a model was written in ERDAS IMAGINE, that when executed for each pair of NDVI and NDVI quality assurance images:

- restored the original NDVI values of each pixel in the NDVI image using equation 4.2
- identified all pixels in the NDVI quality assurance image whose values did not match the 384 different decimal numbers previously identified
- identified all pixels in the NDVI image whose locations corresponded to the locations of the pixels identified in the NDVI quality assurance image in the previous step, and changed their NDVI values to two

Similarly to MODIS, two images were created for each S-10 data file of VEGETATION, a NDVI image and a status map which provided information regarding the data quality of its respective NDVI image. The data quality information was stored in the form of an 8-bit binary number with the first bit being the most significant one. The description of the different binary numbers is provided in table 4.9. The pixel values of the status map were the values of the 8-bit binary numbers converted to the decimal system. For the purpose of this study it was decided to use only NDVI data that:

- were collected under clear conditions
- were collected over areas not covered by ice/snow
- were derived from spectral data of good radiometric quality

Two binary numbers described the above criteria: 00011111, and 00001111 or otherwise 248 and 240 when converted to the decimal system using the first bit as the least significant.

Consequently a model was written and run for every VEGETATION NDVI image in ERDAS IMANIGE. The model:

- restored the original NDVI values of each pixel in the NDVI images using equation 4.3
- identified the pixels in status map images whose values did not equal 248 or 240
- replaced the existing NDVI value to two of each pixel in the NDVI image that corresponded with pixels in the status map that were identified in the previous step

Table 4.8: Layout of MODIS NDVI quality assurance 16-bit binary number

Bit	Data quality measurement	Bit value
0-1	NDVI quality	00 NDVI produced, good quality 01 NDVI produced, but check QA 10 Most likely cloudy pixel 11 Pixel not produced
2-5	VI usefulness four bit range	0000 Highest quality 1100 Descending quality 1101 No atmospheric correction 1110 Lowest quality 1111 Not useful
6-7	Aerosol quantity	00 Climatology 01 Low 10 Average 11 High
8	Adjacency correction	1 Yes 0 No
9	Atmosphere BRDF correction	1 Yes 0 No
10	Mixed clouds	1 Yes 0 No
11-12	Land/water flag	00 Ocean 01 Coast 10 Wetland 11 Land
13	Possible snow/ice	1 Yes 0 No
14	Possible shadow	1 Yes 0 No
15	Composite method for NDVI	0 BRDF 1 CVMVC

Table 4.9: Layout of VEGETATION status map 8-bit binary number

Bit number	Data quality measurement	Bit value
0-1	Cloud and shadow coverage	00 Clear 01 Shadow 10 Uncertain 11 Cloud
2	Ice/snow coverage	1 Yes 0 No
3	Water/Land	1 Land 0 Water
4	Radiometric quality of SWIR	1 Good 0 Bad
5	Radiometric quality of B3	1 Good 0 Bad
6	Radiometric quality of B2	1 Good 0 Bad
7	Radiometric quality of B0	1 Good 0 Bad

At the end of this processing stage, all scaled NDVI values were restored to their original NDVI values, and all pixels whose NDVI values were not calculated based on good quality measurements were given the value two.

4.5.2.4 Data mosaic and layerstack

The composite NDVI datasets of AVHRR and VEGETATION provided data over all seven study sites in a single file for every composite period. In the case of MODIS however, NDVI data collected over the seven study sites for each composite period were available in seven separate files. Thus image processes that could be run only once for the AVHRR and VEGETATION, had to be run seven times for MODIS. In order to minimize image processing time and simplify data handling, all MODIS NDVI data collected over the same composite periods were mosaiced together in single images; the mosaic function of ERDAS IMAGINE was used.

Image processing times and data handling simplicity were further improved by placing all available NDVI data collected by each sensor over a year in a single multi-layer file. The layerstack function of ERDAS IMAGINE was used to stack all NDVI data

collected by each sensor over each yearly period; data were stacked in chronological order beginning with the earliest date.

4.5.2.5 Data extraction

Before deriving an empirical relation between the NDVI values of the three sensors, care had to be taken to ensure that the NDVI values used to derive the empirical relations were recorded from each sensor over the same time and areas. At this stage of the image processing however the pixels of each of the three sensors' datasets were not only of different size but were also expressed in different units. The pixel size of the AVHRR dataset was 8 km, while in the MODIS and VEGETATION datasets it was approximately 0.0083°.

Towards solving this mismatch all the datasets were initially re-projected to a common geographical projection (datum: WGS84, spheroid: WGS84). In this way the pixel sizes of all datasets were expressed in the same units (decimal degrees (dd)), and the same set of study site coordinates (table 4.2) could be used to extract data from all three datasets. The re-projection was performed using the re-project function of ERDAS IMAGINE (a rigorous transformation and nearest neighbour resampling method were used).

Next, the image degradation function of ERDAS IMAGINE was used, to resample the datasets of MODIS and VEGETATION to an increased pixel size that matched that of the AVHRR dataset (about 0.07 dd). The value of each newly created pixel was calculated by taking the mean value of the original pixels located within its area.

Finally, the "pixel to ASCII …" function of ERDAS IMAGINE was used to extract NDVI data from every sensor's yearly multi-temporal dataset over the seven study sites. The data were then imported to MSExcel for further processing.

4.5.3 MODIS data interpolated to a 10-day composite interval

The MODIS dataset was created using a 16-day composite time interval as opposed to the datasets of AVHRR and VEGETATION which were based on a 10-day interval. Thus data from the MODIS dataset were available at different chronological steps, and were based on measurements taken at different dates, than the data available from the AVHRR and VEGETATION datasets. Consequently NDVI data from the MODIS dataset could not be compared directly with NDVI data from the other two sensors.

In order to solve this chronological mismatch, it was decided to estimate the NDVI values the MODIS dataset would have had if it was created using a 10-day composite interval. The MODIS NDVI values were estimated on a 10-day interval by linearly interpolating between the closest available MODIS 16-day composite NDVI values from before and after the 10-day step. Data that had previously been flagged as "bad quality" (given a NDVI value of two) were not used in the interpolation.

4.5.4 Simple linear regression

Equations describing the relationship between the valid composite NDVI values of the three sensors' datasets over common observations (same targets and composite periods) were derived by performing a simple linear regression analysis. Between the data extracted from the datasets of AVHRR and VEGETATION, 1057 valid common observations were found, while the number of valid common observations between the data extracted from AVHRR and MODIS, and MODIS and VEGETATION were 562 and 671 respectively.

4.5.5 Test of significant differences

The equations derived from the regression analysis between the NDVI values extracted from the sensors' datasets (empirical regression) were tested for significant statistical difference against the respective equations derived from the regression analysis between the sensors' simulated NDVI values (simulated regression), and against a one-

to-one relationship. The reason for doing so was to test whether the violation of assumptions made in the simulated regression caused significant difference in the empirical regression, and whether composite NDVI values from one sensor could be directly used with the composite NDVI values of another.

The significance test was performed by calculating the 95% confidence interval (CI) of each regressions scale and constant coefficient, according to the following equation:

$$95\%\ \text{coefficient CI} = \text{coefficient value} \pm T(n-2, p<0.05)(\text{coefficient SE}) \quad (4.1)$$

$T(n-2,p<0.05)$= Value of the t distribution for n-2 degrees of freedom at 5% risk
n= Number of observations

In the event that the 95% CI of both scale and constant coefficients of two regressions overlapped, then the regression equations were not considered significantly different. Also in the event that the value of one was within the 95% CI of the scale coefficient of a regression, and zero within the 95% CI of the regression constant coefficient, then the regression equation was not considered to be significantly different than a one-to-one relationship.

4.6 Results

Scatter plots depicting the relationship between the NDVI values extracted from the three sensors' datasets are displayed in figures 4.6, 4.7, and 4.8. All regressions were found to be significant (SL<0.001) and could explain more than 95% of variation between the NDVI values (R^2>0.95). The equations and statistics derived from the performed simple linear regressions are given in table 4.10.

Table 4.10: Statistics of the regression analysis between the NDVI values of AVHRR, MODIS and VEGETATION.

	Equation	R^2	Slope SE	Constant SE	SE	SL
MODIS/AVHRR	MODIS=1.0824AVHRR+0.0115	0.9641	0.00883	0.003847	0.055652	<0.001
VGT/AVHRR	VGT=0.9954AVHRR-0.0091	0.9655	0.005792	0.002585	0.050944	<0.001
MODIS/VGT	MODIS=1.0424VGT+0.0312	0.9517	0.009076	0.003911	0.063879	<0.001

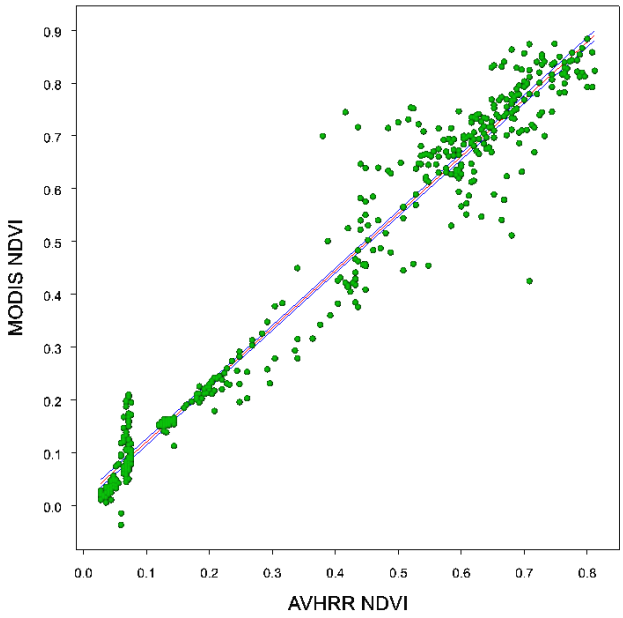

Figure 4.6: Scatter plot of the regression relationship between the NDVI values of AVHRR and MODIS (The trendline and 95% CI are displayed in red and blue respectively).

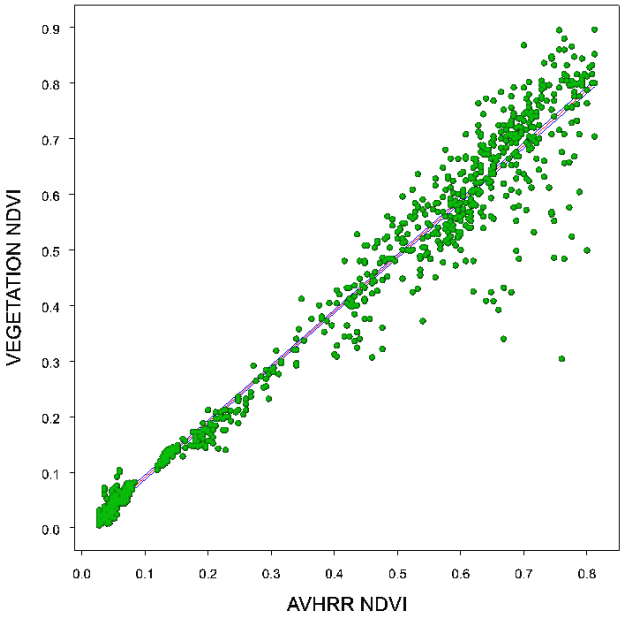

Figure 4.7: Scatter plot of the regression relationship between the NDVI values of AVHRR and VEGETATION (The trendline and 95% CI are displayed in red and blue respectively).

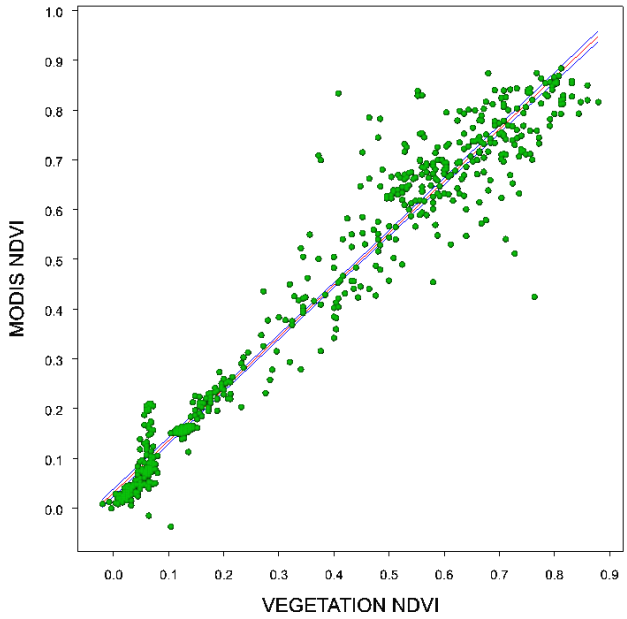

Figure 4.8: Scatter plot of the regression relationship between the NDVI values of MODIS and VEGETATION (The trendline and 95% CI are displayed in red and blue respectively).

The empirical regression between AVHRR and MODIS composite NDVI data was found to be significantly different from both the simulated regression and the one-to-one relationship. The empirical regression between AVHRR and VEGETATION composite NDVI data was not found to be significantly different from the simulated regression, but was significantly different from the one-to-one relationship. And finally the empirical regression between VEGETATION and MODIS composite NDVI data was not found to be significantly different than the simulated regression, but was significantly different than the one-to-one relationship. The 95% CI of the regression coefficients are given in tables 4.11, 4.12 and 4.13

Table 4.11: 95% Confidence interval range of the scale and constant coefficients of simulated and empirical regressions between NDVI values from AVHRR and MODIS.

MODIS/AVHRR	Simulated regression	Empirical regression
Scale lower 95% CI	1.06501	1.00154
Scale higher 95% CI	1.0997	1.05556
Constant lower 95% CI	0.00397	-0.019
Constant higher 95% CI	0.01908	0.01834

Table 4.12: 95% Confidence interval range of the scale and constant coefficients of simulated and empirical regressions between NDVI values from AVHRR and VEGETATION

VEGETATION/AVHRR	Simulated regression	Empirical regression
Scale lower 95% CI	0.961375	0.984059
Scale higher 95% CI	1.049089	1.00679
Constant lower 95% CI	-0.03901	-0.01415
Constant higher 95% CI	0.021553	-0.004

Table 4.13: 95% Confidence interval range of the scale and constant coefficients of simulated and empirical regressions between NDVI values from VEGETATION and MODIS.

MODIS/VEGETATION	Simulated regression	Empirical regression
Scale lower 95% CI	0.988813	1.024597
Scale higher 95% CI	1.055253	1.060241
Constant lower 95% CI	-0.01338	0.023535
Constant higher 95% CI	0.032175	0.038895

4.7 Discussion

4.7.1 MODIS/AVHRR regression

More than 96% of MODIS composite NDVI variation could be explained by respective AVHRR data. The majority of NDVI values extracted from the two sensors datasets followed the relationship of the derived regression equation; however a few observations deviated from it (outliers). Such outliers could be seen in figure 4.6; points located considerably further away from the regression line.

Such deviations from the regression relationship between the NDVI values of the two sensors could have been caused by a variety of things. One such thing was believed to be the use of cloud contaminated data which the cloud detection criteria had failed to identify. Cloud detection is not always successful, and cloud contaminated pixels may not have been detected; particularly pixels covered with low altitude and/or sub-pixel clouds. NDVI data based on such cloud contaminated measurements have considerably lower values than normal. Hence, if cloud contaminated data have not been properly identified by the cloud detection criteria of a sensor's dataset, then the calculated NDVI based on that data would be considerably lower than would be expected in relation to the respective cloud-free composite NDVI value of the other sensor.

Outliers could also have been caused by the use of poorly atmospherically corrected data. Variations in the atmospheric content can cause significant variations in the NDVI measurements, aerosol scattering alone could cause NDVI value variations in the order of 0.2 units (Goward et al., 1991; Teillet, 1989). Out of the two sensors' datasets only MODIS NDVI data were atmospherically corrected; therefore the use of poorly atmospherically corrected data (e.g. due to poorly estimated aerosol atmospheric content) would have affected only the NDVI values of MODIS dataset, and the NDVI value relationship between the two sensors datasets would deviate from the normal relationship described by the regression equation, creating outliers. Moreover, unusual atmospheric conditions (e.g. sand storms) would have changed the normal (under normal atmospheric conditions) NDVI values of AVHRR considerably, while the NDVI values of the MODIS dataset would have not, due to the fact that the MODIS data in most cases were

well atmospherically corrected. Hence, unusual atmospheric conditions could also have been the cause of outliers.

Another possible cause of outliers could have been that in some cases the only NDVI observation available within a compositing time period could have been collected at high viewing and/or solar zenith angles or in the case of MODIS may have not been enough to help normalise the BRDF effects. Due to atmospheric contamination and land cover surface anisotropy bidirectional reflectance effects, such composite NDVI values could have considerably different values than composite NDVI values normalised for BRDF effects or based on measurements at lower viewing and/or solar zenith angles (Holben 1986, Goward et al. 1991, Gutman 1991, Cihlar et al. 1994a, Burgess and Pairman 1997, Li et al. 1996).

In figure 4.6 it can be seen that for several observations over relatively low composite NDVI values, the composite NDVI values of MODIS exhibit a greater value range than the respective composite NDVI values of AVHRR. These outliers were believed to have been caused by NDVI measurements collected over sparsely vegetated areas at high solar zenith angles. The bidirectional effects due to high solar zenith angles are stronger over sparsely vegetated areas (Asrar, 1984; Kaufman et al., 2000) which have low NDVI values. In addition to that, high solar zenith angles increase the length of the atmospheric path (hence, the magnitude of the atmospheric contamination) which lowers the measured NDVI values (Cihlar et al., 1994a, 1994b). NDVI data collected by AVHRR are not atmospherically corrected and therefore it is less likely that the MVC methodology would select observation collected at high solar zenith angles; but even if such observations were selected the atmospheric contamination would reduce/counteract the magnitude of the bidirectional reflectance effects. On the other hand MODIS NDVI measurements are atmospherically corrected before being composited, as such the NDVI measurements are not reduced by atmospheric contamination, and the probability of the compositing methodology of MODIS to select NDVI observations at high solar zenith angles is not reduced. Furthermore, if such NDVI observations were collected over sparsely vegetated areas, then they are likely to be affected by bidirectional reflectance effects (which are not reduced by atmospheric contamination) and as such exhibit a wider range of NDVI values.

Overall, the proportion of outliers found was low and considering the high value of the correlation coefficient it was not believed that the outliers had to be removed from the regression. Besides the outliers, several observations were scattered at short distances around the regression line. This was expected because the two datasets' NDVI values were not expected to be perfectly correlated. Moreover, it was believed that some of these deviations from the regression line were caused by seasonal change in the relationship of two sensors' NDVI values. This is because due to the sensors' different spectral bands, NDVI measurements taken by the two sensors do not capture seasonal changes in vegetation spectral properties due to biophysical and biochemical changes equally.

The MODIS NDVI values were generally higher than the respective AVHRR ones, which was as expected according to the previous theoretical analysis in Chapter 2 (section 2.3.3) due to differences in the relative spectral response of the sensors' red and NIR bands, and also due to the fact that the NDVI values of MODIS were not as depressed by atmospheric contamination as the respective AVHRR NDVI values. The empirical regression was found to be significantly different to the simulated regression and the one-to-one relationship.

The simulated and empirical regressions were different, due to the fact that the assumptions made in the simulation were violated. The main reasons for the difference between the simulated and empirical regressions were believed to be: i) the fact that the NDVI values of MODIS were calculated from atmospherically corrected data unlike the respective values of AVHRR, and ii) that NDVI measurements of the two sensors were likely to have been unequally affected by different sun-target-sensor geometry and/or cloud contamination.

The measurements of HyMap used for the simulation of the sensors' NDVI values, were taken at an altitude of a few kilometres, therefore as far as atmospheric contamination was concerned they were mainly affected by aerosols and Rayleigh scattering. Aerosols and Rayleigh scattering increase the values of the measured reflectance in the red spectral region and hence cause an underestimation of NDVI values. Therefore the simulated NDVI values for MODIS and AVHRR were underestimated. In the empirical regression however, the MODIS NDVI data were atmospherically corrected unlike the respective AVHRR data. Therefore, the MODIS

NDVI values would have higher values than the ones predicted by the simulated regression.

Moreover, AVHRR and MODIS NDVI data used in the empirical regression were collected from much higher altitudes than the data collected by HyMap; as such these data were also affected by other atmospheric contaminants higher in the atmospheric column, mainly water vapour and ozone. Water vapour causes absorption in the NIR spectral region, and consequently causes NDVI values to be underestimated. Studies have shown that the reflectance values of AVHRR NIR spectral band can be reduced by 10-30% due to water absorption alone (Luo and Trishchenko, 2005; Tanre et al., 1992). Ozone on the other hand causes absorption in the red spectral region and thus increases the values of calculated NDVI. Between the two, the effect of water vapour is stronger and overall NDVI values are underestimated when calculated from data not atmospherically corrected. HyMap data were only mildly affected by water vapour or ozone due to the relatively low altitude of the sensor, and therefore the simulated NDVI values of AVHRR and MODIS NDVI were not underestimated. In the empirical regression however AVHRR NDVI data were affected and consequently underestimated unlike the respective NDVI values of MODIS which were based on atmospherically corrected data where the effects of water vapour and ozone had been removed. Hence, again the MODIS NDVI values used in the empirical regression would be higher than the values predicted by the simulated regression in relation to the AVHRR NDVI values.

Additionally, the data used in the simulated regression were simulated from measurements taken by HyMap; therefore, the simulated NDVI values of each sensor were based on measurements taken under the same sun-target-sensor geometry and were equally affected by cloud contamination, unlike the NDVI data used in the empirical regression. Consequently this could have caused considerable differences between the sensors' simulated and empirical composite NDVI relationships.

The empirical regression was also found to be significantly different to the one-to-one relationship. Therefore data from the NDVI composite dataset of AVHRR should not be used without previous processing/adjustment with data from the NDVI composite dataset of MODIS.

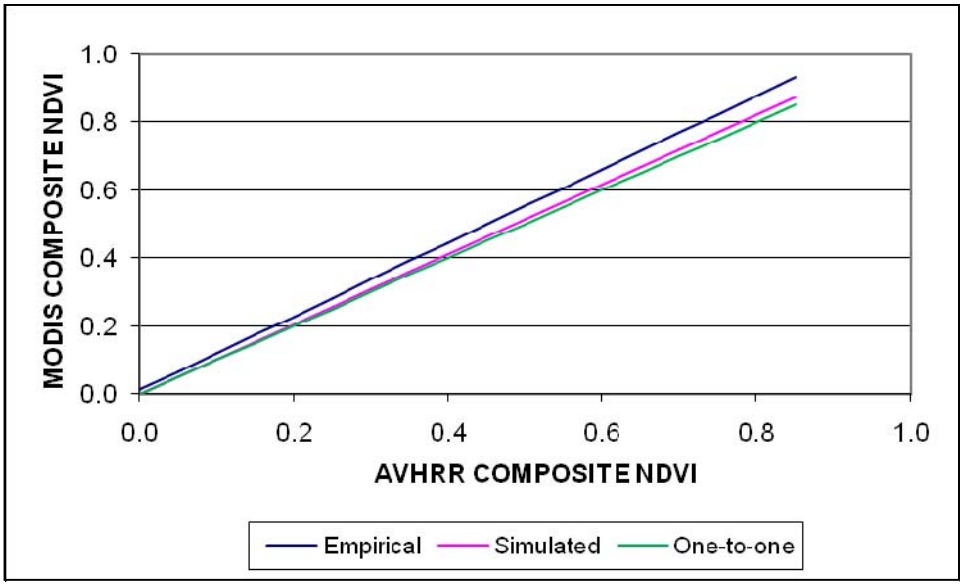

Figure 4.9: Empirical, simulated and one-to-one relationship between the NDVI values of MODIS and AVHRR

4.7.2 VEGETATION/AVHRR regression

The regression analysis between the NDVI values of the VEGETATION and AVHRR composite datasets, revealed that more than 96% of variance in the VEGETATION dataset could be explained by the AVHRR dataset. A few outliers in the MODIS/AVHRR empirical regression can be seen on the scatter plot (figure 4.7).

The main reason behind the majority of the outliers was believed to have been caused by the use of measurements taken over cloud contaminated areas. As already mentioned cloud detection is not always successful; this was expected to be particularly true for the case of VEGETATION mostly due to the sensor's lack of thermal bands (Latifovic et al., 2004). Hence, proportionally more NDVI data depressed by cloud contamination were expected to be found in the NDVI composite dataset of VEGETATION than in that of AVHRR. This was believed to be the reason why the majority of outliers were located under the regression line.

Similarly to the outliers found in the empirical regression between AVHRR and MODIS, some of the outliers in the empirical regression between AVHRR and VEGETATION could have been caused by poorly atmospherically corrected

VEGETATION data, or unusual atmospheric conditions which would affect mainly the NDVI values of the AVHRR dataset since unlike the dataset of VEGETATION, the NDVI values were not calculated using atmospherically corrected measurements.

Again similarly to the outliers found in the regression between AVHRR and MODIS, some outliers in the regression between AVHRR and VEGETATION were likely to have been caused by the use of NDVI data collected by the two sensors at considerably different sun-target-sensor geometry, which in turn could result in considerably different NDVI values due to surface anisotropy bidirectional reflectance effects.

Also due to the fact that the VEGETATION MVC methodology selected the NDVI observation before the NDVI were atmospherically corrected, the chance of selecting NDVI observations at high solar zenith angles was reduced (because atmospheric contamination would have reduced the NDVI values at high solar zenith angles); hence, outliers were not observed at the lower NDVI values of the regression between the AVHRR and VEGETATION MVC NDVI data (figure 4.7), as was the case between MODIS and AVHRR (figure 4.6).

The outliers found were only a very small proportion of the observations used in the regression, something that can also be seen by the very good fit of regression (R^2>0.96), and as such it was not thought that their removal from the regression was necessary.

The empirical and simulated regressions between the sensors' composite NDVI values were not significantly different at a 95% CI, despite the violation of the assumptions adopted in the simulated regression. A reason behind this result was believed to be the fact that VEGETATION data have been used to intercalibrate the NDVI composite dataset of AVHRR and also because the AVHRR dataset was processed in order to match the dynamic range of the VEGETATION NDVI dataset (Tucker et al., 2005).

However the difference between the empirical regression and one-to-one relationship was found to be significant, and NDVI data from the AVHRR dataset have to be adjusted (e.g. using the derived empirical regression) before they can be used with the NDVI data of the VEGETATION dataset. The one-to-one relationship and the simulated and empirical regression lines are displayed in figure 4.10.

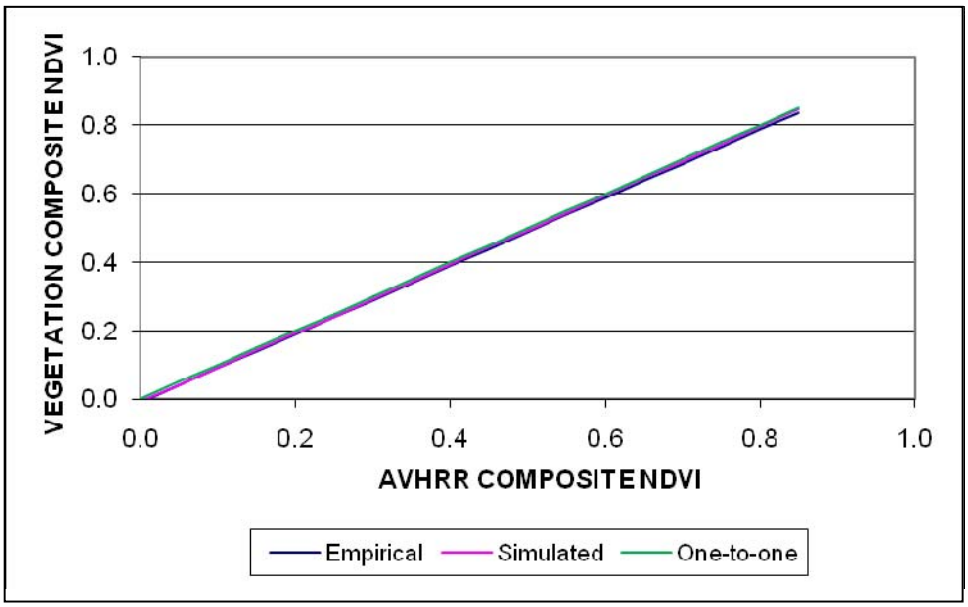

Figure 4.10: Empirical, simulated and one-to-one relationship between the NDVI values of VEGETATION and AVHRR

4.7.3 MODIS/VEGETATION regression

More than 95% of variation in the NDVI values extracted from the MODIS NDVI composite dataset could be explained by the NDVI values extracted from the VEGETATION NDVI composite dataset. The few outliers that could be seen in figure 4.8, similar to the other empirical regressions were believed to have been caused by the use of cloud contaminated data that were not successfully identified by the cloud detection criteria, variations in the quality of the atmospheric correction processes, and probably the use of NDVI data collected by each sensor at significantly different sun-target-sensor geometry.

The chance that the compositing methodology of MODIS would select NDVI observations at high solar zenith angles was higher than that for VEGETATION; because the NDVI observations of the former were not selected by its compositing methodology before being atmospherically corrected, unlike the latter (atmospheric contamination reduces the values of NDVI measurements). Therefore bidirectional reflectance effects caused by solar zenith angles over land cover surfaces with low NDVI values were more

pronounced in the MODIS composite NDVI dataset than that of VEGETATION. This can be seen in figure 4.8 where for VEGETATION composite NDVI values of about 0.05, the respective MODIS composite NDVI values range from about 0.05 to 0.2.

Considering that the proportion of outliers was relatively low, they were not removed from the regression, following the same approach adopted in the previous empirical regressions.

The empirical regression between the two sensors' composite NDVI values was not found to be significantly different than the simulated regression between the two sensors' simulated NDVI values. The main factors that were believed likely to cause significant differences between the empirical and simulated regressions of two sensors' composite NDVI values were mainly possible differences in sun-target-sensor geometry during the measurements of the two sensors, and possible differences between the success of the sensors' process at masking cloud contaminated data and removing atmospheric contribution. Regardless, the effect of these factors did not result in an empirical regression between the sensors' composite NDVI data, significantly different (with a 95% CI) to the simulated regression of the sensors' NDVI values.

The empirical regression however was found to be significantly different from the one-to-one relationship of the two sensor's NDVI composite datasets. Consequently before using NDVI composite data from both sensors' datasets, one of the sensor's dataset NDVI values would have to be adjusted to fit the NDVI values of the other sensor's dataset. The one-to-one relationship and the simulated and empirical regression lines are displayed in figure 4.11.

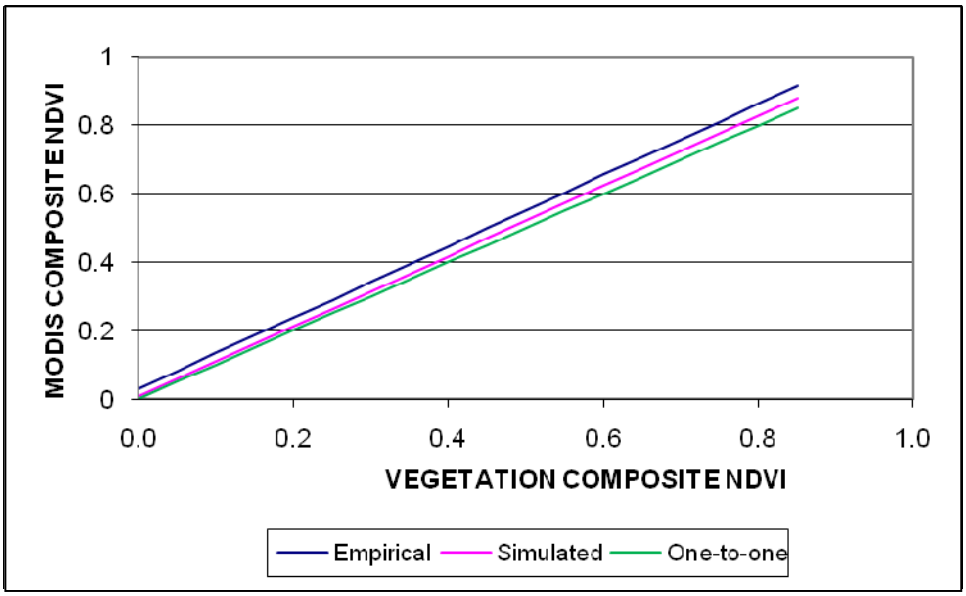

Figure 4.11: Empirical, simulated and one-to-one relationship between the NDVI values of MODIS and VEGETATION

4.8 Conclusions

The empirical regressions developed between the composite NDVI values of the three sensors' datasets over seven homogeneous sites in Africa were found to be significant, and significantly different to one-to-one relationships. This result demonstrates the fact that the composite NDVI values of the three sensors for observations over the same targets and compositing period are not equal with each other, and as such they can not be used in conjunction with each other in applications requiring such data, unless they are previously adjusted. In addition to that the developed empirical regressions showed that more than 95% of variance in the NDVI dataset of one sensor could be explained by the NDVI dataset of another sensor. Thus it was considered possible that empirical regressions such as the ones developed in this part of the study, could be used to predict with fairly good accuracy the composite NDVI value of one sensor based on the composite NDVI value of another sensor over the same site and date.

Therefore, it was also considered possible that through the use of empirical regressions the historical composite NDVI datasets of MODIS and VEGETATION could potentially be extended to the past when the sensors were not yet operational, based on the historical composite NDVI dataset of AVHRR. In turn that could enable the use of MODIS and VEGETATION in applications that require historical composite NDVI records longer than those they currently have; provided that the simulation accuracy meets the requirements of the application. For instance applications such as fire risk assessment (Dwyer et al., 2000; Gabban et al., 2006; Illera et al., 1996; Maselli et al., 2003; San-Miguel-Ayanz, 2002 ; Stroppiana et al., 2000), desertification monitoring (Hobbs, 1995 ; Tripathy et al., 1996; Weiss et al., 2001) or yield assessment (Domenikiotis et al., 2004). Moreover it was also considered possible that through the use of empirical regressions the composite NDVI datasets of the three sensors could become interchangeable, and in the event that data from one or even two sensors became unavailable, applications that require continuous up-to-date composite NDVI data such as disaster monitoring applications, could continue to operate uninterrupted using composite NDVI data collected by the remaining sensor(s).

Nevertheless, although the empirical regressions developed in this part of the study could be used to simulate composite NDVI data for any of the three sensors over the seven selected sites over Africa with fairly good accuracy, it was not certain that the same regression equations could be used to simulate composite NDVI data for the three sensors with equal accuracy over different sites; especially considering that the seven selected sites over Africa were homogeneous and differences between the sensors' composite NDVI values caused by the their different spatial resolution and image registration accuracies were minimised. In addition to that, the simulation accuracy requirements may vary between applications, and those achieved using the empirical regressions may be sufficient for some applications but not for some others.

In order to test these possibilities it was decided in the next part of the study to develop empirical regressions between the sensors' composite NDVI values over a series of different sites in Africa and compare the newly derived empirical regressions with the regression equations derived in this part of the study. In the event that the two sets of empirical regressions were not found significantly different then that would provide

evidence to support the more general use of the empirical regression equations developed here. Moreover in the next part of the study the simulation accuracy requirements of the VPI methodology over a series of sites were to be assessed in order to test whether the simulation could meet the accuracy requirements.

4.9 Future work

As time passes more and more data are becoming available from all three sensors over the same areas and time; consequently these data could be used in the development of further empirical regressions between the sensors' NDVI composite values, which due to the greater amount of data used for their development are likely to be more accurate.

The results of this study were based on data collected over seven study sites. It is recommended that in the future, these results are more thoroughly validated by using data extracted from more sites. Future studies could also be directed towards researching the relationship between the three sensors' composite NDVI data measured over specific land-cover classes. It is possible that specialised regressions developed using NDVI data measured over specific land-cover classes, could describe the relationship between the sensors' composite NDVI data measured over a certain land-cover class more accurately than generic regressions (developed using NDVI data collected over a variety of targets). Similarly, future research on the relationship of the sensors' composite NDVI data measured during specific seasons could help develop specialised regressions that potentially describe that relationship more accurately during these seasons than generic regressions (developed using NDVI data measured during throughout the year). Even more specialised regressions could be developed by researching the relationship between the sensors' composite NDVI data measured over specific land-cover classes and seasons, which may be able to describe that relationship even more accurately.

CHAPTER FIVE

5 Drought monitoring

5.1 Background

In Chapter 2 it was hypothesised that out of MODIS VEGETATION and AVHRR, drought conditions would be most accurately represented when using NDVI data collected by MODIS and least by AVHRR. In this Chapter this hypothesis is tested with experimental results.

5.2 Introduction

The assessment of the three sensors' (AVHRR, MODIS and VEGETATION) characteristics in Chapter 2 revealed that they are not equally equipped at detecting stress-related changes in the spectral properties of vegetation (e.g. due to drought). It was hypothesised that NDVI data collected by MODIS would help detect drought conditions more accurately than NDVI data collected by VEGETATION or AVHRR using a methodology such as the VPI; and similarly VPI results based on VEGETATION NDVI data were expected to be more accurate than VPI results based on AVHRR data. However, this hypothesis was not supported by experimental data and the magnitude of difference between the three sensors' NDVI data capacity to detect drought conditions using a methodology such as the VPI was unknown.

In Chapter 4, the composite NDVI values of the three sensors were found to be highly correlated with each other based on assessments carried out using both simulated and experimental data. Consequently, since the VPI methodology depends on composite NDVI data, it was suspected that the three sensors would have similar VPI results over the same sites and dates. Nevertheless, despite the expected similarity of the sensors' VPI

results, it was possible that some sensors could help monitor drought conditions more accurately than others (using the VPI methodology).

However before the three sensors' relative capacity to accurately monitor drought conditions using the VPI methodology could be compared, there were some questions that had to be answered. In order to use the VPI methodology over a certain site and date of the year, it is required that the distribution of rainfall over that site and date through the years is determined based on sufficiently long historical NDVI records. At the time of the study MODIS and VEGETATION did not have such long historical NDVI records. Moreover, if the capacity of the three sensors in detecting drought conditions using the VPI methodology were to be compared objectively, the VPI results of each sensor would have to be based on the same duration of historical observations.

In Chapter 4, empirical regressions were developed for simulating composite NDVI values for MODIS and VEGETATION based on composite NDVI measurements collected by AVHRR over the same sites and time. However, these empirical regressions were developed over specific sites and it was not certain whether their use could help simulate composite NDVI data for MODIS and VEGETATION over different sites successfully. It was also not known how accurate the simulation of the composite NDVI values should be so that the VPI methodology would not produce misleading results.

In order to help find answers to these questions experimental data were needed. It was decided that empirical regressions had to be developed between composite NDVI data collected by AVHRR, MODIS and VEGETATION over a series of sites and dates (suitable for the VPI methodology) and then be compared to the respective empirical regressions developed in the previous part of the study. In the event that empirical regressions were not found to be significantly different to the respective empirical regressions developed in the previous part of the study, then that would support the validity of the latter, and as such they could be used to simulate the historical composite NDVI records of MODIS and VEGETATION. If on the other hand the empirical regressions developed in this part of the study were found to be significantly different to the respective empirical regressions developed in the Chapter 4, then that would indicate that it may be necessary to develop new empirical regressions over different sites, and the

empirical regressions developed in this part of the study would be used to provide MODIS and VEGETATION with historical composite NDVI data.

Consequently, the VPI methodology was to be applied over the selected sites and dates for each sensor, and the relationships between the VPI results and the composite NDVI values used to produce them were to be derived for each selected site and date. From these relationships between VPI results and composite NDVI values the sensitivity of the VPI results to composite NDVI value fluctuations were to be estimated. If the sensitivity of the VPI results to composite NDVI value fluctuations was found to be higher than the accuracy the historical composite NDVI data could be simulated for MODIS and/or VEGETATION over a certain site and date, then VPI results based on such simulated historical composite NDVI data would not be reliable.

If the simulation of the historical composite NDVI records of MODIS and VEGETATION was found to be sufficiently accurate for the needs of the VPI methodology over a considerable number of sites and dates, then the sensors' VPI results over these sites and dates could be used for determining which sensor is more likely to produce the most accurate drought monitoring results using the VPI methodology. The relative capacity of the sensors to accurately monitor drought conditions using the VPI methodology was to be assessed by comparing the VPI results of the three sensors over the same sites and dates against VPI results calculated from rainfall data collected over the same sites and dates.

The sites used in the analysis had to be selected from vegetated regions susceptible to drought conditions; because the VPI methodology is not be applicable over regions where vegetation is not dependant on rainfall, and consequently would not show signs of stress during drought periods. For the purpose of this part of the study it was decided to select sites from the region of Ethiopia. Vegetation in Ethiopia is primarily rain-fed including crops. Approximately 10% of the total area of the country is cultivated and only about 2% of this cultivated area is irrigated (AQUASTAT, 2005; CIA, 2006) using almost entirely surface water. Hence, crops in Ethiopia are particularly dependant on rainfall and very susceptible to drought conditions. This combined with the facts that i) 80% of Ethiopia's population is employed in the agricultural sector and ii) Ethiopia is the third most populous country in Africa, mean that the impact of drought can be particularly

damaging in this country. The susceptibility of Ethiopia to drought conditions is evident in the country's history; most notably the drought-related famines in 1974 and 1984 when approximately 200,000 and more than a million people were believed to have perished, respectively.

5.3 Study area

Ethiopia is located in the horn of Africa (longitudes: 32˚59'26"E-47˚59'17"E, latitudes: 14˚48'24"N-3˚24'24"N), extending 1,127,127 km^2, and bordering Somalia and Djibouti to the east, Kenya to the south, Eritrea to the north, and Sudan to the west (figure 5.1).

The country is dominated by a complex of high mountains and plateaus. The central plateau of the country, also known as the Ethiopian Plateau, has an average elevation of about 1680 m and is divided by the Great Rift Valley running from southwest to northeast. The Great Rift Valley is surrounded by steppe, lowlands and semi-deserts and numerous lakes can be found within it. The northern part of the Great Rift Valley, also known as the Denakil Depression, drops to about 125 m below sea level and is the lowest and hottest part of the country. The highest peak of the country is Ras Dashen which rises to about 4620 m and is located at the midst of the Simen mountain range in the north of the country.

There are three climatic zones in the country, determined by elevation. Areas below 1830 m are within the tropical zone also known as "Kolla". In this zone the average annual temperature and rainfall is about 27˚ C and 510 mm respectively. Areas with elevation between 1,830 m and 2,440 m are within the subtropical zone also known as "Woina dega". In the subtropical zone the average annual temperature is about 22˚ C and the annual rainfall ranges between 510 and 1530 mm. Finally, areas above 2440 m are within the cool zone known as "Dega". In the cool zone, the average annual temperature is about 16˚C and the annual rainfall ranges between 1270 and 1280 mm (Teklehaimanot, 2007). Normally the rainy season lasts from mid June to mid September, the rest of the year is dry, with the exception of occasional showers around February and March.

Figure 5.1: Map of Ethiopia (source: CIA the World Factbook)

According to an FAO report (1996) the vegetation distribution of the country is as follows. Areas below 500 m are sparsely vegetated and dominated by desert and semi-desert scrubland. Areas between 500 and 1,900 m are mainly covered with Acacia – Commiphora woodland species, particularly in the north, southeast and central parts of the country. Areas east of the Great Rift Valley at elevations between 1,500 and 2,600 m are covered with humid mixed forest. Humid broad-leaved forest is found mainly in south-western parts of the country at elevations between 1,500 and 2,500 m. Evergreen forest occurs in the western part of Ethiopia at altitudes between 450 and 600 m. Broad-leaved deciduous woodland occurs at altitudes between 500 and 1,900 m in the north-western, western and south-western parts of the country. Dry evergreen montane forest and grassland occurs in the northern part of the country at altitudes between 2,100 and 3,200 m, in the central and western parts of the country at altitudes between 1,900 and 3,200 m, and in the southern and south-eastern parts of the country at altitudes between 1,500 and 2,200 m. Evergreen shrub-land can be found in the lower parts of the dry evergreen montane forest and grassland. Areas above 3,200 m are covered with

Afroalpine and sub-Afroalpine vegetation. Finally along the banks of perennial rivers and the shorelines of some lakes, riparian and swamp vegetation occurs.

5.4 Data

5.4.1 Test sites and rainfall data

The selection of sites over Ethiopia for the purpose of this part of the study was based on two criteria:

1. The sites had to be equally spread across the extent of the study are so that the sensors' composite NDVI values and VPI results would be assessed across a representative range of the environmental conditions of the study area.
2. Historical rainfall data needed to be available for each site, spanning at least over the same time period as the NDVI data used in the VPI methodology.

Rainfall data have been collected by the Ethiopian National Meteorological Agency (NMA) for several decades over hundreds of stations across the country. Information was provided for 767 stations on the website of NMA (http://www.ethiomet.gov.et/index.php?Page_No=2&item=5 (06 August 2006)); specifically, the name/code, location coordinates, and operational time period were given for each station. The information given for each station was reviewed, and 84 candidate stations which were operational within the period 1981-2003/2004 (it was possible that the website had not been updated recently, but no station appeared to have rainfall data beyond 2004) were identified; the names, coordinates and operational time-period of each of the 84 identified stations are provided in the Appendix C.

Table 5.1: Name, code name, and coordinates of each of the selected rainfall stations

ID	Name	Code	Longitude (in dd)	Latitude (in dd)
1	Agarfa	BAAGAR14	39.82	7.283
2	Bolo Giorgis	SHBOLO14	39.43	8.82
3	Delo Sebro	BADELO14	40.47	7.25
4	Derba	SHDERB14	38.64	9.43
5	Didu Gordomo	ILDIDU14	35.52	8.4
6	Ginchi	SHGINC14	38.12	9.03
7	Guranda Meta	SHGURA14	38.77	8.98
8	Kone	WEKONE14	36.78	8.68
9	Kora	HAKORA14	40.53	9.12
10	Meteso	KFMETE14	36.88	7.43
11	Teji	SHTEJI14	38.37	8.8
12	Toke Erenso	SHTOKE14	37.62	8.97
13	Yambero	ILYAMB14	36.45	8.27
14	Zequala	SHZEQU14	38.87	8.53
15	Chena	KFCHEN14	35.85	7.17
16	Durame	SHDURA14	37.95	7.2
17	Gibe Farm	SHGIBE14	37.58	8.23
18	Koshe	SHKOSH14	38.53	8.02
19	Enselale	SHENSE14	38.42	8.93
20	Kutaber	WOKUTA14	39.53	11.27

It was not financially feasible to acquire the rainfall data from all 84 stations; hence, it was decided to select 20 stations out of the 84. The selection was based on the location of the stations. The 20 stations which provided the most even distribution across Ethiopia out of the 84 available stations were selected. However, when the NMA was contacted it was discovered that the operation of some of the selected rainfall stations was not always continuous and rainfall data were missing for some years. Consequently, some of the originally selected stations which had significant data gaps had to be replaced. As a result the choice of stations was narrowed and the stations which were finally selected were not as evenly distributed across Ethiopia as would have been preferred (figure 5.2). The name and coordinates of each of the selected stations are displayed in table 5.1. Once purchased from the NMA, the rainfall data for each station was received in the form of a spreadsheet detailing the cumulative rainfall measured by the rainfall station for each 10 day period between 1981 and 2002.

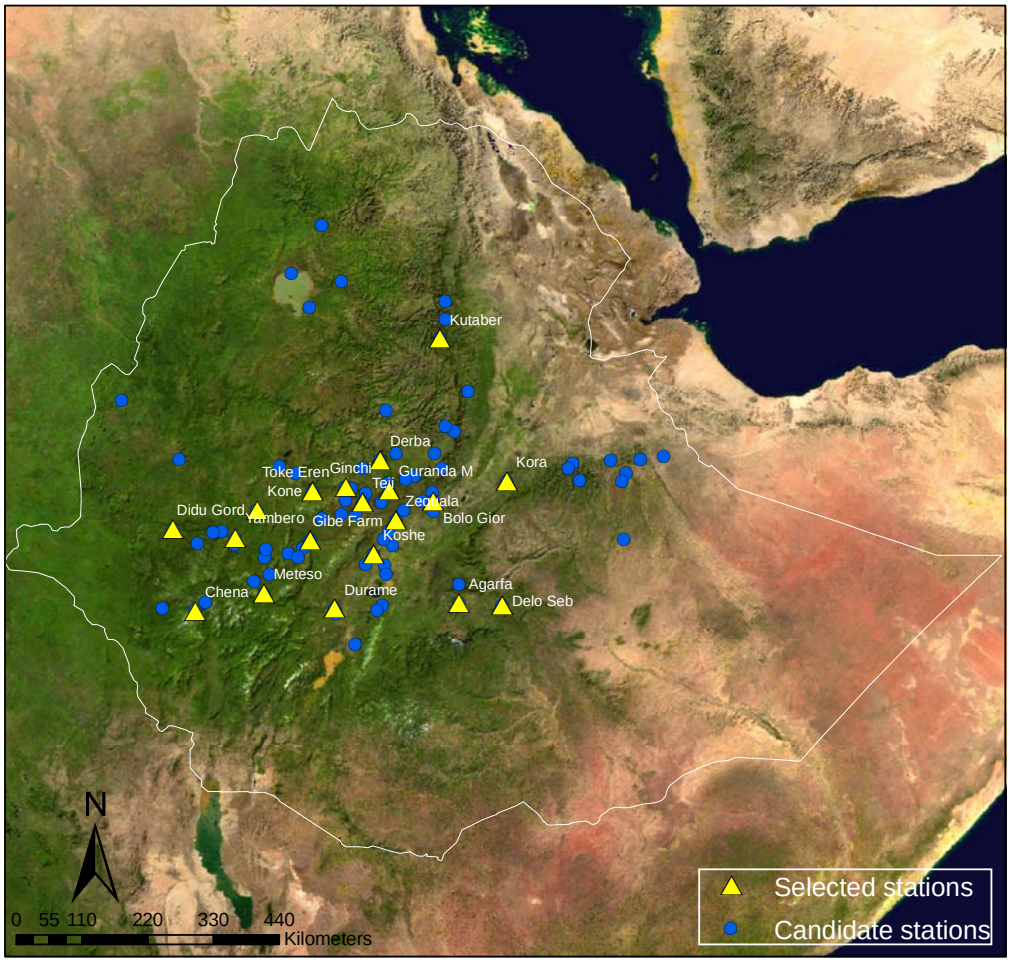

Figure 5.2: Candidate and selected rainfall stations in Ethiopia, displayed over an image composite of MODIS

5.4.2 Sensor data

Due to constraints in rainfall data availability beyond 2003 for the majority of rainfall stations and the fact that at the time of this part of the study SPOT had announced that data collected by VEGETATION-2 after 2003 were being recalibrated by VITO (VEGETATION, 2006) because it was discovered that the on-board calibration system of VEGETATION-2 was not performing as expected, it was decided to limit the VPI assessment up to the end of 2002.

The sensors' composite NDVI datasets needed for this part of the study were practically the same as those used in Chapter 4. Hence, the GIMMS MVC NDVI dataset

was used for AVHRR, the MOD13A2 products were used for MODIS, and the S-10 products were used for VEGETATION. The descriptions of these datasets have already been provided in the Chapter 4.

The two main differences between the composite NDVI datasets used in this part of the study and the previously used datasets were that: i) in this part of the study AVHRR MVC NDVI data were needed to be acquired and processed since 1981 instead of 1998 and ii) the extent of the MOD13A2 products used in the data simulation did not cover the location of the rainfall stations, hence other MOD13A2 products whose extent did cover the locations of the 20 selected rainfall stations within the 2000-2002 time period, had to be acquired and processed.

5.4.3 GLC2000

Drought conditions are detected with the VPI methodology by assessing the health status of vegetation by means of comparing the NDVI value measured over a vegetated area to previously measured NDVI values over the same area and time period over the years of available historical data. Therefore, the VPI methodology provides meaningful results only over vegetated areas. Moreover as previously mentioned the VPI methodology can successfully identify drought conditions over vegetated areas that are dependant on rainfall for water.

It was decided to use the GLC2000 map of Africa (Mayaux et al., 2003) in order to identify and remove from further analysis any possible test sites located over non-vegetated or irrigated areas. The GLC2000 map of Africa was chosen because it was the most recent map of Africa at the time of the study which was freely available and at a spatial resolution comparable to that of the three sensors (1km). The GLC2000 map of Africa was produced using a DEM and imagery collected by VEGETATION, the Synthetic Aperture Radar (SAR) onboard the European Remote Sensing satellites one and two (ERS-1 and ERS-2) and the Japanese Earth Resources Satellite one (JERS-1), and the Defence Meteorological Satellite Program (DMSP) Operational Linescan System (OLS). For further details regarding the production of the dataset the reader is referred to Mayaux et al., 2003.

The map covered the whole of Africa, was georeferenced using a geographic projection and the WGS84 spheroid and had a spatial resolution of about 1 km at the Equator (0.00892857 dd). The CLG2000 map of Africa could be downloaded from the JRC's GLC2000 product webpage in either ESRI TIFF or binary format (http://www-gvm.jrc.it/glc2000/Products/fullproduct.asp (02 September 2006)).

5.5 Methodology

5.5.1 Acquisition of sensor NDVI data

AVHRR 10-day MVC NDVI data for the whole of Africa for the period between April 1998 and December 2002, were already acquired and processed in the previous part of this study. In this part of the study however, the whole historical MVC NDVI record of AVHRR until December 2002 was needed; hence the remainder of the historical record dating from July 1981 to April 1998 had to be acquired and consequently processed. The data were downloaded from the FEWS NET ADDS website (http://earlywarning.cr.usgs.gov/adds/datatheme.php (20 May 2005)) in BIL format; in total 603 files were downloaded.

The MODIS MOD13A2 products that were used in the data simulation part of this study (Chapter 4) could not be used in this part of the study, because the extent of these products did not cover the 20 selected rainfall stations in Ethiopia. The search engine of the EOS Data Gateway website (http://edcimswww.cr.usgs.gov/pub/imswelcome/ (06 October 2006) was used to identify the MOD13A2 products whose extent covered the location of all 20 rainfall stations; for each 16-day composite period the extent of all 20 stations was covered by four MOD13A2 products. Consequently, for the time period between 16/02/2000 and 31/12/2002, 288 files were needed. The files were downloaded in EOS-HDF format from the EOS Data Gateway website.

The operational composite NDVI data of VEGETATION collected over Africa from the start of the sensor's operation in April 1998 until December 2002 were already acquired and processed in the data simulation part (Chapter 4) of the present study.

5.5.2 Image processing

The operational composite NDVI data of VEGETATION that were processed in Chapter 4 covered the whole of Africa, including the 20 selected test sites in Ethiopia. Hence for the purpose of this part of the study the only image processing step that remained before extracting the composite NDVI data over the 20 test sites was to mask out any non-vegetated and irrigated areas. This was done by importing the GLC2000 map of Africa to ERDAS IMAGINE and then using the Mask function to mask out any areas in the composite NDVI dataset of VEGETATION which spatially coincided (the GLC2000 map and the VEGETATION composite NDVI dataset shared the same projection system) with the non-vegetated and irrigated land cover classes of GLC2000 (classes 20 and 22 to 27; the classification scheme of GLC2000 of Africa is given in the Appendix C).

The image processing required for the AVHRR and MODIS composite NDVI data was identical to the one followed in Chapter 4, the reader is referred to section 4.5.2 for more details. In regard to the image quality assurance stage of AVHRR's image processing, seven AVHRR MVC NDVI images were identified as distorted within the time period 01/06/1981 – 31/12/2002, and had to be removed; the dates of these composite images are given in table 5.2. Subsequently, similarly to the VEGETATION composite NDVI dataset, the GLC2000 map was used to mask out any areas from the composite NDVI images of AVHRR and MODIS which were non-vegetated or irrigated.

Finally the "pixel to ASCII…" function of ERDAS IMAGINE was used to extract the composite NDVI values over the 20 test sites from each composite NDVI dataset and every 10-day period when data were available. It should be stated out that at this point of the image processing it was discovered that the test site at Guranda Meta (id: 7) was located in an area classified as non-vegetated by the GLC2000 map and hence data from that site were removed from further analysis.

Table 5.2: MVC NDVI data from AVHRR with significant geometric or radiometric distortion

Year	Month	Dekad
1983	June	2nd
1987	January	1st
1990	July	1st
1990	December	3rd
1991	April	3rd
1991	June	2nd
1996	May	1st

5.5.3 Interpolation of MODIS' 16-day composite NDVI data to 10-day composite interval

As explained in Chapter 4 the MOD13A2 product was based on a 16 day composite period as opposed to the 10 day period used by AVHRR and VEGETATION. Hence for compatibility reasons, the 16-day composite NDVI values of MODIS were interpolated to 10-day composite intervals. The same process was previously performed in the Chapter 4 of this study; the reader is referred to section 4.5.3 for more details.

5.5.4 Selection of dekads to be used for the calculation of VPI over each of the selected sites

In earlier studies in Zambia (Sannier et al., 1998a) and Ethiopia (Tamene, 1996), VPI results based on MVC NDVI data collected by AVHRR over 30 and 14 rainfall stations respectively, were found to be highly correlated with VPI results based on rainfall data collected at the respective stations. In these studies the VPI results based on the AVHRR MVC NDVI data were calculated over the dekads when vegetation growth was expected to be at its peak (Sannier et al., 1998a; Tamene, 1996). Considering the success of the two studies, it was also decided to calculate and consequently compare the VPI of each sensor over each selected site for the dekad when vegetation growth was expected to be at its peak. In order to identify these dekads the average yearly NDVI value of each

dekad and test site was calculated from the extracted composite data of AVHRR and a yearly average temporal NDVI profile of each test site was plotted (figure 5.3).

It can be seen in figure 5.3 that the yearly average NDVI temporal profile of eight test sites (Delo Sebro, Ginchi, Kora, Meteso, Yambero, Chena, Durame and Kutaber) had two peaks (labelled A and B from here on); this is because these sites have two growing seasons which are the result of two rainy seasons. Hence, for sites with dual rainy seasons two dates were selected, one for each NDVI peak (table 5.3).

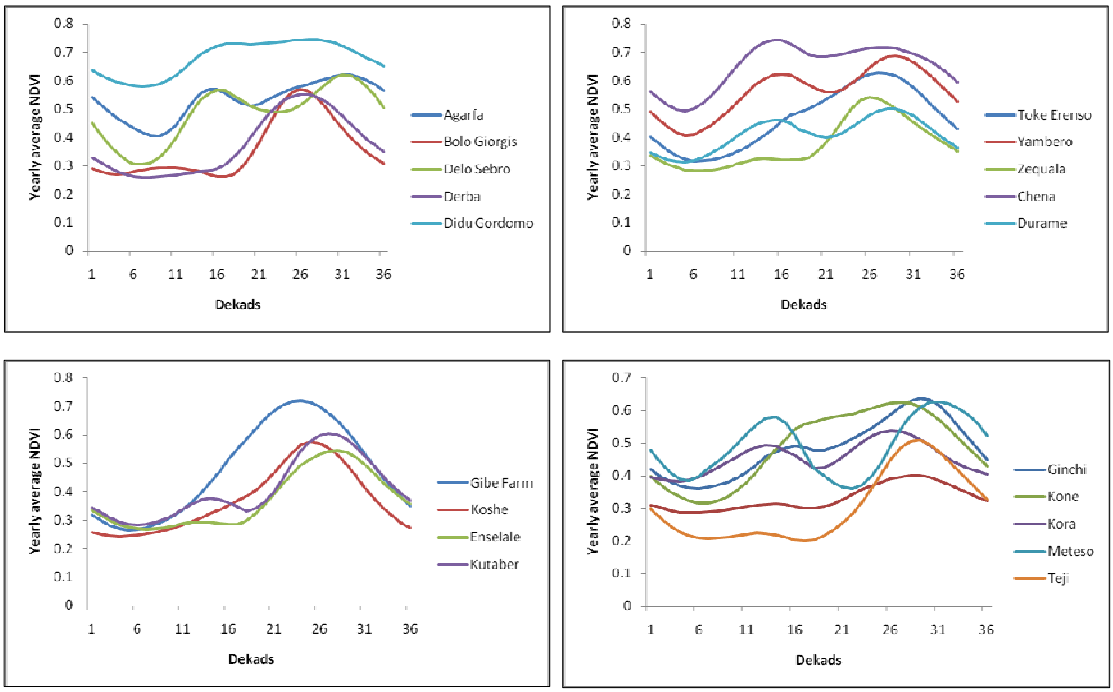

Figure 5.3: Temporal yearly average AVHRR MVC NDVI profiles of the 19 selected test sites (using a 10-day step)

Table 5.3: Selected NDVI peak dekads for the 19 test sites

Site	NDVI peak dekad A	NDVI peak dekad B
Agarfa	15	31
Bolo Giorgis	26	N/A
Chena	15	28
Delo Sebro	16	31
Derba	26	N/A
Didu Gordomo	16	N/A
Durame	15	29
Enselale	28	N/A
Gibe Farm	24	N/A
Ginchi	16	29
Kone	27	N/A
Kora	13	26
Koshe	25	N/A
Kutaber	14	27
Meteso	14	30
Teji	29	N/A
Toke Erenso	27	N/A
Yambero	16	29
Zequala	26	N/A

5.5.4 Simulation of the historical composite NDVI records of MODIS and VEGETATION

Regression analysis was performed between all valid composite NDVI values of the three sensors, collected over the selected sites and dekads of Ethiopia within the period of the first dekad of March, 2000 until the last dekad of December, 2002 (the period when operational composite NDVI data were available for all three sensors). The resulting empirical regressions (Ethiopian regressions) between the composite NDVI values of MODIS and AVHRR, and VEGETATION and AVHRR were then compared against the respective regression equations derived in Chapter 4 (table 4.10) (continental regressions). In the event that the Ethiopian regressions were significantly different (95% CI) to the continental regressions, then the historical composite NDVI records of MODIS and VEGETATION were to be simulated using the Ethiopian regressions; otherwise, MODIS and VEGETATION historical composite NDVI records were to be simulated using the continental regressions. The significance difference test was performed according to the process already described in section 4.5.5.

The historical composite NDVI records of MODIS and VEGETATION over the selected sites and dekads of Ethiopia were simulated based on composite NDVI data collected by AVHRR over the same sites and dekads. Composite NDVI data were simulated for each sensor and selected site for the time period between the first dekad of July, 1981 (the first dekad of available AVHRR composite NDVI data) and the dekad when each sensor became operational (the first dekad of March, 2000 and the first dekad of April, 1998 for MODIS and VEGETATION respectively).

5.5.5 VPI calculation

The VPI expresses a probability (p) of having a composite NDVI value over a specific site and dekad which is lower or equal to the measured one. It is calculated based on Weibull's (1939) formula (5.1); all valid composite NDVI values (n) recorded over the specific site and dekad are ranked in ascending order, then the rank (m) of the composite NDVI value, measured over the dekad the VPI is calculated for, is divided by the total number (n) of valid composite NDVI values plus one.

$$VPI = p = \frac{m}{n+1} \quad \text{(Weibull, 1939)} \qquad (5.1)$$

A high VPI values suggests that the measured composite NDVI value over a certain site and dekad is comparably higher to most of the previously recorded composite NDVI values over the same site and dekad. Consequently, vegetation health over the specific site and dekad is above the historical average, suggesting favourable conditions and hence no drought signs. Vice versa, low VPI values suggest vegetation stress probably caused by drought, while VPI values about 0.5 suggest normal conditions. Sannier et al. (1998) classified the calculated VPI values into five classes according to table 5.4; nevertheless, it was decided not to further classify the calculated VPI values but leave them in their original values, so that possible differences between the three sensors' VPI values over the same sites and dekads were not masked.

Table 5.4: VPI classes defined by Sannier et al. (1998)

VPI Class	Probability range
Very low	$p \leq 0.2$
Low	$0.2 < p \leq 0.4$
Average	$0.4 < p \leq 0.6$
High	$0.6 < p \leq 0.8$
Very high	$p > 0.8$

The VPI values were calculated for each sensor over the selected sites and dekads of Ethiopia. Moreover, in order to reduce possible differences between the VPI results of the three sensors over the same sites and dekads, caused not by the sensors' technical characteristics but by the use of different historical composite NDVI records, it was decided to remove any composite NDVI value from the historical composite NDVI records of all sensors for which a valid composite NDVI measurement did not exist in all sensors' historical records.

5.5.6 Comparison between the achieved and required historical composite NDVI simulation

In order to determine whether the historical composite NDVI records of MODIS and VEGETATION were simulated sufficiently accurately for the needs of the VPI methodology over the selected sites and dekads of Ethiopia, two steps had to be taken:

1. The prediction accuracies of the regressions used for the simulations of the historical composite NDVI data had to be estimated.
2. The sensitivity of the VPI results to fluctuations of the composite NDVI values had to be estimated for each sensor and selected site and dekad.

The prediction accuracy (or estimation error) of the regressions for a 95% CI were calculated using the following equation:

Prediction accuracy of the regression = ±T(n, p<0.05)(Regression SE) (5.2)

T(n-2, p<0.05)= Value of the t distribution for n-2 degrees of freedom at 5% risk

n= Number of observations

Regression SE= Standard error of the regressions/standard error of the estimate

The sensitivity of each of the sensors' VPI results to fluctuations of the composite NDVI values over the selected sites and dekads of Ethiopia was estimated by plotting all available valid composite NDVI values collected over each site and dekad against the respective VPI values which were calculated from them. A third order polynomial was then fitted to the scatter plot using the least squares method. That polynomial was then used to calculate the NDVI values that would result in different VPI classes (VPI values of 0.2, 0.4, 0.6 and 0.8, according to table 5.4). The sensitivity of each of the sensors' VPI results to fluctuations of the composite NDVI values over the selected sites and dekads of Ethiopia was then estimated by calculating the difference between the calculated NDVI values that would result in different VPI classes.

Consequently, the prediction accuracies (or prediction error) of the regressions between composite NDVI values of MODIS and AVHRR , and VEGETATION and AVHRR over the selected sites and dekads were compared to the estimated VPI sensitivity of each sensor over each selected site and dekad. The sites and dekads for which the VPI sensitivity of MODIS and/or VEGETATION was found to be greater than the prediction error of their simulated composite NDVI data, had to be removed from the analysis. This is because, over these sites and dekads the historical composite NDVI values of MODIS and VEGETATION could have been simulated with prediction errors significant enough to result in VPI values that could range over one VPI class away from the VPI class that would have been predicted if the simulation was perfectly accurate. Consequently, the VPI results of MODIS and VEGETATION over such sites and dekads were not considered reliable.

5.5.7 Relative comparison of the three sensors' capacity to accurately monitor drought conditions over the selected sites and dekads

If a sufficient number of selected sites and dekads were not removed after the comparison of MODIS and VEGETATION simulated composite NDVI data accuracy to the VPI sensitivity of each site and dekad, then the sensors' relative capacity to accurately monitor drought conditions using the VPI methodology was to be assessed by comparing the sensors' VPI results over the remaining sites and dekads against VPI results calculated based on rainfall measurements collected over these sites.

Due to the fact that the majority of the historical composite NDVI data of MODIS and VEGETATION used in the VPI methodology were simulated based on MVC NDVI data from AVHRR, it was expected that differences between the VPI results of the sensors would be less pronounced than they would have been if only operational composite NDVI data collected from each sensor were available and used. However, possible differences between the VPI results of the three sensors were likely to be more obvious over the dates when operational composite NDVI data collected by each sensor were available; hence, it was decided to limit the comparison of the three sensors' VPI results within the dates when operational composite NDVI data were available for all three sensors.

The sensors' VPI results over each selected site and dekad were to be compared against the rainfall-based VPI results over the respective sites and dekads. The rainfall-based VPI results were be to calculated using the same methodology as the NDVI-based VPI; only instead of composite NDVI measurements, cumulative rainfall were to be used. For each test site and year, rainfall data were to be cumulated starting from the dekad for which the yearly average temporal NDVI profile starts to rise (indicating the start of the rainy season) up to two dekads before NDVI profile reaches its peak (two cumulative periods were to be used in sites where two rainy seasons/NDVI peaks were observed). NDVI-based VPI results describe drought conditions as they were several days before the measurement of the composite NDVI value used for the calculation of the NDVI-based VPI; because the vegetation's response to rainfall is not immediate but can be delayed by several days depending on factors such as soil, vegetation type and other environmental conditions (e.g. temperature). Due to lack of additional information the exact length of

the NDVI response lag to rainfall for each test site and rainy season could not be determined; instead, it was decided to use a default lag period of two dekads. The dekads for which rainfall data were cumulated for each site are displayed in table 5.5. Additionally, cumulative rainfall data which were available over sites and dekads when composite NDVI data in the next two dekads were not available were to be removed from the analysis, and vice versa. This was done so that the calculation of both rainfall-based and NDVI-based VPI results was based on the same observations.

The Spearman rank correlation was to be used to determine which sensor's VPI results were more closely correlated to the rainfall-based VPI results. Sannier et al. (1998) validated the NDVI-based VPI results of AVHRR over 30 rainfall stations in Zambia against VPI results calculated from cumulative rainfall data. A Spearman rank correlation was performed between the respective NDVI-based and rainfall-based VPI results of each site. In the present study this approach could not be implemented as there were only a few NDVI-based VPI measurements per selected site and dekad over the 2000-2002 time period. Instead, all available NDVI-based VPI results of each sensor over the selected sites and dates during the 2000-2002 period were to be correlated (Spearman rank) against the respective rainfall-based VPI results.

However, in the event that the majority of selected sites and dekads had to be removed from the analysis, then based on the available experimental data of this study a quantitative assessment of the sensors' relative capacity to accurately monitor drought conditions over the selected sites and dekads of Ethiopia would not be able to be achieved. Instead, in such an event it was decided to assess the sensors' relative capacity to monitor drought conditions by comparing the rainfall and composite NDVI temporal profiles of each sensor over the selected sites during the 2000-2002 period.

Table 5.5: Time periods in dekads for which rainfall data were accumulated for the calculation of the rainfall-based VPI results of each site

Site	Rainfall cumulative period A (in dekads)	Rainfall cumulative period B (in dekads)
Agarfa	9-13	20-29
Bolo Giorgis	17-24	N/A
Chena	5-13	20-26
Delo Sebro	8-14	23-29
Derba	16-24	N/A
Didu Gordomo	8-14	N/A
Durame	5-13	21-27
Enselale	17-26	N/A
Gibe Farm	6-22	N/A
Ginchi	6-14	18-27
Kone	7-25	N/A
Kora	5-11	18-24
Koshe	4-23	N/A
Kutaber	6-12	18-25
Meteso	5-12	22-28
Teji	17-27	N/A
Toke Erenso	7-25	N/A
Yambero	5-14	22-27
Zequala	18-24	N/A

It should be noted that NDVI values measured over vegetated areas do not depend solely on the amount of rainfall the observed vegetated area had received; moreover the vegetation's response to rainfall can be delayed by a length of time dependant on several factors such as soil and vegetation type or environmental temperature. Furthermore, biophysical and biochemical changes to vegetation properties, and consequently to NDVI values, are not as rapid as the changes in the amount of rainfall received over an area could be. For instance, if a vegetated area received a normal amount of rainfall (for the time of year and area) over a time period of several dekads apart from one dekad when there was no rainfall, then it should not be expected that the NDVI values measured over that vegetated area and time period would have normal NDVI values (for the time of year and area), then drop to zero over the dekad when there was no rainfall and have normal NDVI values again the next dekad. It is more likely that the recorded NDVI values over that area would have approximately (because other factors than rainfall may also affect the recorded NDVI values) normal values, then drop slightly below normal (depends on

the vegetation's growth stage and resilience to drought, water within the soil and environmental temperature among other factors) for a length of time after the dekad when no rainfall was recorded, and then gradually recover to its normal NDVI values. Moreover, the NDVI values recorded by the sensors may not always be representing the true NDVI values of the observed vegetated areas, mainly due to possible errors in cloud masking, atmospheric correction, calibration and effects caused by high illumination and observation angles. Hence, a very close match between the NDVI and rainfall temporal profiles should not be expected.

The rainfall values used for each site and dekad were to be the accumulated amount of rainfall received by each site over the last five dekads. This way the magnitude of potential mismatches between the NDVI and rainfall temporal profiles caused by rapid changes in rainfall would be reduced. It is likely that over several sites vegetation is affected by the amount of rainfall it received over time periods longer than five dekads; however, the accumulation of the rainfall was limited to a five dekad period due to gaps in the rainfall data. The sensor whose composite NDVI temporal profile matches the rainfall data temporal profile most closely over each selected site and dekad would be considered to have the highest capacity for monitoring drought conditions.

5.6 Results

The results of the regression analysis between the three sensors' composite NDVI values over the selected sites and dekads over Ethiopia are displayed in table 5.6, while the scatter plots of the regressions are displayed in figure 5.4. All regressions had more than 99% significance level. By comparing the Ethiopian regression (table 5.6) with the continental regressions (table 4.10), it was found that the regression between composite NDVI values of MODIS and AVHRR and MODIS and VEGETATION over the selected sites and dekads (table 5.3) in Ethiopia, were not significantly different at a 95% CI from their respective continental ones derived in Chapter 4. As far as the Ethiopian and continental regressions between the composite NDVI values of VEGETATION and AVHRR were concerned, the slope coefficient values of the two regressions were not significantly different at a 95% CI but the constant coefficient values were.

Consequently the historical composite NDVI record of MODIS was simulated using the continental regression derived in Chapter 4; while the historical composite NDVI record of VEGETATION was simulated using the Ethiopian regression.

Table 5.6: Regression analysis results between the composite NDVI values of the three sensors over the selected sites and dekads over Ethiopia.

Equation	R^2	Slope SE	Constant SE	SE	SL
MODIS =1.0692966AVHRR+0.047285	0.572586882	0.11548	0.068192	0.088891	<0.001
VEGETATION =0.856472AVHRR+0.121958	0.735450899	0.06421	0.037916	0.049425	<0.001
MODIS =1.194068VEGETATION-0.07117	0.712157494	0.094892	0.059622	0.072948	<0.001

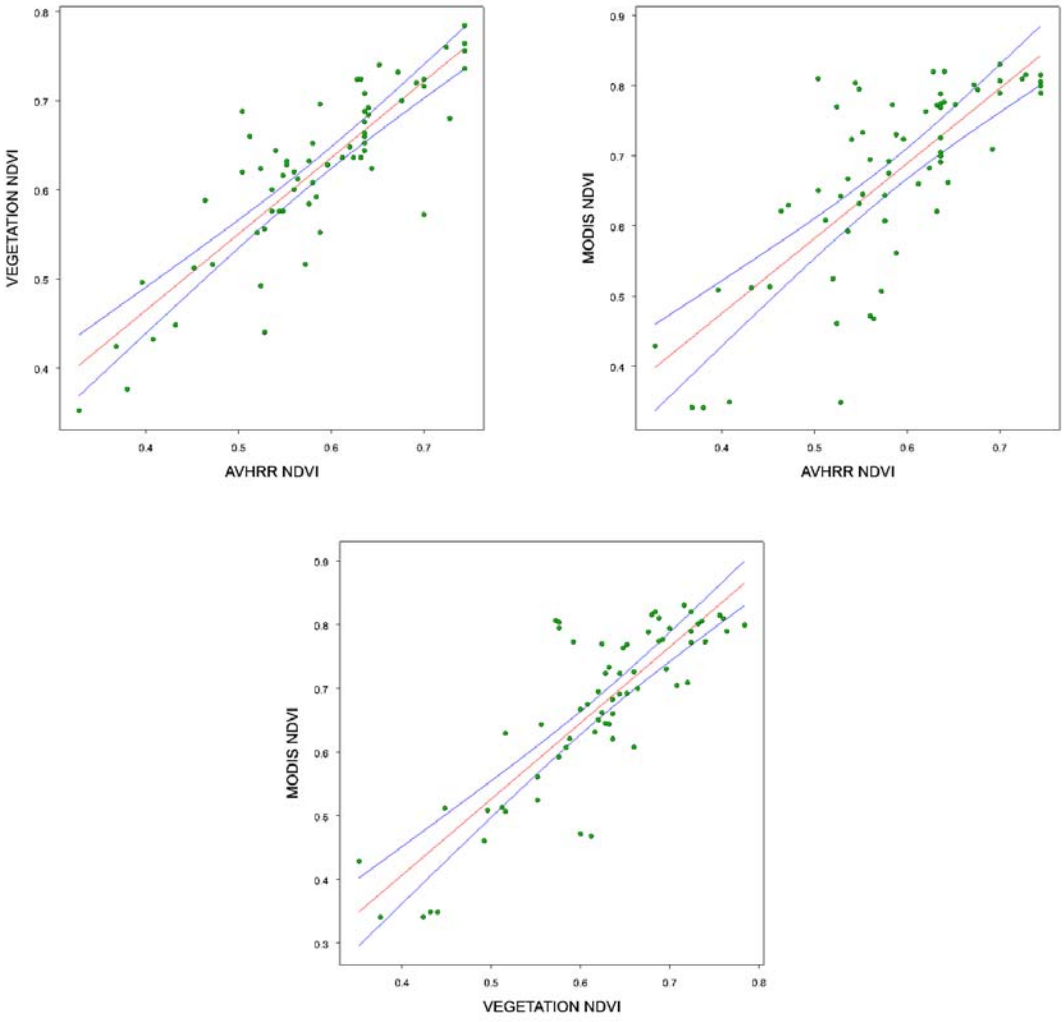

Figure 5.4: Scatter plots between the composite NDVI values of the three sensors over the selected sites and dates over Ethiopia (Trendlines and 95% CI are displayed in red and blue respectively).

The prediction accuracy of each of the continental regressions between the composite NDVI values of MODIS and AVHRR, and MODIS and VEGETATION, as well as the prediction accuracy of the Ethiopian regression between VEGETATION and AVHRR were calculated for a 95% CI according to equation 5.2; the results are displayed in table 5.7.

Table 5.7: 95% CI Accuracies of the regressions between the NDVI values of the three sensors over the selected sites and dekads over Ethiopia.

Regression	SE	95% CI Accuracy
MODIS NDVI/AVHRR NDVI	0.055652	±0.109078
VGT NDVI/AVHRR NDVI	0.049425	±0.09885
MODIS NDVI/VGT NDVI	0.063879	±0.125203

As a further step, the sensitivity of the VPI results of each sensor, selected site and dekad to composite NDVI value fluctuations needed to be estimated. According to the methodology, all available valid composite NDVI values of each sensor, selected site and dekad were plotted against the respective VPI values derived from these NDVI observations. Then, using the least square methodology, third order polynomials were fitted to each scatter plot to approximate the VPI/NDVI relationships; two examples are given in figure 5.5. The derived polynomial of each sensor and selected site and dekad was then used to calculate the composite NDVI values that would result in different VPI classes (VPI values of 0.2, 0.4, 0.6 and 0.8). These NDVI values for each sensor and selected site and dekad are displayed in tables 5.8, 5.9 and 5.10.

It can be seen in tables 5.8, 5.9 and 5.10 that the difference between the NDVI values that would result in different VPI classes for every sensor, selected site and dekad were very small. In the majority of cases, composite NDVI values differences as little as 0.05 would result in different VPI classes. As such the VPI sensitivity to NDVI values was very high over the selected sites and dates for all sensors. Composite NDVI values for MODIS and VEGETATION could not be simulated within accuracies less than 0.05 (table 5.8).

Hence, according to the methodology, the relative capacity of the three sensor's to monitor drought conditions was assessed by visually comparing the NDVI temporal profiles of each selected site and dekad against their respective rainfall temporal profiles.

The rainfall and NDVI temporal profiles of each sensor and site are displayed in figures 5.6, 5.7 and 5.8.

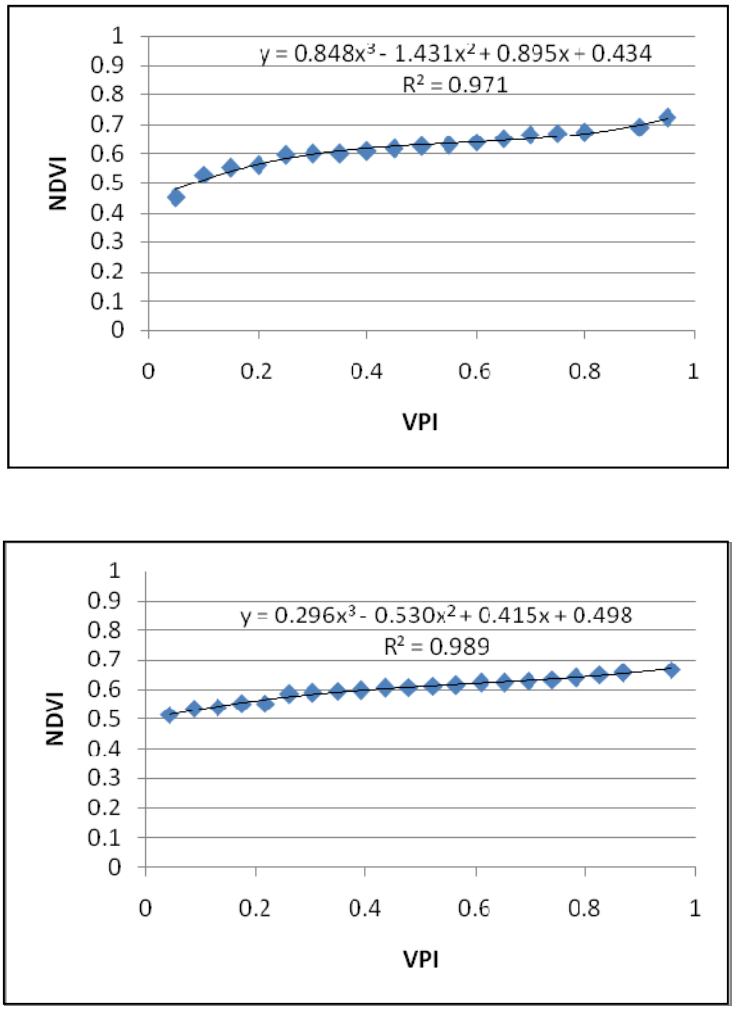

Figure 5.5: Two examples of VPI/NDVI relations. The top scatter plot displays the relation between the VPI/NDVI values of AVHRR over Agarfa for the 15th dekad, and the bottom one the relation between the VPI/NDVI values of AVHRR over Bolo Giorgis for the 26th dekad.

Table 5.8: Results of the VPI/NDVI relation analysis for AVHRR over the selected sites and dekads of Ethiopia.

Site	Dekad	Polynomial	NDVI value that would result in the following VPI values:			
			0.2	0.4	0.6	0.8
Agarfa	15	$y = 0.916x^3 - 1.581x^2 + 1.022x + 0.365$	0.5135	0.5795	0.6069	0.6398
Agarfa	31	$y = 0.789x^3 - 1.441x^2 + 0.986x + 0.418$	0.5639	0.6323	0.6613	0.6885
Bolo Giorgis	26	$y = 0.482x^3 - 0.853x^2 + 0.568x + 0.455$	0.5383	0.5766	0.5928	0.6103
Chena	15	$y = 0.395x^3 - 0.703x^2 + 0.472x + 0.643$	0.7124	0.7446	0.7584	0.7729
Chena	28	$y = 0.205x^3 - 0.368x^2 + 0.311x + 0.634$	0.6831	0.7126	0.7324	0.7522
Delo	31	$y = 0.552x^3 - 0.943x^2 + 0.615x + 0.497$	0.5867	0.6274	0.6458	0.6681
Delo Sebro	16	$y = 0.530x^3 - 0.946x^2 + 0.692x + 0.406$	0.5108	0.5654	0.5951	0.6255
Derba	26	$y = 0.130x^3 - 0.234x^2 + 0.233x + 0.484$	0.5223	0.5481	0.5676	0.5872
Didu Gordomo	16	$y = 0.356x^3 - 0.569x^2 + 0.375x + 0.637$	0.6921	0.7187	0.7341	0.7551
Durame	15	$y = 0.380x^3 - 0.702x^2 + 0.522x + 0.346$	0.4254	0.4668	0.4886	0.5089
Durame	29	$y = 0.545x^3 - 0.847x^2 + 0.487x + 0.408$	0.4759	0.5022	0.5130	0.5346
Enselale	28	$y = 0.265x^3 - 0.431x^2 + 0.347x + 0.452$	0.5063	0.5388	0.5623	0.5894
Gibe	24	$y = 0.825x^3 - 1.386x^2 + 0.819x + 0.572$	0.6870	0.7306	0.7426	0.7626
Ginchi	16	$y = 0.038x^3 - 0.063x^2 + 0.212x + 0.401$	0.4412	0.4782	0.5137	0.5497
Ginchi	29	$y = 0.626x^3 - 0.959x^2 + 0.553x + 0.529$	0.6062	0.6368	0.6508	0.6782
Kone	27	$y = 0.169x^3 - 0.376x^2 + 0.342x + 0.540$	0.5947	0.6275	0.6463	0.6595
Kora	13	$y = 0.601x^3 - 0.966x^2 + 0.758x + 0.289$	0.4068	0.4761	0.5259	0.5849
Kora	26	$y = 1.181x^3 - 1.751x^2 + 0.895x + 0.384$	0.5024	0.5374	0.5457	0.5840
Koshe	25	$y = 0.019x^3 - 0.058x^2 + 0.18x + 0.505$	0.5388	0.5689	0.5962	0.6216
Kutaber	14	$y = 0.612x^3 - 0.892x^2 + 0.512x + 0.271$	0.3426	0.3722	0.3893	0.4231
Kutaber	27	$y = 0.630x^3 - 0.994x^2 + 0.621x + 0.473$	0.5625	0.6027	0.6238	0.6562
Meteso	14	$y = 0.750x^3 - 1.055x^2 + 0.717x + 0.409$	0.5162	0.5750	0.6214	0.6914
Meteso	30	$y = 0.491x^3 - 1.013x^2 + 0.930x + 0.38$	0.5294	0.6213	0.6794	0.7271
Teji	29	$y = 0.394x^3 - 0.709x^2 + 0.499x + 0.403$	0.4776	0.5144	0.5323	0.5502
Toke Erenso	27	$y = 0.897x^3 - 1.486x^2 + 0.851x + 0.475$	0.5929	0.6350	0.6444	0.6640
Yambero	16	$y = 0.678x^3 - 1.079x^2 + 0.642x + 0.493$	0.5837	0.6206	0.6362	0.6632
Yambero	29	$y = 0.485x^3 - 0.825x^2 + 0.546x + 0.576$	0.6561	0.6934	0.7114	0.7331
Zequala	26	$y = 0.180x^3 - 0.238x^2 + 0.267x + 0.447$	0.4923	0.5272	0.5604	0.6004

Table 5.9: Results of the VPI/NDVI relation analysis for MODIS over the selected sites and dekads of Ethiopia.

Site	Dekad	Polynomial	NDVI value that would result in the following VPI values:			
			0.2	0.4	0.6	0.8
Agarfa	15	$y = 1.058x^3 - 1.848x^2 + 1.212x + 0.373$	0.5499	0.6298	0.6634	0.7016
Agarfa	31	$y = 0.871x^3 - 1.577x^2 + 1.069x + 0.464$	0.6217	0.6950	0.7258	0.7559
Bolo Giorgis	26	$y = 0.263x^3 - 0.543x^2 + 0.501x + 0.487$	0.5676	0.6174	0.6489	0.6749
Chena	15	$y = 0.448x^3 - 0.789x^2 + 0.518x + 0.709$	0.7846	0.8186	0.8325	0.8478
Chena	28	$y = 0.292x^3 - 0.539x^2 + 0.413x + 0.691$	0.7544	0.7886	0.8078	0.8259
Delo	31	$y = 0.676x^3 - 1.172x^2 + 0.743x + 0.544$	0.6511	0.6969	0.7139	0.7344
Delo Sebro	16	$y = 0.528x^3 - 0.990x^2 + 0.769x + 0.439$	0.5574	0.6220	0.6580	0.6909
Derba	26	$y = 0.993x^3 - 1.243x^2 + 0.594x + 0.512$	0.5890	0.6143	0.6354	0.7001
Didu Gordomo	16	$y = 0.564x^3 - 0.880x^2 + 0.501x + 0.699$	0.7685	0.7947	0.8046	0.8254
Durame	15	$y = 0.600x^3 - 0.992x^2 + 0.653x + 0.378$	0.4737	0.5189	0.5423	0.5727
Durame	29	$y = 1.091x^3 - 1.490x^2 + 0.705x + 0.445$	0.5351	0.5584	0.5673	0.6140
Enselale	28	$y = 0.258x^3 - 0.430x^2 + 0.377x + 0.502$	0.5623	0.6005	0.6291	0.6605
Gibe	24	$y = 0.892x^3 - 1.475x^2 + 0.862x + 0.633$	0.7535	0.7989	0.8119	0.8353
Ginchi	16	$y = 0.617x^3 - 0.998x^2 + 0.702x + 0.356$	0.4614	0.5166	0.5512	0.5948
Ginchi	29	$y = 0.541x^3 - 0.867x^2 + 0.565x + 0.575$	0.6576	0.6969	0.7187	0.7491
Kone	27	$y = 0.709x^3 - 1.033x^2 + 0.589x + 0.579$	0.6612	0.6947	0.7137	0.7521
Kora	13	$y = 0.702x^3 - 1.053x^2 + 0.751x + 0.357$	0.4707	0.5338	0.5802	0.6433
Kora	26	$y = 1.068x^3 - 1.509x^2 + 0.782x + 0.452$	0.5566	0.5917	0.6086	0.6587
Koshe	25	$y = 0.468x^3 - 0.870x^2 + 0.633x + 0.488$	0.5835	0.6320	0.6557	0.6772
Kutaber	14	$y = 0.380x^3 - 0.514x^2 + 0.382x + 0.299$	0.3579	0.3939	0.4252	0.4702
Kutaber	27	$y = 0.337x^3 - 0.557x^2 + 0.485x + 0.538$	0.6154	0.6644	0.7013	0.7421
Meteso	14	$y = 0.812x^3 - 1.142x^2 + 0.776x + 0.454$	0.5700	0.6336	0.6839	0.7597
Meteso	30	$y = 0.729x^3 - 1.473x^2 + 1.193x + 0.417$	0.6025	0.7052	0.7600	0.8019
Teji	29	$y = 0.963x^3 - 1.410x^2 + 0.749x + 0.433$	0.5341	0.5686	0.5828	0.6229
Toke Erenso	27	$y = 0.739x^3 - 1.265x^2 + 0.804x + 0.534$	0.6501	0.7005	0.7206	0.7460
Yambero	16	$y = 0.608x^3 - 0.984x^2 + 0.645x + 0.552$	0.6465	0.6915	0.7161	0.7495
Yambero	29	$y = 0.430x^3 - 0.797x^2 + 0.579x + 0.635$	0.7224	0.7666	0.7884	0.8083
Zequala	26	$y = 0.114x^3 - 0.202x^2 + 0.313x + 0.493$	0.5484	0.5932	0.6327	0.6725

Table 5.10: Results of the VPI/NDVI relation analysis for VEGETATION over the selected sites and dekads of Ethiopia.

Site	Dekad	Polynomial	NDVI value that would result in the following VPI values:			
			0.2	0.4	0.6	0.8
Agarfa	15	$y = 0.848x^3 - 1.431x^2 + 0.895x + 0.434$	0.5625	0.6173	0.6390	0.6683
Agarfa	31	$y = 0.597x^3 - 1.133x^2 + 0.815x + 0.481$	0.6035	0.6639	0.6911	0.7135
Bolo Giorgis	26	$y = 0.296x^3 - 0.530x^2 + 0.415x + 0.498$	0.5622	0.5981	0.6201	0.6424
Chena	15	$y = 0.432x^3 - 0.794x^2 + 0.532x + 0.645$	0.7231	0.7584	0.7717	0.7836
Chena	28	$y = 0.762x^3 - 1.422x^2 + 0.944x + 0.526$	0.6640	0.7248	0.7451	0.7613
Delo	31	$y = 0.371x^3 - 0.659x^2 + 0.474x + 0.551$	0.6224	0.6589	0.6783	0.6984
Delo Sebro	16	$y = 0.413x^3 - 0.764x^2 + 0.589x + 0.467$	0.5575	0.6068	0.6346	0.6607
Derba	26	$y = 0.063x^3 - 0.128x^2 + 0.171x + 0.539$	0.5686	0.5910	0.6091	0.6261
Didu Gordomo	16	$y = 0.385x^3 - 0.574x^2 + 0.346x + 0.665$	0.7143	0.7362	0.7491	0.7716
Durame	15	$y = 0.345x^3 - 0.659x^2 + 0.501x + 0.401$	0.4776	0.5180	0.5389	0.5567
Durame	29	$y = 2.349x^3 - 3.821x^2 + 1.965x + 0.251$	0.5100	0.5760	0.5618	0.5802
Enselale	28	$y = 0.880x^3 - 1.474x^2 + 0.860x + 0.429$	0.5491	0.5935	0.6044	0.6242
Gibe	24	$y = 0.953x^3 - 1.648x^2 + 0.972x + 0.563$	0.6991	0.7491	0.7588	0.7738
Ginchi	16	$y = 0.199x^3 - 0.320x^2 + 0.341x + 0.416$	0.4730	0.5139	0.5484	0.5859
Ginchi	29	$y = 1.242x^3 - 2.11x^2 + 1.200x + 0.444$	0.6095	0.6659	0.6727	0.6895
Kone	27	$y = 0.232x^3 - 0.406x^2 + 0.327x + 0.579$	0.6300	0.6597	0.6792	0.6995
Kora	13	$y = 0.923x^3 - 1.501x^2 + 0.969x + 0.331$	0.4721	0.5375	0.5714	0.6181
Kora	26	$y = 1.037x^3 - 1.566x^2 + 0.849x + 0.431$	0.5465	0.5864	0.6006	0.6389
Koshe	25	$y = 0.198x^3 - 0.296x^2 + 0.244x + 0.546$	0.5845	0.6089	0.6286	0.6531
Kutaber	14	$y = 0.795x^3 - 1.251x^2 + 0.726x + 0.292$	0.3935	0.4331	0.4490	0.4792
Kutaber	27	$y = 0.556x^3 - 0.808x^2 + 0.488x + 0.532$	0.6017	0.6335	0.6540	0.6900
Meteso	14	$y = 0.462x^3 - 0.647x^2 + 0.537x + 0.465$	0.5502	0.6058	0.6541	0.7171
Meteso	30	$y = 1.214x^3 - 2.141x^2 + 1.348x + 0.418$	0.6117	0.6923	0.7183	0.7477
Teji	29	$y = 0.483x^3 - 0.811x^2 + 0.513x + 0.452$	0.5260	0.5584	0.5722	0.5907
Toke Erenso	27	$y = 0.874x^3 - 1.359x^2 + 0.745x + 0.528$	0.6296	0.6645	0.6745	0.7017
Yambero	16	$y = 0.703x^3 - 1.084x^2 + 0.628x + 0.531$	0.6189	0.6538	0.6694	0.6996
Yambero	29	$y = 0.849x^3 - 1.467x^2 + 0.865x + 0.564$	0.6851	0.7296	0.7383	0.7518
Zequala	26	$y = -0.012x^3 + 0.009x^2 + 0.171x + 0.509$	0.5435	0.5781	0.6122	0.6454

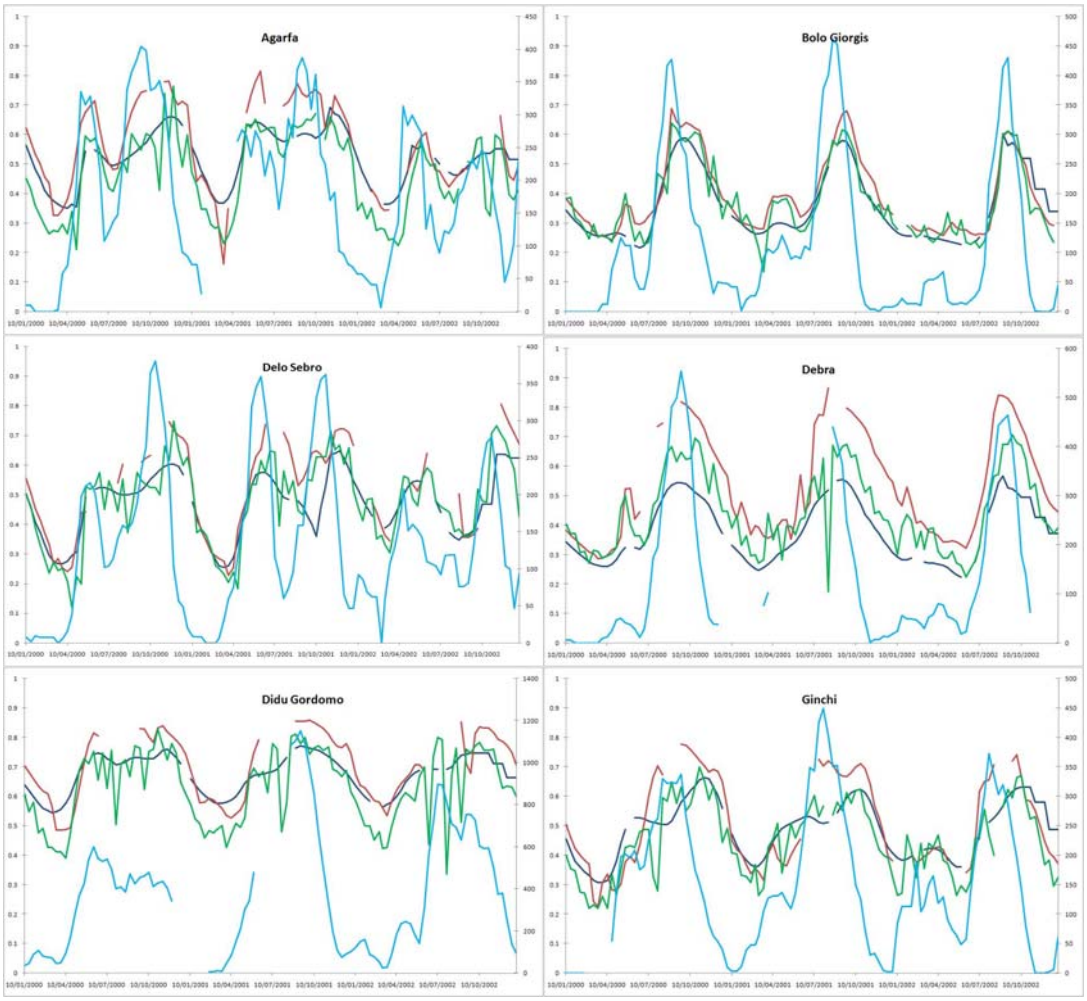

Figure 5.6: NDVI and rainfall temporal profiles of the selected sites over Ethiopia, during the 2000-2002 period. The NDVI temporal profiles of AVHRR, MODIS and VEGETATION are displayed with dark blue, purple and green colour lines respectively, while rainfall profiles are displayed with light blue colour lines. The left and right vertical axes display NDVI and accumulated rainfall in mm, respectively. The horizontal axis displays the dekads from the beginning of 2000 until the end of 2002.

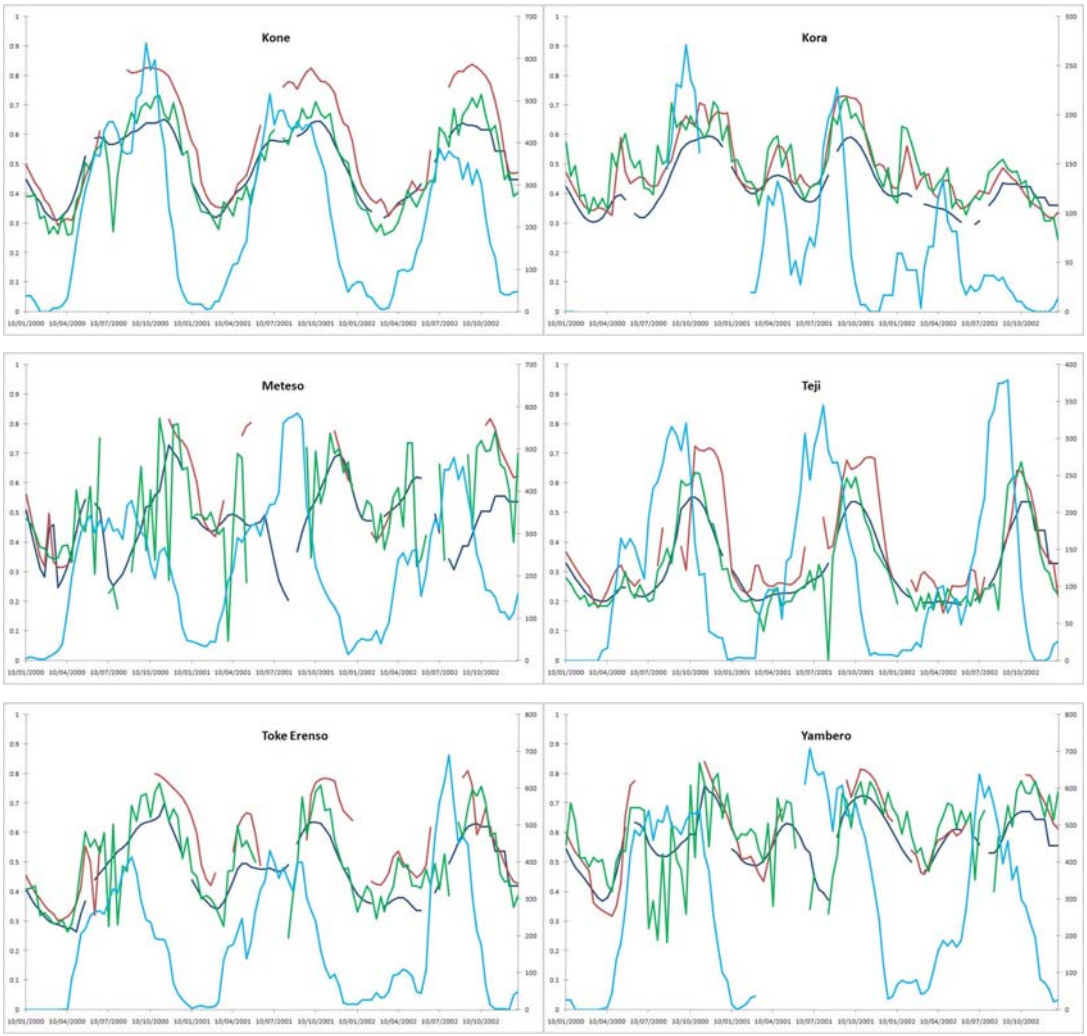

Figure 5.7: NDVI and rainfall temporal profiles of the selected sites over Ethiopia, during the 2000-2002 period. The NDVI temporal profiles of AVHRR, MODIS and VEGETATION are displayed with dark blue, purple and green colour lines respectively, while rainfall profiles are displayed with light blue colour lines. The left and right vertical axes display NDVI and accumulated rainfall in mm, respectively. The horizontal axis displays the dekads from the beginning of 2000 until the end of 2002.

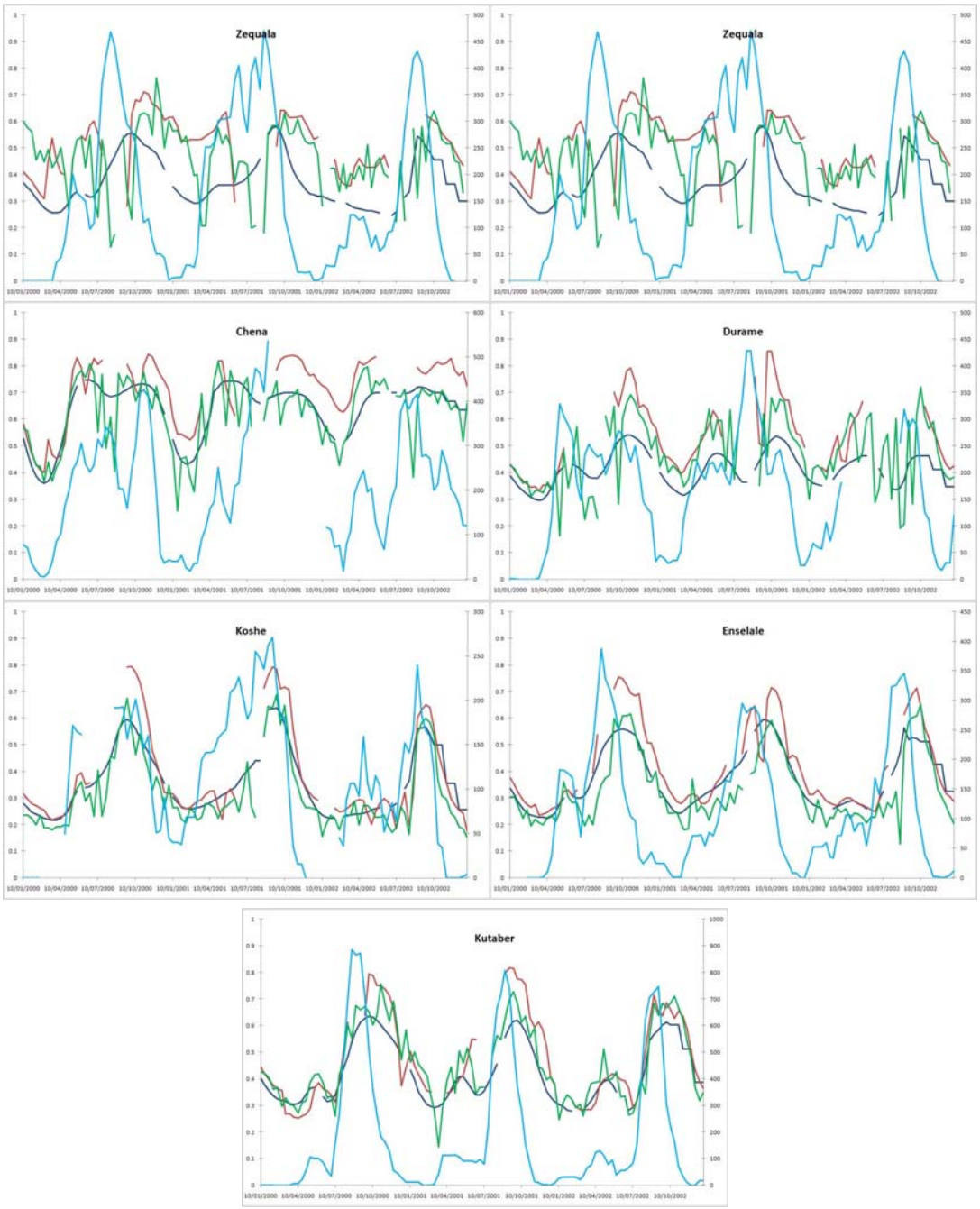

Figure 5.8: NDVI and rainfall temporal profiles of the selected sites over Ethiopia, during the 2000-2002 period. The NDVI temporal profiles of AVHRR, MODIS and VEGETATION are displayed with dark blue, purple and green colour lines respectively, while rainfall profiles are displayed with light blue colour lines. The left and right vertical axes display NDVI and accumulated rainfall in mm, respectively. The horizontal axis displays the dekads from the beginning of 2000 until the end of 2002.

Overall the NDVI temporal profiles of the sensors followed a similar pattern to that of the rainfall temporal profiles over the same sites, indicating that the NDVI values of all three sensors are good indicators of the amount of rainfall received over vegetated areas. A closer comparison of their NDVI profiles however, revealed that the NDVI temporal profile of AVHRR was the smoothest, suggesting that small fluctuations in rainfall were not easily detected. This can be seen more clearly over sites such as Bolo Giorgis; it can be seen from the MODIS and VEGETATION NDVI rainfall temporal profiles over the site, that there were actually two growing seasons instead of one according to table 5.3 which was based on the yearly average NDVI profiles of AVHRR. The first growing season peaking at about the 15th dekad of the year was overlooked because the NDVI response of AVHRR was quite faint, compared to the more defined responses of MODIS and VEGETATION.

On the other hand the NDVI temporal profiles of VEGETATION had sharp and considerable NDVI value fluctuations between consecutive dekads over the same sites. Although the general pattern of the NDVI profiles followed the pattern of the rainfall profiles, the sharp NDVI value fluctuations were not consistent with fluctuations in the rainfall data, and in some cases were too great to be real. One such unrealistic case can be seen in the Debra site, where for the 22nd dekad of 2001 the NDVI values recorded by VEGETATION dropped from 0.63 to 0.17 and then increased to 0.67 for the 23rd dekad of the same year. Such rapid value fluctuations were more likely to be caused by cloud contaminated data which were not properly identified and removed during the cloud masking process.

Out of the three sensors, the NDVI temporal profile of MODIS seemed to match the temporal profile of rainfall better. The NDVI response of MODIS was more sensitive to rainfall fluctuations than AVHRR, and it contained less temporal noise (such as cloud contaminated data) than VEGETATION.

5.7 Discussion

The results show that the Ethiopian and continental regressions were not significantly different with a 95% CI apart from the respective regressions between VEGETATION and AVHRR which were barely significantly different at a 95% CI. This is evidence to support use of the continental regressions developed in Chapter 4 at other sites than the ones they were developed for.

The slight significant difference that was found between the Ethiopian and continental regressions between the composite NDVI values of VEGETATION and AVHRR were believed to be the result of a relatively higher proportion of outliers in the Ethiopian regressions; something which can be seen from the lower values of the coefficients of determination achieved in the Ethiopian regressions (table 5.7) than the respective continental regressions (table 4.10). The increased proportion of outliers in the Ethiopian regressions, were believed to have been caused mainly because:

- The continental regressions were based on observations over homogenous sites while the sites used in the Ethiopian regressions were not necessarily homogenous. Therefore a greater portion of outliers could have been caused in the Ethiopian regressions due to the sensors' different spatial resolution and possible image registration inaccuracies, meaning that the Ethiopian regressions were more likely to have been based on observations over different land cover composition by each sensor, than the continental regressions.
- The continental regressions were based on observations collected over certain sites though all dekads of the year. However, the composite NDVI values selected for the VPI methodology were collected over specific dekads of the year when the highest NDVI values of each site were expected. It is possible that differences between the sensors' composite NDVI values were higher when vegetation was at its peak.
- The Ethiopian regressions were based on NDVI observations collected over each selected site at about the dates when rainfall and vegetation were expected to be at their peak, as opposed to the continental regressions which were based on observations collected over the whole year. Due to this, there was a considerably

higher chance that the proportion of cloud contaminated observations used in the Ethiopian regressions was higher than that of the continental regressions, because higher rainfall is directly linked with higher cloud cover and the chance of using cloud contaminated data which were not successfully removed was therefore increased due to the increased proportion of cloud contaminated data.

It was also found that the VPI was highly sensitive to composite NDVI value fluctuations over the selected sites and dekads. Composite NDVI value fluctuations as little as 0.05 could result in different VPI classes. Such composite NDVI accuracy requirements were considered to be too high to realistically be met by the NDVI simulation. In fact such accuracy requirements were considered to be too high even for the composite NDVI measurements of AVHRR, let alone simulated composite NDVI values based on them. The added effect of factors such as cloud and atmospheric contamination, radiometric noise, calibration inaccuracies, varying sun-target-sensor geometry, varying spatial resolution across the scan line and image registration inaccuracies were very likely to cause composite NDVI inaccuracies of about or greater than 0.05.

To test whether the required accuracy of composite NDVI values over the selected sites and dekads for the VPI methodology was too high even for non-simulated data, it was decided to validate the AVHRR composite NDVI-based VPI results over the selected sites and dekads against the respective rainfall-based VPI results. The NDVI-based VPI results were calculated using all available composite NDVI data of AVHRR over the selected sites and dekads according to table 5.3 within the 1981-2002 time period; while the rainfall-based VPI results were calculated using all available rainfall data over the selected sites and dekads according to table 5.5 also within the 1981-2002 period. Then correlation of NDVI-based and rainfall-based VPI results over each of the selected sites and dekads, was tested using the Spearman rank correlation.

Table 5.11: Spearman rank correlation coefficients achieved in the correlations between AVHRR composite NDVI-based and rainfall-based VPI results over the selected sites and dekads of Ethiopia.

Site	Growing season A	Growing season B
Agarfa	0.542857	0.597523
Bolo Giorgis	-0.14737	N/A
Delo Sebro	0.304386	0.108442
Derba	0.181203	N/A
Didu Gordomo	0.421053	N/A
Ginchi	-0.04747	-0.34887
Kone	-0.08701	N/A
Kora	0.786765	0.467544
Meteso	0.25387	0.37807
Teji	0.138312	N/A
Toke Erenso	-0.2332	N/A
Yambero	0.346429	-0.26015
Zequala	-0.16827	N/A
Chena	0.243873	0.407519
Durame	-0.32843	-0.57218
Gibe Farm	-0.38045	N/A
Koshe	-0.29412	N/A
Enselale	0.279503	N/A
Kutaber	0.405882	0.182456

The Spearman rank correlation coefficients achieved for each correlation between the NDVI-based and rainfall-based VPI results of every selected site and dekad are displayed in table 5.11. Overall the correlation between the NDVI-based and rainfall-based VPI results was particularly low with the exception of a few sites and dekads where the correlation was moderate (e.g. Agarfa) or high (e.g. Kora, growing season A).

A possible factor that may have lowered the correlation between the NDVI-based and rainfall-based VPI results was that the rainfall data had not been validated by the NMA for errors (such as typographical errors) that occasionally occur when data are transferred from paper to Excel spreadsheets (personal communication with the NMA), and therefore could have contained errors that may have reduced the correlation between NDVI-based and rainfall-based VPI results over the selected sites and dekads. However, it was considered very unlikely that this was the sole reason for the particularly low Spearman rank correlation coefficients achieved in the majority of selected sites and dekads.

The primary cause for the particularly low correlations achieved between the NDVI-based and rainfall-based VPI results, was also believed to be the high sensitivity of the VPI to composite NDVI value fluctuations over the selected sites and dekads. The VPI was so highly sensitive because the majority of valid historical composite NDVI values used for the VPI calculation over each selected site and dekad in Ethiopia were within a very narrow range. Consequently small fluctuations in the composite NDVI values resulted in significantly different rank positions and therefore VPI values. The fact that the majority of composite NDVI values available over each selected site and dekad had similar values was further demonstrated by calculating their standard deviation (SD) (table 5.12); it can be seen that the lower the SD value of each site and dekad the higher their sensitivity to composite NDVI value fluctuations and the lower spearman rank correlation coefficients achieved against the respective rainfall-based VPI results.

A possible reason why this may have happened could be that, the majority of historical composite NDVI data collected over the majority of each selected site and dekad were collected under similar/normal rainfall conditions, and therefore the collected composite NDVI values over each of these sites and dekads were also similar (assuming that the composite NDVI data were collected over vegetated areas that are respondent to rainfall). In such a case however, the assumption of the VPI methodology that the available historical composite NDVI data over each site and dekad are sufficient to help distinguish between a range of drought conditions is violated, and consequently the VPI results based on such historical composite NDVI data are invalid. For instance, if the majority of valid historical composite NDVI values available over a certain site and dekad were collected under normal rainfall conditions (and consequently had similar values), were to be used to calculated the VPI, the VPI results would indicate extreme rainfall conditions for the group of lower and higher values of the available normal composite NDVI values, which would be false.

The values of the Spearman rank correlation coefficients obtained in this part of the study between the AVHRR composite NDVI-based VPI results and the respective rainfall-based VPI results over the selected sites and dekads, were particularly low compared to the high Spearman rank correlation coefficients obtained over similar studies in Zambia (Sannier et al., 1998a) and Ethiopia (Tamene, 1996) which were also

based on AVHRR composite NDVI and rainfall data. The main difference between the present study and the studies in Zambia and Ethiopia however, was that the composite NDVI values used for the calculation of the VPI in the current study were extracted from a single pixel location for every selected site and dekad (following the same methodology adopted by the Global Monitoring for Food Security (GMFS) (GMFS, 2006)) as opposed to the studies in Zambia and Ethiopia where the extracted composite NDVI values used for the calculation of the VPI were not based on NDVI measurements over single pixel locations, but were the mean composite NDVI value of an area covered with the same land cover class as that at the location for which composite NDVI data were extracted. It is possible that composite NDVI observations over a single location are likely to be less representative than composite NDVI values based on observations over a greater area covered with the same land cover class, and as such better suited for use with the VPI methodology. Therefore it was considered possible that the valid composite NDVI values available over each selected site and dekad may have been observed under a representative range of drought conditions, but the composite NDVI values collected over single pixel locations may have not been representative. Thus, it was considered possible that had the AVHRR composite NDVI-based VPI values been calculated using historical composite NDVI values based on greater area observations instead of pixel locations, then correlation between NDVI-based and rainfall-based VPI results over the same sites and dekads could have been much higher, in agreement with the results of the VPI studies in Zambia (Sannier et al., 1998a) and Ethiopia (Tamene, 1996).

Therefore, either because the rainfall data may not have been very accurate, or the considerable possibility that the VPI analysis was not valid, (either because the majority of valid composite NDVI data available over the majority of the selected sites and dekads were collected under similar rainfall conditions, or because they were extracted from pixel locations and as such they may have not been representative of the condition of the vegetation in relation to rainfall availability stress) the sensors' capacity to monitor drought conditions using the VPI methodology could not have been assessed by means of validating the NDVI-based results of each sensor against the respective rainfall-based VPI results over each selected site and dekad as originally intended, and further research was needed.

Table 5.12: Standard deviation (SD) values of all the available valid composite NDVI values used by each sensor for the VPI methodology over each of the selected sites and dekads of Ethiopia.

Site	Dekad	AVHRR SD	MODIS SD	VGT SD
Agarfa	15	0.07414	0.087299	0.062957
Agarfa	31	0.072541	0.078993	0.062968
Bolo Giorgis	26	0.042034	0.054914	0.042257
Chena	15	0.036157	0.038243	0.037151
Chena	28	0.036446	0.039414	0.062577
Delo	31	0.047322	0.051015	0.041863
Delo Sebro	16	0.062611	0.071012	0.055572
Derba	26	0.032466	0.070681	0.028205
Didu Gordomo	16	0.034553	0.035251	0.032711
Durame	15	0.045852	0.056105	0.043384
Durame	29	0.036388	0.056397	0.089153
Enselale	28	0.042052	0.050003	0.051325
Gibe	24	0.049146	0.052858	0.052581
Ginchi	16	0.051801	0.072264	0.055631
Ginchi	29	0.044227	0.051557	0.064322
Kone	27	0.03351	0.054912	0.03683
Kora	13	0.092762	0.09184	0.08328
Kora	26	0.058745	0.066666	0.06148
Koshe	25	0.040132	0.056496	0.035565
Kutaber	14	0.047705	0.058631	0.053472
Kutaber	27	0.054055	0.064793	0.050311
Meteso	14	0.093257	0.100941	0.084815
Meteso	30	0.102223	0.108438	0.085802
Teji	29	0.041893	0.058784	0.039292
Toke Erenso	27	0.049373	0.058365	0.048464
Yambero	16	0.049017	0.059447	0.049095
Yambero	29	0.042925	0.047418	0.04761
Zequala	26	0.053458	0.060815	0.048242

The relative capacity of the sensors' data at monitoring drought conditions using the VPI methodology was limited to assessing the sensors' NDVI responsiveness to rainfall by means of visually comparing the rainfall and composite NDVI temporal profiles of each sensor over each site. The VPI methodology relies on the responsiveness of NDVI

values to rainfall in order to assess drought conditions; therefore, the sensor with the most responsive NDVI data to rainfall is more likely to help produce the most accurate VPI results. Based on the visual inspection of the profiles, MODIS was deemed to be the sensor with the most responsive NDVI data to rainfall, mainly because it seemed to be more sensitive at detecting biophysical and biochemical changes over vegetation likely to have been triggered by water availability than AVHRR, and contained less temporal data noise than VEGETATION. The primary source of VEGETATION's temporal data noise was believed to be caused by cloud contaminated data and could potentially be reduced either with improved cloud detection processes or the use of temporal filters such as a high order polynomial fitted over a temporally consecutive number of observations.

5.8 Conclusions

The results of this part of the study confirmed the validity of the continental regressions developed in the previous part of the study (Chapter 4) for simulating composite NDVI data for one sensor based on composite NDVI data collected by another sensor over the same area and date. Hence, it was considered possible that the use of these regressions in conjunction with the historical composite NDVI data of AVHRR could help extend the historical composite NDVI records of MODIS and VEGETATION and enable their use in applications that require historical composite NDVI records longer than those currently available, provided that the considered applications do not require historical composite NDVI values at higher precision than the achievable simulation accuracy of the regressions. Moreover, it was believed that the regressions could also be helpful in cases when composite NDVI data become unavailable from a particular sensor; in such cases if a particular monitoring application can no longer receive composite NDVI data from the sensor it was using, then it could continue its operation by simulating the composite NDVI values the application would have received from the sensor based on data collected by another sensor.

The VPI values calculated based on NDVI data collected over the selected sites and dekads of Ethiopia and the VPI values calculated based on rainfall data collected over the

respective sites and dekads were not correlated. The reason for this was attributed to three possible causes: i) there may have been errors in the rainfall data ii) the VPI methodology may not be suitable for pixel based analysis and iii) vegetation conditions may have not changed significantly over the selected sites and dekads during the 1981-2002 period. Due to this the NDVI based VPI values of the sensors over the selected sites and dekads could not be compared with the rainfall based VPI values over the respective sites and dekads.

The hypothesis that out of MODIS VEGETATION and AVHRR, drought conditions would be most accurately represented when using NDVI data collected by MODIS and least by AVHRR was tested by comparing the temporal composite NDVI profiles of each sensor against the respective temporal rainfall profiles of each selected site. The temporal composite NDVI profiles of MODIS matched the temporal rainfall profiles over the respective sites more closely than those of VEGETATION and AVHRR, confirming the hypothesis. However, the temporal composite NDVI profiles of VEGETATION did not match the respective temporal rainfall profiles as closely as AVHRR due to unexpected sharp fluctuations in the composite NDVI values of VEGETATION's temporal profile believed to have been caused by clouds which have not been successfully detected and masked; hence the hypothesis was not confirmed for VEGETATION.

5.9 Future work

The poor correlation between the NDVI and rainfall based VPI values calculated over the selected sites and dekads was not expected, as a result the original intent of this part of the study to compare the three sensors' capacity to monitor drought using the VPI methodology by means of identifying which of the three sensors' NDVI based VPI values matched more closely the rainfall based VPI values over most of the selected sites and dekads, was not realised. In the future it would be interesting to examine the possible reasons behind this poor correlation.

It should be investigated whether the rainfall data used in this study contained errors by comparing them against a validated version of the rainfall data from the NMA (the NMA was in the process of validating the rainfall data at the time of this study (personal

communication with the NMA)) . In the event that validated rainfall data can not be acquired from the NMA, the existing rainfall data could be cross-validated against other sources of information such as the rainfall datasets which have recently been released by FAO as part of the Climate Impact on Agriculture (CLIMPAG) project. In the event that the validated rainfall data are found to be significantly different to the rainfall data used in the present study, then the rainfall-based VPI results could be recalculated and tested for correlation against the respective NDVI-based VPI results. If the NDVI based VPI values and the VPI values based on the validated rainfall data are poorly correlated again then a different reason must have caused the poor correlation.

Another possibility is that NDVI and rainfall based VPI values are best correlated when the NDVI based VPI values are calculated using mean composite NDVI values extracted over large areas covered with the same land cover class as the investigated sites (this methodology was applied in the studies of Sannier et al., 1998a and Tamene, 1996) instead of using composite NDVI values collected over single pixel locations.

In the event that the NDVI based VPI values using the above methodology are again found to be poorly correlated with VPI values based on rainfall data over the respective sites and dekads, then it should be investigated whether between the 1981-2002 period the vegetation over the selected sites was not affected by droughts and therefore the VPI methodology could not have had valid results over these sites. In such case, rainfall and NDVI data should be used that have been collected over a new set of sites where drought conditions have been recorded in the period between 1981 and 2002. The NDVI based VPI could then be calculated over these new sites using both the single pixel and mean area composite NDVI value methodologies. The NDVI based VPI values derived based on at least one of the two methodologies should be correlated with the rainfall based VPI values over the same sites and dekads. Subsequently, it would be possible to calculate the NDVI based VPI values for each sensor over each site and dekads and realise the initial intent of this part of the study. What is more, based on the results of such a possible future study it should be possible to determine whether it is better to calculate the VPI based on composite NDVI values collected over single pixel locations or based on the mean of composite NDVI values collected over areas covered with the same land cover class as the site monitored.

After having determined the cause of the poor correlation between the NDVI and rainfall based VPI values over the selected sites and dekads of this study, similar studies over other sites and dekads should provide further experimental data over which to base the relative assessment of the three sensors' capacity to monitor drought. Such studies would be particularly interesting in the future when the historical composite NDVI records of the three sensors would be further extended, and any bias in the comparison caused by the extension of MODIS and VEGETATION historical composite NDVI records based on NDVI data collected by AVHRR, would be further minimised.

CHAPTER SIX

6 Summary

6.1 Background

The aim of this study was to identify which of the three most operational low resolution sensors at the time the study was most likely to help produce the most accurate results in land cover mapping and drought monitoring applications at 1 km spatial resolution. Initially a hypothesis regarding the expected relative performance of the sensors in such applications was formed based on a theoretical assessment of the sensors' characteristics. Subsequently, this hypothesis was tested with experimental results. The relative effectiveness of the sensors' SRBs in mapping land cover at 1 km spatial resolution was assessed over the UK and Greece, and the relative effectiveness of the sensors in monitoring drought conditions at 1 km spatial resolution using the VPI methodology was assessed over Ethiopia. However, at the time of the study only the AVHRR had sufficiently long historical NDVI records to meet the requirements of the VPI methodology. Hence, it was also researched whether the historical NDVI records of MODIS and VEGETATION could be extended based on the historical NDVI record of AVHRR.

6.2 Review

The theoretical assessment of the three sensors' characteristics (Chapter 2) led to the hypothesis that land cover mapping and drought monitoring applications at 1 km spatial resolutions would probably produce the most accurate results when based on data collected by MODIS, followed by VEGETATION and lastly AVHRR.

Towards testing with experimental results the part of the hypothesis regarding the expected performance of the sensors in land cover mapping applications (Chapter 3), a classification methodology was developed which allowed for the objective comparison of

the sensors' SRBs relative capacity to map land cover at 1 km spatial resolution, with the minimum possible human input. It was aimed to minimize the human input as much as possible so that the methodology could be fully replicable without bias introduced by the human factor. In order to help assess the sensors' relative capacity in mapping land cover over a range of environmental conditions, the methodology was applied over a series of dates over study areas in the UK and Greece. The classification accuracy of each land cover map produced using data collected by each sensor over the same study area and date was assessed. The sensor which produced the most accurate land cover maps over most study areas and dates was MODIS, followed by VEGETATION and then AVHRR, confirming the hypothesis.

In addition to the confirmation of the hypothesis regarding the expected relative performance of the three sensors in land cover mapping, the analysis of the experimental results also shown that:

- At 1 km spatial resolution sensors are more likely to successfully identify the dominant land cover class in a square km area than the mixture of land cover classes present within it.
- The use of more than the first seven SRBs of MODIS is not likely to significantly improve the accuracy of land cover mapping, particularly over study areas with high heterogeneity.
- Land cover maps based on multidate data were more accurate than maps based on single date data.
- Over study areas of high heterogeneity land cover maps based on VEGETATION data may be more accurate than maps based on MODIS data due to the higher image registration accuracy of the former.

Towards extending the historical NDVI records of MODIS and VEGETATION using the historical NDVI record of AVHRR (Chapter 4), regression analysis was performed between the composite NDVI values collected by each sensor over eight sites in Africa within the period when the operation of the sensors overlapped. It was discovered that the relationship between the composite NDVI values collected by each sensor over the same site and composite period is highly linear. Subsequently the extension of the historical composite NDVI records of MODIS and VEGETATION through the use of the

regressions developed in this part of the study and the historical composite NDVI record of AVHRR was considered possible. This result was further confirmed by the results of a similar regression analysis between the composite NDVI data of the three sensors over 20 sites in Ethiopia (Chapter 5).

The study intended to test the hypothesis regarding the sensors' relative capacity to monitor drought conditions using the VPI methodology by comparing which of the sensors' VPI values over 19 selected sites and dekads of Ethiopia would match more closely the VPI values calculated over the respective sites and dekads using rainfall data. However, the original intent of the study could not be realised because it was unexpectedly discovered that the correlation between the NDVI and rainfall based VPI values over the selected sites and dekads, was poor. This poor correlation was believed to be the result of three possible causes: i) errors in the rainfall data ii) use of composite NDVI data in the VPI methodology which have been extracted from single pixel locations instead of using the mean composite NDVI value of areas covered with the same land cover class as the location monitored. iii) selection of sites that may have not been affected by drought conditions during the 1981-2002 period. However, the capacity of the VPI methodology to monitor drought conditions is directly linked to the responsiveness of NDVI to rainfall. Based on that it was alternatively decided to assess the sensors' relative capacity to monitor drought conditions using the VPI methodology by assessing which of the three sensors' temporal composite NDVI profiles matched more closely the temporal rainfall profiles of the respective sites. The result of the assessment confirmed part of the hypothesis that drought monitoring based on the VPI methodology would most likely produce the most accurate results when based on NDVI data collected by MODIS. The results also show that VPI results based on NDVI data collected by VEGETATION may not be as accurate as those based on NDVI data collected by AVHRR, due to cloud contamination problems in the NDVI data collected by the former sensor. The detection of cloud contaminated data may have been more successful if VEGETATION was equipped with TEBs.

References

Ackerman S., Strabala K., Menzel P., Frey R., Moeller C., Gumley L., Baum B., Schaaf C., Riggs G., and Welch R., 1996. Discriminating Clear-sky from Cloud with MODIS Algorithm Theoretical Basis Document V3 http://eospso.gsfc.nasa.gov/atbd/modistables.html (14 January 2004)

Achard F., Eva H. and Mayaux P., 2001. Tropical forest mapping from coarse spatial resolution satellite data: production and accuracy assessment issues. International Journal of Remote Sensing, Vol. 22, no. 14, pp. 2741–2762

Agrawal S., Joshi P.K., Shukla Y. and Roy P.S., 2003. Spot–Vegetation multi temporal data for classifying vegetation in South Central Asia. Current Science, 84, pp. 1440–1448.

Agresti A., 1990. Categorical Data Analysis, John Wiley & Sons.

Allen J.D.,1990. A Look at the Remote Sensing Applications Program of the National Agricultural Statistics Service. Jour. of Official Stat. VI, 4, pp. 393-409.

Anonymous, 1948. Forest resources of the world. Unasylva 2, 4, pp. 161-182

Anonymous, 1950. Forest resources of the world - supplementary data of the original FAO study. Unasylva 4, 2, pp. 57-59

Anonymous, 1954. Forest resources of the world. Unasylva 8, 3, pp. 129-141.

AQUASTAT survey, 2005. Ethiopia, Irrigation in Africa in figures. http://www.fao.org/ag/agl/aglw/aquastat/countries/ethiopia/index.stm (13 Octomber 2006)

Asrar G., Fuchs M., Kanemasu E.T., and Hatfield J.L., 1984. Estimating absorbed photosynthetic radiation and leaf area index from spectral reflectance in wheat. Agronomy Journal, 76, pp. 300-306

Asrar G., and Dozier J., 1994, EOS: Science Strategy for the Earth Observing System (Woodbury, NY: American Institute of Physics).

Bamber J., 2006. CCRS-Fundamentals of remote sensing. http://www.ggy.bris.ac.uk/personal/JonathanBamber/teaching/ccrs_tutorial/tutorial/chap1/c1p4e.html (4 February 2006)

Baret F., Guyot G., 1991. Potentials and limits of vegetation indices for LAI and APAR assessment. Remote Sensing of Environment 35, pp. 161–173.

Baret F., Jacquemoud S., Guyot G., and Leprieur C., 1992. Modelled analysis of the biophysical nature of spectral shifts and comparison with information content of broad bands. Remote Sensing of the Environment, 41, pp. 133-142.

Barnes J.C. and Smallwood M.D., 19 http://www.cnes-tv.com/dossiers/spot5/va/pdf/technique_va.pdf82. TIROS-N Sereis Direct Readout Services

Barnes W.L., Pagano T.S. and Salomonson V.V., 1998. Prelaunch Characteristics of the Moderate Resolution Imaging Spectroradiometer (MODIS) on EOS-AM1. IEEE Transactions On Geoscience And Remote Sensing, 36, 4

Barnsley M. J., 1984. Effects of the nadir view angles on the detected spectral response of vegetation canopies. International Journal of Remote Sensing, 5, pp. 715-728.

Bartalev S., Belward A.S., Erchov D. and Isaev A.S., 2003. A new SPOT4-VEGETATION derived land cover map of Northern Eurasia. International Journal of Remote Sensing, 24, pp. 1977–1982.

Bartholomé E., Belward A.S., Achard F., Bartalev S., Carmona-Moreno C., Eva H., Fritz S., Gregoire J.-M., Mayaux P. and Stibig H.-J., 2002, GLC 2000—Global Land Cover Mapping for the Year 2000—project Status November 2002. Publications of the European Commission, EUR 20524 EN (Luxembourg: Office for Official Publications of the European Communities).

Bartholomé E., and Belward A.S., 2005. GLC2000: a new approach to global land cover mapping from Earth observation data. International Journal of Remote Sensing, Vol. 26, No. 9, pp. 1959-1977

Bartholomé E., 2004. The GLC 2000 land-cover map and beyond: Lessons learnt, strengths, weaknesses, possible improvements. In Proceedings, VEGETATION 2004 conference, Antwerp (B), 24-26 March 2004

Bauer M.E., Daughtry C.S.T., and Vanderbilt V.C. 1981. Spectral-agronimic relationships of corn, soybean, and wheat canopies, SR-P1-04187. Laboratory for Applications of Remote Sensing, Purdue University, West Lafayette, Indiana, 17pp.

Bauer M. E., Burk T. E., Ek A. R., Coppin P. R., Lime S. D., Walsh T. A., and Walters D. K., 1994. Satellite inventory of Minnesota forest resources. Photogrammetric Engineering and Remote Sensing, 60, pp. 287– 298.

Beaubien J., and Simard G., 1993, Methodologie de classification des donnees AVHRR pour la surveillance du couvert vegetal. Proceedings of the 16th Canadian Remote Sensing Symposium, Sherbrooke, Québec, 7–10 June 1993 (Québec: Canadian Remote Sensing Society), pp. 597–603.

Becker, F. and Li Z.L., 1990. Towards a local split window method over land surface, International Journal of Remote Sensing, 3, 369-393

Begue A., 1993. Leaf area index, intercepted photosynthetically active radiation and spectral vegetation indices: a sensitivity analysis for regular-clumped canopies. Remote Sensing of Environment, 46, pp. 45-59

Belward A., and Loveland T.R., 1995. The IGBP 1-km land cover project. In Proceedings of the 21st Annual Conference of the Remote Sensing Society, Southampton, UK, pp. 1099-1106

Belward A. S., 1996, The IGBP-DIS Global 1 km Land Cover Data Set (DISCover): proposal and implementation plans. IGBP-DIS Working Paper 13, International Geosphere–Biosphere Programme Data and Information System Office, Toulouse, France.

Berk A., Bernstein L.S., and Robinson D.C., 1989. MODTRAN: A moderate resolution model for LOWTRAN 7. Hanscom Air Force Base, Massachusetts: Air Force Geophysics Laboratory

Berthelot B. and Dedieu G., 2000. Operational method to correct VEGETATION satellite measurements from atmospheric effects, IGARS'2000, IEEE 2000 International, 2, pp. 831 - 833

Betts A.K., Ball J.H., Beljaars A.C.M., Miller M.J. and Viterbo P.A., 1996. The land-surface atmosphere interaction: a review based on observational and global modelling perspectives. Journal of Geophysical Research, 101, pp. 7209–7225.

Blackburn G.A., 1998. Spectral indices for estimating photosynthetic pigment concentrations: a test using senescent tree leaves, International Journal of Remote Sensing, 19, 4, pp. 657-675

Blackburn G.A., 1999. Relationships between Spectral Reflectance and Pigment Concentrations in Stacks of Deciduous Broadleaves. Remote Sensing of Environment, 70, pp. 224-227

Blackburn G.A. and Steele C.M. 1999. Towards the remote sensing of matorral vegetation physiology: relationships between spectral reflectance, pigment, and biophysical characteristics of semiarid bushland canopies. Remote Sensing of Environment. 70, pp. 278-292.

Bork E.W., West N.E., Price K.P., 1999. Calibration of broad- and narrow-band spectral variables for ranglenad cover component quantification. International Journal of Remote Sensing 20, 18, pp. 3641-3662

Bowers T. L., and Rowan L. C., 1996, Remote mineralogic and lithologic mapping of the Ice River Alkaline Complex, British Columbia, Canada, using AVIRIS data. Photogrammetric Engineering and Remote Sensing, 62, pp. 1379–1385.

Boyd D. S., and Duane W. J., 2001. Exploring spatial and temporal variation in middle infrared reflectance (at 3.75 mm) measured from the tropical forests of West Africa. International Journal of Remote Sensing, 22, 10, pp. 1861– 1878.

Braswell B.H., Hagen S.C., Frolking S.E., and Salas W.A., 2003. A multivariable approach for mapping sub-pixel land cover distributions using MISR and MODIS: Application in the Brazilian Amazon region. Remote Sensing of Environment, 87, pp. 243-256

Briottet X., Diligeard E., Snter R.and Deuze J.L., 1997. VEGETATION: Calibration of the Blue and Red Channels Using Rayleigh Scattering over Open Oceans, Proc. EUROPTO, European Symposium on Aerospace Remote Sensing, London

Brodley, C. E., and Utgoff, P. E., 1992. Multivariate versus univariate decision trees. Technical report 92-8. Department of Computer Science, University of Massachusetts, Amherst, MA, USA.

Broge N.H., Leblanc E., 2000. Comparing prediction power and stability of broadband and hyperspectral vegetation indices for estimation of green leaf area index and canopy chlorophyll density. Remote Sensing of Environment 76, pp. 156-172.

Brown J. F., Loveland T. R., Ohlen D. O., and Zhu Z., 1999. The global land-cover characteristics database: the user's perspective. Photogrammetric Engineering and Remote Sensing, 65, pp. 1069–1074.

Burgess D. W., and Pairman D., 1997, Bidirectional reflectance effects in NOAA AVHRR data. International Journal of Remote Sensing, 18, pp. 2815–2825.

Campbell J.B., 1996. Introduction to Remote Sensing, 2nd edition, Taylor and Francis, London

Cann A.J., 2004. Correlation. http://www-micro.msb.le.ac.uk/1010/DH3.html (6 May 2006)

Canters F., 1997. Evaluating the uncertainty of area estimates derived from fuzzy land-cover classification. Photogrammetric Engineering and Remote Sensing, 63, pp. 403–414.

Carder K.L., Chen F.R., Cannizzaro J.P., Campbell J.W. and Mitchell B.G., 2004. Performance of the MODIS semi-analytical ocean color algorithm for chlorophyll-a. Advances in Space Research, Vol.33, 7, pp. 1152-1159.

Carter G. A., 1994. Ratios of leaf reflectances in narrow wavebands as indicators of plant stress. International Journal of Remote Sensing, 15, pp. 697– 703.

Carter G. A.,1998. Reflectance bands and indices for remote estimation of photosynthesis and stomatal conductance in pine canopies. Remote Sensing of Environment, 63, pp. 61– 72.

Ceccato P., Flasse S, Tarantola S., Jacquemoud S. and Grégoire J-M., 2001. Detecting vegetation leaf water content using reflectance in the optical domain. Remote Sensing of Environment Vol. 77, 1, pp. 22-33

Champeaux J.L., Mucher C.A., Steunnocher K., Griguolo S., Wester K., Goutorbe J-P., Kressler F. Heunks C. and Van Katwijk V.F., 2000. The PELCOM Project: a 1-km pan European land cover database for environmental monitoring and use in meteorological models. IEEE 2000 International, Vol. 5, pp. 1915 - 1917

Changnon S.A. 1999. Impacts of 1997-98 El Niño -generated weather in the United States. Bulletin of the American Meteorological Society 80, 1, pp. 1819-1827.

Chapin F. S. III, Zavaleta E. S., Eviner V. T., Naylor R. L., Vitousek P. M., Reynolds H. L., Hooper D. U., Lavorel S., Sala O. E., Hobbie S. E., Mack M. C., and Diaz S., 2000. Consequences of changing biodiversity. Nature, 405, 234– 242.

Chen X., Tateishi R., and Wang C., 1999. Development o a 1-km landcover dataset of China using AVHRR data. ISPRS Journal of Photogrammetry and Remote Sensing, 54, pp. 305-316

Choudhury B. J.,1987. Relationships between vegetation indices, radiation absorption, and net photosynthesis evaluated by a sensitivity analysis. Remote Sensing of Environment, 22, pp. 209-233.

CIA, 2006. CIA The World Factbook. https://www.cia.gov/cia/publications/factbook/index.html (12 January 2006)

Cihlar J., Manak D., D'Iorio M., 1994. Evaluation of compositing algorithms for AVHRR data over land. IEEE Transactions on Geoscience and Remote Sensing 32, pp. 427–437.

Cihlar J.,Manak D., and Voisin N., 1994b. AVHRR bidirectionale reflectance effects and compositing. Remote Sensing of Environment, 48, pp. 77–88.

Cihlar J., Hung L., and Xiao Q., 1996, Land cover classification with AVHRR multichannel composites in northern environments. Remote Sensing of Environment, 58, pp. 36–51.

Cihlar J., Xiao Q., Beaubien J., Fung K., and Latifovic R., 1998, Classification by Progressive Generalization: a new automated methodology for remote sensing multichannel data. International Journal of Remote Sensing, 19, pp. 2685–2704.

Cihlar J., and Beaubien J., 1998, Land Cover of Canada 1995 Version 1.1. Digital data set documentation, Natural Resources Canada, Ottawa, Ontario.

Cihlar J., 2000. Land cover mapping of large areas from satellites: status and research priorities. International Journal of Remote Sensing, Vol. 21, 6 & 7, pp. 1093-1114

Cinderby S., 2002. Description of 2002 revised SEI land cover map. http://www.york.ac.uk/inst/sei/APS/projects.html (21 May 2006)

Clark W.C., 1985. Scales of climate impacts, in The Sensitivity of Natural Ecosystems and Agriculture to Climate Change. International Institute for Applied Systems Analysis, Laxenburg, Austria

Clark R. N., Swayze G. A., Gallagher A. J., King T. V. V. and Calvin W. M., 1993. The U.S. Geological Survey Digital Spectral Library, Version 1: 0.2 to 3.0 microns, U.S. Geol. Surv. Open File Rep., 93– 592, 1340 pp

Cloudhury B.J., 1987. Relationships between vegetation indices, radiation absorption and net photosynthesis evaluated by sensitivity analysis. Remote Sensing of Environment, 22, pp. 209-233

Coakley J.A., Jr., and Bretherton F.P., 1982. Cloud cover from high-resolution scanner data: detecting and allowing for partially filled fields of view. J. Geophys. Res., 87, pp. 4917-4932

Cochran W.G., 1977. Sampling techniques. John Wiley & Sons, New York, NY.

Cohen J., 1960. A coefficient of agreement for nominal scales. Educational and Psychological Measurement, 20, pp. 37–46

Collins W., 1978. Remote sensing of crop type and maturity. Photogrammetric Engineering and Remote Sensing, 26, pp. 43- 55.

Congalton R.G., and Green K., 1999. Assessing the Accuracy of Remotely Sensed Data: Principles and Practices. Lewis Publishers.

Cosnefroy H., Leroy M. and Briottet X., 1996. Selection and Characterization of Saharan and Arabian Desert Sites fir the Calibration of Optical Satellite Sensors. Remote Sensing of Environment, 58, pp. 101-114

Costa M. H., and Foley J. A., 2000. Combined effects of deforestation and doubled atmospheric CO2 concentrations on the climate of Amazonia. Journal of Climate, 13, 1, pp. 18– 34.

Cracknell A.P. and Hayes L.W., 1993. Atmospheric corrections to Passive Satellite Remote Sensing Data. Chapter 8 in Introduction to Remote Sensing, London: Taylor & Francis, pp. 116-158

Cracknell A.P.,1997. The Advanced Very High Resolution Radiometer, Taylor and Francis, London, 1997.

Cracknell A.P., 1999. Twenty years of publication of the International Journal of Remote Sensing. International Journal of Remote Sensing, Vol. 20, 18, pp. 3485-3491

Cracknell A.P., 2001. The exciting and totally unanticipated success of the AVHRR in applications for which it was never intended. Adv. Space Res. Vol. 28, 1, pp. 233-240

Curran P.J., 1983. Multispectral remote sensing for estimation of green leaf area index. Phil. Trans. Roy. Meteorol. Soc. A, 309, pp. 257-27

Curran P.J., 1985. Principles of Remote Sensing. London and New York, Longman

Curran P. J., 1994. Imaging spectrometry. Progress in Physical Geography, 18, 2, pp. 247– 266.

Dabrowska-Zielinska K., Kogan F.N., Ciolkosz A., Gruszczynska M. and Kowalik W., 2002. Modelling of crop growth conditions and crop yield in Poland using AVHRR-based indices. International Journal of Remote Sensing, Vol. 23, 6, pp. 1109-1123

Dalezios N.R., Papazafiriou Z.G., Papamichail D.M., Karacostas, T.S., 1991. Drought assessment for the potential of precipitation enhancement in Northern Greece. Theor. Appl. Clim. 44, 2, pp. 75– 88.

Dalezios N.R., Loukas A., Vasiliades L., Liakopoulos E., 2000. Severity-duration-frequency analysis of droughts and wet periods in Greece. Hydrol. Sci. J. 45, 5, pp. 751–769.

Daughtry C.S.T., Gallo K.D., and Bauer M.E., 1982. Spectral estimates of solar radiation intercepted by corn canopies. AgRISTARS Tech. Report sr-PZ-04236, Purdue Univ., West Lafayette, IN.

Dawson T. P., and Curran P. J., 1998. A new technique for interpolating the reflectance red edge position. International Journal of Remote Sensing, 19(11), 2133–2139.

De Badts E., 2002, Global Land Cover 2000: an evaluation of the SPOT VEGETATION sensor for land use mapping. Thesis report GIRS 2002-41, Wageningen University, The Netherlands.

Deering D. W., Rouse J. W., Haas R. H., and Schell J. A., 1975, Measuring `forage production' of grazing units from Landsat MSS data. Proceedings of the 10th International Symposium on Remote Sensing of Environment (Ann Arbor, MI: ERIM), Vol. II, pp. 1169- 1178.

Defelice T. P, Lloyd D., Meyer D.J., Baltzer T.T. And Piraino P., 2003 . Water vapour correction of the daily 1 km AVHRR global land dataset: part I – validation and use of the Water Vapour input field. International Journal of Remote Sensing, Vol. 24, 11, pp. 2365–2375

DeFries R. S., and Townshend J. R. G., 1994a. Global land cover: comparison of ground-based data sets to classifications with AVHRR data, in Environmental Remote Sensing from Regional to Global Scales (G. Foody and P. Curran, Eds.), Wiley, Chichester, pp. 84-110.

DeFries R.S. and Townshend J.G.R., 1994b. NDVI derived land cover classification at a global scale. International Journal of Remote Sensing, 5, pp. 3567-3586

DeFries R., Hansen M., and Townshend J., 1995. Global Discrimination of Land Cover Types from Metrics Derived from AVHRR Pathfinder Data. Remote Sensing of Environment, 54, pp. 209-222

DeFries R.S., and Belward A.S., 2000. Global and regional land cover characterization from satellite data: an introduction to the Special Issue. International Journal of Remote Sensing, Vol. 21, 6 & 7, pp. 1083-1092

DeFries R.S., Hansen M., Townshend J.G.R., and Sohlberg R., 1998. Global land cover classification at 8 km resolution: the use of training data derived from Landsat imagery in decision tree classifiers. International Journal of Remote Sensing, 19, pp. 3141-3168

DeFries R.S., Hansen M.C., Townshend J.R.G., Janetos A.C. and Loveland T.R., 2000. A new global 1-km dataset of percentage tree cover derived from remote sensing. Global Change Biology, 6, pp. 247-254

Delincé J., 2000. Outline of project LUCAS.- Eurostat Working Document ESTAT/LAND/33, WP Land Use Statistics May 2000 Area frame surveys 25

Delincé J., 2001. A European approach to area frame survey. Proceedings of the Conference on Agricultural and Environmental Statistical Applications in Rome (CAESAR), June 5-7, Vol. 2 pp. XXV.1-10.

Demetriades-Shah T. H., Steven M. D., and Clark J. A., 1990. High resolution derivative spectra in remote sensing. Remote Sensing of the Environment, 33, pp. 55-64.

Di Gregorio A., and Jansen L. J. M., 2000. Land cover classification system (LCCS) (pp. 180). Rome: F.A.O.

Diallo O., Diouf A., Hanan N.P., Ndiave A., and Presvost Y., 1991. AVHRR monitoring of savannah primary production in Senegal, West Africa. International Journal of Remote Sensing, 12, pp. 125-133

Dickinson R. E., and Henderson-Sellers A., 1988. Modelling tropical deforestation: a study of GCM land-surface parameterizations. Quarterly Journal of the Royal Meteorological Society, 114, pp. 439–462.

Dillegeard E., Briottet X., Deuze J.L. and Santer R., 1996. SPOT calibration of XS1 and XS2 channels using Rayleigh scattering over clear oceans, Proc. SPIE, 2957, pp. 373-379

Dinguirard M. and Slater P.N., 1998. Calibration of space-multispectral imaging sensors: A review, Remote Sensing of Environment 86, pp. 194-205

Domenikiotis C., Spiliotopoulos M., Tsiros E., Dalezios N.R., 2004. Early cotton yield assessment by the use of the NOAA/AVHRR derived Vegetation Condition Index in Greece. International Journal of Remote Sensing 25, pp. 2807–2817.

Driese K. L., Reiners W. A., Merrill E. H., and Gerow K. G., 1997, A digital land cover map of Wyoming, USA: a tool for vegetation analysis. Journal of Vegetation Science, 8, pp. 133–146.

Duchemin B., Goubier J., and Courrier G. 1999. Monitoring Phenological Key Stages and Cycle Duration of Temperate Deciduous Forest Ecosystems with NOAA/AVHRR Data. Remote Sensing of Environment, 67, pp. 68-82

Duchemin B., Maisongrande P., Dedieu G ., Leroy M., Roujean J .L., Bicheron P., Hautecoeur O., and Lacaze R., 2000. A 10-days compositing method accounting for bidirectional effects. Proceedings of the VEGETATION 2000, Belgirate Italy (3 – 6 April 2000), pp. 313 – 318.

Duchemin B., Berthelot B., Dedieu G., Leroy M., and Maisongrande P., 2002. Normalisation of directional effects in 10-day global syntheses derived from VEGETATION/SPOT: II. Validation of an operational method on actual data sets. Remote Sensing of Environment 8, pp. 101-113.

Duggin M.J., 1985. Factors limiting the discrimination and quantification of terrestrial features using remotely sensed radiance. International Journal of Remote Sensing, 6, pp. 3-21

Dwyer E., Pinnock S., Gregoire J.-M., and Pereira J.M.C., 2000, Global spatial and temporal distribution of vegetation fire as determined from satellite observations. International Journal of Remote Sensing, 21, pp. 1289–1302.

Dymond J. R., Begue A. and Loseen D., 2001. Monitoring land at regional and national scales and the role of remote sensing. JAG Vol. 3, 2

Eastwood J. A., Plummer S.E., Wyatt B.K. and Stocks B.J., 1998. The potential of SPOT-Vegetation data for fire scar detection in boreal forests. International Journal of Remote Sensing, Vol. 19, 18, pp. 3681 – 3687

EEA, 2006a, CLC1990. http://dataservice.eea.europa.eu/dataservice/available2.asp?type=findkeyword&theme=CLC1990 (20 March 2006)

EEA, 2006b. Land cover Part1. http://reports.eea.europa.eu/COR0-part1/en/land_coverPart1.pdf (20 March 2006)
EEA, 2006c. CLC time coverage reference EEA153861. http://dataservice.eea.europa.eu/dataservice/metadetails.asp?id=820 (20 March 2006)
EEA, 2006d. The thematic accuracy of CORINE land cover 2000 Assessment using LUCAS (land use/cover area frame statistical survey). EEA Technical report, No 7/2006
Eidenshink J. C., Faundeen J. L., 1994. The 1-km AVHRR global land data set: First stages in implementation. International Journal of Remote Sensing 15, pp. 3443–3462.
Elvidge C.D., Chen, Z., and Groeneveld, D.P. 1993. Detection of trace quantities of green vegetation in 1990 AVIRIS data. Remote Sensing of Environment. 44, pp. 271-279
Elvidge C. D., and Chen Z.,1995. Comparison of broadband and narrowband red and near-infrared vegetation indices. Remote Sensing of Environment, 54, pp. 38– 48.
Emberson L. and Cinderby S., 2002. The Stockholm Environment Institute (SEI) land cover map: Potential application within UN/ECE pollutant deposition and effects work. http://www.sei.se/atmosphere/Land-cover_document.pdf (30 March 2006)
EM-DAT, 2007. Disaster Profile for Droughts. http://www.em-dat.net/disasters/Visualisation/profiles/natural-table-emdat_disasters.php?dis_type=Drought&Submit=Display+Disaster+Profile (30 December 2007)
Erbertseder T., Tungalagsaikhan P., Bittner M., Meisner R., Schroedter M. and Dech S., 1999. Towards an operational atmospheric correction for AVHRR landsurface products. Geoscience and Remote Sensing Symposium, 1999. IGARSS '99 Proceedings. IEEE 1999 International, Hamburg, Germany, Vol. 4, pp. 2227-2229
ERS-1, 1989. Reference Manual, Technical note, ESA, DC-MA-EOS-ED-0001.
ESA, 1992. Remote sensing map of Europe (1:6,000,000). European Space Agency / ESTEC, Noordijk.
ESA, 2007. ESA-Living planet Programme-MetOp. http://www.esa.int/esaLP/LPmetop.html (30 December 2007)
Eva H.D., Belward A.S., De Miranda E.E., Di Bella C.M., Gond V., Huber O., Jones S., Sgrenzaroli M. and Fritz S., 2004. A land cover map of South America. Global Change Biology, 10, pp. 732–745.f
Eyles G.O., Jessen M.R., Shepherd T.G., Brown L.J. and Stephens P.R., 1993. Land monitoring guidelines for Environment Waikato. Landcare Research contract report LC9394/26. Landcare Research, Christchurch.
FAO, 1946. Forestry and forest products: World situation 1937-1946. FAO, Rome.
FAO, 1947. The growth of the world's forests. Unasylva 1, 1, 27-36.
FAO, 1960. The world's forest resources. Unasylva 14, 3.
FAO, 1963. World Forest Inventory. FAO, Rome.
FAO, 1996. Ethiopia: country report to the FAO international technical conference on plant genetics resources, Leipzig, Germany
FAO, 2005. Global Forest Resources Assessment 2005. ftp://ftp.fao.org/docrep/fao/008/A0400E/A0400E00.pdf (25 January 2006)

FAO, 2000. Crop production statistics. http://www.fao.org. (December 2000)
FAO-Agristat, 1990. FAO Vol. 1, United Nations
FAO-Cartographia, 1980. Land use map of Europe (1:2,500,000) Cartographia, Budapest
Fell F., Fischer J., Preusker R. and Schröder T., 2001. Automated atmospheric correction of AVHRR channel 1 and 2 data using dark surface targets. In: Proceedings of the International Geoscience and Remote Sensing Symposium (IGARSS), Sydney, Australia, 2001.
Fensholt R., 2004. Earth observation of vegetation status in the Sahelian and Sudanian West Africa: comparison of TERRA MODIS and NOAA AVHRR satellite data. International Journal of Remote Sensing, 25, pp. 1641-1659
Fensholt R., and Sandholt I., 2005. Evaluation of MODIS and NOAA AVHRR vegetation indices with in situ measurements in a semi-arid environment. International Journal of Remote Sensing, Vol. 26, No. 12, pp. 2561-2594
Fleig A. J., Heath D. F., Klenk K. F., Oslik N., Lee K. D., Park H., Bartia P. K., Gordon D., 1983. User's guide for the Solar Backscattered Ultraviolet (SBUV) and the Total Ozone Mapping Spectrometer (TOMS) RUT-S and RUT-T data Sets. October 31, 1978 to November 1980. NASA Reference Publication 1112
Fleischmann C. G., and Walsh S. J., 1991,Multi-temporal AVHRR digital data: an approach for landcover mapping of heterogeneous landscapes. Geocarto International, 4, pp. 5–20.
Fleiss J.L., Cohen J., and Everitt B.S., 1969. Large-sample standard errors of kappa and weighted kappa. Psychological Bulletin, Vol. 72, pp. 323-327
Foody G.M., 1996a. Fuzzy modelling of vegetation from remotely sensed imagery. Ecological Modelling, 85, pp. 3-12
Foody G. M., 1996b. Approaches for the production and evaluation of fuzzy land cover classification from remotely-sensed data. International Journal of Remote Sensing, 17, pp. 1317– 1340.
Foody G. M., and Arora M. K., 1997. An evaluation of some factors affecting the accuracy of classification by an artificial neural network. International Journal of Remote Sensing, 18, pp. 799– 810.
Foody G. M., 1999. The continuum of classification fuzziness in thematic mapping. Photogrammetric Engineering and Remote Sensing, 65, pp. 443– 451.
Foody G.M., 2002. Status of land cover classification accuracy assessment. Remote Sensing of Environment, 80, pp. 185-201.
Forster B. C., and Best P., 1994. Estimation of SPOT P-mode point spread function and derivation of a deconvolution filter. ISPRS Journal of Photogrammetry and Remote Sensing, 49, pp. 32– 42.
Fraser R. S., Bahethi O. P., and Al-Abbas A. H., 1977. The effect of the atmosphere on classification of satellite observations to identify surface features. Remote Sensing of Environment, 6, pp. 229-238
Fraser R.S., and Kaufman Y.J., 1986. Calibration of satellite sensors after launch. Appl Opt., 25, pp. 1177-1185
Fraser R.H., and Latifovic R., 2003. Coarse Resolution Satellite Mapping of Insect-Induced Tree Defoliation and Mortality 2003 IEEE International Geoscience and Remote Sensing SymposiumJuly 21-25, 2003 Toulouse, France, Vol. II, pp. 978 – 978

Friedl M.A., Michaelsen J., Davis F.W., Walker H., and Schimel D.S., 1994. Estimating grassland biomass and leaf area index using ground and satellite data. International Journal of Remote Sensing 15, pp. 1401-1420

Friedl M.A., and Brodley C.E., 1997. Decision tree classification of land-cover from remotely sensed data, Remote Sensing of Environment 61, 3, pp. 399-409

Friedl M.A., McIver D.K., Hodges J.C.F., Zhang X. Y., Muchoney D., Strahler A.H., Woodcock C.E., Gopal S., Schneider A., Cooper A., Baccini A., Gao F. and Schaaf C., 2002. Global land cover mapping from MODIS: algorithms and early results, Remote Sensing of Environment, Vol. 83, 1-2, pp. 287-302

Fritz S., Bartholomé E., Belward A., Hartley A., Stibig H-J., Eva H., et al., 2003. Harmonization, mosaicking, and production of the Global Land Cover 2000 database. Ispra, Italy Joint Research Center (JRC).

Fuller R.M., Smith G.M., Sanderson J.M., Hill R.A. and Thomson, A.G., 2002. Land Cover Map 2000: construction of a parcel-based vector map from satellite images. Cartographic Journal, 39, pp. 15-25

Gabban A., San-Miguel-Ayanz J., Barbosa P., and Liberta G., 2006. Analysis of NOAA-AVHRR NDVI inter-annual variability for forest fire risk estimation. International Journal of Remote Sensing, Vol. 27, No. 8, pp. 1725–1732.

Gallego F.J., 1995. Sampling frames of square segments. Report EUR 16317. Joint Research Centre, European Commission, Brussels.

Gallego F.J., 1998, On the feasibility of diachronic regression estimators with ground survey and Landsat TM data. International Journal of Remote Sensing. Vol. 19, n. 8, pp. 1621-1625.

Gallego F.J., 1999. CROP AREA ESTIMATION IN THE MARS PROJECT. Conference on ten years of the MARS Project, Brussels

Gallo K., Ji L., Reed B., Dwyer J., and Eidenshink, J., 2004. Comparison of MODIS and AVHRR 16-day normalized difference vegetation index composite data. Geophysical Research Letters, 31, 7, L07502.

Gamon J.A., Field C.B., Goulden M.L., Griffin K.L., Hartley A.E., Joel G., Penuelas J., Valentini, R., 1995. Relationships between NDVI, canopy structure, and photosynthesis in three Californian vegetation types. Ecological Applications 5, 1, pp. 28– 41.

Gao B.C., 2000. A Practical Method for Simulating AVHRR-Consistent NDVI Data Series Using Narrow MODIS Channels n the 0.5-1.0 mm Spectral Range. IEEE transactions on geoscience and remote sensing, Vol. 38, 4, pp. 1969-1975

Gausman H. W., 1973. Reflectance, transmittance, and absorptance of light by subcellular particles of spinach (Spinacia oleracea L.) leaves. Agronomy Journal, 65, pp. 551– 553.

Giglio L., Descloitres J., Justice C.O. and Kaufman Y.J., 2003. An Enhanced Contextual Fire Detection Algorithm for MODIS. Remote Sensing of Environment, Vol. 87, 2-3, pp. 273-282.

Giovacchini A., Brunetti A., 1992, Agricultural Statistics by Remote Sensing in Italy: an Ultimate Cost Analysis. Conference on the application of remote sensing to agricultural statistics. Belgirate. Office for Publications of the E.C. Luxembourg.

Giri C., Defourny P., and Shrestha S., 2003. Land cover characterization and mapping of continental Southeast Asia using multi-resolution satellite sensor data. International Journal of Remote Sensing, 24, 21, pp. 4181– 4196.

Giri C., Zhu Z., and Reed B., 2005. A comparative analysis of the Global Land Cover 2000 and MODIS land cover data sets. Remote Sensing of Environment 94, pp. 123-132

Gitelson A.A., Merzlyak M.N., 1996. Signature analysis of leaf reflectance spectra: Algorithm development for remote sensing of chlorophyll, Journal of plant physiology, 148, 3-4, pp. 494-500.

Gitelson A.A., and Kaufman Y.J., 1998. MODIS NDVI optimization to fit the AVHRR data series—Spectral considerations: Short communication. Remote Sensing of Environment 66, pp. 343–350.

GMFS, 2006. Vegetation productivity indicator, ESA ESRIN Contract No. 19402/05/I-LG, http://www.gmfs.info/publications/documents/GMFS_S5_ProductSheet_VPI.pdf

Gond V. and Bartholomé E., 2001. Classifying land cover types with VEGETATION data in dryland: a case study in Burkina Faso. Proceedings of the VEGETATION 2000 Conference, Belgirate, Italy, 3–6 April 2000, G. Saint (Ed.) (Toulouse: CNES and Ispra: Joint Research Centre), pp. 443–444.

Goodrum G., Kidwell K.B. and Winston W., 2000. NOAA KLM USER'S GUIDE. US Department of Commerce, National Climatic Center, Satellite Data Service Division , Washington, D.C.

Gopal S., Sklarew D.M., and Lambin E., 1994. Fuzzy-neural network in multi-temporal classification of land-cover change in the Sahel. In Proceeding of the DOSES Workshop on New Tools for Spatial Analysis, Lisbon, Portugal, DOSES, EUROSTAT, ECSC-EC-EAEC, Brussels, Luxembourg, pp. 55-58

Gopal S., Woodcock C.E., and Strahler A.H., 1999. Fuzzy Neual Network Classification of Global Land Cover from a 1° AVHRR Data Set. Remote Sensing of Environmen 67, pp. 230-243

Gordon H.R., Brown J.W., Brown O.B., Evans R.H., and Clark D.K., 1983. Nimbus-7 CZCS: reduction in its radiometric sensitivity with time. Appl. Opt., 22, 24, pp. 3929-3931

Goward S.N., Tucker C.J. and Dye D.G., 1985. North American vegetation patterns observed with NOAA-7 advanced very high resolution radiometer, Vegetatio 64, pp. 3-14

Goward S.N., and Dye D.G., 1987. Evaluating North American net primary productivity with satellite observations. Adv. Space Res., 7, 11, pp. 165-174

Goward S.N., Markham B., Dye D.G., Dulaney W., and Yang J., 1991. Normalized Difference Vegetation Index measurements from the Advanced Very high Resolution Radiometer. Remote Sensing of Environment, 35, pp. 257-277

Goward S.N., and Huemmrich K.F., 1992. Vegetation canopy PAR absorbance and the normalized difference vegetation index : An assessment using the SAIL model. Remote Sensing of Environment, 39, pp. 119–140

Goward, D. G., Turner, S., Dye, D. G., Liang, J. 1994. University of Maryland improved Global Vegetation Index. International Journal of Remote Sensing 15, pp. 3365–3395.

Gray T.I., and McCrary D.G., 1981. The environmental vegetation index, a tool potentially useful for arid land management. AgRISTARS Report EW-N1-04076 JSC-17132

Guo X., and Richard P., 2004. Assessing Canadian prairie drought with satellite and climate data. Environmental Informatics Archives, 2, pp. 422-430

Gutman G.G., 1991. Vegetation Indices from AVHRR Data: Am update and future Prospects. Remote Sensing of Environment, 35, pp. 121-136

Gutman G.G., Tarpley D., and Ohring G., 1987. Cloud screening for determination of land surface characteristics in reduced resolution satellite data set. International Journal of Remote Sensing, 8, 6, pp. 859-870

Hack B., and English R., 1996. National land cover Mapping by remote sensing. World Development, 24, 5, pp. 845-855

Hall D.K., Riggs G.A. and Salomonson V.V., 1995. Development of methods for mapping global snow cover using moderate resolution imaging spectroradiometer data. Remote Sensing of Environment, Vol. 54, 2, pp. 127-140.

Hall F.G., Strebel D.E., Nickeson J.E., and Goetz S.J., 1991. Radiometric rectification: Toward a common radiometric response among multidate, multisenseor images. Remote Sensing of Environment, 35, pp. 11-27

Han K.-S., Champeaux J.-L. and Roujean J.-L., 2004. A land cover classification product over France at 1 km resolution using SPOT/VEGETATION data. Remote Sensing of Environment, 92, pp. 52–66.

Hansen M., Dubayah R., and DeFries R., 1996. Classification trees: An alternative to traditional land cover classifiers. International Journal of Remote Sensing, 17, pp. 1075-1081

Hansen M.C., and Reed B., 2000. A comparison of the IGBP DISCover and University of Maryland 1 km global land cover products. International Journal of Remote Sensing, Vol. 21, No 6 & 7, pp. 1365-1373

Hansen M.C., DeFries R.S., Townshend J.R.G., and Sohlberg R., 2000. Global land cover classification at 1 km spatial resolution using a classification tree approach. International Journal of Remote Sensing, 21, 6-7, pp. 1331-1364

Hay G.J., Niemann K.O., Goodenough D.G., 1997. Spatial thresholds, image-objects, and upscaling: a multi-scale evaluation. Remote Sensing of Environment, 62, pp. 1–19.

Hayward K., 2002. Crop insurance as a risk management tool for dryland agriculture . Proceedings of Soils and Crops 2002. Saskatoon, Saskatchewan, Canada. February 17-18.

Heidinger A.K., Cao C., and Sullivan J.T., 2002. Using Moderate Resolution Imaging Spectrometer (MODIS) to calibrate advanced very high resolution radiometer reflectance channels. Journal of Geophysical Research, Vol. 107, D23, 4702

Heidinger A. K., Sullivan J. T. and Rao N., 2002b. Calibration of visible and nearinfrared channels of the NOAA-12 AVHRR using time-series of observations over deserts. International Journal of Remote Sensing, Vol. 24, 18, pp. 3635-3649

Henderson-Sellers A., Wilson M., Thomas G., and Dickinson R., 1986, Current, global land surface data sets for use in climate-related studies. Technical Report, NCAR, Boulder, CO, USA

Henry P., Dinguirard M. and Bodilis M., 1993. SPOT multi-temporal calibration over stable deserts areas. Proc. SPIE, International Symposium on Optical Engineering and Photonics, 1938, Orlando.

Henry P., Gentet T., Arnaud M., and Andersson C., 1996. The VEGETATION system: A global Earth monitoring from SPOT satellites. Acta Astronautica Vol. 38, No 4-8, pp. 487-492

Henry P. and Meygret A., 2001a. Calibration of VEGETATION cameras on-board SPOT4. Proceedings of the VEGETATION 2000 conference, Belgirate, Italy, 3–6 April 2000, G. Saint (Ed.) (Toulouse: CNES and Ispra: Joint Research Centre), pp. 23–32.

Henry P. and Meygret A., 2001b. Calibration of HRVIR and VEGETATION cameras on SPOT4. Adv. Space Res. Vol. 28, No. 1, pp. 49-58

Henry P., Reulet J.F. and Tavera F., 2004. VEGETATION system: Operational status and performance. VEGETATION international user conference, Antwerp, 24-26 March, 2004

Hillger D. and Toth G., 2006. Polar-orbiting weather satellites. http://www.cira.colostate.edu/ramm/hillger/polar-wx.htm#tiros-n (4 March 2006)

Hodges J., 2002. Validation of the consistent year V003 MODIS land cover product. http://www-modis.bu.edu/landcover/userguidelc/consistent.htm

Hobbs T. J., 1995. The use of NOAA-AVHRR NDVI data to assess herbage production in the arid rangelands of Central Australia. International Journal of Remote Sensing, 16, 1289-1302.

Holben B. N., 1986. Characteristics of Maximum-value Composite Images from Temporal AVHRR data, International Journal of Remote Sensing, 7, 1417-1434.

Holben B.N., Eck T.F., and Frasher R.S., 1991. Temporal and spatial variability of aerosol optical depth in the Sahel region in relation to vegetation remote sensing. International Journal of Remote Sensing, 12, 1147-1163

Holben B.N., Vermote E., Kaufman Y.J., Tanre D., and Kalb V., 1992. Aerosol retrieval overland from AVHRR data-Application for atmospheric correction. I.E.E.E. Transactions on Geoscience and Remote Sensing, 30, 212-221

Homer C. G., Ramsey R. D., Edwards T. C. Jr, and Falconer A., 1997, Landscape cover type modelling using a multi-scene Thematic Mapper mosaic. Photogrammetric Engineering and Remote Sensing, 63, 59–67.

Horler D. N. H., Dockray M., and Barber J., 1983. The red edge of plant leaf reflectance. International Journal of Remote Sensing, 4, 273- 288.

Houghton R. A., Skole D. L., Nobre C. A., Hackler J. L., Lawrence K. T., and Chomentowski W. H., 2000. Annual fluxes of carbon from deforestation and regrowth in the Brazilian Amazon. Science, 403, 301– 304.

Hsieh P-F., Lee L. C., and Chen N-Y., 2001. Effect of Spatial Resolution on Classification Errors of Pure and Mixed Pixels in Remote Sensing., IEEE Transactions on Geoscience and Remote Sensing, Vol. 39, No 12, pp. 2657-2663

Hu C., Chen Z., Clayton T.D., Swarzenski P., Brock J.C. and Muller-Karger F.E., 2005. Erratum to "Assessment of estuarine water-quality indicators using MODIS medium-resolution bands: Initial results from Tampa Bay, FL" [Remote Sensing of Environment 93(2004) 423-441], Remote Sensing of Environment, Vol. 94, 3, Pages 425-427.

Huang C., Townshend J.R.G., Liang S., Kalluri S.N.V., and DeFries R.S., 2002. Impact of sensors' point spread function on land cover characterization: assessment and deconvolution. Remote Sensing of Environment, 80, 203-212

Huete A.R., Justice C.O., and Van Leeuwen W.J.D., 1999. MODIS Vegetation Index (MOD 13). Version 3. Algorithm Theoretical Basis Document. http://modis.gsfc.nasa.gov/data/atbd/land_atbd.html

Huh O.K., 1991. Limitations and capabilities of the NOAA satellite advanced very high resolution radiometer (AVHRR) for remote sensing of the Earth's surface. Preventive Veterinay Medicine 11: 167-183.

Hutchison K.D., 2003. Applications of MODIS satellite data and products for monitoring air quality in the state of Texas, Atmospheric Environment, Vol. 37, 17, Pages 2403-2412.

HyVista, 2007. HyMap Sensor. http://www.hyvista.com/hyvistaweb/subPage.php?pageid=23 (15 January 2007)

Ichoku C., Kaufman Y.J., Remer L.A. and Levy R., 2004. Global aerosol remote sensing from MODIS, Advances in Space Research, Vol. 34, 4, Pages 820-827.

Illera P., Fernandez A., and Delgrado, J.A., 1996, Temporal evolution of the NDVI as an indicator of forest fire danger. International Journal of Remote Sensing, 17, pp. 1093–1105.

Jackson R.D., 1983. Spectral indices in n-space. Remote Sensing of Environment, 13, pp. 1401-1429

Jakubauskas M. E., and Price K. P.,1997. Empirical relationships between biotic and spectral factors of Yellowstone lodgepole pine forests. Photogrammetric Engineering and Remote Sensing, 63, 12, pp. 1375–1381.

James M. E., and Kalluri S. N. V., 1994. The Pathfinder AVHRR land data set: An improved coarse resolution data set for terrestrial monitoring. International Journal of Remote Sensing, 15, pp. 3347-3363

Janetos A. C., and Justice C. O., 2000. Land cover and global productivity: A measurement strategy for the NASA programme. International Journal of Remote Sensing, 21, pp. 1491– 1512.

Jensen J.R., Cowen D., Narumalani S., Weatherbee O., and Althausen J., 1993. Evaluation of CoastWatch Change Detection Protocol in South Carolina. Photogrammetric Engineering and Remote Sensing, 59, 6, 1039-1046

Jensen J.R., 1996. Introductory digital image processing: A remote sensing perspective (pp. 236–238). New Jersey: Prentice.

Jensen J. R., 2000. Remote sensing of the environment: An earth resource perspective. Upper Saddle River, NJ: Prentice-Hall.

Jensen J.R., 2005. Electromagnetic Radiation Principles and Radiometric Correction. Chapter 6 in Introductory Digital Image Processing A Remote Sensing Perspective. 3rd Edition, Upper Saddle River, NJ: Pearson Prentice Hall.

Ji R., Xie B.Y., Li D.M., Li Z. and Zhang X., 2004. Use of MODIS data to monitor the oriental migratory locust plague, Agriculture, Ecosystems & Environment, Vol. 104, 3, pp. 615-620.

Johnson G.E., Achutuni V.R., Thiruvengadachari S., and Kogan F., 1993. The Role of NOAA Satellite Data in Drought Early Warning and Monitoring, in book Drought

Assessment, Management, and Planning: Theory and Case Studies. Ed. Wilhite D.A., Kluwer Academic Publishers, Boston/Dordrecht/London, pp. 31-49

Johnson S.G., 2006. Visible/Infrared Imager Radiometer Suite (VIIRS) National Polar-orbiting Operational Environmental Satellite System Business Development, Raytheon Company, Space and Airborne Systems, Santa Barbara Remote Sensing, 75 Coromar Drive, B-30, M/S-73 Goleta, California

Johnson, G.E. A. Van Dijk, and C.M. Sakamoto, 1987: The use of AVHRR data in operational agricultural assessment in Africa. Geocarto International, 1:41-60

Justice C.O., Townshend J.R.G., Holben B.N. and Tucker C.J., 1985. Analysis of the phenology of global vegetation using meteorological satellite data. International Journal of Remote Sensing, 6, pp. 1271-1318

Karaska M. A., Huguenin R. L., Van Blaricom D., and Savitsky B., 1995. Subpixel classification of cypress and tupelo trees in TM imagery. Proceedings of the 1995 ACSM/ASPRS Annual Convention and Exposition, 3, pp. 856– 865.

Kaufman Y.J., and Sendra C., 1988. Automatic atmospheric correction. International Journal of Remote Sensing, 9, pp. 1357-1381

Kaufman Y.J., and Holben B.N., 1993. Calibration of the AVHRR visible and near-IR bands by atmospheric scattering, ocean glint and desert reflection. International Journal of Remote Sensing, 14, pp. 21-52

Kaufman Y.J. and Tanre D., 1998. Algorithm for remote sensing of aerosol from MODIS. MODIS Algorithm Theoretical Basis Document.

Kaufmann R.K., Zhou L., Knyazikhin Y., Shabanov N., Myneni R., and Tucker C.J., 2000. Effect of orbital drift and sensor changes on the time series of AVHRR vegetation index data. IEEE Transactions on Geoscience and Remote Sensing, 38, pp. 2584-2597

Kavzoglu T., 2001. An investigation of the design and use of feed-forward artificial neural networks in the classification of remotely sensed images. PhD thesis, University of Nottingham, Nottingham, UK.

Kawata Y., Ohtani A., Kusaka T. and Ueno S., 1990. Classification Accuracy for the MOS-1 MESSR Data Before and After the Atmospheric Correction. IEEE Transactions on Geoscience and Remote Sensing, 28, pp. 755-760

Kelly P. M., and White J.M., 1993, Preprocessing remotely-sensed data for efficient analysis and classification. Knowledge-based systems in aerospace and industry: applications of artificial intelligence. Proceedings SPIE, pp. 24–30.

Kempler S., 2006a. GES DISC DAAC Data Guide:
Total Ozone Mapping Spectrometer (TOMS) Level 2 Orbital Ozone and Reflectivity Data Set (Version 7),
http://daac.gsfc.nasa.gov/guides/GSFC/guide/tomsl2_dataset.gd.shtml#7. (26 August 2006)

Kempler S., 2006b. NDVI Data from AVHRR Land Pathfinder.
http://daac.gsfc.nasa.gov/interdisc/readmes/pal_NDVI.shtml (26 August 2006)

Kennedy P. J., Belward, A. S. and Grigoire, J-M., 1994. An improved approach to fire monitoring in West Africa using AVHRR data. International Journal of Remote Sensing, 15, pp. 2235-255.

Kidwell K B. 1984. NOAA polar orbital data users' guide (TIROS-N, NOAA 6,7,8). NOAA National Climate Center, Washington, D.C.

Kidwell K.B., 1990. Global Vegetation Index User's Guide, U.S. Department of Commerce, NOAA, Washington, D.C.

Kidwel K.B., 1998. NOAA Polar Orbiter Data (TIROS-N, NOOA-6, NOOA-7, NOOA-8, NOOA-9, NOOA-10, NOAA-11, NOAA-12, NOOA-13, NOAA-14) Users Guide: Washington, D.C., NOAA/NESDIS.

Kim H.H. and Elman G.C., 1990. Normalization of satellite imagery. Int. J. Remote Sensing, 8, pp. 1331-1347

Kimes D.S., Holben B.N., Tucker C.J. and Newcomb W.W., 1984. Optimal Directional View Angles for Remote-Sensing Missions. International Journal of Remote Sensing, Vol.5, pp. 887-908.

Kimes D. S., Newcomb W. W., Tucker C. J., Zonneveld I. S., Van Wijngaarden W., De Leeuw J., and Epema G. F., 1985. Directional reflectance factor distribution for cover types of Northern Africa. Remote Sensing of Environment, 18, 1-19.

King M., 2006. MODIS Atmosphere, Cloud Mask. http://modis-atmos.gsfc.nasa.gov/MOD35_L2/format.html (27 May 2006)

Klein A.G. and Barnett A.C., 2003. Validation of daily MODIS snow cover maps of the Upper Rio Grande River Basin for the 2000-2001 snow year. Remote Sensing of Environment, Vol. 86, 2, pp. 162-176.

Kleinn C., Coralles L., Morales D., 2002. Forest area in Costa Rica: a comparative study oftropical forest cover estimates over time. Environmental Monitoring and Assessment 73, pp. 17–40.

Kneizys F.X., Shettle E.P., Gallery W.O., Chetwynd J.H., Abreu L.W., Selby J.E.A., Clough S.A. and Fenn R.W.,1983. Atmospheric transmittance/radiance: computer code LOWTRAN 6. Air Force Geophysics Laboratroy, Report AFGL-TR-83-0187, Hanscom AFB, MA.

Kneizys F.X., Shettle E.P., Abreu L.W., Chetwynd J.H., Andreson G.P., Gallery W.O., Selby J.E.A. and Clough S.A., 1988. User's guide to LOWTRAN 7. Hanscom Air Force Base, Massachusetts: Air Force Geophysics Laboratory

Kogan F.N., 1990a. Remote sensing of weather impacts on vegetation in non-homogeneous areas. International Journal of Remote Sensing, 11, 8, pp. 1405-1419

Kogan F.N., 1990b. Monitoring the 1988 US Drought from Satellite, I : Proceedings 5th Conference on Satellite Meteorology and Oceanography, London, 3-7/09/1990, pp. 186

Kogan F.N., and Sullivan J., 1993. Development of global drought-watch system using NOAA/AVHRR data, Adv. Space Res., 13, 5

Kogan F. N., 1994. NOAA plays leadership role in developing satellite technology for drought watch. Earth Obs. Mag. September, pp. 18–21.

Kogan F.N., 1995a. Application of vegetation index and brightness temperature for drought detection. Adv. Space Res. Vol. 15, No. 11, pp. 91-100

Kogan F.N., 1995b. Droughts of the Late 1980s in the United States as Derived from NOAA Polar Orbiting Satellite Data. Bull. Of Am. Met. Soc., 76, pp. 655-668

Kogan F. N., 1997. Global drought watch from space. Bulletin of American Meteorological Society 78, pp. 621–636.

Kogan F. N., 2000. Contribution of remote sensing to drought early warning. In Early warning systems for drought preparedness and drought management, ed. D.A. Wilhite and D.A. Wood. 75–87. Geneva: World Meteorological Organization.

Kogan F. N., and Zhu X., 2001. Evolution of long-term errors in NDVI time series: 1985–1999. Advances in Space Research 28, pp. 149–153.

Koomanoff V.A., 1989. Analysis of global vegetation patterns: a comparison between remotely data and a conventional map, Biogeography Research Series, Report #890201. Department of Geography, University of Maryland, college Park

Kumar L., Schmidt K.S., Dury S., and Skidmore A.K., 2001. Review of hyperspectral remote sensing and vegetation science. In Van Der Meer, F. (editor). Hyperspectral remote sensing (Kluwer Academic Press: Dordrecht).

Kummer D.M., 1992. Deforestation in the Postwar Philippines. University ofChicago, Chicago (Geography Research Paper 234).

Lambert N. J., Ardo J., Rock B. N., and Vogelmann J. E.,1995. Spectral characterization and regression-based classification of forest damage in Norway spruce stands in the Czech Republic using Landsat Thematic Mapper data. International Journal of Remote Sensing, 16, pp. 1261– 1287.

Lambin E.F., and Ehrlich, 1996a. The surface temperature-vegetation index space for land cover and land-cover change analysis. International Journal of Remote Sensing, 17, 3, pp. 463-487

Lambin E.F., and Ehrlich, 1996b. Borad scale land-cover classification and interannual climatic variability. International Journal of Remote Sensing, 17, 5, pp. 845-862

Laporte N.T., Goetz S.J., Justice C.O., and Heinicke M., 1998. A new land cover map of central Africa derived from multi-resolution, multi-temporal AVHRR, data. International Journal of Remote Sensing, Vol. 19, No. 18, pp. 3537-3550

Latifovic R., Zhu Z.-L., Cihlar J., Giri C. and Olthof I., 2004. Land cover mapping of North and Central America—Global Land Cover 2000. Remote Sensing of Environment, 89, pp. 116–127.

Latty R. S., R. Nelson, B. Markham, D. Williams, D. Toll, and J. Iorns, 1985. Performance comparison between information extraction techniques using variable spatial resolution data. Photogramm. Eng. Remote Sensing, Vol. 51, no. 9, pp. 1459–1470

Ledwith M., 2003. Land cover classification using SPOT Vegetation 10-day composite images—Baltic Sea catchment basin. http://www.lantmateriet. se/cms/files/pdf/pdf/ geografisk_information%5CMMA_article_glc2000.pdf (22 June 2005).

Lee T. Y., and Kaufman Y. J., 1986, Non-Lambertian effects on remote sensing of surface reflectance and vegetation index. IEEE Transactions on Geoscience and Remote Sensing, 24, pp. 699-708.

Leeuwen van W. J. D., Huete A. R., Duncan J., and Franklin J., 1994. Radiative transfer in shrub savanna sites in Niger -- preliminary results from HAPEX IISahel: 3. Optical dynamics and vegetation index sensitivity to biomass and plant cover. Agricultural and Forest Meteorology, 69, pp. 267-288.

Lenney M.P., Woodcock C.E., and Hamdi H., 1996. The status of agricultural lands in Egypt: The use of multitemporal NDVI features derived from Landsat TM. Remote Sensing of Environment 56, 1, pp. 8-20

Leroy M., Dedieu G., Roujean J.L., Berthelot B., Hautecoeur O., Bicheron P. and Lacaze R., 1998. Improved atmospheric corrections and data compositing methods for surface reflectance retrieval, Final report for the VEGETATION Preparatory Programme

Leuning R., Cleugh H.A., Zegelin S.J. and Hughes D., 2005. Carbon and water fluxes over a temperate Eucalyptus forest and a tropical wet/dry savanna in Australia: measurements and comparison with MODIS remote sensing estimates, Agricultural and Forest Meteorology, Vol. 129, 3-4, pp. 151-173.

Li Z., Cihlar J., Zheng X., Moreau L., and Ly H., 1996, The bidirectional effects of AVHRR measurements over Boreal regions. IEEE Transactions on Geoscience and Remote Sensing, 34, pp. 1308–1322.

Liang S., Fallah-Adl H., Kalluri S., Jaja J., Kaufman Y.J., and Townshend J.R.G., 1997. An operational atmospheric correction of landsat ETM+ land surface imagery:II. Validation and applications. IEEE Transactions on Geoscience and Remote Sensing, 40, 2736-2746.

Liang S., 2001. Land-cover classification methods for multi-year AVHRR data. International Journal of Remote Sensing, Vol. 22, No 8, pp. 1479-1493

Liang S., 2004. Quantitative Remote Sensing of Land Surfaces. John Wiley & Sons, Inc, Hoboken, New Jersey

Lillesand T.M., and Kiefer R.W., 2000. Remote Sensing and Image Interpretation, 4th ed. Wiley, New York, 721 pp.

Lim A., Liew S.C. and Kwoh L.K., 2004. Retrieval of Land Surface Temperature in the Humid Tropics from MODIS Data by Modeling the Atmospheric Transmission and Thermal Emission. Proc. 2004 IEEE International Geoscience and Remote Sensing Symposium, September 20 - 24, 2004, Anchorage, Alaska, USA

Linsley R. K., Kohler M.A. and Paulhus J.L.H., 1975. Hydrology for Engineers, New York, Toronto, London:McGraw-Hill.

Lioubimtseva E., 2003. An evaluation of VEGETATION-1 imagery for broad-scale landscape mapping of Russia: effects of resolution on landscape pattern. Landscape and Urban Planning 65, pp187-200

Lloyd D., 1990. A phenological classification of terrestrial vegetation cover using shortwave vegetation index imagery. International Journal of Remote Sensing, 11, 12, pp. 2269-2270.

Loeb N.G., 1997. In-flight calibration of NOAA AVHRR visible and near-IR bands over Greenland and Antarctica. International Journal of Remote Sensing, Vol. 18, No. 3, pp. 477-490

Los S.O., Justice C.O., and Tucker C.J., 1994. A global 1°x1° NDVI data set for climate studies derived from the GIMMS continental NDVI data. International Journal of Remote Sensing, 15, pp. 3493-3618

Los S.N., 1998. Estimation of the ratio of sensor degradation between NOAA AVHRR channels 1 and 2 from monthly NDVI composites. IEEE Transactions on Geoscience and Remote Sensing, 36, pp. 206-213

Loveland T. R., Merchant J. W., Ohlen D. O., and Brown J. F., 1991. Development of a land-cover characteristics database for the conterminous U.S., Photogramm. Eng. Remote Sens. 57, 11, pp. 1453-1463

Loveland T.R., Merchant J.W., Brown J.F., Ohlen D.O., Reed B.C., Olson P. and Hutchinson J., 1995. Seasonal land-cover of the United States. Annals Association of American Geographers, 85, pp. 339-355

Loveland T. R., and Belward A. S., 1997. The IGBP-DIS global 1 km land cover dataset, DISCover: first results. International Journal of Remote Sensing, 18, pp. 3289–3295.

Loveland T. R., Estes J. E., and Scepan J., 1999. Global land cover mapping and validation—foreword. Photogrammetric Engineering and Remote Sensing, 65, 9, pp. 1011– 1012.

Loveland T.R., Reed B.C., Brown J.F., Ohlen D.O., Zhu Z., Yang L. and Merchant J.W., 2000. Development of a global land cover characteristics database and IGBP DISCover from 1 km AVHRR data. International Journal of Remote Sensing 21, 6-7, pp. 1303-1365

Lucas, 2003. The Lucas survey. European statisticians monitor territory. Luxembourg: Office for Official Publications of the European Communities, 2003, ISBN 92-894-4984-5, Cat. No. KS-AZ-03-001-EN-N ISSN 1725-0714

Luo Y. P. and Trishchenko, A., 2005. Comparison of Atmospheric Correction Results for AVHRR, VGT and MODIS Reflective Bands Used for Land Applications. American Geophysical Union, Fall Meeting 2005, abstract #A23A-0929

Lupo F., Reginster I. and Lambin E.F., 2002. Monitoring natural disasters and " hot spots " of land-cover changes with SPOT VEGETATION data to assess regions at risks, Proceedings of the 21st EARSeL Symposium " Observing Our Environment From Space : New Solutions For A New Millennium ", Paris, 14-16 May 2001 ; Ed. G. Bégni, AA. Balkema Publishers, Lisse, pp. 333,-336/429 MA, 118pp.

Lyon J.G., Yuan D., Lunetta R.S. and Elvidge C.D., 1998. A change detection experiment using vegetation indices, Photogramm. Eng. Remote Sens., 64, pp. 143-150.

Maccherone B. and Cardwell S., 2006a. MODIS Web. http://modis.gsfc.nasa.gov/about/ (8 July 2006)

Maccherone B. and Cardwell S., 2006b. MODIS Web. http://modis.gsfc.nasa.gov/about/specifications.php (8 July 2006)

Maccherone B. and Cardwell S., 2006c. MODIS Web. http://modis.gsfc.nasa.gov/data/dataprod/index.php (8 July 2006)

Mackay G., Steven M.D. and Clark J.A., 1998. An atmospheric correction procedure for the ATSR-2 visible and near-infrared land surface data. International Journal of Remote Sensing, Vol. 19, No. 15, pp. 2949-2968

Maisongrande P., Duchemin B. and Dedieu G., 2004. VEGETATION/SPOT: an operational mission for the Earth monitoring; presentation of new standard products. International Journal of Remote Sensing, Vol. 25, No. 1, pp. 9–14

Malingreau, J. P., 1986, Global vegetation dynamics: satellite observations over Asia. International Journal of Remote Sensing, 7, pp. 1121–1146.

Malingreau J.P., Tucker C. J., and Laporte N., 1989, AVHRR for monitoring global tropical deforestation. International Journal of Remote Sensing, 10, pp. 855–867.

Markham B. L., 1985. The Landsat sensors' spatial responses. IEEE Transactions on Geoscience and Remote Sensing, GE-23, pp. 864– 875.

Maselli F., Romanelli S., Bottai L., and Zipoli G., 2003. Estimation of Dynamic Fire Risk by the Use of NOAA-AVHRR NDVI Images. Remote Sensing of Environment, 86, pp. 187-197.

Mather A. S., 2005. Assessing the world's forests. Global Environmental Change 15, pp. 267-280

Matson M., Stephens G., Robinson J., 1987. Fire detection using data from the NOAA-N satellites. International Journal of Remote Sensing, Vol. 8. No. 7, pp. 961-970

Matthews E., 1983. Global vegetation and land-use: new high-resolution databases for climate studies. Journal of Climate and Applied Meteorology, 22, pp. 474-487

Mauser W., and Bach H.., 1995. Imaging spectroscopy in hydrology and agriculture – determination of model parameters. In: J. Hill, & J. Megier (Eds.), Imaging spectrometry – a tool for environmental observations (pp. 261- 283). Dordrecht, The Netherlands: Kluwer Academic Publishers.

Mayaux P., and Lambin E., 1995. Estimation of tropical forest area from coarse spatial resolution data: a two-step correction function for proportional errors due to spatial aggregation. Remote Sensing of Environment, 53, pp. 1–16.

Mayaux P., Gond V. and Bartholomé E., 2000. A near-real time forest-cover map of Madagascar derived from SPOT-4 VEGETATION data International Journal of Remote Sensing Vol. 21, 16, pp3139 – 3144

Mayaux P., Bartholomé E., Massart M., and Belward A. S., 2002. The land cover of Africa for the year 2000. LUCC Newsletter, 8

Mayaux P., Bartholomé E., Cabral A., Cherlet M., Defourny P., Di Gregorio A., Diallo O., Massart M., Nonguierma A., Pekel J.-F., Pretorius C., Vancutsem C. and Vasconcelos M., 2003. The Land Cover Map for Africa in the Year 2000. GLC2000 database, European Commision Joint Research Centre, http://www-gem.jrc.it/glc2000 (14 December 2006)

Mayaux P., Bartholomé E., Fritz S. and Belward A., 2004. A new land-cover map of Africa for the year 2000. Journal of Biogeography, 31, pp. 1–17.

Mayaux P., Eva H., Gallego J., Strahler A.H., Herold M., Agrawal S., Naumov S., De Miranda E.E., Di Bella C.M., Ordoyne C., Kopin Y. and Roy P.S., 2006. Validation of the global land cover 2000 map**.** Geoscience and Remote Sensing, IEEE Transactions, Vol. 44, 7, pp. 1728 - 1739

McGwire K., Minor T., Fenstermaker L., 2000. Hyperspectral Mixture Modeling for Quantifying Sparse Vegetation Cover in Arid Environments, 72, 3, pp. 360-374.

Menzel W.P. Seemann S.W., Li J.and Gumley L.E., 2002. MODIS atmospheric profile retrieval algorithm theoretical basis document, Version 6. http://earth.engr.ccny.cuny.edu/noaa/wc/atbd_mod07.pdf (23 July 2003)

Merchant J. W., Yang L., and Yang W., 1994. Validation of continentalscale continentalscale land cover data bases developed from AVHRR data. In: Proceedings of Pecora 12 land information from space-based systems pp. 63–72). Bethesda: ASPRS.

Meyer D. J., Fenno J. L., Baltzer T. T., Hollaren D. M., and Rockvam, T. J., 2003, Correcting for Rayleigh scattering and ozone absorption in the 1-kilometer AVHRR global land data set. International Journal of Remote Sensing, in press.

Meyer-Roux J., Vossen P., 1994. The first phase of the MARS Project, 1988-1993:overview, methods and results, The Mars Project: overview and perspectives, Office for Publications of the EC. Luxembourg, pp. 33-81.

Meygret A., Dimguirard M. and Henry P., 1997. Eleven Years of Experience and Data in Calibrating SPOT HRV Cameras, Proc ISPRS, Hanover

Meygret A., Briottet X., Henry P., Hagolle O., and Santer R., 2000. Calibration of SPOT4-HRVIR and Vegetation cameras over the Rayleigh Scattering, Proc. SPIE'00, San Diego, USA, 2000, in prep.

Moody A. and Woodcock C.E., 1995. Scale-dependent errors in the estimation of land-cover proportions: implications for global land-cover datasets. Photogramm. Eng. Remote Sens. 60, pp. 585– 594.

Moody A., 1998. Using landscape spatial relationships to improve estimates of land-cover area from coarse-resolution remote sensing. Remote Sensing of Environment, 64, pp. 202–220.

Mucher C.A., Champeaux J. L., Steinnocher K. T., Griguolo S., Wester K., Heunks C., Winiwater W., Kressler F. P., Goutorbe J. P., Ten Brink B., Van Katwijk V. F., Furberg O., Perdigao V., and Nieuwenhuis G. J. A., 2001. Development of a consistent methodology to derive land cover information on a European scale from remote sensing for environmental modeling. The PELCOM Report. Centre for Geo-Information (CGI), Wageningen university, Wageningen, The Netherlands 2001.

Mucher S., Steinnocher K., Chapeaux J-L., Griguolo S., Wester K., Heunks C and Van Katwijk V., 2000. Establishment of a 1-km Pan-european Land Cover Database for Environmental Monitoring. IAPRS., Vol. XXXIII, Amsterdam, 2000

Muchoney D., Borak J., Chi H., Friedl M., Gopal S., Hodges J., Morrow N. and Strahler A., 2000. Application of the MODIS global supervised classification model to vegetation and land cover mapping of Central America. International Journal of Remote Sensing, Vol. 21, No. 6, pp. 1115-1138

Muller S. V., Walker D. A., Nelson F. E., Auerach N. A., Bockheim J. G., Guyer S., and Sherba, D., 1998. Accuracy assessment of a land-cover map of the Kuparuk river basin, Alaska: considerations for remote regions. Photogrammetric Engineering and Remote Sensing, 64, pp. 619– 628.

Myneni R. B., and Williams D. L., 1994. On the relationship between FAPAR and NDVI. Remote Sensing of the Environment, 49, pp. 200-211.

Myneni R.B., Hall F.G., Sellers P.J., and Marshak A.L., 1995. The interpretation of spectral vegetation indexes. IEEE Transactions on Geoscience and Remote Sensing, 33, pp. 481-486

NASA, 2003. NASA FTP site. ftp://ftp.mcst.ssai.biz/pub/permanent/MCST/PFM_L1B_LUT_4-30-99/ (17 February 2003)

Neckel H., and Labs D., 1984. The Solar Spectrum Between 3300 and 12500 . Solar Physics, Vol. 90, pp. 205-258.

Nelson R., and Holben B., 1986. Identifying deforestation in Brazil using multiresolution satellite data. International Journal of Remote Sensing, 7, 3, pp. 429–448.

Nemani R., Pierce L.L, Running S.W., and Goward S.N., 1993. Developping satellite derived estimates of surface moisture status. J. Appl. Meteorol., 32, pp. 548-557

Nemani R. R., and Running S. W., 1995, Satellite monitoring of global land cover changes and their impact on climate. Climate Change, 31, pp. 395- 413.
Nemani R., and Running S., 1997, Land cover characterization using multitemporal red, near-IR, and thermal-IR data from NOAA/AVHRR. Ecological Applications, 7, pp. 79–90.
NGDC (National Geophysical Data Center), 1993. 5 minute gridded world elevation. NGDC data announcement DA 93- MGG-01. Boulder.
Nishihama M., Wolfe R., Solomon D., Patt F., Blanchette J., Fleig A., and Masuoka E., 1997. MODIS Level 1A Earth Location: Algorithm Theoretical Basis Document Version 3.0., SDST-092
NOAA, 2006. POES Status. http://www.oso.noaa.gov/poesstatus/ (3 December 2006)
Nobre, C. A., Sellers, P. J., and Shukla, J., 1991, Amazonian deforestation and regional climate change. Journal of Climate, 4, pp. 957–988.
O'Brien K. L., 1996, Tropical deforestation and climate change. Progress in Physical Geography, 20, pp. 311–332.
Obasi G.O.P., 1994. WMO's Role in the international Decade for Natural Disaster Reduction, Bull. Amer. Meteor. Soc., 75, pp. 1655-1661.
Oguro Y., Tsuchiya K., and Suga Y., 1999. Comparison of land cover features observed with different satellite sensors over a semi-arid land in central Australia. Advances in Space Research., 23, 8, pp. 1401-1404
Olson C. E., 1967. Optical remote sensing of the moisture content in fine forest fuels. 1st Report N8036-1-F. Ann Arbor, MI: University of Michigan.
Olson J.S., and Wattas J., 1982. Major world ecosystem complexes. In D.B. Jones (Ed.), Earth's vegetation and atmospheric carbon dioxide. Carbon dioxide review (pp 388-399). Oxford: Oxford Univ. Press
Ouaidrari H., and Vermote E., 1999. Operational atmospheric correction of Landsat TM data. Remote Sensing of Environment, 70, pp. 4–15.
Ozer P., Tychon B. and Touré S., 2000. SPOT – 4 VEGETATION potentialities for food early warning systems and famine reduction in the Sahel. 1st Earsel workshop on remote sensing for developing countries"" Ghent (B) pp. 167-172
Pal M., and Mather P.M., 2003. An assessment of the effectiveness of decision tree methods for land cover classification. Remote Sensing of Environment, 86, pp. 554-565
Palmer W.C., 1965. Meteorological Drought. Research Paper no. 45, US Department of Commerce Weather Bureau, Washington, DC.
Passot X., 2000. VEGETATION image processing methods in the CTIV VEGETATION system engineer – CNES - Toulouse
Pekel J.-F., Vancutsem C. and Defourny P., 2003. Pan-European land cover derived from 366 daily SPOT VEGETATION images. GLC 2000 'Final Results' Workshop, Ispra (I) 24–26 March 2003.
Penner J. E., 1994. Atmospheric chemistry and air quality. In:W. B. Meyer, B. L. Turner II (Eds.), Changes in land use and land cover: a global perspective (pp. 175– 209). Cambridge: Cambridge University Press.
Penuelas J., Filella I., Biel C., Serrano L., and Save R., 1993. The reflectance at the 950–970 region as an indicator of plant water status. International Journal of Remote Sensing, 14, 10, pp. 1887– 1905.

Persson R., 1974. World Forest Resources: Review ofthe World's Forest Resources in the Early 1970s, Research Note 17. Royal College ofForestry, Stockholm.

Peterson D.L., Spanner M.A., Running S.W., and Teuber K.B., 1987. Relationship of Thematic Mapper Simulator data to leaf area index of temperate coniferous forest. Remote Sensing of Environment, 22, pp. 323-341

Phulpin T., Lavenu F., Bellan M.F., Mougenot B. and Blasco F., 2002. Using SPOT-4 HRVIR and VEGETATION sensors to assess impact of tropical forest fires in Roraima, Brazil. International Journal of Remote Sensing, Vol. 23, 10, pp. 1943 – 1966

Pinzon J., Brown M.E., Tucker C.J., 2005. Satellite time series correction of orbital drift artifacts using empirical mode decomposition. In EMD and its applications, N.E. Huangand S.S.P. Shen (Eds) (Singapore: World Scientific Publishers)

Pokrant H., 1991, Land cover map of Canada derived from AVHRR images. Manitoba Remote Sensing Centre, Winnipeg, MB, Canada.

Potter C., Davidson E., Nepstad D., and de Carvalho C. R., 2001. Ecosystem modeling and dynamic effects of deforestation on trace gas fluxes in Amazon tropical forests. Forest Ecology and Management, 152, pp. 97– 117.

Prata A.J., Caselles V., Coll C., Sobrino J.A. and Ottle C., 1995. Thermal remote sensing of land surface temperature from satellites: Current status and future prospects, Remote Sens. Reviews, 12, pp. 175-224

Price J.C., 2003. Comparing MODIS and ETM+ data for regional and global land classification. Remote Sensing of Environment, 86, pp. 491-499

Prince S. D., 1991. A model of regional primary production for use with coarse resolution satellite data. International Journal of Remote Sensing, 12, pp. 1313–1330.

Privette J. L., Fowler C., Wick G. A., Baldwin D., and Emery W. J., 1995. Effects of orbital drift on advanced very high resolution radiometer produces: Normalized difference vegetation index and sea surface temperature. Remote Sensing of Environment, Vol. 53, pp. 164 171.

Rahman H. and Dedieu G., 1994. SMAC: A Simplified Method for the Atmospheric Correction of Satellite Measurements in the Solar Spectrum., International Journal of Remote Sensing, 15, l, pp. 123-143.

Rao K.P., Holmes S.J., Anderson R.K., Winston J.S., and Lehr P.E., 1990. Weather Satelites: System , Data, and Environmental Applications, American Meteorological Society, Boston.

Rao C. R. N., and Chen J., 1995. Inter-satellite calibration linkages for the visible and near-infrared channels of the Advanced Very High Resolution Radiometer on the NOAA-7-9, and -11 spacecrafts. International Journal of Remote Sensing, 16, pp. 1931-1942

Rao C. R. N., and Chen J., 1996. Post-launch calibration of the visible and near infrared channels of the advanced very high resolution radiometer on the NOAA-14 spacecraft. International Journal of Remote Sensing, 17, pp. 2743–2747

Rao C.R.N., and Chen J., 1999. Revised post-launch calibration of the visible and near-infrared channels of the Advanced Very High Resolution Radiometer on the NOAA-14 spacecraft. International Journal of Remote Sensing, 20, pp. 3485-3491

Reed B. C., 1997. Applications of the U.S. Geological Survey's global land cover product. Acta Astronautica, 41, 4–10, pp. 671– 680

Reed B. D., Brown J. F., VanderZee D., Loveland T. R., Merchant J. W., and Ohlen D. O., 1994. Measuring phenological variability from satellite imagery, J. Veg. Sci. 5, pp. 703-714.

Rees W.G., 2001. Physical principles of remote sensing. 2nd edition. Cambridge University Press, Cambridge.

Reichenbach S.E., and Li J., 2001. Restoration and Reconstruction from Overlapping Images for Multi-Image Fussion. IEEE Transactions On Geoscience And Remote Sensing, Vol. 39, 4, pp. 769-780

Richards J.A., 1992. Remote Sensing Digital Image Analysis. Apringer-Verlag, Cambridge, UK.

Richards J.A., 1993. Remote Sensing Digital Image Analysis An introduction. 2nd Edition, Springer-Verlag, Berlin, Heidelberg, New York

Riebsame, W.E., S.A. Changnon, and T.R. Karl., 1990. Drought and Natural Resource Management in the United States: Impacts and Implications of the 1987-1989 Drought. Westview Press, Boulder, Colorado.

Riemann, R., Hoppus, M., and Lister, A., 2000. Using arrays of small ground sample plots to assess the accuracy of Landsat TM-derived forest-cover maps. In: G. B. M. Heuvelink, M. J. P. M. Lemmens (Eds.), Proceedings of the 4th International Symposium on Spatial Accuracy Assessment in Natural Resources and Environmental Sciences (pp. 541– 548). Delft: Delft University Press.

Roujean M., Leroy M., and Deschamps P.Y., 1992. A bidirectional reflectance model of the Earth's surface for the correction of remote sensing data. J. Geophy. Res. 97, 20, pp. 455-468

Rouse J. W., Haas R. H., Schell J. A., Deering D. W., and Harlan J. C., 1974. Monitoring the vernal advancement of retrogradation of natural vegetation. NASA/GSFC, Type III, Final Report, Greenbelt, MD.

Roy D.P., Lewis P.E. and Justice C.O., 2002. Burned area mapping using multi-temporal moderate spatial resolution data--a bi-directional reflectance model-based expectation approach, Remote Sensing of Environment, Vol. 83,1-2, pp. 263-286.

Running S.W., and Nemani R.R., 1988. Relating seasonal patterns of the AVHRR vegetation index to simulated photosynthesis and transpiration of forest in different climates. Remote Sensing of Environment, 24, pp. 347-367

Running S.W., Justice C.O., Salomonson V., Hall D., Barker J., Kaufmann Y.J., Strahler A.H., Huete A.R., Muller J.P., Vanderbilt V., Wan Z.M., Teillet P. and Carneggie D., 1994a. Terrestrial remote sensing science and algorithms planned for EOS/MODIS. International Journal of Remote Sensing, 15, 17, pp. 3587-3620

Running S. W., Loveland T., and Pierce L. L., 1994b. A vegetation classification logic based on remote sensing for use in global biogeochemical models. Ambio, 23, pp. 77– 81.

Running S.W., Loveland T.R., Pierce L.L., Nemani R.R., and Hunt Jr. E.R., 1995. A remote sensing based vegetation classification logic for Global Land cover Analysis. Remote Sensing of Environment, 51, pp. 39-48

Russell P.B., Livingston J.M., Dutton E.G., Pueschel R.F., Reagan J.A., DeFoor T.E., Box M.A., Allen D., Pilewskie, Herman B.M., Kinne S.A., and Hoffman D.J.,

1993. Pinatubo and pre-Pinatubo optical depth spectra:Mauna Loa measurements, compositions, inferred particle siz distributions, radiative effects, and relationship to lidar data. J. Geophys. Res., 98, pp. 22969-22985

Saint, G., 1992, VEGETATION onboard SPOT 4: mission spécifications. Report No. 92102, Laboratoire d'etudes et de recherches en teledetection spatiale, Toulouse, France.

Saint G., 1994. VEGETATION onboard SPOT 4: mission specifications, Version 3, IUC documentation, May 1995

Saint G., 1997. The VEGETATION Programme, CNES-JRC/SAI

Saleous N.Z., Vermote E.F., Justice C.O., Townshend J.R.G., Tucker C.J. and Goward S.N., 2000. Improvements in the global biospheric record from the advanced very high resolution radiometer. International Journal of Remote Sensing, 21, pp. 1251-1278.

San-Miguel-Ayanz J., 2002, Methodologies for the evaluation of forest fire risk: from longterm (static) to dynamic indices. In Forest Fires: Ecology and Control, pp. 117–132

Sannier C.A.D., Taylor J.C., Du Plessis W. and Campbell K., 1998a. Real-time vegetation monitoring with NOAA-AVHRR in Southern Africa for wildlife management and food security assessment., International Journal of Remote Sensing Vol. 19, No. 4, pp. 621- 639

Sannier C.A.D., Taylor J.C., and Campbell K., 1998b. Compatibility of FAO-ARTEMIS and NASA Pathfinder AVHRR Land NDVI data archives for the African continent. International Journal of Remote Sensing 19, 17, pp. 3441-3450

Saunders R.U., and Kriebel K.T., 1988. An improved method for detecting clear sky and cloudy radiances from AVHRR data. International Journal of Remote Sensing, 9, pp. 123-150.

Scepan J., 1999. Thematic validation of high-resolution global land-cover data sets. Photogrammetric Engineering and Remote Sensing, 65, 9, pp. 1051-1060.

Scepan J., Menz G., and Hansen M. C., 1999. The DISCover validation image interpretation process. Photogrammetric Engineering and Remote Sensing, 65, pp. 1075– 1081.

Schepers J. S., Blackmer T. M., Wilhelm W. W., and Resende M., 1996. Transmittance and reflectance measurements of corn leaves from plants with different nitrogen and water supply. Journal of Plant Physiology, 148, pp. 523– 529.

Schmullius C.C., Plummer S. and Quegan S., 2003. The SIBERIA-II Project, Greenhouse Gas Accounting and the Global Project Context 2003 IEEE International Geoscience and Remote Sensing SymposiumJuly 21-25, 2003 Toulouse, France, Vol. I, pp. 485 – 487

Schott J.R., 1997. Remote Sensing The Image Chain Approach. New York, Oxford University Press.

Schowengerdt R. A., 1997. Remote sensing: models and methods for image processing. San Diego: Academic Press.

Schroedter M., Olesen F. and Fischer H., 2003. Determination of land surface temperature distributions from single channel IR measurements: an effective spatial interpolation method for the use of TOVS, ECMWF and radiosonde

profiles in the atmospheric correction scheme. International Journal of Remote Sensing, Vol. 24, No. 6, pp. 1189-1196
Schwalb A., 1978. The TIROS-N/NOAA A-G Satellite Series. NOAA Tech Memo.
Seelan S.K., Laguette S., Casady G.M. and Seielstad G.A.,2003. Remote sensing applications for precision agriculture: A learning community approach, Remote Sensing of Environment, Vol. 88,1-2, pp. 157-169.
SEI, 2006. SEI Land Cover Map of Europe. http://www.york.ac.uk/inst/sei/gis/land-use.html (21 May 2006)
Seiler R.A., Kogan F., and Sullivan J., 1998. AVHRR-based vegetation and temperature condition indices for drought detection in Argentina. Adv. Space Res. Vol. 21, No. 3, pp. 481-484.
Sellers P. J., 1985. Canopy reflectance, photosynthesis, and transpiration. International Journal of Remote Sensing, 6, pp. 1335-1372.
Seller P.J., Berry J.A., Collatz G.J., Field C.B., and Hall F.G., 1992. Canopy Reflectance, Photosynthesis, and Transpiration. III. AReanalysis Using Improved Leaf Models and a New Canopy Intergration Scheme., Remote Sensing of Environment 42, pp. 187-216
Sellers P. J., Randall D.A. and Collatz G.J., 1996. A revised land surface parameterization (SiB2) for atmospheric GCMs. Part 1: Model formulation. Journal of Climate 9, pp. 676–705.
Sellers, P. J., Bounoua L., Collatz G. J., Randall D. A., Dazlich D. A., Los S. O., Berry J. A., Fung I., Tucker C. J., Field C. B., and Jensen T. G., 1996, Comparison of radiative and physiological effects of doubled atmospheric CO2 on climate. Science, 271, pp. 1402–1406.
Singh R.P., Roy S. and Kogan F., 2003. Vegetation and temperature condition indices from NOAA AVHRR data for drought monitoring over India. International Journal of Remote Sensing, Vol. 24, 22, pp. 4393-4402
Skole D. L., 1994. Data on global land-cover change: acquisition, assessment and analysis. In: W. B. Meyer, B. L. Turner II (Eds.), Changes in land use and land cover: a global perspective (pp. 437– 471). Cambridge: Cambridge University Press.
Smith G.M., and Milton E.J., 1999. The use of Empirical Line Method to Calibrate Remotely Sensed Data to Reflectance. International Journal of Remote Sensing, 20, pp. 2653-2662
Smith G.M., Brown N.J. and Cooper J., 2004. NBN Access to LCM2000-lite. Centre for Ecology and Hydrology, Monks Wood, Abbots Ripton, Huntingdon, Cambs PE28 2LS
Smith, J. A., Lin, T. L., and Ranson, K. J., 1980, The Lambertian assumption and Landsat data. Photogrammetric Engineering and Remote Sensing, 46, pp. 1183-1189.
Smith D. E., Christodoulidis D. C., Kolenkiewicz R., Dunn P. J., Klosko S. M., 1985. A global geodetic reference frame from Lageos ranging (SL5.1AP). Journal of Geophysical Research, 90, pp. 9221
Smith W.L., Woolf H.M., Hayden C.M. and Schreiner A.J., 1985. The Simultaneous Retrieval Export Package, Technical Report, 2ndInt. TOVS Study Conf, Igls, pp. 224-253

Song C., Woodcock C. E., Soto K. C., Lenney M.P. and Macomber S.A., 2001. Classification and Change detection Using Landsat TM Data: When and How to correct Atmospheric effects? Remote Sensing of Environment, 75, pp. 230-244

SPOT-4 CNES, 2006. The Vegetation instrument. http://spot4.cnes.fr/spot4_gb/vegetati.htm (24 April 2006)

SPOT-5 CNES, 2006a. Technical features of SPOT 5 system. http://www.cnes-tv.net/dossiers/spot5/va/pdf/technique_va.pdf (24 February 2006)

SPOT-5 CNES, 2006b. SPOT-5 Observing Earth. http://spot5.cnes.fr/gb/satellite/satellite.htm (4 May 2006)

SPOT-VEGETATION, 2006a. VEGETATION Programme. http://spot-vegetation.com/vegetationprogramme/index.htm (6 May 2006)

SPOT-VEGETATION, 2006b. User guide. http://www.spot-vegetation.com/vegetationprogramme/Pages/TheVegetationSystem/userguide/userguide.htm (6 May 2006)

Stehman S. V., 1997. Selecting and interpreting measures of thematic classification accuracy. Remote Sensing of Environment, 62, pp. 77– 89.

Steitz D., Kenitzer A., Diller G., Henry K., Ainsworth D. and Neiman M., 1998. Terra: Flagship of the Earth Observing System. National Aerunautics and Space Administration

Stibig H-J., Beuchle R. and Achard F., 2003. Mapping of the tropical forest cover of insular Southeast Asia from SPOT4-Vegetation images. International Journal of Remote Sensing, Vol. 24, no. 18, pp. 3651-3662.

Strahler A., Muchoney D., Borak J., Friedl M., Gopal S., Lambin E. and Moody A., 1999a. MODIS Land Cover Product Algorithm Theoretical Basis Document (ATBD) Version 5.0. MODIS Land Cover and Land-Cover Change, Boston University Boston, MA.

Strahler A. H., Muller J.P., Lucht W., Barker Schaaf, C., Tsang T., Gao F., Li X., Lewis P., Barnsley M., Strugnell N., Hu B., Hyman A., D'entremont R. P., Chen L., Liu Y., Mciver D., Liang S., Disney M., Hobson P., Dunderdale M., and Roberts G., 1999b. MODIS Product ID: MOD43 MODIS BRDF/Albedo Product: Algorithm Theoretical Basis Document Version 5.0. NASA GSFC, Greenbelt, MD, USA.

Stroppiana D., Pinnock S., and Gregoire J.-M., 2000. The Global Fire Product: daily fire occurrence from April 1992 to December 1993 derived from NOAA AVHRR data. International Journal of Remote Sensing, 21, pp. 1279–1288.

Su Z., Yacob A., Wen J., Roerink G., He Y., Gao B., Boogaard H., and Van Diepen C., 2003. Assessing relative soil moisture with remote sensing data: theory, experimental validation, and application to drought monitoring over the North China Plain. Physics and Chemistry of the Earth, 28, pp. 89-101

Tamene L., 1996. Vegetation status monitoring using NOAA-AVHRR NDVI in Ethiopia. MSc thesis, Silsoe College, Cranfield Unversity.

Tarne D., Deroo C. , P. Duhaut Herman M., Morcrette J.J., Perbos J. and Deschamps P.Y., 1990. A description of a computer code to simulate the satellite signal in the solar spectrum: the 5s code. International Journal of Remote Sensing, Vol. 11, pp. 659-668.

Tanre D., Holben B.N. and Kaufman Y.J., 1992. Atmospheric Correction Algorithm for NOAA-AVHRR Products: Theory and Application. IEEE Transactions on Geoscience and Remote Sensing, 30, No. 2, pp. 231-248

Tarpley J.P., Schnieder S.R., and Money R.L., 1984. Global vegetation indices from NOAA-7 Meteorological satellite, J, Climate and Applied Meteorology, 23, pp. 491

Tateishi R., Zhu L. and Sato H.P., 2003, The Land Cover for Central Asia for the Year 2000. GLC2000 database, European Commission Joint Research Centre, Ispra, Italy.

Tatem A.J., Goetz S.J. and Hay S.I., 2004. Terra and Aqua: new data for epidemiology and public health, International Journal of Applied Earth Observation and Geoinformation, Vol. 6, 1, pp. 33-46.

Taylor J., Sannier C., Delincé J, Gallego F.J., 1997. Regional Crop Inventories in Europe Assisted by Remote Sensing: 1988-1993, Synthesis Report. Office for Publications of the EC. Luxembourg.

Teillet P., 1989. Surface reflectance retrieval using atmospheric correction algorithms. Proc. IGARSS'89 and the 12th Canadian Symposium on Remote Sensing, Vancouver, Canada, pp. pp. 864-867.

Teillet P. M., Staenz K., Willams D. J., 1997. Effects of spectral, spatial, and radiometric characteristics on remote sensing vegetation indices of forested regions. Remote Sensing of Environment, 61, pp. 139–149.

Teklehaimanot T., 2006. Ethiopian Treasures. http://www.ethiopiantreasures.toucansurf.com/index.htm (20 December 2006)

Thenkabail P.S., Ward A.D., and Lyon J.G., 1995. Landsat-5 Thematic Mapper models of soybean and corn crop characteristics. International Journal of Remote Sensing, 15, pp. 49-61.

Thenkabail P.S., Smith R.B. and De Pauw E., 1999a. Hyperspectral vegetation indices for determining agricultural crop characteristics. CEO research publication series No. 1. Center of Earth Observation, Yale University Press, New Haven, CT

Thenkabail P. S., 1999b. Characterisation of the alternative to slash-and burn benchmark research area representing the Congolese rainforests of Africa using near-real-time SPOT HRV data. International Journal of Remote Sensing, 20, 5, pp. 839–877.

Thenkabail P.S., Smith R.B. and De Pauw E., 2000. Hyperspectral Vegetation Indices and Their Relationship with Agricultural Crop Characteristics. Remote Sensing of Environment, 71, pp. 158-182.

Thenkabail P. S., Smith R. B., De-Pauw E., 2002a. Evaluation of narrowband and broadband vegetation indices for determining optimal hyperspectral wavebands for agricultural crop characterization. Photogrammetric Engineering and Remote Sensing, 68, pp. 607–621.

Thenkabail P.S., Enclona E.A., Ashton M.S., and Van Der Meer B., 2002b. Accuracy Assessments and Optimal Hyperspectral Wavebands for Vegetation and Agriculture in 400-2500 Nanometers. In review for publication in the book chapter "Remote Sensing and GIS Accuracy Assessment" based on the accuracy assessment symposium organized by USEPA that was held at Las Vegas, NV during December 11-13, 2001 (in review).

Thenkabail P.S., Lin T., Hall J., Ashton M., Harris D. 2002c. Detecting floristic changes across topographic gradients and moisture regimes in a central African rain forest using IKONOS and ETM+ satellite imagery. Forest Ecology and management (in review).

Thenkabail P. S., Gamage M. S. D. N., Smakhtin V. U., 2004a. The use of remote sensing data for drought assessment and monitoring in Southwest Asia. Research Report 85. Colombo, Sri Lanka: International Water Management Institute.

Thenkabail P.S., Enclona E.A., Ashton M. S., Legg C., Jean De Dieu M., 2004b. Hyperion, IKONOS, ALI, and ETM+ sensors in the study of African rainforests. Remote Sensing of Environment, 90, pp. 23–43.

Thenkabail P.S., Enclona E.A., Ashton M.S., and Van Der Meer B., 2004c. Accuracy Assessments of hyperspectral waveband performance for vegetation analysis applications. Remote Sensing of Environment 91, pp. 354-376

Todd W. J., Gehring D. G., and Haman J. F., 1980. Landsat wildland mapping accuracy. Photogrammetric Engineering and Remote Sensing, 46, pp. 509– 520.

Toll D., 1985. Effect of Landsat thematic mapper sensor parameters on land cover classification. Remote Sensing of Environment, Vol. 17, pp. 129–140.

Townshend J. R. G., 1981. Spatial resolution of satellite images. Progress in Physical Geography, 5, pp. 33–55.

Townshend J., Goff T., and Tucker C., 1985, Multitemporal dimensionality of images of Normalized Difference Vegetation Index at Continental Scales. IEEE Transactions on Geoscience and Remote Sensing, 23, pp. 888–895.

Townshend J. R. G., C. O. Justice and Kalb V.T, 1987. Characterization and classification of South American land cover types using satellite data. International Journal of Remote Sensing, 8, pp. 1189-1207.

Townshend J.R.G., and Justice C.O., 1988. Selecting the spatial resolution of satellite sensors required for global monitoring of land transformations. International Journal of Remote Sensing, 92, pp. 187-236.

Townshend J.R.G., Justice C., Li W., Gurney C. and McManus J., 1991. Global land cover classification by remote sensing: Present capabilities and future possibilities. Remote Sensing of Environment 35, pp. 243-255

Townshend J. R. G., 1992. Improved Global Data for Land Applications: A Proposal for a New High Resolution Data Set, Report No. 20, International Geosphere-Biosphere Program, Stockholm.

Townshend J. R. G., Justice C. O., Skole D., Malingreau J.-P., Cihlar J., Teillet P., Sadowski F., and Ruttenberg S., 1994, The 1 km AVHRR global data set: needs of the International Geosphere–Biosphere Programme. International Journal of Remote Sensing, 15, pp. 3417–3441.

Townshend J. R. G., Huang C., Kalluri S. N. V., DeFries R. S., Liang S., and Yang K., 2000. Beware of per-pixel characterization of land cover. International Journal of Remote Sensing, 21, pp. 839–843.

Townshend J.R.G., and Justice C.O., 2002. Towards operational monitoring of terrestrial systems by moderate-resolution remote sensing, Remote Sensing of Environment, 83, pp. 351-259

Tripathy G. K., Ghosh T. K., and Shah S. D., 1996. Monitoring of desertification process in Karnataka state India using multitemporal remote sensing and ancillary

information using GIS. International Journal of Remote Sensing, 17, pp. 2243-2257.
Tucker C.J., 1979. Red and photographic infrared linear combinations for monitoring vegetation. Remote Sensing of Environment, 8, pp. 127-150.
Tucker C.J., Townshend J.R.G., and Goff T. E., 1985. African land cover classification using satellite data, Science 227, pp. 233-250
Tucker C. J., and P.J.Sellers, 1986. Satellite remote sensing of primary production, International Journal of Remote Sensing 7, 1395-1416.
Tucker C. J., and Choudhury B. J., 1987. Satellite remote sensing of drought conditions. Remote Sensing of Environment, 23, pp. 243–251.
Tucker C.J., and Townshend J.R.G., 2000. Strategies for monitoring tropical deforestation using satellite data. International Journal of Remote Sensing, Vol. 21 No. 7, pp. 1461-1471
Tucker C.J., Dregne H.E., and Newcomb W.W., 1991. Expansion and contraction of the Saharan desert from 1980 to 1990. Science, 253, pp. 299-301
Tucker C.J., Newcomb W.W., and Dregne H.E., 1994. Improved data sets for determination of desert spatial extent. International Journal of Remote Sensing, 15, pp. 3519-3545.
Tucker C. J., 1996, History of the use of AVHRR data for land applications. In Advances in the Use of NOAA AVHRR Data for Land Applications, edited by G. D'Souza A.S. Belward, and J.-P. Malingreau (Dordrecht: Kluwer Academic), pp. 1–19.
Tucker C.J., Pinzon J.E., Brown M.E., Slayback D., Pak E.W., Mahoney R., Vermote E., El Saleous N., 2005. An Extended AVHRR 8-km NDVI Data Set Compatible with MODIS and SPOT Vegetation NDVI Data. International Journal of Remote Sensing, 26, 20, pp. 4485-4498.
Tupper A., Carn S., Davey J., Kamada Y., Potts R., Prata F. and Tokuno M., 2004. An evaluation of volcanic cloud detection techniques during recent significant eruptions in the western & lsquo Ring of Fire. Remote Sensing of Environment, Vol. 91, 1, pp. 27-46.
UN, 2002. Report of the World Summit on Sustainable Development. Johannesburg, South Africa, 26 August to 4 September 2002, pp. 178, New York, ISBN 92– 1-104521–5.
UN, 2004. World Population to 2300, United Nations Department of Economic and Social Affairs/Population Division, New York
Unganai, L.S.,and Kogan, F.N., 1998. Drought monitoring and corn yield estimation in Southern Africa from AVHRR data. Remote Sensing of Environment, 63, pp. 219–232.
van Dijk A.,1985. A Crop Condition and Crop Yield Estimation Method Based on NOAA/AVHRR Satellite Data, Unpublished PhD thesis, University of Missouri-Columbia.
VEGETATION, 2006. Note to users of VEGETATION data: problems with radiometric calibration of VEGETATION 2 data. http://www.vgt.vito.be/Recalibration/newcalibrationvgt2_final.pdf (21 July 2006)
Vermote E., Santer R., Deschamps P.Y. and Herman M., 1992. In-flight Calibration of Large Field-of-View Sensors at Short Wavelengths using Rayleigh Scattering. International Journal of Remote Sensing, 13, pp. 3409-3429

Vermote E., and Kaufman Y.J., 1995. Absolute Calibration of AVHRR Visible and Near Infrared Cahnnels using Ocean and Cloud Views. International Journal of Remote Sensing, 16, pp. 2317-2340.

Vermote E., Tanre D., Deuze J. L., Herman M., and Morcrette J. J., 1996. 6S User Guide, version 1

Vermote E.F., Saleous N.El., Justice C.O., Kaufman Y.J., Privette J.L., Remer L., Roger J.C., and Tanre D., 1997a. Atmospheric correction of visible to middle-infrared EOD-MODIS data over land surfaces: Background, operational algorithm and validation. Journal of Geophysical research, Vol. 102, No D14, pp. 17131-17141.

Vermote E., Saleous N.E., Kaufman Y.J., and Dutton E., 1997b. Data preprocessing: stratospheric aerosol perturbing effect on the remote sensing of vegetation: correction method for the composite NDVI after the Pinatubo eruption. Remote Sensing Reviews, 15, pp. 7-21

Vermote E., Tanre D., Deuze J.L., Herman M., and Mocrette J.J., 1997c. Second Simulation of the Satellite Signal in the Solar Spectrum (6S): an overview. IEEE Transactions on Geoscience and Remote Sensing, 35, 3, pp. 675-686.

Vermote E.F. and Vermeulen A., 1999. Atmospheric correction algorithm: Spectral reflectances (MOD09). NASA contract NAS5-96062

Veroustraete F., Bartholomé E. and Verstraeten W.W., 2005. Proceedings of the 2nd International VEGETATION user conference. http://www.vgt.vito.be/vgtapen/proceedings/00intro.pdf (25 March 2006)

Viera A. J. and Garrett J. M., 2005. Understanding Interobserver Agreement: The Kappa Statistic. Family Medicince, Vol. 37, No. 5, pp. 360-363

Vierling, L. A., Deering, D. W., and Eck, T. F., 1997. Differences in Arctic tundra vegetation type and phenology as seen using bidirectional radiometry in the early growing season. Remote Sensing of Environment, 60, pp. 71-82.

Viovy N., 2000. Automatic Classification of Time Series (ACTS): a new clustering method for remote sensing time series. International Journal of Remote Sensing, Vol. 21, 6 & 7, pp. 1537-1560

Vitousek P. M., 1994. Beyond global warming: ecology and global change. Ecology, 75, pp. 1861– 1876.

Vogelmann J. E., Sohl T., and Howard S. M., 1998, Regional characterization of land cover using multiple sources of data. Photogrammetric Engineering and Remote Sensing, 64, pp. 45–57.

Walker G. K., Sud Y. C., and Atlas R., 1995. Impact of the ongoing Amazonian deforestation on local precipitation—A GCM simulation study. Bulletin of the American Meteorological Society, 76, 3, pp. 346– 361.

Walter-Shea, E. A., Privette, J. L., Cornell, D., Mesarch, M. A., and Hays, C. J., 1997. Relations between spectral vegetation indices and leaf area and absorbed radiation in alfalfa. Remote Sensing of Environment, 61, pp. 162-177.

Walthall C.L., Norman J.M., Welles J.M., Campbell G., and Blad B.L.,1985. Simple equation to approximate the bi-directional reflectance from vegetative canopies and bare soil surfaces, Applied Optics, 24, 3, pp. 383-387.

Wan Z. and Dozier J. 1996. A Generalized Split Window Algorithm for Retrieving Land Surface Temperature from Space. IEEE Transactions on Geoscience and Remote Sensing, Vol. 34, No. 4, pp. 892-905

Wan Z. and Li Z.-L., 1997. A physics-based algorithm for retrieving land-surface emissivity and temperature from EOS/MODIS data. IEEE Transactions on Geoscience and Remote Sensing, Vol. 35, 4, pp. 980-996.
Wan Z., 1999. MODIS Land-Surface Temperature Algorithm Theoretical Basis Document (LST ATBD)
Wan Z., 2006. MODIS Land Surface Products Users' Guide.
Weibull W., 1939, A statistical Theory of the Strength of Materials, Ing. Vetenskapsakad. Handl. (Stockh.), 151, 15
Weiss E., Marsh S.E., and Pfirman E.S., 2001. Application of NOAA-AVHRR NDVI time-series data to assess changes in Saudi Arabia's rangelands. International Journal of Remote Sensing, 2001, Vol. 22, no. 6, pp. 1005-1027
Weiss J.L., Gutzler D.S., Coonrod J.E.A.and Dahm C.N. 2004. Long-term vegetation monitoring with NDVI in a diverse semi-arid setting, central New Mexico, USA. Journal of Arid Environments, 58, pp. 249-272
Wheaton E.E., 2000. Canadian Prairie Drought Impacts and Experiences in Drought. A Global Assessment - Volume 1 ed. D.A Wilhite (London: Routledge) 312-330.
Wiegand C.J., Richardson A.J., Escobar D.E. and Gerbermann A.H., 1991. Vegetation indices in crop assessments. Remote Sensing of Environment, 35, pp. 105-119.
Wikipedia, 2006a. United Kingdom. http://en.wikipedia.org/wiki/Uk (9 January 2006)
Wilhite D. A., and Glantz M. H., 1985. Understanding the drought phenomenon: the role of definitions. In Planning for Drought (D. A. Wilhite and W. E. Easterling, Eds) Westview Press, Boulder, CO.
Wilhite D. A., 1993. Planning for drought: a methodology, drought assessment, management and planning: theory and case studies. In Drought Assessment, Management and Planning: Theory and Case Studies (D. A. Wilhite, Ed.), Kluwer Academic, Boston, pp. 87–109.
Wilkinson G. G., 1997. Open questions in neurocomputing for earth observation. Neuro-computational in remote sensing data analysis (pp. 3 – 13). Berlin: Springer-Verlag.
Williams C. S., and Becklund, O. A., 1989. Introduction to the optical transfer function. New York: Wiley.
Wilson M., and Henderson-Sellers A., 1985. A global archive of land cover and soil data for use in general circulation climate models. Journal of Climatology, 5, 119-143
WMO (World Meteorological Organization), 1994. Quarterly Bulletin, Geneva.
Wolfe R.E., Roy D.P., and Vermote, E., 1998. MODIS land data storage, gridding, and compositing methodology: Level 2 grid. IEEE Transactions on Geoscience and Remote Sensing, 36, 4, pp. 1324-1338.
Woodcock C.E., and Strahler A.H., 1987. The factor of scale in remote sensing. Remote Sensing of Environment, 21, pp. 311–332.
Wright R., Flynn L., Garbeil H., Harris A. and Pilger E., 2002. Automated volcanic eruption detection using MODIS. Remote Sensing of Environment, Vol. 82, 1, pp. 135-155.
Wu B., Xu W., Huang H. and Yan C., 2002, Global Land Cover 2000—China window. GLC 2000 'First Results' Workshop, Ispra, Italy, 18–22 March 2002
Xiangming X., Braswell B., Zhang O., Boles S., Frolking S. and Moore B III, 2003. Sensitivity of vegetation indices to atmospheric aerosols: continental-scale

observations in Northern Asia Remote Sensing of Environment Vol. 84, 3, pp. 385-392.

Xiao X., Shen Z., and Qin X., 2001. Assessing the potential of VEGETATION sensor data for mapping snow and ice cover: a Normalized Difference Snow and Ice Index. International Journal of Remote Sensing Vol. 22, 13, pp. 2479 – 2487

Xiao X., Boles S., Frolking S., Salas W., Moore B. III , Li C. , He L. and ZhaoR., 2002a. Observation of flooding and rice transplanting of paddy rice fields at the site to landscape scales in China using VEGETATION sensor data International Journal of Remote Sensing Vol. 23, 15, pp. 3009 – 3022

Xiao X., Moore B. III, Qin X., Shen X. and Boles S., 2002b. Large-scale observations of alpine snow and ice cover in Asia: Using multi-temporal VEGETATION sensor data. International Journal of Remote Sensing Vol. 23, 11, pp. 2213 – 2228

Xiao X., Zhang O., Saleska S., Hutyra L., De Camargo P., Wofsy S., Frolking S., Boles S., Keller M. and Moore B. III, 2005. Satellite-based modeling of gross primary production in a seasonally moist tropical evergreen forest. Remote Sensing of Environment, Vol. 94, 1, pp. 105-122.

Xiong J., Salomonson V., Sun J., Wu A., Barnes W. and Guenther B., 2004. Inter-comparison of Terra and Aqua MODIS. CEOS-IVOS at ESA/ESTEC, Noordwijk, Netherlands , 12-14 October, 2004.

Xiong X., Sun J., Esposito J., Guenther B., and Barnes W., 2002a. MODIS Reflective Solar Bands Calibration Algorithm and On-orbit Performance. Science Systems and Applications, Inc., 10210 Greenbelt Road, Suite 600, Lanham, MD 20706; Lockheed Martin Corporation, 8455 Colesville Road, Suite 960, Silver Sprine, MD 20910; Laboratory for Hydrospheric Processes, NASA/GSFC, Greenbelt, MD 20771

Xiong X., Chiang K., Guenther B., and Barnes W., 2002b. MODIS Thermal Emissive Bands Calibration Algorithm and On-orbit Performance. Science Systems and Applications, Inc., 10210 Greenbelt Road, Suite 600, Lanham, MD 20706; Lockheed Martin Corporation, 8455 Colesville Road, Suite 960, Silver Sprine, MD 20910; Laboratory for Hydrospheric Processes, NASA/GSFC, Greenbelt, MD 20771

Xiong X., Chiang K., Esposito J., Guenther B., and Barnes W., 2002c. MODIS on-orbit Calibration and Characterization. Science Systems and Applications, Inc., 10210 Greenbelt Road, Suite 600, Lanham, MD 20706; Lockheed Martin Corporation, 8455 Colesville Road, Suite 960, Silver Sprine, MD 20910; Laboratory for Hydrospheric Processes, NASA/GSFC, Greenbelt, MD 20771

Xiong X., Toller G., Chiang K., Sun J., Esposito J. and Barnes W., 2005. MODIS Level 1B Algorithm Theoretical Basis Document. MODIS Characterization Support Team.

Xue, Y., 1996, The impact of desertification in the Mongolian and the Inner Mongolian Grassland on the regional climate. Journal of Climate, 9, pp. 2173–2189

Yukuan S., Longxun C., and Min D., 1994, Numerical simulation for the impact of deforestation on climate in China and its neighboring regions. Advances in Atmospheric Sciences, 11, pp. 212–234.

Zhan X., DeFries R., Townshend J.R.G., Dimiceli C., Hansen M., Huang C., and Sohlberg R., 2000. The 250m global land cover change product from the

Moderate Resolution Imaging Spectroradiometer of NASA's Earth Observing System. International Journal of Remote Sensing, Vol. 21, 6 & 7, pp. 1433-1460

Zhan X., Sohlberg R.A., Townshend J.R.G., DiMiceli C., Carroll M.L., Eastman J.C., Hansen M.C. and DeFries R.S., 2002. Detection of land cover changes using MODIS 250 m data. Remote Sensing of Environment, Vol. 83, 1-2, pp. 336-350.

Zhang F., Wu B. and Liu C., 2003. Using Time Series of SPOT VGT NDVI for Crop Yield Forecasting 2003. IEEE International Geoscience and Remote Sensing Symposium July 21-25, 2003 Toulouse, France, Vol. I, pp. 386 – 388

Zhang X., Friedl M.A., Schaaf C.B., Strahler A.H., Hodges J.C.F., Gao F., Reed B.C. and Huete A.,2003. Monitoring vegetation phenology using MODIS. Remote Sensing of Environment, Vol. 84, 3, pp. 471-475.

Zon R., Sparhawk W.W., 1923. Forest Resources of the World. McGraw-Hill, New York.

Appendices

Appendix A, Theoretical comparison

MODIS PRODUCTS (http://modis.gsfc.nasa.gov/data/dataprod/index.php(20/3/2002)

Calibration

MOD 01 - Level-1A Radiance Counts
MOD 02 - Level-1B Calibrated Geolocated Radiances
MOD 03 - Geolocation Data Set

Atmosphere

MOD 04 - Aerosol Product
MOD 05 - Total Precipitable Water (Water Vapour)
MOD 06 - Cloud Product
MOD 07 - Atmospheric Profiles
MOD 08 - Gridded Atmospheric Product
MOD 35 - Cloud Mask

Land

MOD 09 - Surface Reflectance
MOD 11 - Land Surface Temperature & Emissivity
MOD 12 - Land Cover/Land Cover Change
MOD 13 - Gridded Vegetation Indices (Max NDVI & Integrated MVI)
MOD 14 - Thermail Anomalies, Fires & Biomass Burning
MOD 15 - Leaf Area Index & FPAR
MOD 16 - Evapotranspiration
MOD 17 - Net Photosynthesis and Primary Productivity
MOD 43 - Surface Reflectance
MOD 44 - Vegetation Cover Conversion

Cryosphere

MOD 10 - Snow Cover

MOD 29 - Sea Ice Cover

Ocean

MOD 18 - Normalized Water-leaving Radiance

MOD 19 - Pigment Concentration

MOD 20 - Chlorophyll Fluorescence

MOD 21 - Chlorophyll_a Pigment Concentration

MOD 22 - Photosynthetically Available Radiation (PAR)

MOD 23 - Suspended-Solids Concentration

MOD 24 - Organic Matter Concentration

MOD 25 - Coccolith Concentration

MOD 26 - Ocean Water Attenuation Coefficient

MOD 27 - Ocean Primary Productivity

MOD 28 - Sea Surface Temperature

MOD 31 - Phycoerythrin Concentration

MOD 36 - Total Absorption Coefficient

MOD 37 - Ocean Aerosol Properties

MOD 39 - Clear Water Epsilon

AVHRR RED BAND SIMULATION DATA

Wavelength	Winter Barley	Sugar beet	Forest	Pasture	Winter wheat	Bare soil	Winter OSR	Urban	Exoterrestrial irradiance	Normalised sensor response
0.4400	6.4533	7.9980	2.1950	7.5700	6.4530	7.8910	5.3890	8.3130	1799.5	1.16E-03
0.4420	6.0843	7.5926	2.3046	7.1794	6.0272	7.6370	5.2240	8.1442	1989.0	8.49E-04
0.4440	5.7153	7.1872	2.4142	6.7888	5.6015	7.3830	5.0590	7.9754	1974.5	5.34E-05
0.4460	5.3463	6.7818	2.5238	6.3982	5.1757	7.1290	4.8939	7.8066	1888.5	2.30E-04
0.4480	4.9772	6.3764	2.6334	6.0076	4.7500	6.8750	4.7289	7.6378	2059.5	4.66E-04
0.4520	4.5415	5.8931	2.7018	5.5646	4.2560	6.5584	4.5000	7.3949	2059.5	8.38E-05
0.4540	4.4747	5.8152	2.6606	5.5122	4.1877	6.4958	4.4361	7.3208	2008.5	5.55E-04
0.4560	4.4079	5.7373	2.6194	5.4598	4.1195	6.4332	4.3722	7.2467	2090.5	5.63E-04
0.4580	4.3412	5.6594	2.5782	5.4074	4.0512	6.3706	4.3082	7.1726	2070.5	6.58E-05
0.4600	4.2744	5.5815	2.5370	5.3550	3.9829	6.3080	4.2443	7.0985	2059.0	4.96E-04
0.4620	4.2076	5.5036	2.4958	5.3026	3.9147	6.2454	4.1804	7.0244	2115.0	4.31E-04
0.4640	4.1409	5.4257	2.4546	5.2502	3.8464	6.1828	4.1165	6.9503	2042.5	6.03E-04
0.4660	4.0741	5.3478	2.4134	5.1978	3.7782	6.1202	4.0526	6.8762	2015.5	5.21E-04
0.4680	4.0073	5.2699	2.3722	5.1454	3.7099	6.0576	3.9887	6.8021	2038.5	1.05E-04
0.4700	3.9406	5.1920	2.3310	5.0930	3.6417	5.9950	3.9248	6.7280	1966.5	1.53E-04
0.4720	3.8538	5.0838	2.2914	5.0360	3.5636	5.9290	3.8571	6.6094	2064.0	2.08E-05
0.4760	3.6802	4.8674	2.2122	4.9220	3.4075	5.7970	3.7218	6.3722	2020.0	8.18E-05
0.4780	3.5934	4.7592	2.1726	4.8650	3.3294	5.7310	3.6541	6.2536	2076.5	1.93E-04
0.4800	3.5066	4.6510	2.1330	4.8080	3.2513	5.6650	3.5864	6.1350	2090.5	8.76E-05
0.4820	3.5048	4.6563	2.1274	4.8271	3.2477	5.6734	3.5921	6.1311	2092.0	4.02E-04
0.4840	3.5031	4.6616	2.1218	4.8462	3.2441	5.6818	3.5977	6.1272	2028.0	6.32E-04
0.4860	3.5014	4.6669	2.1162	4.8653	3.2405	5.6902	3.6033	6.1233	1757.5	2.14E-04
0.4900	3.4979	4.6775	2.1050	4.9035	3.2332	5.7070	3.6146	6.1155	2017.5	2.46E-05
0.4920	3.4962	4.6828	2.0994	4.9226	3.2296	5.7154	3.6202	6.1116	1929.0	5.22E-04
0.4940	3.4945	4.6881	2.0938	4.9417	3.2260	5.7238	3.6259	6.1077	2007.0	1.48E-04
0.4980	3.4911	4.6987	2.0826	4.9799	3.2187	5.7406	3.6371	6.0999	1975.0	2.90E-04
0.5000	3.4893	4.7040	2.0770	4.9990	3.2151	5.7490	3.6428	6.0960	1946.5	1.06E-04
0.5020	3.5848	4.8468	2.1358	5.1432	3.3177	5.8436	3.8080	6.1728	1885.0	2.52E-04
0.5040	3.6803	4.9896	2.1946	5.2874	3.4203	5.9382	3.9731	6.2496	1934.0	2.47E-04
0.5060	3.7757	5.1324	2.2534	5.4316	3.5229	6.0328	4.1383	6.3264	2011.0	2.50E-04
0.5080	3.8712	5.2752	2.3122	5.5758	3.6255	6.1274	4.3035	6.4032	1945.5	2.76E-04
0.5100	3.9667	5.4180	2.3710	5.7200	3.7281	6.2220	4.4687	6.4800	1964.5	3.22E-04
0.5120	4.0963	5.6055	2.4709	5.8753	3.8711	6.3333	4.6571	6.5750	1965.0	2.13E-04
0.5140	4.2258	5.7930	2.5708	6.0306	4.0141	6.4446	4.8455	6.6700	1899.5	1.68E-04
0.5160	4.3554	5.9805	2.6707	6.1859	4.1571	6.5559	5.0339	6.7650	1815.0	9.79E-05
0.5180	4.4850	6.1680	2.7706	6.3412	4.3002	6.6672	5.2223	6.8600	1718.5	2.84E-04
0.5200	4.6146	6.3555	2.8705	6.4965	4.4432	6.7785	5.4107	6.9550	1861.5	2.59E-04
0.5220	4.7442	6.5430	2.9704	6.6518	4.5862	6.8898	5.5991	7.0500	1897.0	2.30E-04
0.5240	4.8738	6.7305	3.0703	6.8071	4.7292	7.0011	5.7875	7.1450	1959.5	1.85E-04
0.5260	5.0034	6.9180	3.1702	6.9624	4.8722	7.1124	5.9759	7.2400	1832.5	2.49E-04
0.5280	5.1330	7.1055	3.2701	7.1177	5.0152	7.2237	6.1643	7.3350	1895.0	1.62E-04
0.5300	5.2626	7.2930	3.3700	7.2730	5.1582	7.3350	6.3527	7.4300	1968.5	2.15E-04
0.5320	5.4960	7.6440	3.5388	7.5738	5.4172	7.5934	6.7010	7.6690	1899.0	5.90E-05
0.5340	5.7294	7.9950	3.7076	7.8746	5.6763	7.8518	7.0493	7.9080	1923.0	1.51E-04
0.5360	5.9628	8.3460	3.8764	8.1754	5.9353	8.1102	7.3976	8.1470	1963.5	3.21E-04

0.5380	6.1962	8.6970	4.0452	8.4762	6.1943	8.3686	7.7459	8.3860	1925.5	2.91E-04
0.5400	6.4297	9.0480	4.2140	8.7770	6.4533	8.6270	8.0942	8.6250	1832.0	1.58E-04
0.5420	6.4684	9.1151	4.2362	8.8563	6.4890	8.7077	8.1671	8.6882	1885.0	1.83E-04
0.5440	6.5072	9.1822	4.2584	8.9356	6.5248	8.7884	8.2400	8.7514	1911.0	3.77E-04
0.5460	6.5459	9.2493	4.2806	9.0149	6.5605	8.8691	8.3129	8.8146	1922.5	2.90E-04
0.5480	6.5846	9.3164	4.3028	9.0942	6.5962	8.9498	8.3857	8.8778	1880.0	1.84E-04
0.5500	6.6234	9.3835	4.3250	9.1735	6.6319	9.0305	8.4586	8.9410	1911.0	1.64E-04
0.5520	6.6621	9.4506	4.3472	9.2528	6.6676	9.1112	8.5315	9.0042	1890.5	2.24E-04
0.5540	6.7009	9.5177	4.3694	9.3321	6.7033	9.1919	8.6044	9.0674	1922.5	2.27E-04
0.5560	6.7396	9.5848	4.3916	9.4114	6.7390	9.2726	8.6772	9.1306	1891.5	3.50E-04
0.5580	6.7784	9.6519	4.4138	9.4907	6.7747	9.3533	8.7501	9.1938	1848.0	2.72E-04
0.5600	6.8171	9.7190	4.4360	9.5700	6.8104	9.4340	8.8230	9.2570	1857.0	2.23E-04
0.5620	6.7272	9.6062	4.3402	9.5688	6.6792	9.4992	8.7382	9.2872	1869.0	3.61E-04
0.5640	6.6374	9.4934	4.2444	9.5676	6.5480	9.5644	8.6534	9.3174	1889.5	5.43E-04
0.5660	6.5475	9.3806	4.1486	9.5664	6.4167	9.6296	8.5686	9.3476	1845.0	7.81E-04
0.5680	6.4576	9.2678	4.0528	9.5652	6.2855	9.6948	8.4838	9.3778	1880.5	8.79E-04
0.5700	6.3678	9.1550	3.9570	9.5640	6.1542	9.7600	8.3990	9.4080	1846.0	1.38E-03
0.5720	6.3068	9.0795	3.9015	9.5407	6.0780	9.7689	8.3258	9.3937	1890.0	2.34E-03
0.5740	6.2459	9.0040	3.8460	9.5174	6.0018	9.7778	8.2525	9.3794	1903.5	4.04E-03
0.5760	6.1850	8.9285	3.7905	9.4941	5.9256	9.7867	8.1793	9.3651	1870.0	7.63E-03
0.5780	6.1240	8.8530	3.7350	9.4708	5.8494	9.7956	8.1061	9.3508	1851.5	1.58E-02
0.5800	6.0631	8.7775	3.6795	9.4475	5.7732	9.8045	8.0328	9.3365	1865.0	3.66E-02
0.5820	6.0022	8.7020	3.6240	9.4242	5.6970	9.8134	7.9596	9.3222	1895.0	8.95E-02
0.5840	5.9412	8.6265	3.5685	9.4009	5.6207	9.8223	7.8864	9.3079	1890.5	2.28E-01
0.5860	5.8803	8.5510	3.5130	9.3776	5.5445	9.8312	7.8131	9.2936	1838.0	4.82E-01
0.5880	5.8194	8.4755	3.4575	9.3543	5.4683	9.8401	7.7399	9.2793	1830.0	6.71E-01
0.5900	5.7584	8.4000	3.4020	9.3310	5.3921	9.8490	7.6667	9.2650	1742.0	7.04E-01
0.5920	5.7305	8.3667	3.3796	9.3290	5.3556	9.8740	7.6233	9.2626	1828.5	7.00E-01
0.5940	5.7026	8.3334	3.3572	9.3270	5.3191	9.8990	7.5800	9.2602	1815.5	7.11E-01
0.5960	5.6747	8.3001	3.3348	9.3250	5.2825	9.9240	7.5366	9.2578	1824.5	7.41E-01
0.5980	5.6468	8.2668	3.3124	9.3230	5.2460	9.9490	7.4932	9.2554	1799.5	7.76E-01
0.6000	5.6189	8.2335	3.2900	9.3210	5.2095	9.9740	7.4499	9.2530	1788.4	8.07E-01
0.6020	5.5910	8.2002	3.2676	9.3190	5.1730	9.9990	7.4065	9.2506	1735.6	8.23E-01
0.6040	5.5631	8.1669	3.2452	9.3170	5.1365	10.0240	7.3632	9.2482	1797.6	8.30E-01
0.6060	5.5352	8.1336	3.2228	9.3150	5.0999	10.0490	7.3198	9.2458	1771.6	8.35E-01
0.6080	5.5072	8.1003	3.2004	9.3130	5.0634	10.0740	7.2765	9.2434	1751.0	8.43E-01
0.6100	5.4793	8.0670	3.1780	9.3110	5.0269	10.0990	7.2331	9.2410	1728.0	8.48E-01
0.6120	5.4161	7.9904	3.1224	9.3096	4.9448	10.1554	7.1444	9.2458	1730.0	8.53E-01
0.6140	5.3528	7.9138	3.0668	9.3082	4.8628	10.2118	7.0558	9.2506	1685.0	8.73E-01
0.6160	5.2895	7.8372	3.0112	9.3068	4.7807	10.2682	6.9671	9.2554	1661.0	9.00E-01
0.6180	5.2263	7.7606	2.9556	9.3054	4.6986	10.3246	6.8784	9.2602	1699.9	9.22E-01
0.6200	5.1630	7.6840	2.9000	9.3040	4.6166	10.3810	6.7898	9.2650	1716.2	9.35E-01
0.6220	5.1353	7.6608	2.8849	9.3000	4.5863	10.4084	6.7551	9.2576	1697.9	9.43E-01
0.6240	5.1077	7.6376	2.8698	9.2960	4.5560	10.4358	6.7204	9.2502	1661.5	9.49E-01
0.6260	5.0800	7.6144	2.8547	9.2920	4.5258	10.4632	6.6856	9.2428	1661.6	9.54E-01
0.6280	5.0524	7.5912	2.8396	9.2880	4.4955	10.4906	6.6509	9.2354	1716.2	9.63E-01
0.6300	5.0247	7.5680	2.8245	9.2840	4.4653	10.5180	6.6162	9.2280	1679.6	9.79E-01
0.6320	4.9971	7.5448	2.8094	9.2800	4.4350	10.5454	6.5815	9.2206	1659.5	9.86E-01
0.6340	4.9694	7.5216	2.7943	9.2760	4.4048	10.5728	6.5468	9.2132	1665.3	9.91E-01
0.6360	4.9418	7.4984	2.7792	9.2720	4.3745	10.6002	6.5121	9.2058	1666.5	9.95E-01

0.6380	4.9141	7.4752	2.7641	9.2680	4.3443	10.6276	6.4774	9.1984	1685.6	9.98E-01
0.6400	4.8864	7.4520	2.7490	9.2640	4.3140	10.6550	6.4427	9.1910	1640.2	9.99E-01
0.6420	4.8115	7.3832	2.6968	9.2116	4.2361	10.6968	6.3086	9.1868	1634.0	1.00E+00
0.6440	4.7366	7.3144	2.6446	9.1592	4.1582	10.7386	6.1746	9.1826	1636.0	9.99E-01
0.6460	4.6616	7.2456	2.5924	9.1068	4.0803	10.7804	6.0405	9.1784	1621.1	9.96E-01
0.6480	4.5867	7.1768	2.5402	9.0544	4.0024	10.8222	5.9065	9.1742	1633.6	9.94E-01
0.6500	4.5118	7.1080	2.4880	9.0020	3.9246	10.8640	5.7724	9.1700	1574.3	9.90E-01
0.6520	4.4713	7.0667	2.4663	8.9670	3.8843	10.8721	5.6830	9.1573	1626.1	9.85E-01
0.6540	4.4307	7.0254	2.4446	8.9320	3.8441	10.8802	5.5935	9.1446	1593.8	9.83E-01
0.6560	4.3902	6.9841	2.4229	8.8970	3.8038	10.8883	5.5041	9.1319	1349.8	9.75E-01
0.6580	4.3497	6.9428	2.4012	8.8620	3.7636	10.8964	5.4146	9.1192	1544.8	9.68E-01
0.6600	4.3092	6.9015	2.3795	8.8270	3.7233	10.9045	5.3252	9.1065	1578.3	9.39E-01
0.6620	4.2686	6.8602	2.3578	8.7920	3.6831	10.9126	5.2357	9.0938	1597.0	9.03E-01
0.6640	4.2281	6.8189	2.3361	8.7570	3.6428	10.9207	5.1463	9.0811	1558.0	8.72E-01
0.6660	4.1876	6.7776	2.3144	8.7220	3.6026	10.9288	5.0568	9.0684	1566.2	8.58E-01
0.6680	4.1471	6.7363	2.2927	8.6870	3.5624	10.9369	4.9673	9.0557	1555.1	8.67E-01
0.6700	4.1066	6.6950	2.2710	8.6520	3.5221	10.9450	4.8779	9.0430	1553.8	9.05E-01
0.6720	4.1041	6.6884	2.2710	8.6756	3.5208	10.9592	4.8525	9.0146	1540.7	9.55E-01
0.6740	4.1016	6.6818	2.2710	8.6992	3.5195	10.9734	4.8270	8.9862	1532.8	9.54E-01
0.6760	4.0991	6.6752	2.2710	8.7228	3.5182	10.9876	4.8016	8.9578	1526.7	8.24E-01
0.6780	4.0966	6.6686	2.2710	8.7464	3.5169	11.0018	4.7762	8.9294	1519.8	5.58E-01
0.6800	4.0941	6.6620	2.2710	8.7700	3.5156	11.0160	4.7508	8.9010	1514.9	3.24E-01
0.6820	4.2899	6.8698	2.4158	9.0069	3.7250	11.0850	5.0840	8.9314	1509.9	1.75E-01
0.6840	4.4857	7.0776	2.5606	9.2438	3.9344	11.1540	5.4173	8.9618	1505.8	9.41E-02
0.6860	4.6814	7.2854	2.7054	9.4807	4.1438	11.2230	5.7505	8.9922	1502.9	5.24E-02
0.6880	4.8772	7.4932	2.8502	9.7176	4.3532	11.2920	6.0838	9.0226	1499.9	3.02E-02
0.6900	5.0730	7.7010	2.9950	9.9545	4.5626	11.3610	6.4171	9.0530	1506.4	1.83E-02
0.6920	5.2688	7.9088	3.1398	10.1914	4.7720	11.4300	6.7503	9.0834	1495.0	1.16E-02
0.6940	5.4646	8.1166	3.2846	10.4283	4.9814	11.4990	7.0836	9.1138	1498.0	7.53E-03
0.6960	5.6603	8.3244	3.4294	10.6652	5.1908	11.5680	7.4168	9.1442	1489.0	4.93E-03
0.6980	5.8561	8.5322	3.5742	10.9021	5.4002	11.6370	7.7501	9.1746	1459.6	3.34E-03
0.7000	6.0519	8.7400	3.7190	11.1390	5.6096	11.7060	8.0833	9.2050	1484.3	2.23E-03
0.7020	7.1440	10.0658	4.6840	12.2826	6.8494	12.3360	9.5865	9.7086	1455.5	1.55E-03
0.7040	8.2361	11.3916	5.6490	13.4262	8.0893	12.9660	11.0896	10.2122	1469.1	1.07E-03
0.7060	9.3282	12.7174	6.6140	14.5698	9.3292	13.5960	12.5928	10.7158	1470.4	8.13E-04
0.7080	10.4202	14.0432	7.5790	15.7134	10.5691	14.2260	14.0960	11.2194	1454.0	6.94E-04
0.7100	11.5123	15.3690	8.5440	16.8570	11.8090	14.8560	15.5991	11.7230	1427.0	4.66E-04
0.7180	17.3191	20.1354	13.3907	20.1663	18.4698	17.0565	20.4506	13.4966	1398.1	8.84E-05
0.7240	21.6741	23.7102	17.0257	22.6483	23.4654	18.7069	24.0891	14.8268	1388.6	6.13E-06
0.7580	37.7178	35.2971	29.5309	31.6118	41.7208	24.8411	36.3684	19.3964	1271.0	1.20E-05
0.8100	48.3372	40.1830	36.2180	37.5320	53.4945	29.1185	42.5766	21.8875	1095.0	4.68E-05
0.8220	48.7432	40.3108	36.4142	38.1524	53.8242	29.4560	42.8345	22.0336	1053.0	7.45E-05

AVHRR NIR BAND SIMULATION DATA

Wavelength	Winter Barley	Sugar beet	Forest	Pasture	Winter wheat	Bare soil	Winter OSR	Urban	Exoterrestrial irradiance	Normalised sensor response
0.5000	3.4893	4.7040	2.0770	4.9990	3.2151	5.7490	3.6428	6.0960	1946.5	3.89E-04
0.5040	3.6803	4.9896	2.1946	5.2874	3.4203	5.9382	3.9731	6.2496	1934.0	1.25E-04
0.5080	3.8712	5.2752	2.3122	5.5758	3.6255	6.1274	4.3035	6.4032	1945.5	2.19E-04
0.5120	4.0963	5.6055	2.4709	5.8753	3.8711	6.3333	4.6571	6.5750	1965.0	3.00E-04
0.5160	4.3554	5.9805	2.6707	6.1859	4.1571	6.5559	5.0339	6.7650	1815.0	9.49E-05
0.5200	4.6146	6.3555	2.8705	6.4965	4.4432	6.7785	5.4107	6.9550	1861.5	1.02E-04
0.5280	5.1330	7.1055	3.2701	7.1177	5.0152	7.2237	6.1643	7.3350	1895.0	6.32E-05
0.5400	6.4297	9.0480	4.2140	8.7770	6.4533	8.6270	8.0942	8.6250	1832.0	2.73E-05
0.5520	6.6621	9.4506	4.3472	9.2528	6.6676	9.1112	8.5315	9.0042	1890.5	7.25E-05
0.5640	6.6374	9.4934	4.2444	9.5676	6.5480	9.5644	8.6534	9.3174	1889.5	1.85E-05
0.5680	6.4576	9.2678	4.0528	9.5652	6.2855	9.6948	8.4838	9.3778	1880.5	4.81E-05
0.5720	6.3068	9.0795	3.9015	9.5407	6.0780	9.7689	8.3258	9.3937	1890.0	8.15E-05
0.5760	6.1850	8.9285	3.7905	9.4941	5.9256	9.7867	8.1793	9.3651	1870.0	1.29E-05
0.5800	6.0631	8.7775	3.6795	9.4475	5.7732	9.8045	8.0328	9.3365	1865.0	1.35E-05
0.6240	5.1077	7.6376	2.8698	9.2960	4.5560	10.4358	6.7204	9.2502	1661.5	1.05E-05
0.6400	4.8864	7.4520	2.7490	9.2640	4.3140	10.6550	6.4427	9.1910	1640.2	1.10E-05
0.6560	4.3902	6.9841	2.4229	8.8970	3.8038	10.8883	5.5041	9.1319	1349.8	1.32E-05
0.6600	4.3092	6.9015	2.3795	8.8270	3.7233	10.9045	5.3252	9.1065	1578.3	3.22E-06
0.6640	4.2281	6.8189	2.3361	8.7570	3.6428	10.9207	5.1463	9.0811	1558.0	4.03E-05
0.6680	4.1471	6.7363	2.2927	8.6870	3.5624	10.9369	4.9673	9.0557	1555.1	6.38E-05
0.6720	4.1041	6.6884	2.2710	8.6756	3.5208	10.9592	4.8525	9.0146	1540.7	1.16E-04
0.6760	4.0991	6.6752	2.2710	8.7228	3.5182	10.9876	4.8016	8.9578	1526.7	1.34E-04
0.6800	4.0941	6.6620	2.2710	8.7700	3.5156	11.0160	4.7508	8.9010	1514.9	2.08E-04
0.6840	4.4857	7.0776	2.5606	9.2438	3.9344	11.1540	5.4173	8.9618	1505.8	3.21E-04
0.6880	4.8772	7.4932	2.8502	9.7176	4.3532	11.2920	6.0838	9.0226	1499.9	7.83E-04
0.6920	5.2688	7.9088	3.1398	10.1914	4.7720	11.4300	6.7503	9.0834	1495.0	1.95E-03
0.6960	5.6603	8.3244	3.4294	10.6652	5.1908	11.5680	7.4168	9.1442	1489.0	5.39E-03
0.7000	6.0519	8.7400	3.7190	11.1390	5.6096	11.7060	8.0833	9.2050	1484.3	1.44E-02
0.7040	8.2361	11.3916	5.6490	13.4262	8.0893	12.9660	11.0896	10.2122	1469.1	3.50E-02
0.7080	10.4202	14.0432	7.5790	15.7134	10.5691	14.2260	14.0960	11.2194	1454.0	7.84E-02
0.7120	12.4847	16.3287	9.4187	17.5176	12.9287	15.2621	16.5749	12.0620	1415.4	1.49E-01
0.7160	14.4295	18.2481	11.1681	18.8388	15.1681	16.0743	18.5265	12.7400	1403.0	2.26E-01
0.7200	16.3742	20.1675	12.9175	20.1600	17.4076	16.8865	20.4781	13.4180	1387.8	3.00E-01
0.7240	18.3190	22.0869	14.6669	21.4812	19.6470	17.6987	22.4296	14.0960	1388.6	3.65E-01
0.7280	20.2637	24.0063	16.4163	22.8024	21.8864	18.5109	24.3812	14.7740	1372.0	4.20E-01
0.7320	23.6464	26.6214	19.1766	24.6238	25.7623	19.7552	27.0440	15.7652	1358.1	4.95E-01
0.7360	28.4670	29.9322	22.9478	26.9454	31.2746	21.4316	30.4180	17.0696	1335.1	6.16E-01
0.7400	33.2876	33.2430	26.7190	29.2670	36.7870	23.1080	33.7920	18.3740	1308.0	7.62E-01
0.7440	34.9824	34.1548	27.9046	30.0156	38.7725	23.7142	34.7694	18.7832	1322.8	8.81E-01
0.7480	36.6773	35.0666	29.0902	30.7642	40.7579	24.3204	35.7468	19.1924	1321.8	9.20E-01
0.7520	38.3722	35.9784	30.2758	31.5128	42.7434	24.9266	36.7241	19.6016	1285.0	9.03E-01
0.7560	40.0671	36.8902	31.4614	32.2614	44.7289	25.5328	37.7015	20.0108	1280.0	8.76E-01
0.7600	41.7620	37.8020	32.6470	33.0100	46.7143	26.1390	38.6789	20.4200	1257.0	8.58E-01
0.7640	43.3564	38.3872	33.5462	33.8096	48.4518	26.7402	39.5093	20.7488	1243.0	8.66E-01
0.7680	44.9507	38.9724	34.4454	34.6092	50.1892	27.3414	40.3397	21.0776	1224.0	9.15E-01

0.7720	45.8987	39.3255	34.9808	35.1270	51.2049	27.7127	40.8559	21.2782	1206.0	9.62E-01
0.7760	46.2002	39.4465	35.1524	35.3630	51.4990	27.8541	41.0579	21.3506	1186.0	9.94E-01
0.7800	46.5018	39.5675	35.3240	35.5990	51.7931	27.9955	41.2599	21.4230	1212.0	9.97E-01
0.7840	46.8033	39.6885	35.4956	35.8350	52.0871	28.1369	41.4620	21.4954	1207.0	9.89E-01
0.7880	47.1049	39.8095	35.6672	36.0710	52.3812	28.2783	41.6640	21.5678	1191.0	9.89E-01
0.7920	47.4155	39.9140	35.8208	36.3678	52.6692	28.4562	41.8880	21.6396	1149.0	9.90E-01
0.7960	47.7353	40.0020	35.9564	36.7254	52.9511	28.6706	42.1341	21.7108	1161.0	9.81E-01
0.8000	48.0550	40.0900	36.0920	37.0830	53.2330	28.8850	42.3801	21.7820	1143.0	9.73E-01
0.8040	48.1679	40.1272	36.1424	37.2626	53.3376	28.9784	42.4587	21.8242	1137.0	9.76E-01
0.8080	48.2807	40.1644	36.1928	37.4422	53.4422	29.0718	42.5373	21.8664	1110.0	9.86E-01
0.8120	48.3936	40.2016	36.2432	37.6218	53.5468	29.1652	42.6158	21.9086	1091.0	9.95E-01
0.8160	48.5065	40.2388	36.2936	37.8014	53.6514	29.2586	42.6944	21.9508	1080.0	9.99E-01
0.8200	48.6193	40.2760	36.3440	37.9810	53.7560	29.3520	42.7730	21.9930	1069.0	9.99E-01
0.8240	48.8671	40.3456	36.4844	38.3238	53.8924	29.5600	42.8960	22.0742	1072.0	1.00E+00
0.8280	49.1149	40.4152	36.6248	38.6666	54.0288	29.7680	43.0190	22.1554	1060.0	9.98E-01
0.8320	49.3070	40.4710	36.7364	38.9313	54.1536	29.9252	43.1246	22.2075	1047.0	9.95E-01
0.8360	49.4435	40.5130	36.8192	39.1179	54.2668	30.0316	43.2128	22.2305	1019.0	9.91E-01
0.8400	49.5801	40.5550	36.9020	39.3045	54.3801	30.1380	43.3011	22.2535	1017.0	9.86E-01
0.8440	49.7166	40.5970	36.9848	39.4911	54.4933	30.2444	43.3894	22.2765	990.7	9.80E-01
0.8480	49.8531	40.6390	37.0676	39.6777	54.6065	30.3508	43.4776	22.2995	1003.0	9.69E-01
0.8520	50.0306	40.6910	37.2036	39.9310	54.7570	30.4798	43.5951	22.3610	957.1	9.55E-01
0.8560	50.2493	40.7530	37.3928	40.2510	54.9449	30.6314	43.7417	22.4610	939.2	9.41E-01
0.8600	50.4679	40.8150	37.5820	40.5710	55.1328	30.7830	43.8883	22.5610	959.0	9.30E-01
0.8640	50.5474	40.8482	37.6230	40.7414	55.1942	30.8698	43.9266	22.5918	912.5	9.23E-01
0.8680	50.6269	40.8814	37.6640	40.9118	55.2556	30.9566	43.9650	22.6226	953.1	9.22E-01
0.8720	50.7064	40.9146	37.7050	41.0822	55.3170	31.0434	44.0033	22.6534	944.2	9.30E-01
0.8760	50.7859	40.9478	37.7460	41.2526	55.3785	31.1302	44.0416	22.6842	949.1	9.41E-01
0.8800	50.8654	40.9810	37.7870	41.4230	55.4399	31.2170	44.0799	22.7150	926.3	9.52E-01
0.8840	50.9328	41.0378	37.8924	41.5872	55.5056	31.3208	44.1218	22.7908	928.3	9.51E-01
0.8880	51.0002	41.0946	37.9978	41.7514	55.5714	31.4246	44.1637	22.8666	915.4	9.44E-01
0.8920	51.0675	41.1514	38.1032	41.9156	55.6372	31.5284	44.2056	22.9424	902.6	9.28E-01
0.8960	51.1349	41.2082	38.2086	42.0798	55.7029	31.6322	44.2474	23.0182	910.5	9.10E-01
0.9000	51.2022	41.2650	38.3140	42.2440	55.7687	31.7360	44.2893	23.0940	880.8	8.94E-01
0.9040	51.1724	41.3334	38.2252	42.5376	55.6922	31.8956	44.2198	23.1124	872.8	8.89E-01
0.9080	51.1426	41.4018	38.1364	42.8312	55.6158	32.0552	44.1502	23.1308	846.1	8.92E-01
0.9120	51.0865	41.4344	38.1159	43.0428	55.5547	32.1667	44.0785	23.1577	864.9	9.04E-01
0.9160	51.0041	41.4312	38.1637	43.1724	55.5090	32.2301	44.0047	23.1931	852.0	9.12E-01
0.9200	50.9218	41.4280	38.2115	43.3020	55.4633	32.2935	43.9308	23.2285	827.3	9.15E-01
0.9240	50.8394	41.4248	38.2593	43.4316	55.4176	32.3569	43.8570	23.2639	826.3	9.04E-01
0.9280	50.7571	41.4216	38.3071	43.5612	55.3719	32.4203	43.7831	23.2993	837.2	8.80E-01
0.9320	50.3954	41.3686	38.2490	43.8164	54.9930	32.5922	43.4316	23.3440	840.1	8.49E-01
0.9360	49.7544	41.2658	38.0850	44.1972	54.2809	32.8726	42.8023	23.3980	812.4	8.20E-01
0.9400	49.1134	41.1630	37.9210	44.5780	53.5688	33.1530	42.1730	23.4520	813.4	7.95E-01
0.9440	48.5633	40.9028	37.6714	44.6552	52.9438	33.1426	41.6158	23.4398	814.4	7.66E-01
0.9480	48.0131	40.6426	37.4218	44.7324	52.3187	33.1322	41.0585	23.4276	793.6	7.48E-01
0.9520	47.4629	40.3824	37.1722	44.8096	51.6937	33.1218	40.5013	23.4154	788.6	7.37E-01
0.9560	46.9127	40.1222	36.9226	44.8868	51.0687	33.1114	39.9440	23.4032	791.6	7.29E-01
0.9600	46.3626	39.8620	36.6730	44.9640	50.4437	33.1010	39.3868	23.3910	784.7	7.19E-01
0.9640	45.9010	39.6408	36.5938	45.0924	50.0010	33.0986	38.8761	23.3398	777.2	7.04E-01
0.9680	45.4394	39.4196	36.5146	45.2208	49.5584	33.0962	38.3654	23.2886	771.7	6.81E-01

0.9720	45.2464	39.3328	36.5162	45.3380	49.3674	33.1107	38.1339	23.2702	771.9	6.47E-01
0.9760	45.3220	39.3804	36.5986	45.4440	49.4279	33.1421	38.1817	23.2846	760.4	5.83E-01
0.9800	45.3976	39.4280	36.6810	45.5500	49.4884	33.1735	38.2296	23.2990	752.4	4.78E-01
0.9840	45.4732	39.4756	36.7634	45.6560	49.5490	33.2049	38.2774	23.3134	749.2	3.62E-01
0.9880	45.5489	39.5232	36.8458	45.7620	49.6095	33.2363	38.3252	23.3278	742.9	2.61E-01
0.9920	45.7102	39.6055	36.9632	45.8843	49.7599	33.2953	38.4616	23.3569	738.7	1.84E-01
0.9960	45.9572	39.7225	37.1156	46.0229	50.0000	33.3819	38.6867	23.4007	733.6	1.26E-01
1.0000	46.2042	39.8395	37.2680	46.1615	50.2402	33.4685	38.9117	23.4445	728.0	7.84E-02
1.0040	46.4512	39.9565	37.4204	46.3001	50.4803	33.5551	39.1368	23.4883	709.7	4.37E-02
1.0080	46.6983	40.0735	37.5728	46.4387	50.7205	33.6417	39.3618	23.5321	714.5	2.17E-02
1.0120	47.1519	40.2922	37.7992	46.6336	51.1643	33.7880	39.7822	23.6022	709.5	1.01E-02
1.0160	47.8120	40.6126	38.0996	46.8848	51.8118	33.9940	40.3979	23.6986	697.1	4.64E-03
1.0200	48.4722	40.9330	38.4000	47.1360	52.4593	34.2000	41.0137	23.7950	691.0	2.17E-03
1.0240	48.8350	41.0928	38.5750	47.2844	52.8239	34.2936	41.3586	23.8464	694.0	1.02E-03
1.0280	49.1979	41.2526	38.7500	47.4328	53.1884	34.3872	41.7036	23.8978	690.5	5.08E-04
1.0320	49.5607	41.4124	38.9250	47.5812	53.5530	34.4808	42.0485	23.9492	682.3	2.39E-04
1.0360	49.9235	41.5722	39.1000	47.7296	53.9176	34.5744	42.3935	24.0006	675.4	1.45E-04
1.0400	50.2863	41.7320	39.2750	47.8780	54.2821	34.6680	42.7384	24.0520	664.4	5.13E-05
1.0440	50.8015	41.9168	39.4706	48.0452	54.8062	34.8124	43.2673	24.1092	666.3	8.53E-06

MODIS RED BAND SIMULATION DATA

Wavelength	Winter Barley	Sugar beet	Forest	Pasture	Winter wheat	Bare soil	Winter OSR	Urban	Extraterrestrial irradiance	Normalised sensors response
0.6120	5.4161	7.9904	3.1224	9.3096	4.9448	10.1554	7.1444	9.2458	1730.0	2.87E-03
0.6140	5.3528	7.9138	3.0668	9.3082	4.8628	10.2118	7.0558	9.2506	1685.0	8.93E-03
0.6170	5.2579	7.7989	2.9834	9.3061	4.7397	10.2964	6.9228	9.2578	1680.5	7.02E-02
0.6190	5.1946	7.7223	2.9278	9.3047	4.6576	10.3528	6.8341	9.2626	1700.6	2.34E-01
0.6220	5.1353	7.6608	2.8849	9.3000	4.5863	10.4084	6.7551	9.2576	1697.9	6.22E-01
0.6240	5.1077	7.6376	2.8698	9.2960	4.5560	10.4358	6.7204	9.2502	1661.5	7.04E-01
0.6270	5.0662	7.6028	2.8472	9.2900	4.5107	10.4769	6.6683	9.2391	1688.9	7.07E-01
0.6290	5.0386	7.5796	2.8321	9.2860	4.4804	10.5043	6.6336	9.2317	1697.9	7.16E-01
0.6320	4.9971	7.5448	2.8094	9.2800	4.4350	10.5454	6.5815	9.2206	1659.5	7.29E-01
0.6340	4.9694	7.5216	2.7943	9.2760	4.4048	10.5728	6.5468	9.2132	1665.3	7.32E-01
0.6370	4.9279	7.4868	2.7717	9.2700	4.3594	10.6139	6.4947	9.2021	1676.1	7.46E-01
0.6390	4.9003	7.4636	2.7566	9.2660	4.3291	10.6413	6.4600	9.1947	1662.9	7.47E-01
0.6420	4.8115	7.3832	2.6968	9.2116	4.2361	10.6968	6.3086	9.1868	1634.0	7.59E-01
0.6440	4.7366	7.3144	2.6446	9.1592	4.1582	10.7386	6.1746	9.1826	1636.0	7.72E-01
0.6470	4.6242	7.2112	2.5663	9.0806	4.0414	10.8013	5.9735	9.1763	1627.3	8.38E-01
0.6490	4.5492	7.1424	2.5141	9.0282	3.9635	10.8431	5.8395	9.1721	1604.0	8.74E-01
0.6520	4.4713	7.0667	2.4663	8.9670	3.8843	10.8721	5.6830	9.1573	1626.1	9.45E-01
0.6540	4.4307	7.0254	2.4446	8.9320	3.8441	10.8802	5.5935	9.1446	1593.8	9.76E-01
0.6570	4.3700	6.9635	2.4121	8.8795	3.7837	10.8924	5.4594	9.1256	1447.3	1.00E+00
0.6590	4.3294	6.9222	2.3904	8.8445	3.7435	10.9005	5.3699	9.1129	1561.6	9.70E-01
0.6620	4.2686	6.8602	2.3578	8.7920	3.6831	10.9126	5.2357	9.0938	1597.0	8.30E-01
0.6640	4.2281	6.8189	2.3361	8.7570	3.6428	10.9207	5.1463	9.0811	1558.0	7.55E-01
0.6670	4.1673	6.7570	2.3036	8.7045	3.5825	10.9329	5.0121	9.0621	1560.7	5.89E-01
0.6690	4.1268	6.7157	2.2819	8.6695	3.5422	10.9410	4.9226	9.0494	1554.5	4.33E-01
0.6720	4.1041	6.6884	2.2710	8.6756	3.5208	10.9592	4.8525	9.0146	1540.7	2.00E-01
0.6740	4.1016	6.6818	2.2710	8.6992	3.5195	10.9734	4.8270	8.9862	1532.8	1.10E-01
0.6770	4.0978	6.6719	2.2710	8.7346	3.5175	10.9947	4.7889	8.9436	1523.3	4.14E-02
0.6790	4.0954	6.6653	2.2710	8.7582	3.5162	11.0089	4.7635	8.9152	1517.4	2.05E-02
0.6820	4.2899	6.8698	2.4158	9.0069	3.7250	11.0850	5.0840	8.9314	1509.9	6.19E-03

MODIS NIR BAND SIMULATION DATA

Wavelength	Winter Barley	Sugar beet	Forest	Pasture	Winter wheat	Bare soil	Winter OSR	Urban	Extraterrestrial irradiance	Normalised sensors response
0.8190	48.5911	40.2667	36.3314	37.9361	53.7299	29.3287	42.7534	21.9825	1072.5	6.79E-03
0.8220	48.7432	40.3108	36.4142	38.1524	53.8242	29.4560	42.8345	22.0336	1053.0	1.60E-02
0.8240	48.8671	40.3456	36.4844	38.3238	53.8924	29.5600	42.8960	22.0742	1072.0	3.11E-02
0.8270	49.0529	40.3978	36.5897	38.5809	53.9947	29.7160	42.9882	22.1351	1064.0	7.75E-02
0.8290	49.1768	40.4326	36.6599	38.7523	54.0629	29.8200	43.0497	22.1757	1046.5	1.26E-01
0.8320	49.3070	40.4710	36.7364	38.9313	54.1536	29.9252	43.1246	22.2075	1047.0	2.04E-01
0.8340	49.3753	40.4920	36.7778	39.0246	54.2102	29.9784	43.1687	22.2190	1028.0	2.50E-01
0.8370	49.4777	40.5235	36.8399	39.1646	54.2951	30.0582	43.2349	22.2363	1028.5	3.72E-01
0.8390	49.5459	40.5445	36.8813	39.2579	54.3518	30.1114	43.2790	22.2478	1027.5	5.13E-01
0.8420	49.6483	40.5760	36.9434	39.3978	54.4367	30.1912	43.3452	22.2650	1020.0	7.70E-01
0.8440	49.7166	40.5970	36.9848	39.4911	54.4933	30.2444	43.3894	22.2765	990.7	8.81E-01
0.8470	49.8190	40.6285	37.0469	39.6311	54.5782	30.3242	43.4556	22.2938	1002.0	9.20E-01
0.8490	49.8872	40.6495	37.0883	39.7244	54.6348	30.3774	43.4997	22.3053	985.0	9.20E-01
0.8520	50.0306	40.6910	37.2036	39.9310	54.7570	30.4798	43.5951	22.3610	957.1	9.24E-01
0.8540	50.1400	40.7220	37.2982	40.0910	54.8510	30.5556	43.6684	22.4110	867.9	9.34E-01
0.8570	50.3039	40.7685	37.4401	40.3310	54.9919	30.6693	43.7784	22.4860	962.0	9.50E-01
0.8590	50.4132	40.7995	37.5347	40.4910	55.0858	30.7451	43.8517	22.5360	971.9	9.74E-01
0.8620	50.5076	40.8316	37.6025	40.6562	55.1635	30.8264	43.9075	22.5764	975.9	1.00E+00
0.8640	50.5474	40.8482	37.6230	40.7414	55.1942	30.8698	43.9266	22.5918	912.5	9.91E-01
0.8670	50.6070	40.8731	37.6538	40.8692	55.2403	30.9349	43.9554	22.6149	916.0	9.47E-01
0.8690	50.6468	40.8897	37.6743	40.9544	55.2710	30.9783	43.9745	22.6303	952.1	9.09E-01
0.8720	50.7064	40.9146	37.7050	41.0822	55.3170	31.0434	44.0033	22.6534	944.2	8.54E-01
0.8740	50.7462	40.9312	37.7255	41.1674	55.3478	31.0868	44.0224	22.6688	947.1	7.12E-01
0.8770	50.8058	40.9561	37.7563	41.2952	55.3938	31.1519	44.0512	22.6919	937.2	3.52E-01
0.8790	50.8456	40.9727	37.7768	41.3804	55.4245	31.1953	44.0703	22.7073	925.8	1.96E-01
0.8820	50.8991	41.0094	37.8397	41.5051	55.4728	31.2689	44.1008	22.7529	914.5	9.52E-02
0.8840	50.9328	41.0378	37.8924	41.5872	55.5056	31.3208	44.1218	22.7908	928.3	6.66E-02
0.8870	50.9833	41.0804	37.9715	41.7104	55.5550	31.3987	44.1532	22.8477	914.5	4.35E-02
0.8890	51.0170	41.1088	38.0242	41.7925	55.5878	31.4506	44.1741	22.8856	913.5	3.52E-02
0.8920	51.0675	41.1514	38.1032	41.9156	55.6372	31.5284	44.2056	22.9424	905.6	2.48E-02
0.8940	51.1012	41.1798	38.1559	41.9977	55.6700	31.5803	44.2265	22.9803	905.5	1.92E-02
0.8970	51.1517	41.2224	38.2350	42.1209	55.7194	31.6582	44.2579	23.0372	898.1	1.24E-02

VGT RED BAND SIMULATION DATA

Wavelength	Winter Barley	Sugar beet	Forest	Pasture	Winter wheat	Bare soil	Winter OSR	Urban	Extraterrestrial irradiance	Normalised sensors response
0.5800	6.0631	8.7775	3.6795	9.4475	5.7732	9.8045	8.0328	9.3365	1865.0	0.00E+00
0.5900	5.7584	8.4000	3.4020	9.3310	5.3921	9.8490	7.6667	9.2650	1742.0	0.00E+00
0.6000	5.6189	8.2335	3.2900	9.3210	5.2095	9.9740	7.4499	9.2530	1789.2	8.00E-03
0.6100	5.4793	8.0670	3.1780	9.3110	5.0269	10.0990	7.2331	9.2410	1728.0	1.60E-01
0.6200	5.1630	7.6840	2.9000	9.3040	4.6166	10.3810	6.7898	9.2650	1716.2	6.08E-01
0.6300	5.0247	7.5680	2.8245	9.2840	4.4653	10.5180	6.6162	9.2280	1684.3	8.16E-01
0.6400	4.8864	7.4520	2.7490	9.2640	4.3140	10.6550	6.4427	9.1910	1640.2	8.56E-01
0.6500	4.5118	7.1080	2.4880	9.0020	3.9246	10.8640	5.7724	9.1700	1610.0	8.96E-01
0.6600	4.3092	6.9015	2.3795	8.8270	3.7233	10.9045	5.3252	9.1065	1578.3	9.52E-01
0.6700	4.1066	6.6950	2.2710	8.6520	3.5221	10.9450	4.8779	9.0430	1553.4	1.00E+00
0.6800	4.0941	6.6620	2.2710	8.7700	3.5156	11.0160	4.7508	8.9010	1514.0	9.68E-01
0.6900	5.0730	7.7010	2.9950	9.9545	4.5626	11.3610	6.4171	9.0530	1511.4	7.76E-01
0.7000	6.0519	8.7400	3.7190	11.1390	5.6096	11.7060	8.0833	9.2050	1478.8	4.80E-01
0.7100	11.5123	15.3690	8.5440	16.8570	11.8090	14.8560	15.5991	11.7230	1435.8	2.56E-01
0.7200	16.3742	20.1675	12.9175	20.1600	17.4076	16.8865	20.4781	13.4180	1387.3	1.28E-01
0.7300	21.2361	24.9660	17.2910	23.4630	23.0061	18.9170	25.3570	15.1130	1354.4	5.60E-02
0.7400	33.2876	33.2430	26.7190	29.2670	36.7870	23.1080	33.7920	18.3740	1304.8	2.40E-02
0.7500	37.5248	35.5225	29.6830	31.1385	41.7507	24.6235	36.2354	19.3970	1298.8	8.00E-03
0.7600	41.7620	37.8020	32.6470	33.0100	46.7143	26.1390	38.6789	20.4200	1257.0	8.00E-03
0.7700	45.7479	39.2650	34.8950	35.0090	51.0579	27.6420	40.7549	21.2420	1215.0	0.00E+00

VGT NIR BAND SIMULATION DATA

Wavelength	Winter Barley	Sugar beet	Forest	Pasture	Winter wheat	Bare soil	Winter OSR	Urban	Extraterrestrial irradiance	Normalised sensors response
0.7300	21.2361	24.9660	17.2910	23.4630	23.0061	18.9170	25.3570	15.1130	1354.4	0.00E+00
0.7400	33.2876	33.2430	26.7190	29.2670	36.7870	23.1080	33.7920	18.3740	1304.8	1.20E-02
0.7500	37.5248	35.5225	29.6830	31.1385	41.7507	24.6235	36.2354	19.3970	1298.8	4.82E-02
0.7600	41.7620	37.8020	32.6470	33.0100	46.7143	26.1390	38.6789	20.4200	1257.0	1.69E-01
0.7700	45.7479	39.2650	34.8950	35.0090	51.0579	27.6420	40.7549	21.2420	1215.0	3.98E-01
0.7800	46.5018	39.5675	35.3240	35.5990	51.7931	27.9955	41.2599	21.4230	1212.0	6.51E-01
0.7900	47.2557	39.8700	35.7530	36.1890	52.5282	28.3490	41.7650	21.6040	1174.0	8.43E-01
0.8000	48.0550	40.0900	36.0920	37.0830	53.2330	28.8850	42.3801	21.7820	1143.0	9.52E-01
0.8100	48.3372	40.1830	36.2180	37.5320	53.4945	29.1185	42.5766	21.8875	1095.0	1.00E+00
0.8200	48.6193	40.2760	36.3440	37.9810	53.7560	29.3520	42.7730	21.9930	1069.0	1.00E+00
0.8300	49.2388	40.4500	36.6950	38.8380	54.0970	29.8720	43.0804	22.1960	1033.0	1.00E+00
0.8400	49.5801	40.5550	36.9020	39.3045	54.3801	30.1380	43.3011	22.2535	1017.0	1.00E+00
0.8500	49.9213	40.6600	37.1090	39.7710	54.6631	30.4040	43.5218	22.3110	967.0	9.88E-01
0.8600	50.4679	40.8150	37.5820	40.5710	55.1328	30.7830	43.8883	22.5610	959.0	9.64E-01
0.8700	50.6667	40.8980	37.6845	40.9970	55.2863	31.0000	43.9841	22.6380	951.1	9.28E-01
0.8800	50.8654	40.9810	37.7870	41.4230	55.4399	31.2170	44.0799	22.7150	926.3	8.43E-01
0.8900	51.0338	41.1230	38.0505	41.8335	55.6043	31.4765	44.1846	22.9045	911.5	6.39E-01
0.9000	51.2022	41.2650	38.3140	42.2440	55.7687	31.7360	44.2893	23.0940	880.8	3.37E-01
0.9100	51.1277	41.4360	38.0920	42.9780	55.5776	32.1350	44.1154	23.1400	857.0	1.45E-01
0.9200	50.9218	41.4280	38.2115	43.3020	55.4633	32.2935	43.9308	23.2285	827.3	6.02E-02
0.9300	50.7159	41.4200	38.3310	43.6260	55.3490	32.4520	43.7462	23.3170	832.2	2.41E-02
0.9400	49.1134	41.1630	37.9210	44.5780	53.5688	33.1530	42.1730	23.4520	813.4	1.20E-02
0.9500	47.7380	40.5125	37.2970	44.7710	52.0062	33.1270	40.7799	23.4215	795.6	1.20E-02
0.9600	46.3626	39.8620	36.6730	44.9640	50.4437	33.1010	39.3868	23.3910	784.7	0.00E+00

Appendix B, Land cover mapping

GLC2000 CLASSIFICATION SCHEME
(http://www-gvm.jrc.it/glc2000/Legend/GLC2000_legend_summary.doc (14 December 2006)

	GLC Global Class (according to LCCS terminology)
1	Tree Cover, broadleaved, evergreen
2	Tree Cover, broadleaved, deciduous, closed
3	Tree Cover, broadleaved, deciduous, open
4	Tree Cover, needle-leaved, evergreen
5	Tree Cover, needle-leaved, deciduous
6	Tree Cover, mixed leaf type
7	Tree Cover, regularly flooded, fresh water
8	Tree Cover, regularly flooded, saline water
9	Mosaic: Tree cover / Other natural vegetation
10	Tree Cover, burnt
11	Shrub Cover, closed-open, evergreen
12	Shrub Cover, closed-open, deciduous
13	Herbaceous Cover, closed-open
14	Sparse Herbaceous or sparse Shrub Cover
15	Regularly flooded Shrub and/or Herbaceous Cover
16	Cultivated and managed areas
17	Mosaic: Cropland / Tree Cover / Other natural vegetation
18	Mosaic: Cropland / Shrub or Grass Cover
19	Bare Areas
20	Water Bodies
21	Snow and Ice
22	Artificial surfaces and associated areas

IGBP DISCover CLASSIFICATION SCHEME (Belward 1996)

Code	Class name
1	Evergreen Needleleaf Forest
2	Evergreen Broadleaf Forest
3	Deciduous Needleleaf Forest
4	Deciduous Broadleaf Forest
5	Mixed Forests
6	Closed Shrublands
7	Open Shrublands
8	Woody Savannas
9	Savannas
10	Grasslands
11	Persistent Wetlands
12	Croplands
13	Urban and Built-Up
14	Cropland/Other vegetation Mosaic
15	Snow and Ice
16	Barren or Sparsely Vegetated
17	Water

METRICS USED BY Hansen et al., 2000

1) Maximum NDVI value
2) Minimum NDVI value of 8 greenest months
3) Mean NDVI value of 8 greenest months
4) Amplitude of NDVI over 8 greenest months
5) Mean NDVI value of 4 warmest months
6) NDVI value of warmest month
7) Maximum channel 1 value of 8 greenest months
8) Minimum channel 1 value of 8 greenest months
9) Mean channel 1 value of 8 greenest months
10) Amplitude of channel 1 over 8 greenest months
11) Channel 1 value from month of maximum NDVI
12) Mean channel 1 value of 4 warmest months
13) Channel 1 value of warmest month
14) Maximum channel 2 value of 8 greenest months
15) Minimum channel 2 value of 8 greenest months
16) Mean channel 2 value of 8 greenest months
17) Amplitude of channel 2 over 8 greenest months
18) Channel 2 value from month of maximum NDVI
19) Mean channel 2 value of 4 warmest months
20) Channel 2 value of warmest month
21) Maximum channel 3 value of 8 greenest months
22) Minimum channel 3 value of 8 greenest months
23) Mean channel 3 value of 8 greenest months
24) Amplitude of channel 3 over 8 greenest months
25) Channel 3 value from month of maximum NDVI
26) Mean channel 3 value of 4 warmest months
27) Channel 3 value of warmest month
28) Maximum channel 4 value of 8 greenest months
29) Minimum channel 4 value of 8 greenest months
30) Mean channel 4 value of 8 greenest months
31) Amplitude of channel 4 over 8 greenest months
32) Channel 4 value from month of maximum NDVI
33) Mean channel 4 value of 4 warmest months
34) Channel 4 value of warmest month
35) Maximum channel 5 value of 8 greenest months
36) Minimum channel 5 value of 8 greenest months
37) Mean channel 5 value of 8 greenest months
38) Amplitude of channel 5 over 8 greenest months
39) Channel 5 value from month of maximum NDVI
40) Mean channel 5 value of 4 warmest months
41) Channel 5 value of warmest month

CLASSIFICATION SCHEME USED BY Hansen et al., 2000

Code	Class name
1	Needleleaf evergreen forest
2	Broadleaf evergreen forest
3	Needleleaf deciduous forest
4	Broadleaf deciduous forest
5	Mixed forest
6	Woodland
7	Wooded grassland
8	Closed shrubland
9	Open shrubland
10	Grassland
11	Cropland
12	Bare ground
14	Urban/built-up areas

CLASSIFICATION SCHEME USED BY DeFries and Townshend, 1994b

Code	Class name
0	Water
1	Broadleaf evergreen forest
2	Coniferous evergreen forest and woodland
3	High latitude deciduous forest and woodland
4	Tundra
5	Mixed coniferous forest and woodland
6	Wooded grassland
7	Grassland
8	Bare ground
9	Shrubs and bare ground
10	Cultivated crops
11	Broadleaf deciduous forest and woodland
12	Data unavailable

METRICS USED BY DeFries et al., 1995

1. Maximum NDVI in year
2. Mean NDVI in year
3. NDVI amplitude
4. NDVI threshold
5. Total length of growing season (length of time NDVI>NDVI threshold)
6. Fraction of total growing season in greenup (number of months in greenup period/total number of months in growing season)
7. Rate of greenup (increase in NDVI during greenup/months of greenup)
8. Rate of senescence (decrease in NDVI during senescence/months of senescence)
9. Integrated NDVI over growing season
10. Integrated NDVI in greenup/ integrated NDVI in senescence
11. AVHRR Band 1 value corresponding to maximum NDVI
12. AVHRR Band 2 value corresponding to maximum NDVI
13. Maximum surface temperature
14. Surface temperature at maximum NDVI
15. Maximum surface temperature surface temperature at maximum NDVI
16. Maximum surface temperature surface temperature at beginning of growing season

CLASSIFICATION SCHEME USED BY DeFried et al., 1995

Code	Class name
1	Broadleaf evergreen non seasonal
2	Broadleaf evergreen seasonal
3	High altitude deciduous forest and woodland
4	Coniferous evergreen forest and woodland open canopy
5	Coniferous evergreen forest and woodland closed canopy
6	Broadleaf deciduous forest and woodland
7	Mixed deciduous and evergreen forest
8	Wooded grassland
9	Grassland
10	Tundra
11	Cultivated crops
12	Shrubs and bare ground
13	Bare ground

CLASSIFICATION SCHEME USED BY DeFries et al., 1998

Code	Class name
1	Evergreen needleleaf forests
2	Evergreen broadleaf forests
3	Deciduous needleleaf forests
4	Deciduous broadleaf forests
5	Mixed forests
6	Woodlands
7	Wooded grasslands/shrublands
8	Closed bushlands or shrublands
9	Open shrublands
10	Grasses
11	Croplands
12	Bare
13	Mosses and lichens

MODIS12 LAND COVER CLASSIFICATION SCHEME (Friedl et al., 1999)

	IGBP	SiB2	BGC	LAI/FPAR
1	Evergreen Needleleaf Forests	Needleleaf-Evergreen Trees	Evergreen Needleleaf	Needle Forests
2	Deciduous Needleleaf Forests	Needleleaf-Deciduous Trees	Deciduous Needleleaf	Needle Forests
3	Evergreen Broadleaf Forests	Broadleaf-Evergreen Trees	Evergreen Broadleaf	Leaf Forests
4	Deciduous Broadleaf Forests	Broadleaf-Deciduous Trees	Deciduous Broadleaf	Leaf Forests
5	Mixed Forests	Broadleaf and Needleleaf Trees		
6	Woody Savannas	C-4 Grassland	Savannas	Savanna
7	Savannas	C-4 Grassland	Savannas	Savanna
8	Grasslands	C-4 Grassland	Grasses	Grasses/Cereal Crops
9	Closed Shrublands	Dwarf Trees and Shrubs		Shrubland
10	Open Shrublands	Shrubs with Bare Soil		Shrublands
11	Croplands	Agriculture or C-3 Grassland		Broadleaf Crops
12	Cropland/Natural vegetation Mosaics			
13	Permanent Wetlands			
14	Urban and Built-Up Lands			

PELCOM CLASSIFICATION SCHEME (Mucher et al., 2000)

Code	Class name
1	Coniferous forest
2	Deciduous forest
3	Mixed forest
4	Grassland
5	Rainfed arable land
6	Irrigated arable land
7	Permanent crops
8	Shrubland
9	Barren land
10	Permanent Ice and Snow
11	Wetlands
12	Inland waters
13	Sea
14	Urban areas

LUCAS CLASSIFICATION SCHEME

Level 1	Description	Level 2	Description	Level 3	Description
A	Artificial Land	A1	Built-up areas	A11	Buildings with 1 to 3 floors
				A12	Buildings with more than 3 floors
				A13	Greenhouses
		A2	Artificial non built-up areas	A21	Non built-up area features
				A22	Non built-up linear features
B	Cropland	B1	Cereals	B11	Common wheat
				B12	Durum Wheat
				B13	Barley
				B14	Rye
				B15	Oats
				B16	Maize
				B17	Rice
				B18	Other cereals
		B2	Root crops	B21	Potatoes
				B22	Sugar beet
				B23	Other root crops
		B3	Non permanent Industrial crops	B31	Sunflower
				B32	Rape seeds
				B33	Soya
				B34	Cotton
				B35	Other fibre and oleaginous crops
				B36	Tobacco
				B37	Other non permanent industrial

					crops
		B4	Dry pulses, vegetables and flowers	B41	Dry pulses
				B42	Tomatoes
				B43	Other fresh vegetables
				B44	Floriculture and ornamental plants
		B5	Temporary, artificial Pastures	B50	Temporary, artificial pastures
		B6	Fallow land	B60	Fallow land
		B7	Permanent crops: fruit trees, berries	B71	Apple fruit
				B72	Pear fruit
				B73	Cherry fruit
				B74	Nuts trees
				B75	Other fruit trees and berries
				B76	Oranges
				B77	Other citrus fruit
		B8	Other permanent crops	B81	Olive groves
				B82	Vineyards
				B83	Nurseries
				B84	Permanent industrial crops
C	Woodland	C1	Forest area	C11	Broad-leaved forest
				C12	Coniferous forest
				C13	Mixed forest
		C2	Other wooded area	C21	Other broad-leaved wooded area
				C22	Other coniferous wooded area
				C23	Other mixed wooded area
		C3	Poplars, eucalyptus	C30	Poplars, eucalyptus
D	Shrubland			D01	Shrubland with sparse tree cover
				D02	Shrubland without tree cover
E	Permanent			E01	Permanent grassland with sparse

	Grassland		tree/shrub cover
		E02	Permanent grassland without tree/shrub cover
F	Bare land	F00	Bare land
G	Water and wetland	G01	Inland water bodies
		G02	Inland running water
		G03	Coastal water bodies
		G04	Wetland
		G05	Glaciers, permanent snow

LCM2000 LAND COVER CLASSIFICATION SCHEME

(Smith et al., 2004; Land Cover Map 2000 Widespread Broad Habitats and LCM2000 Classes)

Level 1	CODE	Level 2	Level 3
Sea / Estuary	22.1	Sea / Estuary	Sea, estuary
Water (inland)	13.1	Water (inland)	Water (inland)
Littoral rock and sediment	20.1	Littoral rock	Rock & rock with algae
	21.1	Littoral sediment	Mud, sand & sand with algae
	21.2	Saltmarsh	Saltmarsh (Grazed / ungrazed)
Supra-littoral rock and sediment	18.1	Supra-littoral rock	Rock
	19.1	Supra-littoral sediment	Shingle, vegetated shingle, dune, dune shrubs
Bog	12.1	Bog	Bog: shrub, grass/shrub, grass/herb
Dwarf shrub heath	10.1	Dwarf shrub heath	Dense shrub (ericaceous / gorse)
	10.2	Open shrub heath	Open shrub (ericaceous / gorse)
Montane habitats	15.1	Montane habitats	Montane vegatation
Broad-leaved / mixed woodland	1.1	Broad-leaved / mixed woodland	Scrub, open birch & deciduous, mixed, broadleaved evergreen, yew
Coniferous woodland	2.1	Coniferous woodland	Conifers, new plantation & felled
Improved grassland	5.1	Improved grassland	Intensive grazing, hay/ silage cut, grazing marsh
Abandoned and derelict grasslands	5.2	Setaside grass	Grass setaside
	6.1	Rough grass	Rough grass (unmanaged)
Semi-natural & natural grasslands & bracken	6.2	Managed neutral grass	Grass (neutral / unimproved)
	7.1	Calcareous grass	Calcareous (managed, rough)
	8.1	Acid grass	Acid Acid with Juncus Acid Nardus/Festuca/Molinia
	9.1	Bracken	Bracken
Fen, marsh, swamp	11.1	Fen, marsh, swamp	Swamp, fen/marsh, fen willow
Built-up areas, gardens	17.1	Suburban/rural developed	Suburban/rural developed
	17.2	Continuous Urban	Urban residential/commercial
Inland Bare Ground	16.1	Inland Bare Ground	Despoiled / semi-natural

COUNTRIES COVERED BY CLC1990 ver. 2000/12

Albania, Austria, Belgium, Bosnia and Herzegovina, Bulgaria, Czech Republic, Denmark, Estonia, Finland, France, Germany, Greece, Hungary, Ireland, Italy, Latvia, Lithuania, Luxembourg, the Former Yugoslav Republic of Macedonia, Netherlands, Poland, Portugal, Romania, Slovakia, Slovenia, Spain, United Kingdom

CORINE CLASSIFICATION SCHEME

Code	Level1	Level2	Level3
1	Artificial surfaces	Urban fabric	Continuous urban fabric
2	Artificial surfaces	Urban fabric	Discontinuous urban fabric
3	Artificial surfaces	Industrial, commercial and transport units	Industrial or commercial units
4	Artificial surfaces	Industrial, commercial and transport units	Road and rail networks and associated land
5	Artificial surfaces	Industrial, commercial and transport units	Port areas
6	Artificial surfaces	Industrial, commercial and transport units	Airports
7	Artificial surfaces	Mine, dump and construction sites	Mineral extraction sites
8	Artificial surfaces	Mine, dump and construction sites	Dump sites
9	Artificial surfaces	Mine, dump and construction sites	Construction sites
10	Artificial surfaces	Artificial, non-agricultural vegetated areas	Green urban areas
11	Artificial surfaces	Artificial, non-agricultural vegetated areas	Sport and leisure facilities
12	Agricultural areas	Arable land	Non-irrigated arable land
13	Agricultural areas	Arable land	Permanently irrigated land
14	Agricultural areas	Arable land	Rice fields
15	Agricultural areas	Permanent crops	Vineyards
16	Agricultural areas	Permanent crops	Fruit trees and berry plantations
17	Agricultural areas	Permanent crops	Olive groves
18	Agricultural areas	Pastures	Pastures
19	Agricultural areas	Heterogeneous agricultural areas	Annual crops associated with permanent crops
20	Agricultural areas	Heterogeneous agricultural areas	Complex cultivation patterns
21	Agricultural areas	Heterogeneous agricultural areas	Land principally occupied by agriculture, with significant areas of natural

			vegetation
22	Agricultural areas	Heterogeneous agricultural areas	Agro-forestry areas
23	Forest and semi natural areas	Forests	Broad-leaved forest
24	Forest and semi natural areas	Forests	Coniferous forest
25	Forest and semi natural areas	Forests	Mixed forest
26	Forest and semi natural areas	Scrub and/or herbaceous vegetation associations	Natural grasslands
27	Forest and semi natural areas	Scrub and/or herbaceous vegetation associations	Moors and heathland
28	Forest and semi natural areas	Scrub and/or herbaceous vegetation associations	Sclerophyllous vegetation
29	Forest and semi natural areas	Scrub and/or herbaceous vegetation associations	Transitional woodland-shrub
30	Forest and semi natural areas	Open spaces with little or no vegetation	Beaches, dunes, sands
31	Forest and semi natural areas	Open spaces with little or no vegetation	Bare rocks
32	Forest and semi natural areas	Open spaces with little or no vegetation	Sparsely vegetated areas
33	Forest and semi natural areas	Open spaces with little or no vegetation	Burnt areas
34	Forest and semi natural areas	Open spaces with little or no vegetation	Glaciers and perpetual snow
35	Wetlands	Inland wetlands	Inland marshes
36	Wetlands	Inland wetlands	Peat bogs
37	Wetlands	Maritime wetlands	Salt marshes
38	Wetlands	Maritime wetlands	Salines
39	Wetlands	Maritime wetlands	Intertidal flats
40	Water bodies	Inland waters	Water courses
41	Water bodies	Inland waters	Water bodies
42	Water bodies	Marine waters	Coastal lagoons
43	Water bodies	Marine waters	Estuaries
44	Water bodies	Marine waters	Sea and ocean
49	NODATA	NODATA	NODATA
50	Sea and ocean	Sea and ocean	Sea and ocean

LAND COVER CLASSIFICATION CONFUSION MATRICES

The inclusion of the full land cover class names in the confusion matrices was impractical for display purposes and the land cover names have been replaced by code numbers. The land cover class – code number association used is provided in the following tables. Additionally the abbreviations P.A. and U.A. found in the matrices, stand for produced and user accuracy respectively.

UK Dominant class classification scheme

Code	Land cover class
1	Urban/Built-up
2	Agriculture
3	Grassland
4	Broad-leaved
5	Coniferous
6	Mixed forest
7	Moors and heathland
8	Transitional woodland-shrub
9	Bare soil/sparsely vegetated
10	Inland marshes
11	Peat bogs
12	Salt marshes
13	Intertidal flats
14	Water bodies
15	Estuaries

Greek Dominant class classification scheme

Code	Land cover class
1	Urban/Built-up
2	Bare soil/sparsely vegetated
3	Agriculture
4	Sclerophyllous vegetation
5	Grassland
6	Broad-leaved
7	Coniferous
8	Mixed forest
9	Moors and heathland
10	Transitional woodland-shrub
11	Water bodies
12	Inland marshes
13	Peat bogs
14	Salt marshes
15	Salines

UK Combination class classification scheme

Code	Land cover class
1	Urban/Built-up
2	Grassland
3	Agriculture
4	Broad-leaved
5	Coniferous
6	Moors and heathland
7	Peat bogs
8	Water bodies
9	Estuaries
10	Grassland & Moors and heathland
11	Urban/Built-up & Grassland
12	Agriculture & Grassland
13	Moors and heathland & Peat bogs
14	Grassland & Peat bogs
15	Grassland & Coniferous
16	Grassland & Broad-leaved
17	Coniferous & Moors and heathland
18	Urban/Built-up & Agriculture
19	Agriculture & Broad-leaved
20	Urban/Built-up, Agriculture & Grassland
21	Agriculture, Grassland & Broad-leaved

AVHRR CONFUSION MATRIX (11% SAMPLE)
UK STUDY AREA
DATE:13/07/2003
COMBINATION CLASS CLASSIFICATION SCHEME

		REFERENCE																					
		1	2	3	4	5	6	7	8	9	10	11	12	13	14	15	16	17	18	19	20	21	U.A
CLASSFIED	1	**419**	169	118	1	0	1	0	0	8	3	82	143	0	0	2	22	0	43	5	20	2	40.37%
	2	344	**6039**	1080	60	127	511	5	3	24	494	256	1722	10	8	231	476	54	92	37	59	73	51.59%
	3	161	724	**3442**	33	18	115	5	4	28	66	87	1336	5	3	20	53	12	183	63	42	30	53.53%
	4	0	0	0	**0**	0	0	0	0	0	0	0	0	0	0	0	0	0	0	0	0	0	N/A
	5	0	0	0	0	**4**	4	0	0	0	0	0	0	0	0	0	0	1	0	0	0	0	44.44%
	6	17	672	84	8	316	**1460**	14	25	36	410	13	123	41	4	112	24	104	7	4	2	2	41.98%
	7	0	0	0	0	0	0	**0**	0	0	0	0	0	0	0	0	0	0	0	0	0	0	N/A
	8	0	0	0	0	0	0	0	**0**	0	0	0	0	0	0	0	0	0	0	0	0	0	N/A
	9	4	15	14	0	3	18	0	8	**110**	4	1	8	1	0	0	1	1	1	0	0	0	58.20%
	10	0	0	0	0	0	1	0	0	0	**1**	0	1	1	0	0	0	0	0	0	0	0	25.00%
	11	0	0	0	0	0	0	0	0	0	0	**0**	1	0	0	0	0	0	0	0	0	0	0.00%
	12	16	177	163	5	2	1	1	0	1	2	11	**234**	0	0	3	16	0	16	7	8	4	35.08%
	13	0	0	0	0	0	0	0	0	0	0	0	0	**0**	0	0	0	0	0	0	0	0	N/A
	14	0	0	0	0	0	0	0	0	0	0	0	0	0	**0**	0	0	0	0	0	0	0	N/A
	15	0	0	0	0	0	0	0	0	0	0	0	0	0	0	**0**	0	0	0	0	0	0	N/A
	16	0	0	0	0	0	0	0	0	0	0	0	0	0	0	0	**0**	0	0	0	0	0	N/A
	17	0	0	0	0	0	0	0	0	0	0	0	0	0	0	0	0	**0**	0	0	0	0	N/A
	18	0	0	0	0	0	0	0	0	0	0	0	0	0	0	0	0	0	**3**	0	0	0	100.00%
	19	0	0	0	0	0	0	0	0	0	0	0	0	0	0	0	0	0	0	**0**	0	0	N/A
	20	0	0	0	0	0	0	0	0	0	0	0	0	0	0	0	0	0	0	0	**0**	0	N/A
	21	0	0	0	0	0	0	0	0	0	0	0	0	0	0	0	0	0	0	0	0	**0**	N/A
	P.A	43.60%	77.46%	70.23%	0.00%	0.85%	69.16%	0.00%	0.00%	53.14%	0.10%	0.00%	6.56%	0.00%	0.00%	0.00%	0.00%	0.00%	0.87%	0.00%	0.00%	0.00%	**49.79%**

AVHRR CONFUSION MATRIX (11% SAMPLE)
UK STUDY AREA
DATE:16/04/2003
COMBINATION CLASS CLASSIFICATION SCHEME

		REFERENCE																					
		1	2	3	4	5	6	7	8	9	10	11	12	13	14	15	16	17	18	19	20	21	U.A
CLASSFIED	1	**474**	138	172	1	56	112	4	10	26	52	78	103	5	4	29	12	22	60	3	7	2	34.60%
	2	147	**7597**	908	77	143	336	47	6	1	415	208	1734	3	59	238	456	32	52	33	37	67	60.31%
	3	296	921	**3623**	16	48	231	12	4	10	150	149	1661	15	17	36	52	19	231	72	54	32	47.37%
	4	0	0	0	**0**	0	0	0	0	0	0	0	0	0	0	0	0	0	0	0	0	0	N/A
	5	24	116	37	3	**228**	104	6	17	10	34	0	26	1	2	46	10	51	3	0	2	0	31.67%
	6	44	318	153	9	88	**1099**	60	5	1	257	26	66	16	29	61	26	59	18	2	3	0	46.97%
	7	0	0	0	0	0	0	**0**	0	0	0	0	0	0	0	0	0	0	0	0	0	0	N/A
	8	0	0	0	0	0	0	0	**0**	0	0	0	0	0	0	0	0	0	0	0	0	0	N/A
	9	10	19	17	1	2	4	0	56	**122**	2	4	13	0	0	0	1	1	2	0	0	0	48.03%
	10	0	0	0	0	0	0	0	0	0	**0**	0	0	0	0	0	0	0	0	0	0	0	N/A
	11	0	0	0	0	0	0	0	0	0	0	**0**	0	0	0	0	0	0	0	0	0	0	N/A
	12	21	282	269	5	2	1	0	0	0	5	28	**365**	0	1	3	17	0	16	8	5	13	35.06%
	13	0	0	0	0	0	0	0	0	0	0	0	0	**0**	0	0	0	0	0	0	0	0	N/A
	14	0	0	0	0	0	0	0	0	0	0	0	0	0	**0**	0	0	0	0	0	0	0	N/A
	15	0	0	0	0	0	0	0	0	0	0	0	0	0	0	**0**	0	0	0	0	0	0	N/A
	16	0	0	0	0	0	0	0	0	0	0	0	0	0	0	0	**0**	0	0	0	0	0	N/A
	17	0	0	0	0	0	0	0	0	0	0	0	0	0	0	0	0	**0**	0	0	0	0	N/A
	18	0	0	0	0	0	0	0	0	0	0	0	0	0	0	0	0	0	**0**	0	0	0	N/A
	19	0	0	0	0	0	0	0	0	0	0	0	0	0	0	0	0	0	0	**0**	0	0	N/A
	20	0	0	0	0	0	0	0	0	0	0	0	0	0	0	0	0	0	0	0	**0**	0	N/A
	21	0	0	0	0	0	0	0	0	0	0	0	0	0	0	0	0	0	0	0	0	**0**	N/A
	P.A	46.65%	80.90%	69.96%	0.00%	40.21%	58.24%	0.00%	0.00%	71.76%	0.00%	0.00%	9.20%	0.00%	0.00%	0.00%	0.00%	0.00%	0.00%	0.00%	0.00%	0.00%	**52.01%**

AVHRR CONFUSION MATRIX (11% SAMPLE)
UK STUDY AREA
DATE:17/03/2003
COMBINATION CLASS CLASSIFICATION SCHEME

		REFERENCE																					
		1	2	3	4	5	6	7	8	9	10	11	12	13	14	15	16	17	18	19	20	21	U.A
CLASSFIED	1	**532**	106	116	2	25	54	5	4	7	23	96	96	1	2	15	6	6	52	1	18	4	45.43%
	2	167	**9724**	959	82	120	490	203	4	3	522	272	2472	19	211	230	458	48	46	50	50	83	59.98%
	3	168	420	**2706**	10	9	54	1	1	0	40	84	1013	3	6	19	30	6	175	44	37	17	55.87%
	4	0	0	0	**0**	0	0	0	0	0	0	0	0	0	0	0	0	0	0	0	0	0	N/A
	5	37	130	7	1	**212**	170	13	47	23	53	14	17	6	4	43	7	53	0	0	0	0	25.33%
	6	11	485	38	15	130	**1228**	201	9	2	311	21	61	49	60	73	47	67	2	4	4	3	43.53%
	7	0	7	0	1	1	9	**20**	0	0	3	1	1	1	13	2	1	1	0	0	0	0	32.79%
	8	0	4	0	0	0	17	1	**41**	33	6	0	1	2	0	1	0	1	0	0	0	0	38.32%
	9	4	2	4	0	0	0	0	0	**9**	0	0	3	0	0	0	0	0	0	0	0	0	40.91%
	10	1	5	0	0	0	6	1	0	0	**11**	0	0	1	0	0	1	0	0	0	0	0	42.31%
	11	0	0	0	0	0	0	0	0	0	0	**0**	0	0	0	0	0	0	0	0	0	0	N/A
	12	19	138	138	1	4	17	0	0	0	8	23	**211**	0	0	5	8	2	9	3	3	4	35.58%
	13	0	0	0	0	0	0	0	0	0	0	0	0	**0**	0	0	0	0	0	0	0	0	N/A
	14	0	0	0	0	0	0	0	0	0	0	0	0	0	**0**	0	0	0	0	0	0	0	N/A
	15	0	0	0	0	0	1	0	1	0	2	0	0	0	1	**0**	1	0	0	0	0	0	0.00%
	16	0	0	0	0	0	0	0	0	0	0	0	0	0	0	0	**0**	0	0	0	0	0	N/A
	17	0	0	0	0	1	0	0	0	0	0	0	0	0	0	0	0	**0**	0	0	0	0	0.00%
	18	0	0	0	0	0	0	0	0	0	0	0	0	0	0	0	0	0	**0**	0	0	0	N/A
	19	0	0	0	0	0	0	0	0	0	0	0	0	0	0	0	0	0	0	**0**	0	0	N/A
	20	0	0	0	0	0	0	0	0	0	0	0	0	0	0	0	0	0	0	0	**0**	0	N/A
	21	0	0	0	0	0	0	0	0	0	0	0	0	0	0	0	0	0	0	0	0	**0**	N/A
	P.A	56.66%	88.23%	68.20%	0.00%	42.23%	60.02%	4.49%	38.32%	11.69%	1.12%	0.00%	5.45%	0.00%	0.00%	0.00%	0.00%	0.00%	0.00%	0.00%	0.00%	0.00%	**55.03%**

AVHRR CONFUSION MATRIX (11% SAMPLE)
UK STUDY AREA
DATE:18/04/2003
COMBINATION CLASS CLASSIFICATION SCHEME

		REFERENCE																					
		1	2	3	4	5	6	7	8	9	10	11	12	13	14	15	16	17	18	19	20	21	U.A
CLASSFIED	1	**366**	139	143	0	57	54	14	3	18	34	46	60	3	4	25	5	19	34	4	8	0	35.33%
	2	203	**9743**	2076	98	157	489	242	20	22	522	237	3043	34	218	228	463	64	89	57	68	85	53.66%
	3	396	1519	**2686**	13	120	278	78	9	10	256	187	1263	8	68	87	73	32	205	40	49	17	36.33%
	4	0	0	0	**0**	0	0	0	0	0	0	0	0	0	0	0	0	0	0	0	0	0	N/A
	5	16	120	31	4	**201**	130	11	21	16	40	1	21	3	3	39	9	43	3	0	2	0	28.15%
	6	30	345	146	19	121	**1682**	242	17	1	340	10	67	52	74	61	32	73	8	5	3	4	50.48%
	7	0	0	0	0	0	0	**0**	0	0	0	0	0	0	0	0	0	0	0	0	0	0	N/A
	8	15	29	20	0	8	10	2	**105**	86	2	4	19	0	2	1	1	0	5	0	0	0	33.98%
	9	0	0	0	0	0	0	0	0	**0**	0	0	0	0	0	0	0	0	0	0	0	0	N/A
	10	0	0	0	0	0	0	0	0	0	**0**	0	0	0	0	0	0	0	0	0	0	0	N/A
	11	0	0	0	0	0	0	0	0	0	0	**0**	0	0	0	0	0	0	0	0	0	0	N/A
	12	6	35	29	0	0	6	3	0	0	8	5	**58**	0	2	2	1	2	1	1	1	1	36.02%
	13	0	0	0	0	0	0	0	0	0	0	0	0	**0**	0	0	0	0	0	0	0	0	N/A
	14	0	0	0	0	0	0	0	0	0	0	0	0	0	**0**	0	0	0	0	0	0	0	N/A
	15	0	0	0	0	0	0	0	0	0	0	0	0	0	0	**0**	0	0	0	0	0	0	N/A
	16	0	0	0	0	0	0	0	0	0	0	0	0	0	0	0	**0**	0	0	0	0	0	N/A
	17	0	0	0	0	0	0	0	0	0	0	0	0	0	0	0	0	**0**	0	0	0	0	N/A
	18	0	0	0	0	0	0	0	0	0	0	0	0	0	0	0	0	0	**0**	0	0	0	N/A
	19	0	0	0	0	0	0	0	0	0	0	0	0	0	0	0	0	0	0	**0**	0	0	N/A
	20	0	0	0	0	0	0	0	0	0	0	0	0	0	0	0	0	0	0	0	**0**	0	N/A
	21	0	0	0	0	0	0	0	0	0	0	0	0	0	0	0	0	0	0	0	0	**0**	N/A
	P.A	35.47%	81.67%	52.35%	0.00%	30.27%	63.50%	0.00%	60.00%	0.00%	0.00%	0.00%	1.28%	0.00%	0.00%	0.00%	0.00%	0.00%	0.00%	0.00%	0.00%	0.00%	**47.71%**

AVHRR CONFUSION MATRIX (11% SAMPLE)
UK STUDY AREA
DATE:19/03/2003
COMBINATION CLASS CLASSIFICATION SCHEME

		REFERENCE																					
		1	2	3	4	5	6	7	8	9	10	11	12	13	14	15	16	17	18	19	20	21	U.A
CLASSFIED	1	**519**	102	183	3	24	80	3	5	8	22	64	59	7	1	12	6	8	72	1	7	1	43.72%
	2	47	**5698**	812	53	45	325	14	0	0	400	150	1779	14	17	148	375	27	40	43	27	71	56.50%
	3	261	620	**3139**	24	18	162	12	1	0	98	160	1090	13	7	24	65	4	196	72	53	36	51.84%
	4	0	0	0	**0**	0	0	0	0	0	0	0	0	0	0	0	0	0	0	0	0	0	N/A
	5	9	59	9	3	**283**	115	6	23	15	46	2	10	1	0	39	1	72	4	0	0	0	40.60%
	6	14	315	63	28	148	**1314**	44	5	0	274	16	90	24	10	69	43	74	2	2	2	5	51.69%
	7	0	0	0	0	0	0	**0**	0	0	0	0	0	0	0	0	0	0	0	0	0	0	N/A
	8	0	0	0	0	0	0	0	**0**	0	0	0	0	0	0	0	0	0	0	0	0	0	N/A
	9	4	8	2	0	0	7	0	9	**109**	0	0	3	0	0	0	0	0	1	0	1	0	75.69%
	10	0	0	0	0	0	0	0	0	0	**0**	0	0	0	0	0	0	0	0	0	0	0	N/A
	11	0	1	0	0	0	0	0	0	0	0	**1**	0	0	0	0	0	0	0	0	0	0	50.00%
	12	16	159	134	5	4	14	0	0	0	17	10	**236**	1	0	9	25	1	13	3	3	4	36.09%
	13	0	0	0	0	0	0	0	0	0	0	0	0	**0**	0	0	0	0	0	0	0	0	N/A
	14	0	0	0	0	0	0	0	0	0	0	0	0	0	**0**	0	0	0	0	0	0	0	N/A
	15	0	0	0	0	1	0	0	0	0	0	1	0	0	0	**1**	0	1	0	0	0	0	25.00%
	16	0	0	0	0	0	0	0	0	0	0	0	0	0	0	0	**0**	0	0	0	0	0	N/A
	17	0	0	0	0	0	0	0	0	0	0	0	0	0	0	0	0	**0**	0	0	0	0	N/A
	18	0	0	0	0	0	0	0	0	0	0	0	0	0	0	0	0	0	**0**	0	0	0	N/A
	19	0	0	0	0	0	0	0	0	0	0	0	0	0	0	0	0	0	0	**0**	0	0	N/A
	20	0	0	0	0	0	0	0	0	0	0	0	0	0	0	0	0	0	0	0	**0**	0	N/A
	21	0	0	0	0	0	0	0	0	0	0	0	0	0	0	0	0	0	0	0	0	**0**	N/A
	P.A	59.66%	81.84%	72.29%	0.00%	54.11%	65.15%	0.00%	0.00%	82.58%	0.00%	0.25%	7.22%	0.00%	0.00%	0.33%	0.00%	0.00%	0.00%	0.00%	0.00%	0.00%	**52.88%**

AVHRR CONFUSION MATRIX (11% SAMPLE)
UK STUDY AREA
DATE:22/03/2003
COMBINATION CLASS CLASSIFICATION SCHEME

CLASSFIED \ REFERENCE	1	2	3	4	5	6	7	8	9	10	11	12	13	14	15	16	17	18	19	20	21	U.A
1	**525**	133	148	1	31	66	2	1	19	23	61	72	1	0	18	14	3	76	3	11	3	43.35%
2	112	**5280**	906	77	72	227	6	2	1	272	166	1554	4	7	108	431	19	53	47	35	66	55.90%
3	191	929	**3348**	18	27	121	2	0	7	94	142	1392	5	3	42	73	8	173	59	46	43	49.80%
4	0	0	0	**0**	0	0	0	0	0	0	0	0	0	0	0	0	0	0	0	0	0	N/A
5	2	48	5	1	**82**	66	1	4	0	16	0	10	2	1	28	3	18	0	0	0	0	28.57%
6	9	134	31	14	60	**252**	3	1	8	77	5	44	4	4	31	24	24	5	2	0	1	34.38%
7	0	0	0	0	0	0	**0**	0	0	0	0	0	0	0	0	0	0	0	0	0	0	N/A
8	0	0	0	0	0	0	0	**0**	0	0	0	0	0	0	0	0	0	0	0	0	0	N/A
9	5	18	6	2	7	15	0	1	**64**	1	3	11	0	0	0	1	0	3	0	0	0	46.72%
10	1	0	1	0	1	0	0	0	0	**4**	0	1	0	0	1	1	0	0	0	0	0	40.00%
11	1	1	1	0	1	0	0	0	0	0	**2**	3	0	0	1	0	0	0	0	0	0	20.00%
12	21	134	119	4	2	4	0	0	0	5	17	**174**	0	0	4	4	0	13	2	3	4	34.12%
13	0	0	0	0	0	0	0	0	0	0	0	0	**0**	0	0	0	0	0	0	0	0	N/A
14	0	0	0	0	0	0	0	0	0	0	0	0	0	**0**	0	0	0	0	0	0	0	N/A
15	0	0	0	0	0	1	0	0	0	2	0	0	0	0	**0**	1	0	0	0	0	0	0.00%
16	0	0	0	0	0	0	0	0	0	0	0	0	0	0	0	**0**	0	0	0	0	0	N/A
17	0	0	0	0	0	0	0	0	0	0	0	0	0	0	0	0	**0**	0	0	0	0	N/A
18	0	0	0	0	0	0	0	0	0	0	0	0	0	0	0	0	0	**0**	0	0	0	N/A
19	0	0	0	0	0	0	0	0	0	0	0	0	0	0	0	0	0	0	**0**	0	0	N/A
20	0	0	0	0	0	0	0	0	0	0	0	0	0	0	0	0	0	0	0	**0**	0	N/A
21	0	0	0	0	0	0	0	0	0	0	0	0	0	0	0	0	0	0	0	0	**0**	N/A
P.A	60.55%	79.08%	73.34%	0.00%	28.98%	33.51%	0.00%	0.00%	64.65%	0.81%	0.51%	5.34%	0.00%	0.00%	0.00%	0.00%	0.00%	0.00%	0.00%	0.00%	0.00%	**51.03%**

AVHRR CONFUSION MATRIX (11% SAMPLE)
UK STUDY AREA
DATE:23/03/2003
COMBINATION CLASS CLASSIFICATION SCHEME

		REFERENCE																					
		1	2	3	4	5	6	7	8	9	10	11	12	13	14	15	16	17	18	19	20	21	U.A
CLASSFIED	1	**447**	118	158	14	53	52	0	1	16	19	64	96	1	0	14	19	16	37	2	9	0	39.35%
	2	135	**5538**	1136	49	75	338	1	4	3	375	199	1664	3	8	126	339	26	73	27	53	59	54.13%
	3	300	1390	**3115**	37	62	224	2	1	5	193	166	1508	5	5	58	135	17	186	71	48	34	41.19%
	4	0	0	0	**0**	0	0	0	0	0	0	0	0	0	0	0	0	0	0	0	0	0	N/A
	5	16	77	19	2	**164**	136	0	7	13	27	6	16	0	0	57	9	52	5	0	0	0	27.06%
	6	18	241	85	13	94	**648**	2	1	1	137	8	60	4	3	51	28	39	5	5	4	3	44.69%
	7	0	0	0	0	0	0	**0**	0	0	0	0	0	0	0	0	0	0	0	0	0	0	N/A
	8	0	0	0	0	0	0	0	**0**	0	0	0	0	0	0	0	0	0	0	0	0	0	N/A
	9	2	1	9	0	0	0	0	1	**69**	0	1	5	0	0	0	0	0	0	0	0	0	78.41%
	10	0	0	0	0	0	0	0	0	0	**0**	0	0	0	0	0	0	0	0	0	0	0	N/A
	11	0	0	0	0	1	0	0	0	0	0	**1**	0	0	0	0	0	0	0	0	0	0	50.00%
	12	9	98	115	1	2	15	0	0	0	2	10	**149**	0	1	5	11	0	10	4	3	5	33.86%
	13	0	0	0	0	0	0	0	0	0	0	0	0	**0**	0	0	0	0	0	0	0	0	N/A
	14	0	0	0	0	0	0	0	0	0	0	0	0	0	**0**	0	0	0	0	0	0	0	N/A
	15	0	0	0	0	0	0	0	0	0	0	0	0	0	0	**0**	0	0	0	0	0	0	N/A
	16	0	0	0	0	0	0	0	0	0	0	0	0	0	0	0	**0**	0	0	0	0	0	N/A
	17	0	0	0	0	0	0	0	0	0	0	0	0	0	0	0	0	**0**	0	0	0	0	N/A
	18	0	0	0	0	0	0	0	0	0	0	0	1	0	0	0	0	0	**0**	0	0	0	0.00%
	19	0	0	0	0	0	0	0	0	0	0	0	0	0	0	0	0	0	0	**0**	0	0	N/A
	20	0	0	0	0	0	0	0	0	0	0	0	0	0	0	0	0	0	0	0	**0**	0	N/A
	21	0	0	0	0	0	0	0	0	0	0	0	0	0	0	0	0	0	0	0	0	**0**	N/A
	P.A	48.22%	74.21%	67.18%	0.00%	36.36%	45.86%	0.00%	0.00%	64.49%	0.00%	0.22%	4.26%	0.00%	0.00%	0.00%	0.00%	0.00%	0.00%	0.00%	0.00%	0.00%	**47.09%**

AVHRR CONFUSION MATRIX (11% SAMPLE)
UK STUDY AREA
DATE:MULTIDATE
COMBINATION CLASS CLASSIFICATION SCHEME

CLASSFIED \ REFERENCE	1	2	3	4	5	6	7	8	9	10	11	12	13	14	15	16	17	18	19	20	21	U.A
1	**460**	84	84	3	1	2	1	0	2	3	69	84	0	0	2	20	0	43	3	22	3	51.92%
2	124	**4894**	619	57	73	329	0	1	4	363	142	1214	4	11	134	352	30	45	22	37	31	57.67%
3	117	556	**3060**	17	16	36	0	3	5	27	84	1144	1	0	9	45	0	147	54	35	28	56.84%
4	0	0	0	**0**	0	0	0	0	0	0	0	0	0	0	0	0	0	0	0	0	0	N/A
5	0	35	6	3	**115**	77	0	3	6	12	0	8	1	0	21	3	23	0	1	0	0	36.62%
6	4	216	33	6	115	**722**	0	0	1	112	8	49	5	1	51	12	36	3	0	0	3	52.43%
7	0	0	0	0	0	0	**0**	0	0	0	0	0	0	0	0	0	0	0	0	0	0	N/A
8	0	0	0	0	0	0	0	**0**	0	0	0	0	0	0	0	0	0	0	0	0	0	N/A
9	1	3	11	0	1	0	0	3	**29**	0	0	3	0	0	0	1	0	2	0	0	0	53.70%
10	0	0	0	0	0	0	0	0	0	**1**	0	0	0	0	0	0	0	0	0	0	0	100.00%
11	0	0	0	0	0	0	0	0	0	0	**0**	0	0	0	0	0	0	0	0	0	0	N/A
12	33	282	310	9	1	11	0	0	0	11	31	**426**	0	0	0	27	0	26	12	12	13	35.38%
13	0	0	0	0	0	0	0	0	0	0	0	0	**0**	0	0	0	0	0	0	0	0	N/A
14	0	0	0	0	0	0	0	0	0	0	0	0	0	**0**	0	0	0	0	0	0	0	N/A
15	2	3	2	0	0	0	0	0	0	0	0	1	0	0	**1**	2	1	0	0	0	1	7.69%
16	0	0	0	0	0	0	0	0	0	0	0	0	0	0	0	**0**	0	0	0	0	0	N/A
17	0	0	0	0	0	0	0	0	0	0	0	0	0	0	0	0	**0**	0	0	0	0	N/A
18	0	0	0	0	0	0	0	0	0	0	0	0	0	0	0	0	0	**0**	0	0	0	N/A
19	0	0	0	0	0	0	0	0	0	0	0	0	0	0	0	0	0	0	**0**	0	0	N/A
20	0	0	0	0	0	0	0	0	0	0	0	0	0	0	0	0	0	0	0	**0**	0	N/A
21	0	0	0	0	0	0	0	0	0	0	0	0	0	0	0	0	0	0	0	0	**0**	N/A
P.A	62.08%	80.59%	74.18%	0.00%	35.71%	61.34%	0.00%	0.00%	61.70%	0.19%	0.00%	14.54%	0.00%	0.00%	0.46%	0.00%	0.00%	0.00%	0.00%	0.00%	0.00%	**54.79%**

MODIS1 CONFUSION MATRIX (11% SAMPLE)
UK STUDY AREA
DATE:13/07/2003
COMBINATION CLASS CLASSIFICATION SCHEME

		REFERENCE																					
		1	2	3	4	5	6	7	8	9	10	11	12	13	14	15	16	17	18	19	20	21	U.A
CLASSFIED	1	**430**	114	124	4	10	59	2	5	26	13	82	101	4	0	0	12	2	54	4	19	1	40.34%
	2	98	**6129**	889	53	132	476	12	9	14	577	159	1484	7	13	222	436	53	45	30	31	51	56.13%
	3	211	874	**3619**	28	7	26	1	1	17	12	137	1518	0	0	24	80	3	203	71	60	40	52.21%
	4	0	0	0	**0**	0	0	0	0	0	0	0	0	0	0	0	0	0	0	0	0	0	N/A
	5	0	0	0	0	**1**	0	0	0	0	0	0	0	0	0	0	0	0	0	0	0	0	100.00%
	6	29	393	23	13	306	**1493**	7	16	9	368	9	38	41	1	119	25	111	3	1	4	2	49.58%
	7	0	0	0	0	0	0	**0**	0	0	0	0	0	0	0	0	0	0	0	0	0	0	N/A
	8	0	0	0	0	0	0	0	**0**	0	0	0	0	0	0	0	0	0	0	0	0	0	N/A
	9	28	41	28	0	10	25	2	9	**130**	6	4	22	3	0	3	2	3	2	1	3	0	40.37%
	10	1	2	0	0	0	2	1	0	0	**5**	1	0	0	0	0	0	0	0	0	0	0	41.67%
	11	3	1	0	0	0	0	0	0	0	0	**4**	1	0	0	0	0	0	2	0	0	0	36.36%
	12	24	221	207	6	1	0	0	0	1	3	28	**377**	0	1	2	27	1	20	11	7	13	39.68%
	13	0	0	0	0	0	0	0	0	0	0	0	0	**0**	0	0	0	0	0	0	0	0	N/A
	14	0	0	0	0	0	0	0	0	0	0	0	0	0	**0**	0	0	0	0	0	0	0	N/A
	15	1	0	0	0	0	0	0	0	0	0	0	0	0	0	**1**	0	0	0	0	0	0	50.00%
	16	0	0	0	0	0	0	0	0	0	0	0	0	0	0	0	**0**	0	0	0	0	0	N/A
	17	0	0	0	0	0	0	0	0	0	0	0	0	0	0	0	0	**0**	0	0	0	0	N/A
	18	0	0	2	0	0	0	0	0	0	0	0	0	0	0	0	0	0	**0**	0	0	0	0.00%
	19	127	12	11	0	0	18	0	0	7	2	15	14	0	0	0	0	0	5	**0**	1	0	0.00%
	20	0	0	0	0	0	0	0	0	0	0	0	0	0	0	0	0	0	0	0	**0**	0	N/A
	21	0	0	0	0	0	0	0	0	0	0	0	0	0	0	0	0	0	0	0	0	**0**	N/A
	P.A	45.17%	78.71%	73.81%	0.00%	0.21%	71.13%	0.00%	0.00%	63.73%	0.51%	0.91%	10.60%	0.00%	0.00%	0.27%	0.00%	0.00%	0.00%	0.00%	0.00%	0.00%	**52.00%**

MODIS1 CONFUSION MATRIX (11% SAMPLE)
UK STUDY AREA
DATE:16/04/2003
COMBINATION CLASS CLASSIFICATION SCHEME

		REFERENCE																					
		1	2	3	4	5	6	7	8	9	10	11	12	13	14	15	16	17	18	19	20	21	U.A
CLASSFIED	1	**295**	111	118	3	75	153	9	19	26	38	52	50	4	4	16	5	18	40	3	13	3	27.96%
	2	198	**7666**	1918	76	157	198	52	6	10	379	217	2476	4	77	236	438	41	79	57	41	67	53.26%
	3	240	1173	**2579**	22	99	211	32	8	5	189	155	1100	4	18	90	106	40	187	52	46	37	40.34%
	4	0	0	0	**0**	0	0	0	0	0	0	0	0	0	0	0	0	0	0	0	0	0	N/A
	5	3	17	6	2	**30**	21	0	0	0	3	1	7	0	1	11	2	1	2	0	0	0	28.04%
	6	243	247	415	4	196	**1260**	29	17	7	283	46	128	28	11	49	14	81	49	2	5	3	40.42%
	7	0	0	0	0	0	0	**0**	0	0	0	0	0	0	0	0	0	0	0	0	0	0	N/A
	8	12	19	13	0	4	7	1	**45**	31	1	2	9	0	0	2	2	1	4	1	0	0	29.22%
	9	5	16	6	0	0	0	0	1	**75**	0	5	10	0	0	0	2	0	5	0	2	0	59.06%
	10	2	11	4	0	0	6	2	0	0	**9**	1	4	0	0	2	0	0	0	0	0	0	21.95%
	11	0	0	0	0	0	0	0	0	0	1	**2**	0	0	0	0	0	0	0	0	0	0	66.67%
	12	7	101	88	3	2	5	3	0	0	4	11	**164**	0	0	2	8	1	5	4	4	4	39.42%
	13	0	0	0	0	0	0	0	0	0	0	0	0	**0**	0	0	0	0	0	0	0	0	N/A
	14	0	0	0	0	0	0	0	0	0	0	0	0	0	**0**	0	0	0	0	0	0	0	N/A
	15	0	0	0	0	0	0	0	0	0	0	0	0	0	0	**0**	0	0	0	0	0	0	N/A
	16	0	0	0	0	0	0	0	0	0	0	0	0	0	0	0	**0**	0	0	0	0	0	N/A
	17	0	0	0	0	0	0	0	0	0	0	0	0	0	0	0	0	**0**	0	0	0	0	N/A
	18	0	0	1	0	0	0	0	0	0	0	0	1	0	0	0	0	0	**0**	0	0	0	0.00%
	19	0	0	0	0	0	0	0	0	0	0	0	0	0	0	0	0	0	0	**0**	0	0	N/A
	20	0	0	0	0	0	0	0	0	0	0	0	0	0	0	0	0	0	0	0	**0**	0	N/A
	21	0	0	0	0	0	0	0	0	0	0	0	0	0	0	0	0	0	0	0	0	**0**	N/A
	P.A	29.35%	81.89%	50.10%	0.00%	5.33%	67.71%	0.00%	46.88%	48.70%	0.99%	0.41%	4.15%	0.00%	0.00%	0.00%	0.00%	0.00%	0.00%	0.00%	0.00%	0.00%	**46.98%**

MODIS1 CONFUSION MATRIX (11% SAMPLE)
UK STUDY AREA
DATE:17/03/2003
COMBINATION CLASS CLASSIFICATION SCHEME

CLASSFIED \ REFERENCE	1	2	3	4	5	6	7	8	9	10	11	12	13	14	15	16	17	18	19	20	21	U.A
1	**177**	25	76	2	0	50	5	4	6	12	25	19	2	1	1	3	0	17	2	3	0	41.16%
2	161	**9812**	1344	70	206	389	287	19	13	427	263	2706	15	242	271	441	73	62	45	50	74	57.82%
3	253	606	**2145**	9	54	556	101	12	9	270	108	750	36	32	36	47	28	148	34	42	21	40.49%
4	0	0	0	**0**	0	0	0	0	0	0	0	0	0	0	0	0	0	0	0	0	0	N/A
5	4	27	0	6	**45**	18	0	0	1	7	0	3	0	0	10	6	4	0	0	1	0	34.09%
6	310	373	246	22	183	**969**	42	65	23	212	80	140	22	15	56	43	70	40	12	12	12	32.88%
7	0	3	1	0	0	2	**6**	0	0	2	1	7	0	0	1	0	0	1	0	0	0	25.00%
8	0	0	0	0	0	0	0	**0**	0	0	0	0	0	0	0	0	0	0	0	0	0	N/A
9	7	24	2	0	2	15	0	5	**25**	9	3	10	1	2	2	1	1	1	0	1	0	22.52%
10	1	0	0	0	0	1	0	0	0	**0**	0	0	0	0	0	1	0	0	0	0	0	0.00%
11	0	0	0	0	0	0	0	0	0	0	**0**	0	0	0	0	0	0	0	0	0	0	N/A
12	8	112	95	1	7	20	5	1	1	23	14	**186**	3	5	8	13	6	9	6	3	3	35.16%
13	0	0	0	0	0	0	0	0	0	0	0	0	**0**	0	0	0	0	0	0	0	0	N/A
14	0	0	0	0	0	0	0	0	0	0	1	0	0	**0**	0	0	0	0	0	0	0	0.00%
15	0	0	0	0	0	0	0	0	0	0	0	0	0	0	**0**	0	0	0	0	0	0	N/A
16	0	0	0	0	0	0	0	0	0	0	0	0	0	0	0	**1**	0	0	0	0	0	100.00%
17	0	0	0	0	0	0	0	0	0	0	0	0	0	0	0	0	**0**	0	0	0	0	N/A
18	0	0	1	0	0	0	0	0	0	0	1	0	0	0	0	0	0	**0**	0	0	0	0.00%
19	0	0	0	0	0	0	0	0	0	0	0	0	0	0	0	0	0	0	**0**	0	0	N/A
20	0	0	0	0	0	0	0	0	0	0	0	0	0	0	0	0	0	0	0	**0**	0	N/A
21	0	0	0	0	0	0	0	0	0	0	0	0	0	0	0	0	0	0	0	0	**0**	N/A
P.A	19.22%	89.35%	54.86%	0.00%	9.05%	47.97%	1.35%	0.00%	32.05%	0.00%	0.00%	4.87%	0.00%	0.00%	0.00%	0.18%	0.00%	0.00%	0.00%	0.00%	0.00%	**50.54%**

MODIS1 CONFUSION MATRIX (11% SAMPLE)
UK STUDY AREA
DATE:18/04/2003
COMBINATION CLASS CLASSIFICATION SCHEME

		REFERENCE																					
		1	2	3	4	5	6	7	8	9	10	11	12	13	14	15	16	17	18	19	20	21	U.A
CLASSFIED	1	**154**	39	40	1	3	56	6	1	9	18	9	17	6	3	5	2	10	8	1	3	0	39.39%
	2	143	**9775**	1875	71	119	194	178	22	8	325	223	2952	4	203	211	383	38	80	41	53	62	57.64%
	3	299	1397	**2704**	43	157	419	245	17	18	348	167	1185	30	109	134	146	48	196	54	60	35	34.62%
	4	0	0	0	**0**	0	0	0	0	0	0	0	0	0	0	0	0	0	0	0	0	0	N/A
	5	0	6	5	2	**16**	4	1	1	0	2	1	3	0	0	7	3	1	0	0	0	1	30.19%
	6	410	483	318	14	349	**1911**	114	78	62	453	59	105	57	43	67	25	127	44	4	8	3	40.37%
	7	1	4	6	0	1	3	**16**	0	0	3	1	2	0	1	0	0	0	1	1	0	0	40.00%
	8	0	0	0	0	0	0	0	**0**	0	0	0	0	0	0	0	0	0	0	0	0	0	N/A
	9	10	14	6	0	1	14	0	55	**44**	7	1	11	2	0	0	2	1	1	0	0	0	26.04%
	10	1	6	0	0	3	2	0	0	0	**11**	1	0	0	0	1	0	0	0	0	0	0	44.00%
	11	0	0	0	0	0	0	0	0	0	0	**0**	0	0	0	0	0	0	0	0	0	0	N/A
	12	7	123	103	2	8	5	9	0	3	9	11	**174**	1	7	9	14	0	6	6	3	3	34.59%
	13	0	0	0	0	0	0	0	0	0	0	0	0	**0**	0	0	0	0	0	0	0	0	N/A
	14	0	0	0	0	0	0	0	0	0	0	0	0	0	**0**	0	0	0	0	0	0	0	N/A
	15	0	0	0	0	0	0	0	0	0	0	0	0	0	0	**0**	0	0	0	0	0	0	N/A
	16	0	0	0	0	0	0	0	0	0	0	0	0	0	0	0	**0**	0	0	0	0	0	N/A
	17	0	0	0	0	0	0	0	0	0	0	0	0	0	0	0	0	**0**	0	0	0	0	N/A
	18	0	0	0	0	0	0	0	0	0	0	0	0	0	0	0	0	0	**0**	0	0	0	N/A
	19	0	0	0	0	0	0	0	0	0	0	0	0	0	0	0	0	0	0	**0**	0	0	N/A
	20	0	0	0	0	0	0	0	0	0	0	0	0	0	0	0	0	0	0	0	**0**	0	N/A
	21	0	0	0	0	0	0	0	0	0	0	0	0	0	0	0	0	0	0	0	0	**0**	N/A
	P.A	15.02%	82.51%	53.47%	0.00%	2.44%	73.27%	2.81%	0.00%	30.56%	0.94%	0.00%	3.91%	0.00%	0.00%	0.00%	0.00%	0.00%	0.00%	0.00%	0.00%	0.00%	**48.25%**

MODIS1 CONFUSION MATRIX (11% SAMPLE)
UK STUDY AREA
DATE:19/03/2003
COMBINATION CLASS CLASSIFICATION SCHEME

		REFERENCE																					
		1	2	3	4	5	6	7	8	9	10	11	12	13	14	15	16	17	18	19	20	21	U.A
CLASSFIED	1	**222**	40	84	0	3	85	3	3	16	35	20	16	4	2	1	4	1	18	0	6	0	39.43%
	2	125	**5559**	1156	67	115	223	25	7	3	296	210	1874	3	13	170	379	37	60	55	35	72	53.02%
	3	298	830	**2636**	20	77	579	34	5	3	277	116	979	34	14	53	76	38	186	54	37	37	41.30%
	4	0	0	0	**0**	0	0	0	0	0	0	0	0	0	0	0	0	0	0	0	0	0	N/A
	5	4	22	2	2	**50**	24	0	0	0	5	1	4	0	0	8	2	7	0	0	0	0	38.17%
	6	187	319	310	29	262	**1033**	6	19	16	213	42	156	17	8	69	39	101	42	12	9	8	35.66%
	7	0	0	0	0	0	0	**2**	0	0	1	0	1	0	0	0	0	0	0	0	0	0	50.00%
	8	0	0	0	0	0	0	0	**0**	0	0	0	0	0	0	0	0	0	0	0	0	0	N/A
	9	5	30	6	0	4	27	2	7	**94**	9	2	9	2	0	0	1	0	1	1	2	0	46.53%
	10	0	7	2	0	0	5	0	0	0	**3**	0	4	0	0	0	0	1	1	0	0	0	13.04%
	11	0	0	0	0	0	0	0	0	0	0	**0**	0	0	0	0	0	0	0	0	0	0	N/A
	12	16	109	95	1	13	23	6	0	1	11	12	**171**	0	0	7	12	3	10	3	3	2	34.34%
	13	0	0	0	0	0	0	0	0	0	0	0	0	**0**	0	0	0	0	0	0	0	0	N/A
	14	0	0	0	0	0	0	0	0	0	0	0	0	0	**0**	0	0	0	0	0	0	0	N/A
	15	0	1	0	0	0	0	0	0	0	0	0	0	0	0	**0**	0	0	0	0	0	0	0.00%
	16	0	0	0	0	0	0	0	0	0	0	0	1	0	0	0	**1**	0	0	0	0	0	50.00%
	17	0	0	0	0	0	0	0	0	0	0	0	0	0	0	0	0	**0**	0	0	0	0	N/A
	18	1	0	0	0	0	0	0	0	0	0	0	0	0	0	0	0	0	**1**	0	0	0	50.00%
	19	0	0	0	0	0	0	0	0	0	0	0	0	0	0	0	0	0	0	**0**	0	0	N/A
	20	0	0	0	0	0	0	0	0	0	0	0	0	0	0	0	0	0	0	0	**0**	0	N/A
	21	0	0	0	0	0	0	0	0	0	0	0	0	0	0	0	0	0	0	0	0	**0**	N/A
	P.A	25.87%	80.37%	61.43%	0.00%	9.54%	51.68%	2.56%	0.00%	70.68%	0.35%	0.00%	5.32%	0.00%	0.00%	0.00%	0.19%	0.00%	0.31%	0.00%	0.00%	0.00%	**46.12%**

MODIS1 CONFUSION MATRIX (11% SAMPLE)
UK STUDY AREA
DATE:22/03/2003
COMBINATION CLASS CLASSIFICATION SCHEME

CLASSFIED \ REFERENCE	1	2	3	4	5	6	7	8	9	10	11	12	13	14	15	16	17	18	19	20	21	U.A
1	**359**	107	176	6	13	64	3	2	21	33	37	73	1	1	4	10	7	42	3	7	1	37.01%
2	182	**5365**	1232	78	104	203	2	2	5	224	206	1804	4	5	138	418	28	66	50	36	60	52.54%
3	266	902	**2986**	17	52	175	9	2	12	142	144	1128	7	5	36	73	12	183	52	44	45	47.46%
4	0	0	0	**1**	0	0	0	0	0	0	0	0	0	0	0	0	0	0	0	0	0	100.00%
5	0	4	0	0	**8**	3	0	0	0	1	0	1	1	0	4	3	0	0	0	0	0	32.00%
6	40	133	41	14	94	**273**	1	1	0	79	8	55	3	3	41	25	26	6	1	2	3	32.16%
7	0	0	0	0	0	0	**0**	0	0	0	0	0	0	0	0	0	0	0	0	0	0	N/A
8	0	0	0	0	0	0	0	**0**	0	0	0	0	0	0	0	0	0	0	0	0	0	N/A
9	10	35	9	1	6	14	0	2	**57**	5	2	12	0	0	0	0	0	3	1	0	0	36.31%
10	0	0	1	0	0	0	0	0	0	**2**	0	0	0	0	0	1	0	0	0	0	0	50.00%
11	1	0	1	0	0	0	0	0	0	0	**0**	0	0	0	0	0	0	0	0	0	0	0.00%
12	23	134	109	0	6	14	0	0	1	11	7	**197**	0	1	5	15	0	17	4	5	4	35.62%
13	0	0	0	0	0	0	0	0	0	0	0	0	**0**	0	0	0	0	0	0	0	0	N/A
14	0	0	0	0	0	0	0	0	0	0	0	0	0	**0**	0	0	0	0	0	0	0	N/A
15	0	0	0	0	0	0	0	0	0	0	0	0	0	0	**0**	0	0	0	0	0	0	N/A
16	0	3	3	0	0	0	0	0	0	1	1	1	0	0	0	**0**	0	0	0	0	0	0.00%
17	0	0	0	0	0	0	0	0	0	0	0	0	0	0	0	0	**0**	0	0	0	0	N/A
18	0	1	1	0	0	1	0	0	0	0	0	0	0	0	0	0	0	**3**	0	0	0	50.00%
19	0	0	0	0	0	0	0	0	0	0	0	0	0	0	0	0	0	0	**0**	0	0	N/A
20	0	0	0	0	0	0	0	0	0	0	0	0	0	0	0	0	0	0	0	**0**	0	N/A
21	0	0	0	0	0	0	0	0	0	0	0	0	0	0	0	0	0	0	0	0	**0**	N/A
P.A	40.75%	80.27%	65.50%	0.85%	2.83%	36.55%	0.00%	0.00%	59.38%	0.40%	0.00%	6.02%	0.00%	0.00%	0.00%	0.00%	0.00%	0.94%	0.00%	0.00%	0.00%	**48.49%**

MODIS1 CONFUSION MATRIX (11% SAMPLE)
UK STUDY AREA
DATE:23/03/2003
COMBINATION CLASS CLASSIFICATION SCHEME

		REFERENCE																					
		1	2	3	4	5	6	7	8	9	10	11	12	13	14	15	16	17	18	19	20	21	U.A
CLASSFIED	1	**396**	66	149	3	35	114	2	5	16	25	43	54	1	0	8	9	24	38	3	2	1	39.84%
	2	128	**5882**	1408	56	89	190	1	3	3	314	191	1950	2	13	156	373	28	62	49	54	62	53.40%
	3	279	1156	**2790**	31	117	420	2	2	3	276	170	1180	10	3	78	106	41	180	45	50	26	40.06%
	4	0	0	0	**0**	0	0	0	0	0	0	0	0	0	0	0	0	0	0	0	0	0	N/A
	5	0	0	0	0	**0**	0	0	0	0	0	0	0	0	0	0	0	0	0	0	0	0	N/A
	6	115	181	154	18	204	**661**	0	5	7	115	45	73	2	0	62	37	56	27	3	7	6	37.18%
	7	0	0	0	0	0	0	**0**	0	0	0	0	0	0	0	0	0	0	0	0	0	0	N/A
	8	0	0	0	0	0	0	0	**0**	0	0	0	0	0	0	0	0	0	0	0	0	0	N/A
	9	8	3	5	0	1	0	0	0	**94**	0	2	2	0	0	0	2	1	3	0	0	0	77.69%
	10	0	0	2	0	0	1	0	0	0	**1**	0	1	0	0	0	0	0	0	0	0	0	20.00%
	11	0	0	0	0	0	0	0	0	0	0	**0**	0	0	0	0	0	0	0	0	0	0	N/A
	12	18	128	144	4	3	10	0	0	0	11	10	**241**	0	0	4	14	1	10	8	7	4	39.06%
	13	0	0	0	0	0	0	0	0	0	0	0	0	**0**	0	0	0	0	0	0	0	0	N/A
	14	0	0	0	0	0	0	0	0	0	0	0	0	0	**0**	0	0	0	0	0	0	0	N/A
	15	0	0	0	0	0	0	0	0	0	0	0	0	0	0	**0**	0	0	0	0	0	0	N/A
	16	0	2	0	0	0	0	0	0	0	0	0	1	0	0	1	**1**	0	0	0	0	0	20.00%
	17	0	0	0	0	0	0	0	0	0	0	0	0	0	0	0	0	**0**	0	0	0	0	N/A
	18	0	0	0	0	0	0	0	0	0	0	0	0	0	0	0	0	0	**1**	0	0	0	100.00%
	19	0	0	0	0	0	0	0	0	0	0	0	0	0	0	0	0	0	0	**0**	0	0	N/A
	20	0	0	0	0	0	0	0	0	0	0	0	0	0	0	0	0	0	0	0	**0**	0	N/A
	21	0	0	0	0	0	0	0	0	0	0	0	0	0	0	0	0	0	0	0	0	**0**	N/A
	P.A	41.95%	79.29%	59.97%	0.00%	0.00%	47.35%	0.00%	0.00%	76.42%	0.13%	0.00%	6.88%	0.00%	0.00%	0.00%	0.18%	0.00%	0.31%	0.00%	0.00%	0.00%	**46.82%**

MODIS1 CONFUSION MATRIX (11% SAMPLE)
UK STUDY AREA
DATE:MULTIDATE
COMBINATION CLASS CLASSIFICATION SCHEME

		REFERENCE																					
		1	2	3	4	5	6	7	8	9	10	11	12	13	14	15	16	17	18	19	20	21	U.A
CLASSFIED	1	**425**	32	72	1	5	27	0	1	3	4	49	19	0	0	1	3	0	31	2	12	2	61.68%
	2	45	**4929**	515	57	69	202	0	1	0	300	110	1140	2	8	140	326	23	19	20	29	30	61.88%
	3	209	543	**3185**	18	34	62	0	2	8	46	142	1195	0	3	20	68	8	199	55	55	25	54.19%
	4	0	0	0	**0**	0	0	0	0	0	0	0	0	0	0	0	0	0	0	0	0	0	N/A
	5	0	0	0	0	**0**	0	0	0	0	1	0	0	0	0	1	0	0	0	0	0	0	0.00%
	6	51	160	30	10	203	**861**	1	3	0	155	9	27	9	0	47	14	61	9	0	2	2	52.06%
	7	0	0	0	0	0	0	**0**	0	0	0	0	0	0	0	0	0	0	0	0	0	0	N/A
	8	0	0	0	0	0	0	0	**0**	0	0	0	0	0	0	0	0	0	0	0	0	0	N/A
	9	4	2	3	0	0	0	0	2	**33**	0	0	2	0	0	0	1	0	0	0	0	0	70.21%
	10	0	3	1	0	3	4	0	0	0	**5**	0	1	0	0	0	0	0	1	0	0	0	27.78%
	11	2	1	3	0	0	0	0	0	0	0	**3**	0	0	0	0	0	0	0	0	0	1	30.00%
	12	10	330	291	5	0	2	0	0	1	16	16	**514**	0	1	4	36	0	9	13	6	17	40.44%
	13	0	0	0	0	0	0	0	0	0	0	0	0	**0**	0	0	0	0	0	0	0	0	N/A
	14	0	0	0	0	0	0	0	0	0	0	0	0	0	**0**	0	0	0	0	0	0	0	N/A
	15	0	0	0	0	0	0	0	0	0	0	0	0	0	0	**0**	0	0	0	0	0	0	N/A
	16	1	6	0	2	0	1	0	0	0	0	1	2	0	0	1	**4**	0	1	0	1	0	20.00%
	17	0	0	0	0	0	0	0	0	0	0	0	0	0	0	0	0	**0**	0	0	0	0	N/A
	18	0	0	0	0	0	0	0	0	0	0	0	0	0	0	0	0	0	**0**	0	0	0	N/A
	19	0	0	0	0	0	0	0	0	0	0	0	0	0	0	0	0	0	0	**0**	0	0	N/A
	20	0	0	0	0	0	0	0	0	0	0	0	0	0	0	0	0	0	0	0	**0**	0	N/A
	21	0	0	0	0	0	0	0	0	0	0	0	0	0	0	0	0	0	0	0	0	**0**	N/A
	P.A	56.89%	82.07%	77.68%	0.00%	0.00%	74.29%	0.00%	0.00%	73.33%	0.95%	0.91%	17.72%	0.00%	0.00%	0.00%	0.88%	0.00%	0.00%	0.00%	0.00%	0.00%	**56.74%**

MODIS2 CONFUSION MATRIX (11% SAMPLE)
UK STUDY AREA
DATE:13/07/2003
COMBINATION CLASS CLASSIFICATION SCHEME

CLASSFIED \ REFERENCE	1	2	3	4	5	6	7	8	9	10	11	12	13	14	15	16	17	18	19	20	21	U.A
1	**562**	85	85	1	4	16	1	2	17	4	91	77	0	0	0	14	2	52	3	17	1	54.35%
2	112	**6355**	472	67	155	382	14	6	20	516	188	1355	6	15	229	466	54	33	19	37	54	60.21%
3	220	469	**3849**	18	17	25	0	4	31	20	115	1308	0	0	32	44	6	218	72	51	32	58.93%
4	0	0	1	**0**	0	0	0	0	0	0	0	0	0	0	0	0	0	0	0	0	0	0.00%
5	3	61	5	3	**106**	62	1	2	4	26	0	8	2	0	25	6	14	1	0	0	0	32.22%
6	6	309	15	1	178	**1583**	9	21	13	391	0	33	51	0	61	3	93	2	0	0	1	57.15%
7	0	0	0	0	0	0	**0**	0	0	0	0	0	0	0	0	0	0	0	0	0	0	N/A
8	0	0	0	0	0	0	0	**0**	0	0	0	0	0	0	0	0	0	0	0	0	0	N/A
9	18	29	27	0	2	6	0	4	**119**	2	2	15	0	0	1	2	0	1	1	3	0	51.29%
10	0	5	0	0	0	2	0	0	1	**2**	0	0	0	0	1	0	0	0	0	0	0	18.18%
11	0	0	0	0	0	0	0	0	0	0	**0**	0	0	0	0	0	0	0	0	0	0	N/A
12	44	465	482	14	3	11	0	1	1	12	59	**780**	0	0	12	52	1	35	21	20	21	38.35%
13	0	0	0	0	0	0	0	0	0	0	0	0	**0**	0	0	0	0	0	0	0	0	N/A
14	0	0	0	0	0	0	0	0	0	0	0	0	0	**0**	0	0	0	0	0	0	0	N/A
15	0	0	0	0	0	0	0	0	0	0	0	0	0	0	**1**	0	0	0	0	0	0	100.00%
16	0	5	0	3	1	0	0	0	0	1	2	3	0	0	1	**3**	0	1	0	0	0	15.00%
17	0	0	0	0	0	0	0	0	0	0	0	0	0	0	0	0	**0**	0	0	0	0	N/A
18	1	0	0	0	0	0	0	0	0	0	0	1	0	0	0	0	0	**1**	0	0	0	33.33%
19	0	0	0	0	0	0	0	0	0	0	0	0	0	0	0	0	0	0	**0**	0	0	N/A
20	0	0	0	0	0	0	0	0	0	0	0	0	0	0	0	0	0	0	0	**0**	0	N/A
21	0	0	0	0	0	0	0	0	0	0	0	0	0	0	0	0	0	0	0	0	**0**	N/A
P.A	58.18%	81.65%	77.98%	0.00%	22.75%	75.85%	0.00%	0.00%	57.77%	0.21%	0.00%	21.79%	0.00%	0.00%	0.28%	0.51%	0.00%	0.29%	0.00%	0.00%	0.00%	**56.80%**

MODIS2 CONFUSION MATRIX (11% SAMPLE)
UK STUDY AREA
DATE:16/04/2003
COMBINATION CLASS CLASSIFICATION SCHEME

		REFERENCE																					
		1	2	3	4	5	6	7	8	9	10	11	12	13	14	15	16	17	18	19	20	21	U.A
CLASSFIED	1	**552**	86	130	7	12	7	0	2	7	4	87	83	0	0	1	5	4	71	6	15	6	50.88%
	2	148	**7911**	725	67	196	291	73	20	19	483	197	1755	5	85	294	444	48	49	25	31	57	61.22%
	3	246	598	**3838**	16	18	12	3	3	5	21	131	1438	0	0	13	69	3	232	73	48	35	56.42%
	4	0	0	0	**0**	0	0	0	0	0	0	0	0	0	0	0	0	0	0	0	0	0	N/A
	5	9	96	13	5	**197**	77	5	4	3	30	6	22	2	3	36	10	40	2	0	0	0	35.18%
	6	8	237	12	2	125	**1454**	39	22	3	325	6	16	32	17	46	8	74	1	0	0	1	59.88%
	7	0	3	0	0	0	0	**2**	0	0	0	0	0	0	2	0	0	0	0	0	0	0	28.57%
	8	0	0	0	0	0	0	0	**0**	0	0	0	0	0	0	0	0	0	0	0	0	0	N/A
	9	17	36	25	0	4	6	1	45	**107**	2	8	19	0	0	2	4	1	10	1	2	0	36.90%
	10	0	11	0	0	4	11	1	0	0	**20**	0	0	0	2	3	0	6	0	0	0	0	34.48%
	11	0	0	0	0	0	0	0	0	0	0	**1**	0	0	0	0	0	0	0	0	0	0	100.00%
	12	29	379	438	12	9	6	0	1	0	21	52	**660**	0	2	16	23	4	16	14	13	14	38.62%
	13	0	0	0	0	0	0	0	0	0	0	0	0	**0**	0	0	0	0	0	0	0	0	N/A
	14	0	0	0	0	0	0	0	0	0	0	0	0	0	**0**	0	0	0	0	0	0	0	N/A
	15	0	0	0	0	0	0	0	0	0	0	0	0	0	0	**0**	0	0	0	0	0	0	N/A
	16	0	1	3	1	1	0	0	0	0	0	0	1	0	0	2	**4**	0	0	0	0	0	30.77%
	17	0	0	0	0	0	0	0	0	0	0	0	0	0	0	0	0	**0**	0	0	0	0	N/A
	18	1	2	1	0	0	0	0	0	0	0	0	0	0	0	0	1	0	**1**	0	0	0	16.67%
	19	0	0	0	0	0	0	0	0	0	0	0	0	0	0	0	0	0	0	**0**	0	0	N/A
	20	0	0	0	0	0	0	0	0	0	0	0	0	0	0	0	0	0	0	0	**0**	0	N/A
	21	0	0	0	0	0	0	0	0	0	0	0	0	0	0	0	0	0	0	0	0	**0**	N/A
	P.A	54.65%	84.52%	74.02%	0.00%	34.81%	78.00%	1.61%	0.00%	74.31%	2.21%	0.20%	16.52%	0.00%	0.00%	0.00%	0.70%	0.00%	0.26%	0.00%	0.00%	0.00%	**56.98%**

MODIS2 CONFUSION MATRIX (11% SAMPLE)
UK STUDY AREA
DATE:17/03/2003
COMBINATION CLASS CLASSIFICATION SCHEME

CLASSFIED \ REFERENCE	1	2	3	4	5	6	7	8	9	10	11	12	13	14	15	16	17	18	19	20	21	U.A
1	**559**	63	119	5	4	3	0	2	3	5	99	85	1	1	2	12	0	53	3	17	7	53.60%
2	127	**9711**	579	73	186	418	192	36	20	529	244	1987	13	226	271	437	74	34	32	39	64	63.50%
3	177	346	**2785**	12	4	7	0	0	4	6	93	1033	0	1	10	39	0	167	55	40	18	58.06%
4	0	0	0	**0**	0	0	0	0	0	0	0	0	0	0	0	0	0	0	0	0	0	N/A
5	2	76	1	3	**185**	112	1	2	5	39	0	6	2	2	52	6	28	0	0	0	0	35.44%
6	22	322	26	10	101	**1448**	78	45	17	362	11	35	51	25	39	21	72	4	1	1	1	53.79%
7	0	54	16	0	12	41	**171**	1	0	22	0	10	12	41	7	1	5	0	0	0	0	43.51%
8	0	10	3	0	0	5	2	**14**	2	5	0	1	0	0	0	2	2	1	0	2	0	28.57%
9	7	24	2	0	2	15	1	5	**26**	10	3	10	1	2	2	1	1	1	0	1	0	22.81%
10	0	7	0	0	2	8	0	0	0	**6**	0	0	1	1	0	0	0	0	0	0	0	24.00%
11	0	0	0	0	0	0	0	0	0	0	**0**	0	0	0	0	0	0	0	0	0	0	N/A
12	38	371	390	10	4	1	1	0	0	3	53	**659**	0	1	5	44	2	24	10	13	20	39.96%
13	0	0	0	0	0	0	0	0	0	0	0	0	**0**	0	0	0	0	0	0	0	0	N/A
14	0	1	0	0	0	0	0	0	0	0	0	0	0	**1**	0	0	0	0	0	0	0	50.00%
15	0	0	0	0	0	0	0	0	0	0	0	0	0	0	**0**	0	0	0	0	0	0	N/A
16	0	0	0	0	0	0	0	0	0	0	0	0	0	0	0	**0**	0	0	0	0	0	N/A
17	0	0	0	0	0	0	0	0	0	0	0	0	0	0	0	0	**0**	0	0	0	0	N/A
18	0	0	0	0	0	0	0	0	0	0	0	0	0	0	0	0	0	**0**	0	0	0	N/A
19	0	0	0	0	0	0	0	0	0	0	0	0	0	0	0	0	0	0	**0**	0	0	N/A
20	0	0	0	0	0	0	0	0	0	0	0	0	0	0	0	0	0	0	0	**0**	0	N/A
21	0	0	0	0	0	0	0	0	0	0	0	0	0	0	0	0	0	0	0	0	**0**	N/A
P.A	59.98%	88.40%	71.03%	0.00%	37.00%	70.36%	38.34%	13.33%	33.77%	0.61%	0.00%	17.22%	0.00%	0.33%	0.00%	0.00%	0.00%	0.00%	0.00%	0.00%	0.00%	**58.56%**

MODIS2 CONFUSION MATRIX (11% SAMPLE)
UK STUDY AREA
DATE:18/04/2003
COMBINATION CLASS CLASSIFICATION SCHEME

		REFERENCE																					
		1	2	3	4	5	6	7	8	9	10	11	12	13	14	15	16	17	18	19	20	21	U.A
CLASSFIED	1	**581**	77	162	3	6	8	0	1	6	4	69	61	0	0	0	12	2	51	5	11	2	54.76%
	2	141	**10089**	803	75	232	331	191	78	61	516	230	2157	9	236	303	429	64	57	36	44	63	62.49%
	3	244	502	**3522**	24	14	14	1	3	11	23	124	1322	0	4	26	49	4	206	50	53	24	56.62%
	4	0	0	0	**0**	0	0	0	0	0	0	0	0	0	0	0	0	0	0	0	0	0	N/A
	5	3	88	19	10	**223**	101	9	5	4	48	4	16	2	1	43	10	43	1	0	0	1	35.34%
	6	17	412	21	5	149	**2093**	73	26	11	528	8	17	72	27	41	15	99	4	1	3	0	57.79%
	7	0	105	24	0	24	56	**308**	5	0	30	0	11	14	104	7	2	13	0	0	0	1	43.75%
	8	0	0	0	0	0	0	0	**0**	0	0	0	0	0	0	0	0	0	0	0	0	0	N/A
	9	9	20	10	0	1	12	0	57	**51**	7	1	12	2	0	0	3	1	1	0	1	0	27.13%
	10	0	12	2	0	3	13	9	1	0	**21**	0	1	3	3	2	0	1	0	0	0	0	29.58%
	11	2	2	1	1	1	0	0	0	0	0	**2**	1	0	0	1	0	0	0	1	0	0	16.67%
	12	34	542	518	11	8	5	0	1	1	19	50	**846**	0	0	15	55	2	23	13	15	13	38.97%
	13	0	0	0	0	0	0	0	0	0	0	0	0	**0**	0	0	0	0	0	0	0	0	N/A
	14	0	0	0	0	0	0	0	0	0	0	0	0	0	**0**	0	0	0	0	0	0	0	N/A
	15	0	1	1	0	1	2	1	0	0	1	0	1	0	0	**2**	0	2	0	0	0	0	16.67%
	16	0	3	0	1	0	0	0	0	0	0	0	0	0	0	0	**3**	0	0	0	0	1	37.50%
	17	0	0	0	0	0	0	0	0	0	0	0	0	0	0	0	0	**0**	0	0	0	0	N/A
	18	0	0	0	0	0	0	0	0	0	0	0	0	0	0	0	0	0	**0**	0	0	0	N/A
	19	0	0	0	0	0	0	0	0	0	0	0	0	0	0	0	0	0	0	**0**	0	0	N/A
	20	0	0	0	0	0	0	0	0	0	0	0	0	0	0	0	0	0	0	0	**0**	0	N/A
	21	0	0	0	0	0	0	0	0	0	0	0	0	0	0	0	0	0	0	0	0	**0**	N/A
	P.A	56.35%	85.12%	69.29%	0.00%	33.69%	79.43%	52.03%	0.00%	35.17%	1.75%	0.41%	19.03%	0.00%	0.00%	0.45%	0.52%	0.00%	0.00%	0.00%	0.00%	0.00%	**57.52%**

MODIS2 CONFUSION MATRIX (11% SAMPLE)
UK STUDY AREA
DATE:19/03/2003
COMBINATION CLASS CLASSIFICATION SCHEME

CLASSFIED \ REFERENCE	1	2	3	4	5	6	7	8	9	10	11	12	13	14	15	16	17	18	19	20	21	U.A
1	**419**	51	149	2	2	3	0	1	7	5	54	42	0	0	1	4	0	57	5	14	2	51.22%
2	121	**5662**	391	63	183	323	37	13	20	387	182	1265	7	20	201	397	56	23	23	18	54	59.94%
3	276	399	**3294**	23	12	9	1	0	3	18	98	1196	0	0	16	46	3	216	74	48	31	57.16%
4	0	1	0	**1**	0	0	0	0	0	0	0	1	0	0	0	0	0	0	0	0	0	33.33%
5	2	100	7	6	**248**	111	1	6	1	43	0	14	2	3	59	4	48	0	0	0	1	37.80%
6	15	328	27	14	75	**1562**	28	22	26	384	4	22	52	10	23	25	76	3	1	0	0	57.92%
7	0	6	0	0	1	5	**12**	0	0	3	0	0	0	2	0	0	2	0	0	0	0	38.71%
8	0	0	0	0	0	0	0	**0**	0	0	0	0	0	0	0	0	0	0	0	0	0	N/A
9	4	11	2	0	2	3	0	2	**75**	2	2	5	1	0	0	1	0	0	0	2	0	66.96%
10	0	7	0	0	1	5	0	0	0	**13**	0	2	0	0	0	0	3	0	0	0	0	41.94%
11	2	0	0	0	0	0	0	0	0	0	**1**	0	0	0	0	0	0	0	0	0	0	33.33%
12	37	413	497	11	9	12	0	0	0	12	71	**735**	0	1	8	46	3	29	22	11	31	37.73%
13	0	0	0	0	0	0	0	0	0	0	0	0	**0**	0	0	0	0	0	0	0	0	N/A
14	0	0	0	0	0	0	0	0	0	0	0	0	0	**0**	0	0	0	0	0	0	0	N/A
15	0	0	0	0	0	0	0	0	0	0	0	0	0	0	**0**	0	0	0	0	0	0	N/A
16	0	0	0	0	0	0	0	0	0	0	0	0	0	0	0	**0**	0	0	0	0	0	N/A
17	0	0	0	0	0	0	0	0	0	0	0	0	0	0	0	0	**0**	0	0	0	0	N/A
18	0	0	0	0	0	0	0	0	0	0	0	0	0	0	0	0	0	**0**	0	0	0	N/A
19	0	0	0	0	0	0	0	0	0	0	0	0	0	0	0	0	0	0	**0**	0	0	N/A
20	0	0	0	0	0	0	0	0	0	0	0	0	0	0	0	0	0	0	0	**0**	0	N/A
21	0	0	0	0	0	0	0	0	0	0	0	0	0	0	0	0	0	0	0	0	**0**	N/A
P.A	47.83%	81.14%	75.43%	0.83%	46.53%	76.83%	15.19%	0.00%	56.82%	1.50%	0.24%	22.39%	0.00%	0.00%	0.00%	0.00%	0.00%	0.00%	0.00%	0.00%	0.00%	**55.90%**

MODIS2 CONFUSION MATRIX (11% SAMPLE)
UK STUDY AREA
DATE:22/03/2003
COMBINATION CLASS CLASSIFICATION SCHEME

CLASSFIED \ REFERENCE	1	2	3	4	5	6	7	8	9	10	11	12	13	14	15	16	17	18	19	20	21	U.A
1	**441**	81	141	2	3	6	1	0	8	2	68	83	0	0	0	6	1	69	5	11	3	47.37%
2	116	**5471**	470	78	136	238	6	4	16	312	169	1216	10	8	165	430	36	42	32	25	55	60.55%
3	222	528	**3519**	14	18	20	2	0	3	11	119	1285	0	0	12	62	1	184	50	46	47	57.28%
4	0	0	0	**0**	0	0	0	0	0	0	0	0	0	0	0	0	0	0	0	0	0	N/A
5	0	34	3	6	**81**	45	0	0	0	14	0	17	1	1	37	5	13	0	1	0	1	31.27%
6	8	183	22	4	36	**445**	6	4	1	137	4	20	5	6	14	7	21	0	0	1	0	48.16%
7	0	0	0	0	0	0	**0**	0	0	0	0	0	0	0	0	0	0	0	0	0	0	N/A
8	0	0	0	0	0	0	0	**0**	0	0	0	0	0	0	0	0	0	0	0	0	0	N/A
9	9	28	5	1	2	3	0	0	**64**	3	2	8	0	0	0	0	0	3	0	0	0	50.00%
10	1	2	0	0	0	1	0	0	0	**7**	0	1	0	0	0	1	0	0	0	0	0	53.85%
11	2	0	1	0	1	0	0	0	0	0	**1**	2	0	0	0	0	0	1	0	0	1	11.11%
12	39	375	430	13	8	3	0	0	4	11	46	**640**	0	0	7	36	2	23	22	12	10	38.07%
13	0	0	0	0	0	0	0	0	0	0	0	0	**0**	0	0	0	0	0	0	0	0	N/A
14	0	0	0	0	0	0	0	0	0	0	0	0	0	**0**	0	0	0	0	0	0	0	N/A
15	0	0	0	0	0	0	0	0	0	0	0	0	0	0	**0**	0	0	0	0	0	0	N/A
16	0	1	1	0	0	0	0	0	0	0	0	0	0	0	0	**1**	0	0	0	0	0	33.33%
17	0	0	0	0	0	0	0	0	0	0	0	0	0	0	0	0	**0**	0	0	0	0	N/A
18	0	0	0	0	0	0	0	0	0	0	0	0	0	0	0	0	0	**1**	0	0	0	100.00%
19	38	1	6	0	0	0	0	0	1	0	0	1	0	0	0	0	0	5	**0**	0	0	0.00%
20	0	0	0	0	0	0	0	0	0	0	0	0	0	0	0	0	0	0	0	**0**	0	N/A
21	0	0	0	0	0	0	0	0	0	0	0	0	0	0	0	0	0	0	0	0	**0**	N/A
P.A	50.34%	81.61%	76.53%	0.00%	28.42%	58.48%	0.00%	0.00%	65.98%	1.41%	0.24%	19.55%	0.00%	0.00%	0.00%	0.18%	0.00%	0.30%	0.00%	0.00%	0.00%	**55.64%**

MODIS2 CONFUSION MATRIX (11% SAMPLE)
UK STUDY AREA
DATE:23/03/2003
COMBINATION CLASS CLASSIFICATION SCHEME

CLASSFIED \ REFERENCE	1	2	3	4	5	6	7	8	9	10	11	12	13	14	15	16	17	18	19	20	21	U.A
1	**510**	62	96	2	4	7	0	2	1	4	82	61	0	0	3	8	1	55	4	8	4	55.80%
2	104	**6298**	289	78	182	323	1	2	4	474	206	1157	6	15	212	412	47	22	20	28	42	63.48%
3	242	355	**3672**	15	11	6	2	0	7	7	92	1278	0	1	9	43	1	203	58	50	18	60.49%
4	0	1	0	**2**	0	0	0	0	0	0	0	0	0	0	1	1	0	0	0	0	1	33.33%
5	3	43	7	4	**173**	56	1	6	4	14	1	13	2	0	44	9	33	1	1	1	0	41.59%
6	11	176	6	3	58	**990**	1	4	2	212	9	10	7	1	27	21	63	1	0	1	1	61.72%
7	0	0	0	0	0	0	**0**	0	0	0	0	0	0	0	0	0	0	0	0	0	0	N/A
8	0	0	0	0	0	0	0	**0**	0	0	0	0	0	0	0	0	0	0	0	0	0	N/A
9	12	6	7	0	0	1	0	0	**104**	0	3	4	0	0	2	1	1	5	0	0	0	71.23%
10	0	21	1	1	3	15	0	0	0	**23**	0	5	0	0	2	2	1	0	0	0	0	31.08%
11	2	0	2	0	0	0	0	0	0	0	**5**	0	0	0	0	0	0	1	0	0	0	50.00%
12	45	484	580	7	7	5	0	1	0	16	60	**948**	0	0	5	43	3	30	25	30	32	40.84%
13	0	0	0	0	0	0	0	0	0	0	0	0	**0**	0	0	0	0	0	0	0	0	N/A
14	0	0	0	0	0	0	0	0	0	0	0	0	0	**0**	0	0	0	0	0	0	0	N/A
15	0	2	0	0	5	1	0	0	0	1	0	1	0	0	**9**	0	1	0	0	0	0	45.00%
16	0	0	0	0	0	0	0	0	0	0	0	0	0	0	0	**2**	0	0	0	0	0	100.00%
17	0	0	0	0	0	0	0	0	0	0	0	0	0	0	0	0	**0**	0	0	0	0	N/A
18	0	0	0	0	0	0	0	0	0	0	0	0	0	0	0	0	0	**0**	0	0	0	N/A
19	0	0	0	0	0	0	0	0	0	0	0	0	0	0	0	0	0	0	**0**	0	0	N/A
20	0	0	0	0	0	0	0	0	0	0	0	0	0	0	0	0	0	0	0	**0**	0	N/A
21	0	0	0	0	0	0	0	0	0	0	0	0	0	0	0	0	0	0	0	0	**0**	N/A
P.A	54.90%	84.56%	78.80%	1.79%	39.05%	70.51%	0.00%	0.00%	85.25%	3.06%	1.09%	27.26%	0.00%	0.00%	2.87%	0.37%	0.00%	0.00%	0.00%	0.00%	0.00%	**59.22%**

MODIS2 CONFUSION MATRIX (11% SAMPLE)
UK STUDY AREA
DATE:MULTIDATE
COMBINATION CLASS CLASSIFICATION SCHEME

		REFERENCE																					
		1	2	3	4	5	6	7	8	9	10	11	12	13	14	15	16	17	18	19	20	21	U.A
CLASSFIED	1	**497**	53	85	2	6	1	0	1	0	4	69	42	0	0	1	11	0	42	4	11	3	59.74%
	2	76	**5044**	332	57	99	205	1	1	2	317	132	996	2	11	141	338	26	25	20	29	35	63.94%
	3	124	293	**3180**	8	10	11	0	3	5	5	84	1027	0	0	12	30	3	171	53	46	22	62.51%
	4	0	0	1	**1**	0	0	0	0	0	0	1	2	0	0	0	1	0	0	0	0	0	16.67%
	5	3	44	7	3	**154**	93	0	4	0	24	0	11	0	0	33	3	29	1	0	0	1	37.56%
	6	0	111	3	4	37	**854**	0	0	1	146	2	10	9	0	21	10	30	0	1	0	0	68.93%
	7	0	0	0	0	0	0	**0**	0	0	0	0	0	0	0	0	0	0	0	0	0	0	N/A
	8	0	0	0	0	0	0	0	**0**	0	0	0	0	0	0	0	0	0	0	0	0	0	N/A
	9	5	5	7	0	2	1	0	0	**37**	0	0	4	0	0	0	2	1	2	0	0	0	56.06%
	10	0	3	0	0	0	3	0	0	0	**6**	0	0	0	0	0	0	0	0	0	0	0	50.00%
	11	1	1	3	0	0	0	0	0	0	0	**4**	2	0	0	0	0	0	0	0	1	0	33.33%
	12	35	493	511	13	5	2	0	1	0	22	43	**862**	0	1	10	61	2	28	12	18	18	40.34%
	13	0	0	0	0	0	0	0	0	0	0	0	0	**0**	0	0	0	0	0	0	0	0	N/A
	14	0	0	0	0	0	0	0	0	0	0	0	0	0	**0**	0	0	0	0	0	0	0	N/A
	15	0	0	0	0	0	0	0	0	0	0	0	0	0	0	**0**	0	0	0	0	0	0	N/A
	16	1	0	0	4	1	1	0	0	0	1	0	0	0	0	2	**0**	0	0	0	0	0	0.00%
	17	0	0	0	0	0	0	0	0	0	0	0	0	0	0	0	0	**0**	0	0	0	0	N/A
	18	0	0	0	0	0	0	0	0	0	0	0	0	0	0	0	0	0	**0**	0	0	0	N/A
	19	0	0	0	0	0	0	0	0	0	0	0	0	0	0	0	0	0	0	**0**	0	0	N/A
	20	0	0	0	0	0	0	0	0	0	0	0	0	0	0	0	0	0	0	0	**0**	0	N/A
	21	0	0	0	0	0	0	0	0	0	0	0	0	0	0	0	0	0	0	0	0	**0**	N/A
	P.A	66.98%	83.41%	77.02%	1.09%	49.04%	72.93%	0.00%	0.00%	82.22%	1.14%	1.19%	29.16%	0.00%	0.00%	0.00%	0.00%	0.00%	0.00%	0.00%	0.00%	0.00%	**60.11%**

MODIS3 CONFUSION MATRIX (11% SAMPLE)
UK STUDY AREA
DATE:13/07/2003
COMBINATION CLASS CLASSIFICATION SCHEME

		REFERENCE																					
		1	2	3	4	5	6	7	8	9	10	11	12	13	14	15	16	17	18	19	20	21	U.A
CLASSFIED	1	**574**	142	171	1	4	17	1	1	33	7	100	138	1	0	2	16	0	72	7	21	1	43.85%
	2	125	**6291**	441	62	159	341	12	8	7	492	187	1351	4	12	223	454	56	39	20	36	56	60.63%
	3	201	437	**3737**	19	9	22	2	4	26	19	103	1185	0	0	30	43	5	194	70	50	27	60.44%
	4	0	0	0	**0**	0	0	0	0	0	0	0	0	0	0	0	0	0	0	0	0	0	N/A
	5	5	56	6	6	**106**	65	0	6	3	26	3	6	2	0	31	7	19	1	0	0	0	30.46%
	6	1	270	15	2	168	**1604**	8	13	12	392	0	24	50	1	55	3	82	1	0	0	1	59.36%
	7	0	0	0	0	0	0	**0**	0	0	0	0	0	0	0	0	0	0	0	0	0	0	N/A
	8	0	0	0	0	0	0	0	**0**	0	0	0	0	0	0	0	0	0	0	0	0	0	N/A
	9	18	26	22	0	3	10	1	6	**119**	3	1	16	0	0	2	2	0	2	0	1	0	51.29%
	10	2	22	0	0	0	20	1	1	0	**28**	0	1	0	0	3	1	1	0	0	0	0	35.00%
	11	0	1	0	0	0	0	0	0	0	0	**0**	0	0	0	0	0	0	0	0	0	0	0.00%
	12	46	491	508	13	4	9	0	1	1	11	57	**793**	0	2	15	46	3	36	18	21	20	37.85%
	13	0	0	0	0	0	0	0	0	0	0	0	0	**0**	0	0	0	0	0	0	0	0	N/A
	14	0	0	0	0	0	0	0	0	0	0	0	0	0	**0**	0	0	0	0	0	0	0	N/A
	15	0	2	0	0	3	0	0	0	1	0	0	0	0	0	**3**	0	0	0	0	0	0	33.33%
	16	0	4	0	2	1	2	0	0	0	0	0	0	0	0	0	**12**	1	0	0	0	1	52.17%
	17	0	0	0	0	0	0	0	0	0	0	0	0	0	0	0	0	**0**	0	0	0	0	N/A
	18	0	0	0	0	0	0	0	0	0	0	0	0	0	0	0	0	0	**0**	0	0	0	N/A
	19	0	0	0	0	0	0	0	0	0	0	0	0	0	0	0	0	0	0	**0**	0	0	N/A
	20	0	0	0	0	0	0	0	0	0	0	0	0	0	0	0	0	0	0	0	**0**	0	N/A
	21	0	0	0	0	0	0	0	0	0	0	0	0	0	0	0	0	0	0	0	0	**0**	N/A
	P.A	59.05%	81.26%	76.27%	0.00%	23.19%	76.75%	0.00%	0.00%	58.91%	2.86%	0.00%	22.57%	0.00%	0.00%	0.82%	2.05%	0.00%	0.00%	0.00%	0.00%	0.00%	**56.80%**

MODIS3 CONFUSION MATRIX (11% SAMPLE)
UK STUDY AREA
DATE:16/04/2003
COMBINATION CLASS CLASSIFICATION SCHEME

		REFERENCE																					
		1	2	3	4	5	6	7	8	9	10	11	12	13	14	15	16	17	18	19	20	21	U.A
CLASSFIED	1	**526**	82	143	2	9	21	0	2	12	8	88	74	1	0	4	6	1	65	4	18	6	49.07%
	2	139	**7873**	791	62	172	286	40	16	18	493	216	1750	5	55	275	440	42	55	30	28	55	61.31%
	3	259	683	**3753**	31	27	37	2	3	6	21	141	1479	0	1	20	72	9	231	66	47	37	54.19%
	4	0	1	2	**3**	3	0	0	0	0	0	0	2	0	0	0	0	1	0	1	0	0	23.08%
	5	7	59	9	3	**186**	73	4	5	1	21	2	8	1	1	34	7	37	2	0	0	0	40.43%
	6	26	262	40	2	145	**1403**	36	25	12	324	11	28	25	20	57	10	83	4	0	1	1	55.79%
	7	0	20	3	0	5	14	**44**	0	0	13	0	6	4	21	3	0	2	0	0	0	0	32.59%
	8	3	11	3	0	3	6	1	**43**	10	1	0	4	0	0	2	0	2	0	0	1	0	47.78%
	9	10	14	14	0	2	2	0	4	**114**	0	4	11	0	0	0	3	1	7	1	0	0	60.96%
	10	0	5	0	0	0	4	0	0	0	**7**	0	0	0	0	1	0	1	0	0	0	0	38.89%
	11	0	0	0	0	0	0	0	0	0	0	**0**	0	0	0	0	0	0	0	0	0	0	N/A
	12	37	381	444	3	10	16	1	0	0	18	30	**633**	0	0	15	31	2	17	17	15	16	37.54%
	13	0	0	0	0	0	0	0	0	0	0	0	0	**0**	0	0	0	0	0	0	0	0	N/A
	14	0	4	1	0	0	3	2	0	0	0	0	0	1	**10**	0	0	0	0	0	0	0	47.62%
	15	0	0	0	0	1	0	0	0	0	0	0	0	0	0	**0**	0	0	0	0	0	0	0.00%
	16	0	0	1	0	0	0	0	0	0	0	0	0	0	0	1	**3**	0	0	0	0	0	60.00%
	17	0	0	0	0	0	0	0	0	0	0	0	0	0	0	0	0	**1**	0	0	0	0	100.00%
	18	0	0	2	0	0	0	0	0	0	0	0	0	0	0	0	0	0	**0**	0	0	0	0.00%
	19	0	0	0	0	0	0	0	0	0	0	0	0	0	0	0	0	0	0	**0**	0	0	N/A
	20	0	0	0	0	0	0	0	0	0	0	0	0	0	0	0	0	0	0	0	**0**	0	N/A
	21	0	0	0	0	0	0	0	0	0	0	0	0	0	0	0	0	0	0	0	0	**0**	N/A
	P.A	52.23%	83.80%	72.09%	2.83%	33.04%	75.23%	33.85%	43.88%	65.90%	0.77%	0.00%	15.84%	0.00%	9.26%	0.00%	0.52%	0.55%	0.00%	0.00%	0.00%	0.00%	**56.21%**

MODIS3 CONFUSION MATRIX (11% SAMPLE)
UK STUDY AREA
DATE:17/03/2003
COMBINATION CLASS CLASSIFICATION SCHEME

CLASSFIED \ REFERENCE	1	2	3	4	5	6	7	8	9	10	11	12	13	14	15	16	17	18	19	20	21	U.A
1	**525**	99	129	9	5	12	2	1	5	10	97	110	0	0	3	13	0	55	5	13	7	47.73%
2	163	**9674**	592	64	169	352	183	49	28	474	246	2019	10	217	264	443	69	37	35	37	57	63.72%
3	175	342	**2831**	12	2	3	0	0	3	4	111	1020	0	0	10	43	0	176	44	46	27	58.38%
4	0	6	4	**8**	4	6	0	0	0	1	0	1	0	0	4	6	2	0	2	1	0	17.78%
5	2	70	0	1	**165**	95	0	2	0	39	0	1	2	2	51	7	21	0	0	0	0	36.03%
6	16	322	13	12	141	**1537**	93	32	14	399	10	20	50	31	38	17	82	2	2	0	1	54.27%
7	0	60	12	0	10	38	**152**	3	0	17	0	14	12	46	8	1	7	0	0	0	0	40.00%
8	4	16	4	0	0	4	3	**16**	2	3	0	1	1	2	0	0	1	0	0	0	0	28.07%
9	9	15	5	0	1	0	0	1	**24**	1	2	10	0	0	1	1	0	2	0	1	0	32.88%
10	0	11	0	0	1	11	0	1	0	**24**	0	0	1	1	1	1	2	0	0	0	0	44.44%
11	0	0	0	0	0	0	0	0	0	0	**0**	0	0	0	0	0	0	0	0	0	0	N/A
12	39	370	354	9	3	4	1	0	0	8	38	**645**	0	0	4	29	0	15	13	14	16	41.29%
13	0	0	0	0	0	0	0	0	0	0	0	0	**0**	0	0	0	0	0	0	0	0	N/A
14	0	3	1	0	0	0	2	0	0	2	0	0	0	**1**	0	0	0	0	0	0	0	11.11%
15	0	0	0	0	0	0	0	0	0	0	0	0	0	0	**0**	0	0	0	0	0	0	N/A
16	0	0	0	0	0	0	0	0	0	0	0	0	0	0	0	**0**	0	0	0	0	0	N/A
17	0	0	0	0	0	0	0	0	0	0	0	0	0	0	0	0	**0**	0	0	0	0	N/A
18	0	0	0	0	0	0	0	0	0	0	0	0	0	0	0	0	0	**0**	0	0	0	N/A
19	0	0	0	0	0	0	0	0	0	0	0	0	0	0	0	0	0	0	**0**	0	0	N/A
20	0	0	0	0	0	0	0	0	0	0	0	0	0	0	0	0	0	0	0	**0**	0	N/A
21	0	0	0	0	0	0	0	0	0	0	0	0	0	0	0	0	0	0	0	0	**0**	N/A
P.A	56.27%	88.04%	71.76%	6.96%	32.93%	74.54%	34.86%	15.24%	31.58%	2.44%	0.00%	16.79%	0.00%	0.33%	0.00%	0.00%	0.00%	0.00%	0.00%	0.00%	0.00%	**58.65%**

MODIS3 CONFUSION MATRIX (11% SAMPLE)
UK STUDY AREA
DATE:18/04/2003
COMBINATION CLASS CLASSIFICATION SCHEME

		REFERENCE																					
		1	2	3	4	5	6	7	8	9	10	11	12	13	14	15	16	17	18	19	20	21	U.A
CLASSFIED	1	**558**	106	170	5	14	17	2	3	21	9	68	64	0	0	6	10	2	61	4	10	4	49.21%
	2	182	**10089**	861	76	227	308	214	52	35	500	233	2324	8	255	311	407	65	62	32	43	46	61.78%
	3	234	562	**3533**	22	19	28	1	2	17	28	125	1313	0	1	20	88	3	188	53	58	29	55.87%
	4	0	0	0	**0**	0	0	0	0	0	0	0	0	0	0	0	0	0	0	0	0	0	N/A
	5	3	69	12	9	**176**	59	2	2	1	36	2	11	2	1	33	8	38	0	0	0	1	37.85%
	6	13	405	16	9	196	**2143**	60	33	14	548	4	19	72	22	42	12	106	1	0	1	2	57.64%
	7	4	99	25	0	20	37	**305**	7	1	14	0	17	12	90	7	2	8	0	0	0	0	47.07%
	8	1	18	2	0	0	6	1	**78**	14	8	0	3	1	3	1	0	1	0	0	1	0	56.52%
	9	8	14	8	0	1	8	0	0	**43**	6	1	10	1	0	0	2	1	2	0	0	0	40.95%
	10	1	13	1	0	2	9	3	0	0	**20**	0	0	1	1	1	0	1	0	0	0	0	37.74%
	11	0	0	0	0	0	0	0	0	0	0	**0**	0	0	0	0	0	0	0	0	0	0	N/A
	12	22	519	483	12	4	4	0	0	1	24	44	**736**	0	0	13	53	3	26	17	16	25	36.76%
	13	0	0	0	0	0	0	0	0	0	0	0	0	**0**	0	0	0	0	0	0	0	0	N/A
	14	0	0	0	0	0	0	0	0	0	0	0	0	0	**0**	0	0	0	0	0	0	0	N/A
	15	0	0	0	0	0	0	0	0	0	0	0	0	0	0	**1**	0	1	0	0	0	0	50.00%
	16	0	2	0	0	0	0	0	0	0	0	1	0	0	0	0	**1**	0	0	0	0	0	25.00%
	17	0	0	0	0	0	0	0	0	0	0	0	0	0	0	0	0	**0**	0	0	0	0	N/A
	18	0	0	0	0	0	0	0	0	0	0	0	0	0	0	0	0	0	**0**	0	0	0	N/A
	19	0	0	0	0	0	0	0	0	0	0	0	0	0	0	0	0	0	0	**0**	0	0	N/A
	20	0	0	0	0	0	0	0	0	0	0	0	0	0	0	0	0	0	0	0	**0**	0	N/A
	21	0	0	0	0	0	0	0	0	0	0	0	0	0	0	0	0	0	0	0	0	**0**	N/A
	P.A	54.39%	84.81%	69.13%	0.00%	26.71%	81.83%	51.87%	44.07%	29.25%	1.68%	0.00%	16.37%	0.00%	0.00%	0.23%	0.17%	0.00%	0.00%	0.00%	0.00%	0.00%	**57.18%**

MODIS3 CONFUSION MATRIX (11% SAMPLE)
UK STUDY AREA
DATE:19/03/2003
COMBINATION CLASS CLASSIFICATION SCHEME

		REFERENCE																					
		1	2	3	4	5	6	7	8	9	10	11	12	13	14	15	16	17	18	19	20	21	U.A
CLASSFIED	1	**439**	79	96	4	0	2	0	1	7	1	56	46	0	0	1	10	0	47	2	14	0	54.53%
	2	161	**5754**	428	69	144	284	35	11	21	401	219	1336	13	19	193	404	40	43	36	21	58	59.38%
	3	237	400	**3391**	21	15	14	1	2	7	14	95	1181	2	1	16	57	3	217	67	41	38	58.26%
	4	0	0	0	**0**	0	0	0	0	0	0	0	0	0	0	0	0	0	0	0	0	0	N/A
	5	0	85	8	10	**236**	87	3	4	0	44	1	8	2	2	56	7	40	1	0	0	0	39.73%
	6	4	278	12	7	111	**1601**	17	21	5	376	2	18	42	8	33	15	100	0	1	0	0	60.39%
	7	0	5	0	0	9	3	**23**	0	0	2	0	0	1	3	0	0	1	0	0	0	0	48.94%
	8	0	0	0	0	0	0	0	**0**	0	0	0	0	0	0	0	0	0	0	0	0	0	N/A
	9	3	6	4	0	4	17	0	4	**87**	3	0	3	1	0	0	0	0	0	1	1	0	64.93%
	10	0	2	0	0	1	2	0	0	0	**1**	0	0	0	0	0	0	0	0	0	0	0	16.67%
	11	0	0	0	0	0	0	0	0	0	0	**0**	0	0	0	0	0	0	0	0	0	0	N/A
	12	37	330	427	9	6	12	0	1	3	15	39	**663**	0	0	7	26	2	19	16	15	25	40.13%
	13	0	0	0	0	0	0	0	0	0	0	0	0	**0**	0	0	0	0	0	0	0	0	N/A
	14	0	0	0	0	0	0	0	0	0	0	0	0	0	**0**	0	0	0	0	0	0	0	N/A
	15	0	0	0	0	2	2	0	0	0	0	0	0	0	0	**1**	0	0	0	0	0	0	20.00%
	16	0	3	0	0	0	0	0	0	0	0	1	0	0	0	0	**2**	0	0	1	0	0	28.57%
	17	0	0	0	0	0	0	0	0	0	0	0	0	0	0	0	0	**0**	0	0	0	0	N/A
	18	0	0	0	0	0	0	0	0	0	0	0	0	0	0	0	0	0	**0**	0	0	0	N/A
	19	0	0	0	0	0	0	0	0	0	0	0	0	0	0	0	0	0	0	**0**	0	0	N/A
	20	0	0	0	0	0	0	0	0	0	0	0	0	0	0	0	0	0	0	0	**0**	0	N/A
	21	0	0	0	0	0	0	0	0	0	0	0	0	0	0	0	0	0	0	0	0	**0**	N/A
	P.A	49.83%	82.89%	77.67%	0.00%	44.70%	79.10%	29.11%	0.00%	66.92%	0.12%	0.00%	20.37%	0.00%	0.00%	0.33%	0.38%	0.00%	0.00%	0.00%	0.00%	0.00%	**56.97%**

MODIS3 CONFUSION MATRIX (11% SAMPLE)
UK STUDY AREA
DATE:22/03/2003
COMBINATION CLASS CLASSIFICATION SCHEME

		REFERENCE																					
		1	2	3	4	5	6	7	8	9	10	11	12	13	14	15	16	17	18	19	20	21	U.A
CLASSFIED	1	**480**	116	163	5	3	6	2	0	20	9	75	98	0	0	1	12	1	69	5	7	4	44.61%
	2	148	**5582**	560	74	103	252	7	3	17	318	187	1372	9	8	146	450	27	53	36	29	57	59.14%
	3	200	483	**3511**	12	20	13	1	1	6	15	115	1271	0	0	15	50	1	188	45	51	31	58.24%
	4	0	2	0	**3**	1	1	0	0	0	1	0	0	0	0	1	2	1	0	0	0	0	25.00%
	5	4	33	2	3	**94**	36	0	0	0	16	0	14	2	1	27	5	16	0	2	0	1	36.72%
	6	4	147	14	8	44	**436**	5	5	1	127	0	19	5	6	19	8	22	0	0	0	1	50.06%
	7	0	0	0	0	0	0	**0**	0	0	0	0	0	0	0	0	0	0	0	0	0	0	N/A
	8	0	0	0	0	0	0	0	**0**	0	0	0	0	0	0	0	0	0	0	0	0	0	N/A
	9	5	15	2	1	0	2	0	0	**83**	0	1	4	0	0	0	0	0	1	1	0	0	72.17%
	10	0	0	0	0	1	0	0	0	0	**2**	0	0	0	0	0	0	0	0	0	0	1	50.00%
	11	0	2	1	0	1	0	0	0	0	0	**1**	1	0	0	0	0	0	0	0	0	0	16.67%
	12	30	291	338	2	5	5	0	0	1	9	26	**471**	0	0	3	19	1	13	16	8	19	37.47%
	13	0	0	0	0	0	0	0	0	0	0	0	0	**0**	0	0	0	0	0	0	0	0	N/A
	14	0	0	0	0	0	0	0	0	0	0	0	0	0	**0**	0	0	0	0	0	0	0	N/A
	15	0	6	0	0	8	0	0	0	0	1	0	0	0	0	**12**	0	1	0	0	0	0	42.86%
	16	1	0	0	3	1	0	0	0	0	0	0	2	0	0	0	**4**	0	0	0	0	0	36.36%
	17	0	0	0	0	0	0	0	0	0	0	0	0	0	0	0	0	**0**	0	0	0	0	N/A
	18	0	0	0	0	0	0	0	0	0	0	0	0	0	0	0	0	0	**0**	0	0	0	N/A
	19	0	0	0	0	0	0	0	0	0	0	0	0	0	0	0	0	0	0	**0**	0	0	N/A
	20	0	0	0	0	0	0	0	0	0	0	0	0	0	0	0	0	0	0	0	**0**	0	N/A
	21	0	0	0	0	0	0	0	0	0	0	0	0	0	0	0	0	0	0	0	0	**0**	N/A
	P.A	55.05%	83.60%	76.48%	2.70%	33.45%	58.06%	0.00%	0.00%	64.84%	0.40%	0.25%	14.48%	0.00%	0.00%	5.36%	0.73%	0.00%	0.00%	0.00%	0.00%	0.00%	**55.90%**

MODIS3 CONFUSION MATRIX (11% SAMPLE)
UK STUDY AREA
DATE:23/03/2003
COMBINATION CLASS CLASSIFICATION SCHEME

		REFERENCE																					
		1	2	3	4	5	6	7	8	9	10	11	12	13	14	15	16	17	18	19	20	21	U.A
CLASSFIED	1	**429**	60	80	5	3	9	1	1	3	5	77	44	0	0	2	11	1	44	2	7	4	54.44%
	2	181	**6154**	435	67	151	298	1	2	7	457	213	1324	6	14	193	408	37	33	26	41	49	60.95%
	3	267	397	**3637**	17	9	18	1	0	5	10	118	1303	0	1	13	39	2	217	63	52	21	58.76%
	4	0	0	0	**4**	0	0	0	0	0	0	0	0	0	0	0	1	0	0	0	0	1	66.67%
	5	4	44	2	5	**158**	49	0	6	1	19	1	3	2	0	44	7	30	1	2	0	0	41.80%
	6	5	203	12	5	97	**985**	1	4	3	193	11	24	6	2	42	19	69	0	0	1	1	58.53%
	7	0	0	0	0	0	0	**0**	0	0	0	0	0	0	0	0	0	0	0	0	0	0	N/A
	8	0	0	0	0	0	0	0	**0**	0	0	0	0	0	0	0	0	0	0	0	0	0	N/A
	9	13	5	9	0	1	1	0	1	**103**	0	2	7	0	0	1	0	1	4	0	0	0	69.59%
	10	2	7	0	0	4	16	0	0	0	**22**	1	1	0	0	1	2	1	0	0	0	0	38.60%
	11	0	1	0	0	0	0	0	0	0	0	**0**	0	0	0	0	0	0	0	0	0	0	0.00%
	12	37	435	504	10	10	9	0	1	0	27	26	**780**	0	0	12	41	3	24	15	12	23	39.61%
	13	0	1	0	0	0	0	0	0	0	0	0	0	**0**	0	0	0	0	0	0	0	0	0.00%
	14	0	0	0	0	0	0	0	0	0	0	0	0	0	**0**	0	0	0	0	0	0	0	N/A
	15	0	1	0	0	3	0	0	0	0	0	0	0	0	0	**1**	1	0	0	0	0	0	16.67%
	16	0	0	0	1	0	0	0	0	0	0	0	0	0	0	0	**6**	0	0	0	0	0	85.71%
	17	0	0	0	0	0	0	0	0	0	0	0	0	0	0	0	0	**0**	0	0	0	0	N/A
	18	0	0	0	0	0	0	0	0	0	0	0	0	0	0	0	0	0	**0**	0	0	0	N/A
	19	0	0	0	0	0	0	0	0	0	0	0	0	0	0	0	0	0	0	**0**	0	0	N/A
	20	0	0	0	0	0	0	0	0	0	0	0	0	0	0	0	0	0	0	0	**0**	0	N/A
	21	0	0	0	0	0	0	0	0	0	0	0	0	0	0	0	0	0	0	0	0	**0**	N/A
	P.A	45.74%	84.21%	77.73%	3.51%	36.24%	71.12%	0.00%	0.00%	84.43%	3.00%	0.00%	22.38%	0.00%	0.00%	0.32%	1.12%	0.00%	0.00%	0.00%	0.00%	0.00%	**57.56%**

MODIS3 CONFUSION MATRIX (11% SAMPLE)
UK STUDY AREA
DATE:MULTIDATE
COMBINATION CLASS CLASSIFICATION SCHEME

		REFERENCE																					
		1	2	3	4	5	6	7	8	9	10	11	12	13	14	15	16	17	18	19	20	21	U.A
CLASSFIED	1	**435**	46	67	1	8	5	1	0	8	3	43	30	0	0	3	8	0	34	3	11	4	61.27%
	2	100	**4879**	367	54	81	198	0	3	0	297	150	1042	1	9	133	343	22	35	25	30	38	62.50%
	3	159	335	**3112**	8	13	9	0	2	4	8	91	999	0	0	12	34	1	178	42	41	16	61.45%
	4	0	0	0	**0**	0	0	0	0	0	0	0	0	0	0	0	0	0	0	0	0	0	N/A
	5	0	39	6	4	**139**	37	0	1	0	8	0	3	1	0	34	2	20	0	0	0	1	47.12%
	6	1	110	5	2	60	**899**	0	2	0	159	0	16	9	0	23	4	43	0	0	0	0	67.44%
	7	0	0	0	0	0	0	**0**	0	0	0	0	0	0	0	0	0	0	0	0	0	0	N/A
	8	0	0	0	0	0	0	0	**0**	0	0	0	0	0	0	0	0	0	0	0	0	0	N/A
	9	1	1	2	0	3	1	0	0	**23**	0	0	2	0	0	0	0	0	0	0	0	0	69.70%
	10	0	7	1	0	2	8	0	0	0	**14**	0	0	0	0	3	0	1	0	0	0	0	38.89%
	11	0	0	0	0	0	0	0	0	0	0	**1**	0	0	0	0	0	0	0	0	0	0	100.00%
	12	22	386	447	14	6	5	0	1	2	33	29	**753**	0	2	9	38	4	18	17	18	15	41.40%
	13	0	0	0	0	0	0	0	0	0	0	0	0	**0**	0	0	0	0	0	0	0	0	N/A
	14	0	0	0	0	0	0	0	0	0	0	0	0	0	**0**	0	0	0	0	0	0	0	N/A
	15	0	0	0	0	0	0	0	0	0	0	0	0	0	0	**0**	0	0	0	0	0	0	N/A
	16	0	3	1	3	0	0	0	0	0	0	0	0	0	0	0	**6**	0	0	0	0	0	46.15%
	17	0	0	0	0	0	0	0	0	0	0	0	0	0	0	0	0	**0**	0	0	0	0	N/A
	18	0	0	0	0	0	0	0	0	0	0	0	0	0	0	0	0	0	**0**	0	0	0	N/A
	19	0	0	0	0	0	0	0	0	0	0	0	0	0	0	0	0	0	0	**0**	0	0	N/A
	20	0	0	0	0	0	0	0	0	0	0	0	0	0	0	0	0	0	0	0	**0**	0	N/A
	21	0	0	0	0	0	0	0	0	0	0	0	0	0	0	0	0	0	0	0	0	**0**	N/A
	P.A	60.58%	84.03%	77.64%	0.00%	44.55%	77.37%	0.00%	0.00%	62.16%	2.68%	0.32%	26.47%	0.00%	0.00%	0.00%	1.38%	0.00%	0.00%	0.00%	0.00%	0.00%	**59.97%**

VEGETATION CONFUSION MATRIX (11% SAMPLE)
UK STUDY AREA
DATE:13/07/2003
COMBINATION CLASS CLASSIFICATION SCHEME

		REFERENCE																					
		1	2	3	4	5	6	7	8	9	10	11	12	13	14	15	16	17	18	19	20	21	U.A
CLASSFIED	1	**496**	110	80	2	2	9	0	1	9	5	92	100	0	0	2	13	0	47	2	20	3	49.95%
	2	197	**6298**	445	65	236	625	14	17	61	557	239	1345	15	14	265	465	74	55	17	38	57	56.74%
	3	217	471	**3904**	29	14	6	0	0	31	13	81	1410	0	0	14	60	2	212	71	55	31	58.96%
	4	0	0	0	**0**	0	0	0	0	0	0	0	0	0	0	0	0	0	0	0	0	0	N/A
	5	1	29	11	1	**58**	51	1	4	0	11	1	9	0	0	19	0	13	0	0	0	0	27.75%
	6	15	432	7	3	146	**1398**	11	15	8	385	10	26	42	1	60	15	82	2	0	1	1	52.56%
	7	0	0	0	0	0	0	**0**	0	0	0	0	0	0	0	0	0	0	0	0	0	0	N/A
	8	0	0	0	0	0	0	0	**0**	0	0	0	0	0	0	0	0	0	0	0	0	0	N/A
	9	15	21	10	0	1	8	0	1	**95**	5	3	8	0	0	0	1	0	2	1	1	0	55.23%
	10	0	5	0	0	0	3	0	0	0	**4**	0	0	1	0	0	0	0	0	0	0	0	30.77%
	11	0	0	0	0	0	0	0	0	0	0	**0**	0	0	0	0	0	0	0	0	0	0	N/A
	12	37	438	474	7	9	3	0	2	4	7	33	**680**	0	0	10	43	2	33	24	15	19	36.96%
	13	0	0	0	0	0	0	0	0	0	0	0	0	**0**	0	0	0	0	0	0	0	0	N/A
	14	0	0	0	0	0	0	0	0	0	0	0	0	0	**0**	0	0	0	0	0	0	0	N/A
	15	0	0	0	0	0	0	0	0	0	0	0	0	0	0	**0**	0	0	0	0	0	0	N/A
	16	0	0	0	0	0	0	0	0	0	0	0	0	0	0	0	**0**	0	0	0	0	0	N/A
	17	0	0	0	0	0	0	0	0	0	0	0	0	0	0	0	0	**0**	0	0	0	0	N/A
	18	0	0	0	0	0	0	0	0	0	0	0	0	0	0	0	0	0	**0**	0	0	0	N/A
	19	0	0	0	0	0	0	0	0	0	0	0	0	0	0	0	0	0	0	**0**	0	0	N/A
	20	0	0	0	0	0	0	0	0	0	0	0	0	0	0	0	0	0	0	0	**0**	0	N/A
	21	0	0	0	0	0	0	0	0	0	0	0	0	0	0	0	0	0	0	0	0	**0**	N/A
	P.A	50.72%	80.70%	79.17%	0.00%	12.45%	66.48%	0.00%	0.00%	45.67%	0.41%	0.00%	19.01%	0.00%	0.00%	0.00%	0.00%	0.00%	0.00%	0.00%	0.00%	0.00%	**54.78%**

VEGETATION CONFUSION MATRIX (11% SAMPLE)
UK STUDY AREA
DATE:16/04/2003
COMBINATION CLASS CLASSIFICATION SCHEME

		REFERENCE																					
		1	2	3	4	5	6	7	8	9	10	11	12	13	14	15	16	17	18	19	20	21	U.A
CLASSFIED	1	**446**	106	89	7	14	33	2	4	22	13	85	75	0	3	8	17	7	53	0	9	3	44.78%
	2	168	**7659**	998	72	258	364	82	31	18	467	199	1840	6	81	292	432	55	61	35	28	54	58.02%
	3	306	957	**3672**	26	58	79	8	6	26	75	162	1587	1	7	37	99	15	244	71	60	38	48.74%
	4	0	0	0	**0**	0	0	0	0	0	0	0	0	0	0	0	0	0	0	0	0	0	N/A
	5	5	31	1	2	**51**	23	1	1	0	12	1	2	0	0	9	3	10	1	1	0	0	33.12%
	6	61	264	74	2	168	**1346**	35	30	15	309	11	44	31	15	60	12	94	4	0	1	1	52.23%
	7	0	0	0	0	0	0	**2**	0	0	0	0	0	0	0	0	0	0	0	0	0	0	100.00%
	8	0	0	0	0	0	0	0	**0**	0	0	0	0	0	0	0	0	0	0	0	0	0	N/A
	9	10	59	13	1	4	23	0	26	**89**	17	6	11	1	1	1	2	1	2	0	0	0	33.33%
	10	1	2	0	0	0	0	0	0	0	**3**	0	0	0	0	0	0	0	0	0	0	0	50.00%
	11	0	0	0	0	0	0	0	0	0	0	**0**	0	0	0	0	0	0	0	0	0	0	N/A
	12	11	295	309	1	12	9	2	0	2	14	28	**415**	0	3	5	11	2	17	9	10	19	35.35%
	13	0	0	0	0	0	0	0	0	0	0	0	0	**0**	0	0	0	0	0	0	0	0	N/A
	14	0	0	0	0	0	0	0	0	0	0	0	0	0	**0**	0	0	0	0	0	0	0	N/A
	15	0	0	0	0	0	0	0	0	0	0	0	0	0	0	**0**	0	0	0	0	0	0	N/A
	16	0	0	0	0	0	0	0	0	0	0	0	0	0	0	0	**0**	0	0	0	0	0	N/A
	17	0	0	0	0	0	0	0	0	0	0	0	0	0	0	0	0	**0**	0	0	0	0	N/A
	18	0	0	0	0	0	0	0	0	0	0	0	0	0	0	0	0	0	**0**	0	0	0	N/A
	19	0	0	0	0	0	0	0	0	0	0	0	0	0	0	0	0	0	0	**0**	0	0	N/A
	20	0	0	0	0	0	0	0	0	0	0	0	0	0	0	0	0	0	0	0	**0**	0	N/A
	21	0	0	0	0	0	0	0	0	0	0	0	0	0	0	0	0	0	0	0	0	**0**	N/A
	P.A	44.25%	81.71%	71.22%	0.00%	9.03%	71.71%	1.52%	0.00%	51.74%	0.33%	0.00%	10.44%	0.00%	0.00%	0.00%	0.00%	0.00%	0.00%	0.00%	0.00%	0.00%	**52.81%**

VEGETATION CONFUSION MATRIX (11% SAMPLE)
UK STUDY AREA
DATE:17/03/2003
COMBINATION CLASS CLASSIFICATION SCHEME

CLASSFIED \ REFERENCE	1	2	3	4	5	6	7	8	9	10	11	12	13	14	15	16	17	18	19	20	21	U.A
1	**355**	89	55	7	6	66	8	5	6	13	56	55	2	4	4	9	0	31	4	6	2	45.34%
2	295	**9879**	1132	74	282	645	279	68	50	547	316	2607	37	240	291	461	106	67	45	57	77	56.27%
3	203	462	**2464**	15	24	232	70	5	16	74	87	843	11	23	27	43	11	153	35	36	22	50.74%
4	0	0	0	**0**	0	0	0	0	0	0	0	0	0	0	0	0	0	0	0	0	0	N/A
5	1	23	0	0	**27**	22	0	0	0	14	1	2	0	2	19	0	5	0	0	0	0	23.28%
6	39	400	130	9	143	**1060**	63	26	4	305	21	97	29	23	45	38	60	16	6	6	3	42.01%
7	0	0	0	0	0	0	**0**	0	0	0	0	0	0	0	0	0	0	0	0	0	0	N/A
8	0	0	0	0	0	0	0	**0**	0	0	0	0	0	0	0	0	0	0	0	0	0	N/A
9	0	0	0	0	0	0	0	0	**0**	0	0	0	0	0	0	0	0	0	0	0	0	N/A
10	0	0	0	0	0	0	0	0	0	**0**	0	0	0	0	0	0	0	0	0	0	0	N/A
11	0	0	0	0	0	0	0	0	0	0	**0**	0	0	0	0	0	0	0	0	0	0	N/A
12	27	136	154	7	14	19	26	2	0	16	18	**219**	0	6	4	11	2	18	10	7	4	31.29%
13	0	0	0	0	0	0	0	0	0	0	0	0	**0**	0	0	0	0	0	0	0	0	N/A
14	0	0	0	0	0	0	0	0	0	0	0	0	0	**0**	0	0	0	0	0	0	0	N/A
15	0	0	0	0	0	0	0	0	0	0	0	0	0	0	**0**	0	0	0	0	0	0	N/A
16	0	0	0	0	0	0	0	0	0	0	0	0	0	0	0	**0**	0	0	0	0	0	N/A
17	0	0	0	0	0	0	0	0	0	0	0	0	0	0	0	0	**0**	0	0	0	0	N/A
18	0	0	0	0	0	0	0	0	0	0	0	0	0	0	0	0	0	**0**	0	0	0	N/A
19	0	0	0	0	0	0	0	0	0	0	0	0	0	0	0	0	0	0	**0**	0	0	N/A
20	0	0	0	0	0	0	0	0	0	0	0	0	0	0	0	0	0	0	0	**0**	0	N/A
21	0	0	0	0	0	0	0	0	0	0	0	0	0	0	0	0	0	0	0	0	**0**	N/A
P.A	38.59%	89.90%	62.62%	0.00%	5.44%	51.86%	0.00%	0.00%	0.00%	0.00%	0.00%	5.73%	0.00%	0.00%	0.00%	0.00%	0.00%	0.00%	0.00%	0.00%	0.00%	**52.78%**

VEGETATION CONFUSION MATRIX (11% SAMPLE)
UK STUDY AREA
DATE:18/04/2003
COMBINATION CLASS CLASSIFICATION SCHEME

		REFERENCE																					
		1	2	3	4	5	6	7	8	9	10	11	12	13	14	15	16	17	18	19	20	21	U.A
CLASSFIED	1	**367**	110	125	4	69	120	4	6	24	44	56	66	2	4	12	10	16	32	2	12	0	33.82%
	2	220	**9956**	1325	78	301	527	286	121	93	538	262	2678	15	279	308	425	87	79	47	51	63	56.12%
	3	390	1019	**3204**	39	94	106	10	5	28	115	143	1312	3	6	60	105	27	211	46	49	34	45.73%
	4	0	0	0	**0**	0	0	0	0	0	0	0	0	0	0	0	0	0	0	0	0	0	N/A
	5	3	18	7	1	**12**	9	0	0	0	4	1	4	1	0	8	1	7	0	0	0	0	15.79%
	6	24	430	134	2	160	**1805**	114	38	7	459	5	52	69	34	36	12	91	8	1	1	2	51.81%
	7	4	63	23	0	12	48	**177**	5	2	18	0	18	10	49	6	1	4	0	0	0	0	40.23%
	8	0	0	0	0	0	0	0	**0**	0	0	0	0	0	0	0	0	0	0	0	0	0	N/A
	9	0	0	0	0	0	0	0	0	**0**	0	0	0	0	0	0	0	0	0	0	0	0	N/A
	10	0	0	0	0	0	0	0	0	0	**0**	0	0	0	0	0	0	0	0	0	0	0	N/A
	11	0	0	0	0	0	0	0	0	0	0	**0**	0	0	0	0	0	0	0	0	0	0	N/A
	12	0	17	20	0	4	3	0	0	0	1	2	**22**	0	0	1	2	0	1	0	0	0	30.14%
	13	0	0	0	0	0	0	0	0	0	0	0	0	**0**	0	0	0	0	0	0	0	0	N/A
	14	0	0	0	0	0	0	0	0	0	0	0	0	0	**0**	0	0	0	0	0	0	0	N/A
	15	0	0	0	0	0	0	0	0	0	0	0	0	0	0	**0**	0	0	0	0	0	0	N/A
	16	0	0	0	0	0	0	0	0	0	0	0	0	0	0	0	**0**	0	0	0	0	0	N/A
	17	0	0	0	0	0	0	0	0	0	0	0	0	0	0	0	0	**0**	0	0	0	0	N/A
	18	0	0	0	0	0	0	0	0	0	0	0	0	0	0	0	0	0	**0**	0	0	0	N/A
	19	0	0	0	0	0	0	0	0	0	0	0	0	0	0	0	0	0	0	**0**	0	0	N/A
	20	0	0	0	0	0	0	0	0	0	0	0	0	0	0	0	0	0	0	0	**0**	0	N/A
	21	0	0	0	0	0	0	0	0	0	0	0	0	0	0	0	0	0	0	0	0	**0**	N/A
	P.A	36.41%	85.73%	66.23%	0.00%	1.84%	68.95%	29.95%	0.00%	0.00%	0.00%	0.00%	0.53%	0.00%	0.00%	0.00%	0.00%	0.00%	0.00%	0.00%	0.00%	0.00%	**51.98%**

VEGETATION CONFUSION MATRIX (11% SAMPLE)
UK STUDY AREA
DATE:19/03/2003
COMBINATION CLASS CLASSIFICATION SCHEME

		REFERENCE																					
		1	2	3	4	5	6	7	8	9	10	11	12	13	14	15	16	17	18	19	20	21	U.A
CLASSFIED	1	**349**	98	117	6	21	25	2	3	19	12	54	60	0	1	6	11	6	51	5	9	4	40.63%
	2	203	**5632**	830	80	267	505	28	13	33	432	216	1628	16	20	201	402	79	63	41	38	74	52.14%
	3	252	627	**3120**	23	61	102	1	1	14	67	109	1175	0	0	37	65	9	200	70	35	35	51.97%
	4	0	0	0	**0**	0	0	0	0	0	0	0	0	0	0	0	0	0	0	0	0	0	N/A
	5	0	36	6	0	**42**	36	0	1	0	14	0	8	1	0	13	1	15	0	0	0	1	24.14%
	6	48	330	86	5	127	**1345**	45	25	7	321	19	90	44	12	45	26	76	7	0	3	1	50.53%
	7	0	0	0	0	0	0	**0**	0	0	0	0	0	0	0	0	0	0	0	0	0	0	N/A
	8	0	0	0	0	0	0	0	**0**	0	0	0	0	0	0	0	0	0	0	0	0	0	N/A
	9	8	18	10	0	1	6	0	0	**61**	2	2	7	0	0	0	2	1	1	0	0	0	51.26%
	10	0	0	0	0	0	0	0	0	0	**0**	0	0	0	0	0	0	0	0	0	0	0	N/A
	11	0	0	0	0	0	0	0	0	0	0	**0**	0	0	0	0	0	0	0	0	0	0	N/A
	12	20	254	212	6	6	14	0	0	1	14	15	**343**	0	1	8	18	4	9	9	8	7	36.14%
	13	0	0	0	0	0	0	0	0	0	0	0	0	**0**	0	0	0	0	0	0	0	0	N/A
	14	0	0	0	0	0	0	0	0	0	0	0	0	0	**0**	0	0	0	0	0	0	0	N/A
	15	0	0	0	0	0	0	0	0	0	0	0	0	0	0	**0**	0	0	0	0	0	0	N/A
	16	0	0	0	0	0	0	0	0	0	0	0	0	0	0	0	**0**	0	0	0	0	0	N/A
	17	0	0	0	0	0	0	0	0	0	0	0	0	0	0	0	0	**0**	0	0	0	0	N/A
	18	0	0	0	0	0	0	0	0	0	0	0	0	0	0	0	0	0	**0**	0	0	0	N/A
	19	0	0	0	0	0	0	0	0	0	0	0	0	0	0	0	0	0	0	**0**	0	0	N/A
	20	0	0	0	0	0	0	0	0	0	0	0	0	0	0	0	0	0	0	0	**0**	0	N/A
	21	0	0	0	0	0	0	0	0	0	0	0	0	0	0	0	0	0	0	0	0	**0**	N/A
	P.A	39.66%	80.51%	71.22%	0.00%	8.00%	66.16%	0.00%	0.00%	45.19%	0.00%	0.00%	10.36%	0.00%	0.00%	0.00%	0.00%	0.00%	0.00%	0.00%	0.00%	0.00%	**50.50%**

VEGETATION CONFUSION MATRIX (11% SAMPLE)
UK STUDY AREA
DATE:22/03/2003
COMBINATION CLASS CLASSIFICATION SCHEME

		REFERENCE																					
		1	2	3	4	5	6	7	8	9	10	11	12	13	14	15	16	17	18	19	20	21	U.A
CLASSFIED	1	**396**	85	114	4	7	18	1	1	16	10	65	62	1	0	10	14	4	59	6	9	3	44.75%
	2	183	**5449**	958	80	179	359	1	3	25	338	189	1689	8	10	166	428	41	63	44	28	67	52.86%
	3	275	803	**3320**	27	31	105	5	1	23	53	143	1242	3	1	27	85	4	184	55	54	37	51.25%
	4	0	0	0	**0**	0	0	0	0	0	0	0	0	0	0	0	0	0	0	0	0	0	N/A
	5	0	14	0	0	**25**	8	0	1	0	4	0	6	1	1	8	0	6	0	0	0	0	33.78%
	6	5	134	26	2	41	**254**	7	3	2	85	1	26	3	3	15	7	19	0	0	0	0	40.13%
	7	0	0	0	0	0	0	**0**	0	0	0	0	0	0	0	0	0	0	0	0	0	0	N/A
	8	0	0	0	0	0	0	0	**0**	0	0	0	0	0	0	0	0	0	0	0	0	0	N/A
	9	7	33	8	1	2	5	0	0	**39**	2	1	3	0	0	0	0	0	3	0	1	0	37.14%
	10	0	3	1	0	0	4	0	0	0	**1**	0	0	0	0	0	0	0	0	0	0	0	11.11%
	11	1	2	1	0	0	0	0	0	0	0	**2**	3	0	0	0	0	0	2	0	0	0	18.18%
	12	15	196	175	5	4	6	1	0	4	7	11	**265**	0	0	4	22	0	15	8	1	9	35.43%
	13	0	0	0	0	0	0	0	0	0	0	0	0	**0**	0	0	0	0	0	0	0	0	N/A
	14	0	0	0	0	0	0	0	0	0	0	0	0	0	**0**	0	0	0	0	0	0	0	N/A
	15	0	0	0	0	0	0	0	0	0	0	0	0	0	0	**0**	0	0	0	0	0	0	N/A
	16	0	0	0	0	0	0	0	0	0	0	0	0	0	0	0	**0**	0	0	0	0	0	N/A
	17	0	0	0	0	0	0	0	0	0	0	0	0	0	0	0	0	**0**	0	0	0	0	N/A
	18	0	0	0	0	0	0	0	0	0	0	0	0	0	0	0	0	0	**0**	0	0	0	N/A
	19	0	0	0	0	0	0	0	0	0	0	0	0	0	0	0	0	0	0	**0**	0	0	N/A
	20	0	0	0	0	0	0	0	0	0	0	0	0	0	0	0	0	0	0	0	**0**	0	N/A
	21	0	0	0	0	0	0	0	0	0	0	0	0	0	0	0	0	0	0	0	0	**0**	N/A
	P.A	44.90%	81.10%	72.13%	0.00%	8.65%	33.47%	0.00%	0.00%	35.78%	0.20%	0.49%	8.04%	0.00%	0.00%	0.00%	0.00%	0.00%	0.00%	0.00%	0.00%	0.00%	**50.65%**

VEGETATION CONFUSION MATRIX (11% SAMPLE)
UK STUDY AREA
DATE:23/03/2003
COMBINATION CLASS CLASSIFICATION SCHEME

		REFERENCE																					
		1	2	3	4	5	6	7	8	9	10	11	12	13	14	15	16	17	18	19	20	21	U.A
CLASSFIED	1	**320**	78	82	8	14	39	1	1	9	14	56	63	0	0	6	10	8	26	1	12	2	42.67%
	2	267	**6090**	981	70	277	508	1	6	38	473	240	1656	5	13	222	417	73	77	36	50	58	52.69%
	3	302	792	**3226**	21	64	198	1	3	15	112	131	1297	2	2	39	66	26	192	58	51	29	48.68%
	4	0	0	0	**0**	0	0	0	0	0	0	0	0	0	0	0	0	0	0	0	0	0	N/A
	5	1	13	1	0	**21**	18	1	2	0	2	0	9	1	0	9	0	5	0	0	0	0	25.30%
	6	20	204	128	4	64	**612**	1	3	6	128	10	73	6	2	26	26	35	11	3	1	0	44.90%
	7	0	0	0	0	0	0	**0**	0	0	0	0	0	0	0	0	0	0	0	0	0	0	N/A
	8	0	0	0	0	0	0	0	**0**	0	0	0	0	0	0	0	0	0	0	0	0	0	N/A
	9	4	24	7	0	2	0	0	0	**64**	2	2	8	0	0	1	1	1	1	0	0	0	54.70%
	10	0	2	0	0	0	2	0	0	0	**2**	0	1	0	0	0	0	0	0	0	0	0	28.57%
	11	0	0	0	0	0	0	0	0	0	0	**0**	0	0	0	0	0	0	0	0	0	0	N/A
	12	14	270	250	8	10	28	0	0	0	20	19	**382**	0	0	14	25	2	14	11	3	9	35.40%
	13	0	0	0	0	0	0	0	0	0	0	0	0	**0**	0	0	0	0	0	0	0	0	N/A
	14	0	0	0	0	0	0	0	0	0	0	0	0	0	**0**	0	0	0	0	0	0	0	N/A
	15	0	0	0	0	0	0	0	0	0	0	0	0	0	0	**0**	0	0	0	0	0	0	N/A
	16	0	0	0	0	0	0	0	0	0	0	0	0	0	0	0	**0**	0	0	0	0	0	N/A
	17	0	0	0	0	0	0	0	0	0	0	0	0	0	0	0	0	**0**	0	0	0	0	N/A
	18	0	0	0	0	0	0	0	0	0	0	0	0	0	0	0	0	0	**0**	0	0	0	N/A
	19	0	0	0	0	0	0	0	0	0	0	0	0	0	0	0	0	0	0	**0**	0	0	N/A
	20	0	0	0	0	0	0	0	0	0	0	0	0	0	0	0	0	0	0	0	**0**	0	N/A
	21	0	0	0	0	0	0	0	0	0	0	0	0	0	0	0	0	0	0	0	0	**0**	N/A
	P.A	34.48%	81.49%	69.01%	0.00%	4.65%	43.56%	0.00%	0.00%	48.48%	0.27%	0.00%	10.95%	0.00%	0.00%	0.00%	0.00%	0.00%	0.00%	0.00%	0.00%	0.00%	**49.65%**

VEGETATION CONFUSION MATRIX (11% SAMPLE)
UK STUDY AREA
DATE:MULTIDATE
COMBINATION CLASS CLASSIFICATION SCHEME

		REFERENCE																					
		1	2	3	4	5	6	7	8	9	10	11	12	13	14	15	16	17	18	19	20	21	U.A
CLASSFIED	1	**455**	63	87	1	0	9	0	0	1	3	65	53	0	0	0	7	1	39	4	22	1	56.10%
	2	100	**4960**	375	64	136	294	0	2	6	345	162	1073	1	9	157	351	37	29	17	29	34	60.63%
	3	126	373	**3208**	13	19	15	0	2	20	10	65	1095	0	1	9	42	1	156	49	41	23	60.90%
	4	0	0	0	**0**	0	0	0	0	0	0	0	0	0	0	0	0	0	0	0	0	0	N/A
	5	0	36	6	1	**88**	45	1	2	0	8	0	5	1	0	21	1	14	0	1	0	0	38.26%
	6	3	160	21	2	74	**804**	0	4	2	141	5	17	9	1	22	5	35	2	0	1	1	61.42%
	7	0	0	0	0	0	0	**0**	0	0	0	0	0	0	0	0	0	0	0	0	0	0	N/A
	8	0	0	0	0	0	0	0	**0**	0	0	0	0	0	0	0	0	0	0	0	0	0	N/A
	9	2	18	7	0	1	0	0	0	**21**	0	0	4	0	0	0	1	1	1	0	0	0	37.50%
	10	0	0	0	0	0	0	0	0	0	**2**	0	0	0	0	0	0	0	0	0	0	0	100.00%
	11	0	0	0	0	0	0	0	0	0	0	**0**	0	0	0	0	0	0	0	0	0	0	N/A
	12	39	448	429	15	3	6	0	0	1	11	32	**684**	0	0	7	50	2	32	20	11	22	37.75%
	13	0	0	0	0	0	0	0	0	0	0	0	0	**0**	0	0	0	0	0	0	0	0	N/A
	14	0	0	0	0	0	0	0	0	0	0	0	0	0	**0**	0	0	0	0	0	0	0	N/A
	15	0	0	0	0	0	0	0	0	0	0	0	0	0	0	**0**	0	0	0	0	0	0	N/A
	16	0	0	0	0	0	0	0	0	0	0	0	0	0	0	0	**0**	0	0	0	0	0	N/A
	17	0	0	0	0	0	0	0	0	0	0	0	0	0	0	0	0	**0**	0	0	0	0	N/A
	18	0	0	0	0	0	0	0	0	0	0	0	0	0	0	0	0	0	**0**	0	0	0	N/A
	19	0	0	0	0	0	0	0	0	0	0	0	0	0	0	0	0	0	0	**0**	0	0	N/A
	20	0	0	0	0	0	0	0	0	0	0	0	0	0	0	0	0	0	0	0	**0**	0	N/A
	21	0	0	0	0	0	0	0	0	0	0	0	0	0	0	0	0	0	0	0	0	**0**	N/A
	P.A	62.76%	81.88%	77.62%	0.00%	27.41%	68.54%	0.00%	0.00%	41.18%	0.38%	0.00%	23.34%	0.00%	0.00%	0.00%	0.00%	0.00%	0.00%	0.00%	0.00%	0.00%	**57.85%**

AVHRR CONFUSION MATRIX (11% SAMPLE)
UK STUDY AREA
DATE:13/07/2003
DOMINANT CLASS CLASSIFICATION SCHEME

CLASSIFIED	REFERENCE															
	1	2	3	4	5	6	7	8	9	10	11	12	13	14	15	U.A
1	**568**	234	309	22	1	0	2	1	1	0	0	3	5	2	12	48.97%
2	373	**5022**	1658	115	50	3	184	5	10	4	20	13	28	16	48	66.53%
3	657	2283	**8594**	333	436	7	980	9	19	0	20	8	19	33	40	63.95%
4	0	0	0	**0**	0	0	0	0	0	0	0	0	0	0	0	N/A
5	0	0	10	0	**11**	1	16	2	0	0	0	0	0	0	0	27.50%
6	0	0	0	0	0	**0**	0	0	0	0	0	0	0	0	0	N/A
7	35	152	891	27	405	0	**1626**	10	29	1	41	6	22	47	45	48.73%
8	0	0	0	0	0	0	0	**0**	0	0	0	0	0	0	0	N/A
9	0	0	0	0	0	0	0	0	**0**	0	0	0	0	0	0	N/A
10	0	0	0	0	0	0	0	0	0	**0**	0	0	0	0	0	N/A
11	0	0	0	0	0	0	0	0	0	0	**0**	0	0	0	0	N/A
12	0	0	0	0	0	0	0	0	0	0	0	**0**	0	0	0	N/A
13	4	3	3	0	0	0	1	0	0	0	0	0	**6**	0	1	33.33%
14	0	0	0	0	0	0	0	0	0	0	0	0	0	**0**	0	N/A
15	8	22	26	0	8	0	23	0	1	0	1	0	6	12	**118**	52.44%
P.A	34.53%	65.09%	74.79%	0.00%	1.21%	0.00%	57.42%	0.00%	0.00%	0.00%	0.00%	0.00%	6.98%	0.00%	44.70%	**61.88%**

AVHRR CONFUSION MATRIX (11% SAMPLE)
UK STUDY AREA
DATE:16/04/2003
DOMINANT CLASS CLASSIFICATION SCHEME

		REFERENCE															
		1	2	3	4	5	6	7	8	9	10	11	12	13	14	15	U.A
CLASSIFIED	1	**606**	270	289	13	96	0	166	4	15	0	11	7	17	15	39	39.15%
	2	583	**5426**	2095	95	111	3	367	2	24	2	37	6	10	12	15	61.74%
	3	472	2218	**10373**	323	451	15	729	33	10	2	104	8	8	34	20	70.09%
	4	0	0	0	**0**	0	0	0	0	0	0	0	0	0	0	0	N/A
	5	18	31	171	12	**252**	1	130	12	2	0	7	1	7	26	16	36.73%
	6	0	0	0	0	0	**0**	0	0	0	0	0	0	0	0	0	N/A
	7	53	191	526	34	153	1	**1213**	7	5	1	95	1	0	13	1	52.88%
	8	0	0	0	0	0	0	0	**0**	0	0	0	0	0	0	0	N/A
	9	0	0	0	0	0	0	0	0	**0**	0	0	0	0	0	0	N/A
	10	0	0	0	0	0	0	0	0	0	**0**	0	0	0	0	0	N/A
	11	0	0	0	0	0	0	0	0	0	0	**0**	0	0	0	0	N/A
	12	0	0	0	0	0	0	0	0	0	0	0	**0**	0	0	0	N/A
	13	0	0	0	0	0	0	0	0	0	0	0	0	**0**	0	0	N/A
	14	0	0	0	0	0	0	0	0	0	0	0	0	0	**0**	0	N/A
	15	19	36	41	1	4	0	11	0	4	0	0	9	42	63	**136**	37.16%
	P.A	34.61%	66.40%	76.87%	0.00%	23.62%	0.00%	46.37%	0.00%	0.00%	0.00%	0.00%	0.00%	0.00%	0.00%	59.91%	**63.22%**

AVHRR CONFUSION MATRIX (11% SAMPLE)
UK STUDY AREA
DATE:17/03/2003
DOMINANT CLASS CLASSIFICATION SCHEME

		REFERENCE															
		1	2	3	4	5	6	7	8	9	10	11	12	13	14	15	U.A
CLASSIFIED	1	**671**	215	223	15	46	0	70	4	8	1	9	11	17	12	15	50.95%
	2	330	**3894**	1103	63	46	1	95	0	8	3	7	6	2	8	2	69.94%
	3	534	2507	**13186**	345	444	26	1089	84	53	7	445	14	13	44	24	70.08%
	4	0	0	0	**0**	0	0	0	0	0	0	0	0	0	0	0	N/A
	5	11	9	145	6	**225**	1	207	14	3	0	24	0	6	36	3	32.61%
	6	0	0	0	0	0	**0**	0	0	0	0	0	0	0	0	0	N/A
	7	31	80	721	62	248	4	**1469**	25	30	1	293	1	8	72	21	47.91%
	8	0	0	0	0	0	0	0	**0**	0	0	0	0	0	0	0	N/A
	9	0	0	0	0	0	0	0	0	**0**	0	0	0	0	0	0	N/A
	10	0	0	0	0	0	0	0	0	0	**0**	0	0	0	0	0	N/A
	11	0	1	17	1	1	0	12	1	0	1	**45**	0	0	0	0	56.96%
	12	0	0	0	0	0	0	0	0	0	0	0	**0**	0	0	0	N/A
	13	0	0	0	0	0	0	0	0	0	0	0	0	**0**	0	0	N/A
	14	2	1	15	3	2	0	32	0	0	0	2	0	28	**51**	37	29.48%
	15	8	10	8	1	0	0	1	0	0	0	0	2	19	0	**16**	24.62%
	P.A	42.28%	57.97%	85.52%	0.00%	22.23%	0.00%	49.38%	0.00%	0.00%	0.00%	5.45%	0.00%	0.00%	22.87%	13.56%	**65.69%**

AVHRR CONFUSION MATRIX (11% SAMPLE)
UK STUDY AREA
DATE:18/04/2003
DOMINANT CLASS CLASSIFICATION SCHEME

		REFERENCE															
		1	2	3	4	5	6	7	8	9	10	11	12	13	14	15	U.A
CLASSIFIED	1	**435**	200	214	13	95	2	83	6	5	2	18	5	22	15	24	38.19%
	2	688	**3752**	2433	73	197	5	413	13	23	0	122	7	22	20	16	48.20%
	3	566	4195	**13328**	335	485	14	973	92	39	10	501	13	40	106	64	64.20%
	4	0	0	0	**0**	0	0	0	0	0	0	0	0	0	0	0	N/A
	5	18	49	206	22	**291**	1	225	13	2	1	30	5	10	61	23	30.41%
	6	0	0	0	0	0	**0**	0	0	0	0	0	0	0	0	0	N/A
	7	45	179	632	52	195	1	**2027**	14	43	1	342	0	1	33	2	56.83%
	8	0	0	0	0	0	0	0	**0**	0	0	0	0	0	0	0	N/A
	9	0	0	0	0	0	0	0	0	**0**	0	0	0	0	0	0	N/A
	10	0	0	0	0	0	0	0	0	0	**0**	0	0	0	0	0	N/A
	11	0	0	0	0	0	0	0	0	0	0	**0**	0	0	0	0	N/A
	12	0	0	0	0	0	0	0	0	0	0	0	**0**	0	0	0	N/A
	13	0	0	0	0	0	0	0	0	0	0	0	0	**0**	0	0	N/A
	14	14	23	13	0	5	0	6	1	2	0	1	6	21	**77**	72	31.95%
	15	0	0	0	0	0	0	0	0	0	0	0	0	0	0	**0**	N/A
	P.A	24.63%	44.68%	79.21%	0.00%	22.95%	0.00%	54.39%	0.00%	0.00%	0.00%	0.00%	0.00%	0.00%	24.68%	0.00%	**57.80%**

AVHRR CONFUSION MATRIX (11% SAMPLE)
UK STUDY AREA
DATE:19/03/2003
DOMINANT CLASS CLASSIFICATION SCHEME

CLASSIFIED \ REFERENCE	1	2	3	4	5	6	7	8	9	10	11	12	13	14	15	U.A
1	**717**	311	190	15	39	0	125	1	7	0	11	8	19	15	25	48.35%
2	531	**4349**	1369	121	52	6	249	3	16	3	23	3	4	9	3	64.52%
3	215	2095	**8068**	251	222	9	712	6	3	1	34	3	4	8	2	69.35%
4	0	0	0	**0**	0	0	0	0	0	0	0	0	0	0	0	N/A
5	19	33	189	16	**503**	1	284	26	3	0	14	2	5	55	22	42.92%
6	0	0	0	0	0	**0**	0	0	0	0	0	0	0	0	0	N/A
7	24	96	514	70	171	4	**1406**	10	8	0	67	0	0	7	0	59.15%
8	0	0	0	0	0	0	0	**0**	0	0	0	0	0	0	0	N/A
9	0	0	0	0	0	0	0	0	**0**	0	0	0	0	0	0	N/A
10	0	0	0	0	0	0	0	0	0	**0**	0	0	0	0	0	N/A
11	0	0	0	0	0	0	0	0	0	0	**0**	0	0	0	0	N/A
12	0	0	0	0	0	0	0	0	0	0	0	**0**	0	0	0	N/A
13	11	2	10	1	0	0	5	0	2	0	0	3	**16**	2	12	25.00%
14	0	0	0	0	0	0	0	0	0	0	0	0	0	**0**	0	N/A
15	2	3	3	0	0	0	5	0	0	0	0	2	12	9	**106**	74.65%
P.A	47.20%	63.13%	78.00%	0.00%	50.96%	0.00%	50.47%	0.00%	0.00%	0.00%	0.00%	0.00%	26.67%	0.00%	62.35%	**64.23%**

AVHRR CONFUSION MATRIX (11% SAMPLE)
UK STUDY AREA
DATE:22/03/2003
DOMINANT CLASS CLASSIFICATION SCHEME

		REFERENCE															
		1	2	3	4	5	6	7	8	9	10	11	12	13	14	15	U.A
CLASSIFIED	1	**717**	257	233	13	54	0	71	2	3	1	3	8	12	8	25	50.96%
	2	477	**4782**	1863	113	73	3	186	2	6	3	3	9	7	8	12	63.36%
	3	359	2056	**7355**	333	208	7	493	2	9	1	10	7	27	12	32	67.41%
	4	0	0	0	**0**	0	0	0	0	0	0	0	0	0	0	0	N/A
	5	3	16	94	6	**127**	0	89	2	0	0	2	0	0	12	0	36.18%
	6	0	0	0	0	0	**0**	0	0	0	0	0	0	0	0	0	N/A
	7	11	54	210	28	90	0	**265**	1	2	0	4	2	3	4	10	38.74%
	8	0	0	0	0	0	0	0	**0**	0	0	0	0	0	0	0	N/A
	9	0	0	0	0	0	0	0	0	**0**	0	0	0	0	0	0	N/A
	10	0	0	0	0	0	0	0	0	0	**0**	0	0	0	0	0	N/A
	11	0	0	0	0	0	0	0	0	0	0	**0**	0	0	0	0	N/A
	12	0	0	0	0	0	0	0	0	0	0	0	**0**	0	0	0	N/A
	13	0	0	0	0	0	0	0	0	0	0	0	0	**0**	0	0	N/A
	14	0	0	0	0	0	0	0	0	0	0	0	0	0	**0**	0	N/A
	15	7	9	13	1	5	0	6	0	2	0	0	2	22	1	**58**	46.03%
	P.A	45.55%	66.66%	75.30%	0.00%	22.80%	0.00%	23.87%	0.00%	0.00%	0.00%	0.00%	0.00%	0.00%	0.00%	42.34%	**63.27%**

AVHRR CONFUSION MATRIX (11% SAMPLE)
UK STUDY AREA
DATE:23/03/2003
DOMINANT CLASS CLASSIFICATION SCHEME

		REFERENCE															
		1	2	3	4	5	6	7	8	9	10	11	12	13	14	15	U.A
CLASSIFIED	1	**549**	254	225	26	63	0	59	6	6	0	2	7	4	5	24	44.63%
	2	577	**4619**	2497	153	150	2	337	9	13	1	8	10	9	16	8	54.93%
	3	406	2320	**7653**	246	243	6	671	12	8	3	8	6	6	16	7	65.91%
	4	0	0	0	**0**	0	0	0	0	0	0	0	0	0	0	0	N/A
	5	22	38	154	12	**270**	0	187	8	0	0	2	2	11	15	16	36.64%
	6	0	0	0	0	0	**0**	0	0	0	0	0	0	0	0	0	N/A
	7	15	86	328	31	119	0	**686**	0	0	0	6	0	0	3	3	53.72%
	8	0	0	0	0	0	0	0	**0**	0	0	0	0	0	0	0	N/A
	9	0	0	0	0	0	0	0	0	**0**	0	0	0	0	0	0	N/A
	10	0	0	0	0	0	0	0	0	0	**0**	0	0	0	0	0	N/A
	11	0	0	0	0	0	0	0	0	0	0	**0**	0	0	0	0	N/A
	12	0	0	0	0	0	0	0	0	0	0	0	**0**	0	0	0	N/A
	13	0	0	0	0	0	0	0	0	0	0	0	0	**0**	0	0	N/A
	14	0	0	0	0	0	0	0	0	0	0	0	0	0	**0**	0	N/A
	15	3	16	5	2	0	0	3	0	0	0	0	0	13	2	**72**	62.07%
	P.A	34.92%	62.99%	70.46%	0.00%	31.95%	0.00%	35.31%	0.00%	0.00%	0.00%	0.00%	0.00%	0.00%	0.00%	55.38%	**59.23%**

AVHRR CONFUSION MATRIX (11% SAMPLE)
UK STUDY AREA
DATE:MULTIDATE
DOMINANT CLASS CLASSIFICATION SCHEME

		REFERENCE															
		1	2	3	4	5	6	7	8	9	10	11	12	13	14	15	U.A
CLASSIFIED	1	**508**	126	143	5	3	0	3	0	0	0	1	0	0	0	2	64.22%
	2	282	**4527**	1409	44	22	0	62	0	0	0	0	0	0	3	5	71.25%
	3	246	1491	**6528**	156	160	0	557	0	0	0	3	0	0	1	4	71.38%
	4	0	0	0	**0**	0	0	0	0	0	0	0	0	0	0	0	N/A
	5	0	8	56	5	**142**	0	92	0	0	0	0	0	0	3	6	45.51%
	6	0	0	0	0	0	**0**	0	0	0	0	0	0	0	0	0	N/A
	7	6	46	271	12	137	0	**734**	0	0	0	0	0	0	0	1	60.81%
	8	0	0	0	0	0	0	0	**0**	0	0	0	0	0	0	0	N/A
	9	0	0	0	0	0	0	0	0	**0**	0	0	0	0	0	0	N/A
	10	0	0	0	0	0	0	0	0	0	**0**	0	0	0	0	0	N/A
	11	0	0	0	0	0	0	0	0	0	0	**0**	0	0	0	0	N/A
	12	0	0	0	0	0	0	0	0	0	0	0	**0**	0	0	0	N/A
	13	0	0	0	0	0	0	0	0	0	0	0	0	**0**	0	0	N/A
	14	0	0	0	0	0	0	0	0	0	0	0	0	0	**0**	0	N/A
	15	2	15	4	0	1	0	0	0	0	0	0	0	0	3	**29**	53.70%
	P.A	48.66%	72.86%	77.61%	0.00%	30.54%	N/A	50.69%	N/A	N/A	N/A	0.00%	N/A	N/A	0.00%	61.70%	**69.79%**

MODIS1 CONFUSION MATRIX (11% SAMPLE)
UK STUDY AREA
DATE:13/07/2003
DOMINANT CLASS CLASSIFICATION SCHEME

		REFERENCE															
		1	2	3	4	5	6	7	8	9	10	11	12	13	14	15	U.A
CLASSIFIED	1	**779**	253	260	22	15	1	101	0	20	0	6	15	34	11	49	49.74%
	2	471	**5335**	1880	121	33	1	36	3	5	5	6	8	10	10	32	67.06%
	3	331	2039	**8661**	318	409	8	890	10	13	0	35	8	28	41	58	67.41%
	4	0	1	0	**1**	0	0	0	0	0	0	0	0	0	0	0	50.00%
	5	1	1	2	0	**6**	0	2	0	0	0	0	0	0	0	0	50.00%
	6	0	0	0	0	0	**0**	0	0	0	0	0	0	0	0	0	N/A
	7	45	59	673	38	449	1	**1810**	14	21	0	36	0	4	42	11	56.51%
	8	0	0	0	0	0	0	0	**0**	0	0	0	0	0	0	0	N/A
	9	0	0	0	0	0	0	0	0	**0**	0	0	0	0	0	0	N/A
	10	0	0	0	0	0	0	0	0	0	**0**	0	0	0	0	0	N/A
	11	0	0	0	0	0	0	0	0	0	0	**1**	0	0	0	0	100.00%
	12	0	0	0	0	0	0	0	0	0	0	0	**0**	0	0	0	N/A
	13	0	0	0	0	0	0	0	0	0	0	0	0	**0**	0	0	N/A
	14	0	0	0	0	0	0	0	0	0	0	0	0	0	**0**	0	N/A
	15	12	23	31	0	4	0	12	0	2	0	1	0	9	7	**113**	52.80%
	P.A	47.53%	69.19%	75.27%	0.20%	0.66%	0.00%	63.49%	0.00%	0.00%	0.00%	1.18%	0.00%	0.00%	0.00%	42.97%	**64.74%**

MODIS1 CONFUSION MATRIX (11% SAMPLE)
UK STUDY AREA
DATE:16/04/2003
DOMINANT CLASS CLASSIFICATION SCHEME

		REFERENCE															
		1	2	3	4	5	6	7	8	9	10	11	12	13	14	15	U.A
CLASSIFIED	1	**379**	175	192	15	98	0	201	8	10	0	19	9	15	34	40	31.72%
	2	499	**3670**	2001	97	211	6	304	9	9	0	54	3	7	18	19	53.13%
	3	520	3702	**10650**	336	450	14	535	31	8	5	121	7	9	27	25	64.78%
	4	0	0	0	**0**	0	0	0	0	0	0	0	0	0	0	0	N/A
	5	6	13	37	7	**41**	0	26	1	0	0	1	0	0	0	0	31.06%
	6	0	0	0	0	0	**0**	0	0	0	0	0	0	0	0	0	N/A
	7	318	510	501	24	256	0	**1521**	9	27	0	57	3	13	36	11	46.29%
	8	0	0	0	0	0	0	0	**0**	0	0	0	0	0	0	0	N/A
	9	0	0	0	0	0	0	0	0	**0**	0	0	0	0	0	0	N/A
	10	0	0	0	0	0	0	0	0	0	**0**	0	0	0	0	0	N/A
	11	0	0	0	0	0	0	0	0	0	0	**0**	0	0	0	0	N/A
	12	0	0	0	0	0	0	0	0	0	0	0	**0**	0	0	0	N/A
	13	0	0	0	0	0	0	0	0	0	0	0	0	**0**	0	0	N/A
	14	21	29	38	0	5	0	9	0	2	0	1	5	9	**49**	37	23.90%
	15	16	20	35	0	0	0	0	0	1	0	0	5	24	1	**80**	43.96%
	P.A	21.55%	45.20%	79.16%	0.00%	3.86%	0.00%	58.59%	0.00%	0.00%	0.00%	0.00%	0.00%	0.00%	29.70%	37.74%	**57.82%**

MODIS1 CONFUSION MATRIX (11% SAMPLE)
UK STUDY AREA
DATE:17/03/2003
DOMINANT CLASS CLASSIFICATION SCHEME

		REFERENCE															
		1	2	3	4	5	6	7	8	9	10	11	12	13	14	15	U.A
CLASSIFIED	1	**224**	109	60	5	3	0	71	1	12	0	11	4	15	9	10	41.95%
	2	460	**2975**	1242	76	112	1	815	11	32	2	166	10	22	31	13	49.85%
	3	457	3157	**13372**	328	567	31	875	95	34	7	568	14	33	73	55	68.00%
	4	0	0	0	**0**	0	0	0	0	0	0	0	0	0	0	0	N/A
	5	5	2	33	8	**54**	0	21	7	0	0	2	0	0	3	1	39.71%
	6	0	0	0	0	0	**0**	0	0	0	0	0	0	0	0	0	N/A
	7	422	407	647	77	267	0	**1186**	14	21	4	73	5	30	102	40	35.99%
	8	0	0	0	0	0	0	0	**0**	0	0	0	0	0	0	0	N/A
	9	0	0	0	0	0	0	0	0	**0**	0	0	0	0	0	0	N/A
	10	0	0	0	0	0	0	0	0	0	**0**	0	0	0	0	0	N/A
	11	0	1	4	0	0	0	1	0	0	0	**3**	0	0	0	0	33.33%
	12	0	0	0	0	0	0	0	0	0	0	0	**0**	0	0	0	N/A
	13	0	0	0	0	0	0	0	0	0	0	0	0	**0**	0	0	N/A
	14	0	0	0	0	0	0	0	0	0	0	0	0	0	**0**	0	N/A
	15	0	0	0	0	0	0	0	0	0	0	0	0	0	0	**0**	N/A
	P.A	14.29%	44.73%	87.07%	0.00%	5.38%	0.00%	39.95%	0.00%	0.00%	0.00%	0.36%	0.00%	0.00%	0.00%	0.00%	**60.17%**

MODIS1 CONFUSION MATRIX (11% SAMPLE)
UK STUDY AREA
DATE:18/04/2003
DOMINANT CLASS CLASSIFICATION SCHEME

		REFERENCE															
		1	2	3	4	5	6	7	8	9	10	11	12	13	14	15	U.A
CLASSIFIED	1	**161**	52	51	3	6	0	72	1	15	1	8	2	7	2	12	40.97%
	2	556	**3718**	2384	131	301	4	643	22	13	2	343	4	12	44	30	45.30%
	3	512	4155	**13397**	303	423	16	537	86	38	7	422	13	43	93	67	66.61%
	4	0	0	0	**0**	0	0	0	0	0	0	0	0	0	0	0	N/A
	5	17	21	40	10	**57**	0	24	0	0	0	4	0	1	3	0	32.20%
	6	0	0	0	0	0	**0**	0	0	0	0	0	0	0	0	0	N/A
	7	495	390	856	47	481	2	**2377**	28	48	4	194	10	28	115	39	46.48%
	8	0	0	0	0	0	0	0	**0**	0	0	0	0	0	0	0	N/A
	9	0	0	0	0	0	0	0	0	**0**	0	0	0	0	0	0	N/A
	10	0	0	0	0	0	0	0	0	0	**0**	0	0	0	0	0	N/A
	11	4	9	15	0	2	0	11	1	0	0	**15**	0	0	0	0	26.32%
	12	0	0	0	0	0	0	0	0	0	0	0	**0**	0	0	0	N/A
	13	0	0	0	0	0	0	0	0	0	0	0	0	**0**	0	0	N/A
	14	0	0	0	0	0	0	0	0	0	0	0	0	0	**0**	0	N/A
	15	17	17	30	0	2	0	29	0	0	0	0	5	18	57	**48**	21.52%
	P.A	9.14%	44.46%	79.87%	0.00%	4.48%	0.00%	64.37%	0.00%	0.00%	0.00%	1.52%	0.00%	0.00%	0.00%	24.49%	**57.68%**

MODIS1 CONFUSION MATRIX (11% SAMPLE)
UK STUDY AREA
DATE:19/03/2003
DOMINANT CLASS CLASSIFICATION SCHEME

		REFERENCE															
		1	2	3	4	5	6	7	8	9	10	11	12	13	14	15	U.A
CLASSIFIED	1	**277**	120	93	5	5	0	120	1	13	1	7	3	14	10	27	39.80%
	2	622	**3782**	1635	97	176	6	885	4	15	1	72	8	13	19	11	51.48%
	3	391	2599	**7983**	302	338	12	588	18	8	2	52	6	23	31	36	64.44%
	4	0	0	1	**0**	1	0	0	0	0	0	0	0	0	0	0	0.00%
	5	3	10	64	7	**95**	0	59	3	0	0	0	0	0	1	0	39.26%
	6	0	0	0	0	0	**0**	0	0	0	0	0	0	0	0	0	N/A
	7	228	373	509	71	373	1	**1131**	19	3	0	17	3	9	41	23	40.38%
	8	0	0	0	0	0	0	0	**0**	0	0	0	0	0	0	0	N/A
	9	0	0	0	0	0	0	0	0	**0**	0	0	0	0	0	0	N/A
	10	0	0	0	0	0	0	0	0	0	**0**	0	0	0	0	0	N/A
	11	0	0	1	0	0	0	1	0	0	0	**1**	0	0	0	0	33.33%
	12	0	0	0	0	0	0	0	0	0	0	0	**0**	0	0	0	N/A
	13	0	0	0	0	0	0	0	0	0	0	0	0	**0**	0	0	N/A
	14	0	0	0	0	0	0	0	0	0	0	0	0	0	**0**	0	N/A
	15	9	5	17	0	3	0	9	0	1	0	0	1	6	3	**73**	57.48%
	P.A	18.10%	54.90%	77.48%	0.00%	9.59%	0.00%	40.49%	0.00%	0.00%	0.00%	0.67%	0.00%	0.00%	0.00%	42.94%	**56.52%**

MODIS1 CONFUSION MATRIX (11% SAMPLE)
UK STUDY AREA
DATE:22/03/2003
DOMINANT CLASS CLASSIFICATION SCHEME

		REFERENCE															
		1	2	3	4	5	6	7	8	9	10	11	12	13	14	15	U.A
CLASSIFIED	1	**486**	275	203	23	31	0	97	0	4	2	3	7	26	6	32	40.67%
	2	605	**4383**	1821	114	106	2	304	1	11	3	8	16	11	15	30	58.99%
	3	425	2412	**7438**	316	271	9	375	6	4	0	9	3	7	12	10	65.84%
	4	0	0	0	**1**	0	0	0	0	0	0	0	0	0	0	0	100.00%
	5	0	5	23	6	**38**	0	27	2	0	0	0	0	0	0	0	37.62%
	6	0	0	0	0	0	**0**	0	0	0	0	0	0	0	0	0	N/A
	7	33	60	204	29	104	0	**277**	1	0	0	3	0	3	7	0	38.42%
	8	0	0	0	0	0	0	0	**0**	0	0	0	0	0	0	0	N/A
	9	0	0	0	0	0	0	0	0	**0**	0	0	0	0	0	0	N/A
	10	0	0	0	0	0	0	0	0	0	**0**	0	0	0	0	0	N/A
	11	0	0	0	0	0	0	0	0	0	0	**0**	0	0	0	0	N/A
	12	0	0	0	0	0	0	0	0	0	0	0	**0**	0	0	0	N/A
	13	0	0	0	0	0	0	0	0	0	0	0	0	**0**	0	0	N/A
	14	0	0	0	0	0	0	0	0	0	0	0	0	0	**0**	0	N/A
	15	18	17	57	1	9	0	23	0	3	0	0	2	30	4	**65**	28.38%
	P.A	31.01%	61.28%	76.32%	0.20%	6.80%	0.00%	25.11%	0.00%	0.00%	0.00%	0.00%	0.00%	0.00%	0.00%	47.45%	**60.49%**

MODIS1 CONFUSION MATRIX (11% SAMPLE)
UK STUDY AREA
DATE:23/03/2003
DOMINANT CLASS CLASSIFICATION SCHEME

		REFERENCE															
		1	2	3	4	5	6	7	8	9	10	11	12	13	14	15	U.A
CLASSIFIED	1	**526**	253	174	20	75	0	187	6	7	0	4	10	9	10	22	40.37%
	2	568	**4106**	2175	139	228	3	619	10	13	3	12	8	7	14	10	51.88%
	3	351	2819	**8196**	267	264	4	461	8	5	1	7	5	1	15	8	66.03%
	4	0	0	0	**2**	0	0	0	0	0	0	0	0	0	0	0	100.00%
	5	0	0	0	0	**0**	0	0	0	0	0	0	0	0	0	0	N/A
	6	0	0	0	0	0	**0**	0	0	0	0	0	0	0	0	0	N/A
	7	127	169	302	48	276	1	**675**	11	1	0	3	0	1	17	8	41.18%
	8	0	0	0	0	0	0	0	**0**	0	0	0	0	0	0	0	N/A
	9	0	0	0	0	0	0	0	0	**0**	0	0	0	0	0	0	N/A
	10	0	0	0	0	0	0	0	0	0	**0**	0	0	0	0	0	N/A
	11	0	0	0	0	0	0	0	0	0	0	**0**	0	0	0	0	N/A
	12	0	0	0	0	0	0	0	0	0	0	0	**0**	0	0	0	N/A
	13	0	0	0	0	0	0	0	0	0	0	0	0	**0**	0	0	N/A
	14	0	0	0	0	0	0	0	0	0	0	0	0	0	**0**	0	N/A
	15	14	12	9	0	2	0	0	0	2	0	0	2	25	0	**97**	59.51%
	P.A	33.17%	55.80%	75.50%	0.42%	0.00%	0.00%	34.76%	0.00%	0.00%	0.00%	0.00%	0.00%	0.00%	0.00%	66.90%	**58.04%**

MODIS1 CONFUSION MATRIX (11% SAMPLE)
UK STUDY AREA
DATE:MULTIDATE
DOMINANT CLASS CLASSIFICATION SCHEME

		REFERENCE															
		1	2	3	4	5	6	7	8	9	10	11	12	13	14	15	U.A
CLASSIFIED	1	**476**	99	70	2	6	0	27	0	0	0	0	0	0	1	2	69.69%
	2	394	**4699**	1459	49	50	0	82	0	0	0	0	0	0	2	9	69.68%
	3	124	1359	**6611**	152	168	0	360	0	0	0	3	0	0	1	1	75.30%
	4	0	0	0	**0**	0	0	0	0	0	0	0	0	0	0	0	N/A
	5	0	0	0	0	**0**	0	0	0	0	0	0	0	0	0	0	N/A
	6	0	0	0	0	0	**0**	0	0	0	0	0	0	0	0	0	N/A
	7	57	41	240	15	243	0	**963**	0	0	0	1	0	0	3	0	61.61%
	8	0	0	0	0	0	0	0	**0**	0	0	0	0	0	0	0	N/A
	9	0	0	0	0	0	0	0	0	**0**	0	0	0	0	0	0	N/A
	10	0	0	0	0	0	0	0	0	0	**0**	0	0	0	0	0	N/A
	11	0	0	0	0	0	0	0	0	0	0	**0**	0	0	0	0	N/A
	12	0	0	0	0	0	0	0	0	0	0	0	**0**	0	0	0	N/A
	13	0	0	0	0	0	0	0	0	0	0	0	0	**0**	0	0	N/A
	14	0	0	0	0	0	0	0	0	0	0	0	0	0	**0**	0	N/A
	15	4	4	4	0	0	0	0	0	0	0	0	0	0	2	**33**	70.21%
	P.A	45.12%	75.77%	78.85%	0.00%	0.00%	N/A	67.25%	N/A	N/A	N/A	0.00%	N/A	N/A	0.00%	73.33%	**71.74%**

MODIS2 CONFUSION MATRIX (11% SAMPLE)
UK STUDY AREA
DATE:13/07/2003
DOMINANT CLASS CLASSIFICATION SCHEME

		REFERENCE															
		1	2	3	4	5	6	7	8	9	10	11	12	13	14	15	U.A
CLASSIFIED	1	**774**	183	181	18	12	1	20	0	7	0	3	5	21	7	25	61.58%
	2	493	**5868**	1519	115	73	0	52	5	4	5	4	15	21	10	47	71.29%
	3	357	1555	**9099**	347	417	9	767	12	14	0	33	8	22	39	44	71.52%
	4	0	0	0	**0**	0	0	0	0	0	0	0	0	0	0	0	N/A
	5	7	15	100	13	**142**	1	97	4	0	0	2	0	1	4	5	36.32%
	6	0	0	0	0	0	**0**	0	0	0	0	0	0	0	0	0	N/A
	7	10	35	539	5	265	0	**1896**	4	34	0	42	0	1	45	13	65.63%
	8	0	0	0	0	0	0	0	**0**	0	0	0	0	0	0	0	N/A
	9	0	0	0	0	0	0	0	0	**0**	0	0	0	0	0	0	N/A
	10	0	0	0	0	0	0	0	0	0	**0**	0	0	0	0	0	N/A
	11	0	0	0	0	0	0	0	0	0	0	**0**	0	0	0	0	N/A
	12	0	0	0	0	0	0	0	0	0	0	0	**0**	0	0	0	N/A
	13	0	0	0	0	0	0	0	0	0	0	0	0	**0**	0	0	N/A
	14	0	0	0	0	0	0	0	0	0	0	0	0	0	**0**	0	N/A
	15	28	49	49	1	3	0	10	0	4	0	1	3	19	6	**130**	42.90%
	P.A	46.38%	76.16%	79.21%	0.00%	15.57%	0.00%	66.71%	0.00%	0.00%	0.00%	0.00%	0.00%	0.00%	0.00%	49.24%	**69.43%**

MODIS2 CONFUSION MATRIX (11% SAMPLE)
UK STUDY AREA
DATE:16/04/2003
DOMINANT CLASS CLASSIFICATION SCHEME

		REFERENCE															
		1	2	3	4	5	6	7	8	9	10	11	12	13	14	15	U.A
CLASSIFIED	1	**721**	241	178	13	16	0	13	0	5	0	1	5	8	4	10	59.34%
	2	560	**5787**	1708	113	70	6	50	1	8	4	4	3	9	13	16	69.29%
	3	443	2059	**10907**	325	529	13	662	34	13	1	149	16	30	68	77	71.17%
	4	0	0	0	**0**	0	0	0	0	0	0	0	0	0	0	0	N/A
	5	10	29	151	13	**233**	1	111	17	4	0	12	2	5	11	7	38.45%
	6	0	0	0	0	0	**0**	0	0	0	0	0	0	0	0	0	N/A
	7	15	27	498	15	220	0	**1782**	7	27	0	80	1	5	41	6	65.42%
	8	0	0	0	0	0	0	0	**0**	0	0	0	0	0	0	0	N/A
	9	0	0	0	0	0	0	0	0	**0**	0	0	0	0	0	0	N/A
	10	0	0	0	0	0	0	0	0	0	**0**	0	0	0	0	0	N/A
	11	0	0	5	0	0	0	0	0	0	0	**5**	0	0	0	0	50.00%
	12	0	0	0	0	0	0	0	0	0	0	0	**0**	0	0	0	N/A
	13	0	0	0	0	0	0	0	0	0	0	0	0	**0**	0	0	N/A
	14	0	0	0	0	0	0	0	0	0	0	0	0	0	**0**	0	N/A
	15	17	23	35	0	1	0	0	0	1	0	0	5	25	25	**86**	39.45%
	P.A	40.83%	70.87%	80.90%	0.00%	21.80%	0.00%	68.07%	0.00%	0.00%	0.00%	1.99%	0.00%	0.00%	0.00%	42.57%	**68.61%**

MODIS2 CONFUSION MATRIX (11% SAMPLE)
UK STUDY AREA
DATE:17/03/2003
DOMINANT CLASS CLASSIFICATION SCHEME

		REFERENCE															
		1	2	3	4	5	6	7	8	9	10	11	12	13	14	15	U.A
CLASSIFIED	1	**731**	240	166	28	8	0	6	1	7	1	1	6	8	8	8	59.97%
	2	414	**4495**	1308	92	29	1	15	1	5	3	0	9	4	6	3	70.40%
	3	419	1859	**13066**	328	498	26	875	85	37	8	416	19	76	135	91	72.84%
	4	0	0	0	**0**	0	0	0	0	0	0	0	0	0	0	0	N/A
	5	2	3	130	8	**261**	1	154	19	0	0	4	0	0	7	6	43.87%
	6	0	0	0	0	0	**0**	0	0	0	0	0	0	0	0	0	N/A
	7	25	47	608	37	186	0	**1866**	11	41	0	150	0	8	62	10	61.16%
	8	0	0	0	0	0	0	0	**0**	0	0	0	0	0	0	0	N/A
	9	0	0	4	0	2	0	0	0	**5**	0	4	0	0	0	0	33.33%
	10	0	0	0	0	0	0	0	0	0	**0**	0	0	0	0	0	N/A
	11	0	42	120	1	38	3	75	10	3	1	**247**	0	2	4	0	45.24%
	12	0	0	0	0	0	0	0	0	0	0	0	**0**	0	0	0	N/A
	13	0	0	0	0	0	0	0	0	0	0	0	0	**0**	0	0	N/A
	14	0	0	0	0	0	0	0	0	0	0	0	0	0	**0**	0	N/A
	15	0	0	0	0	0	0	0	0	0	0	0	0	0	0	**0**	N/A
	P.A	45.95%	67.23%	84.83%	0.00%	25.54%	0.00%	62.39%	0.00%	5.10%	0.00%	30.05%	0.00%	0.00%	0.00%	0.00%	**69.48%**

MODIS2 CONFUSION MATRIX (11% SAMPLE)
UK STUDY AREA
DATE:18/04/2003
DOMINANT CLASS CLASSIFICATION SCHEME

		REFERENCE															
		1	2	3	4	5	6	7	8	9	10	11	12	13	14	15	U.A
CLASSIFIED	1	**736**	244	170	14	12	0	16	0	8	1	0	5	4	7	13	59.84%
	2	550	**5508**	1685	119	61	0	44	3	3	2	3	7	7	13	22	68.62%
	3	428	2515	**13777**	301	568	20	673	104	35	10	428	12	56	144	84	71.92%
	4	0	0	0	**0**	0	0	0	0	0	0	0	0	0	0	0	N/A
	5	10	43	188	34	**353**	0	170	17	1	0	22	3	6	14	8	40.62%
	6	0	0	0	0	0	**0**	0	0	0	0	0	0	0	0	0	N/A
	7	32	43	793	28	230	1	**2716**	5	59	1	161	2	9	67	15	65.26%
	8	0	0	0	0	0	0	0	**0**	0	0	0	0	0	0	0	N/A
	9	0	0	0	0	0	0	0	0	**0**	0	0	0	0	0	0	N/A
	10	0	0	0	0	0	0	0	0	0	**0**	0	0	0	0	0	N/A
	11	0	53	182	1	53	2	79	10	4	0	**398**	0	1	10	0	50.19%
	12	0	0	0	0	0	0	0	0	0	0	0	**0**	0	0	0	N/A
	13	0	0	0	0	0	0	0	0	0	0	0	0	**0**	0	0	N/A
	14	0	0	0	0	0	0	0	0	0	0	0	0	0	**0**	0	N/A
	15	17	23	38	0	3	0	25	0	0	0	0	7	30	59	**54**	21.09%
	P.A	41.51%	65.35%	81.85%	0.00%	27.58%	0.00%	72.95%	0.00%	0.00%	0.00%	39.33%	0.00%	0.00%	0.00%	27.55%	**68.25%**

MODIS2 CONFUSION MATRIX (11% SAMPLE)
UK STUDY AREA
DATE:19/03/2003
DOMINANT CLASS CLASSIFICATION SCHEME

		REFERENCE															
		1	2	3	4	5	6	7	8	9	10	11	12	13	14	15	U.A
CLASSIFIED	1	**539**	208	103	7	3	0	4	0	2	2	0	3	3	2	16	60.43%
	2	605	**5256**	1342	128	54	6	31	3	5	1	2	5	4	7	9	70.47%
	3	349	1393	**8116**	294	420	13	689	19	12	1	79	9	27	30	34	70.67%
	4	0	0	0	**0**	0	0	0	0	0	0	0	0	0	0	0	N/A
	5	2	16	194	20	**356**	0	159	17	0	0	4	0	1	11	1	45.58%
	6	0	0	0	0	0	**0**	0	0	0	0	0	0	0	0	0	N/A
	7	26	41	538	32	165	0	**1907**	5	19	0	53	4	15	54	31	65.99%
	8	0	0	0	0	0	0	0	**0**	0	0	0	0	0	0	0	N/A
	9	0	0	0	0	0	0	0	0	**0**	0	0	0	0	0	0	N/A
	10	0	0	0	0	0	0	0	0	0	**0**	0	0	0	0	0	N/A
	11	0	0	8	0	2	0	9	1	0	0	**13**	0	0	0	0	39.39%
	12	0	0	0	0	0	0	0	0	0	0	0	**0**	0	0	0	N/A
	13	0	0	0	0	0	0	0	0	0	0	0	0	**0**	0	0	N/A
	14	0	0	0	0	0	0	0	0	0	0	0	0	0	**0**	0	N/A
	15	10	6	21	0	3	0	8	0	2	0	0	1	15	3	**77**	52.74%
	P.A	35.21%	75.95%	78.63%	0.00%	35.49%	0.00%	67.94%	0.00%	0.00%	0.00%	8.61%	0.00%	0.00%	0.00%	45.83%	**68.67%**

MODIS2 CONFUSION MATRIX (11% SAMPLE)
UK STUDY AREA
DATE:22/03/2003
DOMINANT CLASS CLASSIFICATION SCHEME

		REFERENCE															
		1	2	3	4	5	6	7	8	9	10	11	12	13	14	15	U.A
CLASSIFIED	1	**629**	224	148	15	8	1	9	0	1	0	1	3	7	2	13	59.28%
	2	544	**5385**	1496	127	53	2	32	0	7	4	2	9	7	7	13	70.04%
	3	362	1523	**7737**	332	318	7	489	8	9	1	13	14	22	27	37	70.99%
	4	0	1	0	**1**	0	0	0	0	0	0	0	0	0	0	0	50.00%
	5	0	16	68	8	**122**	0	54	1	0	0	1	0	1	2	0	44.69%
	6	0	0	0	0	0	**0**	0	0	0	0	0	0	0	0	0	N/A
	7	2	14	272	8	52	1	**498**	1	0	0	4	0	0	5	4	57.84%
	8	0	0	0	0	0	0	0	**0**	0	0	0	0	0	0	0	N/A
	9	0	0	0	0	0	0	0	0	**0**	0	0	0	0	0	0	N/A
	10	0	0	0	0	0	0	0	0	0	**0**	0	0	0	0	0	N/A
	11	0	0	0	0	0	0	0	0	0	0	**0**	0	0	0	0	N/A
	12	0	0	0	0	0	0	0	0	0	0	0	**0**	0	0	0	N/A
	13	0	0	0	0	0	0	0	0	0	0	0	0	**0**	0	0	N/A
	14	0	0	0	0	0	0	0	0	0	0	0	0	0	**0**	0	N/A
	15	10	4	34	0	2	0	7	0	2	0	0	1	25	1	**45**	34.35%
	P.A	40.66%	75.14%	79.31%	0.20%	21.98%	0.00%	45.73%	0.00%	0.00%	0.00%	0.00%	0.00%	0.00%	0.00%	40.18%	**68.93%**

MODIS2 CONFUSION MATRIX (11% SAMPLE)
UK STUDY AREA
DATE:23/03/2003
DOMINANT CLASS CLASSIFICATION SCHEME

		REFERENCE															
		1	2	3	4	5	6	7	8	9	10	11	12	13	14	15	U.A
CLASSIFIED	1	**673**	185	150	12	9	0	11	2	3	0	0	5	3	6	2	63.43%
	2	536	**5923**	1483	107	47	1	24	1	2	3	2	8	4	12	10	72.56%
	3	317	1220	**8776**	301	428	5	629	17	9	1	8	3	4	13	15	74.71%
	4	0	0	0	**0**	0	0	0	0	0	0	0	0	0	0	0	N/A
	5	7	21	111	20	**245**	0	81	9	1	0	1	6	2	12	6	46.93%
	6	0	0	0	0	0	**0**	0	0	0	0	0	0	0	0	0	N/A
	7	24	19	329	34	108	2	**1181**	5	10	0	14	0	2	13	2	67.76%
	8	0	0	0	0	0	0	0	**0**	0	0	0	0	0	0	0	N/A
	9	0	0	0	0	0	0	0	0	**0**	0	0	0	0	0	0	N/A
	10	0	0	0	0	0	0	0	0	0	**0**	0	0	0	0	0	N/A
	11	0	0	0	0	0	0	0	0	0	0	**0**	0	0	0	0	N/A
	12	0	0	0	0	0	0	0	0	0	0	0	**0**	0	0	0	N/A
	13	0	0	0	0	0	0	0	0	0	0	0	0	**0**	0	0	N/A
	14	0	0	0	0	0	0	0	0	0	0	0	0	0	**0**	0	N/A
	15	22	14	17	0	2	0	1	0	2	0	0	3	26	0	**109**	55.61%
	P.A	42.62%	80.24%	80.77%	0.00%	29.20%	0.00%	61.29%	0.00%	0.00%	0.00%	0.00%	0.00%	0.00%	0.00%	75.69%	**72.16%**

MODIS2 CONFUSION MATRIX (11% SAMPLE)
UK STUDY AREA
DATE:MULTIDATE
DOMINANT CLASS CLASSIFICATION SCHEME

		REFERENCE															
		1	2	3	4	5	6	7	8	9	10	11	12	13	14	15	U.A
CLASSIFIED	1	**555**	140	107	5	6	0	4	0	0	0	0	0	0	1	0	67.85%
	2	296	**4922**	1235	44	24	0	14	0	0	0	0	0	0	4	9	75.17%
	3	188	1084	**6740**	159	189	0	338	0	0	0	4	0	0	1	2	77.43%
	4	0	0	0	**0**	0	0	0	0	0	0	0	0	0	0	0	N/A
	5	2	11	73	4	**188**	0	111	0	0	0	0	0	0	3	0	47.96%
	6	0	0	0	0	0	**0**	0	0	0	0	0	0	0	0	0	N/A
	7	1	11	201	4	55	0	**967**	0	0	0	0	0	0	1	1	77.92%
	8	0	0	0	0	0	0	0	**0**	0	0	0	0	0	0	0	N/A
	9	0	0	0	0	0	0	0	0	**0**	0	0	0	0	0	0	N/A
	10	0	0	0	0	0	0	0	0	0	**0**	0	0	0	0	0	N/A
	11	0	0	0	0	0	0	0	0	0	0	**0**	0	0	0	0	N/A
	12	0	0	0	0	0	0	0	0	0	0	0	**0**	0	0	0	N/A
	13	0	0	0	0	0	0	0	0	0	0	0	0	**0**	0	0	N/A
	14	0	0	0	0	0	0	0	0	0	0	0	0	0	**0**	0	N/A
	15	2	4	3	0	0	0	1	0	0	0	0	0	0	0	**33**	76.74%
	P.A	53.16%	79.75%	80.63%	0.00%	40.69%	N/A	67.39%	N/A	N/A	N/A	0.00%	N/A	N/A	0.00%	73.33%	**75.53%**

MODIS3 CONFUSION MATRIX (11% SAMPLE)
UK STUDY AREA
DATE:13/07/2003
DOMINANT CLASS CLASSIFICATION SCHEME

		REFERENCE															
		1	2	3	4	5	6	7	8	9	10	11	12	13	14	15	U.A
CLASSIFIED	1	**743**	293	232	16	6	1	20	0	8	0	3	10	33	5	47	52.43%
	2	471	**5817**	1561	115	62	1	53	4	4	4	6	13	11	11	35	71.22%
	3	385	1485	**8979**	343	437	8	676	12	16	0	30	2	26	37	31	72.02%
	4	0	0	1	**1**	0	0	0	0	0	0	0	0	0	0	0	50.00%
	5	8	10	93	17	**139**	0	94	5	0	0	2	0	1	7	5	36.48%
	6	0	0	0	0	0	**0**	0	0	0	0	0	0	0	0	0	N/A
	7	5	22	551	3	267	1	**1979**	6	29	0	42	0	1	40	8	66.99%
	8	0	0	0	0	0	0	0	**0**	0	0	0	0	0	0	0	N/A
	9	0	0	0	0	0	0	0	0	**0**	0	0	0	0	0	0	N/A
	10	0	0	0	0	0	0	0	0	0	**0**	0	0	0	0	0	N/A
	11	0	0	0	0	0	0	0	0	0	0	**0**	0	0	0	0	N/A
	12	0	0	0	0	0	0	0	0	0	0	0	**0**	0	0	0	N/A
	13	0	0	0	0	0	0	0	0	0	0	0	0	**0**	0	0	N/A
	14	0	0	0	0	0	0	0	0	0	0	0	0	0	**0**	0	N/A
	15	30	43	47	1	5	0	14	0	5	0	2	5	14	9	**132**	43.00%
	P.A	45.25%	75.84%	78.32%	0.20%	15.17%	0.00%	69.78%	0.00%	0.00%	0.00%	0.00%	0.00%	0.00%	0.00%	51.16%	**69.23%**

MODIS3 CONFUSION MATRIX (11% SAMPLE)
UK STUDY AREA
DATE:16/04/2003
DOMINANT CLASS CLASSIFICATION SCHEME

		REFERENCE															
		1	2	3	4	5	6	7	8	9	10	11	12	13	14	15	U.A
CLASSIFIED	1	**679**	224	164	11	18	0	32	0	5	0	0	4	11	5	17	58.03%
	2	589	**5725**	1849	125	88	5	79	2	9	4	3	12	7	12	18	67.14%
	3	410	2082	**10748**	309	462	13	619	28	13	1	93	9	17	40	43	72.20%
	4	1	5	1	**3**	4	0	1	1	0	0	0	0	0	0	0	18.75%
	5	11	20	112	14	**246**	1	123	17	2	0	8	0	3	12	1	43.16%
	6	0	0	0	0	0	**0**	0	0	0	0	0	0	0	0	0	N/A
	7	37	63	497	15	243	1	**1703**	9	29	0	73	1	7	45	18	62.13%
	8	0	0	0	0	0	0	0	**0**	0	0	0	0	0	0	0	N/A
	9	0	0	0	0	0	0	0	0	**0**	0	0	0	0	0	0	N/A
	10	0	0	0	0	0	0	0	0	0	**0**	0	0	0	0	0	N/A
	11	0	7	53	1	7	0	29	0	0	0	**70**	0	0	0	0	41.92%
	12	0	0	0	0	0	0	0	0	0	0	0	**0**	0	0	0	N/A
	13	6	5	3	0	0	0	1	0	0	0	0	2	**17**	0	1	48.57%
	14	4	7	22	0	4	0	8	0	0	0	1	0	3	**47**	13	43.12%
	15	19	27	29	0	0	0	0	0	2	0	0	3	17	3	**117**	53.92%
	P.A	38.67%	70.12%	79.74%	0.63%	22.95%	0.00%	65.63%	0.00%	0.00%	0.00%	28.23%	0.00%	20.73%	28.66%	51.32%	**68.06%**

MODIS3 CONFUSION MATRIX (11% SAMPLE)
UK STUDY AREA
DATE:17/03/2003
DOMINANT CLASS CLASSIFICATION SCHEME

		REFERENCE															
		1	2	3	4	5	6	7	8	9	10	11	12	13	14	15	U.A
CLASSIFIED	1	**668**	244	216	31	13	0	14	0	5	1	2	7	17	5	12	54.09%
	2	410	**4393**	1170	102	27	1	13	1	4	2	1	10	6	7	3	71.43%
	3	458	1953	**13057**	297	448	25	708	77	38	8	409	12	38	104	47	73.86%
	4	1	10	14	**12**	11	0	7	0	0	0	0	0	1	0	0	21.43%
	5	3	1	114	6	**235**	0	135	17	0	0	2	0	0	6	1	45.19%
	6	0	0	0	0	0	**0**	0	0	0	0	0	0	0	0	0	N/A
	7	21	28	648	46	245	1	**2026**	16	44	1	178	0	5	79	22	60.30%
	8	0	0	0	0	0	0	0	**0**	0	0	0	0	0	0	0	N/A
	9	0	0	0	0	0	0	0	0	**0**	0	0	0	0	0	0	N/A
	10	0	0	0	0	0	0	0	0	0	**0**	0	0	0	0	0	N/A
	11	2	35	117	0	36	5	69	12	3	0	**222**	0	2	7	0	43.53%
	12	0	0	0	0	0	0	0	0	0	0	0	**0**	0	0	0	N/A
	13	9	3	19	1	1	0	1	0	0	0	0	2	**18**	0	16	25.71%
	14	1	1	13	0	0	0	3	1	3	0	1	0	0	**10**	0	30.30%
	15	7	13	8	1	1	0	0	0	1	0	0	3	13	3	**16**	24.24%
	P.A	42.28%	65.75%	84.92%	2.42%	23.11%	0.00%	68.08%	0.00%	0.00%	0.00%	27.24%	0.00%	18.00%	4.52%	13.68%	**69.60%**

MODIS3 CONFUSION MATRIX (11% SAMPLE)
UK STUDY AREA
DATE:18/04/2003
DOMINANT CLASS CLASSIFICATION SCHEME

		REFERENCE															
		1	2	3	4	5	6	7	8	9	10	11	12	13	14	15	U.A
CLASSIFIED	1	**737**	320	221	22	26	0	30	3	7	1	3	11	13	11	30	51.36%
	2	496	**5386**	1656	121	50	1	45	4	1	2	2	13	12	8	28	68.83%
	3	465	2516	**13730**	291	573	19	658	97	32	9	442	3	32	105	45	72.20%
	4	0	0	0	**0**	0	0	0	0	0	0	0	0	0	0	0	N/A
	5	9	31	161	26	**303**	0	126	8	1	0	15	0	3	17	2	43.16%
	6	0	0	0	0	0	**0**	0	0	0	0	0	0	0	0	0	N/A
	7	22	42	771	32	269	0	**2761**	7	66	0	145	1	13	74	17	65.43%
	8	0	0	0	0	0	0	0	**0**	0	0	0	0	0	0	0	N/A
	9	0	0	0	0	0	0	0	0	**0**	0	0	0	0	0	0	N/A
	10	0	0	0	0	0	0	0	0	0	**0**	0	0	0	0	0	N/A
	11	4	54	180	0	57	2	56	18	0	1	**404**	0	3	11	1	51.07%
	12	0	0	0	0	0	0	0	0	0	0	0	**0**	0	0	0	N/A
	13	18	11	23	0	0	0	3	0	2	0	0	2	**22**	0	14	23.16%
	14	5	7	30	1	1	1	13	3	2	1	3	0	8	**86**	14	49.14%
	15	13	20	26	0	3	0	17	0	1	0	0	6	10	0	**48**	33.33%
	P.A	41.66%	64.22%	81.74%	0.00%	23.63%	0.00%	74.44%	0.00%	0.00%	0.00%	39.84%	0.00%	18.97%	27.56%	24.12%	**68.24%**

MODIS3 CONFUSION MATRIX (11% SAMPLE)
UK STUDY AREA
DATE:19/03/2003
DOMINANT CLASS CLASSIFICATION SCHEME

		REFERENCE															
		1	2	3	4	5	6	7	8	9	10	11	12	13	14	15	U.A
CLASSIFIED	1	**576**	170	153	12	3	0	3	0	5	0	0	6	4	5	17	60.38%
	2	544	**5303**	1375	118	49	5	52	2	5	3	3	4	11	11	21	70.65%
	3	406	1395	**8106**	293	388	14	625	17	12	1	68	9	29	26	32	70.97%
	4	1	1	4	**6**	0	0	1	0	0	0	0	0	0	1	0	42.86%
	5	0	19	164	24	**315**	0	127	16	0	0	7	0	1	11	0	46.05%
	6	0	0	0	0	0	**0**	0	0	0	0	0	0	0	0	0	N/A
	7	2	28	479	19	217	0	**1945**	7	17	0	45	1	2	51	14	68.80%
	8	0	0	0	0	0	0	0	**0**	0	0	0	0	0	0	0	N/A
	9	0	0	0	0	0	0	0	0	**0**	0	0	0	0	0	0	N/A
	10	0	0	0	0	0	0	0	0	0	**0**	0	0	0	0	0	N/A
	11	0	0	8	0	11	0	8	2	0	0	**27**	0	0	0	0	48.21%
	12	0	0	0	0	0	0	0	0	0	0	0	**0**	0	0	0	N/A
	13	1	1	0	1	1	0	0	0	1	0	0	1	**10**	0	2	55.56%
	14	0	0	0	0	0	0	0	0	0	0	0	0	0	**0**	0	N/A
	15	8	6	7	0	1	0	17	0	0	0	0	1	7	2	**81**	62.31%
	P.A	37.45%	76.60%	78.73%	1.27%	31.98%	0.00%	70.01%	0.00%	0.00%	0.00%	18.00%	0.00%	15.63%	0.00%	48.50%	**69.33%**

MODIS3 CONFUSION MATRIX (11% SAMPLE)
UK STUDY AREA
DATE:22/03/2003
DOMINANT CLASS CLASSIFICATION SCHEME

CLASSIFIED \ REFERENCE	1	2	3	4	5	6	7	8	9	10	11	12	13	14	15	U.A
1	**639**	264	215	15	7	1	11	0	4	1	1	8	19	2	32	52.42%
2	524	**5259**	1415	107	54	2	45	0	6	4	3	13	8	10	16	70.44%
3	394	1620	**7807**	334	280	7	463	4	9	0	12	5	17	22	29	70.95%
4	0	3	10	**16**	7	1	5	0	0	0	0	0	0	1	0	37.21%
5	5	11	59	7	**130**	0	55	3	0	0	1	0	1	1	0	47.62%
6	0	0	0	0	0	**0**	0	0	0	0	0	0	0	0	0	N/A
7	10	22	248	15	70	0	**521**	2	0	0	6	0	1	7	1	57.70%
8	0	0	0	0	0	0	0	**0**	0	0	0	0	0	0	0	N/A
9	0	0	0	0	0	0	0	0	**0**	0	0	0	0	0	0	N/A
10	0	0	0	0	0	0	0	0	0	**0**	0	0	0	0	0	N/A
11	0	0	0	0	0	0	0	0	0	0	**0**	0	0	0	0	N/A
12	0	0	0	0	0	0	0	0	0	0	0	**0**	0	0	0	N/A
13	0	0	0	0	0	0	0	0	0	0	0	0	**0**	0	0	N/A
14	0	0	0	0	0	0	0	0	0	0	0	0	0	**0**	0	N/A
15	10	5	23	1	0	0	3	0	2	0	0	2	24	1	**87**	55.06%
P.A	40.39%	73.20%	79.85%	3.23%	23.72%	0.00%	47.23%	0.00%	0.00%	0.00%	0.00%	0.00%	0.00%	0.00%	52.73%	**68.64%**

MODIS3 CONFUSION MATRIX (11% SAMPLE)
UK STUDY AREA
DATE:23/03/2003
DOMINANT CLASS CLASSIFICATION SCHEME

		REFERENCE															
		1	2	3	4	5	6	7	8	9	10	11	12	13	14	15	U.A
CLASSIFIED	1	**560**	159	156	21	8	0	18	0	2	0	1	3	3	5	6	59.45%
	2	561	**5724**	1451	90	42	2	38	1	4	3	2	15	13	13	19	71.75%
	3	414	1438	**8650**	314	395	5	666	17	8	1	11	4	5	19	14	72.32%
	4	0	0	0	**5**	0	0	0	0	0	0	0	0	0	0	0	100.00%
	5	10	16	98	19	**244**	0	86	7	1	0	1	0	1	10	2	49.29%
	6	0	0	0	0	0	**0**	0	0	0	0	0	0	0	0	0	N/A
	7	10	14	323	24	136	1	**1114**	8	11	0	10	1	1	7	3	66.99%
	8	0	0	0	0	0	0	0	**0**	0	0	0	0	0	0	0	N/A
	9	0	0	0	0	0	0	0	0	**0**	0	0	0	0	0	0	N/A
	10	0	0	0	0	0	0	0	0	0	**0**	0	0	0	0	0	N/A
	11	0	0	0	0	0	0	0	0	0	0	**0**	0	0	0	0	N/A
	12	0	0	0	0	0	0	0	0	0	0	0	**0**	0	0	0	N/A
	13	4	1	0	0	1	0	0	0	0	0	0	1	**13**	0	5	52.00%
	14	0	0	0	0	0	0	0	0	0	0	0	0	0	**0**	0	N/A
	15	10	11	12	0	2	0	1	0	0	0	0	1	6	1	**97**	68.79%
	P.A	35.69%	77.74%	80.92%	1.06%	29.47%	0.00%	57.93%	0.00%	0.00%	0.00%	0.00%	0.00%	30.95%	0.00%	66.44%	**70.69%**

MODIS3 CONFUSION MATRIX (11% SAMPLE)
UK STUDY AREA
DATE:MULTIDATE
DOMINANT CLASS CLASSIFICATION SCHEME

		REFERENCE															
		1	2	3	4	5	6	7	8	9	10	11	12	13	14	15	U.A
CLASSIFIED	1	**473**	103	84	0	6	0	5	0	0	0	1	0	0	0	8	69.56%
	2	325	**4694**	1141	35	22	0	17	0	0	0	0	0	0	3	5	75.20%
	3	212	1186	**6579**	159	177	0	336	0	0	0	3	0	0	3	2	76.00%
	4	0	0	0	**0**	0	0	0	0	0	0	0	0	0	0	0	N/A
	5	0	8	62	6	**165**	0	50	0	0	0	0	0	0	1	0	56.51%
	6	0	0	0	0	0	**0**	0	0	0	0	0	0	0	0	0	N/A
	7	1	12	183	4	78	0	**1008**	0	0	0	0	0	0	2	0	78.26%
	8	0	0	0	0	0	0	0	**0**	0	0	0	0	0	0	0	N/A
	9	0	0	0	0	0	0	0	0	**0**	0	0	0	0	0	0	N/A
	10	0	0	0	0	0	0	0	0	0	**0**	0	0	0	0	0	N/A
	11	0	0	0	0	0	0	0	0	0	0	**0**	0	0	0	0	N/A
	12	0	0	0	0	0	0	0	0	0	0	0	**0**	0	0	0	N/A
	13	0	0	0	0	0	0	0	0	0	0	0	0	**0**	0	0	N/A
	14	0	0	0	0	0	0	0	0	0	0	0	0	0	**0**	0	N/A
	15	1	0	1	0	3	0	1	0	0	0	0	0	0	0	**22**	78.57%
	P.A	46.74%	78.19%	81.73%	0.00%	36.59%	N/A	71.14%	N/A	N/A	N/A	0.00%	N/A	N/A	0.00%	59.46%	**75.30%**

VEGETATION CONFUSION MATRIX (11% SAMPLE)
UK STUDY AREA
DATE:13/07/2003
DOMINANT CLASS CLASSIFICATION SCHEME

		REFERENCE															
		1	2	3	4	5	6	7	8	9	10	11	12	13	14	15	U.A
CLASSIFIED	1	**642**	159	203	15	1	0	9	0	2	0	0	8	6	4	18	60.17%
	2	469	**6027**	1606	139	62	3	24	7	8	4	2	13	22	9	57	71.31%
	3	519	1491	**8959**	324	545	8	1069	13	15	1	44	9	33	59	90	67.98%
	4	0	0	0	**0**	0	0	0	0	0	0	0	0	0	0	0	N/A
	5	2	19	59	4	**105**	0	98	2	0	0	1	0	0	7	0	35.35%
	6	0	0	0	0	0	**0**	0	0	0	0	0	0	0	0	0	N/A
	7	17	20	647	14	186	0	**1631**	5	35	0	36	0	4	29	8	61.97%
	8	0	0	0	0	0	0	0	**0**	0	0	0	0	0	0	0	N/A
	9	0	0	0	0	0	0	0	0	**0**	0	0	0	0	0	0	N/A
	10	0	0	0	0	0	0	0	0	0	**0**	0	0	0	0	0	N/A
	11	0	0	0	0	0	0	0	0	0	0	**0**	0	0	0	0	N/A
	12	0	0	0	0	0	0	0	0	0	0	0	**0**	0	0	0	N/A
	13	0	0	0	0	0	0	0	0	0	0	0	0	**0**	0	0	N/A
	14	0	0	0	0	0	0	0	0	0	0	0	0	0	**0**	0	N/A
	15	15	7	20	1	2	0	11	0	5	0	0	1	19	2	**94**	53.11%
	P.A	38.58%	78.04%	77.95%	0.00%	11.65%	0.00%	57.39%	0.00%	0.00%	0.00%	0.00%	0.00%	0.00%	0.00%	35.21%	**67.66%**

VEGETATION CONFUSION MATRIX (11% SAMPLE)
UK STUDY AREA
DATE:16/04/2003
DOMINANT CLASS CLASSIFICATION SCHEME

		REFERENCE															
		1	2	3	4	5	6	7	8	9	10	11	12	13	14	15	U.A
CLASSIFIED	1	**561**	153	206	16	28	1	39	2	2	1	5	3	11	7	29	52.73%
	2	630	**5465**	2058	126	117	5	121	4	8	2	20	7	11	5	33	63.46%
	3	486	2437	**10605**	316	615	14	745	37	19	2	156	17	34	67	76	67.87%
	4	0	0	0	**0**	0	0	0	0	0	0	0	0	0	0	0	N/A
	5	0	0	22	2	**38**	0	29	2	1	0	1	0	0	3	0	38.78%
	6	0	0	0	0	0	**0**	0	0	0	0	0	0	0	0	0	N/A
	7	71	98	532	19	262	0	**1673**	12	24	0	67	5	7	60	20	58.70%
	8	0	0	0	0	0	0	0	**0**	0	0	0	0	0	0	0	N/A
	9	0	0	0	0	0	0	0	0	**0**	0	0	0	0	0	0	N/A
	10	0	0	0	0	0	0	0	0	0	**0**	0	0	0	0	0	N/A
	11	0	0	0	0	1	0	0	1	0	0	**4**	0	0	0	0	66.67%
	12	0	0	0	0	0	0	0	0	0	0	0	**0**	0	0	0	N/A
	13	0	0	0	0	0	0	0	0	0	0	0	0	**0**	0	0	N/A
	14	0	0	0	0	0	0	0	0	0	0	0	0	0	**0**	0	N/A
	15	12	8	59	1	0	0	5	0	6	0	1	0	20	21	**71**	34.80%
	P.A	31.88%	66.96%	78.66%	0.00%	3.58%	0.00%	64.05%	0.00%	0.00%	0.00%	1.57%	0.00%	0.00%	0.00%	31.00%	**64.71%**

VEGETATION CONFUSION MATRIX (11% SAMPLE)
UK STUDY AREA
DATE:17/03/2003
DOMINANT CLASS CLASSIFICATION SCHEME

		REFERENCE															
		1	2	3	4	5	6	7	8	9	10	11	12	13	14	15	U.A
CLASSIFIED	1	**441**	129	151	19	19	0	91	1	8	0	12	4	4	11	13	48.84%
	2	447	**3584**	1125	80	95	4	339	6	21	4	123	12	16	17	15	60.87%
	3	633	2790	**13469**	353	682	27	1222	111	42	7	573	18	70	143	77	66.62%
	4	0	0	0	**0**	0	0	0	0	0	0	0	0	0	0	0	N/A
	5	2	1	39	0	**39**	0	22	2	0	0	4	0	0	1	1	35.14%
	6	0	0	0	0	0	**0**	0	0	0	0	0	0	0	0	0	N/A
	7	64	192	627	42	186	1	**1302**	9	30	1	110	0	2	49	5	49.69%
	8	0	0	0	0	0	0	0	**0**	0	0	0	0	0	0	0	N/A
	9	0	0	0	0	0	0	0	0	**0**	0	0	0	0	0	0	N/A
	10	0	0	0	0	0	0	0	0	0	**0**	0	0	0	0	0	N/A
	11	0	0	0	0	0	0	0	0	0	0	**0**	0	0	0	0	N/A
	12	0	0	0	0	0	0	0	0	0	0	0	**0**	0	0	0	N/A
	13	1	4	1	0	0	0	1	0	0	0	0	0	**9**	0	5	42.86%
	14	0	0	0	0	0	0	0	0	0	0	0	0	0	**0**	0	N/A
	15	0	0	0	0	0	0	0	0	0	0	0	0	0	0	**0**	N/A
	P.A	27.77%	53.49%	87.39%	0.00%	3.82%	0.00%	43.74%	0.00%	0.00%	0.00%	0.00%	0.00%	8.91%	0.00%	0.00%	**63.32%**

VEGETATION CONFUSION MATRIX (11% SAMPLE)
UK STUDY AREA
DATE:18/04/2003
DOMINANT CLASS CLASSIFICATION SCHEME

		REFERENCE															
		1	2	3	4	5	6	7	8	9	10	11	12	13	14	15	U.A
CLASSIFIED	1	**456**	188	210	23	94	0	149	4	2	1	14	6	9	13	30	38.03%
	2	701	**4736**	2044	136	170	4	171	4	4	3	16	11	16	21	43	58.61%
	3	581	3269	**13729**	322	716	18	1064	113	38	9	558	16	80	190	128	65.91%
	4	0	0	0	**0**	0	0	0	0	0	0	0	0	0	0	0	N/A
	5	10	12	39	2	**28**	0	17	2	0	0	0	1	0	0	0	25.23%
	6	0	0	0	0	0	**0**	0	0	0	0	0	0	0	0	0	N/A
	7	23	151	670	12	241	0	**2259**	6	59	0	193	2	8	77	7	60.92%
	8	0	0	0	0	0	0	0	**0**	0	0	0	0	0	0	0	N/A
	9	0	0	0	0	0	0	0	0	**0**	0	0	0	0	0	0	N/A
	10	0	0	0	0	0	0	0	0	0	**0**	0	0	0	0	0	N/A
	11	5	42	109	0	23	1	69	9	8	1	**220**	0	1	11	1	44.00%
	12	0	0	0	0	0	0	0	0	0	0	0	**0**	0	0	0	N/A
	13	0	0	0	0	0	0	0	0	0	0	0	0	**0**	0	0	N/A
	14	0	0	0	0	0	0	0	0	0	0	0	0	0	**0**	0	N/A
	15	0	0	0	0	0	0	0	0	0	0	0	0	0	0	**0**	N/A
	P.A	25.68%	56.39%	81.72%	0.00%	2.20%	0.00%	60.58%	0.00%	0.00%	0.00%	21.98%	0.00%	0.00%	0.00%	0.00%	**62.24%**

VEGETATION CONFUSION MATRIX (11% SAMPLE)
UK STUDY AREA
DATE:19/03/2003
DOMINANT CLASS CLASSIFICATION SCHEME

		REFERENCE															
		1	2	3	4	5	6	7	8	9	10	11	12	13	14	15	U.A
CLASSIFIED	1	**454**	183	147	10	17	1	34	0	0	0	2	5	11	7	31	50.33%
	2	527	**4578**	1514	125	123	7	163	3	6	3	4	3	8	11	19	64.53%
	3	492	2049	**8081**	319	573	12	935	27	11	1	56	13	33	39	52	63.67%
	4	0	0	0	**0**	0	0	0	0	0	0	0	0	0	0	0	N/A
	5	6	14	52	2	**67**	0	58	2	0	0	1	0	0	2	0	32.84%
	6	0	0	0	0	0	**0**	0	0	0	0	0	0	0	0	0	N/A
	7	43	119	564	26	220	0	**1615**	13	21	0	85	0	3	47	7	58.45%
	8	0	0	0	0	0	0	0	**0**	0	0	0	0	0	0	0	N/A
	9	0	0	0	0	0	0	0	0	**0**	0	0	0	0	0	0	N/A
	10	0	0	0	0	0	0	0	0	0	**0**	0	0	0	0	0	N/A
	11	0	0	0	0	0	0	0	0	0	0	**0**	0	0	0	0	N/A
	12	0	0	0	0	0	0	0	0	0	0	0	**0**	0	0	0	N/A
	13	0	0	0	0	0	0	0	0	0	0	0	0	**0**	0	0	N/A
	14	0	0	0	0	0	0	0	0	0	0	0	0	0	**0**	0	N/A
	15	17	16	30	1	3	0	11	1	2	0	0	1	11	0	**64**	40.76%
	P.A	29.50%	65.79%	77.79%	0.00%	6.68%	0.00%	57.35%	0.00%	0.00%	0.00%	0.00%	0.00%	0.00%	0.00%	36.99%	**62.40%**

VEGETATION CONFUSION MATRIX (11% SAMPLE)
UK STUDY AREA
DATE:22/03/2003
DOMINANT CLASS CLASSIFICATION SCHEME

		REFERENCE															
		1	2	3	4	5	6	7	8	9	10	11	12	13	14	15	U.A
CLASSIFIED	1	**509**	180	155	15	18	0	30	0	1	0	1	1	2	4	16	54.61%
	2	600	**4699**	1707	142	75	3	165	3	9	5	7	13	17	12	28	62.78%
	3	450	2222	**7665**	323	368	8	598	7	13	0	7	12	49	20	79	64.84%
	4	0	0	0	**0**	0	0	0	0	0	0	0	0	0	0	0	N/A
	5	0	7	23	0	**38**	0	15	0	0	0	1	0	0	1	0	44.71%
	6	0	0	0	0	0	**0**	0	0	0	0	0	0	0	0	0	N/A
	7	5	38	202	11	58	0	**299**	0	0	0	7	0	2	7	3	47.31%
	8	0	0	0	0	0	0	0	**0**	0	0	0	0	0	0	0	N/A
	9	0	0	0	0	0	0	0	0	**0**	0	0	0	0	0	0	N/A
	10	0	0	0	0	0	0	0	0	0	**0**	0	0	0	0	0	N/A
	11	0	0	0	0	0	0	0	0	0	0	**0**	0	0	0	0	N/A
	12	0	0	0	0	0	0	0	0	0	0	0	**0**	0	0	0	N/A
	13	0	0	0	0	0	0	0	0	0	0	0	0	**0**	0	0	N/A
	14	0	0	0	0	0	0	0	0	0	0	0	0	0	**0**	0	N/A
	15	4	5	22	1	2	0	9	0	0	0	0	0	5	0	**21**	30.43%
	P.A	32.46%	65.71%	78.42%	0.00%	6.80%	0.00%	26.79%	0.00%	0.00%	0.00%	0.00%	0.00%	0.00%	0.00%	14.29%	**62.93%**

VEGETATION CONFUSION MATRIX (11% SAMPLE)
UK STUDY AREA
DATE:23/03/2003
DOMINANT CLASS CLASSIFICATION SCHEME

		REFERENCE															
		1	2	3	4	5	6	7	8	9	10	11	12	13	14	15	U.A
CLASSIFIED	1	**388**	137	130	16	23	0	43	1	1	0	1	3	1	3	9	51.32%
	2	562	**4761**	1753	113	143	1	281	8	5	1	4	12	13	17	20	61.88%
	3	596	2310	**8688**	324	543	6	926	23	8	3	10	10	18	24	56	64.14%
	4	0	0	0	**0**	0	0	0	0	0	0	0	0	0	0	0	N/A
	5	1	9	21	0	**32**	0	25	0	0	0	1	0	0	6	0	33.68%
	6	0	0	0	0	0	**0**	0	0	0	0	0	0	0	0	0	N/A
	7	30	144	279	20	94	0	**650**	2	13	0	10	0	1	6	4	51.88%
	8	0	0	0	0	0	0	0	**0**	0	0	0	0	0	0	0	N/A
	9	0	0	0	0	0	0	0	0	**0**	0	0	0	0	0	0	N/A
	10	0	0	0	0	0	0	0	0	0	**0**	0	0	0	0	0	N/A
	11	0	0	0	0	0	0	0	0	0	0	**0**	0	0	0	0	N/A
	12	0	0	0	0	0	0	0	0	0	0	0	**0**	0	0	0	N/A
	13	0	0	0	0	0	0	0	0	0	0	0	0	**0**	0	0	N/A
	14	0	0	0	0	0	0	0	0	0	0	0	0	0	**0**	0	N/A
	15	6	16	33	2	4	0	2	1	1	0	0	0	10	0	**66**	46.81%
	P.A	24.51%	64.54%	79.68%	0.00%	3.81%	0.00%	33.73%	0.00%	0.00%	0.00%	0.00%	0.00%	0.00%	0.00%	42.58%	**62.11%**

VEGETATION CONFUSION MATRIX (11% SAMPLE)
UK STUDY AREA
DATE:MULTIDATE
DOMINANT CLASS CLASSIFICATION SCHEME

		REFERENCE															
		1	2	3	4	5	6	7	8	9	10	11	12	13	14	15	U.A
CLASSIFIED	1	**515**	133	128	1	1	0	9	0	0	0	0	0	0	0	1	65.36%
	2	304	**4845**	1255	45	29	0	24	0	0	0	0	0	0	2	21	74.25%
	3	222	1183	**6718**	170	239	0	458	0	0	0	3	0	0	2	20	74.52%
	4	0	0	0	**0**	0	0	0	0	0	0	0	0	0	0	0	N/A
	5	0	15	66	1	**117**	0	76	0	0	0	1	0	0	2	0	42.09%
	6	0	0	0	0	0	**0**	0	0	0	0	0	0	0	0	0	N/A
	7	6	21	212	3	83	0	**877**	0	0	0	0	0	0	4	2	72.60%
	8	0	0	0	0	0	0	0	**0**	0	0	0	0	0	0	0	N/A
	9	0	0	0	0	0	0	0	0	**0**	0	0	0	0	0	0	N/A
	10	0	0	0	0	0	0	0	0	0	**0**	0	0	0	0	0	N/A
	11	0	0	0	0	0	0	0	0	0	0	**0**	0	0	0	0	N/A
	12	0	0	0	0	0	0	0	0	0	0	0	**0**	0	0	0	N/A
	13	0	0	0	0	0	0	0	0	0	0	0	0	**0**	0	0	N/A
	14	0	0	0	0	0	0	0	0	0	0	0	0	0	**0**	0	N/A
	15	1	3	1	0	1	0	0	0	0	0	0	0	0	0	**6**	50.00%
	P.A	49.14%	78.15%	80.17%	0.00%	24.89%	N/A	60.73%	N/A	N/A	N/A	0.00%	N/A	N/A	0.00%	12.00%	**73.36%**

AVHRR CONFUSION MATRIX (11% SAMPLE)
GREEK STUDY AREA
DATE:03/08/2000
DOMINANT CLASS CLASSIFICATION SCHEME

		REFERENCE															
		1	2	3	4	5	6	7	8	9	10	11	12	13	14	15	U.A
CLASSIFIED	1	**0**	0	0	0	0	0	0	0	0	0	0	0	0	0	0	N/A
	2	0	**6**	1	0	1	2	1	2	2	0	0	0	0	0	0	40.00%
	3	160	179	**5726**	1421	1086	760	230	242	156	673	124	6	2	34	0	53.02%
	4	6	41	222	**333**	101	142	54	71	19	116	11	0	0	0	0	29.84%
	5	0	2	18	12	**34**	12	4	3	2	14	0	0	0	0	0	33.66%
	6	11	82	733	621	361	**1463**	406	455	100	670	23	1	1	0	0	29.69%
	7	0	7	45	23	28	74	**185**	81	14	63	4	0	0	0	0	35.31%
	8	0	0	3	2	2	5	0	**11**	1	1	0	0	0	0	0	44.00%
	9	0	0	1	0	0	0	1	0	**3**	1	0	0	0	0	0	50.00%
	10	0	2	5	10	14	14	8	5	3	**23**	0	0	0	0	0	27.38%
	11	2	8	35	26	19	42	13	13	4	24	**64**	0	0	1	0	25.50%
	12	0	0	0	0	0	0	0	0	0	0	0	**0**	0	0	0	N/A
	13	0	0	0	0	0	0	0	0	0	0	0	0	**0**	0	0	N/A
	14	0	0	0	0	0	0	0	0	0	0	0	0	0	**0**	0	N/A
	15	0	0	0	0	0	0	0	0	0	0	0	0	0	0	**0**	N/A
	P.A	0.00%	1.83%	84.34%	13.60%	2.07%	58.19%	20.51%	1.25%	0.99%	1.45%	28.32%	0.00%	0.00%	0.00%	N/A	**43.97%**

AVHRR CONFUSION MATRIX (11% SAMPLE)
GREEK STUDY AREA
DATE:03/10/2001
DOMINANT CLASS CLASSIFICATION SCHEME

		REFERENCE															
		1	2	3	4	5	6	7	8	9	10	11	12	13	14	15	U.A
CLASSIFIED	1	**11**	3	6	0	11	0	2	0	1	2	0	0	0	0	0	30.56%
	2	0	**0**	0	0	0	0	0	0	0	0	0	0	0	0	0	N/A
	3	131	266	**5766**	1407	1293	602	211	195	223	672	53	7	0	30	1	53.11%
	4	9	91	482	**860**	217	298	192	191	80	317	13	0	0	5	0	31.22%
	5	14	11	85	50	**122**	17	2	1	10	24	6	0	0	1	0	35.57%
	6	9	23	409	288	209	**1688**	204	359	67	446	4	3	0	0	0	45.51%
	7	1	29	73	111	48	109	**466**	178	22	126	8	0	0	0	0	39.80%
	8	1	0	21	11	5	17	16	**42**	0	10	0	0	0	0	0	34.15%
	9	0	0	0	0	0	0	0	0	**0**	0	0	0	0	0	0	N/A
	10	1	2	26	23	13	27	11	8	5	**40**	5	0	0	1	0	24.69%
	11	3	6	83	40	15	4	15	13	2	11	**111**	0	0	3	0	36.27%
	12	0	0	0	0	0	0	0	0	0	0	0	**0**	0	0	0	N/A
	13	0	0	0	0	0	0	0	0	0	0	0	0	**0**	0	0	N/A
	14	0	0	0	0	0	0	0	0	0	0	0	0	0	**0**	0	N/A
	15	0	0	0	0	0	0	0	0	0	0	0	0	0	0	**0**	N/A
	P.A	6.11%	0.00%	82.95%	30.82%	6.31%	61.12%	41.64%	4.26%	0.00%	2.43%	55.50%	0.00%	N/A	0.00%	0.00%	**46.79%**

AVHRR CONFUSION MATRIX (11% SAMPLE)
GREEK STUDY AREA
DATE:04/05/2001
DOMINANT CLASS CLASSIFICATION SCHEME

		REFERENCE															
		1	2	3	4	5	6	7	8	9	10	11	12	13	14	15	U.A
CLASSIFIED	1	**14**	3	5	1	7	0	0	0	1	2	1	0	0	1	1	38.89%
	2	0	**5**	2	2	0	1	0	2	1	3	0	0	0	0	0	31.25%
	3	142	204	**5480**	1083	1075	784	185	198	164	612	68	3	3	23	0	54.67%
	4	4	74	393	**914**	223	261	241	223	91	289	12	2	0	3	0	33.48%
	5	1	9	85	44	**138**	69	12	8	14	65	3	0	0	1	0	30.73%
	6	8	23	426	298	249	**1336**	93	246	47	470	7	1	0	1	0	41.68%
	7	2	29	45	90	37	39	**221**	128	24	97	6	0	0	1	0	30.74%
	8	0	0	5	14	0	11	13	**32**	2	8	0	0	0	0	0	37.65%
	9	0	0	2	0	0	0	0	0	**1**	0	0	0	0	0	0	33.33%
	10	0	3	14	13	22	22	8	7	1	**40**	1	0	0	0	0	30.53%
	11	3	4	33	23	12	17	9	10	2	9	**115**	2	0	4	1	47.13%
	12	0	0	0	0	0	0	0	0	0	0	0	**0**	0	0	0	N/A
	13	0	0	0	0	0	0	0	0	0	0	0	0	**0**	0	0	N/A
	14	0	0	0	0	0	0	0	0	0	0	0	0	0	**0**	0	N/A
	15	0	0	0	0	0	0	0	0	0	0	0	0	0	0	**0**	N/A
	P.A	8.05%	1.41%	84.44%	36.83%	7.83%	52.60%	28.26%	3.75%	0.29%	2.51%	53.99%	0.00%	0.00%	0.00%	0.00%	**47.02%**

AVHRR CONFUSION MATRIX (11% SAMPLE)
GREEK STUDY AREA
DATE:04/07/2000
DOMINANT CLASS CLASSIFICATION SCHEME

		REFERENCE															
		1	2	3	4	5	6	7	8	9	10	11	12	13	14	15	U.A
CLASSIFIED	1	**12**	1	9	3	2	0	0	0	0	0	0	0	0	1	0	42.86%
	2	0	**1**	1	0	0	0	0	0	0	1	0	0	0	0	0	33.33%
	3	150	302	**5698**	1699	1366	906	439	410	261	968	134	5	2	29	1	46.06%
	4	2	53	433	**663**	134	158	160	115	39	184	18	1	0	2	0	33.79%
	5	0	0	11	9	**23**	6	0	2	1	3	0	0	0	0	0	41.82%
	6	8	37	441	206	239	**1580**	235	342	55	410	4	1	0	1	0	44.39%
	7	1	3	73	55	28	67	**210**	65	12	51	8	0	0	0	0	36.65%
	8	0	0	2	2	2	3	3	**8**	0	6	0	0	0	0	0	30.77%
	9	0	0	0	1	0	0	0	0	**0**	0	0	0	0	0	0	0.00%
	10	0	5	21	21	16	23	7	8	8	**40**	1	0	0	0	0	26.67%
	11	2	1	27	15	5	1	2	3	0	2	**49**	0	0	1	0	45.37%
	12	0	0	0	0	0	0	0	0	0	0	0	**0**	0	0	0	N/A
	13	0	0	0	0	0	0	0	0	0	0	0	0	**0**	0	0	N/A
	14	0	0	0	0	0	0	0	0	0	0	0	0	0	**0**	0	N/A
	15	0	0	0	0	0	0	0	0	0	0	0	0	0	0	**0**	N/A
	P.A	6.86%	0.25%	84.84%	24.79%	1.27%	57.58%	19.89%	0.84%	0.00%	2.40%	22.90%	0.00%	0.00%	0.00%	0.00%	**43.98%**

AVHRR CONFUSION MATRIX (11% SAMPLE)
GREEK STUDY AREA
DATE:05/06/2000
DOMINANT CLASS CLASSIFICATION SCHEME

		REFERENCE															
		1	2	3	4	5	6	7	8	9	10	11	12	13	14	15	U.A
CLASSIFIED	1	**10**	1	13	10	9	0	1	1	0	0	3	0	0	0	0	20.83%
	2	0	**5**	1	1	0	0	1	0	0	0	0	0	0	0	0	62.50%
	3	114	185	**4948**	1385	1005	741	218	178	113	561	87	7	1	26	2	51.70%
	4	5	87	352	**719**	194	106	166	143	93	207	10	0	0	0	0	34.53%
	5	0	7	18	17	**32**	8	9	4	2	6	0	0	0	0	0	31.07%
	6	12	25	496	204	247	**1290**	169	340	68	479	9	0	0	1	0	38.62%
	7	3	36	42	53	34	45	**193**	96	25	84	0	0	0	0	0	31.59%
	8	2	2	28	11	10	43	38	**54**	7	26	1	0	0	0	0	24.32%
	9	0	0	0	0	0	0	0	0	**0**	0	0	0	0	0	0	N/A
	10	1	7	28	27	24	36	20	31	1	**62**	0	0	0	0	0	26.16%
	11	0	1	11	0	0	1	2	1	0	0	**21**	0	0	0	0	56.76%
	12	0	0	0	0	0	0	0	0	0	0	0	**0**	0	0	0	N/A
	13	0	0	0	0	0	0	0	0	0	0	0	0	**0**	0	0	N/A
	14	0	0	0	0	0	0	0	0	0	0	0	0	0	**0**	0	N/A
	15	0	0	0	0	0	0	0	0	0	0	0	0	0	0	**0**	N/A
	P.A	6.80%	1.40%	83.34%	29.63%	2.06%	56.83%	23.62%	6.37%	0.00%	4.35%	16.03%	0.00%	0.00%	0.00%	0.00%	**45.11%**

AVHRR CONFUSION MATRIX (11% SAMPLE)
GREEK STUDY AREA
DATE:07/07/2000
DOMINANT CLASS CLASSIFICATION SCHEME

		REFERENCE															
		1	2	3	4	5	6	7	8	9	10	11	12	13	14	15	U.A
CLASSIFIED	1	**12**	5	6	0	2	0	0	0	1	0	2	0	0	0	0	42.86%
	2	0	**3**	0	2	0	0	0	0	0	1	0	0	0	0	0	50.00%
	3	163	258	**5824**	1367	1209	806	210	194	177	659	109	7	2	27	1	52.88%
	4	6	80	491	**951**	195	158	187	187	82	272	31	0	0	3	0	35.98%
	5	5	10	67	22	**89**	4	6	3	4	8	2	0	0	3	0	39.91%
	6	11	40	568	271	323	**1783**	301	426	84	553	12	1	0	4	0	40.74%
	7	1	32	73	96	47	88	**380**	136	18	135	6	0	0	0	0	37.55%
	8	0	0	4	4	1	3	3	**9**	2	3	1	0	0	0	0	30.00%
	9	0	2	0	0	0	0	0	0	**2**	0	0	0	0	0	0	50.00%
	10	1	2	21	25	17	24	9	14	2	**57**	0	0	0	0	0	33.14%
	11	1	0	39	15	4	8	10	7	1	9	**71**	2	0	2	0	42.01%
	12	0	0	0	0	0	0	0	0	0	0	0	**0**	0	0	0	N/A
	13	0	0	0	0	0	0	0	0	0	0	0	0	**0**	0	0	N/A
	14	0	0	0	0	0	0	0	0	0	0	0	0	0	**0**	0	N/A
	15	0	0	0	0	0	0	0	0	0	0	0	0	0	0	**0**	N/A
	P.A	6.00%	0.69%	82.11%	34.54%	4.72%	62.04%	34.36%	0.92%	0.54%	3.36%	30.34%	0.00%	0.00%	0.00%	0.00%	**46.66%**

AVHRR CONFUSION MATRIX (11% SAMPLE)
GREEK STUDY AREA
DATE:13/04/2000
DOMINANT CLASS CLASSIFICATION SCHEME

		REFERENCE															
		1	2	3	4	5	6	7	8	9	10	11	12	13	14	15	U.A
CLASSIFIED	1	**0**	0	0	0	0	0	0	0	0	0	0	0	0	0	0	N/A
	2	0	**0**	1	1	0	0	1	0	0	0	0	0	0	0	0	0.00%
	3	98	85	**4520**	1098	709	920	232	297	132	581	116	7	0	18	3	51.27%
	4	5	26	308	**492**	107	185	141	142	60	147	13	0	0	0	0	30.26%
	5	0	2	11	2	**24**	5	0	3	0	6	0	0	0	0	0	45.28%
	6	7	55	414	284	245	**749**	131	194	54	354	22	1	1	0	0	29.83%
	7	0	12	39	59	19	47	**148**	81	19	63	2	0	0	0	0	30.27%
	8	0	0	1	3	3	7	3	**10**	1	7	0	0	0	0	0	28.57%
	9	0	0	0	0	0	0	0	0	**2**	0	0	0	0	0	0	100.00%
	10	0	2	15	15	9	22	3	8	4	**39**	1	0	0	0	0	33.05%
	11	0	0	0	0	0	0	0	0	0	0	**0**	0	0	0	0	N/A
	12	0	0	0	0	0	0	0	0	0	0	0	**0**	0	0	0	N/A
	13	0	0	0	0	0	0	0	0	0	0	0	0	**0**	0	0	N/A
	14	0	0	0	0	0	0	0	0	0	0	0	0	0	**0**	0	N/A
	15	0	0	0	0	0	0	0	0	0	0	0	0	0	0	**0**	N/A
	P.A	0.00%	0.00%	85.14%	25.18%	2.15%	38.71%	22.46%	1.36%	0.74%	3.26%	0.00%	0.00%	0.00%	0.00%	0.00%	**43.83%**

AVHRR CONFUSION MATRIX (11% SAMPLE)
GREEK STUDY AREA
DATE:14/06/2000
DOMINANT CLASS CLASSIFICATION SCHEME

		REFERENCE															
		1	2	3	4	5	6	7	8	9	10	11	12	13	14	15	U.A
CLASSIFIED	1	**0**	0	0	0	0	0	0	0	0	0	0	0	0	0	0	N/A
	2	0	**5**	4	0	0	0	2	0	1	1	0	0	0	0	0	38.46%
	3	105	92	**4239**	1079	669	553	197	207	122	409	65	4	2	27	0	54.56%
	4	10	80	462	**783**	221	117	167	152	59	188	15	0	0	1	0	34.72%
	5	1	21	34	34	**72**	6	17	8	8	24	2	0	0	0	0	31.72%
	6	5	16	251	120	133	**723**	98	234	44	303	6	0	0	0	0	37.40%
	7	1	60	87	123	71	61	**353**	140	50	131	0	0	0	0	0	32.78%
	8	4	1	52	37	15	69	74	**112**	18	32	1	0	0	0	0	26.99%
	9	0	0	3	2	1	0	0	0	**3**	0	0	0	0	0	0	33.33%
	10	0	9	23	10	16	21	13	10	2	**42**	0	0	0	0	0	28.77%
	11	0	0	0	0	0	0	0	0	0	0	**0**	0	0	0	0	N/A
	12	0	0	0	0	0	0	0	0	0	0	0	**0**	0	0	0	N/A
	13	0	0	0	0	0	0	0	0	0	0	0	0	**0**	0	0	N/A
	14	0	0	0	0	0	0	0	0	0	0	0	0	0	**0**	0	N/A
	15	0	0	0	0	0	0	0	0	0	0	0	0	0	0	**0**	N/A
	P.A	0.00%	1.76%	82.23%	35.79%	6.01%	46.65%	38.33%	12.98%	0.98%	3.72%	0.00%	0.00%	0.00%	0.00%	N/A	**45.73%**

AVHRR CONFUSION MATRIX (11% SAMPLE)
GREEK STUDY AREA
DATE:20/08/2000
DOMINANT CLASS CLASSIFICATION SCHEME

		REFERENCE															
		1	2	3	4	5	6	7	8	9	10	11	12	13	14	15	U.A
CLASSIFIED	1	**0**	0	0	0	0	0	0	0	0	0	0	0	0	0	0	N/A
	2	0	**2**	0	0	0	0	0	0	1	0	0	0	0	0	0	66.67%
	3	159	237	**5749**	1631	1274	1077	231	208	168	796	159	10	2	32	0	49.00%
	4	9	99	435	**756**	215	186	188	173	78	259	21	0	0	0	0	31.25%
	5	4	21	100	79	**151**	22	15	7	17	31	8	0	0	0	0	33.19%
	6	9	29	512	213	221	**1403**	205	356	83	435	15	0	0	0	0	40.30%
	7	4	47	106	97	47	69	**470**	177	34	119	5	0	0	0	0	40.00%
	8	1	7	31	16	15	60	51	**69**	10	20	0	0	0	0	0	24.64%
	9	0	0	0	0	0	0	0	0	**0**	0	0	0	0	0	0	N/A
	10	0	2	30	16	15	22	14	10	5	**45**	0	0	0	0	0	28.30%
	11	0	0	9	3	3	0	0	0	1	2	**10**	0	0	0	0	35.71%
	12	0	0	0	0	0	0	0	0	0	0	0	**0**	0	0	0	N/A
	13	0	0	0	0	0	0	0	0	0	0	0	0	**0**	0	0	N/A
	14	0	0	0	0	0	0	0	0	0	0	0	0	0	**0**	0	N/A
	15	0	0	0	0	0	0	0	0	0	0	0	0	0	0	**0**	N/A
	P.A	0.00%	0.45%	82.46%	26.89%	7.78%	49.42%	40.03%	6.90%	0.00%	2.64%	4.59%	0.00%	0.00%	0.00%	N/A	**43.86%**

AVHRR CONFUSION MATRIX (11% SAMPLE)
GREEK STUDY AREA
DATE:23/10/2000
DOMINANT CLASS CLASSIFICATION SCHEME

		REFERENCE															
		1	2	3	4	5	6	7	8	9	10	11	12	13	14	15	U.A
CLASSIFIED	1	**4**	0	2	0	0	0	1	0	0	1	0	0	0	0	0	50.00%
	2	0	**0**	0	0	0	0	0	0	0	0	0	0	0	0	0	N/A
	3	92	151	**3926**	1314	886	877	257	302	133	680	165	9	1	34	0	44.48%
	4	3	63	334	**620**	149	275	166	160	58	224	11	0	1	1	0	30.02%
	5	2	10	37	25	**46**	11	6	8	4	15	3	0	0	0	0	27.54%
	6	3	23	205	193	85	**379**	53	98	31	164	8	0	0	1	0	30.49%
	7	1	23	46	86	47	57	**141**	80	21	76	3	0	0	0	0	24.27%
	8	0	2	11	8	5	9	10	**19**	2	9	0	0	0	0	0	25.33%
	9	0	0	0	0	0	0	0	0	**0**	0	0	0	0	0	0	N/A
	10	0	3	19	21	9	13	10	7	4	**24**	0	0	0	0	0	21.82%
	11	0	0	0	2	0	0	0	0	0	0	**0**	0	0	0	0	0.00%
	12	0	0	0	0	0	0	0	0	0	0	0	**0**	0	0	0	N/A
	13	0	0	0	0	0	0	0	0	0	0	0	0	**0**	0	0	N/A
	14	0	0	0	0	0	0	0	0	0	0	0	0	0	**0**	0	N/A
	15	0	0	0	0	0	0	0	0	0	0	0	0	0	0	**0**	N/A
	P.A	3.81%	0.00%	85.72%	27.32%	3.75%	23.38%	21.89%	2.82%	0.00%	2.01%	0.00%	0.00%	0.00%	0.00%	N/A	**39.45%**

AVHRR CONFUSION MATRIX (11% SAMPLE)
GREEK STUDY AREA
DATE:24/03/2001
DOMINANT CLASS CLASSIFICATION SCHEME

		REFERENCE															
		1	2	3	4	5	6	7	8	9	10	11	12	13	14	15	U.A
CLASSIFIED	1	**0**	0	0	0	0	0	0	0	0	0	0	0	0	0	0	N/A
	2	0	**0**	0	0	0	0	0	0	0	0	0	0	0	0	0	N/A
	3	116	185	**5295**	1451	1109	869	304	291	177	642	177	8	2	32	1	49.68%
	4	12	37	363	**653**	116	164	147	173	54	175	8	1	0	1	0	34.30%
	5	0	0	20	13	**23**	10	7	3	1	8	0	0	0	1	0	26.74%
	6	13	57	633	305	341	**1590**	228	263	73	661	34	0	0	1	0	37.87%
	7	3	22	118	133	48	79	**308**	136	23	106	11	0	0	1	0	31.17%
	8	1	0	4	2	1	3	4	**12**	0	4	0	0	0	0	0	38.71%
	9	1	0	2	0	0	1	0	0	**2**	0	0	0	0	0	0	33.33%
	10	0	1	18	23	9	19	15	9	5	**42**	2	0	0	0	0	29.37%
	11	0	0	0	0	0	0	0	0	0	0	**0**	0	0	0	0	N/A
	12	0	0	0	0	0	0	0	0	0	0	0	**0**	0	0	0	N/A
	13	0	0	0	0	0	0	0	0	0	0	0	0	**0**	0	0	N/A
	14	0	0	0	0	0	0	0	0	0	0	0	0	0	**0**	0	N/A
	15	0	0	0	0	0	0	0	0	0	0	0	0	0	0	**0**	N/A
	P.A	0.00%	0.00%	82.05%	25.31%	1.40%	58.14%	30.40%	1.35%	0.60%	2.56%	0.00%	0.00%	0.00%	0.00%	0.00%	**43.99%**

AVHRR CONFUSION MATRIX (11% SAMPLE)
GREEK STUDY AREA
DATE:25/10/2000
DOMINANT CLASS CLASSIFICATION SCHEME

		REFERENCE															
		1	2	3	4	5	6	7	8	9	10	11	12	13	14	15	U.A
CLASSIFIED	1	**0**	0	0	0	0	0	0	0	0	0	0	0	0	0	0	N/A
	2	0	**6**	1	0	1	2	1	2	2	0	0	0	0	0	0	40.00%
	3	160	179	**5726**	1421	1086	760	230	242	156	673	124	6	2	34	0	53.02%
	4	6	41	222	**333**	101	142	54	71	19	116	11	0	0	0	0	29.84%
	5	0	2	18	12	**34**	12	4	3	2	14	0	0	0	0	0	33.66%
	6	11	82	733	621	361	**1463**	406	455	100	670	23	1	1	0	0	29.69%
	7	0	7	45	23	28	74	**185**	81	14	63	4	0	0	0	0	35.31%
	8	0	0	3	2	2	5	0	**11**	1	1	0	0	0	0	0	44.00%
	9	0	0	1	0	0	0	1	0	**3**	1	0	0	0	0	0	50.00%
	10	0	2	5	10	14	14	8	5	3	**23**	0	0	0	0	0	27.38%
	11	2	8	35	26	19	42	13	13	4	24	**64**	0	0	1	0	25.50%
	12	0	0	0	0	0	0	0	0	0	0	0	**0**	0	0	0	N/A
	13	0	0	0	0	0	0	0	0	0	0	0	0	**0**	0	0	N/A
	14	0	0	0	0	0	0	0	0	0	0	0	0	0	**0**	0	N/A
	15	0	0	0	0	0	0	0	0	0	0	0	0	0	0	**0**	N/A
	P.A	0.00%	1.83%	84.34%	13.60%	2.07%	58.19%	20.51%	1.25%	0.99%	1.45%	28.32%	0.00%	0.00%	0.00%	N/A	**43.97%**

AVHRR CONFUSION MATRIX (11% SAMPLE)
GREEK STUDY AREA
DATE:MULTIDATE
DOMINANT CLASS CLASSIFICATION SCHEME

		REFERENCE															
		1	2	3	4	5	6	7	8	9	10	11	12	13	14	15	U.A
CLASSIFIED	1	**2**	0	1	0	0	0	0	0	0	0	0	0	0	0	0	66.67%
	2	0	**2**	2	1	1	5	0	0	0	1	0	0	0	0	0	16.67%
	3	81	112	**3600**	680	670	382	101	115	108	399	34	1	2	13	0	57.16%
	4	6	50	396	**857**	167	148	156	154	86	260	19	1	0	1	0	37.24%
	5	0	2	16	11	**17**	22	3	6	0	12	0	0	0	1	0	18.89%
	6	11	25	307	180	172	**1411**	106	258	41	383	3	1	0	0	0	48.69%
	7	1	26	38	60	18	33	**212**	101	14	76	5	0	0	1	0	36.24%
	8	0	2	20	23	5	20	28	**57**	3	14	0	0	0	0	0	33.14%
	9	0	0	0	0	0	0	0	0	**0**	0	0	0	0	0	0	N/A
	10	0	3	47	36	31	56	14	22	10	**98**	1	0	0	0	0	30.82%
	11	1	2	15	12	4	3	5	2	2	2	**96**	0	0	1	0	66.21%
	12	0	0	0	0	0	0	0	0	0	0	0	**0**	0	0	0	N/A
	13	0	0	0	0	0	0	0	0	0	0	0	0	**0**	0	0	N/A
	14	0	0	0	0	0	0	0	0	0	0	0	0	0	**0**	0	N/A
	15	0	0	0	0	0	0	0	0	0	0	0	0	0	0	**0**	N/A
	P.A	1.96%	0.89%	81.04%	46.08%	1.57%	67.84%	33.92%	7.97%	0.00%	7.87%	60.76%	0.00%	0.00%	0.00%	N/A	**49.54%**

MODIS1 CONFUSION MATRIX (11% SAMPLE)
GREEK STUDY AREA
DATE:03/08/2000
DOMINANT CLASS CLASSIFICATION SCHEME

		REFERENCE															
		1	2	3	4	5	6	7	8	9	10	11	12	13	14	15	U.A
CLASSIFIED	1	**2**	1	0	1	0	0	1	0	2	0	0	0	0	0	0	28.57%
	2	267	**5621**	1338	1177	609	207	183	181	649	103	10	1	31	0	0	54.17%
	3	40	394	**733**	160	134	134	147	48	205	15	0	0	3	0	0	36.41%
	4	13	91	39	**99**	5	9	2	7	10	0	1	0	0	0	0	35.87%
	5	24	532	248	189	**1574**	146	365	57	492	11	0	0	1	0	0	43.25%
	6	6	77	58	18	50	**383**	90	5	76	6	0	0	0	0	0	49.80%
	7	2	33	13	6	34	39	**62**	4	22	1	0	0	0	0	0	28.70%
	8	0	0	0	1	0	0	0	**1**	0	0	0	0	0	0	0	50.00%
	9	2	27	33	8	25	17	20	4	**68**	1	0	0	0	0	0	33.17%
	10	0	0	0	0	0	0	0	0	0	**1**	0	0	0	0	0	100.00%
	11	0	0	0	0	0	0	0	0	0	0	**0**	0	0	0	0	N/A
	12	0	0	0	0	0	0	0	0	0	0	0	**0**	0	0	0	N/A
	13	0	0	0	0	0	0	0	0	0	0	0	0	**0**	0	0	N/A
	14	0	0	0	0	0	0	0	0	0	0	0	0	0	**0**	0	N/A
	15	0	0	0	0	0	0	0	0	0	0	0	0	0	0	**0**	N/A
	P.A	0.56%	82.95%	29.77%	5.97%	64.75%	40.96%	7.13%	0.33%	4.46%	0.72%	0.00%	0.00%	0.00%	N/A	N/A	**48.81%**

MODIS1 CONFUSION MATRIX (11% SAMPLE)
GREEK STUDY AREA
DATE:03/10/2001
DOMINANT CLASS CLASSIFICATION SCHEME

		REFERENCE															
		1	2	3	4	5	6	7	8	9	10	11	12	13	14	15	U.A
CLASSIFIED	1	**3**	3	3	1	1	1	0	0	1	0	0	0	0	0	0	23.08%
	2	334	**5812**	1689	1444	679	246	206	242	768	94	8	0	30	1	0	50.31%
	3	27	299	**535**	135	203	75	121	41	195	9	0	0	4	0	0	32.54%
	4	1	44	31	**54**	14	5	1	10	19	2	0	0	0	0	0	29.83%
	5	38	557	393	205	**1690**	204	405	86	462	8	1	0	0	0	0	41.74%
	6	23	107	76	47	91	**514**	173	24	115	11	0	0	0	0	0	43.52%
	7	1	23	14	12	50	46	**65**	0	18	1	0	0	0	0	0	28.26%
	8	0	1	2	0	1	0	1	**2**	2	0	0	0	0	0	0	22.22%
	9	1	27	32	21	23	14	17	7	**62**	1	0	0	0	0	0	30.24%
	10	2	70	24	11	2	6	6	1	1	**73**	0	0	5	0	0	36.32%
	11	0	0	0	0	0	0	0	0	0	0	**0**	0	0	0	0	N/A
	12	0	0	0	0	0	0	0	0	0	0	0	**0**	0	0	0	N/A
	13	0	0	0	0	0	0	0	0	0	0	0	0	**0**	0	0	N/A
	14	0	0	0	0	0	0	0	0	0	0	0	0	0	**0**	0	N/A
	15	0	0	0	0	0	0	0	0	0	0	0	0	0	0	**0**	N/A
	P.A	0.70%	83.71%	19.11%	2.80%	61.37%	46.26%	6.53%	0.48%	3.77%	36.68%	0.00%	N/A	0.00%	0.00%	N/A	**45.73%**

MODIS1 CONFUSION MATRIX (11% SAMPLE)
GREEK STUDY AREA
DATE:04/05/2001
DOMINANT CLASS CLASSIFICATION SCHEME

		REFERENCE															
		1	2	3	4	5	6	7	8	9	10	11	12	13	14	15	U.A
CLASSIFIED	1	**10**	1	5	8	0	2	0	3	5	0	0	0	0	0	0	29.41%
	2	240	**5279**	1173	1171	694	208	169	169	627	126	5	2	28	2	0	53.36%
	3	46	270	**632**	179	257	128	130	58	221	9	2	0	0	0	0	32.71%
	4	6	51	34	**71**	30	4	4	6	23	4	0	0	0	0	0	30.47%
	5	18	666	435	200	**1426**	137	356	62	501	15	0	0	0	0	0	37.37%
	6	12	70	84	34	38	**212**	105	7	88	12	0	0	0	0	0	32.02%
	7	1	10	6	3	26	28	**48**	3	16	2	1	0	0	0	0	33.33%
	8	0	2	2	2	2	1	0	**5**	2	0	0	0	0	0	0	31.25%
	9	4	40	41	30	40	29	20	12	**85**	1	0	1	2	0	0	27.87%
	10	3	28	8	5	1	5	2	0	3	**50**	0	0	4	0	0	45.87%
	11	0	0	0	0	0	0	0	0	0	0	**0**	0	0	0	0	N/A
	12	0	0	0	0	0	0	0	0	0	0	0	**0**	0	0	0	N/A
	13	0	0	0	0	0	0	0	0	0	0	0	0	**0**	0	0	N/A
	14	0	0	0	0	0	0	0	0	0	0	0	0	0	**0**	0	N/A
	15	0	0	0	0	0	0	0	0	0	0	0	0	0	0	**0**	N/A
	P.A	2.94%	82.27%	26.12%	4.17%	56.72%	28.12%	5.76%	1.54%	5.41%	22.83%	0.00%	0.00%	0.00%	0.00%	N/A	**45.60%**

MODIS1 CONFUSION MATRIX (11% SAMPLE)
GREEK STUDY AREA
DATE:04/07/2000
DOMINANT CLASS CLASSIFICATION SCHEME

		REFERENCE															
		1	2	3	4	5	6	7	8	9	10	11	12	13	14	15	U.A
CLASSIFIED	1	**5**	1	0	1	0	1	1	0	1	0	0	0	0	0	0	50.00%
	2	278	**5438**	1311	1210	653	238	150	195	682	101	5	1	26	0	0	52.86%
	3	72	503	**1007**	177	126	215	205	87	249	25	0	1	3	0	0	37.72%
	4	4	43	15	**78**	19	5	1	3	16	1	1	0	0	0	0	41.94%
	5	31	620	234	294	**1863**	152	400	67	591	7	0	0	1	0	0	43.73%
	6	5	54	55	20	52	**379**	117	9	78	10	0	0	0	0	0	48.65%
	7	1	24	12	5	45	48	**77**	12	24	1	0	0	0	0	0	30.92%
	8	0	0	0	0	0	0	1	**1**	1	0	0	0	0	0	0	33.33%
	9	3	15	12	8	12	14	5	4	**47**	0	0	0	0	0	0	39.17%
	10	9	71	39	17	1	3	9	6	10	**87**	1	0	4	1	0	33.72%
	11	0	0	0	0	0	0	0	0	0	0	**0**	0	0	0	0	N/A
	12	0	0	0	0	0	0	0	0	0	0	0	**0**	0	0	0	N/A
	13	0	0	0	0	0	0	0	0	0	0	0	0	**0**	0	0	N/A
	14	0	0	0	0	0	0	0	0	0	0	0	0	0	**0**	0	N/A
	15	0	0	0	0	0	0	0	0	0	0	0	0	0	0	**0**	N/A
	P.A	1.23%	80.34%	37.50%	4.31%	67.23%	35.92%	7.97%	0.26%	2.77%	37.50%	0.00%	0.00%	0.00%	0.00%	N/A	**47.72%**

MODIS1 CONFUSION MATRIX (11% SAMPLE)
GREEK STUDY AREA
DATE:05/06/2000
DOMINANT CLASS CLASSIFICATION SCHEME

		REFERENCE															
		1	2	3	4	5	6	7	8	9	10	11	12	13	14	15	U.A
CLASSIFIED	1	**19**	9	6	12	5	3	1	3	3	0	0	0	0	0	0	31.15%
	2	273	**4837**	1518	1132	578	354	250	191	660	51	6	0	20	2	0	49.00%
	3	25	373	**592**	128	82	98	107	51	143	1	1	1	5	0	0	36.84%
	4	10	26	23	**50**	15	3	2	2	12	1	0	0	0	0	0	34.72%
	5	21	467	182	193	**1509**	188	383	49	496	9	0	0	0	0	0	43.15%
	6	1	51	25	8	24	**124**	44	3	34	6	0	0	0	0	0	38.75%
	7	1	44	21	14	39	32	**57**	5	27	0	0	0	0	0	0	23.75%
	8	0	1	5	1	0	0	0	**4**	2	0	0	0	0	0	0	30.77%
	9	0	32	16	12	20	5	2	3	**43**	1	0	0	0	0	0	32.09%
	10	3	35	18	7	2	2	0	0	1	**57**	0	0	2	0	0	44.88%
	11	0	0	0	0	0	0	0	0	0	0	**0**	0	0	0	0	N/A
	12	0	0	0	0	0	0	0	0	0	0	0	**0**	0	0	0	N/A
	13	0	0	0	0	0	0	0	0	0	0	0	0	**0**	0	0	N/A
	14	0	0	0	0	0	0	0	0	0	0	0	0	0	**0**	0	N/A
	15	0	0	0	0	0	0	0	0	0	0	0	0	0	0	**0**	N/A
	P.A	5.38%	82.33%	24.61%	3.21%	66.36%	15.33%	6.74%	1.29%	3.03%	45.24%	0.00%	0.00%	0.00%	0.00%	N/A	**45.53%**

MODIS1 CONFUSION MATRIX (11% SAMPLE)
GREEK STUDY AREA
DATE:07/07/2000
DOMINANT CLASS CLASSIFICATION SCHEME

		REFERENCE															
		1	2	3	4	5	6	7	8	9	10	11	12	13	14	15	U.A
CLASSIFIED	1	**2**	0	0	0	0	0	0	0	0	0	0	0	0	0	0	100.00%
	2	340	**5797**	1598	1297	740	298	245	221	777	115	9	0	26	1	0	50.57%
	3	32	376	**741**	128	135	130	142	55	182	18	0	2	6	0	0	38.06%
	4	21	131	69	**164**	11	23	7	10	20	6	0	0	3	0	0	35.27%
	5	25	551	190	227	**1879**	268	418	69	561	6	0	0	1	0	0	44.79%
	6	6	98	62	25	59	**319**	96	10	68	6	0	0	1	0	0	42.53%
	7	0	16	19	3	16	19	**37**	3	15	1	1	0	0	0	0	28.46%
	8	0	1	1	0	0	0	0	**2**	1	0	0	0	0	0	0	40.00%
	9	5	49	47	17	51	24	23	5	**68**	0	0	0	0	0	0	23.53%
	10	2	42	15	10	6	4	0	0	0	**80**	0	0	2	0	0	49.69%
	11	0	0	0	0	0	0	0	0	0	0	**0**	0	0	0	0	N/A
	12	0	0	0	0	0	0	0	0	0	0	0	**0**	0	0	0	N/A
	13	0	0	0	0	0	0	0	0	0	0	0	0	**0**	0	0	N/A
	14	0	0	0	0	0	0	0	0	0	0	0	0	0	**0**	0	N/A
	15	0	0	0	0	0	0	0	0	0	0	0	0	0	0	**0**	N/A
	P.A	0.46%	82.10%	27.02%	8.77%	64.86%	29.40%	3.82%	0.53%	4.02%	34.48%	0.00%	0.00%	0.00%	0.00%	N/A	**46.83%**

MODIS1 CONFUSION MATRIX (11% SAMPLE)
GREEK STUDY AREA
DATE:13/04/2000
DOMINANT CLASS CLASSIFICATION SCHEME

		REFERENCE															
		1	2	3	4	5	6	7	8	9	10	11	12	13	14	15	U.A
CLASSIFIED	1	**1**	0	0	0	0	0	0	0	0	0	0	0	0	0	0	100.00%
	2	112	**4324**	1033	759	545	158	156	128	476	70	4	1	11	3	0	55.58%
	3	20	345	**578**	98	195	107	165	56	167	6	2	0	0	0	0	33.24%
	4	3	28	14	**35**	14	3	4	7	10	0	0	0	0	0	0	29.66%
	5	38	457	226	205	**1082**	140	204	66	429	20	2	0	3	0	0	37.67%
	6	1	50	43	14	43	**224**	122	3	57	3	0	0	0	0	0	40.00%
	7	4	32	29	8	27	23	**69**	5	24	2	0	0	0	0	0	30.94%
	8	0	1	0	0	1	0	1	**2**	0	0	0	0	0	0	0	40.00%
	9	2	38	24	9	29	6	5	5	**50**	0	0	0	0	0	0	29.76%
	10	4	35	14	2	0	4	2	2	1	**54**	0	0	3	0	0	44.63%
	11	0	0	0	0	0	0	0	0	0	0	**0**	0	0	0	0	N/A
	12	0	0	0	0	0	0	0	0	0	0	0	**0**	0	0	0	N/A
	13	0	0	0	0	0	0	0	0	0	0	0	0	**0**	0	0	N/A
	14	0	0	0	0	0	0	0	0	0	0	0	0	0	**0**	0	N/A
	15	0	0	0	0	0	0	0	0	0	0	0	0	0	0	**0**	N/A
	P.A	0.54%	81.43%	29.47%	3.10%	55.89%	33.68%	9.48%	0.73%	4.12%	34.84%	0.00%	0.00%	0.00%	0.00%	N/A	**47.24%**

MODIS1 CONFUSION MATRIX (11% SAMPLE)
GREEK STUDY AREA
DATE:14/06/2000
DOMINANT CLASS CLASSIFICATION SCHEME

		REFERENCE															
		1	2	3	4	5	6	7	8	9	10	11	12	13	14	15	U.A
CLASSIFIED	1	**2**	3	1	0	1	0	1	0	0	0	0	0	0	0	0	25.00%
	2	233	**4292**	1350	857	358	252	243	184	486	70	4	0	25	0	0	51.38%
	3	20	329	**595**	97	85	118	127	42	156	9	0	2	4	0	0	37.56%
	4	6	37	21	**65**	3	8	2	2	10	0	0	0	0	0	0	42.21%
	5	10	349	144	135	**1057**	194	378	57	380	3	0	0	0	0	0	39.05%
	6	6	90	56	22	67	**362**	117	10	68	4	0	0	0	0	0	45.14%
	7	0	5	6	3	0	6	**12**	2	4	1	0	0	0	0	0	30.77%
	8	0	0	0	0	0	0	0	**4**	0	0	0	0	0	0	0	100.00%
	9	2	18	20	8	13	8	4	4	**42**	1	0	0	0	0	0	35.00%
	10	0	0	0	0	0	0	0	0	0	**0**	0	0	0	0	0	N/A
	11	0	0	0	0	0	0	0	0	0	0	**0**	0	0	0	0	N/A
	12	0	0	0	0	0	0	0	0	0	0	0	**0**	0	0	0	N/A
	13	0	0	0	0	0	0	0	0	0	0	0	0	**0**	0	0	N/A
	14	0	0	0	0	0	0	0	0	0	0	0	0	0	**0**	0	N/A
	15	0	0	0	0	0	0	0	0	0	0	0	0	0	0	**0**	N/A
	P.A	0.72%	83.78%	27.13%	5.48%	66.73%	38.19%	1.36%	1.31%	3.66%	0.00%	0.00%	0.00%	0.00%	N/A	N/A	**46.70%**

MODIS1 CONFUSION MATRIX (11% SAMPLE)
GREEK STUDY AREA
DATE:20/08/2000
DOMINANT CLASS CLASSIFICATION SCHEME

		REFERENCE															
		1	2	3	4	5	6	7	8	9	10	11	12	13	14	15	U.A
CLASSIFIED	1	**1**	2	1	0	1	0	0	0	0	0	0	0	0	0	0	20.00%
	2	316	**5680**	1389	1306	777	197	148	222	686	91	9	1	25	0	0	52.36%
	3	62	507	**960**	217	224	214	199	82	311	17	1	0	2	0	0	34.33%
	4	27	135	64	**180**	5	14	2	10	30	2	0	0	0	0	0	38.38%
	5	17	499	234	189	**1712**	134	377	54	479	14	1	1	1	0	0	46.12%
	6	11	79	76	27	41	**547**	161	20	112	9	0	0	1	0	0	50.46%
	7	2	41	35	15	82	64	**111**	12	45	0	0	0	0	0	0	27.27%
	8	1	0	0	0	1	0	0	**1**	0	0	0	0	0	0	0	33.33%
	9	2	23	22	10	10	11	9	1	**51**	1	0	0	0	0	0	36.43%
	10	4	47	20	8	4	4	5	0	1	**61**	0	0	6	0	0	38.13%
	11	0	0	0	0	0	0	0	0	0	0	**0**	0	0	0	0	N/A
	12	0	0	0	0	0	0	0	0	0	0	0	**0**	0	0	0	N/A
	13	0	0	0	0	0	0	0	0	0	0	0	0	**1**	0	0	100.00%
	14	0	0	0	0	0	0	0	0	0	0	0	0	0	**0**	0	N/A
	15	0	0	0	0	0	0	0	0	0	0	0	0	0	0	**0**	N/A
	P.A	0.23%	80.99%	34.27%	9.22%	59.92%	46.16%	10.97%	0.25%	2.97%	31.28%	0.00%	0.00%	2.78%	N/A	N/A	**47.42%**

MODIS1 CONFUSION MATRIX (11% SAMPLE)
GREEK STUDY AREA
DATE:23/10/2000
DOMINANT CLASS CLASSIFICATION SCHEME

CLASSIFIED \ REFERENCE	1	2	3	4	5	6	7	8	9	10	11	12	13	14	15	U.A
1	**6**	1	0	1	1	1	2	0	0	0	0	0	0	0	0	50.00%
2	206	**3857**	1221	973	547	205	161	147	543	93	6	1	31	0	0	48.27%
3	31	241	**535**	89	210	89	110	38	191	7	1	1	3	0	0	34.61%
4	0	16	12	**23**	3	2	1	3	3	0	0	0	0	0	0	36.51%
5	17	340	371	99	**736**	128	216	39	272	10	1	0	0	0	0	33.02%
6	9	42	65	27	78	**171**	117	11	83	4	0	0	0	0	0	28.17%
7	1	20	14	6	27	19	**44**	4	20	0	0	0	0	0	0	28.39%
8	0	2	3	0	1	1	0	**3**	1	0	0	0	0	0	0	27.27%
9	7	24	30	13	29	19	22	7	**69**	1	0	0	0	0	0	31.22%
10	3	47	22	10	4	8	4	1	3	**84**	0	0	2	0	0	44.68%
11	0	0	0	0	1	0	0	0	0	1	**0**	0	0	0	0	0.00%
12	0	0	0	0	0	0	0	0	0	0	0	**0**	0	0	0	N/A
13	0	0	0	0	0	0	0	0	0	0	0	0	**0**	0	0	N/A
14	0	0	0	0	0	0	0	0	0	0	0	0	0	**0**	0	N/A
15	0	0	0	0	0	0	0	0	0	0	0	0	0	0	**0**	N/A
P.A	2.14%	84.03%	23.54%	1.85%	44.96%	26.59%	6.50%	1.19%	5.82%	42.00%	0.00%	0.00%	0.00%	N/A	N/A	**42.44%**

MODIS1 CONFUSION MATRIX (11% SAMPLE)
GREEK STUDY AREA
DATE:24/03/2001
DOMINANT CLASS CLASSIFICATION SCHEME

		REFERENCE															
		1	2	3	4	5	6	7	8	9	10	11	12	13	14	15	U.A
CLASSIFIED	1	**1**	0	0	0	0	0	0	0	1	0	0	0	0	0	0	50.00%
	2	183	**5028**	1360	1023	620	174	171	177	582	84	7	1	20	1	0	53.31%
	3	19	476	**722**	144	240	131	181	43	191	6	0	1	4	0	0	33.46%
	4	16	65	27	**102**	37	17	9	8	33	1	0	0	0	0	0	32.38%
	5	69	598	291	313	**1668**	254	283	78	610	36	1	0	3	0	0	39.68%
	6	5	102	56	24	91	**369**	171	12	75	7	0	0	0	0	0	40.46%
	7	2	36	37	5	39	42	**65**	4	27	2	0	0	0	0	0	25.10%
	8	0	1	1	0	0	1	1	**3**	0	0	0	0	0	0	0	42.86%
	9	8	44	52	34	55	26	16	9	**95**	3	0	0	0	0	0	27.78%
	10	6	80	40	15	3	13	6	3	6	**95**	0	0	7	0	0	34.67%
	11	0	0	0	0	0	0	0	0	0	0	**0**	0	0	0	0	N/A
	12	0	0	0	0	0	0	0	0	0	0	0	**0**	0	0	0	N/A
	13	0	0	0	0	0	0	0	0	0	0	0	0	**0**	0	0	N/A
	14	0	0	0	0	0	0	0	0	0	0	0	0	0	**0**	0	N/A
	15	0	0	0	0	0	0	0	0	0	0	0	0	0	0	**0**	N/A
	P.A	0.32%	78.20%	27.92%	6.14%	60.59%	35.93%	7.20%	0.89%	5.86%	40.60%	0.00%	0.00%	0.00%	0.00%	N/A	**45.51%**

MODIS1 CONFUSION MATRIX (11% SAMPLE)
GREEK STUDY AREA
DATE:25/10/2000
DOMINANT CLASS CLASSIFICATION SCHEME

		REFERENCE															
		1	2	3	4	5	6	7	8	9	10	11	12	13	14	15	U.A
CLASSIFIED	1	**0**	1	1	0	1	0	0	0	0	0	0	0	0	0	0	0.00%
	2	260	**5529**	1346	1282	900	240	248	191	808	93	5	2	28	0	0	50.58%
	3	16	198	**320**	82	146	64	80	25	126	8	0	0	0	0	0	30.05%
	4	2	28	18	**42**	8	7	4	5	10	1	0	0	0	0	0	33.60%
	5	31	737	556	158	**1270**	183	324	55	405	14	0	1	0	0	0	34.01%
	6	5	94	104	29	122	**350**	167	17	129	10	1	0	0	0	0	34.05%
	7	0	17	17	5	15	17	**24**	0	13	0	0	0	0	0	0	22.22%
	8	1	2	1	0	0	0	1	**3**	1	0	0	0	0	0	0	33.33%
	9	3	40	23	21	18	8	17	6	**62**	0	0	0	0	0	0	31.31%
	10	3	48	22	8	2	3	5	0	4	**79**	0	0	5	0	0	44.13%
	11	0	0	0	0	0	0	0	0	0	0	**0**	0	0	0	0	N/A
	12	0	0	0	0	0	0	0	0	0	0	0	**0**	0	0	0	N/A
	13	0	0	0	0	0	0	0	0	0	0	0	0	**0**	0	0	N/A
	14	0	0	0	0	0	0	0	0	0	0	0	0	0	**0**	0	N/A
	15	0	0	0	0	0	0	0	0	0	0	0	0	0	0	**0**	N/A
	P.A	0.00%	82.60%	13.29%	2.58%	51.17%	40.14%	2.76%	0.99%	3.98%	38.54%	0.00%	0.00%	0.00%	N/A	N/A	**44.18%**

MODIS1 CONFUSION MATRIX (11% SAMPLE)
GREEK STUDY AREA
DATE:MULTIDATE
DOMINANT CLASS CLASSIFICATION SCHEME

		REFERENCE															
		1	2	3	4	5	6	7	8	9	10	11	12	13	14	15	U.A
CLASSIFIED	1	**2**	0	0	0	0	0	0	0	0	0	0	0	0	0	0	100.00%
	2	159	**3677**	940	836	408	158	119	150	479	69	2	1	12	0	0	52.45%
	3	28	206	**427**	99	137	72	81	33	158	8	0	0	2	0	0	34.13%
	4	1	19	13	**24**	12	3	1	5	8	0	0	0	0	0	0	27.91%
	5	29	476	359	179	**1403**	158	333	60	446	10	1	0	0	0	0	40.62%
	6	12	50	52	21	61	**208**	102	12	63	5	0	0	0	0	0	35.49%
	7	1	16	10	5	25	16	**34**	3	10	0	0	0	0	0	0	28.33%
	8	0	0	0	0	1	0	0	**2**	0	0	0	0	0	0	0	66.67%
	9	0	36	30	23	21	11	24	4	**78**	3	0	0	0	0	0	33.91%
	10	4	32	18	3	3	2	1	1	1	**58**	0	1	2	0	0	46.03%
	11	0	0	0	0	0	0	0	0	0	0	**0**	0	0	0	0	N/A
	12	0	0	0	0	0	0	0	0	0	0	0	**0**	0	0	0	N/A
	13	0	0	0	0	0	0	0	0	0	0	0	0	**0**	0	0	N/A
	14	0	0	0	0	0	0	0	0	0	0	0	0	0	**0**	0	N/A
	15	0	0	0	0	0	0	0	0	0	0	0	0	0	0	**0**	N/A
	P.A	0.85%	81.49%	23.09%	2.02%	67.75%	33.12%	4.89%	0.74%	6.28%	37.91%	0.00%	0.00%	0.00%	N/A	N/A	**45.95%**

MODIS2 CONFUSION MATRIX (11% SAMPLE)
GREEK STUDY AREA
DATE:03/08/2000
DOMINANT CLASS CLASSIFICATION SCHEME

		REFERENCE															
		1	2	3	4	5	6	7	8	9	10	11	12	13	14	15	U.A
CLASSIFIED	1	**5**	4	0	0	0	1	0	0	2	0	0	0	0	0	0	41.67%
	2	220	**5470**	1085	903	469	203	195	130	530	120	7	1	34	0	0	58.40%
	3	57	534	**960**	231	205	127	152	62	283	8	1	0	4	0	0	36.59%
	4	36	188	103	**284**	42	16	9	20	60	1	0	0	0	0	0	37.42%
	5	16	391	174	182	**1559**	90	255	52	380	3	3	0	0	0	0	50.21%
	6	11	78	63	26	41	**437**	126	14	109	5	0	0	0	0	0	48.02%
	7	2	54	27	14	54	40	**102**	10	31	2	0	0	0	0	0	30.36%
	8	0	1	2	0	0	0	0	**3**	0	0	0	0	0	0	0	50.00%
	9	6	39	38	32	37	23	20	7	**97**	1	0	0	0	0	0	32.33%
	10	0	0	0	0	0	0	0	0	0	**0**	0	0	0	0	0	N/A
	11	0	0	0	0	0	0	0	0	0	0	**0**	0	0	0	0	N/A
	12	0	0	0	0	0	0	0	0	0	0	0	**0**	0	0	0	N/A
	13	0	0	0	0	0	0	0	0	0	0	0	0	**0**	0	0	N/A
	14	0	0	0	0	0	0	0	0	0	0	0	0	0	**0**	0	N/A
	15	0	0	0	0	0	0	0	0	0	0	0	0	0	0	**0**	N/A
	P.A	1.42%	80.93%	39.15%	16.99%	64.77%	46.64%	11.87%	1.01%	6.50%	0.00%	0.00%	0.00%	0.00%	N/A	N/A	**51.19%**

MODIS2 CONFUSION MATRIX (11% SAMPLE)
GREEK STUDY AREA
DATE:03/10/2001
DOMINANT CLASS CLASSIFICATION SCHEME

		REFERENCE															
		1	2	3	4	5	6	7	8	9	10	11	12	13	14	15	U.A
CLASSIFIED	1	**4**	4	3	3	0	3	0	0	6	0	0	0	0	0	0	17.39%
	2	279	**5711**	1437	1227	609	202	195	203	640	80	7	0	22	0	0	53.82%
	3	52	472	**879**	148	220	127	189	58	257	13	1	0	3	0	0	36.34%
	4	16	116	78	**218**	45	14	6	16	57	5	0	0	4	1	0	37.85%
	5	28	387	249	213	**1658**	142	305	87	410	6	1	0	1	0	0	47.55%
	6	35	104	82	59	103	**552**	183	26	145	11	0	0	0	0	0	42.46%
	7	0	25	11	5	65	37	**84**	2	25	2	0	0	0	0	0	32.81%
	8	1	1	0	1	0	0	0	**1**	0	0	0	0	0	0	0	25.00%
	9	4	43	35	32	61	13	23	12	**93**	0	0	0	0	0	0	29.43%
	10	2	72	27	11	3	6	7	0	2	**81**	0	0	7	0	0	37.16%
	11	0	0	0	0	0	0	0	0	0	0	**0**	0	0	0	0	N/A
	12	0	0	0	0	0	0	0	0	0	0	0	**0**	0	0	0	N/A
	13	0	0	0	0	0	0	0	0	0	0	0	0	**0**	0	0	N/A
	14	0	0	0	0	0	0	0	0	0	0	0	0	0	**0**	0	N/A
	15	0	0	0	0	0	0	0	0	0	0	0	0	0	0	**0**	N/A
	P.A	0.95%	82.35%	31.38%	11.37%	59.99%	50.36%	8.47%	0.25%	5.69%	40.91%	0.00%	N/A	0.00%	0.00%	N/A	**48.31%**

MODIS2 CONFUSION MATRIX (11% SAMPLE)
GREEK STUDY AREA
DATE:04/05/2001
DOMINANT CLASS CLASSIFICATION SCHEME

		REFERENCE															
		1	2	3	4	5	6	7	8	9	10	11	12	13	14	15	U.A
CLASSIFIED	1	**2**	0	1	0	2	0	0	1	0	0	0	0	0	0	0	33.33%
	2	184	**5074**	929	828	396	156	135	127	419	126	7	2	28	2	0	60.31%
	3	64	421	**853**	229	236	141	161	88	288	17	1	0	2	0	0	34.11%
	4	32	147	128	**263**	92	10	9	24	89	0	0	0	0	0	0	33.12%
	5	33	585	378	305	**1658**	95	285	50	521	8	0	1	0	0	0	42.31%
	6	18	77	87	30	31	**267**	128	16	105	9	0	0	0	0	0	34.77%
	7	3	33	18	9	41	57	**88**	6	26	4	0	0	0	0	0	30.88%
	8	0	1	1	0	0	0	0	**2**	0	0	0	0	0	0	0	50.00%
	9	11	40	48	52	47	33	23	17	**105**	0	0	0	0	0	0	27.93%
	10	3	28	8	5	1	5	2	0	3	**52**	0	0	4	0	0	46.85%
	11	0	0	0	0	0	0	0	0	0	0	**0**	0	0	0	0	N/A
	12	0	0	0	0	0	0	0	0	0	0	0	**0**	0	0	0	N/A
	13	0	0	0	0	0	0	0	0	0	0	0	0	**0**	0	0	N/A
	14	0	0	0	0	0	0	0	0	0	0	0	0	0	**0**	0	N/A
	15	0	0	0	0	0	0	0	0	0	0	0	0	0	0	**0**	N/A
	P.A	0.57%	79.21%	34.80%	15.28%	66.21%	34.95%	10.59%	0.60%	6.75%	24.07%	0.00%	0.00%	0.00%	0.00%	N/A	**48.69%**

MODIS2 CONFUSION MATRIX (11% SAMPLE)
GREEK STUDY AREA
DATE:04/07/2000
DOMINANT CLASS CLASSIFICATION SCHEME

		REFERENCE															
		1	2	3	4	5	6	7	8	9	10	11	12	13	14	15	U.A
CLASSIFIED	1	**12**	4	5	3	3	2	0	0	5	0	0	0	0	0	0	35.29%
	2	242	**5300**	1216	944	545	207	167	152	608	139	4	2	30	1	0	55.46%
	3	55	494	**993**	185	114	120	145	96	234	13	0	0	1	0	0	40.53%
	4	27	163	96	**263**	27	10	5	21	50	3	1	0	0	0	0	39.49%
	5	31	541	209	303	**1908**	116	325	68	548	6	0	0	0	0	0	47.05%
	6	23	95	83	41	71	**524**	191	30	133	11	0	0	0	0	0	43.59%
	7	1	42	16	11	38	43	**95**	6	20	1	0	0	0	0	0	34.80%
	8	0	1	0	1	0	0	0	**3**	0	0	0	0	0	0	0	60.00%
	9	5	26	24	26	31	17	18	9	**59**	0	0	0	0	0	0	27.44%
	10	4	31	14	8	0	0	4	2	3	**53**	1	0	3	0	0	43.09%
	11	0	0	0	0	0	0	0	0	0	0	**0**	0	0	0	0	N/A
	12	0	0	0	0	0	0	0	0	0	0	0	**0**	0	0	0	N/A
	13	0	0	0	0	0	0	0	0	0	0	0	0	**0**	0	0	N/A
	14	0	0	0	0	0	0	0	0	0	0	0	0	0	**0**	0	N/A
	15	0	0	0	0	0	0	0	0	0	0	0	0	0	0	**0**	N/A
	P.A	3.00%	79.14%	37.39%	14.73%	69.71%	50.43%	10.00%	0.78%	3.55%	23.45%	0.00%	0.00%	0.00%	0.00%	N/A	**49.57%**

MODIS2 CONFUSION MATRIX (11% SAMPLE)
GREEK STUDY AREA
DATE:05/06/2000
DOMINANT CLASS CLASSIFICATION SCHEME

		REFERENCE															
		1	2	3	4	5	6	7	8	9	10	11	12	13	14	15	U.A
CLASSIFIED	1	**29**	14	14	15	4	1	1	3	9	0	0	0	0	0	0	32.22%
	2	228	**4666**	1248	957	444	273	206	172	585	46	7	1	21	2	0	52.69%
	3	33	475	**831**	170	109	105	107	44	146	3	0	0	3	0	0	41.02%
	4	22	52	52	**121**	43	5	5	11	35	1	0	0	0	0	0	34.87%
	5	23	471	176	203	**1508**	139	346	50	470	9	0	0	0	0	0	44.42%
	6	11	75	31	20	55	**240**	85	11	75	6	0	0	0	0	0	39.41%
	7	3	33	26	5	20	22	**45**	3	14	3	0	0	0	0	0	25.86%
	8	0	0	0	2	0	0	0	**3**	0	0	0	0	0	0	0	60.00%
	9	5	46	27	36	53	12	15	7	**81**	0	0	0	0	0	0	28.72%
	10	3	30	15	6	1	2	0	0	1	**56**	0	0	2	0	0	48.28%
	11	0	0	0	0	0	0	0	0	0	0	**0**	0	0	0	0	N/A
	12	0	0	0	0	0	0	0	0	0	0	0	**0**	0	0	0	N/A
	13	0	0	0	0	0	0	0	0	0	0	0	0	**0**	0	0	N/A
	14	0	0	0	0	0	0	0	0	0	0	0	0	0	**0**	0	N/A
	15	0	0	0	0	0	0	0	0	0	0	0	0	0	0	**0**	N/A
	P.A	8.12%	79.60%	34.34%	7.88%	67.41%	30.04%	5.56%	0.99%	5.72%	45.16%	0.00%	0.00%	0.00%	0.00%	N/A	**47.67%**

MODIS2 CONFUSION MATRIX (11% SAMPLE)
GREEK STUDY AREA
DATE:07/07/2000
DOMINANT CLASS CLASSIFICATION SCHEME

		REFERENCE															
		1	2	3	4	5	6	7	8	9	10	11	12	13	14	15	U.A
CLASSIFIED	1	**6**	4	2	3	3	0	0	1	1	0	0	0	0	0	0	30.00%
	2	277	**5641**	1323	1088	572	271	214	185	653	116	10	1	29	0	0	54.34%
	3	55	510	**957**	187	125	120	145	61	162	17	0	1	3	0	0	40.85%
	4	30	158	102	**224**	25	10	7	19	52	2	0	0	1	0	0	35.56%
	5	34	509	217	293	**1977**	171	342	78	582	6	0	0	1	0	0	46.96%
	6	13	88	52	25	56	**416**	140	17	95	6	0	0	1	0	0	45.76%
	7	2	48	25	9	44	42	**93**	3	20	0	0	0	0	0	0	32.52%
	8	0	0	1	0	0	0	0	**0**	0	0	0	0	0	0	0	0.00%
	9	7	55	43	28	77	39	18	12	**132**	1	1	0	0	0	0	31.96%
	10	2	49	17	11	5	6	1	0	0	**86**	0	0	2	0	0	48.04%
	11	0	0	0	0	0	0	0	0	0	0	**0**	0	0	0	0	N/A
	12	0	0	0	0	0	0	0	0	0	0	0	**0**	0	0	0	N/A
	13	0	0	0	0	0	0	0	0	0	0	0	0	**0**	0	0	N/A
	14	0	0	0	0	0	0	0	0	0	0	0	0	0	**0**	0	N/A
	15	0	0	0	0	0	0	0	0	0	0	0	0	0	0	**0**	N/A
	P.A	1.41%	79.88%	34.94%	11.99%	68.55%	38.70%	9.69%	0.00%	7.78%	36.75%	0.00%	0.00%	0.00%	N/A	N/A	**49.21%**

MODIS2 CONFUSION MATRIX (11% SAMPLE)
GREEK STUDY AREA
DATE:13/04/2000
DOMINANT CLASS CLASSIFICATION SCHEME

		REFERENCE															
		1	2	3	4	5	6	7	8	9	10	11	12	13	14	15	U.A
CLASSIFIED	1	**1**	3	1	1	0	1	1	0	5	0	0	0	0	0	0	7.69%
	2	91	**4249**	829	593	372	149	124	114	349	65	4	1	13	2	0	61.09%
	3	38	356	**775**	151	167	86	155	65	176	5	0	0	0	0	0	39.26%
	4	9	69	40	**114**	43	2	4	9	45	0	0	0	0	0	0	34.03%
	5	25	434	195	216	**1256**	96	209	56	455	11	0	0	0	0	0	42.53%
	6	8	50	41	23	50	**252**	136	6	81	3	1	0	0	0	0	38.71%
	7	1	24	25	4	24	18	**61**	9	19	2	0	0	0	0	0	32.62%
	8	0	1	0	1	1	0	0	**0**	0	0	0	0	0	0	0	0.00%
	9	5	46	31	33	48	18	20	9	**83**	2	1	0	0	0	0	28.04%
	10	3	41	16	3	2	11	6	2	7	**63**	0	0	3	1	0	39.87%
	11	0	0	0	0	0	0	0	0	0	0	**0**	0	0	0	0	N/A
	12	0	0	0	0	0	0	0	0	0	0	0	**0**	0	0	0	N/A
	13	0	0	0	0	0	0	0	0	0	0	0	0	**0**	0	0	N/A
	14	0	0	0	0	0	0	0	0	0	0	0	0	0	**0**	0	N/A
	15	0	0	0	0	0	0	0	0	0	0	0	0	0	0	**0**	N/A
	P.A	0.55%	80.58%	39.68%	10.01%	63.98%	39.81%	8.52%	0.00%	6.80%	41.72%	0.00%	0.00%	0.00%	0.00%	N/A	**50.68%**

MODIS2 CONFUSION MATRIX (11% SAMPLE)
GREEK STUDY AREA
DATE:14/06/2000
DOMINANT CLASS CLASSIFICATION SCHEME

		REFERENCE															
		1	2	3	4	5	6	7	8	9	10	11	12	13	14	15	U.A
CLASSIFIED	1	**7**	2	1	2	1	1	0	1	0	0	0	0	0	0	0	46.67%
	2	213	**4173**	1161	723	282	224	219	147	429	73	3	2	26	0	0	54.37%
	3	25	408	**742**	143	92	75	102	67	134	6	1	0	1	0	0	41.31%
	4	14	77	70	**123**	14	7	1	5	20	0	0	0	0	0	0	37.16%
	5	9	282	147	130	**1045**	107	277	53	357	5	0	0	0	0	0	43.33%
	6	10	73	34	22	39	**427**	128	13	74	2	0	0	0	0	0	51.95%
	7	2	47	23	11	60	60	**112**	5	28	0	0	0	0	0	0	32.18%
	8	0	1	5	1	0	0	0	**5**	1	0	0	0	0	0	0	38.46%
	9	6	48	30	27	39	21	32	6	**92**	2	0	0	0	0	0	30.36%
	10	0	0	0	0	0	0	0	0	0	**0**	0	0	0	0	0	N/A
	11	0	0	0	0	0	0	0	0	0	0	**0**	0	0	0	0	N/A
	12	0	0	0	0	0	0	0	0	0	0	0	**0**	0	0	0	N/A
	13	0	0	0	0	0	0	0	0	0	0	0	0	**0**	0	0	N/A
	14	0	0	0	0	0	0	0	0	0	0	0	0	0	**0**	0	N/A
	15	0	0	0	0	0	0	0	0	0	0	0	0	0	0	**0**	N/A
	P.A	2.45%	81.65%	33.53%	10.41%	66.48%	46.31%	12.86%	1.66%	8.11%	0.00%	0.00%	0.00%	0.00%	N/A	N/A	**49.04%**

MODIS2 CONFUSION MATRIX (11% SAMPLE)
GREEK STUDY AREA
DATE:20/08/2000
DOMINANT CLASS CLASSIFICATION SCHEME

		REFERENCE															
		1	2	3	4	5	6	7	8	9	10	11	12	13	14	15	U.A
CLASSIFIED	1	**4**	2	0	0	0	1	0	0	0	0	0	0	0	0	0	57.14%
	2	274	**5579**	1230	1120	623	189	165	180	630	90	9	2	25	0	0	55.15%
	3	72	606	**1100**	254	221	165	207	91	311	10	0	0	3	0	0	36.18%
	4	35	174	112	**268**	37	15	5	24	58	5	1	0	0	0	0	36.51%
	5	17	422	212	205	**1790**	117	291	58	472	10	0	0	0	0	0	49.81%
	6	24	89	89	29	54	**626**	190	30	153	5	0	0	0	0	0	48.56%
	7	3	30	29	18	89	61	**138**	7	26	5	0	0	0	0	0	33.99%
	8	0	0	0	0	0	0	0	**0**	0	0	0	0	0	0	0	N/A
	9	7	38	28	31	42	11	16	7	**88**	1	0	0	0	0	0	32.71%
	10	4	50	21	8	3	5	6	0	1	**68**	0	0	5	0	0	39.77%
	11	0	0	0	0	0	0	0	0	0	0	**0**	0	0	0	0	N/A
	12	0	0	0	0	0	0	0	0	0	0	0	**0**	0	0	0	N/A
	13	0	0	0	0	0	0	0	0	0	0	0	0	**0**	0	0	N/A
	14	0	0	0	0	0	0	0	0	0	0	0	0	0	**0**	0	N/A
	15	0	0	0	0	0	0	0	0	0	0	0	0	0	0	**0**	N/A
	P.A	0.91%	79.81%	38.99%	13.86%	62.61%	52.61%	13.56%	0.00%	5.06%	35.05%	0.00%	0.00%	0.00%	N/A	N/A	**49.23%**

MODIS2 CONFUSION MATRIX (11% SAMPLE)
GREEK STUDY AREA
DATE:23/10/2000
DOMINANT CLASS CLASSIFICATION SCHEME

		REFERENCE															
		1	2	3	4	5	6	7	8	9	10	11	12	13	14	15	U.A
CLASSIFIED	1	**1**	0	0	0	0	1	0	1	0	0	0	0	0	0	0	33.33%
	2	198	**3719**	1102	853	400	167	132	137	472	81	7	2	31	0	0	50.94%
	3	38	368	**773**	144	164	118	128	44	212	10	1	0	0	0	0	38.65%
	4	3	50	9	**57**	15	2	2	7	17	0	0	0	0	0	0	35.19%
	5	15	270	216	120	**910**	81	208	28	285	5	1	0	0	0	0	42.54%
	6	12	47	76	25	62	**200**	106	17	88	3	0	0	3	0	0	31.30%
	7	2	21	18	4	43	36	**63**	8	19	0	0	0	0	0	0	29.44%
	8	0	2	0	0	0	0	0	**1**	0	1	0	0	0	0	0	25.00%
	9	0	0	0	0	0	0	0	0	**0**	0	0	0	0	0	0	N/A
	10	3	55	26	11	6	9	5	1	4	**97**	0	0	2	0	0	44.29%
	11	0	0	0	0	0	0	0	0	0	0	**0**	0	0	0	0	N/A
	12	0	0	0	0	0	0	0	0	0	0	0	**0**	0	0	0	N/A
	13	0	0	0	0	0	0	0	0	0	0	0	0	**0**	0	0	N/A
	14	0	0	0	0	0	0	0	0	0	0	0	0	0	**0**	0	N/A
	15	0	0	0	0	0	0	0	0	0	0	0	0	0	0	**0**	N/A
	P.A	0.37%	82.06%	34.82%	4.70%	56.88%	32.57%	9.78%	0.41%	0.00%	49.24%	0.00%	0.00%	0.00%	N/A	N/A	**45.90%**

MODIS2 CONFUSION MATRIX (11% SAMPLE)
GREEK STUDY AREA
DATE:24/03/2001
DOMINANT CLASS CLASSIFICATION SCHEME

		REFERENCE															
		1	2	3	4	5	6	7	8	9	10	11	12	13	14	15	U.A
CLASSIFIED	1	**6**	3	1	5	4	4	1	0	0	0	0	0	0	0	0	25.00%
	2	136	**4989**	929	801	367	179	180	125	393	107	9	2	20	1	0	60.56%
	3	54	542	**1155**	236	225	126	185	83	240	11	0	0	4	0	0	40.37%
	4	39	153	101	**248**	82	18	11	29	80	3	0	0	0	0	0	32.46%
	5	50	545	253	298	**1899**	160	256	75	679	21	0	0	2	0	0	44.81%
	6	11	99	79	33	68	**475**	189	16	126	3	0	0	0	0	0	43.22%
	7	2	28	12	5	40	21	**71**	3	12	2	0	0	0	0	0	36.22%
	8	0	0	0	0	0	0	0	**1**	0	0	0	0	0	0	0	100.00%
	9	10	21	33	26	42	24	17	4	**92**	2	0	0	0	0	0	33.95%
	10	4	67	28	10	2	11	4	0	4	**80**	0	0	8	0	0	36.70%
	11	0	0	0	0	0	0	0	0	0	0	**0**	0	0	0	0	N/A
	12	0	0	0	0	0	0	0	0	0	0	0	**0**	0	0	0	N/A
	13	0	0	0	0	0	0	0	0	0	0	0	0	**0**	0	0	N/A
	14	0	0	0	0	0	0	0	0	0	0	0	0	0	**0**	0	N/A
	15	0	0	0	0	0	0	0	0	0	0	0	0	0	0	**0**	N/A
	P.A	1.92%	77.38%	44.58%	14.92%	69.59%	46.66%	7.77%	0.30%	5.66%	34.93%	0.00%	0.00%	0.00%	0.00%	N/A	**50.34%**

MODIS2 CONFUSION MATRIX (11% SAMPLE)
GREEK STUDY AREA
DATE:MULTIDATE
DOMINANT CLASS CLASSIFICATION SCHEME

		REFERENCE															
		1	2	3	4	5	6	7	8	9	10	11	12	13	14	15	U.A
CLASSIFIED	1	**0**	1	0	0	0	0	0	0	0	0	0	0	0	0	0	0.00%
	2	128	**3562**	811	668	410	142	126	138	444	57	2	1	14	0	0	54.77%
	3	36	332	**661**	116	156	104	134	49	186	8	0	0	0	0	0	37.09%
	4	13	95	36	**155**	27	9	3	13	32	5	0	0	0	0	0	39.95%
	5	22	367	208	190	**1344**	111	256	50	400	12	1	0	0	0	0	45.39%
	6	18	50	52	31	57	**233**	112	11	94	7	0	0	0	0	0	35.04%
	7	10	27	30	8	33	20	**53**	4	15	0	0	0	0	0	0	26.50%
	8	0	2	2	0	0	0	0	**1**	1	0	0	0	0	0	0	16.67%
	9	8	38	46	25	35	16	11	11	**78**	3	0	0	0	0	0	28.78%
	10	4	36	17	2	2	2	1	1	0	**63**	0	1	2	0	0	48.09%
	11	0	0	0	0	0	0	0	0	0	0	**0**	0	0	0	0	N/A
	12	0	0	0	0	0	0	0	0	0	0	0	**0**	0	0	0	N/A
	13	0	0	0	0	0	0	0	0	0	0	0	0	**0**	0	0	N/A
	14	0	0	0	0	0	0	0	0	0	0	0	0	0	**0**	0	N/A
	15	0	0	0	0	0	0	0	0	0	0	0	0	0	0	**0**	N/A
	P.A	0.00%	78.98%	35.48%	12.97%	65.12%	36.58%	7.61%	0.36%	6.24%	40.65%	0.00%	0.00%	0.00%	N/A	N/A	**47.64%**

MODIS3 CONFUSION MATRIX (11% SAMPLE)
GREEK STUDY AREA
DATE:03/08/2000
DOMINANT CLASS CLASSIFICATION SCHEME

		REFERENCE															
		1	2	3	4	5	6	7	8	9	10	11	12	13	14	15	U.A
CLASSIFIED	1	**1**	1	0	0	0	0	0	0	0	0	0	0	0	0	0	50.00%
	2	0	**3**	2	3	5	1	2	0	2	2	0	0	0	0	0	15.00%
	3	168	230	**5574**	1244	978	541	189	186	143	582	106	10	1	36	0	55.81%
	4	9	60	482	**926**	195	198	157	194	64	310	15	0	0	1	0	35.47%
	5	1	34	138	80	**257**	32	21	14	26	29	1	0	0	0	0	40.60%
	6	6	9	374	151	159	**1340**	79	214	39	359	3	0	0	0	0	49.03%
	7	5	13	116	44	44	239	**405**	195	20	130	2	0	0	0	0	33.39%
	8	0	2	9	19	5	10	24	**48**	3	34	1	0	0	0	0	30.97%
	9	0	0	0	0	0	0	0	0	**0**	0	0	0	0	0	0	N/A
	10	0	1	17	7	11	22	9	11	3	**60**	2	0	0	0	0	41.96%
	11	0	0	6	1	1	0	0	1	0	0	**6**	0	0	1	0	37.50%
	12	0	0	0	0	1	0	0	0	0	0	0	**1**	0	0	0	50.00%
	13	0	0	0	0	0	0	0	0	0	0	0	0	**0**	0	0	N/A
	14	0	0	0	0	0	0	0	0	0	0	0	0	0	**0**	0	N/A
	15	0	0	0	0	0	0	0	0	0	0	0	0	0	0	**0**	N/A
	P.A	0.53%	0.85%	82.97%	37.41%	15.52%	56.23%	45.71%	5.56%	0.00%	3.98%	4.41%	9.09%	0.00%	0.00%	N/A	**49.22%**

MODIS3 CONFUSION MATRIX (11% SAMPLE)
GREEK STUDY AREA
DATE:03/10/2001
DOMINANT CLASS CLASSIFICATION SCHEME

		REFERENCE															
		1	2	3	4	5	6	7	8	9	10	11	12	13	14	15	U.A
CLASSIFIED	1	**0**	0	0	0	0	0	0	0	0	0	0	0	0	0	0	N/A
	2	0	**1**	0	0	0	0	0	0	0	0	0	0	0	0	0	100.00%
	3	147	273	**5533**	1529	1343	584	180	164	203	651	117	8	0	33	1	51.39%
	4	12	62	493	**861**	155	246	130	227	69	273	13	1	0	2	0	33.84%
	5	0	7	35	20	**69**	37	7	7	15	18	1	0	0	0	0	31.94%
	6	8	38	471	297	231	**1731**	206	365	86	489	17	0	0	1	0	43.93%
	7	3	30	108	57	58	114	**552**	188	25	130	5	0	0	0	0	43.46%
	8	0	0	3	3	0	6	5	**15**	0	11	0	0	0	0	0	34.88%
	9	0	3	0	0	1	0	1	0	**3**	3	0	0	0	0	0	27.27%
	10	1	11	46	43	47	64	31	33	13	**88**	0	0	0	0	0	23.34%
	11	1	1	31	7	3	1	2	6	1	0	**48**	0	0	2	0	46.60%
	12	0	0	0	0	0	0	0	0	0	0	0	**0**	0	0	0	N/A
	13	0	0	0	0	0	0	0	0	0	0	0	0	**0**	0	0	N/A
	14	0	0	0	0	0	0	0	0	0	0	0	0	0	**0**	0	N/A
	15	0	0	0	0	0	0	0	0	0	0	0	0	0	0	**0**	N/A
	P.A	0.00%	0.23%	82.34%	30.56%	3.62%	62.20%	49.55%	1.49%	0.72%	5.29%	23.88%	0.00%	N/A	0.00%	0.00%	**46.19%**

MODIS3 CONFUSION MATRIX
GREEK STUDY AREA
DATE:04/05/2001
DOMINANT CLASS CLASSIFICATION SCHEME

		REFERENCE															
		1	2	3	4	5	6	7	8	9	10	11	12	13	14	15	U.A
CLASSIFIED	1	**4**	0	3	0	0	0	0	0	0	0	0	0	0	0	0	57.14%
	2	15	**99**	35	20	40	41	31	23	11	38	0	0	0	0	0	28.05%
	3	977	1826	**40315**	9446	9076	6262	1369	1288	1233	5144	819	65	10	157	14	51.69%
	4	43	409	3353	**6068**	1464	1825	1389	1291	754	1933	99	11	2	13	0	32.53%
	5	8	51	350	191	**670**	170	41	39	52	193	9	0	0	1	0	37.75%
	6	81	172	4244	2257	1574	**10907**	816	2223	361	3416	92	2	0	3	0	41.71%
	7	8	98	382	618	191	389	**1685**	822	96	784	44	0	0	8	0	32.88%
	8	8	17	218	127	65	354	628	**724**	40	234	19	0	0	0	0	29.75%
	9	1	3	8	7	7	5	2	1	**23**	9	0	0	0	0	0	34.85%
	10	9	50	407	224	214	351	101	93	68	**688**	14	1	0	0	0	30.99%
	11	18	44	390	215	82	48	64	35	12	31	**692**	7	2	46	3	40.97%
	12	0	0	0	0	0	0	0	0	0	0	0	**0**	0	0	0	N/A
	13	0	0	0	0	0	0	0	0	0	0	0	0	**0**	0	0	N/A
	14	0	0	3	2	1	0	0	0	0	0	1	0	0	**4**	0	36.36%
	15	0	0	0	0	0	0	0	0	0	0	0	0	0	0	**0**	N/A
	P.A	0.34%	3.58%	81.10%	31.65%	5.01%	53.59%	27.51%	11.07%	0.87%	5.52%	38.68%	0.00%	0.00%	1.72%	0.00%	**45.34%**

MODIS3 CONFUSION MATRIX (11% SAMPLE)
GREEK STUDY AREA
DATE:04/05/2001
DOMINANT CLASS CLASSIFICATION SCHEME

		REFERENCE															
		1	2	3	4	5	6	7	8	9	10	11	12	13	14	15	U.A
CLASSIFIED	1	**1**	0	0	0	0	0	0	0	0	0	0	0	0	0	0	100.00%
	2	2	**17**	4	2	5	6	8	2	0	4	0	0	0	0	0	34.00%
	3	127	226	**5034**	1183	1138	746	157	155	161	628	96	7	2	25	1	51.97%
	4	3	42	435	**771**	181	238	161	177	97	261	18	0	0	1	0	32.33%
	5	2	9	48	30	**79**	23	4	2	4	23	3	0	0	1	0	34.65%
	6	16	24	530	300	210	**1343**	113	292	40	421	10	0	0	0	0	40.71%
	7	2	8	37	64	21	48	**208**	96	14	95	4	0	0	0	0	34.84%
	8	2	5	32	21	11	36	83	**88**	8	33	1	0	0	0	0	27.50%
	9	0	1	0	0	1	1	0	0	**2**	1	0	0	0	0	0	33.33%
	10	2	4	46	28	26	48	15	11	6	**90**	1	0	0	0	0	32.49%
	11	4	6	49	20	9	7	8	4	3	6	**85**	1	1	7	1	40.28%
	12	0	0	0	0	0	0	0	0	0	0	0	**0**	0	0	0	N/A
	13	0	0	0	0	0	0	0	0	0	0	0	0	**0**	0	0	N/A
	14	0	0	0	1	0	0	0	0	0	0	0	0	0	**0**	0	0.00%
	15	0	0	0	0	0	0	0	0	0	0	0	0	0	0	**0**	N/A
	P.A	0.62%	4.97%	81.00%	31.86%	4.70%	53.81%	27.48%	10.64%	0.60%	5.76%	38.99%	0.00%	0.00%	0.00%	0.00%	**45.24%**

MODIS3 CONFUSION MATRIX (11% SAMPLE)
GREEK STUDY AREA
DATE:04/07/2000
DOMINANT CLASS CLASSIFICATION SCHEME

		REFERENCE															
		1	2	3	4	5	6	7	8	9	10	11	12	13	14	15	U.A
CLASSIFIED	1	**23**	2	24	0	7	0	1	0	0	1	1	1	0	1	0	37.70%
	2	1	**29**	9	10	13	4	8	3	7	15	0	0	0	0	0	29.29%
	3	116	203	**5082**	1183	1014	667	188	156	139	608	90	5	2	27	0	53.61%
	4	9	60	599	**1049**	216	145	146	185	102	263	20	0	0	1	0	37.53%
	5	3	39	106	57	**187**	39	8	5	28	54	0	0	0	0	0	35.55%
	6	7	29	434	199	250	**1661**	124	267	52	459	5	0	0	0	0	47.63%
	7	3	24	107	69	38	139	**465**	242	29	122	10	0	0	0	0	37.26%
	8	1	2	20	7	4	20	14	**48**	5	11	1	0	0	0	0	36.09%
	9	0	0	0	0	0	0	0	0	**0**	0	0	0	0	0	0	N/A
	10	0	8	28	33	29	36	27	28	11	**105**	1	0	0	0	0	34.31%
	11	5	5	63	36	11	5	3	7	7	10	**101**	1	0	5	1	38.85%
	12	0	0	0	0	0	0	0	0	0	0	0	**0**	0	0	0	N/A
	13	0	0	0	0	0	0	0	0	0	0	0	0	**0**	0	0	N/A
	14	0	0	0	0	0	0	0	0	0	0	0	0	0	**0**	0	N/A
	15	0	0	0	0	0	0	0	0	0	0	0	0	0	0	**0**	N/A
	P.A	13.69%	7.23%	78.52%	39.69%	10.57%	61.16%	47.26%	5.10%	0.00%	6.37%	44.10%	0.00%	0.00%	0.00%	0.00%	**47.57%**

MODIS3 CONFUSION MATRIX (11% SAMPLE)
GREEK STUDY AREA
DATE:05/06/2000
DOMINANT CLASS CLASSIFICATION SCHEME

		REFERENCE															
		1	2	3	4	5	6	7	8	9	10	11	12	13	14	15	U.A
CLASSIFIED	1	**0**	0	0	0	0	0	0	0	0	0	0	0	0	0	0	N/A
	2	0	**0**	0	0	0	0	0	0	0	0	0	0	0	0	0	N/A
	3	115	266	**4914**	1569	1169	657	331	261	193	699	66	7	1	25	0	47.83%
	4	3	20	377	**590**	94	100	89	109	46	129	5	0	0	1	0	37.75%
	5	0	38	43	32	**54**	17	10	5	12	27	0	0	0	0	0	22.69%
	6	8	16	438	162	190	**1429**	258	389	43	463	12	0	0	0	0	41.93%
	7	0	9	40	49	17	24	**109**	57	9	52	4	0	0	0	0	29.46%
	8	0	0	1	2	1	0	0	**3**	0	0	0	0	0	0	0	42.86%
	9	0	0	0	1	0	0	0	0	**0**	0	0	0	0	0	0	0.00%
	10	1	7	32	23	24	33	12	14	9	**70**	1	0	0	0	0	30.97%
	11	1	2	25	19	6	2	2	0	0	2	**39**	0	0	1	0	39.39%
	12	0	0	0	0	0	0	0	0	0	0	0	**0**	0	0	0	N/A
	13	0	0	0	0	0	0	0	0	0	0	0	0	**0**	0	0	N/A
	14	0	0	0	0	0	0	0	0	0	0	0	0	0	**0**	0	N/A
	15	0	0	0	0	0	0	0	0	0	0	0	0	0	1	**1**	50.00%
	P.A	0.00%	0.00%	83.71%	24.11%	3.47%	63.17%	13.44%	0.36%	0.00%	4.85%	30.71%	0.00%	0.00%	0.00%	100.00%	**44.54%**

MODIS3 CONFUSION MATRIX (11% SAMPLE)
GREEK STUDY AREA
DATE:07/07/2000
DOMINANT CLASS CLASSIFICATION SCHEME

		REFERENCE															
		1	2	3	4	5	6	7	8	9	10	11	12	13	14	15	U.A
CLASSIFIED	1	**0**	0	0	0	0	0	0	0	0	0	0	0	0	0	0	N/A
	2	1	**18**	8	6	13	4	5	1	2	9	0	0	0	0	0	26.87%
	3	158	301	**5602**	1469	1135	710	278	218	185	734	85	7	0	27	1	51.35%
	4	8	34	510	**883**	212	124	132	148	51	184	14	1	1	4	0	38.29%
	5	1	18	79	49	**147**	12	10	4	23	23	1	0	0	0	0	40.05%
	6	15	39	667	278	289	**1808**	399	413	84	581	111	2	0	6	0	38.53%
	7	1	11	31	51	17	8	**95**	27	7	51	0	0	1	0	0	31.67%
	8	1	0	4	7	0	6	5	**25**	0	3	0	0	0	0	0	49.02%
	9	0	0	0	0	0	0	1	0	**1**	0	0	0	0	0	0	50.00%
	10	0	5	30	23	29	32	15	11	9	**71**	1	0	0	0	0	31.42%
	11	0	0	2	1	1	0	1	0	1	0	**11**	0	0	0	0	64.71%
	12	0	0	0	0	0	0	0	0	0	0	0	**0**	0	0	0	N/A
	13	0	0	0	0	0	0	0	0	0	0	0	0	**0**	0	0	N/A
	14	0	0	0	0	0	0	0	0	0	0	0	0	0	**0**	0	N/A
	15	0	0	0	0	0	0	0	0	0	0	0	0	0	0	**0**	N/A
	P.A	0.00%	4.23%	80.80%	31.91%	7.98%	66.86%	10.10%	2.95%	0.28%	4.29%	4.93%	0.00%	0.00%	0.00%	0.00%	**45.73%**

MODIS3 CONFUSION MATRIX (11% SAMPLE)
GREEK STUDY AREA
DATE:13/04/2000
DOMINANT CLASS CLASSIFICATION SCHEME

		REFERENCE															
		1	2	3	4	5	6	7	8	9	10	11	12	13	14	15	U.A
CLASSIFIED	1	**0**	0	0	1	0	0	0	0	0	0	0	0	0	0	0	0.00%
	2	0	**4**	0	0	1	0	0	0	0	0	0	0	0	0	0	80.00%
	3	91	116	**4108**	1019	772	502	162	168	169	469	78	6	1	12	3	53.52%
	4	7	28	451	**674**	102	223	174	203	56	197	7	2	0	0	0	31.73%
	5	0	3	57	8	**53**	32	3	3	5	43	1	0	0	0	0	25.48%
	6	4	15	378	156	159	**1105**	84	166	30	386	11	0	0	0	0	44.31%
	7	0	9	61	55	14	55	**203**	143	6	77	5	0	0	0	0	32.32%
	8	0	0	6	4	1	15	6	**31**	2	9	0	0	0	0	0	41.89%
	9	0	0	0	0	0	0	0	0	**1**	0	0	0	0	0	0	100.00%
	10	1	5	12	13	5	6	5	5	3	**24**	1	0	0	0	0	30.00%
	11	5	4	44	25	3	3	15	10	2	4	**48**	0	0	3	0	28.92%
	12	0	0	0	0	0	0	0	0	0	0	0	**0**	0	0	0	N/A
	13	0	0	0	0	0	0	0	0	0	0	0	0	**0**	0	0	N/A
	14	0	0	0	0	0	0	0	0	0	0	0	0	0	**0**	0	N/A
	15	0	0	0	0	0	0	0	0	0	0	0	0	0	0	**0**	N/A
	P.A	0.00%	2.17%	80.28%	34.48%	4.77%	56.93%	31.13%	4.25%	0.36%	1.99%	31.79%	0.00%	0.00%	0.00%	0.00%	**46.45%**

MODIS3 CONFUSION MATRIX (11% SAMPLE)
GREEK STUDY AREA
DATE:14/06/2000
DOMINANT CLASS CLASSIFICATION SCHEME

		REFERENCE															
		1	2	3	4	5	6	7	8	9	10	11	12	13	14	15	U.A
CLASSIFIED	1	**0**	0	0	0	0	0	0	0	0	0	0	0	0	0	0	N/A
	2	0	**7**	3	1	1	0	4	0	0	2	0	0	0	0	0	38.89%
	3	98	231	**4104**	1208	758	367	204	210	175	492	27	4	2	21	0	51.94%
	4	5	24	443	**711**	159	79	108	129	61	154	2	0	0	2	0	37.88%
	5	2	8	58	37	**79**	0	14	1	6	11	0	0	0	0	0	36.57%
	6	8	14	394	219	142	**957**	408	352	48	385	52	0	0	1	0	32.11%
	7	0	5	16	27	13	5	**52**	24	3	22	0	0	0	0	0	31.14%
	8	0	3	13	19	2	4	12	**33**	5	17	0	0	0	0	0	30.56%
	9	0	0	0	0	0	0	0	0	**0**	0	0	0	0	0	0	N/A
	10	0	2	33	21	21	31	21	18	5	**43**	0	0	0	0	0	22.05%
	11	1	2	0	2	0	0	0	0	0	0	**3**	0	0	0	0	37.50%
	12	0	0	0	0	0	0	0	0	0	0	0	**0**	0	0	0	N/A
	13	0	0	0	0	0	0	0	0	0	0	0	0	**0**	0	0	N/A
	14	0	0	1	0	0	0	0	0	0	0	0	0	0	**1**	0	50.00%
	15	0	0	0	0	0	0	0	0	0	0	0	0	0	0	**0**	N/A
	P.A	0.00%	2.36%	81.03%	31.67%	6.72%	66.32%	6.32%	4.30%	0.00%	3.82%	3.57%	0.00%	0.00%	4.00%	N/A	**44.46%**

MODIS3 CONFUSION MATRIX (11% SAMPLE)
GREEK STUDY AREA
DATE:20/08/2000
DOMINANT CLASS CLASSIFICATION SCHEME

		REFERENCE															
		1	2	3	4	5	6	7	8	9	10	11	12	13	14	15	U.A
CLASSIFIED	1	**2**	0	0	0	1	0	0	0	0	0	0	0	0	0	0	66.67%
	2	0	**24**	5	8	13	4	4	3	6	9	0	0	0	0	0	31.58%
	3	147	292	**5498**	1452	1232	701	181	163	175	694	82	7	2	27	0	51.61%
	4	9	46	446	**844**	156	210	162	194	66	289	21	0	0	0	0	34.55%
	5	5	23	173	116	**241**	59	21	4	26	45	2	1	0	3	0	33.52%
	6	7	12	430	227	199	**1784**	159	410	71	490	12	1	0	0	0	46.92%
	7	3	19	107	114	37	78	**625**	211	28	139	5	0	0	0	0	45.75%
	8	0	2	12	1	2	8	7	**11**	2	6	0	0	0	0	0	21.57%
	9	0	10	6	8	14	1	1	3	**18**	7	0	0	0	0	0	26.47%
	10	0	2	13	15	14	12	6	7	6	**42**	0	0	0	0	0	35.90%
	11	1	2	40	17	5	5	6	4	1	1	**72**	1	0	5	0	45.00%
	12	0	0	0	0	0	0	0	0	0	0	0	**0**	0	0	0	N/A
	13	0	0	0	0	0	0	0	0	0	0	0	0	**0**	0	0	N/A
	14	0	0	0	0	0	0	0	0	0	0	0	0	0	**1**	0	100.00%
	15	0	0	0	0	0	0	0	0	0	0	0	0	0	0	**0**	N/A
	P.A	1.15%	5.56%	81.69%	30.12%	12.59%	62.33%	53.33%	1.09%	4.51%	2.44%	37.11%	0.00%	0.00%	2.78%	N/A	**47.08%**

MODIS3 CONFUSION MATRIX (11% SAMPLE)
GREEK STUDY AREA
DATE:23/10/2000
DOMINANT CLASS CLASSIFICATION SCHEME

		REFERENCE															
		1	2	3	4	5	6	7	8	9	10	11	12	13	14	15	U.A
CLASSIFIED	1	**0**	0	0	0	0	0	0	0	0	0	0	0	0	0	0	N/A
	2	0	**4**	1	0	2	1	0	0	0	2	0	0	0	0	0	40.00%
	3	79	192	**3421**	1147	843	515	152	150	142	493	94	8	1	25	0	47.11%
	4	6	40	374	**700**	150	258	145	164	50	251	16	0	1	3	0	32.44%
	5	0	0	0	4	**4**	1	1	0	1	0	0	0	0	0	0	36.36%
	6	2	13	188	248	94	**685**	85	162	32	241	1	0	0	0	0	39.12%
	7	2	10	34	54	22	78	**173**	107	14	90	3	0	0	0	0	29.47%
	8	0	4	23	23	10	63	60	**71**	7	34	0	0	0	0	0	24.07%
	9	0	0	0	1	1	1	1	0	**1**	0	0	0	0	0	0	20.00%
	10	0	6	34	24	21	29	22	24	5	**58**	1	0	0	0	0	25.89%
	11	5	1	52	21	11	6	12	7	1	4	**78**	1	0	4	0	38.42%
	12	0	0	0	0	0	0	0	0	0	0	0	**0**	0	0	0	N/A
	13	0	0	0	0	0	0	0	0	0	0	0	0	**0**	0	0	N/A
	14	0	0	0	0	0	0	0	0	0	0	0	0	0	**0**	0	N/A
	15	0	0	0	0	0	0	0	0	0	0	0	0	0	0	**0**	N/A
	P.A	0.00%	1.48%	82.89%	31.50%	0.35%	41.84%	26.57%	10.36%	0.40%	4.94%	40.41%	0.00%	0.00%	0.00%	N/A	**41.54%**

MODIS3 CONFUSION MATRIX (11% SAMPLE)
GREEK STUDY AREA
DATE:24/03/2001
DOMINANT CLASS CLASSIFICATION SCHEME

		REFERENCE															
		1	2	3	4	5	6	7	8	9	10	11	12	13	14	15	U.A
CLASSIFIED	1	**1**	0	0	0	0	0	0	0	0	0	0	0	0	0	0	100.00%
	2	0	**9**	2	2	4	1	4	0	1	0	0	0	0	0	0	39.13%
	3	109	144	**5005**	1155	950	555	167	146	150	523	99	8	2	23	1	55.38%
	4	8	55	558	**941**	194	263	164	198	75	264	8	0	0	0	0	34.49%
	5	2	35	145	93	**212**	54	16	11	27	87	3	0	0	1	0	30.90%
	6	13	41	501	212	230	**1686**	200	307	68	525	11	0	0	0	0	44.44%
	7	4	10	120	132	41	144	**433**	216	12	143	9	0	0	0	0	34.26%
	8	0	0	1	0	0	4	1	**14**	0	3	1	0	0	0	0	58.33%
	9	0	0	1	0	0	0	0	0	**1**	0	0	0	0	0	0	50.00%
	10	1	10	40	23	19	54	11	11	6	**98**	3	0	0	0	0	35.51%
	11	6	3	75	34	12	3	12	6	0	6	**93**	1	0	9	0	35.77%
	12	0	0	0	0	0	0	0	0	0	0	0	**0**	0	0	0	N/A
	13	0	0	0	0	0	0	0	0	0	0	0	0	**0**	0	0	N/A
	14	0	0	0	0	0	0	0	0	0	0	0	0	0	**0**	0	N/A
	15	0	0	0	0	0	0	0	0	0	0	0	0	0	0	**0**	N/A
	P.A	0.69%	2.93%	77.62%	36.30%	12.76%	61.00%	42.96%	1.54%	0.29%	5.94%	40.97%	0.00%	0.00%	0.00%	0.00%	**46.94%**

MODIS3 CONFUSION MATRIX (11% SAMPLE)
GREEK STUDY AREA
DATE:25/10/2000
DOMINANT CLASS CLASSIFICATION SCHEME

		REFERENCE															
		1	2	3	4	5	6	7	8	9	10	11	12	13	14	15	U.A
CLASSIFIED	1	**0**	0	0	0	0	0	0	0	0	0	0	0	0	0	0	N/A
	2	0	**10**	1	6	2	2	1	0	4	2	0	0	0	0	0	35.71%
	3	144	212	**5543**	1344	1156	655	190	227	167	670	98	4	3	33	0	53.06%
	4	7	28	333	**594**	115	200	58	102	33	175	16	1	0	0	0	35.74%
	5	2	4	56	29	**79**	31	8	4	9	36	0	0	0	0	0	30.62%
	6	5	36	490	326	201	**1424**	176	313	58	459	9	1	0	0	0	40.71%
	7	3	6	62	52	30	101	**400**	155	16	106	6	0	0	0	0	42.69%
	8	1	1	27	16	6	38	26	**55**	6	27	0	0	0	0	0	27.09%
	9	0	0	2	1	1	1	0	0	**0**	1	0	0	0	0	0	0.00%
	10	2	8	47	46	27	56	25	23	6	**99**	2	0	0	0	0	29.03%
	11	1	1	18	5	3	1	1	5	0	2	**79**	0	0	4	0	65.83%
	12	0	0	0	0	0	0	0	0	0	0	0	**0**	0	0	0	N/A
	13	0	0	0	0	0	0	0	0	0	0	0	0	**0**	0	0	N/A
	14	0	0	0	0	0	0	0	0	0	0	0	0	0	**0**	0	N/A
	15	0	0	0	0	0	0	0	0	0	0	0	0	0	0	**0**	N/A
	P.A	0.00%	3.27%	84.25%	24.56%	4.88%	56.76%	45.20%	6.22%	0.00%	6.28%	37.62%	0.00%	0.00%	0.00%	N/A	**47.33%**

MODIS3 CONFUSION MATRIX (11% SAMPLE)
GREEK STUDY AREA
DATE:MULTIDATE
DOMINANT CLASS CLASSIFICATION SCHEME

		REFERENCE															
		1	2	3	4	5	6	7	8	9	10	11	12	13	14	15	U.A
CLASSIFIED	1	**0**	0	0	0	0	0	0	0	0	0	0	0	0	0	0	N/A
	2	0	**1**	1	0	0	0	0	0	0	1	0	0	0	0	0	33.33%
	3	66	138	**3342**	857	681	496	114	96	142	458	62	2	1	15	0	51.65%
	4	6	31	400	**651**	167	139	134	133	80	207	15	0	0	1	0	33.15%
	5	1	11	71	39	**92**	14	5	10	10	20	0	0	1	0	0	33.58%
	6	14	32	405	228	174	**1337**	232	331	37	460	12	0	0	1	0	40.97%
	7	1	4	20	41	6	25	**99**	65	8	35	9	0	0	0	0	31.63%
	8	1	1	11	26	5	19	12	**28**	0	10	1	0	0	0	0	24.56%
	9	0	0	0	0	0	0	0	0	**0**	0	0	0	0	0	0	N/A
	10	0	3	24	11	17	17	7	14	4	**52**	0	1	0	0	0	34.67%
	11	2	2	23	11	1	2	2	3	1	0	**57**	0	0	1	0	54.29%
	12	0	0	0	0	0	0	0	0	0	0	0	**0**	0	0	0	N/A
	13	0	0	0	0	0	0	0	0	0	0	0	0	**0**	0	0	N/A
	14	0	0	0	0	0	0	0	0	0	0	0	0	0	**0**	0	N/A
	15	0	0	0	0	0	0	0	0	0	0	0	0	0	0	**0**	N/A
	P.A	0.00%	0.45%	77.78%	34.92%	8.05%	65.25%	16.36%	4.12%	0.00%	4.18%	36.54%	0.00%	0.00%	0.00%	N/A	**44.71%**

VEGETATION CONFUSION MATRIX (11% SAMPLE)
GREEK STUDY AREA
DATE:03/08/2000
DOMINANT CLASS CLASSIFICATION SCHEME

		REFERENCE															
		1	2	3	4	5	6	7	8	9	10	11	12	13	14	15	U.A
CLASSIFIED	1	**6**	2	12	5	3	1	2	1	0	0	1	0	0	0	0	18.18%
	2	0	**9**	5	5	6	0	1	3	1	3	0	0	0	0	0	27.27%
	3	109	152	**4887**	848	852	671	180	246	85	546	53	6	0	20	0	56.46%
	4	18	91	611	**839**	202	157	118	144	60	245	11	1	0	6	0	33.52%
	5	1	26	136	37	**168**	26	12	7	15	51	2	0	0	0	0	34.93%
	6	12	21	580	177	193	**1454**	125	245	52	417	9	2	0	0	0	44.23%
	7	4	25	126	59	40	73	**401**	136	19	104	10	0	0	1	0	40.18%
	8	2	3	65	13	10	51	41	**73**	7	26	0	0	0	1	0	25.00%
	9	0	1	0	0	1	0	2	1	**2**	2	0	0	0	0	0	22.22%
	10	1	11	52	42	31	69	29	19	12	**101**	3	0	0	0	0	27.30%
	11	1	0	12	3	1	6	2	0	0	2	**51**	1	0	1	0	63.75%
	12	0	0	0	0	0	0	0	0	0	0	0	**0**	0	0	0	N/A
	13	0	0	0	0	0	0	0	0	0	0	0	0	**0**	0	0	N/A
	14	0	0	0	0	0	0	0	0	0	0	0	0	0	**0**	0	N/A
	15	0	0	0	0	0	0	0	0	0	0	0	0	0	0	**0**	N/A
	P.A	3.90%	2.64%	75.35%	41.37%	11.15%	57.97%	43.92%	8.34%	0.79%	6.75%	36.43%	0.00%	N/A	0.00%	N/A	**47.73%**

VEGETATION CONFUSION MATRIX (11% SAMPLE)
GREEK STUDY AREA
DATE:03/10/2001
DOMINANT CLASS CLASSIFICATION SCHEME

		REFERENCE															
		1	2	3	4	5	6	7	8	9	10	11	12	13	14	15	U.A
CLASSIFIED	1	**12**	2	13	0	1	0	0	0	0	1	1	0	0	1	0	38.71%
	2	1	**1**	0	0	1	0	0	0	0	0	0	0	0	0	0	33.33%
	3	145	295	**5727**	1385	1257	571	187	142	183	603	94	8	0	25	1	53.91%
	4	13	53	461	**911**	159	225	181	205	91	297	11	2	0	5	0	34.85%
	5	2	34	143	91	**263**	42	10	1	26	51	4	0	0	0	0	39.43%
	6	2	23	386	274	192	**1747**	133	317	67	470	3	0	0	1	0	48.33%
	7	2	11	64	71	19	54	**495**	185	16	94	3	0	0	0	0	48.82%
	8	1	3	25	17	12	69	70	**117**	12	24	0	0	0	0	0	33.43%
	9	0	0	0	0	0	0	0	0	**0**	0	0	0	0	0	0	N/A
	10	0	4	46	35	23	59	7	12	16	**82**	0	0	0	0	0	28.87%
	11	4	2	50	26	7	2	2	7	1	4	**84**	0	0	8	0	42.64%
	12	0	0	0	0	0	0	0	0	0	0	0	**0**	0	0	0	N/A
	13	0	0	0	0	0	0	0	0	0	0	0	0	**0**	0	0	N/A
	14	0	0	0	0	0	0	0	0	0	0	0	0	0	**0**	0	N/A
	15	0	0	0	0	0	0	0	0	0	0	0	0	0	0	**0**	N/A
	P.A	6.59%	0.23%	82.82%	32.42%	13.60%	63.09%	45.62%	11.87%	0.00%	5.04%	42.00%	0.00%	N/A	0.00%	0.00%	**48.66%**

VEGETATION CONFUSION MATRIX (11% SAMPLE)
GREEK STUDY AREA
DATE:04/05/2001
DOMINANT CLASS CLASSIFICATION SCHEME

		REFERENCE															
		1	2	3	4	5	6	7	8	9	10	11	12	13	14	15	U.A
CLASSIFIED	1	**22**	6	6	0	2	2	0	0	3	1	0	0	0	0	1	51.16%
	2	1	**6**	2	3	0	1	0	0	1	0	0	0	0	0	0	42.86%
	3	129	217	**5258**	1029	906	515	161	133	130	517	51	5	3	23	1	57.92%
	4	1	50	418	**867**	179	210	195	209	95	270	12	1	0	2	0	34.56%
	5	7	35	205	133	**364**	89	12	11	28	106	0	0	0	1	0	36.73%
	6	8	21	449	267	220	**1612**	91	250	54	519	4	0	0	0	0	46.12%
	7	2	4	44	80	22	37	**255**	141	5	78	3	0	0	0	0	38.00%
	8	0	2	18	31	2	37	48	**63**	4	25	1	0	0	0	0	27.27%
	9	0	0	0	0	0	0	0	0	**0**	0	0	0	0	0	0	N/A
	10	3	12	38	39	50	40	6	13	16	**75**	0	0	0	1	0	25.60%
	11	1	6	57	25	13	5	1	4	3	5	**134**	2	0	6	0	51.15%
	12	0	0	0	0	0	0	0	0	0	0	0	**0**	0	0	0	N/A
	13	0	0	0	0	0	0	0	0	0	0	0	0	**0**	0	0	N/A
	14	0	0	0	0	0	0	0	0	0	0	0	0	0	**0**	0	N/A
	15	0	0	0	0	0	0	0	0	0	0	0	0	0	0	**0**	N/A
	P.A	12.64%	1.67%	80.95%	35.04%	20.71%	63.27%	33.16%	7.65%	0.00%	4.70%	65.37%	0.00%	0.00%	0.00%	0.00%	**49.22%**

VEGETATION CONFUSION MATRIX (11% SAMPLE)
GREEK STUDY AREA
DATE:04/07/2000
DOMINANT CLASS CLASSIFICATION SCHEME

		REFERENCE															
		1	2	3	4	5	6	7	8	9	10	11	12	13	14	15	U.A
CLASSIFIED	1	**16**	3	10	0	2	0	0	0	0	0	1	1	0	1	1	45.71%
	2	0	**3**	2	2	1	1	2	0	0	6	1	0	0	0	0	16.67%
	3	133	243	**5470**	1089	919	485	151	149	145	539	54	4	2	25	0	58.14%
	4	6	84	533	**1120**	234	91	167	159	105	263	22	0	0	1	0	40.22%
	5	3	32	200	141	**340**	47	15	7	25	65	9	0	0	1	0	38.42%
	6	6	23	354	197	249	**1942**	89	265	64	524	4	2	0	0	0	52.22%
	7	1	10	53	73	14	33	**536**	163	21	117	5	0	0	1	0	52.19%
	8	0	0	55	21	6	101	67	**193**	6	42	1	0	0	1	0	39.15%
	9	0	0	0	0	0	0	0	0	**0**	0	0	0	0	0	0	N/A
	10	0	8	48	51	52	69	28	25	18	**129**	1	0	0	1	0	30.00%
	11	3	5	36	18	12	2	4	3	3	4	**126**	0	0	2	0	57.80%
	12	0	0	0	0	0	0	0	0	0	0	0	**0**	0	0	0	N/A
	13	0	0	0	0	0	0	0	0	0	0	0	0	**0**	0	0	N/A
	14	0	0	1	0	0	0	0	0	0	0	0	0	0	**1**	0	50.00%
	15	0	0	0	0	0	0	0	0	0	0	0	0	0	0	**0**	N/A
	P.A	9.52%	0.73%	80.89%	41.30%	18.59%	70.08%	50.61%	20.02%	0.00%	7.64%	56.25%	0.00%	0.00%	2.94%	0.00%	**51.92%**

VEGETATION CONFUSION MATRIX (11% SAMPLE)
GREEK STUDY AREA
DATE:05/06/2000
DOMINANT CLASS CLASSIFICATION SCHEME

		REFERENCE															
		1	2	3	4	5	6	7	8	9	10	11	12	13	14	15	U.A
CLASSIFIED	1	**23**	6	17	1	5	0	0	0	0	0	0	0	0	0	0	44.23%
	2	0	**25**	10	10	15	4	1	0	3	2	0	0	0	0	0	35.71%
	3	104	273	**4876**	1212	903	370	247	187	181	567	44	6	0	18	2	54.24%
	4	9	17	424	**805**	169	75	101	100	57	149	7	0	0	3	0	42.01%
	5	1	26	120	85	**200**	21	5	2	9	35	0	0	0	0	0	39.68%
	6	6	13	336	185	185	**1655**	128	308	43	471	2	0	0	0	0	49.67%
	7	0	6	45	51	9	46	**271**	142	4	71	2	1	1	1	0	41.69%
	8	0	1	16	20	3	32	33	**63**	0	16	2	0	0	0	0	33.87%
	9	0	0	0	0	0	0	0	0	**0**	0	0	0	0	0	0	N/A
	10	2	3	67	48	62	72	23	18	12	**122**	0	0	0	0	0	28.44%
	11	2	0	35	20	9	1	3	3	0	5	**66**	0	0	3	0	44.90%
	12	0	0	0	0	0	0	0	0	0	0	0	**0**	0	0	0	N/A
	13	0	0	0	0	0	0	0	0	0	0	0	0	**0**	0	0	N/A
	14	0	0	0	0	0	0	0	0	0	0	0	0	0	**0**	0	N/A
	15	0	0	0	0	0	0	0	0	0	0	0	0	0	0	**0**	N/A
	P.A	15.65%	6.76%	82.00%	33.03%	12.82%	72.72%	33.37%	7.65%	0.00%	8.48%	53.66%	0.00%	0.00%	0.00%	0.00%	**49.80%**

VEGETATION CONFUSION MATRIX (11% SAMPLE)
GREEK STUDY AREA
DATE:07/07/2000
DOMINANT CLASS CLASSIFICATION SCHEME

		REFERENCE															
		1	2	3	4	5	6	7	8	9	10	11	12	13	14	15	U.A
CLASSIFIED	1	**29**	3	14	0	2	0	0	0	0	0	0	0	0	0	0	60.42%
	2	2	**15**	9	5	9	1	0	0	0	2	0	0	0	0	0	34.88%
	3	138	261	**5549**	1018	877	494	185	135	180	517	75	7	0	26	1	58.64%
	4	11	52	592	**1242**	247	145	180	195	84	283	18	1	0	5	0	40.65%
	5	6	54	277	148	**402**	46	17	4	19	86	1	0	0	0	0	37.92%
	6	7	25	409	184	242	**2022**	128	348	65	519	5	1	1	1	0	51.10%
	7	0	10	57	36	19	42	**491**	149	10	100	5	0	0	1	0	53.37%
	8	1	3	34	19	7	60	57	**115**	5	29	3	0	0	0	0	34.53%
	9	0	1	0	3	0	0	1	1	**1**	1	0	0	0	0	0	12.50%
	10	0	4	88	58	55	67	26	16	12	**149**	1	0	0	1	0	31.24%
	11	4	0	54	34	4	8	7	10	1	8	**128**	2	0	5	0	48.30%
	12	0	0	0	0	0	0	0	0	0	0	0	**0**	0	0	0	N/A
	13	0	0	0	0	0	0	0	0	0	0	0	0	**0**	0	0	N/A
	14	0	0	0	0	0	0	0	0	0	0	0	0	0	**0**	0	N/A
	15	0	0	0	0	0	0	0	0	0	0	0	0	0	0	**0**	N/A
	P.A	14.65%	3.50%	78.34%	45.21%	21.57%	70.09%	44.96%	11.82%	0.27%	8.80%	54.24%	0.00%	0.00%	0.00%	0.00%	**51.67%**

VEGETATION CONFUSION MATRIX (11% SAMPLE)
GREEK STUDY AREA
DATE:13/04/2000
DOMINANT CLASS CLASSIFICATION SCHEME

		REFERENCE															
		1	2	3	4	5	6	7	8	9	10	11	12	13	14	15	U.A
CLASSIFIED	1	**0**	0	0	0	0	0	0	0	0	0	0	0	0	0	0	N/A
	2	0	**0**	0	0	0	0	0	0	0	0	0	0	0	0	0	N/A
	3	88	124	**4419**	850	708	475	88	92	104	402	29	5	1	9	0	59.76%
	4	8	20	369	**747**	110	201	126	188	67	192	5	1	0	3	1	36.65%
	5	0	6	51	17	**70**	50	1	0	2	57	1	0	0	0	0	27.45%
	6	8	30	400	191	233	**1151**	112	230	79	458	9	0	0	0	0	39.68%
	7	0	2	53	92	10	39	**270**	150	12	85	2	0	0	0	0	37.76%
	8	0	0	18	38	4	27	59	**83**	4	16	5	0	0	0	0	32.68%
	9	0	0	0	0	0	0	0	0	**0**	0	0	0	0	0	0	N/A
	10	1	1	19	12	11	22	2	7	2	**28**	0	0	0	0	0	26.67%
	11	7	2	27	16	4	6	13	4	1	5	**103**	1	0	4	2	52.82%
	12	0	0	0	0	0	0	0	0	0	0	0	**0**	0	0	0	N/A
	13	0	0	0	0	0	0	0	0	0	0	0	0	**0**	0	0	N/A
	14	0	0	0	0	0	0	0	0	0	0	0	0	0	**0**	0	N/A
	15	0	0	0	0	0	0	0	0	0	0	0	0	0	0	**0**	N/A
	P.A	0.00%	0.00%	82.51%	38.05%	6.09%	58.40%	40.24%	11.01%	0.00%	2.25%	66.88%	0.00%	0.00%	0.00%	0.00%	**49.59%**

VEGETATION CONFUSION MATRIX (11% SAMPLE)
GREEK STUDY AREA
DATE:14/06/2000
DOMINANT CLASS CLASSIFICATION SCHEME

		REFERENCE															
		1	2	3	4	5	6	7	8	9	10	11	12	13	14	15	U.A
CLASSIFIED	1	**26**	6	12	1	5	0	0	0	0	0	2	0	0	0	0	50.00%
	2	4	**17**	2	6	9	1	1	0	0	1	0	0	0	0	0	41.46%
	3	83	218	**4172**	923	663	257	133	110	149	401	42	3	1	26	0	58.10%
	4	4	30	495	**1022**	232	62	137	148	77	174	6	0	0	3	0	42.76%
	5	1	6	89	49	**116**	12	4	1	5	21	2	0	0	0	0	37.91%
	6	5	12	242	110	115	**1088**	104	273	40	351	0	0	0	0	0	46.50%
	7	1	3	58	67	21	33	**469**	185	13	93	1	0	0	0	0	49.68%
	8	2	0	42	18	6	66	64	**143**	9	38	1	0	1	0	0	36.67%
	9	0	0	0	0	0	0	0	0	**0**	0	0	0	0	0	0	N/A
	10	1	3	42	27	23	39	15	14	7	**58**	0	0	0	0	0	25.33%
	11	1	0	13	10	5	0	3	2	1	2	**32**	0	0	0	0	46.38%
	12	0	0	0	0	0	0	0	0	0	0	0	**0**	0	0	0	N/A
	13	0	0	0	0	0	0	0	0	0	0	0	0	**0**	0	0	N/A
	14	0	0	0	0	0	0	0	0	0	0	0	0	0	**0**	0	N/A
	15	0	0	0	0	0	0	0	0	0	0	0	0	0	0	**0**	N/A
	P.A	20.31%	5.76%	80.74%	45.77%	9.71%	69.83%	50.43%	16.32%	0.00%	5.09%	37.21%	0.00%	0.00%	0.00%	N/A	**51.23%**

VEGETATION CONFUSION MATRIX (11% SAMPLE)
GREEK STUDY AREA
DATE:20/08/2000
DOMINANT CLASS CLASSIFICATION SCHEME

		REFERENCE															
		1	2	3	4	5	6	7	8	9	10	11	12	13	14	15	U.A
CLASSIFIED	1	**22**	5	6	0	1	0	0	0	0	0	0	0	0	0	0	64.71%
	2	0	**0**	0	0	0	0	0	0	0	0	0	0	0	0	0	N/A
	3	137	285	**5644**	1104	1102	544	159	113	164	608	70	7	2	27	0	56.63%
	4	10	80	568	**1182**	235	173	210	197	108	329	24	0	0	3	0	37.90%
	5	13	46	211	156	**366**	30	20	4	36	45	4	0	0	1	0	39.27%
	6	7	15	379	202	175	**1950**	107	310	55	471	4	3	0	3	0	52.97%
	7	0	9	57	81	20	33	**609**	194	22	120	2	0	0	0	0	53.10%
	8	1	1	36	53	9	96	64	**186**	8	48	0	0	0	0	0	37.05%
	9	0	0	0	0	0	1	0	1	**2**	1	0	0	0	0	0	40.00%
	10	0	4	33	26	21	33	11	10	7	**69**	3	0	0	0	0	31.80%
	11	2	0	31	21	9	2	3	5	1	7	**85**	1	0	2	0	50.30%
	12	0	0	0	0	0	0	0	0	0	0	0	**0**	0	0	0	N/A
	13	0	0	0	0	0	0	0	0	0	0	0	0	**0**	0	0	N/A
	14	0	0	0	0	0	0	0	0	0	0	0	0	0	**0**	0	N/A
	15	0	0	0	0	0	0	0	0	0	0	0	0	0	0	**0**	N/A
	P.A	11.46%	0.00%	81.03%	41.84%	18.89%	68.13%	51.48%	18.24%	0.50%	4.06%	44.27%	0.00%	0.00%	0.00%	N/A	**51.16%**

VEGETATION CONFUSION MATRIX (11% SAMPLE)
GREEK STUDY AREA
DATE:23/10/2000
DOMINANT CLASS CLASSIFICATION SCHEME

		REFERENCE															
		1	2	3	4	5	6	7	8	9	10	11	12	13	14	15	U.A
CLASSIFIED	1	**7**	3	6	0	3	0	1	0	0	0	0	0	0	0	0	35.00%
	2	0	**0**	0	0	0	0	0	0	0	0	0	0	0	0	0	N/A
	3	77	191	**3795**	1039	888	601	170	138	132	536	84	7	2	25	0	49.38%
	4	5	40	362	**821**	141	259	118	165	72	273	2	0	0	1	0	36.34%
	5	2	16	55	32	**119**	6	1	1	7	7	0	0	0	4	0	47.60%
	6	5	19	219	203	54	**641**	51	133	28	197	1	1	0	0	0	41.30%
	7	3	3	44	57	10	36	**226**	113	4	64	4	0	0	0	0	40.07%
	8	0	6	18	47	8	37	49	**93**	4	33	0	0	0	0	0	31.53%
	9	0	0	0	0	0	0	0	0	**0**	0	0	0	0	0	0	N/A
	10	1	3	36	28	7	39	13	14	3	**56**	0	0	0	0	0	28.00%
	11	7	0	38	30	8	4	3	5	1	6	**99**	1	0	3	0	48.29%
	12	0	0	0	0	0	0	0	0	0	0	0	**0**	0	0	0	N/A
	13	0	0	0	0	0	0	0	0	0	0	0	0	**0**	0	0	N/A
	14	0	0	0	0	0	0	0	0	0	0	0	0	0	**0**	0	N/A
	15	0	0	0	0	0	0	0	0	0	0	0	0	0	0	**0**	N/A
	P.A	6.54%	0.00%	82.99%	36.38%	9.61%	39.49%	35.76%	14.05%	0.00%	4.78%	52.11%	0.00%	0.00%	0.00%	N/A	**44.95%**

VEGETATION CONFUSION MATRIX (11% SAMPLE)
GREEK STUDY AREA
DATE:24/03/2001
DOMINANT CLASS CLASSIFICATION SCHEME

		REFERENCE															
		1	2	3	4	5	6	7	8	9	10	11	12	13	14	15	U.A
CLASSIFIED	1	**8**	4	3	1	2	4	2	1	1	1	0	0	0	0	0	29.63%
	2	2	**16**	7	14	6	3	1	0	3	4	0	0	0	0	0	28.57%
	3	93	156	**5113**	1047	839	378	156	107	153	389	47	6	1	10	0	60.19%
	4	7	44	460	**992**	169	228	154	194	61	254	9	0	0	1	0	38.55%
	5	8	23	163	73	**234**	62	16	9	12	93	0	0	0	2	0	33.67%
	6	12	41	446	234	291	**1865**	144	263	76	652	15	1	0	4	0	46.12%
	7	4	12	84	96	29	74	**479**	204	5	103	6	0	1	2	0	43.59%
	8	1	1	33	22	6	36	42	**100**	7	26	0	0	0	0	0	36.50%
	9	0	0	0	0	0	0	0	0	**0**	0	0	0	0	0	0	N/A
	10	1	4	37	29	37	60	11	8	7	**74**	1	1	0	0	0	27.41%
	11	9	2	75	58	19	6	11	8	1	12	**150**	1	0	13	1	40.98%
	12	0	0	0	0	0	0	0	0	0	0	0	**0**	0	0	0	N/A
	13	0	0	0	0	0	0	0	0	0	0	0	0	**0**	0	0	N/A
	14	0	0	0	0	0	0	0	0	0	0	0	0	0	**0**	0	N/A
	15	0	0	0	0	0	0	0	0	0	0	0	0	0	0	**0**	N/A
	P.A	5.52%	5.28%	79.63%	38.66%	14.34%	68.67%	47.15%	11.19%	0.00%	4.60%	65.79%	0.00%	0.00%	0.00%	0.00%	**50.46%**

VEGETATION CONFUSION MATRIX (11% SAMPLE)
GREEK STUDY AREA
DATE:25/10/2000
DOMINANT CLASS CLASSIFICATION SCHEME

		REFERENCE															
		1	2	3	4	5	6	7	8	9	10	11	12	13	14	15	U.A
CLASSIFIED	1	**4**	0	3	0	0	0	0	0	0	0	0	0	0	0	0	57.14%
	2	0	**17**	4	3	7	6	1	1	1	10	1	0	0	0	0	33.33%
	3	112	136	**4443**	811	987	993	226	241	82	675	92	6	4	20	0	50.33%
	4	5	24	365	**408**	94	181	70	95	14	132	9	1	1	3	1	29.08%
	5	0	13	142	29	**99**	71	13	13	14	44	2	0	0	1	0	22.45%
	6	9	69	705	350	292	**1398**	164	180	51	498	21	0	0	1	0	37.40%
	7	4	16	131	80	36	96	**262**	101	11	102	12	0	0	1	0	30.75%
	8	1	3	67	15	13	43	16	**22**	7	16	0	0	0	0	0	10.84%
	9	0	0	0	0	0	0	0	0	**0**	0	0	0	0	0	0	N/A
	10	2	11	59	29	25	65	20	12	8	**75**	0	0	0	1	0	24.43%
	11	2	2	22	13	6	2	2	1	0	4	**124**	0	0	5	0	67.76%
	12	0	0	0	0	0	0	0	0	0	0	0	**0**	0	0	0	N/A
	13	0	0	0	0	0	0	0	0	0	0	0	0	**0**	0	0	N/A
	14	0	0	0	0	0	0	0	0	0	0	0	0	0	**0**	0	N/A
	15	0	0	0	0	0	0	0	0	0	0	0	0	0	0	**0**	N/A
	P.A	2.88%	5.84%	74.79%	23.48%	6.35%	48.97%	33.85%	3.30%	0.00%	4.82%	47.51%	0.00%	0.00%	0.00%	0.00%	**42.79%**

VEGETATION CONFUSION MATRIX (11% SAMPLE)
GREEK STUDY AREA
DATE:MULTIDATE
DOMINANT CLASS CLASSIFICATION SCHEME

		REFERENCE															
		1	2	3	4	5	6	7	8	9	10	11	12	13	14	15	U.A
CLASSIFIED	1	**4**	2	3	1	2	0	1	0	0	0	0	0	0	0	0	30.77%
	2	0	**5**	1	1	4	0	1	0	0	3	0	0	0	0	0	33.33%
	3	76	102	**3589**	559	493	272	54	67	88	315	32	2	1	10	0	63.41%
	4	9	47	372	**919**	169	106	125	129	80	222	9	0	0	1	0	42.00%
	5	5	27	115	89	**302**	34	16	8	26	52	1	0	0	0	0	44.74%
	6	5	25	267	168	148	**1528**	56	227	44	389	0	1	0	0	0	53.46%
	7	0	6	41	55	15	20	**288**	125	14	89	2	0	0	0	0	43.97%
	8	0	2	18	27	4	57	42	**111**	3	27	1	0	0	0	0	38.01%
	9	1	0	0	1	3	0	0	0	**3**	0	0	0	0	0	0	37.50%
	10	1	14	68	56	65	82	30	37	18	**166**	1	0	0	0	0	30.86%
	11	1	4	31	11	4	0	1	2	4	1	**112**	0	1	5	0	63.28%
	12	0	0	0	0	0	0	0	0	0	0	0	**0**	0	0	0	N/A
	13	0	0	0	0	0	0	0	0	0	0	0	0	**0**	0	0	N/A
	14	0	1	0	0	0	0	0	0	0	0	1	0	0	**2**	0	50.00%
	15	0	0	0	0	0	0	0	0	0	0	0	0	0	0	**0**	N/A
	P.A	3.92%	2.13%	79.67%	48.70%	24.98%	72.80%	46.91%	15.72%	1.07%	13.13%	70.44%	0.00%	0.00%	11.11%	N/A	**53.73%**

Appendix C, Drought monitoring

GLC2000 AFRICAN MAP CLASSIFICATION SCHEME
(http://www-gvm.jrc.it/glc2000/Products/africa/GLC2000_africa3.pdf (14 December 2006)

	GLC2000 AFRICAN MAP LANDCOVER CLASS
1	Closed evergreen lowland forest
2	Degraded evergreen lowland forest
3	Submontane forest (900 -1500 m)
4	Montane forest (>1500 m)
5	Swamp forest
6	Mangrove
7	Mosaic Forest / Croplands
8	Mosaic Forest / Savanna
9	Closed deciduous forest
10	Deciduous woodland
11	Deciduous shrubland with sparse trees
12	Open deciduous shrubland
13	Closed grassland
14	Open grassland with sparse shrubs
15	Open grassland
16	Sparse grassland
17	Swamp bushland and grassland
18	Croplands (>50%)
19	Croplands with open woody vegetation
20	Irrigated croplands
21	Tree crops
22	Sandy desert and dunes
23	Stony desert
24	Bare rock
25	Salt hardpans
26	Waterbodies
27	Cities

Candidate rainfall stations in Ethiopia

Name	Code	Longitude (in dd)	Latitude (in dd)
Abdela	ILABDE14	36.2500	8.3667
Adamitulu	SHADAM14	38.7000	7.8500
Agarfa	BAAGAR14	39.8167	7.2833
Aleltu	SHALEL14	39.1500	9.2000
Ambuye	KFAMBU14	36.9000	7.9667
Ameya	SHAMEY14	37.7500	8.5667
Aposto/Yekatit-25	SIAPOS14	38.2500	6.6667
Arerti	SHARER14	39.4167	8.9500
Babile	HABABI14	42.3333	9.2333
Bantuliben	SHBANT14	38.2667	8.6167
Bedeno	HABEDE14	41.6333	9.1333
Bisidimo	HABISI14	42.2667	9.1167
Bita Woshi	KFBITA14	36.0000	7.3000
Bologiorgis	SHBOLO14	39.4333	8.8167
Boneya	SHBONE14	38.6500	8.8000
Bulbula	SHBULB14	38.7167	7.7167
Busa	SHBUSA14	38.1167	8.8333
Chacha	SHCHAC14	39.4500	9.5500
Chekorsa	KFCHEK24	36.7333	7.6167
Chelenko	HACHEL14	41.5333	9.4000
Chena	KFCHEN14	35.8500	7.1667
Chinaksen	HACHIN14	42.5500	9.4500
Chora	ILCHOR14	36.1167	8.3500
Dabat	GNDABA14	37.7500	12.9833
Debre Sina	SHDEBR24	39.7500	9.8667
Deder	HADEDE14	41.4667	9.3167
Delo Sebro	BADELO14	40.4667	7.2500
Dera	SHDERA14	38.7167	10.1833
Derba	SHDERB14	38.6333	9.4333
Dertu Liben	SHDERT14	38.9833	8.6833
Didu Gordomo	ILDIDU14	35.5167	8.4000
Dilela	SHDILE14	38.0500	8.6167
Dimtu	KFDIMT14	37.2500	8.0333
Durame	SHDURA14	37.9500	7.2000
Ejere	SHEJER14	39.2667	8.8167
Ejersa Lele	SHEJER34	38.6833	8.2500
Enchini	SHENCH14	38.3667	9.3167
Enselale	SHENSE14	38.4167	8.9333
Fedis	HAFEDI14	42.3000	8.2500
Fugo Leka	ILFUGO14	35.8833	8.1833
Gibe Farm	SHGIBE14	37.5833	8.2333
Ginager	SHGINA14	39.5667	9.3167
Ginchi	SHGINC14	38.1167	9.0333
Gorgora School	GNGORG14	37.3000	12.2500
Guranda Meta	SHGURA14	38.7667	8.9833
Hareto	WEHARE14	37.1167	9.3500

Hena	WEHENA14	35.6000	9.4500
Hombole	SHHOMB14	38.7667	8.3667
Ibnat Police Station	GNIBNA14	38.0500	12.1333
Indento	ARINDE14	39.8167	7.5667
Karakore	SHKARA14	39.9500	10.4667
Kombolcha	HAKOMB14	42.1000	9.4333
Kone	WEKONE14	36.7833	8.6833
Kora	HAKORA14	40.5333	9.1167
Korata	GNKORA14	37.5667	11.7333
Koshe	SHKOSH14	38.5333	8.0167
Kumbi	KFKUMB14	37.4667	8.1167
Kutaber	WOKUTA14	39.5333	11.2667
Kuyera	SHKUYE34	38.6667	7.2500
Lefasa	HALEFA14	42.9000	9.5000
Limu Seka	KFLIMU24	36.9167	8.1000
Medhanalem/Sch	SHMEDH14	38.7500	9.0833
Meki	SHMEKI14	38.8167	8.1500
Menge	WEMENG14	34.7333	10.3333
Meteso	KFMETE14	36.8833	7.4333
Muke Turi	SHMUKE14	38.8667	9.5500
Saja School	KFSAJA14	37.4000	7.9667
Seladingai	SHSELA14	39.6167	9.9500
Sendafa	SHSEND14	39.0167	9.1500
Serbo	KFSERB14	36.9667	7.7167
Setema	ILSETE24	36.4333	8.1667
Shone	SHSHON14	37.9667	7.1333
Teji	SHTEJI14	38.3667	8.8000
Toke Erenso	SHTOKE14	37.6167	8.9667
Tora	SHTORA14	38.4167	7.8667
Wayu	WEWAYU14	37.3667	9.2333
Welenchiti	SHWELE14	39.4333	8.6667
Welenkomi	SHWELE24	38.2000	9.0167
Wendo Genet	SHWEND34	38.5833	7.1667
Woldia	WOWOLD34	39.6167	11.8333
Wurgesa	WOWURG24	39.6167	11.5500
Yambero	ILYAMB14	36.4500	8.2667
Yeki	ILYEKI14	35.3500	7.2000
Zequala	SHZEQU14	38.8667	8.5333